



TECHNISCHE UNIVERSITÄT MÜNCHEN

FAKULTÄT FÜR CHEMIE

FACHBEREICH ORGANISCHE CHEMIE

**The Multifunctional Component Catalyst Principle (MFCCP):
Design of Functional Catalyst Precursors for Systematic Reaction
Development**

Philippe Klein

Vollständiger Abdruck der von der Fakultät für Chemie der Technischen Universität München zur Erlangung des akademischen Grades eines

Doktors der Naturwissenschaften (Dr. rer. nat.)

genehmigten Dissertation.

Vorsitzende(r):

Prof. Dr. Thomas Brück

Prüfer der Dissertation:

1. Prof. Dr. Lukas Hintermann
2. Prof. Dr. Klaus Köhler

Die Dissertation wurde am 28.10.2020 bei der Technischen Universität München eingereicht und durch die Fakultät für Chemie am 08.12.2020 angenommen.

Für meine Eltern und Großeltern.

If you want great success you need to offer great sacrifice.

Otherwise why would you be so lucky?

You can't just carelessly expect things from the universe,

Don Pepijn Schipper.

The present thesis was carried out from October 2016 to October 2020 under the supervision of Prof. Dr. Lukas Hintermann at the Technical University of Munich. This thesis has been funded by the Fonds National de la Recherche (FNR) Luxembourg (project number 11587854).

Parts of this thesis have already been published prior to the submission of the thesis:

P. Klein, V. D. Lechner, T. Schimmel, L. Hintermann,* *Chem. Eur. J.* **2020**, *26*, 176-180, DOI: 10.1002/chem.201904545. For license agreement, see 8.7.1.

Acknowledgment

Every project starts with the idea of a new concept and so did mine. It is never easy to be the first one; the first to climb a mountain, the first to discover a new pharmaceutical, the first in line. This project left me being the first one to synthesize, isolate and apply multifunctional component catalyst precursors. A challenge I could not have tackled without my supervisor. Since December 2015, Prof. Dr. Lukas Hintermann gave me the opportunity to be part of his group. Now it is time for me to say, 'thank you'. While researching in your group, I quickly realized how endless your scientific, practical as well as your general knowledge is. I appreciated the margin you always left for me to work independently in the laboratory. Every discussion with you showed me different points of view, to think outside the box, to consider the unobvious. Even though chemistry can be frustrating at some point, I always enjoyed every new day in our laboratories. Special thanks to you for the large-scale synthesis of the cycloheptatrienyl hexafluorophosphate in Aachen. You are right: the larger the scale, the longer it lasts.

I want to thank the Fonds National de la Recherche (FNR) Luxembourg for the financial support throughout the execution of my thesis (project number 11587854).

A special thanks goes to Sabrina Nietsch and Verena Widhopf who always helped to reduce bureaucracy and paper war to a minimum.

My dear coworkers, my time in the laboratory would not have been as pleasant and fun without every one of you: Dr. Sebastian Koller, Dr. Sebastian Helmbrecht, Dr. Matthias Schreyer, Katja Reinhardt, Nicolas Hilgert, Dr. Tanyu Cheng, Dr. Junlin Zhang, Dr. Zhai Lianjie, Julia Gatzka, Michael Wiedemann, Corvin Lossin, Anna (Frieda) Gradenegger, Lukas Ochmann, Lukas Rast, Donato Pasculli, Theresa Appleson, Christian Weindl and Mateja Markotic. Even though we did not always find a common denominator when it came to music, we all 'accepted' the rather weird taste in music of each other. I will never forget our AK rumbles, which we should put in place on a regular basis. The atmosphere we created is irreplaceable. Both Sebastian's contributed in their own way to my daily laboratory routine. Dear Sebastian (Sasha) H(elmi), I felt very honored to share not only a common laboratory space but also the desk on the opposite side with you. It was a real pleasure for me to work next to you and defend the title of 'cleanest bench space' day by day (even though we did not really have to make any great effort 😊). Time flew so quickly. It is already been more than a year that you, Sebastian K(olli), left the Hintermann laboratory. Not only the scientific discussions we had, but also the pranks we

played on each other (or other people, sorry Helmi 😊) or the time we chilled 'Koller style' are all I am and will be missing during my daily work schedule. Our trip to Ibiza was just about the right thing to calm down and strengthen a friendship we started years ago. Since you left, I particularly enjoy our regular lunch dates to keep us up to date. I also want to thank Katja for every scientific, but also personal discussion we had. Especially, I could always count on you to drink coffee after lunch. A special thanks goes to you for performing my very last experiment during my writing quarantine. Christian was the best Helmi substitute one could wish for. Even though we did not share a long time together in the labs, my remaining research time could not have been any better. Thank you for measuring my residual NMR spectra. I also want to thank Dr. S. Helmbrecht and C. Weindl for helping me translate the acknowledgement of my girlfriend to Bavarian. I thank Dr. Lianjie Zhai for providing $\text{IPr}^*\cdot\text{HCl}$, $\text{IPr}^{\text{OMe}}\cdot\text{HCl}$, and $\text{IPr}^{\text{Me}}\cdot\text{HCl}$. Special thanks to M. Sc. Katja Reinhardt for the extensive synthesis of KatPhos and CyAnPhos, which will be detailed in her projected PhD thesis.

A Ph.D. student would be worthless without his or her little minions. Therefore, I want to thank every single student who supported my research while being at TUM: Sandra Paßreiter, Guro Buas Austli, Kevin Frankiewicz, Markus Weber, Teresa Eisner Lilla Koser and Kristof Hintzer. It was a pleasure for me to teach you my work techniques and I wish you all the best.

I would like to thank everyone who helped me performing analytical measurements of any kind: Jürgen Kudermann for GC-MS or GC-FID, Ulrike Ammari for elemental analysis, Maria Matthews for variable temperature NMR, Philipp Altmann and Christian Jandl for X-ray measurements and refinement. A special thanks is dedicated to my mentor Dr. Alexander Pöthig who introduced me to the field of crystallography.

Every visit at the university's chemical store would not have been as funny as if you, Daniel Lemma, would not have been there.

No matter where I am living right now, I can always count on every one of my friends. I enjoyed every time I met Tobias, Jan, Philipp and Simone not only at the university but also at Ben's Bar or Call Soul or wherever in Munich. Even though you stopped studying chemistry and followed your dreams, I am very happy to stay in regular contact with Lorenz. The friendship Verena and I grew over the last decade is irreplaceable. I thank you for always listening and being there for me. I also want to thank my (former) roommates: Benedikt, Benjamin, Johannes and Melanie. We all shared many years, thoughts, parties, ups and downs all together in Munich. Without you my time in Munich would have been much different. Thanks to Fatih

who helped me looking fresh on a regular basis. I enjoyed every discussion we shared and hope we will keep it up in the future.

The number of times I visited my home country diminished year by year. The friendship I share with Gilles, Tom, Gregory and Tamara since more than a decade still grows day after day. Every time we meet feels like we last met yesterday. Thank you for your support, your jokes, your listening, your empathy, our stories and reminding me who I am.

Ein sehr wichtiger Teil dieser Danksagung gebührt meiner Familie und meinen Verwandten, welche mich pausenlos nicht nur finanziell, sondern auch emotional während meiner Dissertation begleitet haben. Meinen Großeltern, Cecile und Filippo, danke ich für jede Stunde, die wir gemeinsam verbracht haben, sowie jedes leckere Mittagessen, das meine Oma zubereitet hat. Auch wenn meine Schwester, Lynn, die Neuigkeiten aus der Heimat oft etwas sehr ins Extreme zieht, bin ich froh, dass wir in Kontakt bleiben und es immer wieder schaffen uns zu treffen. Ein besonderer Dank gilt Susanne und Siegfried. Ihr habt mich bereits bei unserem ersten Treffen vor über drei Jahren ins Herz geschlossen und mir das Gefühl gegeben ein zweites Zuhause gewonnen zu haben. Ich genieße auch weiterhin jeden einzelnen Besuch bei euch (mit oder ohne Kuchen 😊).

Ohne die Unterstützung meiner Eltern, Antonia und Jean-Marie, hätte mein neuer Lebensabschnitt in München wohl nie beginnen können. Ich danke euch für Finanzspritzen jeglicher Art, jeden gemeinsamen Moment, jedes Tief und jedes Hoch. Ein unendlicher Dank gebührt euch auch dafür, dass ihr mir die Last meiner durchs Studium angehäuften Schulden abgenommen und für mich übernommen habt. Es erfreut mich jedes Mal euch bei jedem Besuch in Luxemburg wiederzusehen und Zeit mit euch zu verbringen, auch wenn es oft nur kurz ist. Meiner Mutter und ihrem Freund Marco möchte ich besonders für die vielen Besuche (fast schon dreistellig) in München danken. Auch wenn wir denselben Weg zum 100ten Mal abgelaufen sind, haben wir doch jedes Mal etwas Neues entdeckt.

A narrischs Dangschen gähd an mei Freindin, d'Sabine. Unsa gemeinsame Gschicht hod scha im erstn Drittl vo meina Promotion agfangt. Ois promovierte Chemikerin host du genau gwisst, wia du mi noch Niederschläg im Labor aufbaun kaast. Dei positive Ausstrahlung gibt ma jedn Dog auf's Neie Kraft zum Durchhoitn und s'Allerbeste aus allem zum mocha. I dank da dafia, dass'd immer fia mi do bist und as schaffst, mein Ruhepol ins Gleichgewicht zum bringa. Ob in Quarantäne, im Urlaub oda einfach nur dahoam, i gfrei mi auf jede weidare Sekundn, die i mit dir an meina Seitn verbringa kaa. In dia hob i mei bessare Häifdn gfundn und i gfrei mi auf unsa gemeinsams Lem in Ludwigshafen oder wo a immer auf dera Wäid.

Abstract

In the first part of the project, the generation of organozinc reagents by insertion of zinc into aryl sulfonates has been investigated. The direct insertion of zinc into the C–X bond of aryl halides has previously been limited to X = iodides and bromides. A NiCl₂–1,4-diazadiene catalyst-system, where diazadiene refers to glyoxal or diacetyl diimines, bipyridines and related ligands, has been developed which enables the insertion of preactivated zinc dust into the C–O bonds of aryl sulfonates (tosylates, mesylates, triflates, sulfamates) or into the C–X bonds of weakly activated aryl electrophiles (X = Cl, SMe). In this manner, aryl zinc sulfonates are readily available by catalytic zincation in either DMF or NMP solution and have been shown to undergo a wide range of catalytic cross-coupling or electrophilic substitution reactions.

The second part of the project was concerned with the focus of current research in homogeneous metal-complex catalysis placed on increasingly efficient catalyst-systems, which convert previously inaccessible substrates or enable novel types of transformations. However, these catalyst systems still usually incorporate unfunctional spectator units which fulfill no specific role in the catalytic cycle. If such spectator components were substituted by substances exerting a specific role instead, the efficiency and overall activity of the catalyst-system could be ameliorated. The application of the resulting multifunctional component catalyst (MFCC) precursors either alone or in combination with other functional additives opens new and efficient ways of catalysis screening.

In palladium cross-coupling catalysis, the combination of a metal precatalyst (Pd(OAc)₂) with an imidazolium salt (Im·HCl) as ligand precursor affords an active catalyst. These separate functional components were combined into single, difunctional salts of the types (ImH)₂[Pd₂Cl₆] or (ImH)₂[PdCl₄] (Im = IMes, IPr, IPr^{*}). The hexachlorodipalladates were structurally characterized by single crystal X-ray analysis. Attempts to create a trifunctional IPrH–Pd–pivalate precursor incorporating an additional CMD (concerted metalation deprotonation) functional component delivered the mesoionic carbene complex [(κ²-IPr)₂Pd₂Cl₂(μ-OPiv)₂]. Application of the precursors (ImH)₂[Pd₂Cl₆], (ImH)₂[PdCl₄], and [(κ²-IPr)₂Pd₂Cl₂(μ-OPiv)₂] (Im = IPr) in catalytic test reactions showed good to excellent activity compared to literature precedent with in situ catalysts.

In developing MFCC precursors, the synthesis of composite salts that provide two or more functionalities to a catalyst-system has been achieved. By combining pre-ligand- or phase-transfer catalyst- (PTC) with CMD-functionality, we have obtained the difunctional salts Im·HOPiv (Im = IMes, IPr) as well as several ammonium carboxylates, e.g. tetrabutyl-

ammonium diisopropyl propionate (NBu₄DiPP) or pivalate (NBu₄OPiv). The application of these composite salts as additives in Pd-catalyzed C–H cross-coupling reactions revealed enhanced reactivity effects.

In a third topic, new pathways for the efficient release of active catalyst from specific precursor components were explored. The ligand precursors in question are a series of P-alkylated air-stable, quaternary phosphonium salts derived from air-sensitive PCy₃, and a selection of Buchwald type ligands. They were obtained by quaternization of the free phosphines with appropriate alkylating reagents of the benzyl-, allyl- or vinyl-type. Combination of these compounds with nucleophiles (amine or NaO^tBu) and a Pd^{II} source (Pd(OAc)₂) efficiently released catalytically active Pd⁰L fragments as demonstrated by ³¹P-NMR spectroscopy. Crystallization of [(Trop)RPCy₂]PF₆ salts (Trop = cyclohepta-2,4,6-trienyl, R = Ar, Cy) revealed a susceptible rearrangement from a cycloheptatrienyl to a norcaradienyl (bicyclo[4.1.0]hepta-2,4-dien-7-yl) species. Compared to free Buchwald ligands, the tropylated versions demonstrated enhanced reactivity in the Suzuki coupling of *p*-chloroanisole with phenyl boronic acid, although the exact reasons for this are not yet evident.

In a fourth focus of the project, a combination of Ir- and Pd-precatalysts offers first examples of dehydrogenative coupling of tertiary amines with aryl bromides to give β-styryl dialkyl amines. Best results were obtained by using an IPr-PEPSI (5.0 mol%)/[Cp*IrCl₂]₂ (2.5 mol%) catalyst-system at 110 °C. For NEt₃ as symmetric substrate, which cannot suffer from competitive dehydrogenation of different alkyl groups, the reaction with 1-naphthyl bromide yielded 54% of (*E*)-*N,N*-diethylstyrylamine, entailing 14% of overarylation side-product. Cyclic, tertiary amines, e.g. *N*-methyl- or *N*-ethylpiperidine, were preferably dehydrogenated inside the 6-membered ring, and not at the *N*-alkyl group. Using 1-naphthyl bromide, Hünig's base (*N,N*-diisopropyl ethylamine) was converted to *N,N*-diisopropyl styrylamine in 24% yield. Dehydrogenation of an isopropyl group occurred as side-reaction, giving 29% of diphenyl allyl derivative.

In a fifth part of the project, the Heck coupling of styrene with chloropyrimidines was chosen as model reaction for testing catalysis screening with MFCC precursors. A 'naked, ligandless' Pd-catalyst already provided 31% of heteroarylated olefin coupling product, whereas the additional introduction of phosphine ligands impeded the cross-coupling, as did NHC- (*N*-heterocyclic carbene) ligands. Application of the difunctional ammonium carboxylates NBu₄OPiv and NBu₄DiPP proved successful by ameliorating the conversion and yielding 47% of the derived pyrimidyl styrene.

Zusammenfassung

Im ersten Teil dieser Arbeit wurde die Bildung von Organozinkreagenzien durch Insertion von Zink in Arylsulfonate untersucht. Die direkte Insertion von Zink in die C–X Bindung von Arylhalogeniden war bisher auf X = Iodid und Bromid limitiert. Ein NiCl₂–1,4-Diazadien Katalysatorsystem, wobei sich Diazadien auf Glyoxal- oder Diacetyldiimine, Bipyridine, oder verwandte Liganden bezieht, wurde entwickelt und ermöglicht die Insertion von präaktiviertem Zink in die C–O Bindung von Arylsulfonaten (Tosylate, Mesylate, Triflate, Sulfamate) oder in die C–X Bindung von schwach aktivierten Arylelektrophilen (X = Cl, SMe). Durch katalytische Zinkierung in DMF oder NMP Lösungen sind auf diese Weise Arylzink Sulfonate leicht zugänglich und gehen eine Vielzahl an katalytischen Kreuzkupplungs- und elektrophilen Substitutionsreaktionen ein.

Im zweiten Teil der Arbeit liegt der Fokus auf der aktuellen Forschung in der homogenen Metallkomplex-Katalyse. Dieser liegt auf immer effizienteren Katalysatorsystemen, welche bisher unzugängliche Substrate umsetzen können oder neuartige Umsetzungstypen ermöglichen. Diese Katalysatorsysteme enthalten oft nicht funktionale Zuschauerseinheiten, welche keine spezifische Rolle im Katalysezyklus einnehmen. Werden solche Komponenten ersetzt durch funktionale Einheiten mit bestimmten Eigenschaften, könnte dadurch sowohl die Effizienz als auch die Aktivität des Katalysatorsystems gesteigert werden. Die Verwendung der resultierenden multifunktionalen Komponenten-Katalysator (MFKK) Präkursoren allein oder in Kombination mit anderen funktionalen Additiven öffnet neue und effiziente Wege des Katalysescreenings.

In der Palladium Kreuzkupplungskatalyse ergibt die Kombination eines Metallpräkatalysators (Pd(OAc)₂) mit einem Imidazolium Salz (Im·HCl) als Ligand-Präkursor einen aktiven Katalysator. Diese separaten, funktionalen Komponenten wurden zu einzelnen, difunktionalen Salzen des Typs (ImH)₂[Pd₂Cl₆] oder (ImH)₂[PdCl₄] (Im = IMes, IPr, IPr^{*}) kombiniert. Die Hexachlordipalladate wurden strukturell durch Einkristall-Röntgenstrukturanalyse charakterisiert. Versuche einen trifunktionalen IPrH–Pd–Pivalat Präkursor, welcher eine zusätzliche funktionale CMD (konzentrierte Metallierung-Deprotonierung) Komponente beinhaltet, ergaben den mesoionischen Carbenkomplex [(κ²-IPr)₂Pd₂Cl₂(μ-OPiv)₂]. Die Anwendung der Präkursoren (ImH)₂[Pd₂Cl₆], (ImH)₂[PdCl₄], und [(κ²-IPr)₂Pd₂Cl₂(μ-OPiv)₂] (Im = IPr) in katalytischen Testreaktionen zeigte gute bis exzellente Aktivität im Vergleich zur Literaturpräzedenz mit in situ Katalysatoren.

In der Entwicklung von MFKK Präkursoren wurde die Synthese von gemischten Salzen, welche einem Katalysatorsystem zwei oder mehr Funktionalitäten zuführen, erreicht. Durch die Kombination von Präligand- oder Phasentransferkatalystor- (PTC) mit CMD-Funktionalität haben wir die difunktionalen Salze Im·HOPiv (Im = IMes, IPr) und mehrere Ammonium-carboxylate, z. B. Tetrabutylammoniumdiisopropylpropionat (NBu₄DiPP) oder -pivalat (NBu₄OPiv), erhalten. Die Verwendung dieser gemischten Salze als Additive in Pd-katalysierten C–H Kreuzkupplungsreaktionen offenbarte verbesserte Reaktivitätseffekte.

In einem dritten Thema wurden neue Wege zur effizienten Freisetzung eines aktiven Katalysators aus spezifischen Präkursorkomponenten untersucht. Die Ligand-Präkursoren, welche dabei in Frage kommen, sind eine Reihe aus P-alkylierten luftstabilen, quaternären Phosphoniumsalzen abgeleitet von luftempfindlichem PCy₃, und einer Reihe an Liganden des Buchwaldtyps. Sie wurden durch Quaternisierung der freien Phosphine mit geeigneten Alkylierungsmitteln des Benzyl-, Allyl- oder Vinyltyps erhalten. Die Kombination dieser Komponenten mit Nukleophilen (Amin oder NaO^tBu) und einer Pd^{II}-Quelle (Pd(OAc)₂) setzte effizient katalytisch aktive Pd⁰L Fragmente frei, welche mit Hilfe von ³¹P-NMR Spektroskopie nachgewiesen wurden. Die Kristallisation von [(Trop)RPCy₂]PF₆ (Trop = Cyclohepta-2,4,6-trienyl, R = Ar, Cy) offenbarte eine mögliche Umlagerung von einer Cycloheptatrienyl- zu einer Norcaradienyl- (Bicyclo[4.1.0]hepta-2,4-dien-7-yl) Spezies. Im Vergleich zu den freien Buchwaldliganden bewiesen die tropylierten Versionen eine verbesserte Reaktivität in der Suzuki-Kupplung von *p*-Chloranisol mit Phenylboronsäure, auch wenn die genauen Gründe bisher nicht geklärt wurden.

Im vierten Teil des Projektes lieferte die Kombination von Ir- und Pd-Präkatalysatoren erste Beispiele einer dehydrierenden Kupplung von tertiären Aminen mit Arylbromiden, welche β -Styryldialkylamine ergibt. Mit Hilfe eines IPr-PEPPSI (5.0 mol%)/[Cp^{*}IrCl₂]₂ (2.5 mol%) Katalysatorsystems bei 110 °C wurden die besten Ergebnisse erzielt. Im Falle von NEt₃ als symmetrisches Substrat, welches keine kompetitive Dehydrierung verschiedener Alkylgruppen eingehen kann, ergab die Reaktion mit 1-Bromnaphthalin 54% (*E*)-*N,N*-Diethylstyrylamin und 14% des Überarylierungsnebenproduktes. Zyklische, tertiäre Amine, z. B. *N*-Methyl- oder *N*-Ethylpiperidin, wurden vorzugsweise im 6-gliedrigen Ring dehydriert und nicht an der *N*-Alkylgruppe. Unter Einsatz von 1-Bromnaphthalin lieferte die Hünig-Base (*N,N*-Diisopropylethylamin) das Produkt *N,N*-Diisopropylstyrylamin in 24% Ausbeute. Die Dehydrierung einer Isopropylgruppe trat als Nebenreaktion auf und ergab 29% des Diphenylallylderivats.

In einem fünften Teil des Projekts wurde die Heck-Kupplung von Styrol mit Chlorpyrimidinen als Modellreaktion zum Testen des Katalysescreenings mit MFKK Präkursoren ausgewählt. Ein „nackter, ligandloser“ Pd-Katalysator lieferte bereits 31% des heteroarylierten Kupplungsprodukts, während der zusätzliche Einsatz eines Phosphin- oder NHC- (*N*-heterozyklisches Carben) Liganden die Kreuzkupplung größtenteils verhinderten. Die Verwendung der difunktionalen Ammoniumcarboxylate, NBu₄OPiv und NBu₄DiPP, erwiesen sich als erfolgreich, indem sie sowohl den Umsatz verbesserten als auch 47% des abgeleiteten Pyrimidylstyrols ergaben.

TABLE OF CONTENTS

1	GENERATION OF ORGANOZINC REAGENTS BY NICKEL-DIAZADIENE-COMPLEX CATALYZED ZINC INSERTION INTO ARYL SULFONATES	1
1.1	ZINC INSERTION IN ORGANIC SYNTHESIS.....	3
1.2	NI-CATALYZED ZINC INSERTION INTO ARYL SULFONATES – HOW IT ALL STARTED.....	4
1.3	REFINED REACTION CONDITIONS AND PROCEDURE.....	8
1.4	TO REACT OR NOT TO REACT – SUBSTRATE SCOPE.....	10
1.5	ZINC SPECIES, WHERE NOW?.....	13
1.6	BEHIND THE SCENES.....	15
1.7	CONCLUSION AND OUTLOOK.....	16
1.8	REFERENCES.....	18
2	THE MULTIFUNCTIONAL COMPONENT CATALYST (MFCC) PRINCIPLE: DEFINITIONS, SCREENING, AND APPLICATION	23
2.1	DEFINING THE MULTIFUNCTIONAL COMPONENT CATALYST PRINCIPLE (MFCCP).....	25
2.2	NEW WAYS OF SCREENING.....	30
2.3	TWO-DIMENSIONAL (2D) MATRIX SCREENING IN PRACTICE.....	32
2.4	CONCLUSION AND OUTLOOK.....	35
2.5	REFERENCES.....	37
3	MULTIFUNCTIONAL CATALYST COMPONENT PRECURSORS: THE NHC-PD-PIVALATE SYSTEM	43
3.1	INTRODUCTION.....	45
3.2	DIFUNCTIONALITY IN A WELL-DEFINED PRECURSOR SALT.....	46
3.2.1	MERGING OF METAL AND LIGAND PRECURSOR.....	46
3.2.2	MERGING OF LIGAND PRECURSOR AND CMD ADDITIVE.....	53
3.2.3	MERGING OF METAL PRECURSOR AND CMD ADDITIVE.....	57
3.3	A TRIFUNCTIONAL NHC-PD-PIVALATE PRECURSOR – CHEERED TOO SOON?.....	59
3.4	MULTIFUNCTIONAL CCP'S IN CATALYSIS.....	66

3.5	CONCLUSION AND OUTLOOK	71
3.6	REFERENCES	75
4	DIFUNCTIONAL ONIUM CARBOXYLATE ADDITIVES FOR CATALYTIC COUPLING.....	83
4.1	INTRODUCTION.....	85
4.2	SYNTHESIS OF DIFUNCTIONAL AMMONIUM CARBOXYLATE ADDITIVES.....	92
4.2.1	CARBOXYLIC ACIDS AND THEIR PERFORMANCE IN CATALYSIS	92
4.2.2	SYNTHESIS OF QUATERNARY AMMONIUM CARBOXYLATES.....	95
4.3	DIFUNCTIONAL ONIUM CARBOXYLATES IN CATALYSIS	102
4.4	CONCLUSION AND OUTLOOK	110
4.5	REFERENCES	113
5	BENZYL, VINYL AND CYCLOHEPTATRIENYL PHOSPHONIUM SALTS: MOLECULAR STOREHOUSE FOR AIR-SENSITIVE LIGANDS.....	123
5.1	INTRODUCTION.....	125
5.2	VINYLIC- AND BENZYLIC- TRICYCLOHEXYLPHOSPHONIUM SALTS: SUITABLE PRECURSORS FOR ACTIVE CATALYST GENERATION.....	131
5.2.1	SYNTHESIS OF VINYLIC- AND BENZYLIC-TRICYCLOHEXYLPHOSPHONIUM SALTS.....	131
5.2.2	ISOMERIZATION OF ALLYL-TYPE PHOSPHONIUM SALTS.....	138
5.2.3	π -COMPLEXATION OF ALKENYLPHOSPHONIUM TO Pd AND RELEASE OF FREE PCY ₃ LIGAND	142
5.2.4	VINYL AND BENZYL PHOSPHONIUM SALTS IN CATALYSIS	145
5.3	CYCLOHEPTATRIENYL PHOSPHONIUM SALTS: SYNTHESIS, REACTIVITY AND A SUSCEPTIBLE REARRANGEMENT	148
5.3.1	SYNTHESIS OF CYCLOHEPTATRIENYL PHOSPHONIUM SALTS	148
5.3.2	CYCLOHEPTATRIENYL IMIDAZOLIUM SALT: A POTENTIAL PRECURSOR FOR THE SYNTHESIS OF BIDENTATE Pd COMPLEXES?	155
5.3.3	CYCLOHEPTATRIENE–NORCARADIENE: A SUSCEPTIBLE REARRANGEMENT	157
5.3.4	REACTIVITY OF TROPYLIUM SALTS: TRANSFER TO Pd METAL CENTER.....	161
5.3.5	CYCLOHEPTATRIENYL PHOSPHONIUM SALTS IN CATALYSIS: INCREASE IN EFFICIENCY?	165

5.4	CONCLUSION AND OUTLOOK.....	168
5.5	REFERENCES	174
6	DUAL METAL CATALYSIS: COMBINING HYDROGEN AUTO TRANSFER AND HECK COUPLING	183
6.1	INTRODUCTION.....	185
6.2	HARNESSING TRIALKYLAMINES AS DONORS IN HECK CROSS-COUPLING VIA A HYDROGEN AUTO TRANSFER PROCESS	189
6.2.1	COINCIDENCE OR GETTING STARTED?	189
6.2.2	CHANGING THE AMINE – REDUCTION OF COMPLEXITY OR NOT?.....	194
6.2.3	DIVERSIFYING THE ARYL BROMIDE – INFLUENCE OF THE SUBSTITUTION PATTERN...	202
6.2.4	PROPOSED MECHANISM.....	206
6.3	HECK CROSS-COUPLING OF STYRENES WITH PYRIMIDYL CHLORIDES	207
6.4	CONCLUSION AND OUTLOOK	212
6.5	REFERENCES	215
7	EXPERIMENTAL SECTION	223
7.1	GENERAL REMARKS.....	225
7.1.1	REAGENTS AND CHEMICALS.....	225
7.1.2	WORK TECHNIQUES	226
7.1.3	ANALYTICS.....	229
7.2	SYNTHESIS PROCEDURES	234
7.2.1	GENERATION OF ORGANOZINC REAGENTS BY NICKEL-DIAZADIENE-COMPLEX CATALYZED ZINC INSERTION INTO ARYL SULFONATES.....	234
7.2.2	THE MULTIFUNCTIONAL COMPONENT CATALYST (MFCC) PRINCIPLE: DEFINITIONS, SCREENING, AND APPLICATION	256
7.2.3	MULTIFUNCTIONAL CATALYST COMPONENT PRECURSORS: THE NHC-Pd-PIVALATE SYSTEM	259
7.2.4	DIFUNCTIONAL ONIUM CARBOXYLATE ADDITIVES FOR CATALYTIC COUPLING	278

7.2.5	VINYL AND BENZYL PCY ₃ -BASED PHOSPHONIUM SALTS: SUITABLE PRECURSORS FOR ACTIVE CATALYST GENERATION	292
7.2.6	CYCLOHEPTATRIENYL PHOSPHONIUM SALTS: SYNTHESIS, REACTIVITY AND A SUSCEPTIBLE REARRANGEMENT	311
7.2.7	ACCESSING TRIALKYLAMINES AS DONORS IN HECK CROSS-COUPLING VIA A HYDROGEN AUTO TRANSFER PROCESS	326
7.2.8	HECK COUPLING OF STYRENE DERIVATIVES WITH PYRIMIDYL CHLORIDES	337
7.3	REFERENCES	338
8	APPENDIX.....	345
8.1	LIST OF ABBREVIATIONS.....	347
8.2	GRAPHS OF HPLC REFERENCE MEASURES FOR CAFFEINE AND PHENYLCAFFEINE.....	355
8.3	X-RAY STRUCTURE DATA	356
8.4	UV/VIS SPECTRUM OF [(TROP)SPHOS]PF ₆	374
8.5	TYPICAL REACTION PROFILE OF A MICROWAVE ASSISTED REACTION.....	374
8.6	EXEMPLARY ANALYSIS OF A QUANTITATIVE NMR SPECTRUM.....	376
8.7	REPRINT PERMISSION	378
8.7.1	GENERATION OF ORGANOZINC REAGENTS BY NICKEL-DIAZADIENE-COMPLEX CATALYZED ZINC INSERTION INTO ARYL SULFONATES.....	378

**1 GENERATION OF ORGANOZINC REAGENTS BY NICKEL-DIAZADIENE-
COMPLEX CATALYZED ZINC INSERTION INTO ARYL SULFONATES**

The following chapter is divided in seven sub-chapters. After introductory words (1.1), the basic concept initiated by Tanja Schimmel at RWTH Aachen as well as extended screening results by Vivien Lechner are depicted (1.2). A refined experimental procedure soon evolved during my PhD studies (1.3). Different aryl sulfonates and derivatives are subjected to the elaborated conditions (1.4). The utility of ArZnOTs reagents is explored by conversion with several electrophiles (1.5). A potential catalytic cycle for catalytic zincation is proposed (1.6). The first chapter ends with a short conclusion and an outlook (1.7). The key results of the following section have already been published.^[1]

1.1 Zinc insertion in organic synthesis

Organometallic zinc reagents are widely used in cross-coupling^[2] and other^[3] reactions. Due to similar electronegativity of carbon and zinc, the nature of their bond is mostly covalent (85%).^[4] Zinc reagents may be prepared by insertion of zinc metal into RX (R = functional group, X = halide). Two general pathways can be differed: either by oxidative addition or by transmetalation reaction. The first example by Frankland^[5] reporting the oxidative addition of zinc metal into alkyl iodides is rather limited due to low reactivity of Zn. Since then, many activation methods have been established to increase the reactivity of zinc metal.^[6] The group of Knochel reported the conversion of allylic or benzylic chlorides to zinc derivatives in very polar solvents.^[7] However, most alkyl or aryl bromides and chlorides are incompatible for direct Zn insertion. Lithium naphthalenide reduction of ZnCl₂ generates the highly reactive Rieke-Zn, which enables zincation of a wide range of organic halides including aromatic bromides.^[8] Whereas the activity of Rieke-Zn decreases over time, a LiCl mediated regioselective ortho insertion depicts mild and practical conditions for zinc incorporation.^[9]

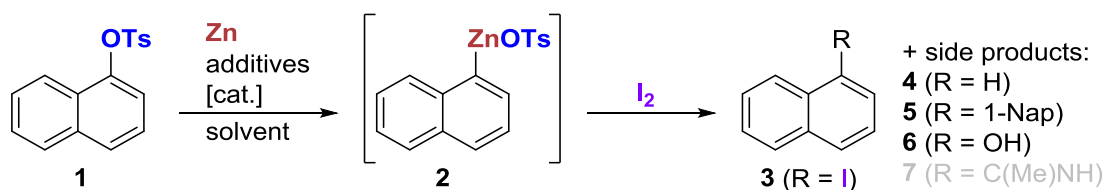
Transmetalation from either magnesium- or lithium-organyls illustrates a convenient method for the generation of organozinc reagents. At low temperatures (<-40 °C), lithium-halogen exchange of aryl iodides and bromides proceeds smoothly with lithium organic bases. Even though aryllithium reagents are less reactive than alkyl analogues, their stability can significantly be further increased by transmetalation with zinc salts (ZnBr₂, ZnCl₂) yielding arylzinc halides.^[10] Trapping of magnesium reagents with ZnX₂ furnishes organozinc species with specific reactivity in C–C cross-coupling or related reactions.^[11]

While the above methods often require activated substrates or rather harsh conditions (Li-naphthalenide, very low temperature), more recent examples of metalation depict metal-

catalyzed magnesium or zinc insertion. Bogdanović et al. described the iron-catalyzed magnesiation^[12] of inactive organochlorides at ambient temperature, which presumably involve a so-called inorganic Grignard reagent^[13] ($[M^I(MgCl)_m \cdot (MgCl_2)_p]$, $m = 1-3$, $p = 0-1$; here: $M = Fe$, $m = 1-2$, $p = 0$). Cobalt-catalyzed zinc insertion into aryl or thienyl halides was reported by the group of Gosmini, depicting an original alternative to previously known zincation.^[14] A Cobalt-Xantphos catalyst system presented by Yoshikai et al.^[15] allows the preparation of arylzinc reagents from aryl iodides, bromides and chlorides and zinc dust. The organometallic compounds resulting from the cited examples were all further subjected to a wide range of metal-catalyzed cross-coupling reactions. Zn-, Mg-, and Li-tetramethylpiperidine (TMP) bases established by the group of Knochel enable the direct substitution of H^+ by M^+ .^[16] Employing this new type of base, even polyfunctional arenes and heteroarenes were efficiently zincated.^[16c] Few literature reports are concerned with metal insertion into non-halogenated substrates, e.g. alkyl phosphates^[17] or sulfonates^[17-18], and benzyl ethers^[19], sulfonates^[19-20] or phosphates^[20a]. Although metal-catalyzed (Ni or Pd) borylation of aryl sulfonates^[21] (mesylate, tosylate and triflate) are numerous, the catalytic zinc insertion into the latter is less common. Even though aromatic chlorides and triflates were zincated in good yields via $CoBr_2$ -bipy catalysis^[22], aryl mesylates only showed minor to no zincation yield.

1.2 Ni-catalyzed zinc insertion into aryl sulfonates – how it all started

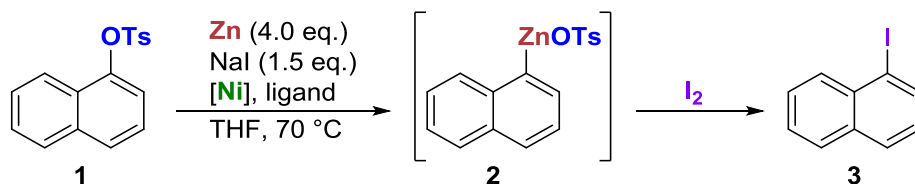
Preliminary work by Tanja Schimmel at RWTH Aachen had revealed the potential of metal catalyzed zinc insertion into aryl sulfonates.^[23] The model substrate, 1-naphthyl tosylate (**1**), was subjected to zinc dust in the presence of various metal precursor complexes and additives. Quenching of the reaction mixture with iodine converted any arylzinc species **2** formed to the iodide **3**. Analysis of the crude material by GC-MS allowed a semi-quantitative listing of the reaction products 1-naphthyl iodide (**3**), naphthalene (**4**), 1,1'-binaphthyl (**5**) and 1-naphthol (**6**). Reactions performed in hot acetonitrile additionally generated 1-methylnaphthalene, 1-cyanonaphthalene as well as imine **7** as side-products.



Scheme 1. Preliminary screening of catalytic zinc insertion into 1-naphthyl tosylate as model substrate (using GC-MS as analytical method).

Among the metal precursors tested, only nickel compounds showed activity. A solvent change from MeCN to THF did not only suppress side-reactions due to MeCN splitting but led to an increase in selectivity. Inspired by Jutand and coworkers^[24], who had reported the Pd- or Ni-catalyzed reductive homocoupling of aryl triflates in the presence of NaI as additive, the latter was incorporated as iodide source for potential halogen-tosylate exchange. In agreement with Jutand et al., Ni-bisphosphane catalysts induced a high degree of homocoupling. Ligand effects were explored to shift the product distribution away from unwanted homocoupling or reduction. First experiments involving a diazadiene (DAD) type ligand, namely 1,4-bis(2,6-diisopropylphenyl)diazabutadiene (IPr-DAD, **L1**), appeared promising (table 1, entry 7).

Table 1. Selected preliminary reaction conditions in the metal-catalyzed zinc insertion of aryl tosylates.^a conv. = conversion; s.p. = side-product.



entry	Ni [mol%]	ligand [mol%]	ArOTs	conv. ^b	ArI	ArH	Ar ₂	s.p.
1	NiCl ₂ (dppe) (10)	-	14	86	30	11	45	
2	NiCl ₂ (dppp) (10)	-	0	100	3	3	89	5% Nap-Ph
3	NiCl ₂ (dppb) (10)	-	51	49	1	4	44	
4	NiCl ₂ (binap) (10)	-	0	100	31	64	5	
5	NiCl ₂ (PPh ₃) ₂ (10)	-	7	93	0	5	88	
6	NiCl ₂ (PPh ₃) ₂ (5)	-	28	72	0	1	71	
7	dried NiCl ₂ (10)	IPr-DAD (30)	9	91	27	44	20	

^aReaction conditions: 400 μmol 1-NapOTs, THF (1 mL), 70 °C, 18-21.5 h; zinc activated with iodine (1 grain). Yields calculated via GC-MS area integration given in mol%. Ar = 1-Nap. ^bConversion (conv.) = 100 mol% – area% of remaining 1-NapOTs.

Refined screening experiments conducted by Vivien Lechner at TUM with anhydrous Ni etherates (NiCl₂(dme) or NiCl₂(diglyme)) as better soluble precatalysts allowed exclusion of water in all steps.^[25] The use of either complex did not affect the outcome of the reaction. Quantitative NMR (q-NMR) of the crude reaction mixture enabled a more precise and superior quantification of all reaction products in comparison to GC-MS. Among the DAD-type ligands tested, diacetyl bis(2,6-diisopropylphenyl)imine (IPr^{Me}-DAD, **L2**) proved superior to **L1** (table 2). Additive NaI quickly fell into disuse, given that its presence was inconsequential. Amidic solvents such as DMF or *N*-methyl-2-pyrrolidone (NMP) enabled the reaction to proceed at room temperature, while also suppressing unwanted homocoupling to biaryl **5**. A metal to ligand ratio of 1:2 gave the most active catalyst. In all cases, zinc dust was activated with either

iodine or 1,2-dichloroethane (DCE). Both activators resulted in virtually identical yields, also highlighting the needlessness of additive NaI in terms of specific iodide effect.

Table 2. Selected conditions of refined screening experiments in the nickel-catalyzed zinc insertion of aryl tosylates.^a cat. = catalyst.

entry	Ni [mol%]	ligand [mol%]	solvent	additive [eq.]	T [°C]	ArI	ArH	Ar ₂
1	NiCl ₂ (diglyme) (10)	L1 (20)	THF	NaI (1.5)	70	62	18	8
2	NiCl ₂ (diglyme) (10)	L2 (20)	THF	NaI (1.5)	70	71	19	5
3	NiCl ₂ (dme) (5)	L2 (10)	DMF	-	r.t.	98	2	0
4	NiCl ₂ (diglyme) (10)	L2 (20)	THF	-	r.t.	86	8	2
5	NiCl ₂ (diglyme) (5)	L2 (10)	THF	-	r.t.	35	3	0
6	NiCl ₂ (diglyme) (5)	L2 (10)	NMP	-	r.t.	80	13	<1
7 ^b	NiCl ₂ (dme) (5)	L2 (10)	DMF	-	r.t.	93	5	0
8	NiCl ₂ (dme) (5)	L2 (5)	DMF	-	r.t.	90	4	0
9	NiCl ₂ (dme) (10)	L2 (30)	THF	NaI (1.5)	70	63	16	2

^aReaction conditions: 1.00 mmol 1-NapOTs, solvent (3 mL). Zinc was activated with iodine (0.5 eq.) by stirring at r.t. until complete discoloration. Spectral yield according to ¹H-NMR with internal standard, given in mol%. Ar = 1-Nap. ^bZinc activation with 1,2-dichloroethane (0.2 eq.); heated to boiling (heat-gun) for one min.

Other open-chain DADs (**L1** to **L4**) or related Schiff bases (**L5** and **L6**) were suitable ligands for the transformation of naphthyl tosylate (**1**) to the zinc species **2** (figure 1). Phenanthroline-type ligands (**L7–L9**) profited from the presence of iodine resulting from the activation step. Even at low catalyst loading (3 mol%) and equimolar Ni to ligand ratio (1:1) a very good conversion of tosylate **1** to zinc species **2** was observed. However, given the necessity of iodine activation as well as the sumptuous design of structurally diverse phenanthroline-based ligands, the latter were not of first choice for further development.

To emphasize the generation of actual ArZnOTs in solution, the reaction was once conducted in [D₇]-DMF using the NiCl₂(dme)-**L2** system. Full 2D NMR analysis of the reaction mixture confirmed the presence of zinc species **2** in solution by complete ¹H- as well as ¹³C-NMR signal sets (quaternary signal at $\delta_C = 156.3$ ppm for C–Zn). Residual water in the deuterated solvent led to the formation of minor amounts of naphthalene. Ligand **L2** was also observed in the reaction mixture. Upon addition of little water to the sample, more naphthalene (**4**) was generated with simultaneous consumption of the zinc species **2**.

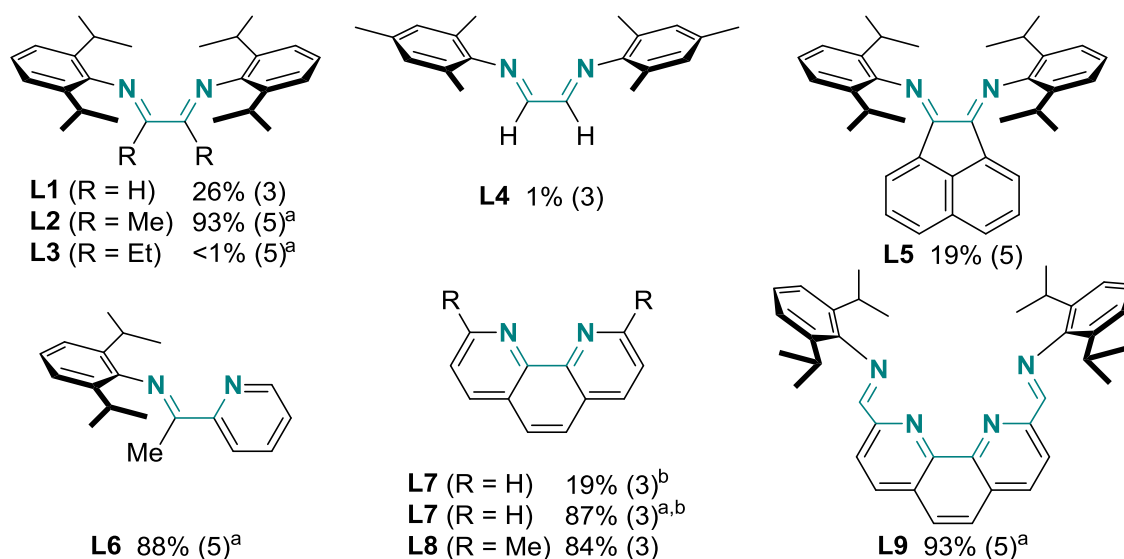


Figure 1. Ligand variation in the Ni-catalyzed zincation of **1**; %-numbers refer to analytically detected yield of 1-NapI (**3**) after quenching with I₂. Scale: 1 mmol 1-NapOTs, DMF (3 mL), r.t., 20 h. Zinc dust activation with iodine (0.5 eq.) by stirring at r.t. until complete discoloration. ^aZinc activation with 1,2-DCE (0.2 eq.), heated to boiling for one min. ^bA metal to ligand ratio 1:1 was used; otherwise a 1:2 ratio was used.

Previous work by V. Lechner had also started to examine the leaving group scope in this nickel-catalyzed zincation. For this purpose, aryl (pseudo-)halides were subjected to the catalytic reaction conditions (figure 2).

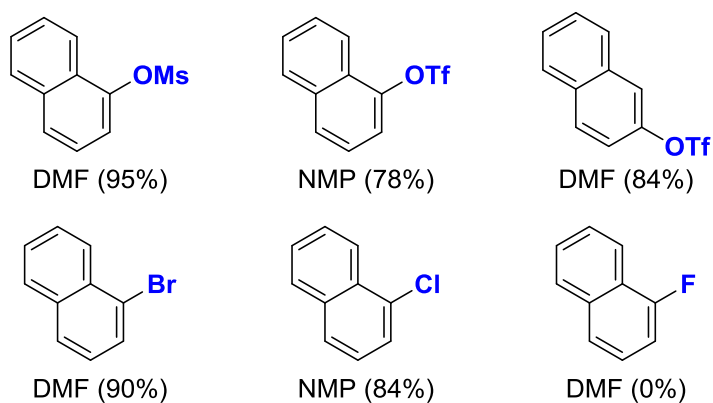


Figure 2. Leaving group scope of the nickel-catalyzed zincation of aryl electrophiles. Reactions were performed on a 1 mmol scale; 5 mol% Ni. Zinc dust was activated with 1,2-DCE (0.2 eq.). Reaction solvent and yield of 1-NapI or 2-NapI (in brackets, determined by q-NMR) after iodolysis (4.0 eq. I₂) are given for each substrate.

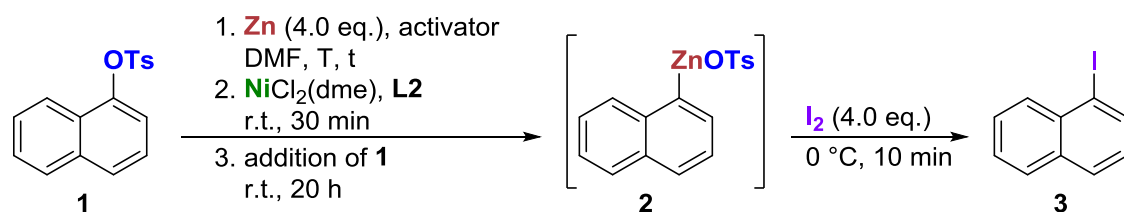
Naphthyl sulfonates including the mesylate or triflate at either 1- or the 2-position were zincated in good to excellent yield. Among the naphthyl halides (1-bromo, 1-chloro, 1-fluoro), only 1-fluoronaphthalene remained untouched, even when heating to 70 °C overnight. Gosmini and coworkers had previously reported a cobalt-catalyzed synthesis of organozinc reagents from

aryl chlorides and sulfonates, although only for unsubstituted or electron-deficient substrates. In their case, aryl triflates as well as aryl chlorides were converted in good yields. However, aryl mesylates afforded a maximum of 36% of ArZnX, and suffered from extensive S–O bond cleavage.^[22]

1.3 Refined reaction conditions and procedure

Since zinc activation with 1,2-dichloroethane requires heating to reflux with a heat-gun, an accurate control of this step was difficult (table 3, entry 1). Further methods were explored to establish fully reproducible conditions. Short stirring (5 min) with catalytic amounts of iodine induced the quantitative conversion of **1** to **3** in the ensuing catalysis but entailed rather high amounts of naphthalene (**4**, entry 2).

Table 3. Concluding screening experiments in the metal-catalyzed zinc insertion of aryl tosylates.^a



entry	activator [eq.]	T [°C]	t [min]	ArOTs	ArI	ArH	Ar ₂	ArOH	comment
1	DCE (0.2)	?	0.5	<1	98	2	<1	<1	heat-gun
2	I ₂ (cat.)	r.t.	5	<1	87	13	<1	<1	
3 ^b	-	r.t.	-	<1	94	6	<1	<1	new DMF
4	-	r.t.	30	<1	89	11	<1	<1	
5	-	100	10	<1	86	13	<1	<1	
6	-	150	10	<1	87	14	<1	<1	
7 ^b	DBE (0.2)	r.t.	5	<1	94	6	<1	<1	5 h reaction
8	DBE (0.2)	50	15	<1	94	6	<1	<1	
9	DBE (0.2)	60	20	<1	97	3	<1	<1	
10	DBE (0.2)	150	10	<1	87	14	<1	<1	
11	DBE (0.2)	?	0.5	91	<1	10	<1	<1	heat-gun

^aReaction conditions: 1.00 mmol 1-NapOTs, DMF (3 mL). Spectral yield according to ¹H-NMR with internal standard, given in mol%. Ar = 1-Nap. ^bReaction conditions were irreproducible. Amount of ArH grew at cost of ArI.

Skipping of the activation step only yielded aryl iodide **3** in excellent yield when solvent from a freshly opened bottle of DMF was used (entry 3). Simple stirring of zinc dust at room temperature or while heating did not affect the outcome of the reaction (entries 4–6). Activation with 1,2-dibromoethane (DBE) proceeded best at 60 °C (entry 9), whereas more naphthalene was produced at higher temperature (entry 10). Already upon addition of the first drops of DBE,

small gas bubbles evolving from the zinc surface could be observed. Zinc activation at ‘heat-gun temperature’ for 30 seconds suppressed the ensuing catalysis (entry 11), which only produced minor amounts of naphthalene. Hence, practical reaction conditions were elaborated and the use of a heat-gun except for drying of glassware became unnecessary. Unless otherwise stated, all upcoming zincations used the conditions described in table 3 entry 9. The detailed general metalation procedure can be found in the experimental section (7.2.1.1).

To broaden the application range and utility of this new reaction, additional diimine or phenanthroline type ligands in combination with NiCl₂(dme) were evaluated (figure 3). Compared with **L2**, use of the open-chain DAD **L1** resulted in lower amounts of aryl iodide **3**. Ligands **L4**, **L6** and **L9** induced high activities similar to those of **L2**.

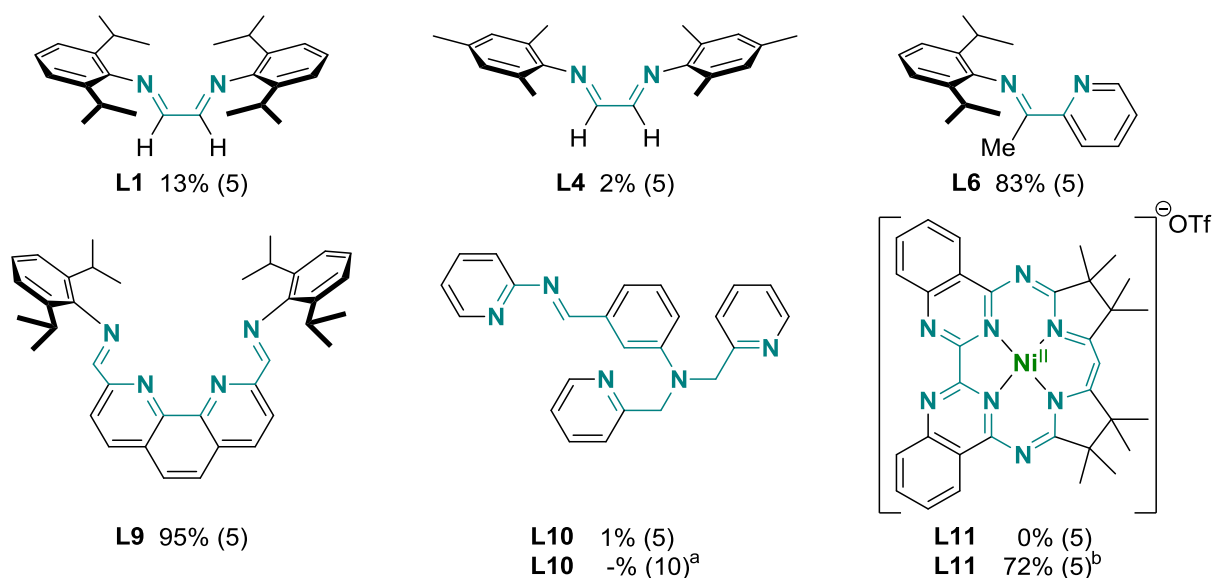


Figure 3. Evaluation of various ligand structures in the catalytic zincation of naphthyl tosylate (**1**). The %-numbers indicate the spectral yield of 1-NapI after iodolysis of the reaction mixture. Values in brackets refer to nickel precatalyst loading in mol%. Scale: 1 mmol 1-NapOTs, DMF (3 mL), r.t., 20 h. Zinc dust activation with 1,2-DBE (0.2 eq.), heated to 60 °C for 20 min. ^aNo q-NMR was conducted as GC-MS claimed no reaction taking place. ^bAdditional NiCl₂(dme) (5 mol%) added.

Catalysis with terpyridyl ligand **L10** left the starting naphthyl tosylate mainly untouched, even at a higher catalyst loading of 10 mol%. The macrocyclic biquinazoline ligand, Mabiq, features a unique scaffold with two distinct coordination sites.^[26] Several redox-active homo- or heterobimetallic complexes of this ligand with metals in formal oxidation states ranging from 0 to +3 have been reported.^[27] In our case, the Ni(Mabiq) triflate salt (**L11**) was investigated, and thus might be reduced to a low-valent and catalytically active species by zinc powder. However, steric crowding at the central coordination site may have blocked any reaction from

taking place. Upon addition of a co-catalytic amount of NiCl₂(dme), good conversion of 1-naphthyl tosylate was achieved. This is readily explained by assuming that the added nickel coordinated to the vacant, external bipyridine moiety of the Mabiq ligand framework, thereby forming a catalytically active complex similar to those with other diimines.

1.4 To react or not to react – substrate scope

A new catalytic reaction proves its practical worth through a broad application range against a variety of variably functionalized starting materials. Thus, the versatility of the zincation was examined with several electron-rich and electron-poor substrates. Most of the aryl tosylates used in this study were easily accessible in almost quantitative yield from phenols and tosyl chloride with aqueous sodium hydroxide according to a procedure by Lei and coworkers.^[28] Substrates containing the hydrolysis-sensitive ester functionality were prepared under non-aqueous conditions using pyridine as base.^[29]

Each tosylate was subjected to the standard metalation conditions (see table 4). Subsequent iodolysis converted any organozinc species present to aryl iodide, which could be accurately quantified by q-NMR. Reactions performing at a good to excellent level (>50%) were also operated on a 2 mmol preparative scale and the product was purified by flash column chromatography. With less successful substrates, the 1 mmol scale analytical run with q-NMR analysis was considered sufficient. Similar to **1** (entry 1), regioisomeric 2-naphthyl as well as *ortho*-biphenyl tosylate were successfully zincated in almost quantitative yield (entries 2 and 3, respectively). The low solubility of *para*-substituted biphenyl sulfonate as well as of the corresponding zinc reagent hindered the conversion of this substrate (entry 4). Simple aryl derivatives, including cresyl and *para-tert*-butylphenyl tosylates, cleanly yielded the desired products (entries 5-9). Larger groups in *ortho*-position of tosylate, like isopropyl, slightly lowered the performance of the transformation (entries 10 and 11). Less bulky carvacryl (5-isopropyl-2-methylphenyl) tosylate could not be isolated in sufficient purity to be subjected to the catalytic zincation conditions. The allyl-substituted tosylate (entry 12) did neither yield aryl iodide nor the ring-closed (dihydro)benzofuran, but simply isomerized to its styryl derivative. Whereas electron-rich methoxy and dialkylamino substrates (entries 13 and 14) were well tolerated, electron-poor nitrile and bis(trifluoromethyl) substitutions impeded the reaction (entries 15 and 16). The *meta,meta*-xylyl tosylate (entry 17) merely converted in trace amounts.

Table 4. Substrate scope of the nickel-catalyzed zincation of aryl tosylates.^a

1. **Zn** (4.0 eq.), DBE (0.2 eq.)
 DMF, 60 °C, 20 min
 2. **NiCl₂(dme)**-**L₂** (1:2)
 r.t., 30 min
 3. addition of **8**
 r.t., 20 h
Metalation

entry	substrate	Ni [mol%]	yield [%] ^b	entry	substrate	Ni [mol%]	yield [%] ^b
1		5	96 ^c (96)	14 ^f		5	96 (99)
2		5	88 ^d (92)	15		5	(7)
3		5	98 (99)	16		5	(2) ^g
4		5	(21)	17		5	(<1)
5		5	85 (88)	18		10	96 (96)
6		5	95 (96)	19		10	75 (78)
7		5	85 (90)	20		5	86 (85)
8		5	90 (93)	21		5	(0) ^h
9		10	76 (80)	22		10	56 (54)
10		10	80 (85)	23		5	77 ⁱ (77)
11		10	77 (77)	24		5	(10) ^j
12		5	(0) ^e	25 ^k		15	88 (89)
13		5	83 (88)	26 ^k		15	(33) ^l

^aReaction conditions according to GP 1.3 (preparative scale, or GP 1.2 for analytical scale, see 7.2.1.1): Zn (4.0 eq.) and DBE (0.2 eq.) were stirred for 20 min at 60 °C; NiCl₂(dme) and **L2** (Ni-**L2** 1:2) were added at r.t. and stirred for 30 min; ArOTs was added and the mixture was stirred for 20 h at r.t.; solvent: DMF (3 mL/mmol).

^bYield of ArI after iodolysis (4.0 eq., 0 °C, 10 min) of ArZnOTs; isolated yield of chromatographically purified material, numbers in brackets, according to quantitative ¹H-NMR against internal standard. ^cArI-ArH 98:2. ^dArI-ArH 95:5. ^e76% starting material, 24% isomerized styryl derivative. ^f1.2 eq. of I₂, short iodolysis (1 min) at 0 °C. ^g3% ArOH detected. ^h2% 5-iodovanillin, 14% ArOH and further decomposition compounds. ⁱIC₆H₄Cl-C₆H₄I₂-PhI 91:6:3. ^j72% ArOH. ^kNMP as solvent. ^lYield of *p*-C₆H₄I₂, 44% IC₆H₄OTs, 5% C₆H₅I.

Ester as well as *ortho*-nitrile type starting materials reacted with excellent yields, and their acceptor substituents were left untouched (entries 18-20). The latter substrates might have profited from coordination of OMe or CN in comparison to the *para*-nitrile derivative (entry 15). The vanillin derived tosylate (entry 21) suffered *ortho*-iodination in the case of work-up, after S–O bond cleavage had taken place under zincation conditions, leading to a rather low spectral recovery. Suffering from potential metal coordination at the nitrogen, the quinoliny-8-tosylate achieved moderate yields at high catalyst loading (entry 22). Chemoselectivity issues were explored with 4-chlorophenyl tosylate as bifunctional substrate in the nickel-catalyzed zincation (entry 23). Indeed, tosylate activation was preferred over C–Cl cleavage. Minor amounts of diiodobenzene arose from double metalation. A chromatographical separation of the aryl iodide mixture was not possible. Reductive S–O bond cleavage was highly preferred with the coumaryl mesylate (entry 24). Even though naphthalene-1,5-ditosylate (entry 25) seemed to hold solubility issues, the challenging twofold metalation was achieved in high yield. The related resorcinol derived disulfonate (entry 26) exhibited similar properties like the naphthalene derivative, yet a double metalation was not completely achieved. The bulk of material stopped to react after a single zincation. Losses in recovery were mainly due to poor solubility of the starting material in the extraction solvent, diethylether.

To broaden the applicability of the catalytic zincation protocol, alternative electrophiles with non-halogen leaving groups (figure 4, compare figure 2) were also explored. Aminosulfonate as well as weakly activated methylthioethers were subjected to the same reaction conditions as the tosylates. Dimethylaminosulfonates were highly active substrates for zincation. Regarding methylthioethers as electrophilic partners, several research groups have already reported Ni- or Pd-catalyzed cross-coupling reactions.^[30] Gosmini and coworkers have reported on the cobalt-catalyzed zincation with such substrates.^[31] Our Ni–DAD system efficiently converted both naphthylthiomethylether regioisomers to the corresponding zinc species entailing neglectable amounts of naphthalene. This appears to be the first catalytic zincation outside the realm of activated heteroarenes. Since dimethylaminosulfonate had delivered a particularly clean reaction with no detectable side-product, the corresponding coumarin derivative, which in case of mesylate activation had failed to cleanly zincate, was synthesized in the hope of a smoother conversion. However, both recovery and yield from this coumaryl substrate were even less satisfactory.

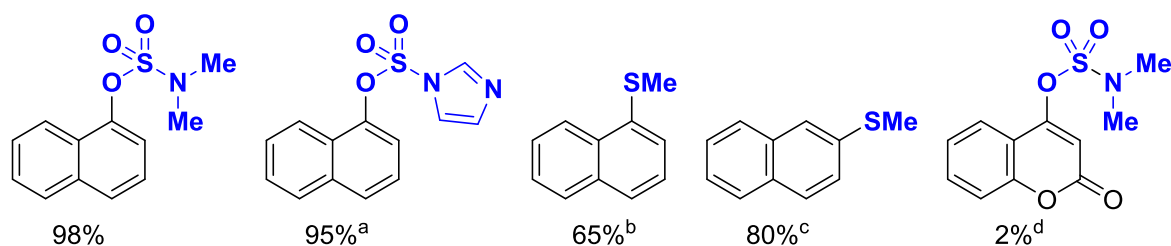


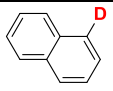
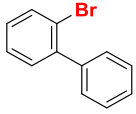
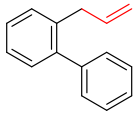
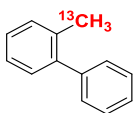
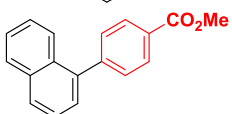
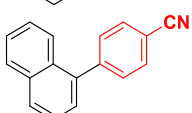
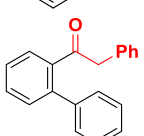
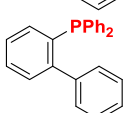
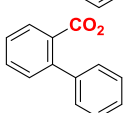
Figure 4. Extended leaving group scope of the Ni-catalyzed zincation. The %-number indicate the spectral yield of 1- or 2-NapI, respectively, after iodolysis (4.0 eq. I₂, 0 °C, 10 min) of the reaction mixture. Scale: 1.00 mmol ArX, NiCl₂(dme)–L2 (1:2, 5 mol% Ni), DMF (3 mL), r.t., 20 h. ^a2% ArX, 3% ArH. ^b31% ArSMe. ^c12% ArSMe, 7% ArH. ^dLow recovery (17%), 15% ArOH.

1.5 Zinc species, where now?

Employing the Ni–DAD catalyst system, a range of substrates was successfully converted to the corresponding arylzinc tosylates, which were further quantified as aryl iodides after iodolysis. In recent years, several research groups have reported on the synthesis of air-stable, easy to handle zinc species.^[32] From such studies, it is known that the reactivity and stability of zinc species is highly dependent on the counter-ion associated to zinc.^[33] To explore the feasibility of ArZnOTs in typical reactions ascribed to organozinc reagents, we subjected two of them, namely 1-naphthyl tosylate (**1**) and 2-biphenyl tosylate (**11**), to various follow-up reactions (table 5). Quenching of arylzinc reagent with excess amounts of D₂O and NBS respectively delivered the desired products in near quantitative yields (entries 1 and 2). Buchwald’s Pd–SPhos catalyst system^[34] allowed room temperature cross-coupling reactions of organozinc reagents with a range of electrophiles in high yields: allylation with allyl bromide (entry 3), methylation with ¹³CH₃I (entry 4), and Negishi coupling with aryl halides proceeded straightforward (entries 5 and 6). Acylation of benzoyl chloride was not tolerated in DMF, presumably due to reaction of the electrophile with solvent. Consequently, a Fukuyama-type acylation^[35] with a less reactive thioester electrophile delivered the desired ketone (entry 7). An attempted synthesis of a Buchwald-type phosphine^[36] in DMF mainly led to decomposition of the phosphine chloride.^[37] This again points to a limitation of application of arylzinc tosylates due to their generation in a nucleophilic amide solvent. However, it had been established in earlier screening results that the synthesis of ArZnOTs is also possible in THF, by using 10 mol% of the Ni catalyst. Even though the nucleophilic solvent was thus removed, and a stoichiometric amount of CuCl·2LiCl^[36a,38] was applied, the reaction in THF only led to minor conversion and the generation of a considerable phosphine oxide fraction (entry 8).

Table 5. Follow-up reaction of the Ni-catalyzed zincation of aryl tosylates.^a **E⁺** = electrophilic reagent.

1. **Zn** (4.0 eq.), DBE (0.2 eq.)
 DMF, 60 °C, 20 min
 2. **NiCl₂(dme)-L₂** (1:2)
 r.t., 30 min
1/11 $\xrightarrow{\text{Metalation}}$ **ArZnOTs** $\xrightarrow[\text{(cat.)}]{\text{E}^+}$ **Ar-E**
 3. addition of **1/11**
 r.t., 20 h
electrophilic quenching

entry	ArOTs	E ⁺ [eq.]	conditions	product	yield [%] ^b
1	1	D ₂ O (xs)	0 °C → r.t. 45 min		91 ^c (92)
2	11	NBS (4.0)	0 °C, 10 min		96 (>99)
3	11	AllylBr (4.0)	[Pd] (3) ^d 0 °C → r.t., 2 d		92 ^e (93)
4	11	¹³ CH ₃ I (2.0)	[Pd] (3) ^d r.t., 4 h		94 ^f (90)
5	1	IC ₆ H ₄ CO ₂ Me (1.0) ^g	[Pd] (2) ^d r.t., 1 h, DMF		95 (>99)
6	1	BrC ₆ H ₄ CN (1.0) ^g	[Pd] (2) ^d r.t., 1 h, DMF		94 (>99)
7	11	PhCH ₂ COSPh (1.0) ^g	[Pd] (5) ^d r.t., 5 h, DMF		71 (74)
8	11^h	PPh ₂ Cl (1.0) ^g	CuCl·2 LiCl (1.0) ⁱ , THF		(37) ^j
9	11	CO ₂ (xs) ^k	r.t., 20 h		j

^aReaction conditions: ArOTs (2.00 mmol), DMF (6 mL). ^bIsolated yield of chromatographically purified material; numbers in brackets according to quantitative ¹H-NMR against internal standard. ^c95% [D]-incorporation at C-1. ^dPd(OAc)₂-SPhos (1:2); Pd loading given in brackets. ^eArAllyl-ArH 95:5. ^fAr¹³CH₃-ArH 87:13, ArH due to acid traces in ¹³CH₃I. ^g1.5 eq. of ArZnOTs added to E⁺. ^hArZnOTs prepared with 10 mol% Ni in THF. ⁱFreshly prepared solution: CuCl and LiCl (1:2) were dried at 150 °C for 3 h under reduced pressure (<2·10⁻¹ mbar) and dissolved in THF (1 M) by stirring for 16 h at r.t. ^jYield determined by integration of ³¹P-NMR signals. 14% phosphine oxide. ^kAdded via CO₂ balloon at the start of the zincation.

The classic synthesis of carboxylic acids from Grignard reactions involves quenching of the organometallic species with solid CO₂.^[39] More recent access pathways consist of the metal-

catalyzed carboxylation^[40] of organometallic reagents or a direct reductive coupling of aryl bromides with CO₂^[41], either at normal or positive pressure of CO₂. However, reactions under CO₂ atmosphere completely failed in the Ni-catalyzed zinc insertion step when using our catalyst system (entry 9), or also with neocuproine as ligand. Neither was carboxylic acid formed when CO₂ was bubbled through a solution of preformed ArZnOTs.

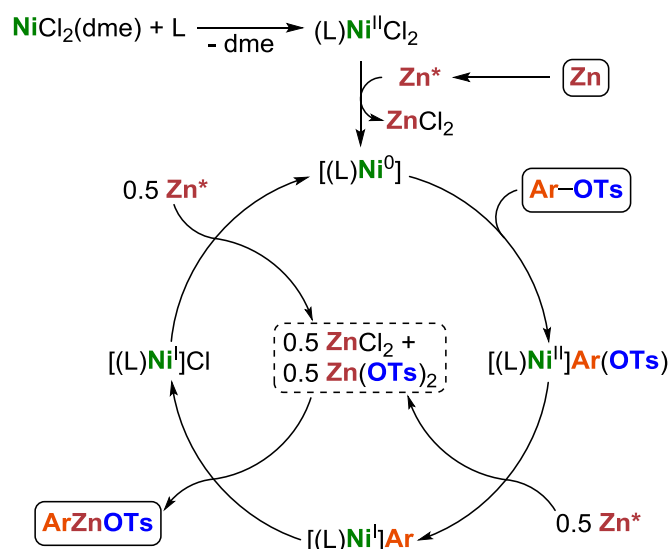
1.6 Behind the scenes

What is actually happening in the catalytic zincation of aryl tosylates? Which species are involved? Those questions arose while looking through literature. Similar to related Ni-chemistry, the Co-catalyzed zincation of aryl bromides presented by the group of Gosmini^[14a] was suggested to involve a dominant Co^I-Co^{III} catalytic cycle.^[42] Later, Yoshikai and coworkers assume a similar reaction mechanism in the generation of aryl zincs from aryl halides.^[15] Taking into account our findings as well as those from earlier work on catalytic zincations^[14,43] and results from studies on Ni-catalyzed reductive coupling reactions,^[41b,43c,44] we propose the following catalytic cycle (scheme 2).

Loss of the ether ligand offers a vacant coordination site for introducing the ligand. (L)Ni^{II}Cl₂, where L stands for diimine **L2**, can be reduced by pre-activated zinc to (L)Ni⁰. Work by tom Dieck suggests that stabilization of the low-valent nickel species as (L)₂Ni⁰ takes place with additional ligand.^[45] The Ni(0) complex will oxidatively add aryl tosylate, generating an arynickel(II) species. Subsequent transmetalation of the aryl group from (L)Ni^{II}ArX to ZnX₂ (X = Cl, OTs) is unfavorable. Namely, it is much more common that aryl transfer proceeds from electropositive (Zn, Mg) to less electropositive (more electron-rich) metal centers (Ni^{II}, Pd^{II}, Pt^{II}).^[46] However, SET-reduction of Ni^{II} to Ni^I with Zn metal as reductant increases the nucleophilicity of the Ni species. Thus, transmetalation of aryl from (L)Ni^IAr to ZnCl(OTs) is more likely, resulting in both ArZnOTs and (L)Ni^ICl. Additional zinc dust readily reduces the latter to Ni⁰, closing the catalytic cycle.

Homocoupling of aryl electrophiles to biaryl poses an unwanted side-reaction in our case. Work by Jutand^[24,47], Durandetti^[48] and Persec^[49] describes the direct synthesis of the latter from reductive coupling of aryl sulfonates, which is thought to involve a Ni^I-Ni^{III} catalytic cycle. Hence, ArOTs oxidatively adds to a preformed Ni^IAr-species and generates biaryl by reductive elimination. Whereas this pathway is preferred with Ni-phosphane^[24,49] catalyst systems, the DAD-type ligands suppress homocoupling of aryl sulfonates. The presence of a π -acceptor

ligand as well as weak donor ligands render the (L)Ni^IX species relatively electron-poor. Particularly, the non-innocent DAD ligand reduces the electron density at Ni. Hence, oxidative addition of ArOTs to (L)Ni^IX is not possible, and reduction to (L)Ni⁰ is necessary.



Scheme 2. Proposed reaction mechanism. L = IPr-MeDAD (**L2**); dme = dimethoxyethane.

1.7 Conclusion and outlook

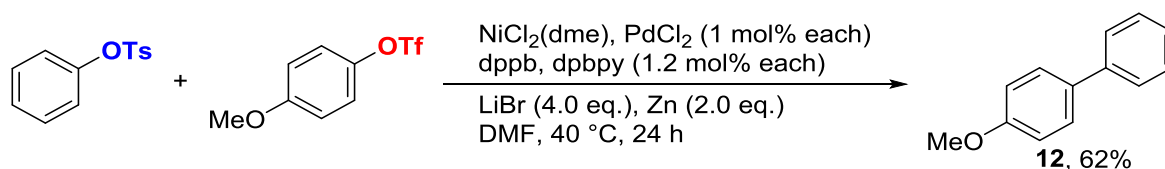
Aryl sulfonates and other deactivated electrophiles were efficiently zincated using the Ni-**L2** (**L2** = IPr-MeDAD) catalyst system developed in this study. Sterically hindered, electro-rich, or -deficient aryl tosylates were converted to the corresponding aryl zinc reagent. Quenching with iodine allowed the quantification of zinc species present, affording high amounts of ArI in most cases. Chemoselective as well as two-fold zincation were both realized. Preferred chemoselectivity of our system could provide useful in the synthesis of natural products in case where an umpolung of the reactive site is needed.

In comparison to other ligands (bipyridines, phenanthrolines, phosphines), DAD-type ligands are readily accessible by simple condensation of commercially available diketones or -aldehydes with a variety of substituted anilines. Hence, a structural modification can easily be realized. While phenanthroline type ligands appear to depend on iodine activation, iodide proved to be superfluous in the case of using DAD ligands, which reduces the complexity of the catalyst system. Treatment of zinc dust with 1,2-dibromoethane turned out to be a mild and efficient method for pre-activation. Among the catalysts and ligands screened, the Ni(Mabiq) triflate salt stands out by showing a peculiar activation effect in case co-catalytic NiCl₂(dme) was added to the inactive complex. This is readily explained by postulating that catalytic

activity depends on an external coordination of nickel to a bipyridine substructure. Since the macrocyclic biquinazoline ligand is capable of hosting different metal atom (Zn, Cu, Fe, Co, Ni),^[26-27,50] it may be possible to modulate the redox activity of the bimetallic complex depending on the metal coordinated inside the macrocycle. The influence exerted on the catalytic zincation would be of interest.

In much of the work performed on Ni-catalyzed reductive coupling reactions, it is assumed that reactions take place at the Ni-center exclusively.^[51] The mechanistic pathway suggested for our catalytic zincation implies that a temporary release of ArZnX is possible, offering a new look on previously published findings, and pointing to applications in a wide range of synthetically useful reactions. It will also be of interest to subject the zinc species generated from our reaction to unexplored classes of electrophiles, either with or without additional Pd-catalyst, to provide the desired products.

Future projects could also include the extension of the substrate scope to heteroaryl^[9b] sulfonates, especially pyrroles and thiophenes, as well as to electrophiles bearing less activated functional groups. Weix et al. have already reported several multi-metallic cross-electrophile reactions of aryl halides with aryl triflates.^[52] Lately, they described the bimetallic one-pot coupling of aryl triflates with aryl tosylates that is believed to involve an in situ generation of ArZnOTs (scheme 3).^[53] The employed metals, Ni and Pd, exhibit complementary reactivity: while Ni reacts preferentially with aryl tosylate, Pd selectively activates aryl triflate. Even though the reaction can also be performed exclusively with Ni, the additional introduction of a Pd-catalyst assures the fast consumption of any aryl zinc species present by cross-coupling with ArOTf. A large excess of the additive LiBr seemed decisive for the reaction to take place, which points to a (pseudo)-halide exchange at the metal center.



Scheme 3. Bimetallic cross-coupling reaction of phenyl tosylate with *p*-anisole triflate to biaryl **12** described by Weix and coworkers.^[53] dppb = 1,4-bis(diphenylphosphino)butane; dpbpy = 4,4'-diphenylbipyridine.

1.8 References

- [1] P. Klein, V. D. Lechner, T. Schimmel, L. Hintermann, *Chem. Eur. J.* **2020**, *26*, 176-180.
- [2] a) E. Negishi, *Acc. Chem. Res.* **1982**, *15*, 340-348; b) C. Han, S. L. Buchwald, *J. Am. Chem. Soc.* **2009**, *131*, 7532-7533; c) V. B. Phapale, D. J. Cárdenas, *Chem. Soc. Rev.* **2009**, *38*, 1598-1607; d) M. M. Heravi, E. Hashemi, N. Nazari, *Mol. Divers.* **2014**, *18*, 441-472.
- [3] a) S. Reformatsky, *Chem. Ber.* **1887**, *20*, 1210-1211; b) S. Reformatsky, *Chem. Ber.* **1895**, *28*, 2842-2847; c) H. E. Simmons, R. D. Smith, *J. Am. Chem. Soc.* **1959**, *81*, 4256-4264; d) A. Fürstner, *Angew. Chem. Int. Ed.* **1993**, *32*, 164-189.
- [4] M. Schlosser, *Organometallics in synthesis: third manual*, John Wiley & Sons, **2013**.
- [5] E. von Frankland, *Liebigs Ann. Chem.* **1849**, *71*, 171-213.
- [6] a) E. Erdik, *Tetrahedron* **1987**, *43*, 2203-2212; b) Q. Cao, J. L. Howard, E. Wheatley, D. L. Browne, *Angew. Chem. Int. Ed.* **2018**, *57*, 11339-11343.
- [7] a) S. C. Berk, M. C. P. Yeh, N. Jeong, P. Knochel, *Organometallics* **1990**, *9*, 3053-3064; b) T. N. Majid, P. Knochel, *Tetrahedron Lett.* **1990**, *31*, 4413-4416.
- [8] L. Zhu, R. M. Wehmeyer, R. D. Rieke, *J. Org. Chem.* **1991**, *56*, 1445-1453.
- [9] a) A. Krasovskiy, V. Malakhov, A. Gavryushin, P. Knochel, *Angew. Chem. Int. Ed.* **2006**, *45*, 6040-6044; b) N. Boudet, S. Sase, P. Sinha, C.-Y. Liu, A. Krasovskiy, P. Knochel, *J. Am. Chem. Soc.* **2007**, *129*, 12358-12359.
- [10] a) C. E. Tucker, T. N. Majid, P. Knochel, *J. Am. Chem. Soc.* **1992**, *114*, 3983-3985; b) P. A. Evans, J. D. Nelson, A. L. Stanley, *J. Org. Chem.* **1995**, *60*, 2298-2301; c) Z.-L. Shen, K. Sommer, P. Knochel, *Synthesis* **2015**, *47*, 2617-2630; d) M. Ketels, D. B. Konrad, K. Karaghiosoff, D. Trauner, P. Knochel, *Org. Lett.* **2017**, *19*, 1666-1669.
- [11] a) R. Giovannini, P. Knochel, *J. Am. Chem. Soc.* **1998**, *120*, 11186-11187; b) F. M. Piller, A. Metzger, M. A. Schade, B. A. Haag, A. Gavryushin, P. Knochel, *Chem. Eur. J.* **2009**, *15*, 7192-7202.
- [12] B. Bogdanović, M. Schwickardi, *Angew. Chem. Int. Ed.* **2000**, *39*, 4610-4612.
- [13] L. E. Aleandri, B. Bogdanovic, P. Bons, C. Duerr, A. Gaidies, T. Hartwig, S. C. Hockett, M. Lagarden, U. Wilczok, R. A. Brand, *Chem. Mater.* **1995**, *7*, 1153-1170.
- [14] a) H. Fillon, C. Gosmini, J. Périchon, *J. Am. Chem. Soc.* **2003**, *125*, 3867-3870; b) C. Gosmini, M. Amatore, S. Claudel, J. Perichon, *Synlett* **2005**, *14*, 2171-2174; c) I.

- Kazmierski, C. Gosmini, J.-M. Paris, J. Périchon, *Tetrahedron Lett.* **2003**, *44*, 6417-6420; d) J. Périchon, C. Gosmini, O. Buriez, Electrochemical Generation and Reaction of Zinc Reagents in *PATAI'S Chemistry of Functional Groups*, John Wiley & Sons, Ltd., Chichester, UK, **2009**.
- [15] M.-Y. Jin, N. Yoshikai, *J. Org. Chem.* **2011**, *76*, 1972-1978.
- [16] a) M. Balkenhohl, R. Greiner, I. S. Makarov, B. Heinz, K. Karaghiosoff, H. Zipse, P. Knochel, *Chem. Eur. J.* **2017**, *23*, 13046-13050; b) G. C. Clososki, C. J. Rohbogner, P. Knochel, *Angew. Chem. Int. Ed.* **2007**, *46*, 7681-7684; c) M. Mosrin, P. Knochel, *Org. Lett.* **2009**, *11*, 1837-1840; d) C. J. Rohbogner, G. C. Clososki, P. Knochel, *Angew. Chem. Int. Ed.* **2008**, *47*, 1503-1507; e) S. H. Wunderlich, P. Knochel, *Angew. Chem. Int. Ed.* **2007**, *46*, 7685-7688.
- [17] C. Jubert, P. Knochel, *J. Org. Chem.* **1992**, *57*, 5425-5431.
- [18] D. Guijarro, G. Guillena, B. Mancheño, M. Yus, *Tetrahedron* **1994**, *50*, 3427-3436.
- [19] T. P. Burns, R. D. Rieke, *J. Org. Chem.* **1987**, *52*, 3674-3680.
- [20] a) S.-H. Kim, R. D. Rieke, *J. Org. Chem.* **2000**, *65*, 2322-2330; b) T. Harada, T. Kaneko, T. Fujiwara, A. Oku, *J. Org. Chem.* **1997**, *62*, 8966-8967.
- [21] a) T. Ishiyama, Y. Itoh, T. Kitano, N. Miyaura, *Tetrahedron Lett.* **1997**, *38*, 3447-3450; b) W. K. Chow, O. Y. Yuen, P. Y. Choy, C. M. So, C. P. Lau, W. T. Wong, F. Y. Kwong, *RSC Adv.* **2013**, *3*, 12518-12539; c) W. K. Chow, C. M. So, C. P. Lau, F. Y. Kwong, *Chem. Eur. J.* **2011**, *17*, 6913-6917; d) G. A. Molander, S. L. Trice, S. M. Kennedy, S. D. Dreher, M. T. Tudge, *J. Am. Chem. Soc.* **2012**, *134*, 11667-11673; e) B. M. Rosen, K. W. Quasdorf, D. A. Wilson, N. Zhang, A.-M. Resmerita, N. K. Garg, V. Percec, *Chem. Rev.* **2011**, *111*, 1346-1416; f) D. A. Wilson, C. J. Wilson, C. Moldoveanu, A.-M. Resmerita, P. Corcoran, L. M. Hoang, B. M. Rosen, V. Percec, *J. Am. Chem. Soc.* **2010**, *132*, 1800-1801.
- [22] I. Kazmierski, C. Gosmini, J.-M. Paris, J. Perichon, *Synlett* **2006**, *6*, 881-884.
- [23] T. Schimmel, *Übergangsmetall-katalysierte Metallierungsreaktionen*, thesis for the First State Examination for Secondary School Teachers, RWTH Aachen (Aachen), **2004**.
- [24] A. Jutand, A. Mosleh, *J. Org. Chem.* **1997**, *62*, 261-274.
- [25] L. Vivien Denise, *Nickel-Catalyzed Synthesis of Arylzinc Reagents from Aryl Sulfonates*, bachelor thesis, Technical University of Munich (Garching bei München), **2016**.

- [26] E. Mueller, G. Bernardinelli, A. Von Zelewsky, *Inorg. Chem.* **1988**, *27*, 4645-4651.
- [27] a) P. Banerjee, A. Company, T. Weyhermüller, E. Bill, C. R. Hess, *Inorg. Chem.* **2009**, *48*, 2944-2955; b) E. V. Puttock, P. Banerjee, M. Kaspar, L. Drennen, D. S. Yufit, E. Bill, S. Sproules, C. R. Hess, *Inorg. Chem.* **2015**, *54*, 5864-5873; c) M. Grübel, I. Bosque, P. J. Altmann, T. Bach, C. R. Hess, *Chem. Sci.* **2018**, *9*, 3313-3317.
- [28] X. Lei, A. Jalla, M. A. A. Shama, J. M. Stafford, B. Cao, *Synthesis* **2015**, *47*, 2578-2585.
- [29] K. M. Khan, S. Rahat, M. I. Choudhary, U. Ghani, S. Perveen, S. Khatoon, A. Dar, A. Malik, *Helv. Chim. Acta* **2002**, *85*, 559-570.
- [30] a) K. Lee, C. M. Counciller, J. P. Stambuli, *Org. Lett.* **2009**, *11*, 1457-1459; b) A. Metzger, L. Melzig, C. Despotopoulou, P. Knochel, *Org. Lett.* **2009**, *11*, 4228-4231; c) M. E. Angiolelli, A. L. Casalnuovo, T. P. Selby, *Synlett* **2000**, *6*, 0905-0907; d) E. Wenkert, T. W. Ferreira, E. L. Michelotti, *J. Chem. Soc., Chem. Commun.* **1979**, 637-638.
- [31] J.-M. Begouin, M. Rivard, C. Gosmini, *Chem. Commun.* **2010**, *46*, 5972-5974.
- [32] a) K. Aikawa, Y. Nakamura, Y. Yokota, W. Toya, K. Mikami, *Chem. Eur. J.* **2015**, *21*, 96-100; b) M. S. Hofmayer, J. M. Hammann, F. H. Lutter, P. Knochel, *Synthesis* **2017**, *49*, 3925-3930; c) C. I. Stathakis, S. Bernhardt, V. Quint, P. Knochel, *Angew. Chem. Int. Ed.* **2012**, *51*, 9428-9432; d) J. M. Hammann, F. H. Lutter, D. Haas, P. Knochel, *Angew. Chem. Int. Ed.* **2017**, *56*, 1082-1086.
- [33] a) A. Hernán-Gómez, E. Herd, E. Hevia, A. R. Kennedy, P. Knochel, K. Koszinowski, S. M. Manolikakes, R. E. Mulvey, C. Schnegelsberg, *Angew. Chem. Int. Ed.* **2014**, *53*, 2706-2710; b) L. C. McCann, M. G. Organ, *Angew. Chem. Int. Ed.* **2014**, *53*, 4386-4389; c) L. Jin, C. Liu, J. Liu, F. Hu, Y. Lan, A. S. Batsanov, J. A. Howard, T. B. Marder, A. Lei, *J. Am. Chem. Soc.* **2009**, *131*, 16656-16657.
- [34] a) T. E. Barder, S. D. Walker, J. R. Martinelli, S. L. Buchwald, *J. Am. Chem. Soc.* **2005**, *127*, 4685-4696; b) R. A. Altman, S. L. Buchwald, *Nat. Protoc.* **2007**, *2*, 3115; c) S. Kozuch, J. M. Martin, *Chem. Commun.* **2011**, *47*, 4935-4937; d) M. M. Heravi, Z. Kheilkordi, V. Zadsirjan, M. Heydari, M. Malmir, *J. Organomet. Chem.* **2018**, *861*, 17-104; e) R. Martin, S. L. Buchwald, *Org. Lett.* **2008**, *10*, 4561-4564.
- [35] a) H. Tokuyama, S. Yokoshima, T. Yamashita, T. Fukuyama, *Tetrahedron Lett.* **1998**, *39*, 3189-3192; b) T. Shimizu, M. Seki, *Tetrahedron Lett.* **2001**, *42*, 429-432; c) Y.

- Mori, M. Seki, *Adv. Synth. Catal.* **2007**, *349*, 2027-2038; d) L. Melzig, A. Metzger, P. Knochel, *Chem. Eur. J.* **2011**, *17*, 2948-2956; e) R. Oost, A. Misale, N. Maulide, *Angew. Chem. Int. Ed.* **2016**, *55*, 4587-4590; f) P. H. Gehrtz, P. Kathe, I. Fleischer, *Chem. Eur. J.* **2018**, *24*, 8774-8778.
- [36] a) D. Gelman, L. Jiang, S. L. Buchwald, *Org. Lett.* **2003**, *5*, 2315-2318; b) W. Wang, G. B. Hammond, B. Xu, *J. Am. Chem. Soc.* **2012**, *134*, 5697-5705.
- [37] V. Morgalyuk, P. Petrovskii, K. Lysenko, E. Nifant'ev, *Russ. J. Gen. Chem.* **2010**, *80*, 100-105.
- [38] a) X. Han, B. M. Stoltz, E. Corey, *J. Am. Chem. Soc.* **1999**, *121*, 7600-7605; b) A. Krasovskiy, P. Knochel, *Angew. Chem. Int. Ed.* **2004**, *43*, 3333-3336; c) M. Kienle, S. R. Dubbaka, V. del Amo, P. Knochel, *Synthesis* **2007**, *8*, 1272-1278.
- [39] D. Bowen, R. Barnes, *Org. Synth* **1941**, *21*, 77-82.
- [40] a) A. Correa, R. Martin, *Angew. Chem. Int. Ed.* **2009**, *48*, 6201-6204; b) M. Börjesson, T. Moragas, D. Gallego, R. Martin, *ACS Catal.* **2016**, *6*, 6739-6749; c) H. Ochiai, M. Jang, K. Hirano, H. Yorimitsu, K. Oshima, *Org. Lett.* **2008**, *10*, 2681-2683.
- [41] a) A. Correa, R. Martin, *J. Am. Chem. Soc.* **2009**, *131*, 15974-15975; b) T. Leon, A. Correa, R. Martin, *J. Am. Chem. Soc.* **2013**, *135*, 1221-1224.
- [42] C. Gosmini, J.-M. Bégouin, A. Moncomble, *Chem. Commun.* **2008**, 3221-3233.
- [43] a) Y. Bourne-Branchu, A. Moncomble, M. Corpet, G. Danoun, C. Gosmini, *Synthesis* **2016**, *48*, 3352-3356; b) C. Gosmini, A. Moncomble, *Isr. J. Chem.* **2010**, *50*, 568-576; c) C. S. Yeung, V. M. Dong, *J. Am. Chem. Soc.* **2008**, *130*, 7826-7827.
- [44] a) T. Fujihara, K. Nogi, T. Xu, J. Terao, Y. Tsuji, *J. Am. Chem. Soc.* **2012**, *134*, 9106-9109; b) F. Rebih, M. Andreini, A. Moncomble, A. Harrison-Marchand, J. Maddaluno, M. Durandetti, *Chem. Eur. J.* **2016**, *22*, 3758-3763; c) Y. Liu, J. Cornella, R. Martin, *J. Am. Chem. Soc.* **2014**, *136*, 11212-11215.
- [45] a) H. tom Dieck, M. Svoboda, T. Greiser, *Z. Naturforsch. B* **1981**, *36*, 823-832; b) H. T. Dieck, J. Dietrich, *Chem. Ber.* **1984**, *117*, 694-701.
- [46] a) N. Miyaura, *J. Organomet. Chem.* **2002**, *653*, 54-57; b) O. Wendt, *Curr. Org. Chem.* **2007**, *11*, 1417-1433; c) A. J. Lennox, G. C. Lloyd-Jones, *Angew. Chem. Int. Ed.* **2013**, *52*, 7362-7370.
- [47] A. Jutand, A. Mosleh, *Synlett* **1993**, *8*, 568-570.
- [48] J. Maddaluno, M. Durandetti, *Synlett* **2015**, *26*, 2385-2388.

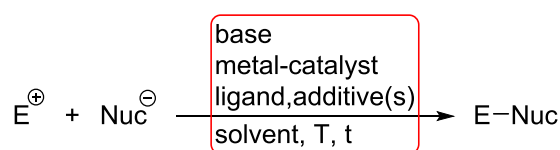
- [49] V. Percec, J.-Y. Bae, M. Zhao, D. H. Hill, *J. Org. Chem.* **1995**, *60*, 176-185.
- [50] H. S. Stark, P. J. Altmann, S. Sproules, C. R. Hess, *Inorg. Chem.* **2018**, *57*, 6401-6409.
- [51] a) L. K. Ackerman, M. M. Lovell, D. J. Weix, *Nature* **2015**, *524*, 454-457; b) A. Correa, R. Martin, *J. Am. Chem. Soc.* **2014**, *136*, 7253-7256; c) Y. Dai, F. Wu, Z. Zang, H. You, H. Gong, *Chem. Eur. J.* **2012**, *18*, 808-812; d) C. Qiu, K. Yao, X. Zhang, H. Gong, *Org. Biomol. Chem.* **2016**, *14*, 11332-11335; e) X. Wang, Y. Dai, H. Gong, Nickel-catalyzed reductive couplings in *Ni- and Fe-Based Cross-Coupling Reactions*, Springer, **2017**, pp. 61-89; f) X. Wang, G. Ma, Y. Peng, C. E. Pitsch, B. J. Moll, T. D. Ly, X. Wang, H. Gong, *J. Am. Chem. Soc.* **2018**, *140*, 14490-14497; g) H. Yin, C. Zhao, H. You, K. Lin, H. Gong, *Chem. Commun.* **2012**, *48*, 7034-7036; h) X. Zhang, H. Liu, X. Hu, G. Tang, J. Zhu, Y. Zhao, *Org. Lett.* **2011**, *13*, 3478-3481; i) C. Zhao, X. Jia, X. Wang, H. Gong, *J. Am. Chem. Soc.* **2014**, *136*, 17645-17651; j) C. Gong, C. Huo, X. Wang, Z. Quan, *Chin. J. Chem.* **2017**, *35*, 1366-1370.
- [52] a) L. Huang, L. K. Ackerman, K. Kang, A. M. Parsons, D. J. Weix, *J. Am. Chem. Soc.* **2019**, *141*, 10978-10983; b) A. M. Olivares, D. J. Weix, *J. Am. Chem. Soc.* **2018**, *140*, 2446-2449.
- [53] K. Kang, L. Huang, D. J. Weix, *J. Am. Chem. Soc.* **2020**, *142*, 10634-10640.

2 THE MULTIFUNCTIONAL COMPONENT CATALYST (MFCC) PRINCIPLE: DEFINITIONS, SCREENING, AND APPLICATION

First, the multifunctional component catalyst (MFCC) principle will be defined (2.1). Recent literature relevant to the topic will be analyzed from our point of view. A new approach for screening of catalytic reactions using multifunctional additives will be presented (2.2). First applications verify the feasibility of our screening approach (2.3). Conclusions and an outlook (2.4) end the chapter.

2.1 Defining the multifunctional component catalyst principle (MFCCP)

In the framework of homogeneous metal-complex catalysis, we set out to define the multifunctional component catalyst principle (MFCCP). A general representation of a reaction in current, homogeneous catalysis is displayed in scheme 4.



Scheme 4. Representation of a typical reaction in homogeneous metal-complex catalysis. E^+ = electrophile; Nuc^- = nucleophile; T = temperature; t = time.

The electrophile (E^+) and nucleophile (Nuc^-) usually do not react with each other to form A–B. However, by taking advantage of a catalyst-system energy barriers can be overcome to realize the desired transformation. In literature, one stumbles across various definitions of a catalyst-system, often referring to every substance which is included in the red rectangle of scheme 4.^[1] Increasing complexity may be prescribed to a catalyst-system depending on how many independently stable, physically separable substances it involves. Such compounds commit a single or several functions, e.g. a base, a ligand, a reductant or any other, designating the task(s) they perform. For example, silver salts have been extensively used as additives in $C_{sp^3}\text{-H}$ cross-coupling reactions,^[2] being known for deprotonation in the case of a carbonate salt, halide abstraction as well as oxidation of metal intermediates. However, a fourth role has been attributed to silver acetate.^[3] Multimetallic interactions of silver and palladium were determined to significantly enhance the activity of the catalyst-system. Another example displays the function of a base which is designated to deprotonate either intermediates or substrate to maintain the turnover of the catalytic cycle. The function as basic activator in ligand deprotonation is often attributed to a base, thus generating the active catalyst species.^[4] Such hidden functionalities render it difficult to draw clear lines between substances, which simply

sustain the existence or actually increase the activity of a catalyst-system, and could be defined as a catalyst-component.

We suggest that a catalyst-system should be defined as positive or negative interplay of catalyst-components, which are independently stable and storable substances. Each catalyst-component carries out a specific task to maintain the activity or existence of the system. Individual components may interfere either directly or indirectly, e.g. react, merge, transform or other. Changes in a system, e.g. removal or substitution of an active element, often have severe impact on its performance or reactivity. Simply thought: a system wraps up all catalyst-components present to one entity (figure 5).

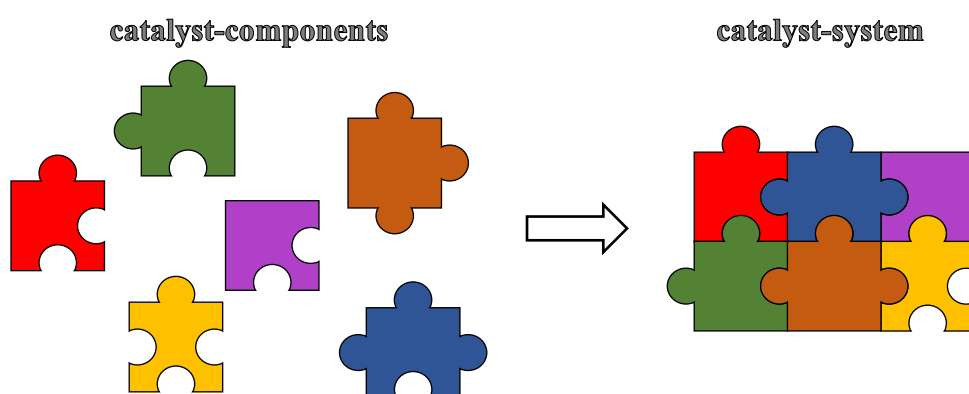


Figure 5. Several catalyst-components merge together to define a catalyst-system. Each color depicts one catalyst-component.

single-component vs. multi-component

Catalyst-systems may either be of single- or multi-component nature. One may ask which substances of a reaction can be defined as component to differ single- and multi-component catalyst-systems. Do reactants (electrophile, nucleophile) as well as product(s) already take part in a catalyst-component? Or is it necessary for a catalyst-component to be involved in catalytic loading? What about solvent(s) or (Lewis) bases/acids which are often present in excess? Several research groups refer to single-^[5] or multi-component^[1c,1e-g] catalysts or reactions. Some include starting materials, base, and solvents, others do not. In our opinion, substrates acting as nucleophile or electrophile delivering a desired product should not be considered as catalyst-component. However, one interesting exception is displayed by the Soai-autocatalysis^[6], which describes the alkylation of pyrimidine-5-carbaldehydes with diisopropylzinc. In the presence of product with minor enantiomeric excess (ee), chiral induction takes place for further turnovers of the catalytic cycle, leading to extremely high ee's

in the end. More and more publications emerge reporting of aqueous^[7] or solvent-free^[8] conditions with the desire to contribute to green chemistry. In chemistry, solvents may have major impact on the outcome of a reaction by (de)stabilizing reactive intermediate, as e.g. in the S_N1 vs. S_N2 mechanistic dichotomy.^[9] Catalysis often relies on the chosen reaction media. In the case of solvent-induced reactivity, e.g. transfer of chirality^[10] via hydrogen bonding or other, the solvent should still be counted as reaction medium and not catalyst-component.

In conclusion, any reagent capable of the following should be added to the list of catalyst-components: assisting the transformation of reagents, reduction of activation barrier, stabilization of intermediates occurring in the catalytic cycle. Physical separation divides components into individually weighable substances. A system constituted of more than one catalyst-component (puzzle piece) is specified as multi-component, else single-component catalyst system.

function – monofunctional vs. multifunctional

In literature, a large variety of catalyst-components can be found, including metals, ligands, base, halide abstractor, CMD (concerted metalation deprotonation) or PTC (phase-transfer catalyst) additive just to name a few. Every catalyst-component can further be classified in an even more precise manner. For example, metals could be separated as main group^[11] or transition^[12] metals according to their position in the periodic table. Any compound, ion or molecule, coordinating a metal center to form a coordination complex is designated as ligand. Most prominent ones are phosphines^[12h,13], NHC^[14] (*N*-heterocyclic carbenes) or bipyridines^[15]. Bases can be divided in organic^[16] or inorganic^[17] ones.^[18] Any of these catalyst-component added to a reaction mixture features an expected behavior, which takes at least one particular position in a system. Thus, catalyst-components exhibit one or more functions, being mono- or multifunctional, respectively. Such functions describe the direct task(s) a substance exhibits, e.g. deprotonation, coordination or other. The list of discrete functionalities could be extended to infinity but should not consist our primary intention at this point. Functions of a catalyst-component can either be spatially separated, e.g. in a salt^[19] or complex^[20], or belong to the same part of the substance. Silver salts are prime examples for difunctional catalyst-components with the ability of Ag(I) for halide abstraction as well as oxidation of inactive metal species.^[21] Catalyst-components ranging from mono- to tetrafunctional are illustrated as puzzle pieces in figure 6. Each puzzle piece can fulfil specific tasks depending on their anchor(s) (function).

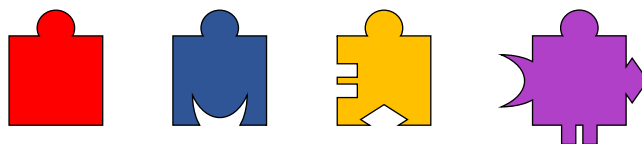
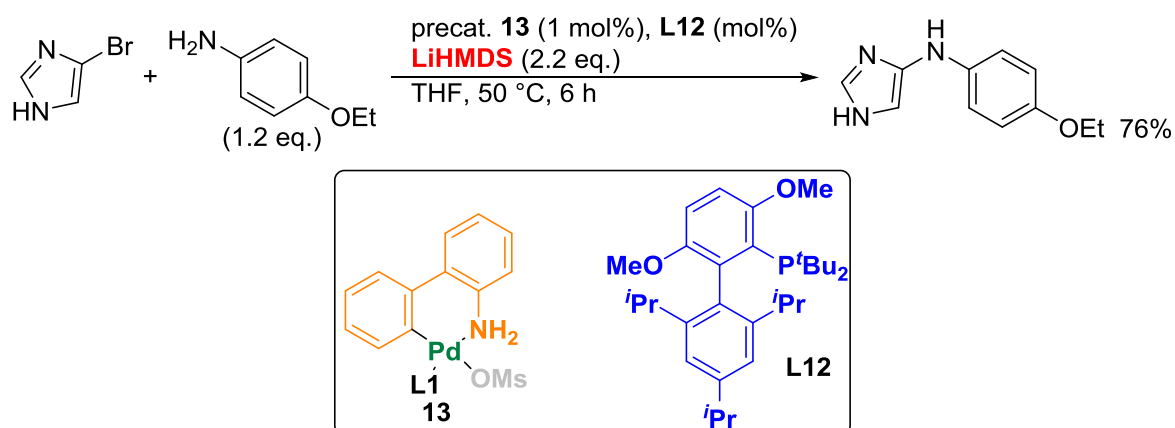


Figure 6. Illustration of **mono**-, **di**-, **tri**-, and **tetra**functional catalyst components.

For example, more than a decade ago Buchwald et al. developed a first class of palladacycles active in catalysis.^[22] After key improvements, precatalysts of four different generations have evolved.^[23] Among these catalyst-systems, we have chosen the amination of unprotected bromoimidazoles as outlined by Buchwald et al. to delineate mono- or multifunctionality (scheme 5).^[24] In this particular reaction, two catalyst-components are present, namely the 3rd generation palladacycle **13**, and the ligand (**L12**, ^tBuBrettPhos). The latter one is monofunctional, since its only function relies in coordination to Pd, thus stabilizing intermediary species. The palladacycle **13** is trifunctional merging **reductant**, **ligand** and **metal center** into one physically separable compound. The involved mesylato ligand is only present due to its weak coordination to Pd. The sulfonate anion allows the complexation of more sterically hindered phosphines leaving the precatalyst with no extra functionality.

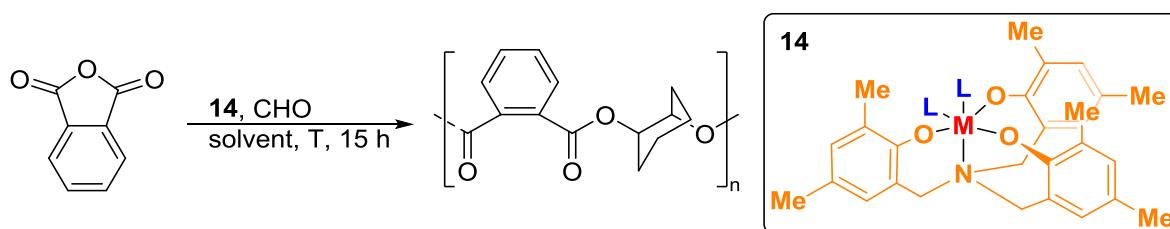


Scheme 5. Pd-catalyzed amination of unprotected bromo-imidazoles reported by the group of Buchwald.^[24] Example shown depicts the coupling of 4-bromo-1*H*-imidazole with electron-rich 4-ethoxyaniline. precat. = precatalyst; **L12** = ^tBuBrettPhos.

However, it is not clear whether the base (**LiHMDS**) takes part in the catalyst-system, since it is not only assuring catalyst-cycle turnover, but also activating the palladacycle **13** in the initial step of the reaction. Via deprotonation of the amino group with subsequent reductive elimination of the carbazole, the Pd(II) center is readily reduced to an active, monoligated Pd(0) species. Therefore, counting LiHMDS as catalyst-component, we would add up to a three-component catalyst-system. The number of functions defining the catalyst-system should be

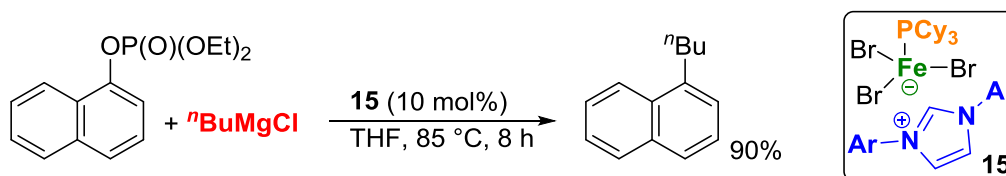
composed of their total sum, here four. Hence, Buchwald employed conditions^[24] could be summarized as *tetrafunctional three-component catalyst system*.

Kleij et al. claim the use of difunctional complexes as one-component catalysts for ring-opening copolymerization of cyclic anhydrides and epoxides (scheme 6).^[4] We agree that the employed catalyst-system is of single-component nature, since the only involved substance is the depicted metal complex **14** (**M** = Co, Mn, or Cr) besides reactants and solvent. However, in our opinion, the catalyst-component **14** is trifunctional, unifying multidentate ligand (**aminotriphenolate**), Lewis acid (**M** = Co, Mn, or Cr), and activator (**L** = DMAP). Functions attributed would comprise coordination, activation as well as (electron pair) acceptor. The work of Kleij et al.^[4] is considered as *trifunctional single-component catalyst system*.



Scheme 6. Ring-opening polymerization published by Kleij et al.^[4] Reaction conditions: **14** (0.25-0.50 mol%) at 65-110 °C in either 8 M THF, 1,2-DCE, toluene, or neat. CHO = cyclohexene oxide (1.0, 1.1, 2.0, or 4.0 eq.); M = Co, Mn, or Cr; L = N,N-dimethylaminopyridine (DMAP).

Sun et al. reported the iron catalysed cross-coupling of aryl phosphates (electrophile) with alkyl Grignard reagents (nucleophile, scheme 7).^[25] Next to these two reactants and the solvent, only one single catalyst-component was added, namely the ionic Fe(II) complex **15**.



Scheme 7. Fe(II)-catalyzed cross-coupling of aryl phosphates with alkyl Grignard reagents described by Sun and coworkers.^[25] Example shown described the coupling of 1-naphthyl phosphate with *n*-butylmagnesium chloride. Ar = 2,6-diisopropylphenyl.

The latter consists of a border case, unifying metal center (**Fe(II)**), and two ligands (**PCy₃** and **imidazolium salt**). One might argue that the complex is trifunctional, since it bears different types of ligands. We suggest that the described salt should be assumed as difunctional, since only two different functionalities, metal center and ligand, are present. However, a second substance exhibits a certain function indispensable for a successful reaction. Besides

functionalization of the phosphate, the hidden base (**Grignard**) exposes the carbene ligand most likely involved in the catalytic conversion, thus taking part in the catalyst-system. Taking our description into account, the work presented by Sun et al.^[25] can be described as *trifunctional two-component catalyst system*.

2.2 New ways of screening

The outcome of chemical reactions is strictly dependent on the involved catalyst-system. Extensive screening efforts seek for optimal conditions to achieve maximal conversion and selectivity to the target material.^[26] Conventional methods rely on one variable (catalyst, ligand, temperature, solvent...) at a time (OVAT) screening, leaving a large number of possible combinations. Since the latter execution is rather exhausting, several groups have taken advantage of high throughput experiments (HTE).^[27] Reactions can either be performed manually or fully automated. Among all possible combinations of catalyst-components, literature precedents for new reactivities often represent good starting points for novel transformations. However, the variation of continuous parameters such as pressure, time, and temperature is limited in batch HTE screening. Microfluidic reactors overcome this challenge while consuming only nanomolar amounts of substances and being limited to screening one reaction at a time.^[28] Possible combinations of catalyst-components are significantly reduced by the Design of Experiments (DoE) methodology.^[29] Based on mathematical calculations, important variables and relations can be deduced to identify viable functionalities for a specific catalytic reaction. This method was further extended to the sequential Design of Experiments (sDoE). Newly generated information from analysis is directly implemented in the development of new conditions, thus a self-optimizing system.^[30] For example, Jensen et al. designed an automated feedback which allowed maximization of yield without loss of catalyst activity in Suzuki-type coupling.^[31]

Next to these methods, we wanted to establish an original approach of screening. By mixing different catalyst-components with individual functions, we hope to discover unprecedented reactivities, e.g. multi-metallic active catalysts similar to reported Pd–Ag interactions^[3,32]. In general, a two-dimensional (2D) matrix should illustrate our proposition for any catalytic conversion (table 6). Any substance, e.g. the solvent, a base, or any other additive, which is not listed in the table but part of the reaction, remains constant. Whereas metal precatalysts define rows of the matrix, catalyst-component of different functionality (additives) will be arranged in

columns. Further arrangements are also possible but will not be part of this thesis. While progressing from left to right, the consecutive combination of additives is expected to reveal the positive or negative influence they exhibit to one another. Metal precatalysts will be used either alone or in combined high–low loading (HiLo). In any case, one metal will be predominant for each row. For HiLo screening, further precursors will be added in considerably lower amounts, e.g. ten times less than the dominant one. This kind of set-up should favor the discovery of hidden multi-metallic interplay. We have depicted one entry of a 2D screening matrix in table 6. Two possibilities emerge from the combination of column 4 and row 3. In both cases, every additive listed so far (additives 1-4) will be involved in a previously fixed stoichiometry (e.g. 10 mol%). Metal 3 will be present in the Hi setting (e.g. 5.0 mol%), either alone or combined in Lo loading (here: 0.5 mol%) with every other metal specified in the matrix.

Table 6. Two-dimensional (2D) screening matrix. Additives are listed horizontally, metals vertically. HiLo = high–low (e.g. 10:1) loading.

	additive 1	additive 2	additive 3	additive 4	additive 5	...
metal 1	combination of additive 1, 2, 3,...			additives 1-4; metal 3 (alone) or metal 3 (Hi), other metals (Lo)		
metal 2						
metal 3						
metal 4						
metal 5						
⋮						

alone or in HiLo
combination of additive 1, 2, 3,...

To visualize our concept, an exemplary two-dimensional (3X3) screening matrix is shown in figure 7. The header of the table includes the corresponding reaction scheme, describing the catalytic conversion which will be optimized. At this point, reactants, fix catalyst-components and conditions (solvent, temperature, time) are depicted. Involved additives which constitute individual rows are listed on the right side of the matrix, metal precatalysts representing columns. Detailed reaction conditions (procedure, analysis) can be found at the bottom of the table. Each intersection of a column and row defines one entry of the matrix, showing which catalyst-components are further added. Every entry summarizes metal precatalyst(s), additive(s), and yield (mol%) for the specific combination. To clarify which entry is being discussed, we adapted conventional numbering from mathematics^[33], i.e. variable $E_{x,y}$ refers to entry of row x and column y. Additive equivalents are indicated in the respective column header. Metal atoms written in subscripts are added in previously defined low (Lo), else in high loading (Hi). One exemplary entry ($E_{2,2}$) is highlighted in red. In this case, Ni- (Hi, 5.0 mol%),

Pd- and **Co**-precatalysts (Lo, 0.5 mol% each), as well as additives **A** and **B** (10.0 mol% each) would be incorporated in the described reaction scheme depicted in the header. While the entry on the left excludes additive **B**, the right one comprises additive **C**.

reaction scheme

educt $\xrightarrow[\text{solvent, T, t}]{\text{reactant(s) catalyst-component(s)}}$ product

metal precat.

	A (10.0)		B (10.0)		C (10.0)	
PdCl₂(MeCN)₂ (5.0)	Pd _{NiCo}	yield	Pd _{NiCo}	yield	Pd _{NiCo}	yield
	A		AB		ABC	
NiCl₂(dme) (5.0)	Ni _{PdCo}	yield	Ni _{PdCo}	yield	Ni _{PdCo}	yield
	A		AB		ABC	
CoBr₂ (5.0)	Co _{PdNi}	yield	Co _{PdNi}	yield	Co _{PdNi}	yield
	A		AB		ABC	

Reaction conditions and additional information. $E_{3,1}$

1 entry indicates yield, additive(s) and metal(s)

list of all additives

Figure 7. Example of a theoretical two-dimensional (2D) screening matrix. precat. = precatalyst (HiLo 10:1).

2.3 Two-dimensional (2D) Matrix screening in practice

Three versions of a 2D matrix were assembled and applied to the arylation of caffeine described by the group of You^[34]. Initial screening experiments are displayed in table 7. Amounts of starting material, reactant, base, and solvent were kept constant for all manipulations.

Table 7. Two-dimensional (2D) 3x3 screening matrix of arylation of caffeine with bromobenzene according to You et al.^[34].

Reaction scheme:

	A (10.0)		B (10.0)		C (10.0)	
PdCl₂(MeCN)₂ (5.0)	Pd	14	Pd	13	Pd	12
	A		AB		ABC	
NiCl₂(dme) (5.0)	Ni	0	Ni	0	Ni	0
	A		AB		ABC	
CoBr₂ (5.0)	Co	0	Co	0	Co	0
	A		AB		ABC	

^aReaction performed with 500 μmol caffeine in DMF (Σ 1.5 mL) according to GP 2.1 (see 7.2.2.1); additive **A** (0.1 M, 0.5 mL) and PhBr (0.75 M, 1.0 mL) were added as solutions (DMF); spectral yield according to ¹H-NMR with internal standard, given in mol%.

Since previous experiments¹ had already confirmed easily comparable arylation results after 2.5 hours at 100 °C, we stuck to the latter conditions. Reaction mixtures were directly filtered

¹ Referring to several master theses at AK Hintermann (P. Klein^[35], L. Rast^[36], J. Rekowski^[37]).

over a short pad of silica gel, eluting with DCM–MeOH (10:1). Crude products were analysed by q-NMR analysis. Limiting our screening to monofunctional catalyst-components, we chose 2-pyridone (**A**), tetrabutylammonium HSO₄ (**B**), and pivalic acid (**C**). Additives were arranged in alphabetic order (**A** to **C**) in columns. Only one metal precatalyst was added for each entry, picking between PdCl₂(MeCN)₂, NiCl₂(dme), and CoBr₂. Reactions involving the latter two precursors (**Ni**, **Co**) proved unreactive (*E*_{2,1}-*E*_{3,3}). The desired product was only observed when Pd metal was present (*E*_{1,1}-*E*_{1,3}). Regarding the three additives, only 2-pyridone seems to practice a positive effect on the coupling (*E*_{1,1}). Additives **B** and **C** did not affect the yield (*E*_{1,2} and *E*_{1,3}).

Since we already knew enhanced reactivity could be expected especially for additives **B** and **C**, we repeated the 2D matrix in reversed order (table 8). To simplify analysis, work-up of reaction mixtures was performed by fast extraction. Washing phase (sat. aq. NaCl solution), extraction solvent (EtOAc) as well as internal standard (1,3,5-trimethoxybenzene) were directly added to the vial. After shaking for 1-2 minutes, samples for q-NMR analysis were withdrawn from the organic layer.²

Table 8. Two-dimensional (2D) 3x3 screening matrix of the arylation of caffeine with bromobenzene according to You et al.^[34], reversed order of additives.

	C (10.0)		B (10.0)		A (10.0)	
Pd Cl ₂ (MeCN) ₂ (5.0)	Pd	39	Pd	48	Pd	13
	C		BC		ABC	
Ni Cl ₂ (dme) (5.0)	Ni	0	Ni	0	Ni	0
	C		BC		ABC	
Co Br ₂ (5.0)	Co	0	Co	0	Co	0
	C		BC		ABC	

A

B

C

^aReaction performed with 500 μmol caffeine in DMF (Σ 1.5 mL) according to GP 2.1 (see 7.2.2.1); additive **C** (0.1 M, 0.5 mL) and PhBr (0.75 M, 1.0 mL) were added as solutions (DMF); spectral yield according to ¹H-NMR with internal standard, given in mol%.

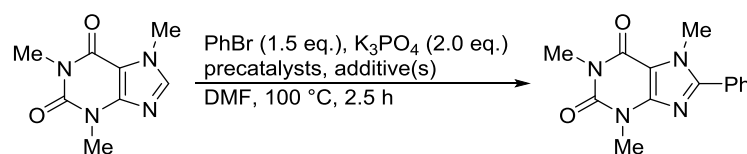
Whereas no conversion was observed for **Ni** and **Co** precatalysts (*E*_{2,1}-*E*_{3,3}), Pd-containing reactions delivered the target material. Compared to entries of table 7 (*E*_{1,1}-*E*_{1,3}), a significant increase in yield was detected for combinations **C** (*E*_{1,1}) and **BC** (*E*_{1,2}). Further addition of

² An extraction with previously weighed amounts of internal standard, educt and product revealed quantitative recovery of phenylcaffeine. Losses in caffeine were observed but will not be indicated in the discussion.

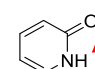
additive **A** remarkably diminished the amount of phenylcaffeine ($E_{1,3}$). Regarding our results obtained so far, we conclude that pivalic acid and NBu_4HSO_4 exhibit a positive influence on the desired conversion. As soon as 2-pyridone takes part, reaction progression is impeded. We suggest that the latter exerts strong coordination to **Pd**, displacing CMD additive **C** and hindering the reaction from taking place. Out of curiosity, we also conducted the arylation involving CuTc (copper (I) thiophene-2-carboxylate) as metal source. Due to the sole recovery of starting material, we decided not to display these reactions in the matrix.

As third option, we wanted to investigate whether any influence induced by multi-metallic interactions could be detected (table 9). For each row, a HiLo setting (10:1) of precatalysts was envisaged. Under argon, greater amounts of metal precursors were previously mixed in the appropriate ratio. Homogeneous solutions or suspensions were added to the vials. Additives **A**, **B**, and **C** were arranged in the same order as in table 7.

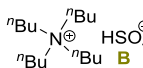
Table 9. Two-dimensional (2D) 3x3 screening matrix of the arylation of caffeine according to You et al.^[34], HiLo setting (10:1).



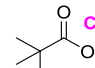
	A (10.0)		B (10.0)		C (10.0)	
Pd $\text{Cl}_2(\text{MeCN})_2$ (5.0)	Pd NiCo	8	Pd NiCo	8	Pd NiCo	16
	A		AB		ABC	
Ni $\text{Cl}_2(\text{dme})$ (5.0)	Ni PdCo	<1	Ni PdCo	<1	Ni PdCo	<1
	A		AB		ABC	
Co Br_2 (5.0)	Co PdNi	<1	Co PdNi	<1	Co PdNi	<1
	A		AB		ABC	



A



B



C

^aReaction performed with 500 μmol caffeine in DMF (Σ 1.5 mL) according to GP 2.2 (see 7.2.2.1); catalyst mixtures were added in HiLo as solution in DMF (0.5 mL); additive **A** (0.1 M, 0.5 mL) and PhBr (1.5 M, 0.5 mL) were added as solutions (DMF); spectral yield according to $^1\text{H-NMR}$ with internal standard, given in mol%.

Reactions with either **Ni** or **Co** in the Hi loading (5.0 mol%) performed poorly ($E_{2,1}$ - $E_{3,3}$), showing minimal conversion. While combinations **A** ($E_{1,1}$) and **AB** ($E_{1,2}$) slightly diminished the yield compared to the mono-metallic version, additional pivalic acid ($E_{1,3}$) afforded similar results than before. The presence of different metal atoms seems to hinder coordination of reactive catalyst-components. However, excessive CMD-additive ($E_{1,3}$) overcomes this barrier.

2.4 Conclusion and outlook

First stages of the multifunctional component catalyst principle (MFCCP) were presented. Definitions were clarified starting from a general point of view. Several catalyst-components, which display physically separable substances, merge to generate a catalyst-system. Depending on the number, one- or multi-component systems can be differentiated. Functions refer to ask one catalyst-component fulfils, e.g. base, metal precatalyst, ligand, or other. Multifunctionality is reached when one catalyst-component exerts several tasks. To underline its potential, literature examples were analyzed according to our outlined principle, and classified as *tetrafunctional three-component*, *trifunctional single-component*, or *trifunctional two-component* catalyst systems.

Opposed to conventional DoE^[29b], OVAT, or HTE^[26] screening, we have depicted a new screening procedure. Reminding of a matrix encountered in mathematics, the screening tables consist of metal precatalysts (rows) by additives (columns). Entries are designated as $E_{x,y}$, where x refers to rows, and y to columns, respectively. At intersections, all encountered catalyst-components (additives), when reading from left to right, will be mixed with metal precursors from the corresponding row. For each individual catalytic reaction, the influences substances exhibit on one another should be easily detectable. A second implementation allows the incorporation of every metal listed in the matrix. While high loading (Hi) is operated to the main metal of a row, others will be involved in predefined, low amounts (Lo), e.g. HiLo setting of 10:1. Unexpected, intermetallic interactions are expected to crystallize.

We chose the C–H-arylation of caffeine with bromobenzene according You et al.^[34] as model reaction. Metal precatalysts ($\text{PdCl}_2(\text{MeCN})_2$, $\text{NiCl}_2(\text{dme})$, CoBr_2) as well as monofunctional additives (2-pyridone, NBu_4HSO_4 , PivOH) were involved. Solely reactions involving Hi setting (5.0 mol%) of Pd afforded detectable amounts of phenylcaffeine. The order of additives in columns was decisive for the extent of conversion. While reactions including 2-pyridone performed poorly, omitting the latter significantly sped up the progression of the reaction. Competitive coordination of PivOH and 2-pyridone to Pd seems deliver a reasonable explanation. At HiLo loading, no intermetallic interactions were observed. We conclude that a sole additive variation is unfavourable in multi-component screening. One has to consider combinations which do not include certain catalyst-components in the design of experiments.

With these results in hand, further studies are necessary and will have to aim at new model reactions. Literature precedents for new transformations should be studied to identify suitable reaction systems. Matrix screening should be extended to further combinations in either way, e.g. permutations of catalyst-components, inclusion of more diverse components or changes of the HiLo ratios. Additives which exhibit a mutually positive influence have to be identified by screening different catalytic reactions. These catalyst-components should be summarized to create a pool of potentially active reagents. By combining most promising ones, the degree of potential functionality exerted upon a catalytic reaction will drastically be increased. Their incorporation in catalysis screening will hopefully speed up the discovery process of new reactions. Even though no breakthrough has yet been achieved, the presented definitions and principle will shape the direction of future investigations. While matrix screening will be of least priority for the remainder of the thesis, our main focus will concentrate on the design, synthesis and efficient release of and from multifunctional precursors.

2.5 References

- [1] a) A. Mittasch, W. Frankenburg, Early studies of multicomponent catalysts in *Advances in catalysis*, Vol. 2, Elsevier, **1950**, pp. 81-104; b) F. Dautzenberg, J. Platteeuw, *J. Catal.* **1970**, *19*, 41-48; c) H. Bloch (Honeywell UOP LLC, Universal Oil Products Co.), US3761531A, **1973**; d) F. Dautzenberg, J. Helle, P. Biloen, W. Sachtler, *J. Catal.* **1980**, *63*, 119-128; e) A. Dömling, I. Ugi, *Angew. Chem. Int. Ed.* **2000**, *39*, 3168-3210; f) J. Zhu, H. Bienaymé, *Multicomponent reactions*, John Wiley & Sons, **2006**; g) J. Toyir, R. Miloua, N. Elkadri, M. Nawdali, H. Toufik, F. Miloua, M. Saito, *Phys. Procedia* **2009**, *2*, 1075-1079; h) K. Chao, Y. Chen, H. Liu, X. Zhang, J. Li, *Energy Fuels* **2012**, *26*, 1152-1159; i) B. Ma, X. Li, D. Li, K. Lin, *Appl. Catal. B* **2019**, *256*, 117865; j) Z. Wei, Y. Liu, Z. Peng, H. Song, Z. Liu, B. Liu, B. Li, B. Yang, S. Lu, *ACS Sustain. Chem. Eng.* **2019**, *7*, 7014-7023.
- [2] a) F.-L. Zhang, K. Hong, T.-J. Li, H. Park, J.-Q. Yu, *Science* **2016**, *351*, 252-256; b) W. Gong, G. Zhang, T. Liu, R. Giri, J.-Q. Yu, *J. Am. Chem. Soc.* **2014**, *136*, 16940-16946; c) H. Park, N. Chekshin, P.-X. Shen, J.-Q. Yu, *ACS Catal.* **2018**, *8*, 9292-9297; d) P. Dolui, J. Das, H. B. Chandrashekar, S. Anjana, D. Maiti, *Angew. Chem. Int. Ed.* **2019**, *58*, 13773-13777; e) H. Lin, X. Pan, A. L. Barsamian, T. M. Kamenecka, T. D. Bannister, *ACS Catal.* **2019**, *9*, 4887-4891.
- [3] M. Anand, R. B. Sunoj, H. F. Schaefer III, *J. Am. Chem. Soc.* **2014**, *136*, 5535-5538.
- [4] C. Martín, A. Pizzolante, E. C. Escudero-Adán, A. W. Kleij, *Eur. J. Inorg. Chem.* **2018**, *18*, 1921-1927.
- [5] a) Q. Shen, J. F. Hartwig, *Org. Lett.* **2008**, *10*, 4109-4112; b) D. Zim, S. L. Buchwald, *Org. Lett.* **2003**, *5*, 2413-2415; c) J. Meléndez, M. North, P. Villuendas, *Chem. Commun.* **2009**, *18*, 2577-2579; d) Y. Yermakov, V. Zakharov, One-component catalysts for polymerization of olefins in *Advances in Catalysis*, Vol. 24, Elsevier, **1975**, pp. 173-219; e) H. Büttner, K. Lau, A. Spannenberg, T. Werner, *ChemCatChem* **2015**, *7*, 459-467.
- [6] K. Soai, T. Shibata, H. Morioka, K. Choji, *Nature* **1995**, *378*, 767-768.
- [7] a) P. N. Taylor, M. J. O'Connell, L. A. McNeill, M. J. Hall, R. T. Aplin, H. L. Anderson, *Angew. Chem. Int. Ed.* **2000**, *39*, 3456-3460; b) Y. Uozumi, Y. Nakai, *Org. Lett.* **2002**, *4*, 2997-3000; c) K. W. Anderson, S. L. Buchwald, *Angew. Chem. Int. Ed.* **2005**, *44*, 6173-6177; d) Y. Uozumi, Y. Matsuura, T. Arakawa, Y. M. Yamada, *Angew. Chem.*

- Int. Ed.* **2009**, *48*, 2708-2710; e) S. M. Rummelt, M. Ranocchiari, J. A. van Bokhoven, *Org. Lett.* **2012**, *14*, 2188-2190; f) C. E. Brocklehurst, F. Gallou, J. C. D. Hartwig, M. Palmieri, D. Ruffle, *Org. Process Res. Dev.* **2018**, *22*, 1453-1457; g) T. Kitanosono, S. Kobayashi, *Chem. Eur. J.* **2020**, *26*, 9408-9429.
- [8] a) D. A. Fulmer, W. C. Shearouse, S. T. Medonza, J. Mack, *Green Chem.* **2009**, *11*, 1821-1825; b) C. M. R. Volla, P. Vogel, *Org. Lett.* **2009**, *11*, 1701-1704; c) R. Thorwirth, A. Stolle, B. Ondruschka, *Green Chem.* **2010**, *12*, 985-991; d) W. Su, J. Yu, Z. Li, Z. Jiang, *J. Org. Chem.* **2011**, *76*, 9144-9150; e) B. J. Tardiff, M. Stradiotto, *Eur. J. Org. Chem.* **2012**, *21*, 3972-3977; f) A. Chartoire, A. Boreux, A. R. Martin, S. P. Nolan, *RSC Adv.* **2013**, *3*, 3840-3843.
- [9] J. Clayden, N. Greeves, S. Warren, *Organic Chemistry*, OUP Oxford, Oxford, **2012**.
- [10] a) W. H. Laarhoven, T. J. Cuppen, *J. Chem. Soc., Perkin Trans. 2* **1978**, 315-318; b) S.-i. Sakurai, K. Okoshi, J. Kumaki, E. Yashima, *J. Am. Chem. Soc.* **2006**, *128*, 5650-5651; c) M. H. Prechtel, J. D. Scholten, B. A. Neto, J. Dupont, *Curr. Org. Chem.* **2009**, *13*, 1259-1277; d) Y. Nagata, T. Kuroda, K. Takagi, M. Suginome, *Chem. Sci.* **2014**, *5*, 4953-4956; e) Y. Fang, E. Ghijsens, O. Ivasenko, H. Cao, A. Noguchi, K. S. Mali, K. Tahara, Y. Tobe, S. De Feyter, *Nat. Chem.* **2016**, *8*, 711-717; f) K. Takaishi, K. Iwachido, T. Ema, *J. Am. Chem. Soc.* **2020**, *142*, 1774-1779.
- [11] a) F. Fairbrother, *J. Chem. Soc. Faraday Trans.* **1941**, *37*, 763b-769; b) A. S. Gothelf, T. Hansen, K. A. Jørgensen, *J. Chem. Soc., Perkin Trans. 1* **2001**, 854-860; c) J. Koller, R. G. Bergman, *Chem. Commun.* **2010**, *46*, 4577-4579; d) M. Nakamura, K. Endo, E. Nakamura, *J. Am. Chem. Soc.* **2003**, *125*, 13002-13003; e) A. Kawata, K. Takata, Y. Kuninobu, K. Takai, *Angew. Chem. Int. Ed.* **2007**, *46*, 7793-7795; f) Y. Bonvin, E. Callens, I. Larrosa, D. A. Henderson, J. Oldham, A. J. Burton, A. G. Barrett, *Org. Lett.* **2005**, *7*, 4549-4552; g) M. Rueping, B. J. Nachtsheim, W. Ieawsuwan, *Adv. Synth. Catal.* **2006**, *348*, 1033-1037.
- [12] a) K. Narasaka, Y. Hayashi, H. Shimadzu, S. Niihata, *J. Am. Chem. Soc.* **1992**, *114*, 8869-8885; b) J. P. Wolfe, S. L. Buchwald, *J. Am. Chem. Soc.* **1997**, *119*, 6054-6058; c) K. Sonogashira, *J. Organomet. Chem.* **2002**, *653*, 46-49; d) J. Montgomery, *Angew. Chem. Int. Ed.* **2004**, *43*, 3890-3908; e) M. F. Kühnel, D. Lentz, *Angew. Chem. Int. Ed.* **2010**, *49*, 2933-2936; f) C.-L. Sun, B.-J. Li, Z.-J. Shi, *Chem. Commun.* **2010**, *46*, 677-685; g) A. G. Sergeev, J. F. Hartwig, *Science* **2011**, *332*, 439-443; h) D. S. Surry, S. L.

- Buchwald, *Chem. Sci.* **2011**, *2*, 27-50; i) S. L. Helmbrecht, J. Schlüter, M. Blazejak, L. Hintermann, *Eur. J. Org. Chem.* **2020**, 2062-2076.
- [13] a) D. S. Surry, S. L. Buchwald, *Angew. Chem. Int. Ed.* **2008**, *47*, 6338-6361; b) M. M. Heravi, Z. Kheilkordi, V. Zadsirjan, M. Heydari, M. Malmir, *J. Organomet. Chem.* **2018**, *861*, 17-104; c) R. Dorel, C. P. Grugel, A. M. Haydl, *Angew. Chem. Int. Ed.* **2019**, *58*, 17118-17129; d) B. C. Hamann, J. F. Hartwig, *J. Am. Chem. Soc.* **1998**, *120*, 7369-7370; e) Q. Shelby, N. Kataoka, G. Mann, J. Hartwig, *J. Am. Chem. Soc.* **2000**, *122*, 10718-10719.
- [14] a) W. A. Herrmann, M. Alison, J. Fischer, C. Köcher, G. R. Artus, *Angew. Chem. Int. Ed.* **1995**, *34*, 2371-2374; b) K. Öfele, W. A. Herrmann, D. Mihalios, M. Alison, E. Herdtweck, T. Priermeier, P. Kiprof, *J. Organomet. Chem.* **1995**, *498*, 1-14; c) W. A. Herrmann, C. Koecher, *Angew. Chem. Int. Ed.* **1997**, *36*, 2162-2187.
- [15] a) S. Derien, E. Dunach, J. Perichon, *J. Am. Chem. Soc.* **1991**, *113*, 8447-8454; b) T. Yamamoto, S. Wakabayashi, K. Osakada, *J. Organomet. Chem.* **1992**, *428*, 223-237; c) A. Correa, R. Martin, *1, 10-Phenanthroline in Encyclopedia of Reagents for Organic Synthesis*, John Wiley & Sons, Ltd., Tarragona, **2001**; d) T. Zell, R. Langer, M. A. Iron, L. Konstantinovski, L. J. Shimon, Y. Diskin-Posner, G. Leitus, E. Balaraman, Y. Ben-David, D. Milstein, *Inorg. Chem.* **2013**, *52*, 9636-9649; e) Y. Shen, Y. Gu, R. Martin, *J. Am. Chem. Soc.* **2018**, *140*, 12200-12209; f) S. Z. Sun, R. Martin, *Angew. Chem. Int. Ed.* **2018**, *57*, 3622-3625.
- [16] a) J. M. Dennis, N. A. White, R. Y. Liu, S. L. Buchwald, *ACS Catal.* **2019**, *9*, 3822-3830; b) S. M. Mennen, J. D. Gipson, Y. R. Kim, S. J. Miller, *J. Am. Chem. Soc.* **2005**, *127*, 1654-1655; c) Y. Su, X. Sun, G. Wu, N. Jiao, *Angew. Chem. Int. Ed.* **2013**, *52*, 9808-9812; d) J. C. Tellis, D. N. Primer, G. A. Molander, *Science* **2014**, *345*, 433-436.
- [17] a) P. Laszlo, *Acc. Chem. Res.* **1986**, *19*, 121-127; b) G. C. Fortman, S. P. Nolan, *Chem. Soc. Rev.* **2011**, *40*, 5151-5169; c) N. P. Reddy, M. Tanaka, *Tetrahedron Lett.* **1997**, *38*, 4807-4810.
- [18] S. Seifert, D. Schmidt, K. Shoyama, F. Würthner, *Angew. Chem. Int. Ed.* **2017**, *56*, 7595-7600.
- [19] a) S. Bouquillon, A. du Moulinet d'Hardemare, M.-T. Averbuch-Pouchot, F. Héning, J. Muzart, *Polyhedron* **1999**, *18*, 3511-3516; b) Y.-C. Xu, J. Zhang, H.-M. Sun, Q. Shen, Y. Zhang, *Dalton Trans.* **2013**, *42*, 8437-8445; c) M. C. Kuhn, A. A. Lapis, G. Machado,

- T. Roisnel, J.-F. Carpentier, B. A. Neto, O. L. Casagrande Jr, *Inorg. Chim. Acta* **2011**, 370, 505-512; d) M. B. Meredith, C. H. McMillen, J. T. Goodman, T. P. Hanusa, *Polyhedron* **2009**, 28, 2355-2358; e) T. Peppel, M. Köckerling, *Z. Anorg. Allg. Chem.* **2010**, 636, 2439-2446; f) C. Zhong, T. Sasaki, A. Jimbo-Kobayashi, E. Fujiwara, A. Kobayashi, M. Tada, Y. Iwasawa, *Bull. Chem. Soc. Jpn.* **2007**, 80, 2365-2374.
- [20] a) C. Valente, M. E. Belowich, N. Hadei, M. G. Organ, *Eur. J. Org. Chem.* **2010**, 23, 4343-4354; b) A. Chartoire, X. Frogneux, A. Boreux, A. M. Slawin, S. P. Nolan, *Organometallics* **2012**, 31, 6947-6951; c) M. Pompeo, R. D. Froese, N. Hadei, M. G. Organ, *Angew. Chem. Int. Ed.* **2012**, 51, 11354-11357.
- [21] a) K. Hirabayashi, A. Mori, J. Kawashima, M. Suguro, Y. Nishihara, T. Hiyama, *J. Org. Chem.* **2000**, 65, 5342-5349; b) A. R. McWilliams, D. P. Gates, M. Edwards, L. M. Liable-Sands, I. Guzei, A. L. Rheingold, I. Manners, *J. Am. Chem. Soc.* **2000**, 122, 8848-8855; c) S. R. Patrick, I. I. Boogaerts, S. Gaillard, A. M. Slawin, S. P. Nolan, *Beilstein J. Org. Chem.* **2011**, 7, 892-896; d) M. Aufiero, F. Proutiere, F. Schoenebeck, *Angew. Chem. Int. Ed.* **2012**, 51, 7226-7230; e) J. Wippich, I. Schnapperelle, T. Bach, *Chem. Commun.* **2015**, 51, 3166-3168.
- [22] M. R. Biscoe, B. P. Fors, S. L. Buchwald, *J. Am. Chem. Soc.* **2008**, 130, 6686-6687.
- [23] a) T. Kinzel, Y. Zhang, S. L. Buchwald, *J. Am. Chem. Soc.* **2010**, 132, 14073-14075; b) N. C. Bruno, M. T. Tudge, S. L. Buchwald, *Chem. Sci.* **2013**, 4, 916-920; c) S. D. Friis, T. Skrydstrup, S. L. Buchwald, *Org. Lett.* **2014**, 16, 4296-4299.
- [24] M. Su, N. Hoshiya, S. L. Buchwald, *Org. Lett.* **2014**, 16, 832-835.
- [25] Z. Li, L. Liu, H.-m. Sun, Q. Shen, Y. Zhang, *Dalton Trans.* **2016**, 45, 17739-17747.
- [26] E. S. Isbrandt, R. J. Sullivan, S. G. Newman, *Angew. Chem. Int. Ed.* **2019**, 58, 7180-7191.
- [27] a) E. C. Hansen, D. J. Pedro, A. C. Wotal, N. J. Gower, J. D. Nelson, S. Caron, D. J. Weix, *Nat. Chem.* **2016**, 8, 1126; b) M. Shevlin, M. R. Friedfeld, H. Sheng, N. A. Pierson, J. M. Hoyt, L.-C. Campeau, P. J. Chirik, *J. Am. Chem. Soc.* **2016**, 138, 3562-3569; c) J. K. Vandavasi, X. Hua, H. B. Halima, S. G. Newman, *Angew. Chem. Int. Ed.* **2017**, 56, 15441-15445; d) A. B. Santanilla, E. L. Regalado, T. Pereira, M. Shevlin, K. Bateman, L.-C. Campeau, J. Schneeweis, S. Berritt, Z.-C. Shi, P. Nantermet, *Science* **2015**, 347, 49-53; e) C. S. Shultz, S. W. Krska, *Acc. Chem. Res.* **2007**, 40, 1320-1326.
- [28] H. Song, D. L. Chen, R. F. Ismagilov, *Angew. Chem. Int. Ed.* **2006**, 45, 7336-7356.

- [29] a) P. M. Murray, S. N. Tyler, J. D. Moseley, *Org. Process Res. Dev.* **2013**, *17*, 40-46;
b) P. Subra, P. Jestin, *Ind. Eng. Chem. Res.* **2000**, *39*, 4178-4184; c) V. K. Aggarwal,
A. C. Staubitz, M. Owen, *Org. Process Res. Dev.* **2006**, *10*, 64-69.
- [30] C. Houben, A. A. Lapkin, *Curr. Opin. Chem. Eng.* **2015**, *9*, 1-7.
- [31] B. J. Reizman, Y.-M. Wang, S. L. Buchwald, K. F. Jensen, *React. Chem. Eng.* **2016**, *1*,
658-666.
- [32] a) G. Chen, Z. Zhuang, G. C. Li, T. G. Saint-Denis, Y. Hsiao, C. L. Joe, J. Q. Yu, *Angew.
Chem. Int. Ed.* **2017**, *56*, 1506-1509; b) W. Feng, T. Wang, D. Liu, X. Wang, Y. Dang,
ACS Catal. **2019**, *9*, 6672-6680.
- [33] H. Anton, R. Chris, *Elementary Linear Algebra 9 th Edition*, Wiley India Pvt. Limited,
2008.
- [34] D. Zhao, W. Wang, S. Lian, F. Yang, J. Lan, J. You, *Chem. Eur. J.* **2009**, *15*, 1337-
1340.
- [35] P. Klein, *The Multi-Component-Catalyst (MCC) Principle: Designing Functional
Catalyst Precursors for Reaction Development*, master thesis, Technical University of
Munich (Garching bei München), **2016**.
- [36] L. Rast, *Additive-effects in Pd-catalyzed C-H transformations*, master thesis, Technical
University of Munich (Garching bei München), **2019**.
- [37] J. Rekowski, *Kinetic effects of CMD-Additives on the C-H arylation of caffeine*, master
thesis, Technical University of Munich (Garching bei München), **2015**.

3 MULTIFUNCTIONAL CATALYST COMPONENT PRECURSORS: THE NHC-PD-PIVALATE SYSTEM

This chapter is subdivided into five parts. A short state of the art overview of established catalyst systems introduces the subject in the first section (3.1). The synthesis of well-defined difunctional salts combining either imidazolium ligand, metal center or CMD-additive (cyclometallation-deprotonation) into one substance is presented (3.2). Unfunctional units, e.g. chloride ligands, in NHC–Pd catalyst precursors are substituted by components exerting a certain role (3.3). Incorporation of our multifunctional component catalyst precursors in state of the art cross-coupling reactions (3.4) demonstrates their utility in catalysis. The conclusion and future outlook (3.5) end chapter 3. To give the full overview of the topic, parts of the preceding master thesis are additionally depicted.^[1]

3.1 Introduction

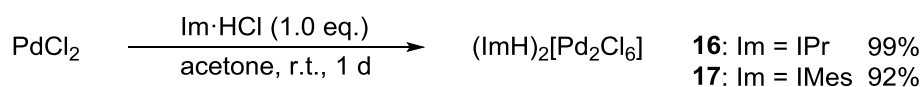
While worldwide waste generation is an omnipresent problem of today's society^[2], chemists seek for atom-economic as well as eco-friendly synthetic methods.^[3] Catalysis offers a great tool to reduce the formation of by-products by selective conversion of starting materials. The efficiency of a catalyst system strictly relies on the interplay of all components. A multitude of factors have to be considered. The generation of catalytically active species from suitable precursors is decisive for a reaction to take place; a problem several research groups have addressed over the years. Unique properties of *N*-heterocyclic carbenes (NHC) in catalysis were demonstrated by the groups of Herrmann^[4], Beller^[5], and Nolan^[6]. Since then, a multitude of publications covering a broad field, e.g. cross-coupling^[7], olefin metathesis^[8], asymmetric (organo-)catalysis^[9], or metallopharmaceuticals^[10], emerged day by day.^[11] The introduction of PEPPSI (pyridine- enhanced precatalyst preparation, stabilization and initiation) precatalysts by Organ et al.^[12] has allowed the synthesis of air-stable, easy to handle metal complexes active in cross-coupling reactions^[13], chiral versions also being reported^[14]. One type of precatalyst has been developed by Buchwald and coworkers.^[15] Four generations of their palladacycles have been established so far.^[16] While ligated aminobiphenyl was methylated, the coordinated chloride ion was replaced with a more weakly binding mesylate counterion. These changes facilitated the activation of the Pd center while expanding the scope of compatible ancillary ligand and decreasing the amount of harmful activation by-products (carbazole). Difunctional nickelates combining imidazolium ligand precursor cations and anionic metallate in fixed ratios have been reported by Sun et al.^[17] (IPrH)₂[NiCl₄] showed superior reactivity in the cross-coupling of Grignard reagents with aryl halides compared to biscarbene Ni(II) or related phosphine complexes. The group of Muzart described ammonium chloropalladates merging

metal center and phase-transfer catalyst (PTC).^[18] The latter aims to increase the catalyst's solubility as well as its activity. Benzene arylation was efficiently demonstrated by Fagnou and coworkers who incorporated pivalic acid as CMD-additive into the catalyst system.^[19] Further examples taking advantage of the carboxylate additive as proton shuttle are widely reported.^[20] Even though these systems are highly active in catalysis, they all contain elements without a specific role. The substitution of co-ligands, counter-ions and other inactive units by components exerting a distinct task would significantly increase the functionality of established catalyst precursors. The resulting multifunctional component catalyst (MFCC) precursors alone or in combination with other multifunctional additives open new ways of catalysis screening. The preparation time of a reaction, e.g. weighing of all reactants or additives, can be remarkably diminished while accelerating the discovery process of new reactions. In the following, structurally well-defined, multifunctional catalyst precursor salts for homogeneous transition metal catalysis are illustrated.

3.2 Difunctionality in a well-defined precursor salt

3.2.1 Merging of metal and ligand precursor

The general aim of this subproject can be described as merging as many functionalities as possible into a stoichiometrically well-defined catalyst precursor salt. The combination of a metal precursor, e.g. Pd(OAc)₂ or Ni(acac)₂, with an imidazolium salt under specific conditions creates an active catalyst system for a range of C-C coupling reactions.^[21] But rather than mixing those separate components, we now want to merge them into a single compound. First MFCC precursors, namely hexachlorodipalladates **16** and **17**, difunctional component catalyst precursors (CCP's) combining imidazolium precursor and Pd cation, were isolated in near quantitative yields as red, air-stable salts (scheme 8).



Scheme 8. Synthesis of hexachlorodipalladates **16** and **17** from PdCl₂.

The sum formula corresponding to a dinuclear species was confirmed by elemental analysis (C, H, N). In the ¹H-NMR spectrum in [D₆]-acetone, the C-2 proton of the imidazolium core is shifted upfield relative to the chloride salt by 2 ppm, whereas all other signals move by insignificant amounts (0.1-0.5 ppm). The structure of palladate **16** was confirmed by X-ray analysis of suitable single crystals (figure 8). Crystal data, as well as collected data for structure

refinement are summarized in the appendix (8.3, table 54f.). The two Pd atoms, which are separated by 3.39(6)-3.41(7) Å, are coordinated in a square planar fashion by four chloride ions forming Cl-Pd-Cl angles close to 90°, where the bridging chloride ions span the smallest angle. Pd-Cl bond distances to bridging atoms are significantly longer (2.32(3)-2.34(2) Å) than terminal ones (2.25(9)-2.28(2) Å). The central core of the imidazolium cations features similar bond lengths and angles to the previously reported structure of IPr·HCl by Arduengo et al.^[22] The constitution of [Pd₂Cl₆]²⁻ is typical and can e.g. be compared to the tetrabutylammonium hexachlorodipalladate synthesized by the group of Muzart.^[18] A dinuclear benzyl-DABCO Pd salt as catalyst precursor for a range of cross-coupling reactions (Suzuki, Sonogashira, Stille) has also been reported by the group of Rafiee.^[23]

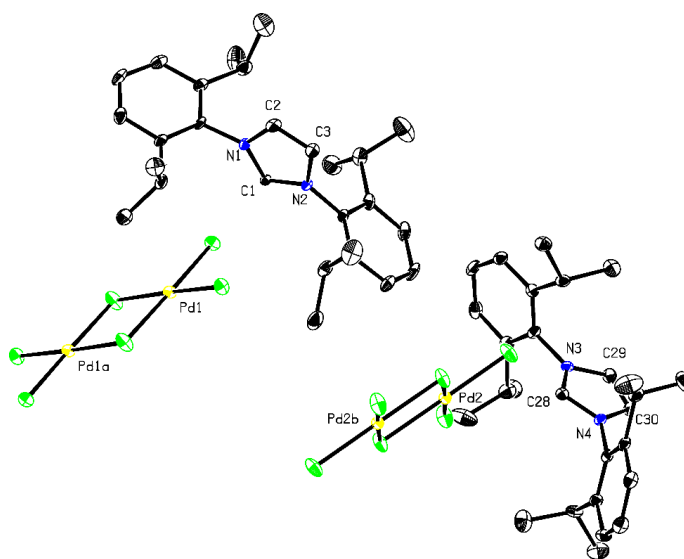
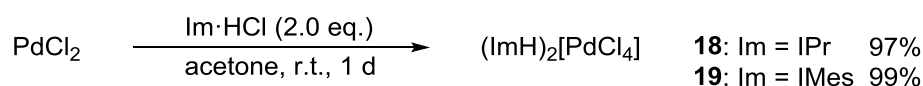


Figure 8. X-Ray crystal structure of (IPrH)₂[Pd₂Cl₆] (**16**). Ellipsoids are shown at 50% probability level. Hydrogen atoms are omitted. Carbon atoms are depicted in grey, nitrogen atoms in blue, chlorine atoms in green and palladium atoms in yellow.

Muzart et al. isolated (NBu₄)₂[Pd₂Cl₆] via recrystallisation of the mononuclear (NBu₄)₂[PdCl₄] species.^[18] ¹H-NMR analysis of the mother liquor indeed revealed the presence of NBu₄Cl. In our case, mononuclear composite salts were isolated by stirring of PdCl₂ with two equivalents of Im·HCl in acetone (scheme 9). Elemental analysis (C, H, N) confirmed the stoichiometry.



Scheme 9. Synthesis of tetrachloropalladates **18** and **19** from PdCl₂.

In the ¹H-NMR spectrum of the bright red solids in [D₆]-acetone, the C-2 proton is considerably shifted downfield compared to the hexachlorodipalladates. This phenomenon is also observed

in the case of the NBu_4 -based chloropalladates. The higher charge density of the dianion leads to a stronger hydrogen-bonding interaction between the anion and H-C(2), which induces the downfield shift. The remaining $^1\text{H-NMR}$ signals are slightly shifted upfield. A comparison of $^1\text{H-NMR}$ shifts of palladate salts with other imidazolium salts is further discussed in a later section (figure 12). Similar to observations by Muzart et al.^[18], recrystallization of IMes tetrachloropalladate **19** delivered crystals of the hexachlorodipalladate **17**, as shown by X-ray crystal structure (figure 9). IMes·HCl must have been eliminated in the process. Crystal data, as well as collected data for structure refinement are summarized in the appendix (8.3, table 56f.). Almost identical values for Pd-Pd or Pd-Cl bond lengths and Cl-Pd-Cl angles compared to **16** were determined. Tetrahedral complexes are less common with palladium(II)^[24], which usually prefer the square-planar coordination.^[25] High charge density at the palladium center of **16** induces the observed elimination which will be favored in apolar solvent, hence reducing the overall density. The relatively small atoms nickel as well as cobalt prefer a tetrahedral coordination.^[25-26] Nickel(II) may also take on square-planar or an intermediate between both geometries.^[25,27] Related nickelates^[17,28] and cobaltates with different cations have been reported.^[29] We stirred $\text{NiCl}_2 \cdot 6\text{H}_2\text{O}$ with $\text{IPr} \cdot \text{HCl}$ (1.0 or 2.0 eq.) in acetone and supposedly³ yielded tetra- and hexachloronickelates quantitatively. In $[\text{D}_6]$ -acetone, the C-2 proton of $[\text{NiCl}_4]^{2-}$ was shifted downfield (0.3 ppm) compared to $[\text{Ni}_2\text{Cl}_6]^{2-}$. Due to deliquescence as well as non-confirmed structure of the salts, application in catalysis was not performed.

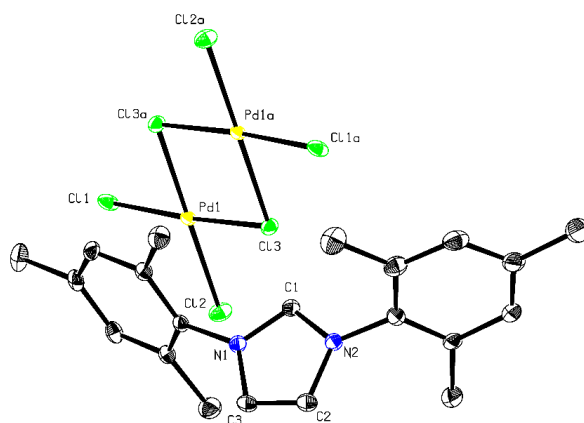
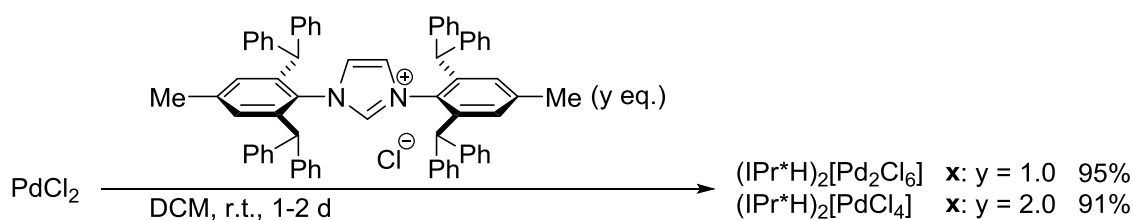


Figure 9. X-ray crystal structure of $(\text{IMesH})_2[\text{Pd}_2\text{Cl}_6]$ (**17**). Ellipsoids are shown at 50% probability level. Hydrogen atoms are omitted. Carbon atoms are depicted in grey, nitrogen atoms in blue, chlorine atoms in green and palladium atoms in yellow.

³ The structures were neither confirmed by elemental nor X-ray analysis.

NHC based catalyst activity is strongly dependent on the specific NHC ligand structure.^[30] Strong σ -donor property of the latter allow the oxidative addition of sterically hindered aryl halides, especially *o,o'*-substituted ones.^[31] Steric hindrance in close proximity to the metal center entails enhanced reductive elimination while stabilizing the catalyst resting state.^[32] Recent examples report the application of highly hindered, yet flexible NHC ligands, namely IPr* (1,3-bis(2,6-benzhydryl-4-methylphenyl)-imidazol-2-ylidene)^[6a,6b,33] and IPr*^{OMe} (*para*-methoxy analogue)^[6c,34]. Similar to its sterically less crowded IPr eponym, hexa- and tetrachloropalladates of IPr*, **20** and **21** respectively, were prepared (scheme 10). Interestingly, the salts show better solubility behavior compared to (IPrH)₂[Pd₂Cl₆] and (IPrH)₂[PdCl₄]. Reaction of PdCl₂ with one equivalent of imidazolium salt in acetone afforded a light pink suspension, which instantly dissolved upon addition of dichloromethane.⁴ Performing the synthesis directly in dichloromethane afforded (IPr*H)₂[Pd₂Cl₆] in excellent yield. Stirring of PdCl₂ with two equivalents of IPr*·HCl in dichloromethane resulted in a light pink suspension. Isolation of the solid confirmed the formation of tetrachloropalladate **21**.



Scheme 10. Synthesis of chloropalladates **20** and **21** from PdCl₂ and IPr*·HCl.

Elemental analysis (C, H, N) of both solids verified the formulae in accord with the proposed structures. Even though the tetrachloropalladate salt **21** is nearly insoluble in dichloromethane, complete dissolution is achieved in chloroform, allowing the comparison of ¹H-NMR shifts. The chemical shift of H-2 proton in the IPr*H-based Pd salts show opposite characteristics to IPrH-based ones: signals of (IPr*H)₂[Pd₂Cl₆] (**20**) are shifted significantly downfield compared to **21**, whereas those of (IPrH)₂[Pd₂Cl₆] (**16**) can be observed upfield in comparison to (IPrH)₂[PdCl₄] (**18**). Steric bulk as well as high electron excess of the IPr*H cation probably induces this observation. In solution, ions of [PdCl₄]²⁻ might also dissociate to [Pd₂Cl₆]²⁻ and Cl⁻. Crystallization of the salts delivered the X-ray structure of (IPr*H)₂[Pd₂Cl₆] in both cases (figure 10). Crystal data, as well as collected data for structure refinement are summarized in the appendix (8.3 table 86f.). Pd-Pd (3.37(1) Å) or Pd-Cl bond lengths (terminal: 2.26(9)-

⁴ Note: IPr*·HCl is completely soluble in dichloromethane, less soluble in acetone.

2.28(3) Å; bridging: 2.32(4)-2.32(5) Å) and Cl-Pd-Cl angles are identical to those described for other hexachlorodipalladates (IPrH and IMesH) in this thesis. Hydrogen bond distances (terminal chloride ions to C2-proton) are remarkably shorter (2.61(2)- 2.62(5) Å) than those observed in (IPrH)₂[Pd₂Cl₆] (2.67(0)-2.87(4) Å), pointing to a stronger interaction of both ions. In the crystal structure of **20**, terminal chloride ions of [Pd₂Cl₆]²⁻ interact via hydrogen bonding with the H-2 proton of IPr^{*}H cations as well as Van der Waals forces with phenyl groups of the benzhydryl moiety (figure 10, left). In the unit cell, [Pd₂Cl₆]²⁻ anions of **20** fill up all four corners as well as the center of the cell, displaying a body centered packaging (figure 10, right).

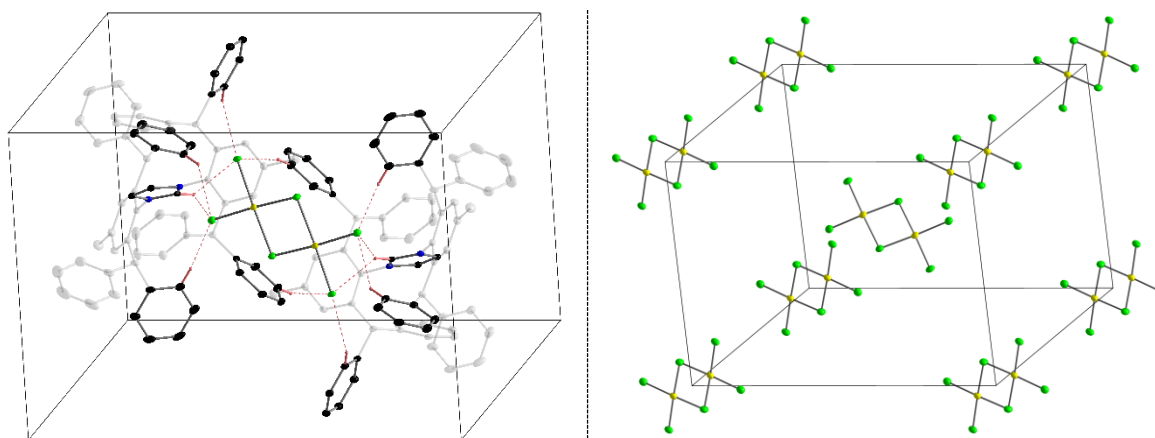
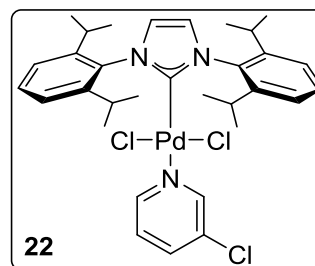
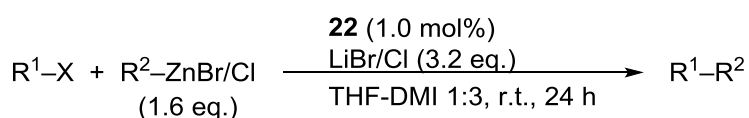


Figure 10. X-ray crystal structure of (IPr^{*}H)₂[Pd₂Cl₆] (**20**); coordination of [Pd₂Cl₆]²⁻ anion by IPr^{*}H cations (left), packaging of anions in the unit cell (right). Ellipsoids are shown at 50% probability level. Except for atoms involved in hydrogen bonding or Van der Waals interactions, hydrogen atoms are omitted. Hydrogen bonding as well as Van der Waals interactions are depicted in light rose. Carbon atoms are depicted in black, (important) hydrogen atoms in light rose, nitrogen atoms in blue, chlorine atoms in green and palladium atoms in yellow.

IPr-PEPPSI: an air- and moisture stable Pd-NHC precatalyst originally introduced by Organ and coworkers^[12] shows enhanced reactivity in a wide range of cross-coupling reactions (scheme 11).^[13c,32,35]



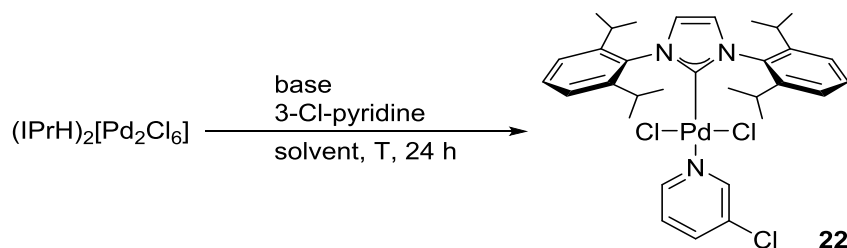
Scheme 11. IPr-PEPPSI catalyzed Negishi cross-coupling reported by Organ et al.^[12a] R¹ = phenyl, *n*-heptyl, *p*-tolyl; X = Cl, Br, I, OTs, OMs, OTf; R² = *n*-butyl, *n*-heptyl, phenyl, *p*-MeOC₆H₄; DMI = 1,3-dimethyl-2-imidazolidinone.

Modifications of the imidazole backbone deliver efficient catalysts, e.g. for selective cross-coupling of secondary organozinc reagents which else tend to undergo unwanted β -hydride elimination.^[36] Organ's original synthesis involves boiling of imidazolium salt and PdCl₂ together with a solid base, mostly K₂CO₃, in co-ligand 3-chloropyridine as solvent (42.1 eq.).^[12a] Even though excess heterocyclic co-ligand was recovered by distillation, handling of this highly toxic reagent should be avoided as far as possible.

We herein present a new synthesis approach for IPr-PEPPSI starting from our hexachlorodipalladate **16**, which does not require excess amounts of the pyridine, but profits of cheap and non-toxic co-solvent (table 10). Each reaction mixture was filtered over a short pad of silica eluting with dichloromethane. Stirring of (IPrH)₂[Pd₂Cl₆] with reduced amounts of 3-chloropyridine (10.5 eq.) afforded the desired complex at 40 °C or ambient temperature in high yields (entries 1-3). The choice of either K₂CO₃ or K₃PO₄ did not affect the outcome of the reaction, even when reducing the amount of base (entries 4 and 5). Equimolar amounts of K₃PO₄ significantly diminished the formation of IPr-PEPPSI (entry 6). Exclusion of inorganic base completely stopped the reaction (entry 7); the pyridine's basicity alone is evidently not strong enough for inducing deprotonation. Lowering of pyridine excess (entry 8) created a requirement for introducing a regular solvent to assure complete mixing of all components. The reaction in dichloromethane first appeared to be irreproducible at ambient temperature (entries 9 and 10). But since initial experiments had been conducted in a non-air-conditioned laboratory during summer, a reaction temperature of over 35 °C had been reached inside the hood while vigorously stirring. Later, it became clear that a little heating was highly beneficial for the reaction progress. Ensuing experiments (entries 11-22) were conducted in the conditioned laboratory either at room temperature (24 °C) or with heating to 40 °C. The use of DBU as organic base was not viable, since it led to formation of a DBU-PdCl₂ species (entry 11), similar to the one reported by Castellón and coworkers.^[37] Whereas the solvent dichloromethane delivered good results at low concentrations (entries 12 and 13), the dipolar solvent DMSO produced impure material (entry 14). Higher reactant concentrations (250 mM) together with slightly larger excesses of 3-chloropyridine (7.5 eq.) and base (3.0 eq.) afforded excellent results (entry 15) at 40 °C, and satisfactory ones at ambient temperature (entry 16). Acetone yielded comparable amounts of product (entries 17 and 18), even with less pyridine (5.0 eq.) involved (entry 19). The experiments so far had all relied on isolated hexachlorodipalladate **16** as starting material. Next, a two-step one-pot synthesis was attempted. By merging the

conditions of two screening experiments (entries 17 and 19), optimal conditions affording IPr-PEPPSI (**22**) in excellent yield were reached (entry 20).

Table 10. Selected screening conditions for the synthesis of IPr-PEPPSI (**22**) from $(\text{IPrH})_2[\text{Pd}_2\text{Cl}_6]$ (**16**).^a K_2CO_3 and K_3PO_4 were dried for at least two hours under reduced pressure (0.8-1.2 mbar) at 300 °C and stored in Schlenk flasks prior use (see 7.1.1).

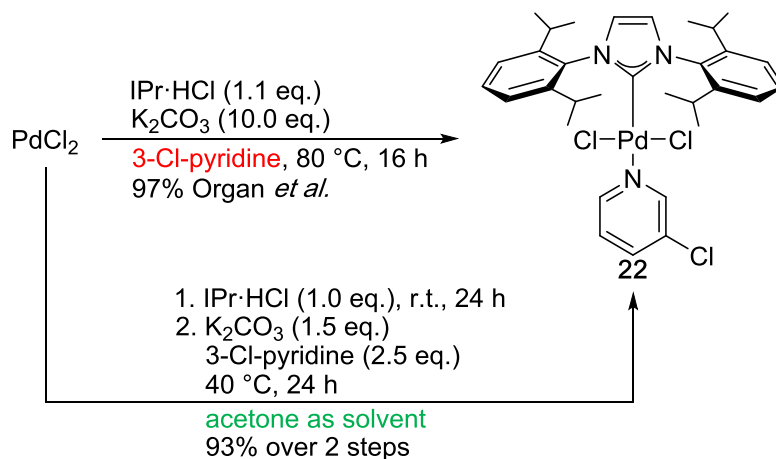


entry	base [eq.]	3-Cl-py [eq.]	T [°C]	solvent [mM]	yield [%] ^b
1	K_2CO_3 (10.0)	10.5	40	- (10.0)	91
2	K_2CO_3 (10.0)	10.5	r.t.	- (10.0)	91
3	K_3PO_4 (10.0)	10.5	r.t.	- (10.0)	90
4	K_3PO_4 (3.0)	10.5	r.t.	- (10.0)	91
5	K_3PO_4 (2.0)	10.5	r.t.	- (10.0)	88
6	K_3PO_4 (1.0)	10.5	r.t.	- (10.0)	54
7	-	10.5	r.t.	- (10.0)	<1
8	K_3PO_4 (3.0)	4.2	r.t.	- (25.0)	83
9	K_3PO_4 (2.0)	2.5	r.t.	DCM (25.0)	25
10	K_3PO_4 (2.0)	5.0	r.t.	DCM (25.0)	83
11	DBU (2.0) ^c	5.0	r.t.	DCM (50.0)	- ^d
12	K_3PO_4 (2.0)	5.0	40	DCM (50.0)	76
13	K_3PO_4 (2.0)	5.0	40	DCM (100)	76/67 ^e
14	K_3PO_4 (2.0)	5.0	40	DMSO (100)	85 ^f
15	K_2CO_3 (3.0)	7.5	40	DCM (250)	90
16	K_2CO_3 (3.0)	7.5	r.t.	DCM (250)	70
17	K_2CO_3 (3.0)	7.5	40	acetone (250)	93
18	K_2CO_3 (3.0)	7.5	r.t.	acetone (125)	57
19	K_2CO_3 (3.0)	5.0	40	acetone (125)	86
20 ^g	K_2CO_3 (1.5)	2.5	40	acetone (250)	90 ^h /93 ⁱ

^aReaction conditions: $(\text{IPrH})_2[\text{Pd}_2\text{Cl}_6]$ (50.0 μmol), base, solvent and 3-chloropyridine were stirred for 24 hours at the indicated time and temperature according to GP 3.1 (see 7.2.3.1).

^bIsolated yield after flash column chromatography (DCM) of the reaction mixture. ^cAddition of DBU (2.0 eq.) at the outset of the reaction. Additional DBU (250 μL) was added after stirring overnight at r.t. ^dNo IPr-PEPPSI isolated. ^e¹H-NMR analysis revealed the presence of a DBU-Pd species. ^f~80% purity. Isolated material contained IPr-HCl (~9%), and unidentified 3-Cl-pyridine Pd species (~9-10%). ^g2-step synthesis starting from PdCl_2 : PdCl_2 and IPr-HCl in acetone were stirred for 24 hours at room temperature. Base and 3-chloropyridine were added and the reaction mixture was stirred for another 24 hours at 40 °C, before purification by flash column chromatography. ^h200 μmol scale. ⁱ1.00 mmol scale.

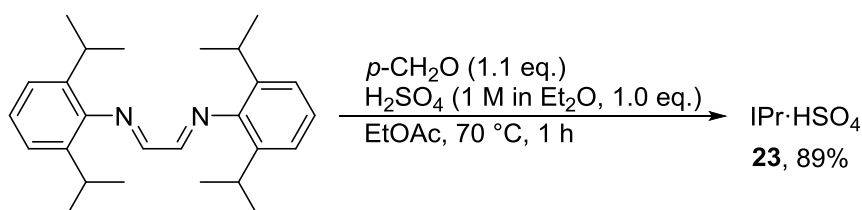
Compared to the usual synthesis reported by the group of Organ^[12], a less toxic and wasteful procedure not involving 3-Cl-pyridine as the solvent was established (Scheme 12). A large excess of base was avoided. Both the isolated (IPrH)₂[Pd₂Cl₆] or an in situ complex from PdCl₂ and IPr·HCl depicted excellent starting material for the synthesis of IPr-PEPPSI (**22**).



Scheme 12. Synthesis of IPr-PEPPSI (**22**) according to Organ *et al.*^[12] and by our new one-pot two-step approach.

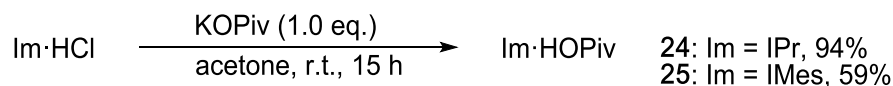
3.2.2 Merging of ligand precursor and CMD additive

Extensive research dealt with the synthesis of NHC precursor imidazolium salts from simple α -diimines.^[38] The majority of the prepared salts incorporate unfunctional anions, e.g. chloride, BF₄⁻, PF₆⁻ or others, whose identity is usually defined by the employed (Lewis) acids. In our project, substitution of non-functional with functional anions would be of utmost interest. During my master thesis, a direct synthesis approach of a difunctional imidazolium involving both a NHC precursor and a CMD additive, (pivalate) was attempted. The use of sulfuric acid as H⁺ source led to the formation of IPr·HSO₄. Further screening of the initial procedure constituted a central element of another master thesis.^[39] Addition of an ethereal solution of sulfuric acid to a suspension of IPr-DAD and *p*-formaldehyde in EtOAc yielded the salt **23** in 89% yield. In the case of IMes, the reaction medium had to be changed to dioxane for further obtained the highest yield, which amounted to 93% of IMes·HSO₄.



Scheme 13. Synthesis of IPr·HSO₄ (**23**) from IPr-DAD and *p*-CH₂O.

The same synthesis protocol could not be transferred to the synthesis of the target bifunctional salt IPr·HOPiv. Alternatively, we envisaged a salt metathesis, starting with IPr·HCl. Stirring of the latter with equimolar amounts of KOiv in acetone afforded IPr·HOPiv (**24**) in 94% yield (scheme 14). KCl is rather insoluble in the involved solvent and could easily be removed by filtration. The pivalate salt (**25**) of the sterically less hindered IMesH cation was obtained in analogy to IPr·HOPiv in 59% yield.



Scheme 14. Synthesis of imidazolium pivalates **24** and **25** by salt metathesis.

The ¹H-NMR spectrum of **24** in [D₆]-acetone displayed a signal at δ_H 11.78 for H-2 of the imidazolium unit that disappeared over time. A similar event had been reported by Magnier et al. for the salt IPr·HF.^[40] They interpreted the disappearance of the C2-proton as being caused by the presence of a hydrogen bond between H-2 of the imidazolium cation and the fluoride anion. In our opinion, H/D-exchange with deuterated solvent is a much more reasonable explanation for the loss of this signal. A saturated solution of IPr·HOPiv (**24**) in [D₆]-acetone was analyzed on a Bruker AVHD-500cr spectrometer with a cryogenic probe for sensitive ¹³C-NMR experiments. In the ¹H-NMR spectrum, a small signal (area = 0.18) for H-2 was detected. The ¹³C-NMR spectrum displayed a triplet (δ 142.7) for the C–D signal at C-2, confirming our hypothesis. Dilution of the sample solution with conventional acetone ([D₆]-acetone–[H₆]-acetone 3:1) led to the reappearance of H-2 (δ 11.47, area = 0.67). A solution of **24** in [D₆]-dimethylsulfoxide gave rise to a spectrum that showed all the expected signals. No H/D exchange with the deuterated solvent was observed. NMR analysis in CDCl₃ revealed a diminished signal for H-2 (δ 9.39, area = 0.70). The residual water signal of the deuterated solvent was shifted remarkably downfield (δ 4.63) as the result of hydrogen-bonding to the pivalate anion. Whereas a solution of IMes·HOPiv (**25**) in [D₆]-acetone showed minor impurities in the ¹H-NMR spectrum, the [D₆]-dimethylsulfoxide solution afforded a pure spectrum. Possibly, the lower steric shielding allows an easier deprotonation of H-2 by pivalate, leading to the decomposition of the free carbene in air.^[44] Since the basicity of pivalate increases in dimethylsulfoxide, the pure spectrum in the latter solvent speaks against the assumption of a free carbene in solution. It is likely that IMes·HOPiv could have reacted with acetone as electrophile.

To gain further insight in the spectral properties of the salts with regard to H-2, a range of imidazolium salts with more or less coordinating counterions was synthesized. The latter were all synthesized via salt metathesis from IPr·HCl in either acetone or water, affording the desired products in near quantitative yields (figure 11).

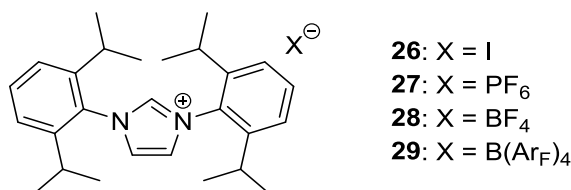
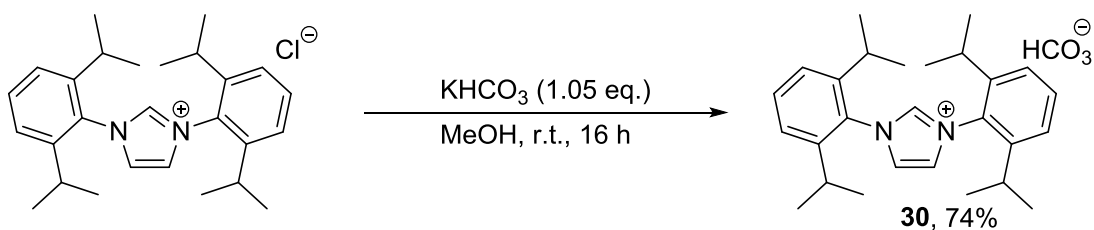


Figure 11. Synthesized imidazolium salts with different anions. Ar_F = 3,5-bis(trifluoromethyl)phenyl.

Solely, the attempted isolation of a perchlorate salt failed due to a minor solubility of potassium perchlorate in acetone, which disabled a complete ion exchange. The latter salt might be obtained according to a procedure by Yi et al.^[41] from IPr·HCl and AgClO₄ with precipitation of AgCl. However, on the account of the explosive nature of perchlorates^[42] in general, the synthesis of this particular imidazolium salt was not conducted.

An attempt to prepare a bicarbonate salt from IPr·HSO₄ and KHCO₃ failed due to similar solubility properties. The groups of Taton and Vignolle have presented the synthesis of several imidazolium bicarbonate salts.^[43] Depending on the solvent used, such salts are in equilibrium with their corresponding imidazolium carboxylate zwitterions. Following the original procedure for IMes- and ⁱPr- based salts by stirring IPr·HCl with KHCO₃ in dry methanol, the desired bicarbonate was obtained in 74% yield (scheme 15).



Scheme 15. Synthesis of imidazolium bicarbonate **30** from IPr·HCl following a procedure by Taton and Vignolle et al.^[43].

In [D₆]-acetone, the salt shows broad signals in the ¹H-NMR spectrum that can be assigned to at least two species.⁵ This behaviour led us to exclude IPr·HCO₃ (**30**) from the comparison of H-2 proton shifts (figure 12). However, only one species is observed in a solution of **30** in [D₄]-methanol; both -N-CH=N⁺- and HCO₃⁻ protons are not detected in the ¹H-NMR spectrum. The

⁵ Partial decomposition may not be excluded.

former one (-N-CH=N⁺-) exchanges rapidly with the deuterated solvent on the NMR time scale. Due to fast equilibrium of HCO₃⁻/CO₂⁻,^[44] a single signal appears for the counterion in the ¹³C-NMR spectrum (δ_C 161.4) and none in the ¹H-NMR spectrum. Imidazolium protons displayed as either broad singlet (δ_C 140.5, -N-CH=N⁺-) or triplet (δ_C 127.1 (t, ²J_{C,D} = 15.3 Hz), NCDCH) as a result of H/D exchange.

For better comparison, equimolar amounts of salt were dissolved in [D₆]-acetone (see 7.2.3.1, general procedure 3.2, for detailed procedure). Due to low solubility, a saturated solution of tetrachloropalladate **18** was submitted to NMR analysis. The shift of H-2 allows to conclude on the coordinating properties of the salts. A cut-out of the relevant chemical shift is shown on the next page (figure 12).

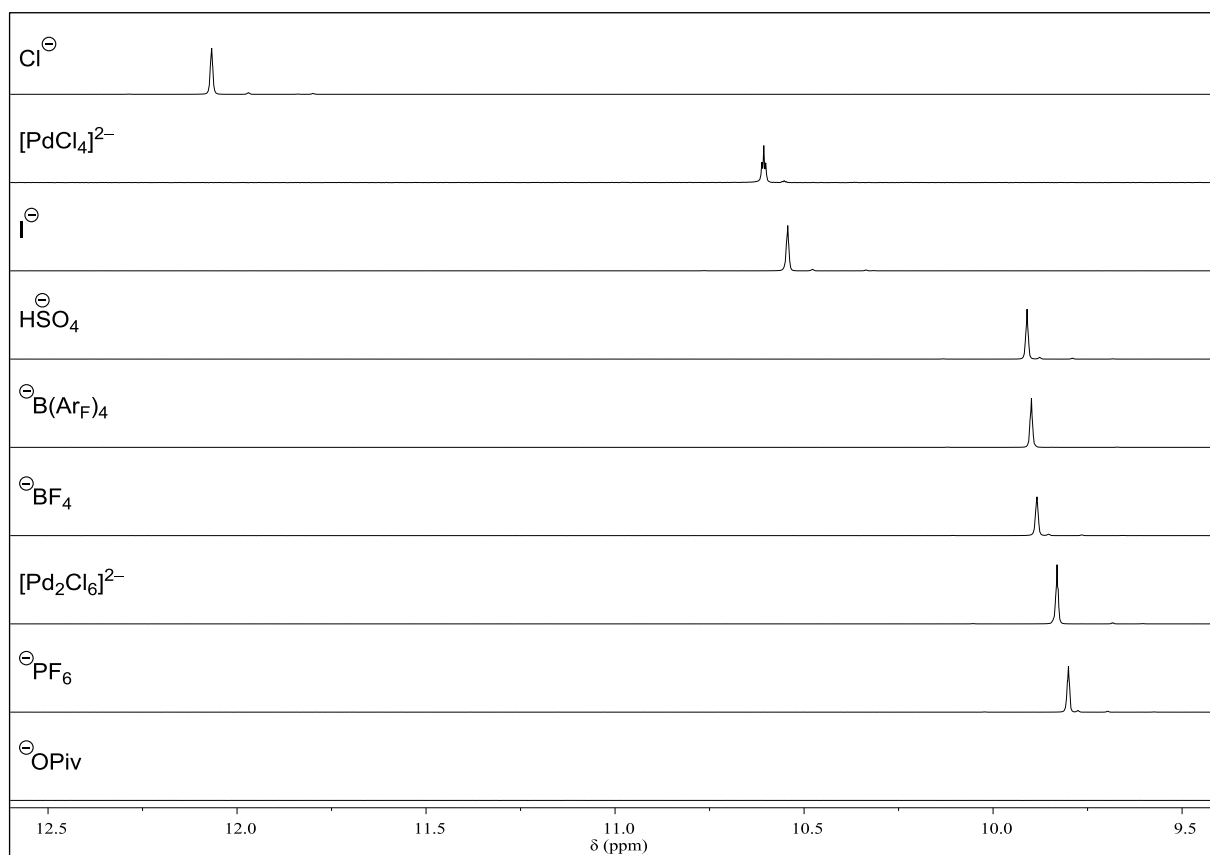


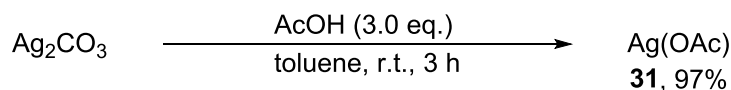
Figure 12. Cut-out of the stacked ¹H-NMR spectra of the H-2 region of different imidazolium salts in [D₆]-acetone, according to GP 3.2 (see 7.2.3.1). Ar_F = 3,5-bis(trifluoromethyl)phenyl.

Among the anions, halides (chloride, iodide) are known for strong hydrogen bonding to polarized C–H donors with bond distances increasing on going from fluoride to iodide.^[45] High charge density at the anion accords the tetrachloropalladate the behaviour of a hydrogen bonding anion, just as chloride or iodide. Judging from our findings concerning the ease of

crystallization, slow dissociation of $[\text{PdCl}_4]^{2-}$ to $[\text{Pd}_2\text{Cl}_6]^{2-}$ and chloride salt (IPr·HCl) is imaginable. Non-nucleophilic ions (PF_6^- , BF_4^- , $\text{B}(\text{Ar}_F)_4^-$) as well as almost dissociated (HSO_4^-) ones manifest a significant upfield shift owing to low interaction with the cation. The hexachlorodipalladate salt **16**, $(\text{IPrH})_2[\text{Pd}_2\text{Cl}_6]$, shows no coordinative properties, similar to PF_6^- . In the case of pivalate, H/D exchanges with the deuterated solvent and completely omits the H-2 in $[\text{D}_6]$ -acetone. Over time (one week) the solution darkened, indicating slow decomposition of the salt. In the carbon NMR, a triplet with very low intensity associated to the C2-carbon in the form of D–C is perceived.

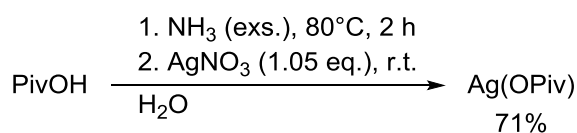
3.2.3 Merging of metal precursor and CMD additive

Among difunctional CCP's, our focus lay on the synthesis of $\text{Pd}(\text{OPiv})_2$ starting from PdCl_2 , which combines metal precursor and CMD additive in one defined compound. For this purpose, we were interested in synthesizing silver carboxylates as synthetic carboxylate metathesis reagents. Besides halide abstraction, combination of $\text{Ag}(\text{OAc})$ with $\text{Pd}(\text{OAc})_2$ exhibits enhanced reactivity allowing $\text{C}(\text{sp}^2)\text{--C}(\text{sp}^3)$ ^[46], $\text{C}_{\text{Ar}}\text{--N}$ or $\text{C}_{\text{Ar}}\text{--O}$ coupling reactions.^[47] $\text{Ag}(\text{OAc})$ is either added as solid or formed in situ^[48] from a silver salt and acetic acid. These transformations often profit from a directing group, e.g. amide, carboxylate or others, facilitating regioselective functionalization.^[46b,48c,49] Authors refer to heterodimeric Pd(II)–Ag(I) species stabilized by chelating ligands and intermetallic Pd–Ag interaction being involved, lowering the activation transition state.^[50] Conventional synthesis methods of silver acetate start from silver nitrate^[51] or silver oxide^[52] in water or the acid itself. We sought for a non-aqueous method involving minor excess of acid. Bright yellow silver carbonate is insoluble in cold toluene, still assuring mixing of all components.^[42] Addition of acetic acid (3.0 eq.) slowly whitens the present solid, indicating the formation of $\text{Ag}(\text{OAc})$ (**31**). Small bubbles occurring from CO_2 via protonation of the carbonate anion were perceived. Simple filtration followed by washing with diethylether affords silver acetate in 97% yield (scheme 16).



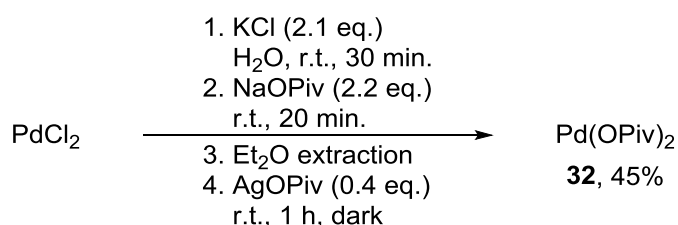
Scheme 16. Synthesis of silver acetate (**31**) from Ag_2CO_3 and acetic acid in toluene.

An even more relevant target for our work was silver pivalate, whose carboxylate unit exerts a powerful CMD effect. The latter was prepared during my master thesis^[1] according to a procedure by Molloy et al.^[53] starting from pivalic acid and silver nitrate in aqueous ammonia (scheme 17). Silver pivalate was isolated in 71% yield and stored under exclusion of light.



Scheme 17. Synthesis of AgOPiv according to a procedure by Molloy and coworkers.^[53]

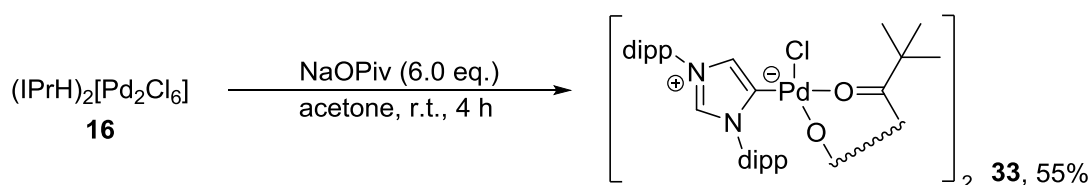
Compared to the acetate, palladium pivalate represents a metal precursor that also includes a strong CMD additive. Following a literature procedure^[54], a large excess (>10 eq.) of pivalic acid was added to a solution of Pd(OAc)₂ in toluene to displace the acetate anion. Azeotropic distillation removes acetic acid and further shifts the reaction equilibrium to the desired product, removing any trace of acetate present. The surplus of pivalic acid can be removed via distillation under reduced pressure at elevated temperature. Due to this rather sumptuous approach, we envisaged a milder procedure at room temperature involving extraction of the product from an aqueous phase. Dissolution of PdCl₂ in water was achieved by the addition of KCl, generating K₂[PdCl₄] in solution.^[55] A prior ion-exchange with sodium pivalate led to the precipitation of a brownish solid. Given the solubility of Pd(OPiv)₂ in diethylether, the latter was chosen as extracting solvent. Elemental analysis (C, H, N) of isolated material revealed a reduced carbon content (0.9%). While KCl is insoluble in ethylether, the ethereal solution might still contain small impurities of residual chloride ions. In that case, silver precipitation was foreseen for assuring full removal. The amount of silver pivalate employed was not optimized, since the exact chloride impurity was not quantified. Even though highest precautions were undertaken to prevent dragging of any water in the extraction step, minor amounts of water present in the ether phase cannot be excluded. Drying agents like Na₂SO₄, MgSO₄ or K₂CO₃ would risk introducing contamination with the listed anions. Therefore, purification including drying of the extract was achieved by simple filtration over a small plug of silica gel. Elemental analysis (C, H, N) of the isolated orange crystals revealed the successful synthesis of Pd(OPiv)₂ (**32**) in excellent purity, albeit in moderate yield (scheme 18).



Scheme 18. Synthesis of Pd(OPiv)₂ (**32**) from PdCl₂ via ion-exchange with NaOPiv and AgOPiv.

3.3 A trifunctional NHC-Pd-pivalate precursor – cheered too soon?

The degree of functionality of our CCP's $(\text{IPrH})_2[\text{Pd}_2\text{Cl}_6]$ or $(\text{IPrH})_2[\text{PdCl}_4]$ is still expandable. Within our current project, our method of choice to introduce additional functionality into CCP's was to replace function-free halide ligands by CMD-active carboxylates. During my master thesis,^[1] the reaction of $(\text{IPrH})_2[\text{Pd}_2\text{Cl}_6]$ (**16**) with sodium pivalate led to a new precatalyst complex which includes three functional components, namely a metal cation, a mesoionic NHC ligand, and coordinated pivalate as CMD-additive (scheme 19). The research literature describes the synthesis of a range of mesoionic carbene complexes and their application in catalysis.^[56] The evaluation of complex **33** in C–H arylation catalysis will be presented in sub-chapter 3.4.



Scheme 19. Ion-exchange reaction of $(\text{IPrH})_2[\text{Pd}_2\text{Cl}_6]$ (**16**) with NaOPiv yielding the mesoionic carbene precatalyst **33**, $(^m\text{IPr})_2\text{Pd}_2\text{Cl}_2(\mu\text{-OPiv})_2$.

Suitable single crystals of **33** for X-ray analysis were grown by slow evaporation of a saturated solution of the precursor in dichloromethane (figure 13). Crystal data as well as collected data for structure refinement is summarized in the appendix (8.3, table 59f.). Two pivalate anions bridge both Pd atoms, each being coordinated in a square planar fashion by the latter, a chloride ion, and a mesoionic, anionic heteroaryl. The metal atoms are separated by 3.02(1) Å. Pd–O bond lengths range from 2.04(1)-2.08(9) Å longer than those reported for the palladium pivalate trimer^[54] (1.98(0) Å). Carboxylate-bridged palladium complexes with phosphine^[57] and NHC ligands^[58] feature significantly longer Pd–O bonds (2.17-2.19 Å), probably occurring from stronger *trans*-effects. Non-bridging carboxylate anions following η^1 -coordination are slightly more distanced from the palladium centers (2.22(6) Å).^[59] Chloride anions fill empty spaces of square planar coordination around the Pd centers. The Pd–Cl bond distance is identical for both Pd atoms (2.27(7) Å), similar to terminal chloride ions of $(\text{IPrH})_2[\text{Pd}_2\text{Cl}_6]$. The mesoionic (anionic) NHC ligand is bound via its backbone to the Pd centers (1.94(4) Å), a comparable Pd–C2 bond distance present in reported IPr-PEPPSI^[12a] (1.96(9) Å). Interestingly, Nolan and coworkers synthesized a palladium complex containing normal and unusual/mesoionic carbene at the same time.^[60] In Nolan's complex, both ligands exhibit somewhat longer Pd–C2 bond

lengths than our complex **33**: 2.01(9) Å for normal NHC ligand, 2.02(1) Å for mesoionic one, owing to minor steric crowding.

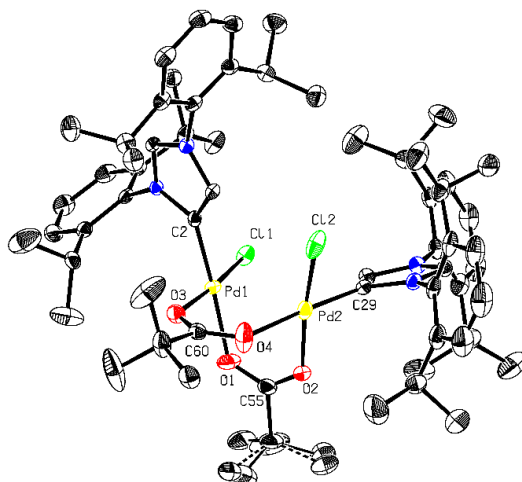
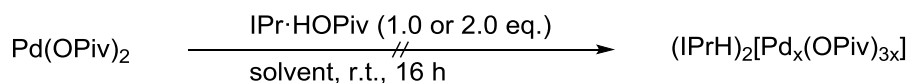


Figure 13. X-ray structure of the mesoionic carbene complex **33**. Two dichloromethane molecules crystallized with the complex but are omitted for sake of clarity. Ellipsoids are shown at 50% probability level. Hydrogen atoms are omitted. Carbon atoms are depicted in grey, nitrogen atoms in blue, chlorine atoms in green, oxygen atoms in red and palladium atoms in yellow. One pivalate group is slightly disordered.

Reducing the sodium pivalate equivalents (2.0, 3.0, or 4.0) in the synthesis of **33** yielded a mesoionic complex of the type (*m*IPr)PdCl₂ or the related dimer, whose crystallization was rather difficult. Further investigation of the synthesis or isolation of the latter compound was not carried out, given that it does not display a higher level of functionality. Conversion of (IPrH₂)[PdCl₄] (**18**) with NaOPiv under identical conditions afforded traces of the mesoionic carbene complex **33**, probably because the reduced solubility of the tetrachloropalladate in acetone prevented an efficient exchange reaction.

In an alternative approach towards obtaining a trifunctional CCP, the synthesis of a stoichiometrically well-defined salt of the type (IPrH)₂[Pd_x(OPiv)_{3x}] (x = 1 or 2) was attempted (scheme 20), similar to the assembly of PdCl₂ and IPr·HCl to (IPrH)₂[Pd₂Cl₆]. Stirring of Pd(OPiv)₂ with IPr·HOPiv in different solvents (acetone, dichloromethane, DMSO) did not yield any desired compound. According to ¹H-NMR analysis, complex **33** was formed in low amounts independent of the solvent involved. This was unexpected, since none of the reaction components (except dichloromethane) contains chlorine. However, traces of chloride might

have been introduced as contamination of either Pd(OPiv)₂ or IPr·HOPiv from prior synthesis,⁶ allowing the generation of **33**.



Scheme 20. Attempted assembly of Pd(OPiv)₂ and IPr·HOPiv; x = 1 or 2 depending of either 1.0 or 2.0 eq. of IPr·HOPiv added. Solvent: acetone, dichloromethane or DMSO.

Further signals at very low intensity were detected in the recorded NMR spectra of the reaction mixtures. Several crude products of the attempted assembly of Pd(OPiv)₂ and IPr·HOPiv (scheme 20) were collected and subjected to crystallizations in a broad set of solvent mixtures. Slow evaporation of acetone from a solution of the latter afforded one tiny crystal. Luckily enough, the crystal was suitable for X-ray analysis revealing its structure: (IPr)PdCl(η²-OPiv) (figure 14). Crystal data, as well as collected data for structure refinement are summarized in the appendix (see 8.3, table 79f.).

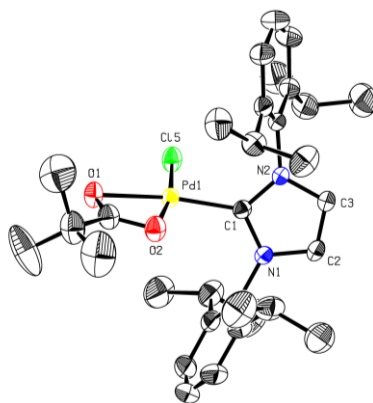


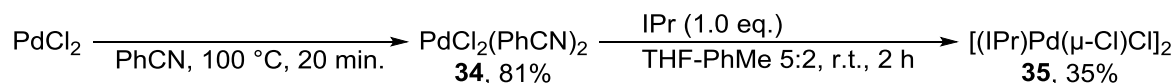
Figure 14. X-ray structure of (IPr)PdCl(η²-OPiv). Ellipsoids are shown at 50% probability level. Hydrogen atoms are omitted. Carbon atoms are depicted in grey, nitrogen atoms in blue, chlorine atom in green, oxygen atoms in red and palladium atoms in yellow.

The complex unifies three elements of functionality, a carbene ligand, Pd metal center and a CMD-additive. Together with a residual non-functional chloride ion the three components arrange in a square-planar fashion around the Pd center. The pivalate coordinates the metal via both oxygen atoms. Whereas the Pd–C1 bond length is slightly shorter (1.93(4) Å) than those reported for IPr-PEPSI^[12a] (1.96(9) Å) or the mesoionic complex (1.94(4) Å), Pd–O distances (2.06(4)-2.15(4) Å) are elongated compared to the latter. Palladium and chlorine atoms are separated by 2.26(9) Å within the range of terminally^[61] bound ones. While most angles vary

⁶ Note: employed Pd(OPiv)₂ was synthesized via a different salt metathesis than the one reported under 3.2.3. Elemental analysis of the incorporated Pd salt showed less satisfactory percentage of carbon and hydrogen.

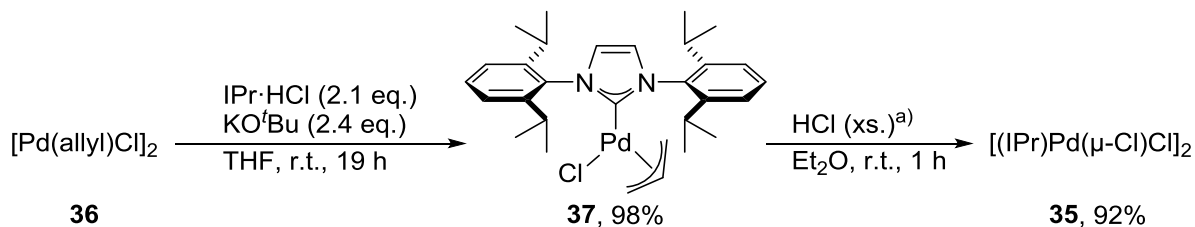
from 87-107°, palladium and oxygen atoms span an acute angle of 62°, owing to structural constitution of the pivalate anion.

Since the synthesis of a salt type trifunctional CCP failed, following experiments were based on ligand exchange reactions bound directly to Pd-carbene complexes. Our focus primarily lay on chloride containing precursors, dimeric [(IPr)Pd(μ-Cl)Cl]₂ or monomeric (IPr)₂PdCl₂. First reported by the group of Nolan^[62], the chlorine bridged Pd complex was prepared following a two-step procedure (scheme 21). Two precursors were necessary for the reported complex: a) free carbene ligand (IPr) accessible via deprotonation of IPr·HCl with KO^tBu^[63], b) PdCl₂(PhCN)₂ (**34**) synthesized by boiling of PdCl₂ in benzonitrile^[64]. The multi-step synthesis and purification of the latter proved rather sumptuous, yielding the dimer **35** in 35% yield. Crystallization was often accompanied with the precipitation of a dark brown solid. Besides, non-neglectable amounts of THF co-crystallized, which could not be removed.



Scheme 21. Two-step synthesis of [(IPr)Pd(μ-Cl)Cl]₂ (**35**) starting from PdCl₂. Following a procedure by Nolan et al.^[63], the free carbene ligand employed in the second step was prepared in 88% yield.

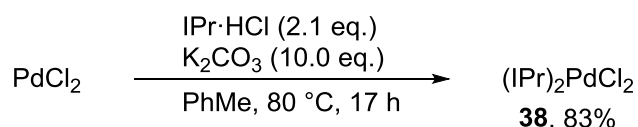
Only one year after Nolan, the group of Sigman published a more convenient method for the preparation of [(IPr)Pd(μ-Cl)Cl]₂.^[65] Even though it involves a three-step procedure, every precursor was easily isolated in near quantitative yield (scheme 22). According to a procedure of Nolan et al.^[66], we first prepared the allyl dimer **36** in 96% yield by adding allyl chloride to an aqueous solution of K₂[PdCl₄]. In situ generation of the IPr carbene allowed the reaction with [Pd(allyl)Cl]₂, affording the Pd(allyl)Cl-carbene complex **37** in 98% yield after flash column chromatography. Stirring of complex **37** with ethereal HCl produces propene via protonolysis, yielding the corresponding dimer **35** in 92%.



Scheme 22. Two-step synthesis of Pd-dimer **35** following a procedure by the group of Sigman.^[65] Allyl dimer **36** was prepared prior according to Nolan et al.^[66] in 96% yield. a) An ethereal solution of HCl (1 M) was used.

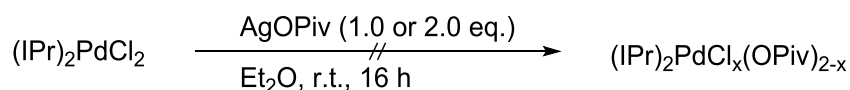
In both cases, the synthesis of the chlorine bridged carbene complex **35** required a detour over several catalyst precursors. We were wondering if a direct synthesis from PdCl₂ would be

possible. Unlike the expected bright orange dimer, the reaction of PdCl₂ with IPr·HCl yielded a yellow solid. Spectroscopic analysis revealed the formation of a well-known Pd complex reported by the group of Fagnou^[67]: (IPr)₂PdCl₂ (**38**). Holding this knowledge, we adapted the equivalents of imidazolium salt to the stoichiometry of the reaction, obtaining 83% of complex **38**. In contrast, (IPrH)₂[Pd₂Cl₆] could not be converted to either (IPr)₂PdCl₂ nor [(IPr)Pd(μ-Cl)Cl] by boiling in the presence of excess K₂CO₃.



Scheme 23. Synthesis of the well-known Pd complex **38**; purification by flash column chromatography simplifies its isolation. Fagnou and coworkers isolated the complex in 51% yield by refluxing a suspension of PdCl₂, IPr·HCl, and Cs₂CO₃ in THF overnight.^[67]

To introduce more functionality into the presented NHC–Pd–Cl complexes, they were subjected to different pivalate sources: PivOH, AgOPiv, and/or NaOPiv. Reaction of the monomeric biscarbene complex (IPr)₂PdCl₂ with AgOPiv only gave recovered starting material (scheme 24). We suggest that the steric crowding around Pd (2 carbene ligands) block pivalate from approaching the metal center. Hence, further studies concerning (IPr)₂PdCl₂ were dropped.



Scheme 24. The halide abstraction with AgOPiv proved unreactive. x = 0 or 1.

However, the dimeric 1:1 complex, [(IPr)Pd(μ-Cl)Cl]₂, reacted even with NaOPiv. Addition of either 2.1 or 4.2 equivalents of the reactant to a solution of the complex in acetone did not affect the outcome of the reaction, yielding an approximately 1:2 mixture of educt and a new species. While the starting material shows rather broad signals in the ¹H-NMR spectrum, sharp peaks of a species with a ligand to pivalate ratio of 1:1 resulted, and the assumption was that (IPr)Pd(OPiv)Cl was formed (figure 15). Extensive crystallization attempts of the mixture only yielded block-shaped crystals of [(IPr)Pd(μ-Cl)Cl], instead.

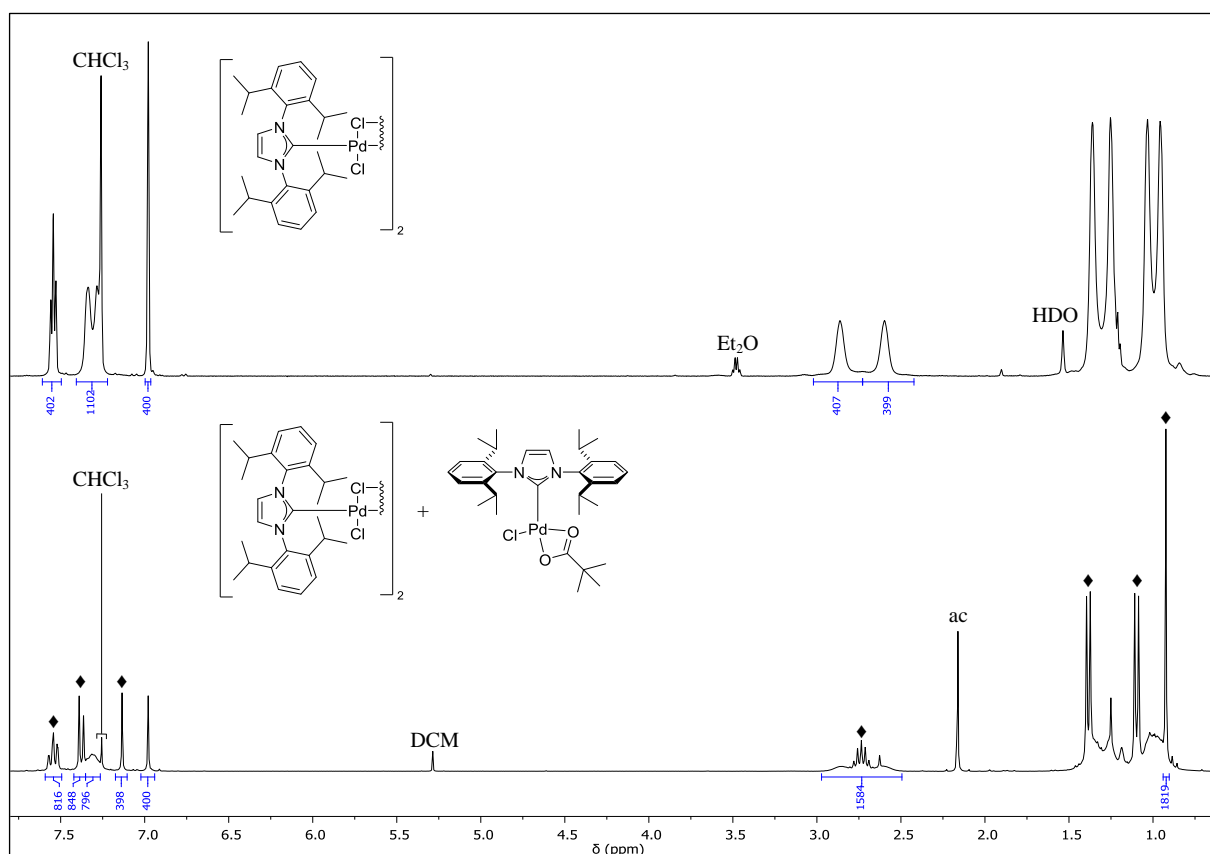
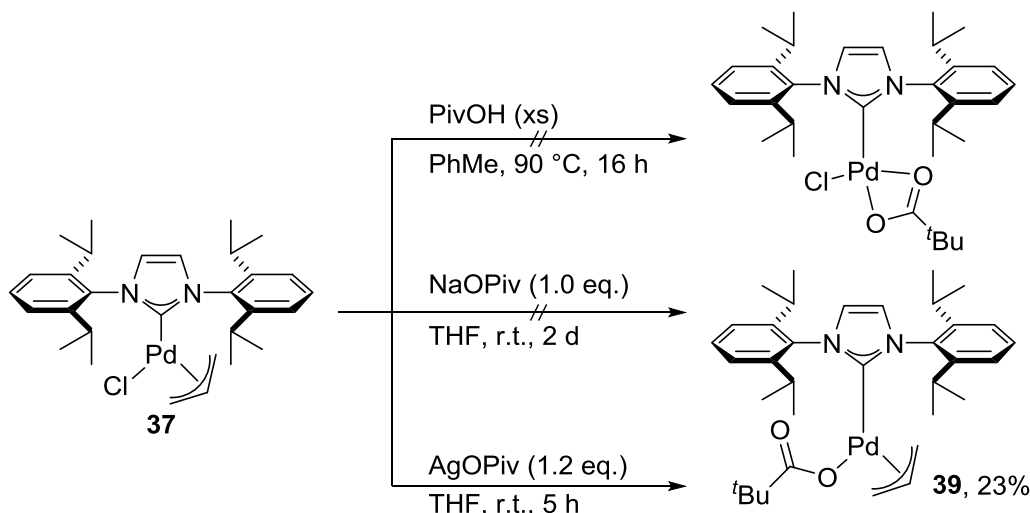


Figure 15. Stacked ¹H-NMR spectra of [(IPr)Pd(μ-Cl)Cl]₂ (top) and after reaction with NaOPiv (4.2 eq., bottom) in CDCl₃. New signals corresponding to (IPr)Pd(OPiv)Cl are marked with ♦. ac = acetone.

The allyl-type carbene complex (IPr)Pd(allyl)Cl features two reactive sites of interest: a) the allyl ligand, which may be removed via protonolysis, as in the synthesis of the dichloro dimer^[65], b) an anionic chloride ligand, which can be activated by halide abstraction. The reaction of (IPr)Pd(allyl)Cl with stoichiometric amounts of pivalic acid in Et₂O or toluene did not proceed, even at elevated temperatures (90 °C) in toluene or with excess of acid (5.0 eq.), much likely due to steric hindrance. Although the complex remained untouched when stirred with NaOPiv, the addition of AgOPiv to a solution of (IPr)Pd(allyl)Cl in THF led to complete consumption of the starting material as indicated by TLC. Spectral analysis of the crude product confirmed the conversion of **37**. Several complex species, whose signals could not be completely separated in the ¹H-NMR, were detected. Crystallization⁷ resulted in the isolation of (IPr)Pd(allyl)(η¹-OPiv) (**39**) along with minor impurities from derived (non-identifiable) complexes in 23% yield. Storing of the mother liquor in the freezer (−25 °C) for several days led to the precipitation of copious amounts of grey or black solid, caused by the decomposition

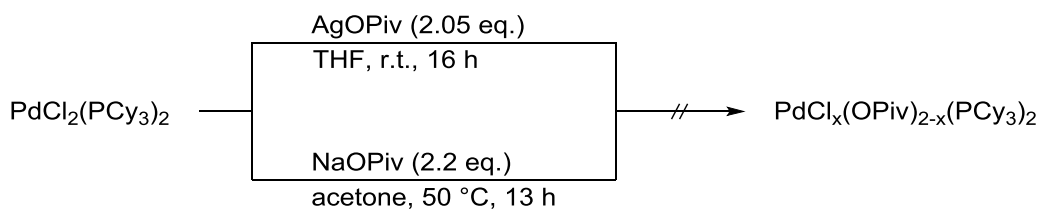
⁷ The isolated material was not suitable for X-ray diffraction. Its appearance consisted more of a powder.

of Pd-complexes or of residual Ag-salts. The negative outcome of these reactions led us to abandon further transformations of complex **37**.



Scheme 25. Complex **37** was subjected to three different conditions, affording two different, identified products in at best moderate yield. The addition of AgOPiv afforded minor amounts of (IPr)Pd(allyl)(η^1 -OPiv) (**39**).

Taking also phosphine-type complexes into consideration, the reactivity of PdCl₂(PCy₃)₂ was exemplarily investigated.⁸ Neither ion-exchange with NaOPiv nor halide abstraction with AgOPiv proved successful. Poor solubility of PdCl₂(PCy₃)₂ might have been the reason for failure. A direct conclusion from ¹H-NMR was not possible due to overlapping of the cyclohexyl signals. Even though the complex was nearly quantitatively converted with the silver salt, ³¹P-NMR analysis revealed a wild mixture of phosphines, including phosphine oxides. Two broad signals (δ 38.6, 44.0) accounting nearly to 60%⁹ of present species especially caught our eyes. We suppose that Pd⁰(PCy₃)_x (x = 1-4) cannot be ruled out as in the case of Pd⁰(PPh₃)₄ generation reported by Kollár and coworkers^[68]. Reduction of Pd^{II} to Pd⁰ might have been induced by partial oxidation of PCy₃. A similar event has been reported by M'Barki et al.^[69] citing the formation of zerovalent palladium from Pd(OAc)₂ and triphenylphosphine.



Scheme 26. The ion-exchange reaction of chloride to pivalate failed along two paths. x = 0 or 1.

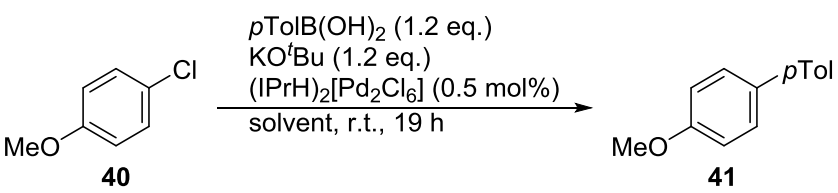
⁸ The Pd precursor was synthesized prior during my master thesis.

⁹ Determined by integration of all signals and setting the total area to 100.

3.4 Multifunctional CCP's in catalysis

To underline the practicability of our CCP's, we sought for promising applications. Suzuki^[70] coupling of aryl (pseudo)-halides with a range of boronic acids turned out to rely on either NHC^[71] or phosphine^[72] bearing Pd catalysts. Related nickel-catalyzed^[73] coupling reactions are also reported but were not in the focus of our interest. We wanted to challenge our IPrH-hexachlorodipalladate precursor **16** by performing the coupling of *p*-chloroanisole (**40**) and *para*-tolyl boronic acid at room temperature and low catalyst loading (0.5 mol%, 1.0 mol% with respect to Pd). Higher reaction temperatures or varied conditions were not envisaged. Depending on the catalyst used in literature, the desired product **41** has been obtained in yields ranging from <5% to >90%.^[71a] While the latter experiments were performed in alcohol, we tested three solvents of different polarity: toluene, dioxane and 2-propanol. Spectral analysis of crude reaction mixtures revealed comparable results (60-68%) in all media (table 11). The low recovery can be explained by partial loss of *p*-chloroanisole at the rotary evaporator. The characteristic smell of this material was recognized in all cases when removing the flask after solvent evaporation.

Table 11. Coupling of *p*-chloroanisole (**40**) with *p*-tolyl boronic acid.^a *p*Tol = *p*-tolyl.



entry	solvent	ArCl [%]	yield [%]	recovery [%]
1	PhMe	25	63	88
2	dioxane	31	60	91
3	2-PrOH	24	68	92

^aReactions performed with 1 mmol of 4-chloroanisole in the indicated solvent (1 mL) according to GP 3.3 (see 7.2.3.1); spectral yield according to ¹H-NMR with internal standard, given in mol%.

Buchwald and coworkers have described the use of monodentate phosphine ligands (DavePhos, JohnPhos, CyJohnPhos,...) in the α -arylation of ketones as being indispensable.^[74] Since, NHC-bearing multifunctional precursor complexes have also proven to be successful in this transformation as reported by the groups of Nolan^[75] and Shi^[76]. Whereas Stradiotto et al.^[77] investigated the α -arylation of acetone with aryl halides and tosylates, employing Mor-DalPhos (phosphine ligand), the group of Ackermann^[78] coupled acetone with imidazolyl sulfonates using a XantPhos/Pd(OAc)₂ catalyst system (diphosphine). To prove the efficiency of our

multifunctional catalyst precursor complexes, we chose the α -arylation of 3-pentanone with *p*-Cl-anisole as model reaction as described by Lu and coworkers (table 12).^[79]

Table 12. α -Arylation of 3-pentanone.^a disubst. = disubstituted; Im = imidazole.

$\text{Me-CH}_2\text{-C(=O)-CH}_2\text{-Me}$ (2.0 eq.) + $p\text{-MeOC}_6\text{H}_4\text{Cl}$ (1.0 eq.)
 precatalyst
 KO^tBu (2.0 eq.)
 PhMe , 80 °C, 3 h

entry	precatalyst [mol%]	additive [mol%]	educt [%]	monosubst. [%]	disubst. [%]	Σ [%]
1	(IPrH) ₂ [Pd ₂ Cl ₆] (0.5)	-	<1	80 (80)	8	89
2	(IPrH) ₂ [PdCl ₄] (1.0)	-	0	81	9	90
3	IPr-PEPPSI (1.0)	-	0	81	8	89
4 ^b	(IPr)PdCl ₂ (Me-Im)	-	-	86	-	-
5 ^c	(IPrH) ₂ [Pd ₂ Cl ₆] (0.5)	-	65	28	1	94
6	(IMesH) ₂ [Pd ₂ Cl ₆] (0.5)	-	88	5	<1	94
7	(IMesH) ₂ [PdCl ₄] (1.0)	-	87	2	<1	90
8	Pd(OAc) ₂ (1.0)	IPr·HSO ₄ (2.0)	67/48	31/55 ^c	0/2 ^c	98/95 ^c
9	Pd(OAc) ₂ (1.0)	IPr·HOPiv (2.0)	54/48	40/48 ^c	<2/2 ^c	96/98 ^c
10 ^e	(IPrH) ₂ [Pd ₂ Cl ₆] (0.5)	-	<1	40	38	79

^aReactions performed with 1.00 mmol of 4-chloroanisole in toluene (1 mL) according to GP 3.4 (see 7.2.3.1). Spectral yield according to ¹H-NMR against internal standard, given in mol%. Isolated yields after flash column chromatography (EtOAc-hexanes 1:50) in brackets. ^bResults reported by Lu et al.^[79] ^cReaction was stirred for 16 h at r.t. ^dSpectral yield after 24 h. ^e700 μ mol of 3-pentanone were reacted with 2.1 eq. of 4-chloroanisole in toluene (1 mL).

The catalyst loading was kept at 1 mol% with respect to Pd for better comparison. The IPrH-hexachlorodipalladate (**16**) showed similar reactivity as the tetrachloropalladate **18**, IPr-PEPPSI and (IPr)PdCl₂(Me-Im), the complex originally used by Lu et al.^[79] (entries 1-4). Reduction of the temperature significantly reduced the conversion (entry 5). Application of IMesH-based chloropalladates (**17**, **19**) did not induce activity even after 24 hours (entries 6-7). The combination of Pd(OAc)₂ with an imidazolium salt (IPr·HSO₄ (**23**), IPr·HOPiv (**24**)) seemed unsatisfactory, even after 24 hours (entries 8 and 9). While increasing the equivalents of chloroanisole employed in the reaction, the group of Lu also described the successful diarylation of ketones. Despite our efforts, the precatalyst (IPrH)₂[Pd₂Cl₆] (**16**) only afforded near identical amounts of mono- or disubstituted ketone with two equivalents of electrophile (entry 10). Recovery losses are owed to the similar boiling point of 3-pentanone (100-101 °C)^[80] compared to toluene (109-111 °C)^[81], allowing for azeotropic removal of the ketone. In addition to the signals of both coupling products, 4-chloroanisole (14%)¹⁰ and its

¹⁰ Percentage calculated on the amount of 4-chloroanisole involved.

homocoupling product (16%)¹⁰ can be detected. We may conclude that our difunctional CCP's exhibited great activity in Heck-type coupling compared to previously established catalyst systems.

In palladium-type cross-coupling chemistry, there seem to be few examples where IMesH-based catalysts are forcedly the best ones among those reported.^[82] An IMes-carbene containing palladacycle, IMes-Pd(dmba)Cl described by the group of Ying efficiently enabled Heck coupling of a range of challenging substrates.^[82c] To test the suitability of our chloropalladates **17** and **19** as catalyst precursors, we envisaged the Heck coupling of two hindered aryl bromides with *tert*-butyl acrylate: mesityl- and isityl bromide (table 52).

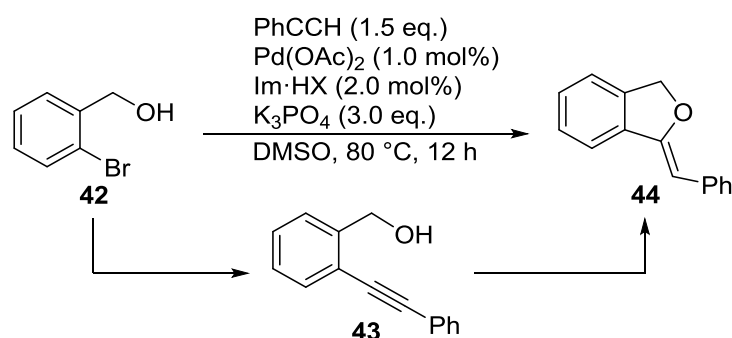
Table 13. Heck coupling of sterically hindered aryl bromides with *tert*-butylacrylate.^a dmba = *N,N*-dimethylbenzylamine.

ArBr		$\begin{array}{c} \text{CH}_2=\text{CH}-\text{CO}_2^t\text{Bu} \text{ (1.2 eq.)} \\ \text{K}_2\text{CO}_3 \text{ (2.0 eq.)} \\ \text{pre-catalyst} \\ \text{NMP, 140 }^\circ\text{C, 18 h} \end{array}$		Ar-CH=CH-CO ₂ ^t Bu		
entry	substrate	precatalyst [mol%]	ArBr [%]	ArH [%]	yield [%]	Σ [%]
1		(IMesH) ₂ [Pd ₂ Cl ₆] (1.0)	84	2	11	95
2		(IMesH) ₂ [PdCl ₄] (2.0)	85	2	11	96
3 ^b		IMes-Pd(dmba)Cl (2.0)	-	-	72/44 ^c	-
4		(IMesH) ₂ [Pd ₂ Cl ₆] (1.0)	79	5	17	101
5		(IPrH) ₂ [Pd ₂ Cl ₆] (1.0)	76	3	21	100
6		(IMesH) ₂ [PdCl ₄] (2.0)	65	5	32	102
7		(IPrH) ₂ [PdCl ₄] (2.0)	60	3	38	101

^aReactions performed with 1.00 mmol of aryl bromide in NMP (400 μL) according to GP 3.5 (see 7.2.3.1). Spectral yield according to ¹H-NMR against internal standard, given in mol%. ^bResults reported by Ying et al.^[82c] ^cReaction performed in air.

Both IMesH-precatalysts showed virtually identical results for the mesityl substrate (entries 1 and 2). The product was accompanied by minor amounts of reduced aryl halide (2%). Employing their IMes-Pd(dmba)Cl precatalyst, Lu et al. were able to convert the sterically more hindered isityl to the desired product in 72% yield (entry 3). The identical reaction in air afforded 44% of target material. Interestingly, our CCP's showed slightly better conversions of the sterically more hindered isityl compared to mesityl (entries 4-7). Regardless of the ligand's nature (IMesH or IPrH), similar results were obtained. In direct comparison of tetra- and hexachloropalladates, an imidazolium ligand to metal ratio of 2:1 was preferred (entries 4 and 6, or entries 5 and 7). Supposedly, poor conversions are due to the alkene coupling partner being rather sensitive towards polymerization and decomposition or reduced catalyst activities.

As pivalate appeared to have only a minor impact in the α -arylation of 3-pentanone, we sought for a more suitable reaction to highlight the CMD-effect. The group of Peris reported the synthesis of three Pd-NHC-pyridine complexes which were applied in a tandem Sonogashira/hydroalkoxylation reaction yielding benzofurans.^[83] The reaction of 2-bromobenzyl alcohol (**42**) with phenylacetylene in combination with Pd(OAc)₂ and one of our imidazolium salts (IPr·HSO₄ or IPr·HOPiv) afforded the desired benzofuran (**44**) in 90-93% spectral yield (scheme 27). Both of our NHC precursors proved superior to the complexes reported by Peris et al.^[83] who obtained **44** in 43-77% yield starting from **42**.¹¹ The CMD-effect of IPr·HOPiv will be demonstrated by monitoring the reaction progression.



Scheme 27. Tandem Sonogashira/hydroalkoxylation reaction of 2-bromobenzyl alcohol (**42**) with phenylacetylene to benzofuran **44**. X = SO₄ or OPiv.

To further underline the CMD-effect, we performed a kinetic study of the above model reaction employing our imidazolium salts. The reaction progress curves are plotted in figure 16 (see 7.2.3.1, general procedure 3.6, for further details). After 70 minutes, almost 60% of starting material was converted when using IPr·HOPiv. The hydroalkoxylation is independent of the anion X in IPr·HX, showing a linear trend. We might assume that no metal is involved in this step of the model reaction, but no investigations proving this assumption were conducted. However, the initial Sonogashira coupling profits from the CMD-effect evoked by the pivalate anion, which accelerates the reaction by 30% and causes a building of intermediate **43**.

¹¹ Peris et al. used Cs₂CO₃ (3.0 eq.) as base.

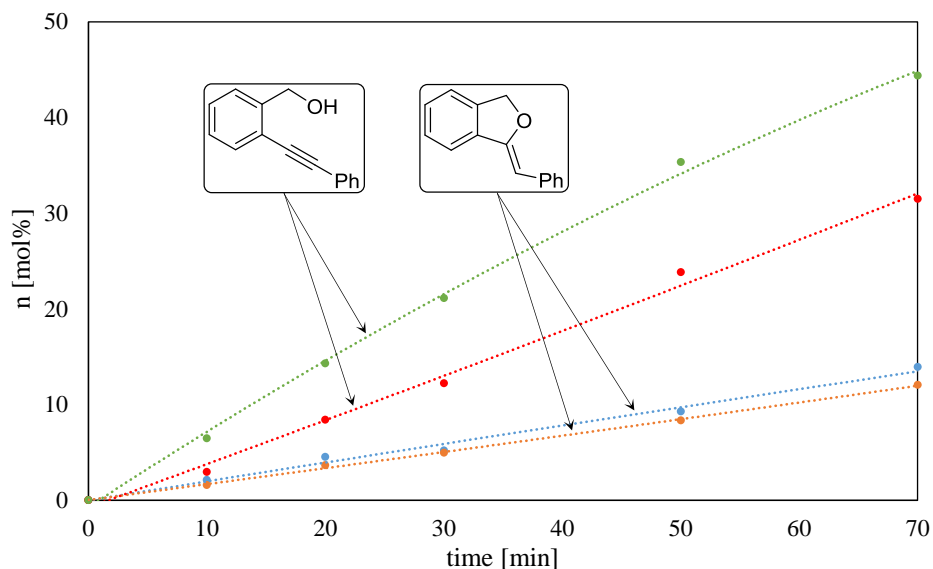


Figure 16. Kinetic study of the tandem Sonogashira/hydroalkoxylation reaction of **42** to **44**. Amount of substance (n) plotted against time (min). **Green:** amount of alkyne **43** using IPr-HOPiv; **red:** amount of alkyne **43** using IPr-HSO₄; **blue:** amount of benzofuran **44** using IPr-HOPiv; **orange:** amount of benzofuran **44** using IPr-HSO₄.

A CMD-additive dependent reaction that displayed a pronounced additive effect is the arylation of caffeine as described by the group of You.^[20a] This turned out to be an ideal model reaction for our purpose.¹² We analyzed the reaction progress during the first six hours by HPLC, allowing us to plot reaction progress for the arylation (figure 17). Reaction temperatures were reduced to 100 °C down from 120 °C in the original work for better comparison. To exclude any CMD-influence derived from the Pd precatalyst, we chose PdCl₂(MeCN)₂ as precursor in combination with different additives. Leaving carboxylate anions completely out of the reaction system effectively shuts down the reaction, showing less than 2% conversion (**orange** curve). Addition of pivalic acid remarkably extremely increased the catalyst's activity and led to quantitative conversion after six hours (**red** curve). In comparison, the combination of PdCl₂(MeCN)₂ with IPr-HOPiv showed satisfactory results, but at a lower rate (**purple** curve). The mesoionic carbene complex **35** showed initial activity, but the reaction seemed to stagnate after four hours (**green** curve). The lower pivalate content in this precursor (Pd–OPiv 1:1) is likely responsible for reduced catalyst activity. Oxidative addition as well as subsequent β-elimination were probably impeded by the NHC-Pd-catalyst's relatively inert structure. Doubling of the catalyst loading resulted in a 1.7 times higher conversion of caffeine (**blue** curve). Enhanced catalyst decomposition due to the high amount of palladium involved is

¹² The applications described in this paragraph were already performed during my master thesis.

likely. For the previous two cases, a complete consumption of caffeine was not achieved after 20 hours, yielding 42% of phenylcaffeine for 2.5 mol%, and 65% for 5.0 mol%, respectively.

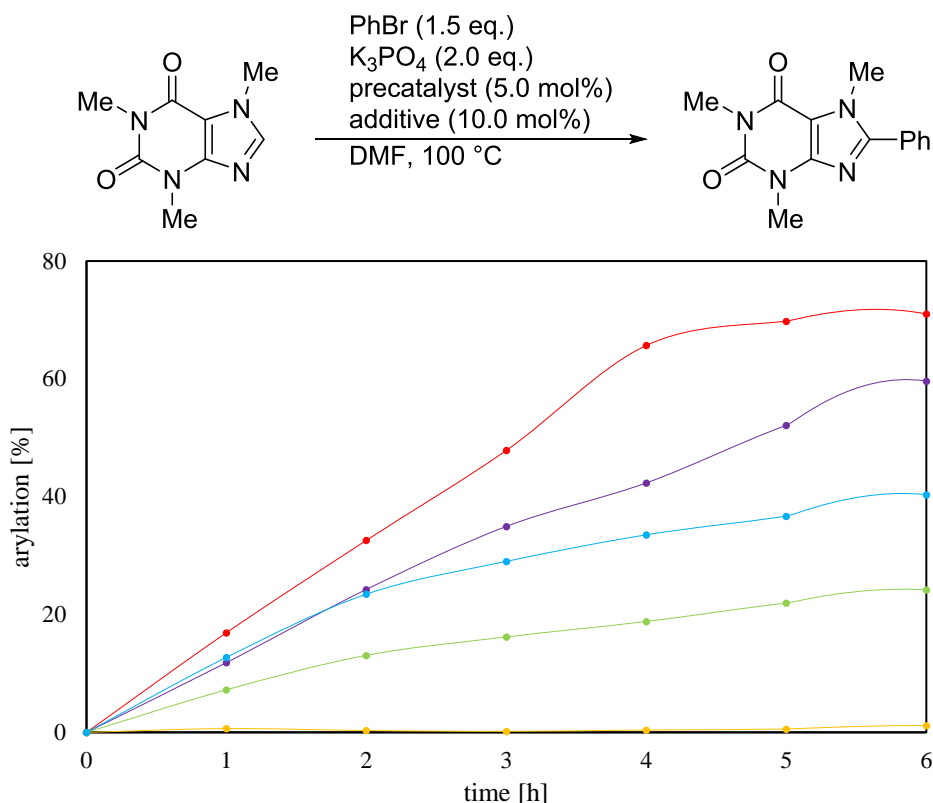


Figure 17. C–H arylation (%) plotted against time (h). Reactions performed with 1.5 mmol of caffeine according to general procedure 3.7 (see 7.2.3.1). **Orange:** PdCl₂(MeCN)₂ (5.0 mol%); **green:** ((*m*)IPr)₂Pd₂Cl₂(μ-OPiv)₂ (2.5 mol%); **blue:** ((*m*)IPr)₂Pd₂Cl₂(μ-OPiv)₂ (5.0 mol%); **purple:** PdCl₂(MeCN)₂ (5.0 mol%), IPr-HOPiv (10.0 mol%); **red:** PdCl₂(MeCN)₂ (5.0 mol%), PivOH (10.0 mol%)

3.5 Conclusion and outlook

Imidazolium chloropalladates containing stoichiometrically well-defined ratios of anion to cation have efficiently been prepared. Tetrachloropalladates tend to eliminate IPr-HCl and generate hexachlorodipalladates during crystallization. The structure of the latter salt has been confirmed by X-ray analysis. Depending on the charge density on the anion, a more or less pronounced hydrogen bonding behavior of the anion towards the imidazolium H-C(2) bond has been demonstrated by comparison of ¹H-NMR shift data with that in some common salts (halide, BF₄, PF₆, BARF). (IPrH)₂[Pd₂Cl₆] (**16**) was readily converted to the established IPr-PEPSI pre-catalyst (**22**) introduced by Organ et al.^[12] in what constitutes a practical new synthesis of this material. The salts IPr-HOPiv (**24**) and IMes·HOPiv (**25**) were designed as difunctional additives for catalysis development, which serve both as ligand precursor and as

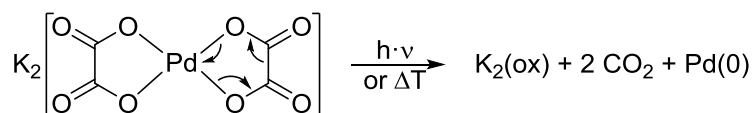
source of CMD-activity. While the IMesH-based salt IMes·HOPiv (**25**) was inherently unstable, IPr·HOPiv (**24**) was isolated in near quantitative yield. The ambient temperature synthesis of Pd(OPiv)₂ (**32**) from PdCl₂ was studied, since this (known) precatalyst is another example for a bifunctional catalyst precursor. A new preparative route to the salt was developed, but while it provided the desired product, it currently suffers from low yield and the unclear state of chloride contamination in the product. Either synthetic or work-up procedures should be varied by substituting extracting solvents and/or purification methods to improve the overall yield. The introduction of a third component of functionality into our precatalysts with the aim to synthesize a complex incorporating imidazolium cation as ligand precursor, a palladate as metal precursor, and a pivalate anion as CMD-additive was partly successful, except that palladium was found to be bound to the NHC-ligand in an ‘abnormal’ fashion, in that the NHC acted as mesoionic carbene. The mesoionic carbene complex **33** was obtained in good yield. On the other hand, a salt-type trifunctional CCP could not be isolated. Minor amounts of chloride impurities led to the formation of a small fraction of (IPr)PdCl(OPiv), as proven by X-ray diffraction. Reaction of the allyl carbene complex **37** with AgOPiv afforded 23% of (IPr)Pd(allyl)(OPiv) (**39**) in a not overly selective reaction.

The suitability of the newly prepared multifunctional component catalyst precursors (MCCP's) for catalysis development was successfully demonstrated. IPrH-based chloropalladates salts showed activity in Suzuki coupling as well as in the α -arylation of 3-pentanone. The results obtained were comparable with those of the established IPr-PEPPSI precatalyst. So far application of the IMesH-based salts were not successful and we generally found it difficult to identify model reactions in which this ligand induced specific and superior catalytic activity at palladium. Heck-type coupling of hindered aryl bromides with *tert*-butyl acrylate showed little conversion with either salt type and imidazolium cation. While showing rather unexceptional results in the α -arylation of ketones, additive salts IPr·HSO₄ (**23**) and IPr·HOPiv (**24**) efficiently converted 2-bromobenzyl alcohol and phenyl acetylene to a benzofuran in a Sonogashira coupling/hydroalkoxylation tandem reaction. The co-catalytic effect of pivalate versus hydrogensulfate was verified in the initial cross-coupling step. Among CMD-dependent reactions, the arylation of caffeine^[20a] turned out as ideal candidate to confirm the effectiveness of pivalate containing precursors. Whereas IPr·HOPiv delivered satisfactory results, the mesoionic carbene precatalyst **33** performed poorly, even at high catalyst loading. It is not quite clear what causes the low catalytic activity of this complex. In any case, the C–H arylation

appears to not profit from a specific ligand effect of the NHC ancillary ligands, and the mesoionic carbene-palladium complex may likewise display low intrinsic activity for this reaction.

The development of other multifunctional CCP's can be envisaged. The combination of palladium carboxylates with phosphines, e.g. $[(\text{Ph}_3\text{P})_2\text{Pd}(\text{OAc})_2]$, is already established in the literature.^[84] Few applications of $[(\text{Ph}_3\text{P})_2\text{Pd}(\text{OAc})_2]$ or related complexes in catalysis are reported leaving room for new reactions.^[85] The trifunctional complex $(\text{PCy}_3)_2\text{Pd}(\text{OPiv})_2$, merging ligand, metal, and CMD-additive sources would still be of high interest in future projects, although its stability and shelf-life may be limited. When $\text{IPr}\cdot\text{HOPiv}$ (**24**) was combined with a Pd-precursor, the formation of a NHC-Pd complex seems inevitable. Therefore, it might be advisable to directly synthesize a $(\text{NHC})\text{Pd}(\text{OPiv})_2$ or a related precatalyst.

A report from the 1990's describes the synthesis of $\text{K}_2[\text{Pd}(\text{ox})_2]\cdot 4\text{H}_2\text{O}$ (ox = oxalate) as precursor for bimetallic $\text{Ag}_2[\text{Pd}(\text{ox})_2]$.^[86] Irradiation or heating of the latter induced the decomposition of the oxalate anion, affording Ag-Pd metal colloids characterized via electron microscopy. One could take advantage of this decomposition to release active Pd(0) for catalysis (scheme 28).¹³ Even if stored under the exclusion of light and in the fridge, the complex $\text{K}_2[\text{Pd}(\text{ox})_2]$ slowly decomposes, yielding a greenish-black solid. Freshly prepared oxalate salt might be combined with imidazolium salts or other cations exhibiting a specific functionality, to generate new trifunctional CCP's. Any trace of chloride (or other halide) present might lead to the already known chloropalladates as side-product. As in the reported $\text{Ag}[\text{Pd}(\text{ox})_2]$ synthesis, a nitrate salt of the introduced cations would be beneficial. As weakly coordinating anions, the latter would not tend to occupy free space around the Pd center.



Scheme 28. Irradiation or heating of the Pd-oxalate precatalysts generates Pd(0) along with $\text{K}_2(\text{ox})$ and CO_2 .

Palladium phthalate, obtained by boiling of metallic Pd and phthalic acid in nitric acid,^[87] could also present a practical precursor to generate Pd(0) by heating, even though harsher conditions would be needed. An increase in functionality would be rather difficult with no exchangeable

¹³ The potassium salt was already synthesized during my master thesis.

cation present. The potassium salt of palladium phthalate has not yet been reported. Additionally, a trapping agent for generated aryne would have to be added. A 1,2-dihydro alternative of palladium phthalate would decompose more easily, leaving benzene, carbon dioxide, and Pd(0). 1,2-Dihydrophthalic acid is available either via electroreduction^[88] or sodium amalgam^[89] in sulfuric acid. Major drawback of these precursors will be the rather high tendency for decomposition due to oxidation of the organic component.

3.6 References

- [1] P. Klein, *The Multi-Component-Catalyst (MCC) Principle: Designing Functional Catalyst Precursors for Reaction Development*, master thesis, Technical University of Munich (Garching bei München), **2016**.
- [2] D. Hoorweg, P. Bhada-Tata, C. Kennedy, *Nature News* **2013**, *502*, 615.
- [3] a) S. U. Son, Y. Jang, J. Park, H. B. Na, H. M. Park, H. J. Yun, J. Lee, T. Hyeon, *J. Am. Chem. Soc.* **2004**, *126*, 5026-5027; b) B. M. Trost, J.-P. Lumb, J. M. Azzarelli, *J. Am. Chem. Soc.* **2011**, *133*, 740-743; c) K. Xu, N. Thieme, B. Breit, *Angew. Chem. Int. Ed.* **2014**, *53*, 2162-2165.
- [4] a) W. A. Herrmann, M. Elison, J. Fischer, C. Köcher, G. R. Artus, *Angew. Chem. Int. Ed.* **1995**, *34*, 2371-2374; b) K. Öfele, W. A. Herrmann, D. Mihailios, M. Elison, E. Herdtweck, T. Priermeier, P. Kiprof, *J. Organomet. Chem.* **1995**, *498*, 1-14; c) W. A. Herrmann, L. J. Goossen, C. Köcher, G. R. Artus, *Angew. Chem. Int. Ed.* **1996**, *35*, 2805-2807; d) W. A. Herrmann, C. Koecher, *Angew. Chem. Int. Ed.* **1997**, *36*, 2162-2187; e) W. A. Herrmann, L. J. Goossen, M. Spiegler, *Organometallics* **1998**, *17*, 2162-2168.
- [5] a) R. Jackstell, M. Gómez Andreu, A. Frisch, K. Selvakumar, A. Zapf, H. Klein, A. Spannenberg, D. Röttger, O. Briel, R. Karch, *Angew. Chem. Int. Ed.* **2002**, *41*, 986-989; b) K. Selvakumar, A. Zapf, M. Beller, *Org. Lett.* **2002**, *4*, 3031-3033; c) K. Selvakumar, A. Zapf, A. Spannenberg, M. Beller, *Chem. Eur. J.* **2002**, *8*, 3901-3906.
- [6] a) A. Chartoire, M. Lesieur, L. Falivene, A. M. Slawin, L. Cavallo, C. S. Cazin, S. P. Nolan, *Chem. Eur. J.* **2012**, *18*, 4517-4521; b) S. Meiries, A. Chartoire, A. M. Slawin, S. P. Nolan, *Organometallics* **2012**, *31*, 3402-3409; c) S. Meiries, K. Speck, D. B. Cordes, A. M. Slawin, S. P. Nolan, *Organometallics* **2013**, *32*, 330-339.
- [7] a) E. A. B. Kantchev, C. J. O'Brien, M. G. Organ, *Angew. Chem. Int. Ed.* **2007**, *46*, 2768-2813; b) S. Wuertz, F. Glorius, *Acc. Chem. Res.* **2008**, *41*, 1523-1533.
- [8] a) T. Weskamp, F. J. Kohl, W. Hieringer, D. Gleich, W. A. Herrmann, *Angew. Chem. Int. Ed.* **1999**, *38*, 2416-2419; b) K. M. Kuhn, J.-B. Bourg, C. K. Chung, S. C. Virgil, R. H. Grubbs, *J. Am. Chem. Soc.* **2009**, *131*, 5313-5320; c) A. Correa, L. Cavallo, *J. Am. Chem. Soc.* **2006**, *128*, 13352-13353.
- [9] a) M. Nakanishi, D. Katayev, C. Besnard, E. P. Kündig, *Angew. Chem. Int. Ed.* **2011**, *50*, 7438-7441; b) D. Shen, Y. Xu, S.-L. Shi, *J. Am. Chem. Soc.* **2019**, *141*, 14938-

- 14945; c) S. S. Sohn, J. W. Bode, *Angew. Chem. Int. Ed.* **2006**, *45*, 6021-6024; d) Y.-R. Zhang, L. He, X. Wu, P.-L. Shao, S. Ye, *Org. Lett.* **2008**, *10*, 277-280; e) M. He, G. J. Uc, J. W. Bode, *J. Am. Chem. Soc.* **2006**, *128*, 15088-15089.
- [10] a) K. M. Hindi, M. J. Panzner, C. A. Tessier, C. L. Cannon, W. J. Youngs, *Chem. Rev.* **2009**, *109*, 3859-3884; b) C. Shahini, G. Achar, S. Budagumpi, M. Tacke, S. A. Patil, *Appl. Organomet. Chem.* **2017**, *31*, e3819; c) S. Ray, R. Mohan, J. K. Singh, M. K. Samantaray, M. M. Shaikh, D. Panda, P. Ghosh, *J. Am. Chem. Soc.* **2007**, *129*, 15042-15053.
- [11] M. N. Hopkinson, C. Richter, M. Schedler, F. Glorius, *Nature* **2014**, *510*, 485-496.
- [12] a) C. J. O'Brien, E. A. B. Kantchev, C. Valente, N. Hadei, G. A. Chass, A. Lough, A. C. Hopkinson, M. G. Organ, *Chem. Eur. J.* **2006**, *12*, 4743-4748; b) M. G. Organ, S. Avola, I. Dubovyk, N. Hadei, E. A. B. Kantchev, C. J. O'Brien, C. Valente, *Chem. Eur. J.* **2006**, *12*, 4749-4755.
- [13] a) M. G. Organ, M. Abdel-Hadi, S. Avola, I. Dubovyk, N. Hadei, E. A. B. Kantchev, C. J. O'Brien, M. Sayah, C. Valente, *Chem. Eur. J.* **2008**, *14*, 2443-2452; b) C. Valente, M. E. Belowich, N. Hadei, M. G. Organ, *Eur. J. Org. Chem.* **2010**, *23*, 4343-4354; c) M. G. Organ, M. Abdel-Hadi, S. Avola, N. Hadei, J. Nasielski, C. J. O'Brien, C. Valente, *Chem. Eur. J.* **2007**, *13*, 150-157.
- [14] a) L. Benhamou, C. Besnard, E. P. Kündig, *Organometallics* **2014**, *33*, 260-266; b) R. Haraguchi, S. Hoshino, T. Yamazaki, S.-i. Fukuzawa, *Chem. Commun.* **2018**, *54*, 2110-2113.
- [15] N. Hazari, P. R. Melvin, M. M. Beromi, *Nat. Rev. Chem.* **2017**, *1*, 1-16.
- [16] a) M. R. Biscoe, B. P. Fors, S. L. Buchwald, *J. Am. Chem. Soc.* **2008**, *130*, 6686-6687; b) T. Kinzel, Y. Zhang, S. L. Buchwald, *J. Am. Chem. Soc.* **2010**, *132*, 14073-14075; c) N. C. Bruno, S. L. Buchwald, *Org. Lett.* **2013**, *15*, 2876-2879; d) C. W. Cheung, D. S. Surry, S. L. Buchwald, *Org. Lett.* **2013**, *15*, 3734-3737; e) S. D. Friis, T. Skrydstrup, S. L. Buchwald, *Org. Lett.* **2014**, *16*, 4296-4299; f) P. G. Gildner, T. J. Colacot, *Organometallics* **2015**, *34*, 5497-5508.
- [17] Y.-C. Xu, J. Zhang, H.-M. Sun, Q. Shen, Y. Zhang, *Dalton Trans.* **2013**, *42*, 8437-8445.
- [18] S. Bouquillon, A. du Moulinet d'Hardemare, M.-T. Averbuch-Pouchot, F. Hénin, J. Muzart, *Polyhedron* **1999**, *18*, 3511-3516.
- [19] M. Lafrance, K. Fagnou, *J. Am. Chem. Soc.* **2006**, *128*, 16496-16497.

- [20] a) D. Zhao, W. Wang, S. Lian, F. Yang, J. Lan, J. You, *Chem. Eur. J.* **2009**, *15*, 1337-1340; b) S. Potavathri, K. C. Pereira, S. I. Gorelsky, A. Pike, A. P. LeBris, B. DeBoef, *J. Am. Chem. Soc.* **2010**, *132*, 14676-14681; c) Q. Zhou, S. Wei, W. Han, *J. Org. Chem.* **2014**, *79*, 1454-1460.
- [21] a) K. Arentsen, S. Caddick, F. G. N. Cloke, A. P. Herring, P. B. Hitchcock, *Tetrahedron Lett.* **2004**, *45*, 3511-3515; b) G. A. Grasa, S. P. Nolan, *Org. Lett.* **2001**, *3*, 119-122; c) A. Schmidt, A. Rahimi, *Chem. Commun.* **2010**, *46*, 2995-2997; d) C. Yang, S. P. Nolan, *Synlett* **2001**, *10*, 1539-1542; e) C. Yang, S. P. Nolan, *Organometallics* **2002**, *21*, 1020-1022; f) V. P. Böhm, T. Weskamp, C. W. Gstöttmayr, W. A. Herrmann, *Angew. Chem. Int. Ed.* **2000**, *39*, 1602-1604.
- [22] A. J. Arduengo III, R. Krafczyk, R. Schmutzler, H. A. Craig, J. R. Goerlich, W. J. Marshall, M. Unverzagt, *Tetrahedron* **1999**, *55*, 14523-14534.
- [23] a) A. R. Hajipour, I. M. Dehbane, F. Rafiee, *Appl. Organomet. Chem.* **2012**, *26*, 743-747; b) A. R. Hajipour, N. Najafi, F. Rafiee, *Appl. Organomet. Chem.* **2013**, *27*, 228-231; c) A. R. Hajipour, F. Rafiee, *Appl. Organomet. Chem.* **2014**, *28*, 595-597; d) F. Rafiee, A. R. Hajipour, *Appl. Organomet. Chem.* **2015**, *29*, 181-184.
- [24] a) M. Olofsson-Mårtensson, M. Kritikos, D. Noréus, *J. Am. Chem. Soc.* **1999**, *121*, 10908-10912; b) J. S. Yeo, J. J. Vittal, T. A. Hor, *Chem. Commun.* **1999**, 1477-1478.
- [25] J. D. Atwood, *Inorganic and organometallic reaction mechanisms*, VCH Publishers, **1997**.
- [26] a) J. A. Davies, *Synthetic coordination chemistry: principles and practice*, World Scientific, **1996**; b) P. B. Hitchcock, K. R. Seddon, T. Welton, *J. Chem. Soc., Dalton Trans.* **1993**, 2639-2643.
- [27] S. Blanchard, F. Neese, E. Bothe, E. Bill, T. Weyhermüller, K. Wieghardt, *Inorg. Chem.* **2005**, *44*, 3636-3656.
- [28] a) M. B. Meredith, C. H. McMillen, J. T. Goodman, T. P. Hanusa, *Polyhedron* **2009**, *28*, 2355-2358; b) M. C. Kuhn, A. A. Lapis, G. Machado, T. Roisnel, J.-F. Carpentier, B. A. Neto, O. L. Casagrande Jr, *Inorg. Chim. Acta* **2011**, *370*, 505-512.
- [29] a) E. Moore, R. Janes, *Metal-ligand bonding*, Royal Society of Chemistry, **2007**; b) T. Poppel, M. Köckerling, *Z. Anorg. Allg. Chem.* **2010**, *636*, 2439-2446; c) C. Zhong, T. Sasaki, A. Jimbo-Kobayashi, E. Fujiwara, A. Kobayashi, M. Tada, Y. Iwasawa, *Bull. Chem. Soc. Jpn.* **2007**, *80*, 2365-2374.

- [30] F. Glorius, N-Heterocyclic carbenes in catalysis—an introduction in *Topics in Organometallic Chemistry*, Springer Nature, **2006**.
- [31] a) N. Marion, E. C. Ecarnot, O. Navarro, D. Amoroso, A. Bell, S. P. Nolan, *J. Org. Chem.* **2006**, *71*, 3816-3821; b) B. M. O’Keefe, N. Simmons, S. F. Martin, *Org. Lett.* **2008**, *10*, 5301-5304.
- [32] G. C. Fortman, S. P. Nolan, *Chem. Soc. Rev.* **2011**, *40*, 5151-5169.
- [33] G. Berthon-Gelloz, M. A. Siegler, A. L. Spek, B. Tinant, J. N. Reek, I. E. Markó, *Dalton Trans.* **2010**, *39*, 1444-1446.
- [34] a) G. Bastug, S. P. Nolan, *J. Org. Chem.* **2013**, *78*, 9303-9308; b) G. Bastug, S. P. Nolan, *Organometallics* **2014**, *33*, 1253-1258; c) A. R. Martin, D. J. Nelson, S. Meiries, A. M. Slawin, S. P. Nolan, *Eur. J. Org. Chem.* **2014**, *15*, 3127-3131.
- [35] a) M. G. Organ, S. Calimsiz, M. Sayah, K. H. Hoi, A. J. Lough, *Angew. Chem. Int. Ed.* **2009**, *48*, 2383-2387; b) K. H. Hoi, J. A. Coggan, M. G. Organ, *Chem. Eur. J.* **2013**, *19*, 843-845; c) M. Pompeo, J. L. Farmer, R. D. Froese, M. G. Organ, *Angew. Chem. Int. Ed.* **2014**, *53*, 3223-3226; d) C. Valente, M. Pompeo, M. Sayah, M. G. Organ, *Org. Process Res. Dev.* **2014**, *18*, 180-190; e) R. Zhong, A. Pöthig, Y. Feng, K. Riener, W. A. Herrmann, F. E. Kühn, *Green Chem.* **2014**, *16*, 4955-4962.
- [36] M. Pompeo, R. D. Froese, N. Hadei, M. G. Organ, *Angew. Chem. Int. Ed.* **2012**, *51*, 11354-11357.
- [37] V. de la Fuente, C. Godard, E. Zangrando, C. Claver, S. Castillon, *Chem. Commun.* **2012**, *48*, 1695-1697.
- [38] a) L. Hintermann, *Beilstein J. Org. Chem.* **2007**, *3*, 22; b) J. R. Struble, J. Kaeobamrung, J. W. Bode, *Org. Lett.* **2008**, *10*, 957-960; c) K. Hirano, S. Urban, C. Wang, F. Glorius, *Org. Lett.* **2009**, *11*, 1019-1022; d) A. M. Voutchkova, L. N. Appelhans, A. R. Chianese, R. H. Crabtree, *J. Am. Chem. Soc.* **2005**, *127*, 17624-17625; e) B. E. Love, J. Ren, *J. Org. Chem.* **1993**, *58*, 5556-5557; f) M. Hans, J. Lorkowski, A. Demonceau, L. Delaude, *Beilstein J. Org. Chem.* **2015**, *11*, 2318-2325; g) S. Meiries, S. P. Nolan, *Synlett* **2014**, *25*, 393-398; h) R. Savka, H. Plenio, *Eur. J. Inorg. Chem.* **2014**, *36*, 6246-6253; i) S. Dierick, D. F. Dewez, I. n. E. Markó, *Organometallics* **2014**, *33*, 677-683; j) S. G. Weber, C. Loos, F. Rominger, B. F. Straub, *Arkivoc* **2012**, *3*, 226-242; k) M. Schmid, R. Eberhardt, J. Kukral, B. Rieger, *Z. Naturforsch. B* **2002**, *57*, 1141-1146.
- [39] L. Rast, *Additive-effects in Pd-catalyzed C-H transformations*, master thesis, Technical University of Munich (Garching bei München), **2019**.

- [40] S. Bouvet, B. Pegot, J. Marrot, E. Magnier, *Tetrahedron Lett.* **2014**, *55*, 826-829.
- [41] S. Wei, X. G. Wei, X. Su, J. You, Y. Ren, *Chem. Eur. J.* **2011**, *17*, 5965-5971.
- [42] A. F. Holleman, *Lehrbuch der anorganischen Chemie*, Walter de Gruyter GmbH & Co KG, **2019**.
- [43] M. v. Fèvre, J. Pinaud, A. Leteneur, Y. Gnanou, J. Vignolle, D. Taton, K. Miqueu, J.-M. Sotiropoulos, *J. Am. Chem. Soc.* **2012**, *134*, 6776-6784.
- [44] F. Mani, M. Peruzzini, P. Stoppioni, *Green Chem.* **2006**, *8*, 995-1000.
- [45] T. Steiner, *Acta Crystallogr. Sect. B: Struct. Sci.* **1998**, *54*, 456-463.
- [46] a) P. Dolui, J. Das, H. B. Chandrashekar, S. Anjana, D. Maiti, *Angew. Chem. Int. Ed.* **2019**, *58*, 13773-13777; b) C. Reddy, N. Bisht, R. Parella, S. A. Babu, *J. Org. Chem.* **2016**, *81*, 12143-12168; c) W. Gong, G. Zhang, T. Liu, R. Giri, J.-Q. Yu, *J. Am. Chem. Soc.* **2014**, *136*, 16940-16946; d) S. Ye, W. Yang, T. Coon, D. Fanning, T. Neubert, D. Stamos, J. Q. Yu, *Chem. Eur. J.* **2016**, *22*, 4748-4752.
- [47] E. M. Beccalli, G. Broggini, M. Martinelli, S. Sottocornola, *Chem. Rev.* **2007**, *107*, 5318-5365.
- [48] a) H. Lin, X. Pan, A. L. Barsamian, T. M. Kamenecka, T. D. Bannister, *ACS Catal.* **2019**, *9*, 4887-4891; b) S. St John-Campbell, J. A. Bull, *Chem. Commun.* **2019**, *55*, 9172-9175; c) F.-L. Zhang, K. Hong, T.-J. Li, H. Park, J.-Q. Yu, *Science* **2016**, *351*, 252-256.
- [49] Y. Wu, Y.-Q. Chen, T. Liu, M. D. Eastgate, J.-Q. Yu, *J. Am. Chem. Soc.* **2016**, *138*, 14554-14557.
- [50] a) M. Anand, R. B. Sunoj, H. F. Schaefer III, *J. Am. Chem. Soc.* **2014**, *136*, 5535-5538; b) W. Feng, T. Wang, D. Liu, X. Wang, Y. Dang, *ACS Catal.* **2019**, *9*, 6672-6680.
- [51] a) D. E. Stephens, J. Lakey-Beitia, G. Chavez, C. Ilie, H. D. Arman, O. V. Larionov, *Chem. Commun.* **2015**, *51*, 9507-9510; b) T. A. Stromnova, D. V. Paschenko, B. Lyubov'I, M. V. Daineko, S. B. Katser, A. V. Churakov, L. G. Kuz'mina, J. A. Howard, *Inorg. Chim. Acta* **2003**, *350*, 283-288.
- [52] P. K. Pramanick, Z. Zhou, Z.-L. Hou, B. Yao, *J. Org. Chem.* **2019**, *84*, 5684-5694.
- [53] D. A. Edwards, R. M. Harker, M. F. Mahon, K. C. Molloy, *Inorg. Chim. Acta* **2002**, *328*, 134-146.
- [54] D. P. Bancroft, F. A. Cotton, L. R. Falvello, W. Schwotzer, *Polyhedron* **1988**, *7*, 615-621.

- [55] J. Tsuji, Palladium Compounds and Complexes Useful in Organic Synthesis in *Organic Synthesis with Palladium Compounds*, Springer, **1980**, pp. 2-3.
- [56] a) E. C. Keske, O. V. Zenkina, R. Wang, C. M. Crudden, *Organometallics* **2012**, *31*, 6215-6221; b) R. H. Crabtree, *Coord. Chem. Rev.* **2013**, *257*, 755-766; c) R. S. Ghadwal, S. O. Reichmann, R. Herbst-Irmer, *Chem. Eur. J.* **2015**, *21*, 4247-4251; d) M. Gazvoda, M. Virant, A. Pevec, D. Urankar, A. Bolje, M. Kočevár, J. Košmrlj, *Chem. Commun.* **2016**, *52*, 1571-1574.
- [57] D. P. Hruszkewycz, J. Wu, N. Hazari, C. D. Incarvito, *J. Am. Chem. Soc.* **2011**, *133*, 3280-3283.
- [58] D. P. Hruszkewycz, J. Wu, J. C. Green, N. Hazari, T. J. Schmeier, *Organometallics* **2012**, *31*, 470-485.
- [59] B. Xiao, T.-J. Gong, Z.-J. Liu, J.-H. Liu, D.-F. Luo, J. Xu, L. Liu, *J. Am. Chem. Soc.* **2011**, *133*, 9250-9253.
- [60] H. Lebel, M. K. Janes, A. B. Charette, S. P. Nolan, *J. Am. Chem. Soc.* **2004**, *126*, 5046-5047.
- [61] a) G. Sim, L. E. Sutton, *Molecular Structure by Diffraction Methods, Vol. 3*, Royal Society of Chemistry, **2007**; b) J. William Suggs, *Palladium: Organometallic Chemistry*, John Wiley & Sons, Ltd., Athens, GA, USA, **2011**.
- [62] M. S. Viciu, R. M. Kissling, E. D. Stevens, S. P. Nolan, *Org. Lett.* **2002**, *4*, 2229-2231.
- [63] L. Jafarpour, E. D. Stevens, S. P. Nolan, *J. Organomet. Chem.* **2000**, *606*, 49-54.
- [64] L. P. Wu, Y. Suenaga, T. Kuroda-Sowa, M. Maekawa, K. Furuichi, M. Munakata, *Inorg. Chim. Acta* **1996**, *248*, 147-152.
- [65] D. R. Jensen, M. S. Sigman, *Org. Lett.* **2003**, *5*, 63-65.
- [66] N. Marion, O. Navarro, J. Mei, E. D. Stevens, N. M. Scott, S. P. Nolan, *J. Am. Chem. Soc.* **2006**, *128*, 4101-4111.
- [67] L.-C. Campeau, P. Thansandote, K. Fagnou, *Org. Lett.* **2005**, *7*, 1857-1860.
- [68] Z. Csákai, R. Skoda-Földes, L. Kollár, *Inorg. Chim. Acta* **1999**, *286*, 93-97.
- [69] a) C. Amatore, A. Jutand, M. A. M'Barki, *Organometallics* **1992**, *11*, 3009-3013; b) C. Amatore, E. Carre, A. Jutand, M. A. M'Barki, *Organometallics* **1995**, *14*, 1818-1826.
- [70] a) N. Miyaura, A. Suzuki, *Chem. Rev.* **1995**, *95*, 2457-2483; b) A. Suzuki, *J. Organomet. Chem.* **1999**, *576*, 147-168; c) A. Suzuki, *J. Organomet. Chem.* **2002**, *653*, 83-90; d) A. Suzuki, *Proc. Jpn. Acad. Ser. B* **2004**, *80*, 359-371.

- [71] a) Z. Jin, S. X. Guo, X. P. Gu, L. L. Qiu, H. B. Song, J. X. Fang, *Adv. Synth. Catal.* **2009**, *351*, 1575-1585; b) T. Wang, L. Liu, K. Xu, H. Xie, H. Shen, W.-X. Zhao, *RSC Adv.* **2016**, *6*, 100690-100695; c) T. Wang, K. Xu, W. Wang, L. Liu, *Transition Met. Chem.* **2018**, *43*, 347-353.
- [72] a) J. H. Li, C. L. Deng, Y. X. Xie, *Synth. Commun.* **2007**, *37*, 2433-2448; b) T. Hoshi, T. Honma, A. Mori, M. Konishi, T. Sato, H. Hagiwara, T. Suzuki, *J. Org. Chem.* **2013**, *78*, 11513-11524; c) C. M. So, C. P. Lau, A. S. Chan, F. Y. Kwong, *J. Org. Chem.* **2008**, *73*, 7731-7734.
- [73] a) V. Percec, G. M. Golding, J. Smidrkal, O. Weichold, *J. Org. Chem.* **2004**, *69*, 3447-3452; b) Z.-Y. Tang, Q.-S. Hu, *J. Am. Chem. Soc.* **2004**, *126*, 3058-3059; c) Z.-Y. Tang, Q.-S. Hu, *J. Org. Chem.* **2006**, *71*, 2167-2169.
- [74] J. M. Fox, X. Huang, A. Chieffi, S. L. Buchwald, *J. Am. Chem. Soc.* **2000**, *122*, 1360-1370.
- [75] M. S. Viciu, R. F. Germaneau, S. P. Nolan, *Org. Lett.* **2002**, *4*, 4053-4056.
- [76] C. Cao, L. Wang, Z. Cai, L. Zhang, J. Guo, G. Pang, Y. Shi, *Eur. J. Org. Chem.* **2011**, *8*, 1570-1574.
- [77] K. D. Hesp, R. J. Lundgren, M. Stradiotto, *J. Am. Chem. Soc.* **2011**, *133*, 5194-5197.
- [78] L. Ackermann, V. P. Mehta, *Chem. Eur. J.* **2012**, *18*, 10230-10233.
- [79] Z.-K. Xiao, H.-Y. Yin, J.-M. Lu, *Inorg. Chim. Acta* **2014**, *423*, 106-108.
- [80] X. Fan, X. Zhang, Y. Zhang, *J. Chem. Res.* **2004**, *2004*, 290-291.
- [81] K. B. Lehmann, F. Flury, N. Engel, N. Estler, N. Frieboes, N. Groß, N. Jordan, N. Klimmer, N. Prillwitz, N. Schulze, *Toxikologie und Hygiene der technischen Lösungsmittel*, Springer-Verlag, **2013**.
- [82] a) H. M. Lee, D. C. Smith, Z. He, E. D. Stevens, C. S. Yi, S. P. Nolan, *Organometallics* **2001**, *20*, 794-797; b) H. van Rensburg, R. P. Tooze, D. F. Foster, S. Otto, *Inorg. Chem.* **2007**, *46*, 1963-1965; c) E. A. B. Kantchev, G.-R. Peh, C. Zhang, J. Y. Ying, *Org. Lett.* **2008**, *10*, 3949-3952; d) N. Marion, S. P. Nolan, *Acc. Chem. Res.* **2008**, *41*, 1440-1449.
- [83] A. Zanardi, J. A. Mata, E. Peris, *Organometallics* **2009**, *28*, 4335-4339.
- [84] a) T. Stephenson, S. Morehouse, A. R. Powell, J. Heffer, G. Wilkinson, *J. Chem. Soc.* **1965**, 3632-3640; b) K. Choki, T. Mori, R. Ravikiran, M. Fujiwara, K. Takahama, K. Watanabe, H. Nonaka, Y. Otake, A. Bell, L. Rhodes (Sumitomo Bakelite Co. Ltd., Promerus LLC), US 7,820,356 B2, **2010**; c) D. U. Heo, D. H. Lee, J. O. Huh, B. J. Jang,

- M. Y. Han, M. W. Jung (LG Chem Ltd.), US 2019/0245149 A1, **2019**; d) N. Thirupathi, D. Amoroso, A. Bell, J. D. Protasiewicz, *Organometallics* **2007**, 26, 3157-3166.
- [85] a) A. Binggeli, V. Breu, D. Bur, W. Fischli, R. Guller, G. Hirth, H.-P. Marki, M. Muller, C. Oefner, H. Stadler (Hoffmann La Roche Inc.), 6,051,712, **2000**; b) B. Forman, R. Beard, I. Dussault, R. Chandraratna (Allergan Sales Inc.), US 2005/0004165 A1, **2005**; c) J. M. Cook, R. V. Edwankar, C. R. Edwankar, S. Huang, H. D. Jain, J. Yang, F. Rivas, H. Zhou (WiSys Technology Foundation Inc.), US 2010/0261711 A1, **2010**.
- [86] K. Torigoe, K. Esumi, *Langmuir* **1993**, 9, 1664-1667.
- [87] Y. Tomida, H. Hashimoto (Canon Inc.), 5,716,618, **1998**.
- [88] T. Ohno, M. Ozaki, A. Inagaki, T. Hirashima, I. Nishiguchi, *Tetrahedron Lett.* **1993**, 34, 2629-2632.
- [89] J. Seo, S. Y. Lee, C. W. Bielawski, *Macromolecules* **2019**, 52, 2923-2931.

4 DIFUNCTIONAL ONIUM CARBOXYLATE ADDITIVES FOR CATALYTIC COUPLING

This chapter is subdivided in four parts. After introductory words on the use of additives in catalysis (4.1), the synthesis of two carboxylic acids with putative reactivity as concerted-metalation-deprotonation (CMD) reagents is described (4.2.1). The combination of promising carboxylic acids with ‘onium’ cations affords multifunctional additives merging CMD- and PTC-properties (4.2.2). Application of these compounds in the arylation of caffeine allows a direct comparison of their activity (4.3). The most promising difunctional CCP, NBu₄DiPP, is involved in state-of-the-art reactions underlining its advantage compared to conventional CMD-additives. A brief outlook concludes the subject (4.4).

4.1 Introduction

Over the years, a variety of catalyst systems have been established, which allow for coupling of more and more sterically hindered substrates to be combined in cross-coupling reactions.^[1] Catalyst systems require or profit from a multitude of different functionalities: metal centers^[2], ligands^[3], bases^[4], halide abstractors^[5], redox-partners^[6], phase transfer catalysts (PTC)^[7], and CMD-additives^[8]. For each new catalyzed reaction, extensive screening efforts are inevitable to discover the optimal interplay of all components. Whereas a multitude of reactions rely on specific steering ligands^[4], this chapter will focus on PTC- and CMD-effects in catalysis.

Reactions in non-homogeneous media suffer from low solubility of certain reagents in one of the phases of the reaction mixture, e.g. in the Suzuki^[9] cross-coupling the base and the organic electrophile are usually soluble in the water or organic phase, but not in both phases. Phase-transfer catalysts or -reagents overcome this barrier, bringing one reagent into a phase where it originally did not dissolve. In case of an efficient transfer mechanism only catalytic amounts of phase-transfer agent is necessary.^[10] A prominent example to describe PTC effects is the reaction of chlorocyclooctane¹⁴ with aqueous sodium cyanide.^[10a,11] After refluxing for several days without phase-transfer catalyst, no obvious reaction had taken place. Only minor amounts of decomposition products emerging from hydrolysis of the cyanide ion, e.g. ammonia or sodium formate, were detected. This is unsurprising if one recons that sodium or potassium salts are typically insoluble in nonpolar organic media.^[12] However, quaternary ammonium salts are soluble in lipophilic solvents depending on their chain length and the nature of their counter-ion. Free ions usually exist in solvents with dielectric constants $\epsilon > 40$ and at high

¹⁴ No additional organic solvent was added to the system.

dilution, e.g. in solvents like water, alcohols, acetonitrile, or DMF^[13]. Larger ions further promote the degree of dissociation. In contrast, ion-pairing is preferred in solvents with $\epsilon < 10-15$, even at high dilution. Aprotic solvents of low polarity are most suitable media for phase-transfer catalysis. In the above outlined example of the reaction of chlorocyclooctane with aqueous sodium cyanide, addition of catalytic amounts of a quaternary ammonium salt (1 wt.%) significantly accelerates the reaction, yielding cyanocyclooctane in near 100% selectivity and conversion within three hours. An illustration of the phase-transfer reaction is depicted in figure 18. The reaction taking place can be subdivided into three basic steps.^[10a] First, the catalyst, Q^+Cl^- , soluble in the organic phase is extracted into the aqueous phase. After anion exchange with cyanide, the ion-pair Q^+CN^- returns to the organic phase via re-extraction. In the above case, the reaction occurs by displacement of anions between Q^+CN^- and the substrate, yielding Q^+Cl^- and cyanocyclooctane. The displaced chloride anion is transferred into the aqueous phase as Q^+Cl^- by the PTC to start a new catalytic cycle.

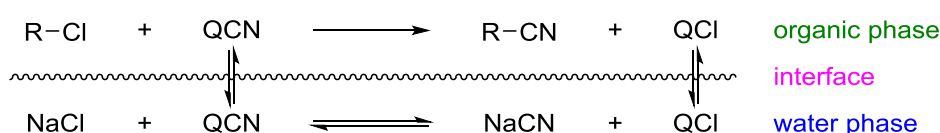


Figure 18. Illustration of the phase-transfer catalyst assisted cyanation of chlorocyclooctane. R = cyclooctane; Q^+ = quaternary ammonium cation.

Crown ethers and cryptands, or cyclic polyethers and -amines in general (figure 19) are particularly interesting in their ability to bind potassium cations.^[12,14] With their aid, hydrophilic salts KY (Y = reactive anion) can be solubilized in the organic phase, allowing the reaction of Y^- with a lipophilic electrophile to take place. Using crown ethers oxidations with $KMnO_4$ in benzene solution^[15] or Finkelstein reactions in fluorous solvents^[16] were achieved. A similar behavior is observed with polyethylene glycols (PEG). A major advantage of PEGs is their much cheaper price compared to crown ethers.¹⁵ Nucleophilic fluorination of alkyl triflates or -halides is possible in dipolar aprotic solvents without the introduction of any catalyst.^[17] However, the smaller potassium analogue was inactive in the S_N2 reaction of 2-(3-methanesulfonyloxypropoxy)naphthalene with KF in MeCN due to the strong Coulombic influence of K^+ on F^- , which reduces its solubility and retards the reaction rate.^[18] The addition of crown ethers in dipolar aprotic solvents (DMF, MeCN) only led to minor conversion. Introduction of bis-terminal hydroxy polyether significantly increased the reaction rate by

¹⁵ Prices at Fisher Scientific Germany (09.07.2020): PEG4000 0.14 €/g; 18-crown-6 2.87 €/g.

activation of both reactants. The cation K^+ is chelated via the ether groups enhancing the solubility of the potassium salt. One hydroxy group reduces the basicity of F^- by hydrogen bonding; the other alcohol group may be involved in activation of the electrophile following similar H-bonding. A chiral version of tetraethylene glycol also enabled the desilylative kinetic resolution of silyl ethers with KF .

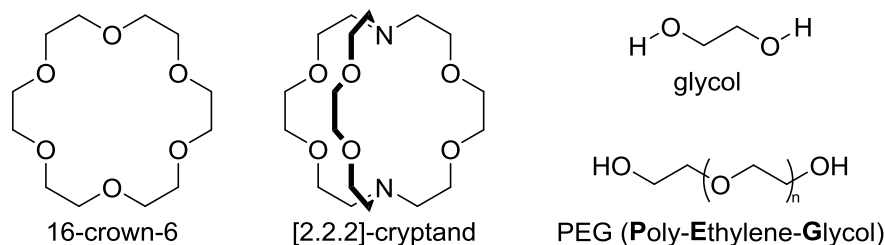


Figure 19. Illustration of a crown ether (left), cryptand (middle), glycol and polyethylene glycols (right).

Hydroxide ions from aqueous concentrated hydroxide solutions or from powdered solids are not extracted into the organic phase.^[10a,12] Deprotonation of the substrate rather occurs at the interphase, anchoring the anion. Phase transfer catalysts can detach anions from the interphase while their original counter-ion passes over to the aqueous one. Additionally, PTCs might assist in the deprotonation by ion-pairing with the anion. Typical phase transfer assisted reactions with hydroxide bases include cyclopropanations^[19], alkylations^[20], or others^[21].

Asymmetric phase transfer catalysis can be performed by introducing chiral cations capable of interacting with reactants (figure 20).^[22] Thus, chiral information from the PTC ion is transferred to the substrate.

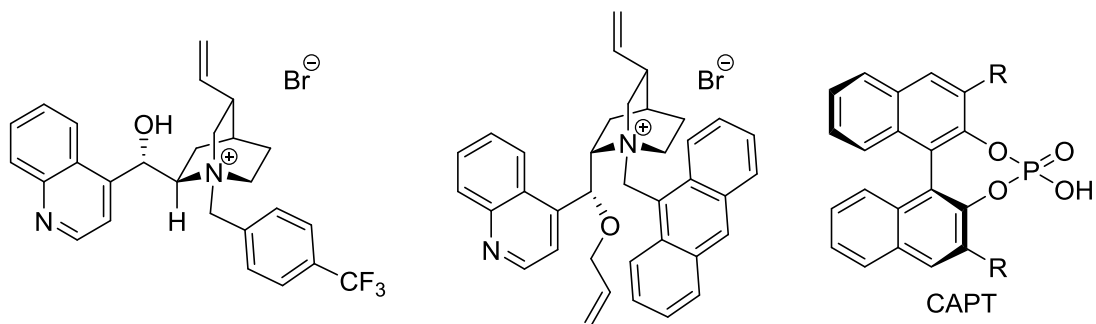
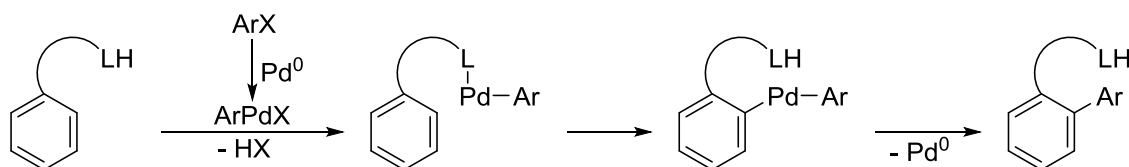


Figure 20. Chiral cinchonidinium salts: a) Merck laboratories^[23] (left) b) Corey^[20d] et al. (middle); chiral anion phase transfer catalyst (CAPT, right) by Toste^[26b-d] and Sigman^[26a-c] et al. R = 2,4,6-tri(*isopropyl*)benzene.

Ground-breaking studies were published by the Merck laboratories describing the asymmetric methylation via chiral cinchonidinium salts.^[23] Almost simultaneously the groups of Corey^[20d] and Lygo^[24] published the enantioselective enolate alkylation using cinchona alkaloids bearing 9-anthrylmethyl groups at the nitrogen. Another approach for introducing chirality by phase

prominent reactions of this type.¹⁷ Whereas early Heck reactions mostly involved aryl iodides or bromides, the scope has been extended to aryl chlorides^[42] over the years. The reaction proceeds via alkyl-palladium intermediates. In case of stereoelectronically hindered β -H-elimination, the palladium center may conduct follow-up reactions, e.g. insertion of alkynes or alkenes.^[43] The group of Trost took advantage of this effect by realizing a Domino-Heck coupling in the synthesis of vitamin D metabolites.^[44] Early literature of Castro et al. cites the palladium-free substitution of aryl iodides with cuprous acetylides in pyridine.^[45] A few decades later, Miura et al. published a similar conversion with catalytic amounts of copper.^[46] However, both cases require harsh conditions with limited compatibility of functional groups. The coupling method later introduced by the group of Sonogashira with Pd metal and co-catalytic copper(I) salt tolerates a wide range of substrates at mild temperature levels (25-100 °C).^[47] Depending on the amine base, copper-free cross-coupling reactions are possible.^[43,47c,48] With functionalized arenes as C-H donors, it is possible to realize selective *ortho*-aryl-aryl couplings. Especially phenols, amines, and heteroarenes act as directing group (scheme 30).^[49] After oxidative addition of an aryl halide to Pd⁰, the resulting Pd^{II} coordinates to the functional group entailing coordination-assisted *ortho*-insertion. Reductive elimination affords the desired biaryl structure.



Scheme 30. *ortho*-C-H arylation in functionalized arenes. L = Lewis base.^[49a]

Electrophilic aromatic substitution (S_EAr) as well as CMD-type mechanisms are the most common pathways in the C-H arylation of (hetero)arenes.^[50] Decisive results in C-H-transformations have been described by the group of Fagnou.^[8f] Incorporation of pivalic acid into the catalyst system allowed the direct arylation of benzene, where the pivalate anion was postulated to play a key role in C-H bond cleavage. The authors assumed that the carboxylate anion acts as proton shuttle from benzene to the inorganic carbonate base. Early studies of C-H bond activation of unactivated arenes already pointed to a concerted proton abstraction mechanism.^[51] Computational DFT studies by Echavarren and coworkers have supported this

¹⁷ The three groups independently published their results nearly at the same time. Heck and Cassar et al. reported their methods as extension of Heck reactions to terminal acetylenes.

hypothesis.^[52] Substitution of coordinated bromide ion by bicarbonate at the Pd center significantly lowers the transition state energy of proton abstraction. Fagnou et al. proposed two possible pathways for the C–H arylation (figure 21).^[8f] One invokes the reversible coordination of pivalate to Pd. Once the aryl bromide oxidatively adds to the Pd⁰ species, deprotonated acid substitutes the bromide ion. Coordinated arene then undergoes a concerted-metalation-deprotonation (CMD) activation step of the C–H bond. According to pathway A, pivalic acid detaches from the metal center. After reductive elimination the coupling product along with Pd⁰ is formed. Pathway B suggests that pivalic acid/pivalate remains bound to Pd throughout the catalytic cycle. Extensive mechanistic and computational studies revealed the general preference of CMD-type mechanisms for electron-rich and deficient substrates, and refute the formation of any σ -Wheland intermediate in a S_EAr mechanism.^[53] Many research groups have taken advantage of the carboxylate assisted CMD-mechanism.^[54] Astonishing results were achieved by the group of You who reported the arylation of heterocycles through C–H bond activation with pivalic acid.^[8a]

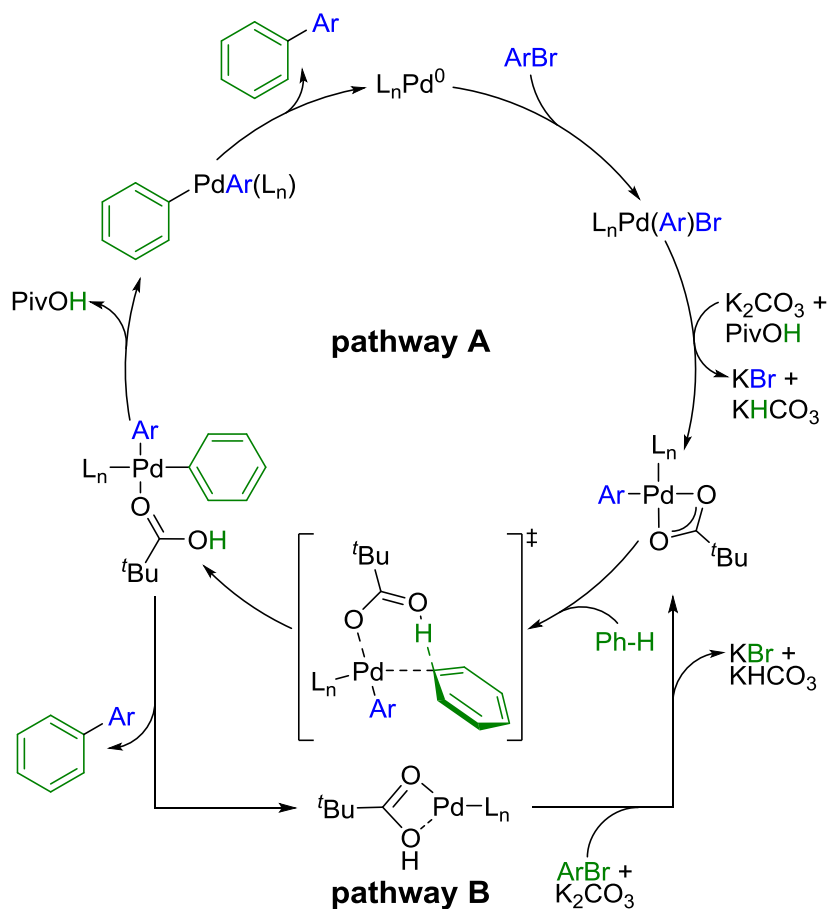


Figure 21. Proposed concerted-metalation-deprotonation (CMD) mechanism by Fagnou et al.^[8f] PR_3 = DavePhos, 2-dicyclohexylphosphino-2'-(*N,N*-dimethylamino)biphenyl; Ar = electron-rich or -deficient aryl group.

CMD-assisted C–H arylation^[55] is being widely used in total synthesis. Besides CMD-activation, a second feature is attributed to carboxylates. Depending on their tail length (8-18 carbon atoms), they can form micelles in aqueous media (figure 22); by virtue of their lipophilic and hydrophilicity structure elements.^[11,56] Three prevalent types of micellar surfactants exist: cationic (ammonium, phosphonium), anionic (sulfate, sulfonate, carboxylate), and nonionic ones (polyoxyethylenes). In aqueous media, the hydrophilic parts of surfactant molecules, e.g. carboxylate groups, are always in contact with the solvent whereas the lipophilic tails arrange in an oil-droplet like shape, minimizing contact of the apolar residues with water.^[57] Non-polar solvents support the formation of inverse micelles. Long chain surfactants may often lead to enhanced reactivity by providing necessary channels for organic reactants to approach aqueous media.

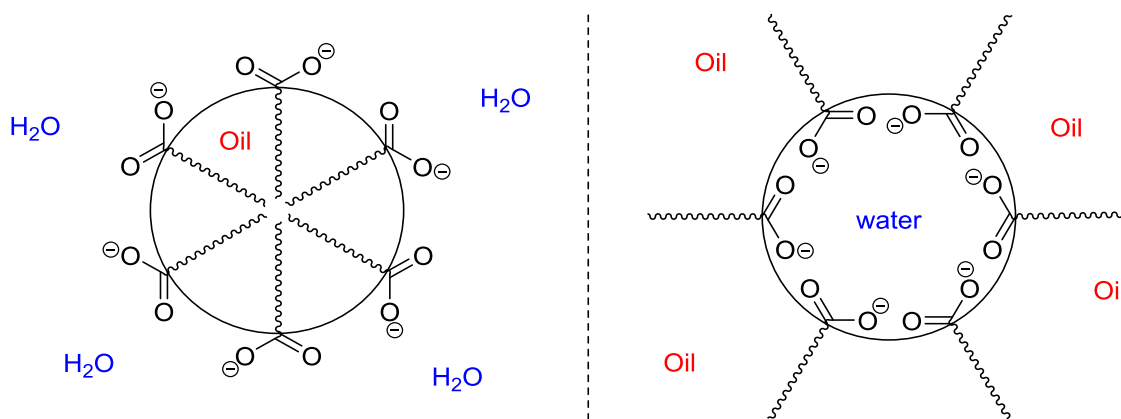
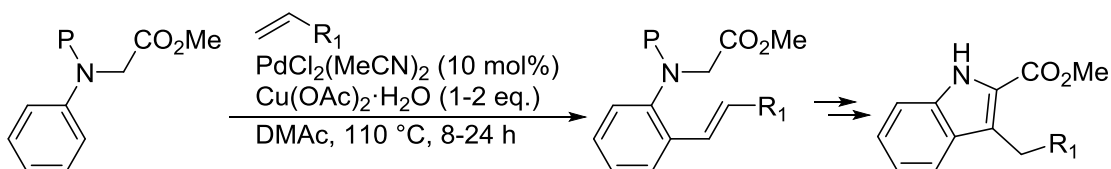


Figure 22. Illustration of a normal micelle (left) and inverse micelle (right) in the case of long-chain carboxylate surfactants. A ball shape arrangement is mostly observed.

Finally, dehydrogenative CH–CH coupling reactions are potentially the most eco-friendly ones, since they formally produce only H₂ or water as waste products. Often involving substrates with activated positions, they allow the efficient synthesis of heterocycles^[58] or biheterocycles^[59]. The group of Gaunt reported the solvent-controlled regioselective C2- or C3-alkenylation of free indoles.^[60] Another approach included an ancillary 3-pyridylsulfonyl group at arylamine nitrogen, providing regioselective C2-Heck alkenylation of functionalized anilines.^[61] Intramolecular Michael addition, subsequent reductive desulfonylation and rearomatization with DDQ afforded the respective indoles (scheme 31).



Scheme 31. *ortho*-Alkenylation of *N*-(2-pyridyl)sulfonyl anilines by the groups of Carretero and Arrayás.^[61] The depicted kind of *N*-alkylated substrate can be transferred to an indole via multi-step synthesis. P = SO₂(2-Py); R₁ = electron-withdrawing group (EWG); DMAc = dimethylacetamide.

Several groups reported applications of tetraalkylammonium carboxylates as nucleophilic oxygen sources in catalysis.^[62] While the ions themselves already showed enhanced reactivity in C–H arylation reactions, we now also want to explore their feasibility as difunctional units for catalyst systems. Pivalic acid as well as long-chain carboxylates often hold low melting and high boiling points^[63], and are difficult to measure in small amounts. Tetraalkylammonium salts, particularly of the chloride type, suffer from high deliquescence.^[64] Our aim consisted in the synthesis of stoichiometrically well-defined, weighable ammonium carboxylate salts as practical additives for catalysis. By combining both ammonium and carboxylate functionalities we expect superior activity in C–H arylation reactions of catalyst system to which the easy to handle additive has been added. Different types of carboxylic acids as well as alkylammonium cations were chosen in order to diversify the properties of the composed salts. The catalytic C–H arylation of caffeine as reported by the group of You^[8a] should provide a stable platform for comparing the effects of each additive in catalysis.

4.2 Synthesis of difunctional ammonium carboxylate additives

4.2.1 Carboxylic acids and their performance in catalysis

A range of carboxylic acids seemed interesting for the synthesis of difunctional onium carboxylates. Next to those cheaply available from chemical suppliers, 2,2-dimethyldecanoic and 2-isopropyl-2,3-dimethylbutanoic acid were previously prepared in our group.^[65] Two specific α -trisubstituted carboxylic acids, acetal **45** and dicarboxylic acid **46** (H₂-esp) additionally raised our attention based on their structural analogy to pivalic acid (figure 23).

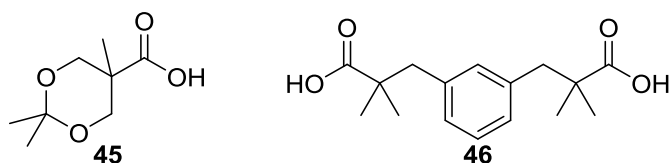
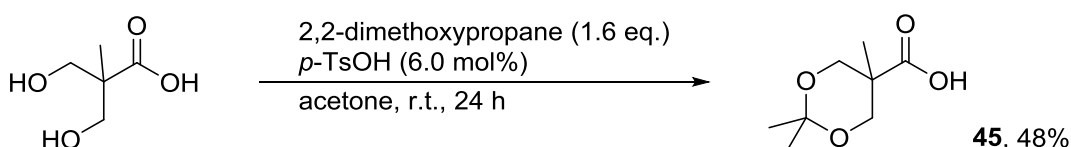


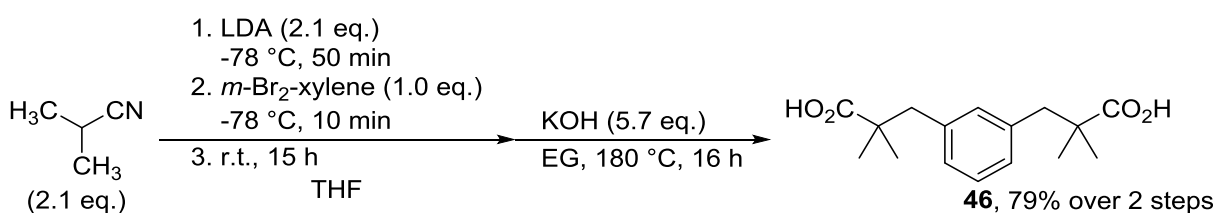
Figure 23. Target carboxylic acids for the subsequent synthesis of difunctional onium carboxylates.

Besides being used as starting material for dendrons^[66], hydrophobic analogues of aspirin^[67], or molecular receptors^[68], acetal **45** might profit from σ -donor effects and steric hindrance from its backbone when applied as CMD-additive in catalysis. Following the procedure by Dhar et al.^[67], the target was isolated in 48% on a large scale (scheme 32). Together with dicarboxylic acid **46**, their evaluation in our model reaction, the arylation of caffeine as described by You^[8a], is presented at the end of this sub-chapter (table 14).



Scheme 32. Acetalization of 2,2-bis(hydroxymethyl)propionic acid to acetal (**45**).

Several metal complexes (Co^[69], Rh^[70], Pd^[71]) bearing H₂-esp (**46**) as ligand have been reported. Originally named after a coworker from the group of Du Bois^[70b], acid **46** features two carboxylate groups. Its superior role over pivalate in the intra- and intermolecular Rh-catalyzed C–H amination arose our interest in potential CMD-reactivity in our arylation reaction. In the case of Du Bois et al., the Rh-units profit from the chelating effect of the ligand, disfavoring complete ligand exchange from the metal centers^[72]. The dicarboxylic acid was readily available via a two-step procedure starting from xylene dibromide (scheme 33).^[69] The intermediary dinitrile as well as the acid were both filtered as solutions over a plug of silica to remove polymeric substances, followed by crystallization. In this manner, flash column chromatography proved unnecessary. A single recrystallization yielded H₂-esp (**46**) in 79% yield over two steps.



Scheme 33. Two-step synthesis of H₂-esp (**46**).^[70b] Whereas Du Bois and coworkers started from the cheaper *m*-Cl₂-xylene, we chose the bromo substrate as it was available in our storage. The intermediary dinitrile was isolated in 81% yield. Saponification of the latter worked in close to quantitative yield. EG = ethylene glycol.

Prior the combination of both acids **45** and **46** with quaternary ammonium salts, their feasibility as CMD additives in the arylation of You^[8a] was investigated. The group of You carried out the arylation of caffeine with bromobenzene in DMF in the presence pivalic acid, resulting in 85%

of phenylcaffeine after seven hours at 120 °C. In previous work¹⁸, we reduced the reaction temperature to 100 °C to get a better insight in the reaction progression. Pd(OAc)₂ was substituted with unfunctional PdCl₂(MeCN)₂ to exclude any CMD-influence by the precatalyst. Reaction progress curves were recorded over five hours by removing small aliquots for HPLC analysis. The aforementioned carboxylic acids (PivOH, Me₂-decanoic acid, ...) proved effective after five hours at 100 °C when the conversion of caffeine had reached completion.

Table 14. Model-reaction testing the performance of CMD additives.^a **A**⁻ = carboxylate anion; caff. = caffeine; Phcaff. = phenylcaffeine.

entry	HA [mol%]	caff. [%] ^b	Phcaff. [%] ^b	recovery [%]
1	acetal 45 (10)	85	12	97
2	H ₂ -esp (5)	96	3	99
3	H ₂ -esp (10)	94	3	97

^aReaction performed with 500 μmol caffeine in DMF (1.5 mL) according to GP 4.2 (see 7.2.4.1).

^bSpectral yield according to ¹H-NMR against internal standard, in mol%.

In contrast, reactions involving acetal **45** and H₂-esp (**46**) were analyzed via q-NMR, allowing a more precise quantification of reaction products, but only after work-up of the reaction. Both test reactions showed little conversion after 14 hours (table 14). Doubling of the H₂-esp (**46**) loading to 10 mol% (20 mol% acid per Pd) did not affect the outcome of the reaction. The groups of Autschbach and Berry^[71] have reported the synthesis of two Pd–esp complexes with different symmetries, namely C_S–Pd₃(esp)₃ and C_{3h}–Pd₃(esp)₃. In the C_S-symmetric complex two esp-ligands lie either above or below the Pd₃ plane, shielding the Pd-atom(s) from any additive or reactant approaching. From our point of view, the cage like species seems relatively stable, impeding the generation of catalytically active Pd(0). Higher loadings of esp ligand probably increase the complex's stability while disfavoring the dissociation of a carboxylate moiety, consequently leaving no vacant coordination site. Due to these results we decided to abandon the synthesis of difunctional onium salts from H₂-esp (**46**) or the acetal **45**.

¹⁸ For the evaluation of those CMD additives, see references [65] and [73].

4.2.2 Synthesis of quaternary ammonium carboxylates

The target additives in this chapter combine two structural elements: the onium and carboxylate component (figure 24). Quaternary ammonium anions potentially exhibit PTC effects, assuring a fast encounter of substrate and reactants. Our target cations range from simple tetraalkylammonium over benzyl trialkylammonium to chiral cinchonidinium units. Each one of them exhibits unique properties of which catalysis may profit. Depending on their hydrocarbon chain lengths and the nature of their counter-ion, varying stability and PTC ability may be attributed to the salts. Especially alkyl chains suffer from Hofmann elimination in alkaline reaction mixtures.^[74] Decomposition due to nucleophilic ion displacement is more common with benzyl, methyl, and allyl substituted quaternary ammonium salts. Among alkyl chains, tetrabutylammonium salts might not offer the highest reactivity but are readily available and inexpensive.^[75] Concerning benzyl trialkylammonium salts, the large benzyl group at the nitrogen increase its lipophilic character. Small methyl groups provide better accessibility of the cationic center, allowing a closer association with the anion, like in the case of methyltrioctylammonium. The latter is most likely to show PTC activity. Aliquat[®] 336, a high molecular weight methyl ammonium salt consisting of a mixture of C₈ and C₁₀ carbon chains (C₈ predominant), efficiently promoted Rh-catalyzed hydrogenation^[76], carbonylation^[77], and Pd-catalyzed Suzuki coupling^[78]. In the total synthesis of Manzamine A, neat Aliquat[®] 336 with potassium acetate achieved nucleophilic substitution of hindered neopentyl bromide.^[79] The cation might be favorable in performing catalytic reactions in water. Cinchona alkaloid-derived quaternary ammonium salts allowed enantioselective alkylations under phase-transfer catalysis.^[20d,23-24] The substrates come in close proximity to the cation due to van der Waals interactions. Thereby, ion pairing simulates the direction for the nucleophilic substitution of primary alkyl halides, delivering high ee's. The group of Corey reisolated the cinchonidinium salt by aqueous extraction for reuse.^[20d] A different example depicts the enantioselective dihydroxylation of olefins using OsO₄ in the presence of a phthalazine-bridged cinchona alkaloid catalyst under Sharpless conditions.^[80] Osmium potentially coordinates the alkylated nitrogen atoms. The crowded chiral cinchona backbone blocks any approach of the olefin, thus inducing face selectivity.

Previous work by L. Rast in our group had depicted good to enhanced catalytic reactivity of the carboxylic acids illustrated in figure 24 as CMD additives. Accelerated conversion was observed for diisopropyl propionic acid as CMD additive.^[65] A major advantage of this acid is

its crystalline state at room temperature. Being used as antiepileptic drug^[81], the liquid valproic acid is readily available. Concerning the long chain decanoic acid, we expect the formation of micelles, increasing the activity of the catalyst, particularly in two-phase systems.

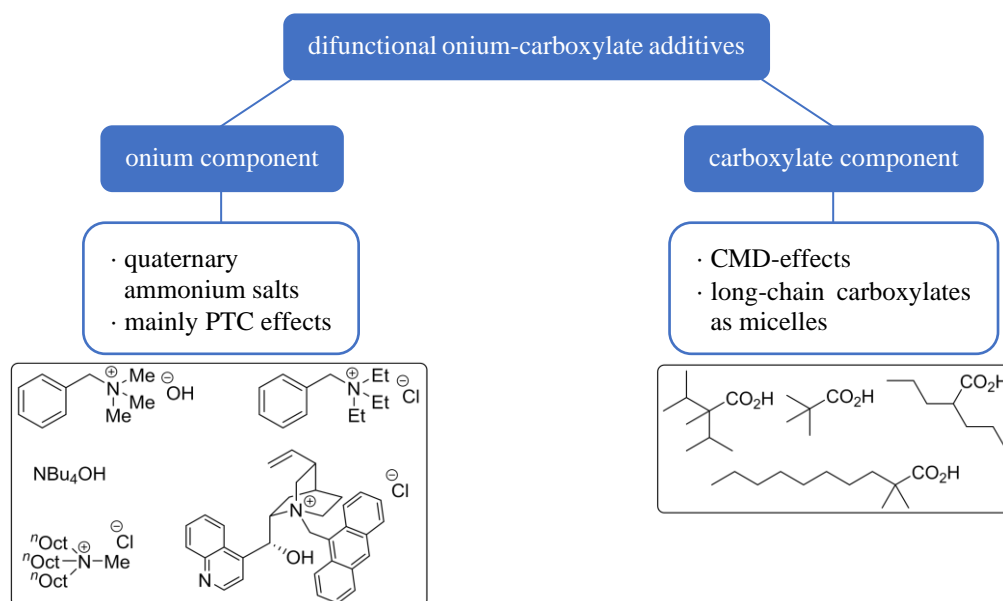


Figure 24. Overview of target difunctional onium carboxylates.

For a meaningful comparison of difunctional salts, we did not envisage to prepare all possible combinations. The main goal was to merge the most promising one, namely diisopropyl propanoic acid (DiPPA), with all of the above ammonium units. The remaining acids will only be combined with the tetrabutyl- and methyltrioctylammonium cations. Titration of carboxylic acids with tetrabutylammonium hydroxide in *i*PrOH against phenolphthalein indicator yielded the corresponding tetrabutylammonium salts in over 90% (table 15).¹⁹ Water was removed via azeotropic distillation with toluene. Diisopropyl propanoic, pivalic, and valproic acid delivered solid salts with increasing deliquescence (entries 1 and 3-4). The onium salt of the long chain carboxylate presented itself as viscous oil or ionic liquid (entry 5). Even after drying for several hours at elevated temperature and reduced pressure, minor amounts of toluene remained dissolved in the valproate and decanoate salt. Combination of diisopropyl propanoic acid with benzyl trimethylammonium hydroxide afforded a crystalline solid in 95% yield (entry 2). Benzyl triethylammonium chloride was first converted to its hydroxide following a procedure^[82] by the group of Pallavicini²⁰. Equimolar reaction with DiPPA resulted in the

¹⁹ The titration was stopped as soon as a light pinkish color was perceived.

²⁰ They reported the synthesis of cetyltrimethylammonium naproxenate from cetyltrimethylammonium hydrogensulfate or chloride and naproacet via precipitation of K₂SO₄ or KCl.

desired product. However, it was accompanied by a significant impurity one could not get rid of. The appearance of diethylbenzylamine (7 mol%) is likely due to decomposition by Hofmann elimination.^[74c] On account of the impurity as well as its rather viscous consistence, further investigations of this salt were abandoned.

Table 15. Synthesis of tetrabutylammonium carboxylates.^a A^- = carboxylate anion.

HA		$\xrightarrow[\textit{iPrOH, r.t., 1 h}]{\text{NBu}_4\text{OH (1.0 eq)}} \text{NBu}_4^+ A^-$	
entry	HA [1.0 eq.]	yield [%]	properties
1		93	solid
2 ^b		95	solid
3		93	solid, hygroscopic
4		97 ^c	solid, highly hygroscopic
5		101 ^d	oil

^aReaction performed with 5.00 or 20.0 mmol of acid in *i*PrOH (1.0 mL/mmol), 3-4 drops of an alcoholic solution of phenolphthalein (0.73 wt.% in *i*PrOH) were added as pH-indicator; isolated yield after purification. ^bBzNMe₃OH (1.0 eq.) was used instead of NBu₄OH. ^c0.2 wt.% toluene. ^d0.6 wt.% toluene.

The five isolated onium carboxylates (table 15, entries 1-5) can be organized according to their physical properties and deliquescence (figure 25). With increasing crystallinity, the hygroscopic nature of the salts decreases. Both diisopropyl propanoates **47** and **48** appear as easily weighable solids which do not quickly absorb water, with tetrabutylammonium slightly superior to the benzyl trimethylammonium derivative. After a few weeks (>4) of storage in a closed container in air, embedded water was clearly perceived while working with the pivalate salt **49**. The valproate salt **50** readily melted while weighing in. Due to easy uptake of water it was stored in a glovebox to facilitate its handling (entry 4). Small amounts of solid difunctional additives pick up moisture more rapid. Formation of small droplets on the spatula could be perceived. Due to its long chain unit, tetrabutylammonium dimethyldecanoate (**51**) remains as ionic liquid at room temperature. The oily nature of this salt impedes an accurate addition in catalysis.

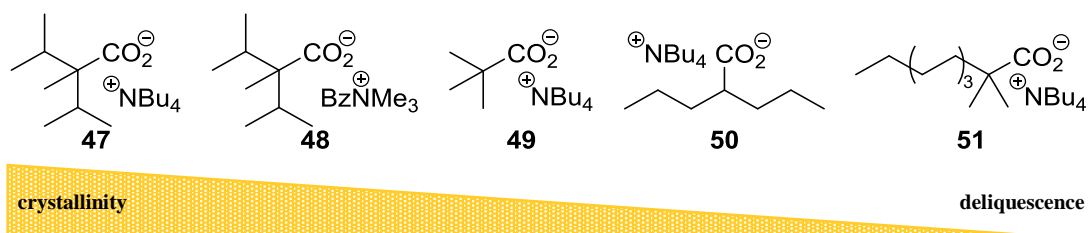


Figure 25. Physical solidity and deliquescence of difunctional onium salts.

Suitable single crystals for X-ray analysis of $47 \cdot 3\text{H}_2\text{O}$ were grown by slow diffusion of hexanes into a saturated solution of the latter in toluene (figure 26). Crystal data, as well as collected data for structure refinement are summarized in the appendix (8.3, table 76f.). Alkyl chains surround the nitrogen atom in a tetrahedral fashion, spanning angles of $111\text{--}112^\circ$. Steric crowding of the cation hampers any approach of the anion: atoms O2 and C14 exhibiting the closest contact distance of $3.41(8) \text{ \AA}$. No interactions between O2 and C14 protons were observed. Hydrogen bonds between three water molecules and the carboxylate can be observed, arranging in a twisted six-membered ring (figure 26 right). Oxygen atoms are separated by $1.83(9)\text{--}2.07(1) \text{ \AA}$. The presence of water supposedly facilitated the dissolution of the salt in toluene. Only by lowering the polarity of the solution, crystallization was induced.

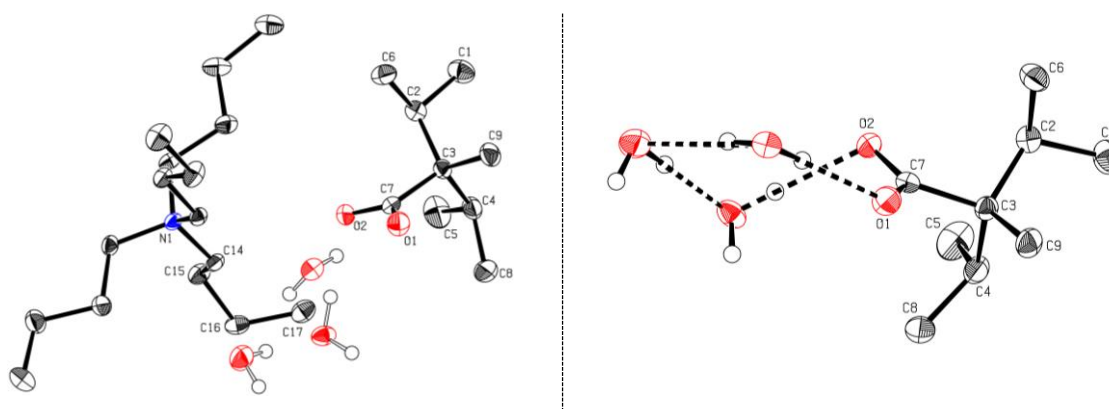


Figure 26. X-ray crystal structure of $47 \cdot 3\text{H}_2\text{O}$. Left: complete structure; right: magnified cutout of water coordination by the carboxylate unit. Ellipsoids are shown at 50% probability level. Hydrogen atoms are omitted except for water molecules. Carbon atoms are depicted in grey, nitrogen atoms in blue, and oxygen atoms in red.

We also wanted to tackle the challenge of combining the above acids with Aliquat[®] 336, which is nominally methyl trioctylammonium chloride, although the alkyl chains are actually a mixture of C8 and C10 alkyl chains.^[83] Avoiding ionic exchange chromatography, Pallavicini and coworkers described the preparation of cetyltrimethylammonium (CTA) naproxenate from $\text{CTA} \cdot \text{HSO}_4$.^[82] Their large-scale synthesis minimized the amount of residual inorganic counter anions ($<500 \text{ ppm}$) originating from the educt. A procedure starting from $\text{CTA} \cdot \text{Cl}$ was also achieved; a final chloride content of 4700 ppm was detected. Following their procedure, we envisaged ion exchange from chloride to hydroxide. The expected compound should then be used as titrant similar to NBu_4OH . Unfortunately, our attempt led to major decomposition of the ammonium cation (figure 27). Analysis of the spectrum revealed the presence of trioctylamine (1.8 mol%), oct-1-ene (2.0 mol%), methyldioctylamine (43.8 mol%), and methyltrioctylammonium salt (52.4 mol%); the values are absolute. Significant amounts of oct-

1-ene might have been removed azeotropically.²¹ Similar results were obtained by Landini et al.^[74c] who studied the stability of quaternary onium salts in the presence of aqueous alkaline solution (50% NaOH). Degradation was already observed at room temperature. Heating to 60 °C led to halfway decomposition of the cation after less than one hour. We suppose our alkaline reaction conditions together with the elevated temperature (60 °C) at the rotary evaporator induced the degradation.

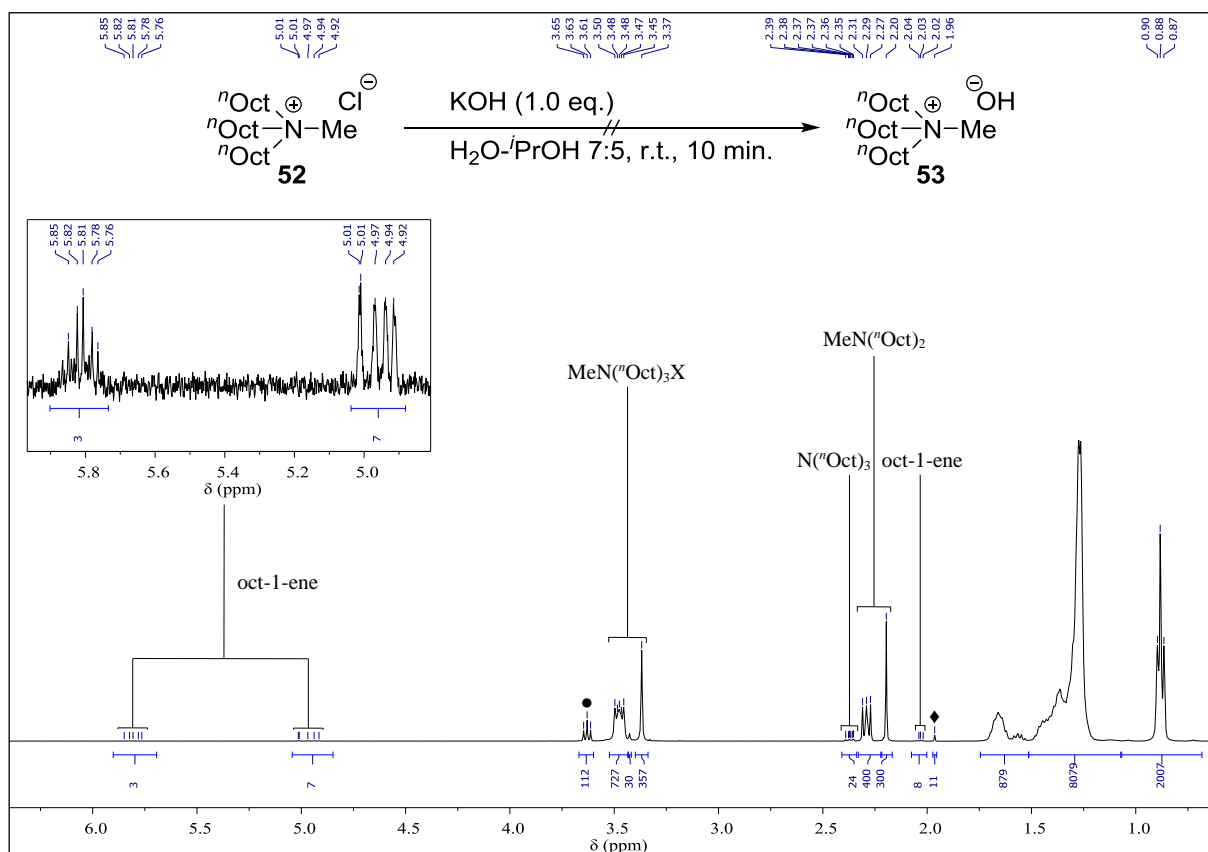
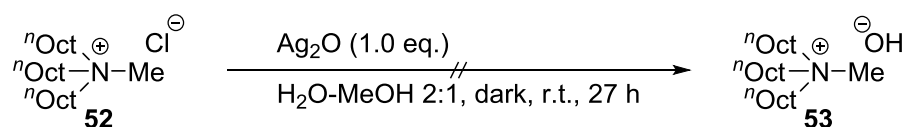


Figure 27. ¹H-NMR spectrum (CDCl₃) of the attempted methyltrioctylammonium hydroxide synthesis from its chloride. Aliquat® 336 is depicted with only C8 alkyl chains for simplicity. Minor amounts of toluene (♦) from azeotropic distillation as well as 1-octanol/1-decanol (●) from the starting material are present in the spectrum. X = Cl or OH.

Recollecting work of Ladenburg et al.^[84], we attempted a milder approach via anion exchange with silver oxide in an aqueous, methanolic medium (scheme 34). Several samples were withdrawn to pursue completion of the reaction by precipitation of AgCl from an acidified aliquot with dilute silver nitrate solution. Due to foaming and clouding while acidulating with

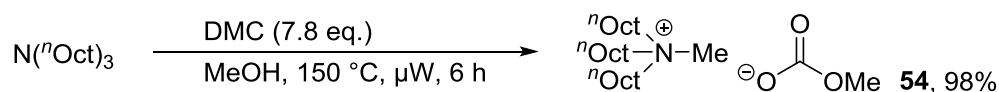
²¹ The reaction was performed in isopropanol. Both solvent evaporation and azeotropic drying with toluene will have removed oct-1-ene.

aqueous HNO₃ and addition of AgNO₃, we considered the ion exchange to be incomplete after six hours of stirring. The suspension was filtered multiple times over a pad of Celite on the next day to remove potential AgCl and residual Ag₂O.²² Removal of the solvent led to a viscous brownish oil which was used for titration of an acid. Sadly, no color change of the pH-indicator was perceived. Incomplete or failed anion exchange was further confirmed by a silver precipitation test. As the age of used Ag₂O was rather indefinable, previous decomposition of the reactant cannot be excluded. Freshly prepared silver hydroxide from silver nitrate would have been beneficial.^[85]



Scheme 34. Silver oxide in an aqueous medium should generate silver hydroxide, conducting the actual ion exchange from chloride to hydroxide.

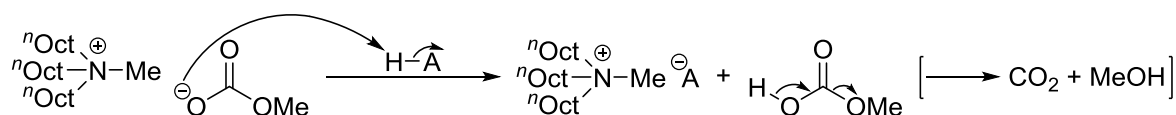
Suffering from these two setbacks, we searched literature for an alternative way to prepare methyltrioctylammonium (MTOA) carboxylates. A clean method was reported by the group of Perosa, describing the halide free synthesis of ionic liquids from MTOA methyl carbonate (**54**).^[86] Other workers^[87] as well as Perosa et al.^[86] prepared the methylammonium salt **54** inside an autoclave. Not having access to one, we took advantage of our microwave reactor which is capable of resisting pressure up to 30 bar. After removal of excessive dimethyl carbonate and methanol, we isolated **54** in 98% yield (scheme 35). Minor amounts of methanol (~1 mol%) and unreacted starting material (~1 mol%) could not be removed. Reactants were only dried for one night over molecular sieves (3 Å and 4 Å). Small quantities of water induced partial hydrolysis of the anion to hydrogen carbonate (9 mol%).



Scheme 35. Microwave synthesis of methyltrioctylammonium (MTOA) methyl carbonate (**54**). DMC = dimethyl carbonate.

Perosa et al. subsequently reacted **54** with Brønsted acids yielding the anion exchanged salts along with methyl hydrogen carbonate.^[86] The latter decomposed to methanol and carbon dioxide as only side-products (scheme 36). Use of water quantitatively converted MTOA methyl carbonate to the hydrogen carbonate salt.

²² A faint silver mirror at the bottom of the Erlenmeyer flask had formed overnight.



Scheme 36. Protonation of the methyl carbonate anion by a Brønsted acid yields the anion exchanged salt. In case of water, hydroxide recombines with CO₂ to give bicarbonate. A⁻ = anion.

Following Perosa's reaction procedures^[86], we investigated the reaction of MTOA methyl carbonate with our acids: diisopropyl propionic, pivalic, valproic, and 2,2-dimethyldecanoic acid (table 16). Due to impurities in MTOA, we used it in small excess. Upon addition of acid to the latter and heating to 50 °C, gas evolution (CO₂) was observed. In evidence of tiny bubbles forming as well as perceptible heat, pivalic acid seemed to be acidic enough for protonation at room temperature. The viscous MTOA methyl carbonate inhibited homogeneous mixing in the beginning. Stirring improved with the progression of the reaction due to stoichiometric amounts of methanol forming. All four salts were obtained as ionic liquids in >100% yield owing to hydrogen carbonate impurity of the educt.

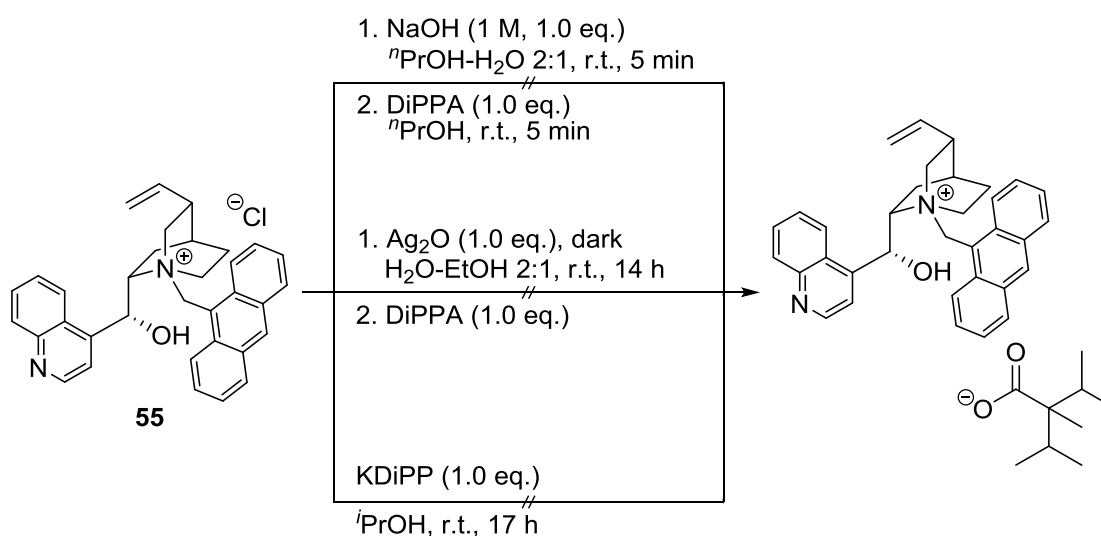
Table 16. Synthesis of methyltriocetylammmonium (MTOA) carboxylates.^a A⁻ = carboxylate anion.

entry	HA [1.0 eq.]	yield [%]	observation
1		107	gas evolution at 50 °C
2		109	gas/heat evolution at r.t.
3		106	gas evolution at 50 °C
4		105	gas evolution at 50 °C

^aReactions performed with 5.00 or 20.0 mmol of HA in ^tPrOH (1 mL/mmol) according to GP 4.1 (see 7.2.4.1); isolated yield after purification.

The last challenge we wanted to tackle consisted in the synthesis of a chiral cinchonidinium carboxylate salt (scheme 37). Ion-exchange of the starting material **55** with either sodium hydroxide^[82] or Ag₂O^[84] were the first options we considered to isolate hydroxide salt **56** for acid titration. Unfortunately, the cinchonidinium salt decomposed under the chosen reaction conditions, leaving us with rather complex ¹H-NMR spectra. Crystallization of reaction mixtures including stoichiometric amounts of acid only afforded unfunctionalized cinchona alkaloid. In the case of the silver salt reaction, no acid was added to the isolated intermediate as its ¹H-NMR spectrum already depicted decomposition of the latter. Another approach relied on a classical ion-exchange in which potassium chloride precipitates. First, we prepared the

corresponding potassium salt of DiPPA via titration against phenolphthalein indicator. Due to limited solubility of both reactants in acetone, we performed the subsequent ion-exchange reaction in *i*PrOH. At 0 °C, potassium chloride should be weakly soluble in the alcohol.²³ After work-up, a slightly sticky, brownish solid was obtained. Purification by precipitation or washing was not achieved. Spectral analysis of the crude product revealed complete consumption of the starting material **55**. However, broad multiplets were observed in the spectrum, pointing to mainly decomposition of the salt. Further investigations were not conducted at this point.



Scheme 37. Attempted syntheses of a chiral cinchonidinium carboxylate salt. Before addition of DiPPA to a supposed cinchonidinium hydroxide solution, solvents and inorganic salts were removed by azeotropic distillation and filtration, respectively. DiPPA = diisopropyl propionic acid; DiPP = diisopropyl propionate.

4.3 Difunctional onium carboxylates in catalysis

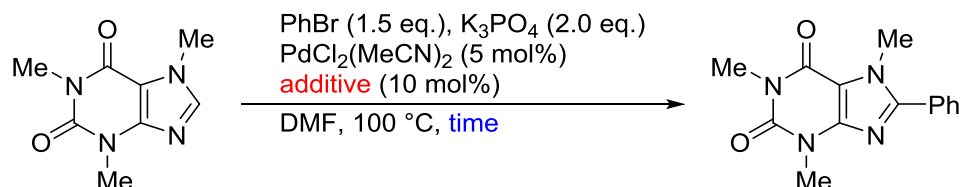
For better comparison of the isolated difunctional onium carboxylates, we envisaged their application as additives in the arylation of caffeine according to You et al.^[8a]. Starting from previously established conditions in our group,^[65,73] we reduced the reaction temperature to 100 °C, since differences in reactivity are best observed at lower reaction rate and in the initial phase of the arylation. Dilution by a factor of three (0.33 M down from 1 M) should also decelerate the progression of the reaction. To remove any CMD-influence due to the Pd precatalyst²⁴, we chose PdCl₂(MeCN)₂ as Pd source. Except for results taken from my master

²³ For comparison, the solubility of NaCl in isopropanol is 16 mg/100 g *i*PrOH.

²⁴ The group of You used Pd(OAc)₂ as metal precursor. Acetate might exhibit a minor CMD effect.

thesis, yields were determined via q-NMR analysis following the procedure described in the general experimental section (7.1.3). After either 2.5 or 13 hours, the reaction mixture was filtered over a short pad of silica, eluting with DCM–MeOH (10:1). Losses in the recovery might be caused by partial sublimation of caffeine at the rotary evaporator.²⁵ Results of the arylation of caffeine are summarized in table 17.

Table 17. Incorporation of difunctional onium carboxylates in the arylation of caffeine described by You^[8a] and coworkers.^a caff. = caffeine; Phcaff. = phenylcaffeine; recov. = recovery.



entry	additive		yield [%] after 2.5 h			yield [%] after 13 h		
	cation	anion	caff.	Phcaff.	recov.	caff.	Phcaff.	recov.
1 ^b	–	–	>99	<1	100	98	1	99
2	H [⊕]		56	35	91	<1 ^b	83 ^b	83 ^b
3	[⊕] NBu ₄		49	47	96	1	88	89
4			51	49	100	7	89	96
5			48	48	96	2	88	90
6			30	66	96	<1	87	87
7	ⁿ Oct [⊕] ⁿ Oct–N–Me ⁿ Oct		45	54	99	5	90	95
8			50	48	98	13	84	97
9			40	54	94	4	91	95
10			25	69	94	<1	92	92
11	BnNMe ₃ [⊕]		27	68	95	<1	87	87

^aReaction performed with 500 μmol caffeine in DMF (1.5 mL) according to GP 4.2 or 4.3 for HPLC (see 7.2.4.1); spectral yield according to ¹H-NMR against internal standard, given in mol%. ^bValues extracted from my master thesis. Yields determined via HPLC according to equations 1.1 to 1.4 described in the general remarks (7.1.3).

In the absence of an additive, the catalytic reaction displayed hardly any conversion (table 17, entry 1), incorporation of pivalic acid (entry 2) improved the coupling of the xanthine with bromobenzene to 35% and 83% yield after 2.5 and 13 hours, respectively. Our difunctional

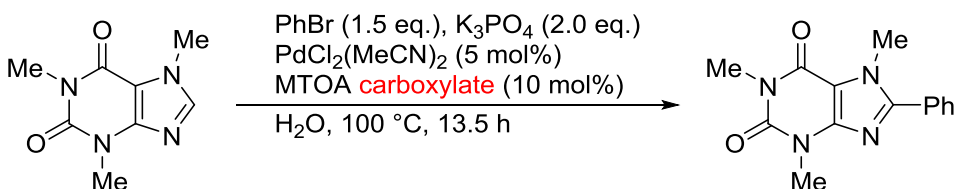
²⁵ Evaporation of residual DMF was performed at 15 mbar and 50 °C. Additionally, condensing drops of solvent at the splash protection were gently heated with the aid of a heat-gun to facilitate their removal.

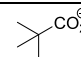
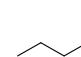
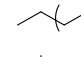
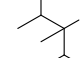
onium carboxylates dramatically accelerated the progression of the reaction in all cases. All salts tested induced near quantitative consumption of caffeine with similar amounts of target material being formed after 13 hours. Differences in reactivity were best observed after 2.5 hours. Tetrabutylammonium salts of pivalic, valproic, and 2,2-dimethyldecanoic acid produced equal quantities of product, reacting 1.4 times faster compared to pivalic acid (entries 3-5). Remarkably, NBu₄DiPP almost doubled the rate of formation of phenylcaffeine, accompanied by an equally high conversion of caffeine (entry 6).

In most instances, MTOA carboxylates, which are ionic liquids, delivered slightly higher yields (entries 7-10). We assume that the model reaction profits from the superior PTC functionality of this cation. To facilitate dropwise dosing MTOA salts by syringe, the ionic liquids were gently heated with the aid of a water bath (45 °C) into order to further liquefy them. Still, ionic liquid type salts impeded an accurate addition, often entailing larger amounts of ions added (1-2 mol%). Even though it would involve an additional preparation step, the precision of salt addition could be increased by the use of stock solutions in DMF. Yet, considering the impurity present in our MTOA salts, namely the hydrogen carbonate anion, use of a minor excess of additive should not implicate crucial differences. Benzyl trimethylammonium DiPP presented identical results to other DiPP salts. Among our difunctional onium carboxylates, diisopropyl propionate additives clearly depicted superior reactivity as well as handling, especially those of tetrabutyl- and benzyl trimethylammonium.

Surfactants promote micellar catalysis in aqueous reaction media without the addition of organic cosolvents.^[76b,89] We wanted to investigate feasibility of arylating of caffeine in water by employing our MTOA salts. Accurate dosing of these viscous compounds was again rather difficult. Unlike in conventional purification by flash column chromatography, reaction mixtures were diluted with saturated aqueous NaCl and subsequently extracted multiple times with dichloromethane. Spectral analysis of crude products revealed no conversion to the desired product for all salts (table 18, entries 1-4). Next to the signals of caffeine, other singlets and multiplets appeared in the spectra. These signals could not be assigned to other xanthine alkaloids, including theophylline, theobromine and paraxanthine, which might have originated by demethylation. Assuming the presence of methyl groups in the unidentified side product, the impurity adds up to an average of 20%. The distressingly low recovery can most likely be blamed to loss of the starting material, including its decomposition products, in the aqueous phase, or to sublimation of the former in the rotary evaporator.

Table 18. Attempted arylation of caffeine in water.^a MTOA = methyltrioctylammonium; caff. = caffeine; Phcaff. = phenylcaffeine; s.p. = side-product.



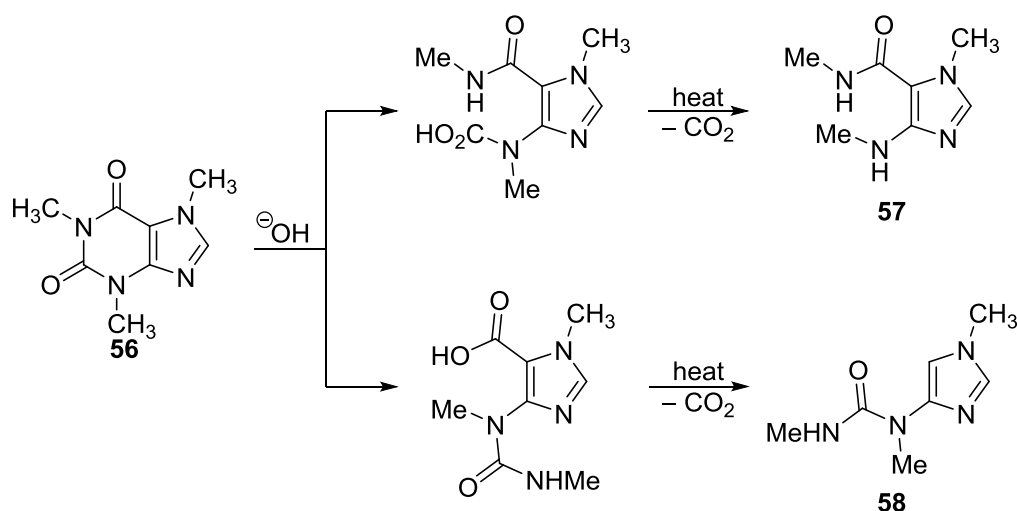
entry	carboxylate	caff. [%]	Phcaff. [%]	s.p. [%]	recov. [%]
1		41	<1	23	64
2		42	<1	24	66
3		45	<1	20	65
4		48	<1	17	65

^aReactions performed with 500 μmol caffeine in water (1.5 mL) according to GP 4.4 (see 7.2.4.1); spectral yield according to $^1\text{H-NMR}$ against internal standard, given in mol%.

The presence of a yet unidentified side product did not satisfy our investigations. With the aid of 2D-NMR analysis (^{13}C , COSY, HSQC, HMBC), we wanted to tackle the identification of the latter. Over time, a decrease in signal intensity was observed, indicating further decomposition taking place. At such low concentrations²⁶ accurate coupling patterns, especially long-range, were not detected. While searching literature concerning the degradation of caffeine^[90], we encountered a paper^[90d] dealing with the behavior of caffeine in alkaline aqueous solution. In dilute hydroxide solution, both carbonyl groups are at risk of nucleophilic attack. The authors clarified the hydrolysis of caffeine (**56**) followed by subsequent decarboxylation (scheme 38). Either way two imidazole compounds were obtained: caffeidine (**57**) or *N*-(4-1-methylimidazolyl)-*N,N'*-dimethylurea (**58**). Comparison of reported NMR shifts with our signal set²⁷ confirmed the presence of imidazole **57** in our crude products, clarifying the riddle. Other derivatives or intermediates of the beneath decomposition cannot be excluded but were not quantified due to overlay of signals of weak intensity. Hence, we concluded to best leave the case unsolved^[91].

²⁶ Most of the crude products except for q-NMR samples (4 counted) were already discarded prior 2D analysis.

²⁷ δ 2.88 (d, $J = 4.6$ Hz, 3H), 3.20 (s, 3H), 3.66 (s, 3H), 6.36 (d, $J = 1.5$ Hz, 1H), 7.18 (d, $J = 1.5$ Hz, 1H), 8.49 (br s, 1H).



Scheme 38. Decomposition of caffeine in alkaline solution reported by Kigasawa et al.^[90d]

Besides the arylation of caffeine, we wanted to employ our most promising difunctional onium carboxylate salt, NBu₄DiPP, in other state-of-the-art coupling reactions. The group of Fagnou described the arylation of benzene for a range of aryl bromides, one of the most prominent examples of CMD additive assisted catalysis.^[8f] While leaving any additional carboxylic acid out only led to <5% conversion, the incorporation of pivalic acid led to enhanced reactivity by acting as proton shuttle. Following their standard procedure, we chose 2-bromonaphthalene and 4-bromoanisole as model substrates to investigate the compatibility of our preferred additive salt NBu₄DiPP (**47**, table 19).

Table 19. Incorporation of NBu₄DiPP in the palladium-catalyzed benzene C–H arylation.^a DavePhos = 2-dicyclohexylphosphino-2'-(*N,N*-dimethylamino)biphenyl; DiPP = diisopropyl propionate; DMAc = dimethylacetamide; recov. = recovery; lit. = literature.

entry	substrate	ArBr [%]	ArH [%]	ArAr [%]	yield [%]	recov. [%]	lit. yield [%]
1		20	22 ^b	<1	57	99	55 ^[8f]
2		18	1 ^c	5	64	93	- ^d

^aReactions performed with 500 μmol of aryl bromide in DMAc (2.9 mL) and benzene (2.5 mL) according to GP 4.5 (see 7.2.4.1); spectral yield according to ¹H-NMR against internal standard, given in mol%. ^bSignals overlay with other compounds. ^cVery small signal in the ¹H-NMR spectrum. ^dNo yield given in the literature for this catalyst system.

As in the case of pivalic acid, 2-bromonaphthalene was converted in good yield along with unreacted and hydrodebrominated aryl halide (entry 1). Fagnou and coworkers used 4-

bromoanisole only for kinetic isotope effect experiments, not indicating the actual yield of the reaction.^[8f] However, regioisomeric 3-bromoanisole afforded 69% of target material. In our case, 4-bromoanisole was arylated in good yield with minor amounts of side-products (entry 2). Losses in recovery were most likely due to the volatility of the aryl bromide and the dehalogenated arene. Even after intense rinsing of glassware in contact with the crude product, the characteristic smell of 4-bromoanisole was still perceived. Further optimization of the reaction, e.g. ligand, metal precatalysts, was not conducted.

Complementary work by the group of Fagnou^[8b] dealt with the arylation of other heterocycles, including (benzo)thiophene, (benzo)furans, imidazoles, and pyrroles. Kinetic experiments revealed the pivotal role of pivalic acid as CMD additive, leading to significantly accelerated reactions. A few years later, Kappe and coworkers reported the microwave assisted arylation of heteroaromatic compounds.^[8c] With reaction temperatures of 180 °C coupling times were remarkably reduced down to a few minutes. To underline the practicability of our NBu₄DiPP salt, we envisaged the coupling of two heterocycles with a few aryl bromides (table 20).

Table 20. Incorporation of NBu₄DiPP in the palladium-catalyzed direct C–H arylation of heteroaromatic compounds.^a HetAr = heteroaromatic arene; DiPP = diisopropyl propionate; DMAc = dimethylacetamide; lit. = literature.

entry	ArBr	HetAr [eq.]	product	t [h]	yield [%]	lit. yield [%]
1				18	42	34 ^b /68 ^c
2				18	13 ^d	<5 ^b /55 ^c
3				4	58	65 ^b /55 ^c
4				18	76	- ^b /55 ^c

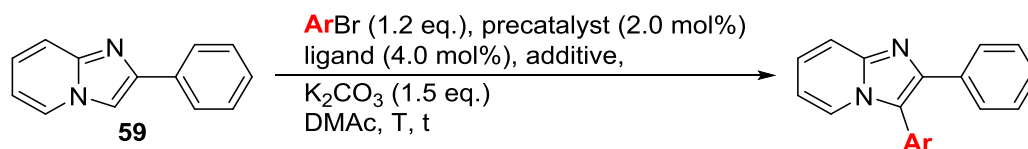
^aReactions performed with 1.00 mmol of aryl bromide (1.0 eq.) in DMAc (2.0 mL) according to GP 4.6 (see 7.2.4.1); spectral yield according to ¹H-NMR with internal standard (1,3,5-trimethoxybenzene), given in mol%. ^bIsolated yield as described by the group of Fagnou.^[8b] Reaction conditions: aryl bromide (1.0 eq.), heterocycle (1.0 eq.), Pd(OAc)₂ (2.0 mol%), PCy₃·HBF₄ (4.0 mol%), PivOH (0.3 eq.) and K₂CO₃ (1.5 eq.) in DMAc (0.3 M) for the indicated time at 100 °C. ^cIsolated yield as described by the group of Kappe.^[8c] Reaction conditions: aryl bromide (1.0 eq.), heterocycle (1.1-1.5 eq.), Pd(OAc)₂ (1.0-2.0 mol%), PCy₃ (2.0-4.0 mol%), PivOH (0.3 eq.) and K₂CO₃ (1.5 eq.) in DMF (0.5 M) for short periods of time (10-60 min) at 180 °C in a sealed vessel using single-mode microwave heating (Monowave 300). ^dAdditional 11% of C3-arylated product.

Due to strong overlay of signals as well as partial loss of reactants by work-up techniques (solubility in water, rotary evaporator), a discussion of recovered or decomposed material is left out. Whereas microwave heating promoted the reactivity of the imidazole ring for C–H arylation (68%),^[8c] the reaction of 1-methylimidazole with 4-bromoanisole yielded 42% of arylated species with our salt (entry 1), within the range of Fagnou et al.^[8b] (34%). None of the bromopyridines (*o*, *m*, *p*) used underwent notable reaction (<5%) under Fagnou's original conditions. Owing to the high temperature employed, Kappe and coworkers enabled the arylation in 55% yield.^[8c] In our case at 100 °C, spectral analysis confirmed the formation of desired 2-substituted benzothiophene (13%) (entry 2), demonstrating higher activity of our salt compared to pivalic acid. Near identical amounts of 2-(benzothiophene-3-yl)pyridine (11%) as side product were also detected. Similar to the reported methods, the less activated electrophile 4-bromoanisole afforded arylated target material in 58% after four hours (entry 3). Unsubstituted benzothiophene was readily converted to the 2-naphthyl derivative in good yield (76%), surpassing Kappe's results obtained at higher temperature^[8c] (entry 4).

Regarding our previous results, NBu₄DiPP efficiently promoted the C–H arylation of several heterocycles. To further highlight the beneficial nature of our difunctional onium carboxylate, we monitored a comparative kinetic profile of a C–H arylation reaction. The groups of Marchand and Bazin prepared 2,3-diarylimidazo[1,2-*a*]pyridines through a Suzuki coupling–direct arylation sequence.^[8d] Our focus lay on the second part of the functionalization. 2-Phenylimidazo[1,2-*a*]pyridine (**59**) was readily available in 64% yield by the one-pot Tschitschibabin method reported by Tomoda et al.^[92] The structural motif of the substrate was particularly interesting due to its characteristic signal shifts and splitting, allowing a straightforward, quantitative ¹H-NMR analysis of crude mixtures. Optimal conditions to run a kinetic study were determined by a small set of screening experiments (table 21). The combination of Pd(OAc)₂ with PCy₃ and our difunctional onium salt quantitatively yielded the desired product with both aryl bromides (entries 1 and 2). Reducing the amount of additive (from 0.3 down to 0.1 equivalents) did not affect the outcome of the reaction (entry 3); in fact even after leaving the latter completely away (entry 4). We supposed that the acetate counterion from the metal precursor exhibits a minor CMD effect. The following entries were deduced from kinetic monitoring of reactions mixtures. To cancel any influence of the precatalyst, PdCl₂(MeCN)₂ in combination with PCy₃ was applied, which showed only moderate conversion after 24 hours (entry 5). Indeed, Pd(OAc)₂ significantly promoted the cross-

coupling with excellent yield after two hours (entry 6). Employing NBu₄DiPP accelerated the reaction, showing quantitative conversion to the arylated heterocycle (entry 7). Regarding our findings, we expected a concurrent coordination of Pd metal between ligand and CMD additive. In fact, by dismissing any additional ligand, we managed an acceleration of the reaction rate, delivering similar amounts of arylated target material after only 15 minutes (entry 8). Under these conditions, the reaction would be too fast for any kinetic study. Small time differences, even seconds, between samples withdrawn would lead to considerable deviations. Whereas lowering of the temperature to 60 °C mainly stopped the reaction (entry 9), optimal conditions were established at 90 °C (entry 10).

Table 21. Incorporation of NBu₄DiPP in the palladium-catalyzed direct C–H arylation of 2-phenylimidazo[1,2-a]pyridine (**59**).^a DMAc = dimethylacetamide; Tol = tolyl; DiPP = diisopropyl propionate.



entry	ArBr	pre-catalyst	ligand	additive [eq.]	T [°C]	t [h]	59 [%]	yield [%]
1	PhBr	Pd(OAc) ₂	PCy ₃	NBu ₄ DiPP (0.3)	100	18	<1	93
2	4-TolBr	Pd(OAc) ₂	PCy ₃	NBu ₄ DiPP (0.3)	100	13	<1	95
3	4-TolBr	Pd(OAc) ₂	PCy ₃	NBu ₄ DiPP (0.1)	100	13	<1	93
4	4-TolBr	Pd(OAc) ₂	PCy ₃	-	100	13	<1	94
5 ^b	4-TolBr	PdCl ₂ (MeCN) ₂	PCy ₃	-	100	24	25	67
6 ^b	4-TolBr	Pd(OAc) ₂	PCy ₃	-	100	2	<1	95
7 ^b	4-TolBr	PdCl ₂ (MeCN) ₂	PCy ₃	NBu ₄ DiPP (0.1)	100	0.5	2	95
8 ^b	4-TolBr	PdCl ₂ (MeCN) ₂	-	NBu ₄ DiPP (0.1)	100	0.25	6	91
9 ^b	4-TolBr	PdCl ₂ (MeCN) ₂	-	NBu ₄ DiPP (0.1)	60	4	89	8
10 ^b	4-TolBr	PdCl ₂ (MeCN) ₂	-	NBu ₄ DiPP (0.1)	90	2	2	93

^aReactions performed with 1.00 mmol of **59** in DMAc (4.0 mL) according to GP 4.7 (7.2.4.1); spectral yield according to ¹H-NMR with internal standard (1,3,5-trimethoxybenzene), given in mol%. ^bKinetic monitoring.

In the following, we compared different conditions to testify the beneficial effect of our difunctional onium carboxylate, NBu₄DiPP as additive in catalysis. The reaction progress is plotted in figure 28 (see 7.2.4.1 – general procedure 4.8 for further details). In all cases, a short initiation phase (5 min) with little conversion is observed. Only after a certain amount of time the reaction mixtures supposedly reached the required temperature for arylation to take place. Whereas Pd(OAc)₂ alone showed slow formation of the product, the reaction profited from both functionalities, the PTC- and the CMD-effect, provided by tetrabutylammonium carboxylates. Again, our promising difunctional onium salt, NBu₄DiPP, proved effective. The latter further

significantly accelerated the rate of the C–H arylation by 20% compared to using NBu₄OPiv as difunctional additive.

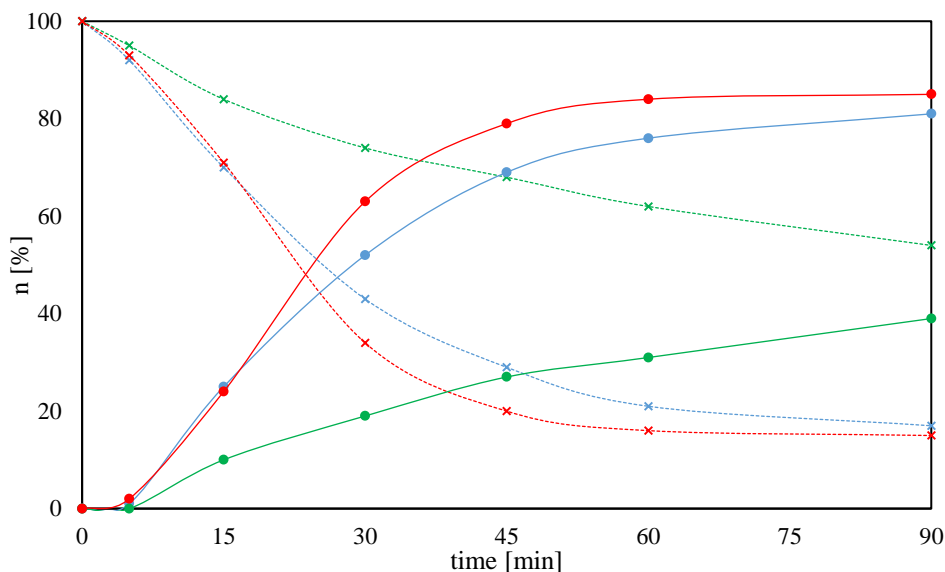


Figure 28. Kinetic study of the C–H arylation of 2-phenylimidazo[1,2-a]pyridine (**59**). Amount of substance (n) plotted against time (min). Dotted line: amount of educt; continuous line: amount of **59**. Green: Pd(OAc)₂; blue: PdCl₂(MeCN)₂, NBu₄OPiv (**49**); red: PdCl₂(MeCN)₂, NBu₄DiPP (**47**).

4.4 Conclusion and outlook

In this chapter, we have proposed to introduce ammonium carboxylate salts as difunctional additives for use in the optimization of catalytic C–H coupling reactions. Such salts are potentially easy to handle and measure out, which makes them convenient additives for catalysis screening. The quaternary ammonium carboxylates can specifically contribute with two or three roles to the improvement of catalytic reactions, namely by inserting (1) a phase-transfer catalyst into the reaction, (2) by providing a CMD-active carboxylate, and (3) by introducing a micelle-forming long-chain carboxylate anion.

Newly synthesized carboxylic acids, acetal **45** and H₂-ESP (**46**), proved minor reactivity in C–H arylation. Further investigations of the latter were not conducted. More promising acids, e.g. PivOH, DiPPA, were combined with ammonium cations leading to difunctional onium carboxylates. Those of NBu₄ or BnNMe₃ were isolated in near quantitative yields via simple titration against phenolphthalein indicator. Initial attempts of merging the cation in Aliquat[®] 336 with carboxylate anions from our acids mostly led to decomposition of the cation. A milder method that excluded any use of strong base solves this synthetic problem. Even though small impurities due to partial hydrolysis of the anion remained, methyltrioctylammonium (MTOA)

methyl carbonate turned out to be an ideal starting material. The anion readily decomposed to easily removable CO₂ and methanol when stirred with carboxylic acids, yielding the carboxylate salts quantitatively. A chiral version of a difunctional ammonium carboxylate could not be isolated. The ease of handling our difunctional onium carboxylates was strongly dependent on the ions involved. MTOA salts presented themselves as ionic liquids. In case of tetrabutylammonium salts, crystallinity decreased with less substituted or long-chain acids. α,α -Diisopropyl propionate salts were easiest to handle, with NBu₄DiPP shown to be more stable than BnNMe₃DiPP.

The application of our salts in C–H coupling reactions allowed for some direct comparisons with established CMD-additives. Compared to pivalic acid itself, enhanced reactivity in the arylation of caffeine was demonstrated, no matter which salt was involved. DiPP salts led to strikingly accelerated conversion of caffeine to phenylcaffeine, underlining the superior role of the difunctional onium carboxylate. MTOA versus tetrabutylammonium compounds showed minor acceleration of the reaction, either owing to superior PTC effects of the cation or greater amounts of ions added. Namely, the viscous nature impeded an accurate dosing of Aliquat[®] derived salts. On the account of surfactants promoting micellar catalysis in water without the addition of organic co-solvents,^[76b,89] we wanted to investigate the arylation of caffeine in aqueous media. Unfortunately, this reaction was unsuitable for the purpose, and no coupling product was detected. The alkaline reaction mixture led to the hydrolysis of the uracil unit followed by decarboxylation. Besides minor amounts of caffeine (57), *N*-(4-1-methylimidazolyl)-*N,N'*-dimethylurea (58) was the major side-product (figure 29).

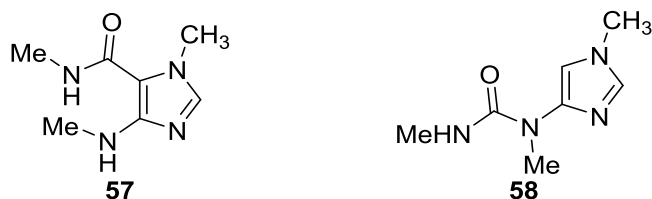


Figure 29. Side-products of the attempted arylation of caffeine in water.

In terms of handling and reactivity, NBu₄DiPP (47) turned out to be the most convincing additive salt. Indeed, benzene as well as several other heterocycles including benzothiophene, and 1-methylimidazol were efficiently arylated in its presence. To underline the superior role played by NBu₄DiPP, we investigated the arylation of 2-phenylimidazo[1,2-*a*]pyridine (59). Enhanced activity was detected when NBu₄DiPP was involved. Kinetic monitoring of the reaction profile revealed a three times faster reaction with NBu₄DiPP compared to Pd(OAc)₂ alone, and 20% faster than NBu₄OPiv (49).

‘Time is money’ has become a common set phrase.^[93] In medicinal chemistry, labeling of pharmaceuticals must occur as fast as possible to prevent any unnecessary decay of the isotope. With half-lives ranging from 20 (¹¹C) to 100 minutes (¹⁸F),^[94] these isotopes are widely used in PET radiology.^[95] Plenty of methods have been established for the synthesis of labelled, aromatic scaffolds.^[96] C–H coupling reactions can strongly profit from both functionalities, PTC and CMD effects. Our difunctional onium carboxylates, especially NBu₄DiPP (**47**), are capable of accelerating C–C-bond forming processes. Potential applications besides preparing PET chemicals lie in accelerating key steps in total syntheses. For example, streptochlorin, a novel antineoplastic agent,^[97] could readily be available via Heck-type C–H coupling of indole with an oxazole electrophile, supported by our additive salt and followed by chlorination (figure 30).

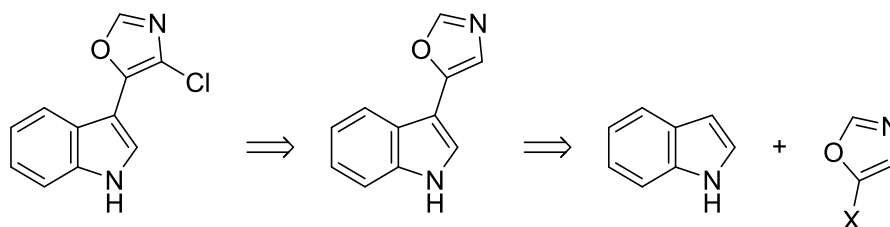


Figure 30. Retrosynthetic sequence of a potential synthesis of streptochlorin. X = leaving group.

Our difunctional onium carboxylates have shown wide application in catalysis, still leaving room for further diversification. Coupling in water which failed with caffeine due to decomposition should be extended to less water- or base-sensitive substrates, e.g. imidazo[1,2-a]pyridines, indoles or other heterocycles. Surfactants including commercially available Kolliphor[®] EL or Triton[™] X-100 as reaction media could also promote the arylation by increased micelle formation.^[89c] Other target anions should include sodium stearate or lauryl sulfate, which can both be expected to display strong micellar effects. Future projects should also tackle the synthesis of chiral carboxylate salts either by introduction of stereochemical information in the cation or anion, e.g. cinchonidinium, *N*-protected amino acids, or axially chiral 1,1'-binaphthyl-2-carboxylic acids. In that manner, the bifunctional role of the additive salts providing both PTC- and CMD-functionality could be complemented with a third role, namely providing chiral induction.

4.5 References

- [1] a) N. Kataoka, Q. Shelby, J. P. Stambuli, J. F. Hartwig, *J. Org. Chem.* **2002**, *67*, 5553-5566; b) G. Altenhoff, R. Goddard, C. W. Lehmann, F. Glorius, *Angew. Chem. Int. Ed.* **2003**, *42*, 3690-3693; c) O. Navarro, R. A. Kelly, S. P. Nolan, *J. Am. Chem. Soc.* **2003**, *125*, 16194-16195; d) W. Su, S. Urgaonkar, P. A. McLaughlin, J. G. Verkade, *J. Am. Chem. Soc.* **2004**, *126*, 16433-16439; e) A. Chartoire, M. Lesieur, L. Falivene, A. M. Slawin, L. Cavallo, C. S. Cazin, S. P. Nolan, *Chem. Eur. J.* **2012**, *18*, 4517-4521; f) G. Bastug, S. P. Nolan, *Organometallics* **2014**, *33*, 1253-1258.
- [2] a) R. Jana, T. P. Pathak, M. S. Sigman, *Chem. Rev.* **2011**, *111*, 1417-1492; b) A. H. Dardir, P. R. Melvin, R. M. Davis, N. Hazari, M. Mohadjer Beromi, *J. Org. Chem.* **2018**, *83*, 469-477; c) A. M. Olivares, D. J. Weix, *J. Am. Chem. Soc.* **2018**, *140*, 2446-2449; d) H. Yue, C. Zhu, M. Rueping, *Angew. Chem. Int. Ed.* **2018**, *54*, 1371-1375; e) T. Zhou, G. Li, S. P. Nolan, M. Szostak, *Org. Lett.* **2019**, *21*, 3304-3309; f) S. L. Helmbrecht, J. Schlüter, M. Blazejak, L. Hintermann, *Eur. J. Org. Chem.* **2020**, 2062-2076; g) M. Schreyer, T. M. Milzarek, M. Wegmann, A. Brunner, L. Hintermann, *ChemCatChem* **2020**, *12*, 152-168.
- [3] a) J. P. Tassone, E. V. England, P. M. MacQueen, M. J. Ferguson, M. Stradiotto, *Angew. Chem. Int. Ed.* **2019**, *58*, 2485-2489; b) E. K. Reeves, J. N. Humke, S. R. Neufeldt, *J. Org. Chem.* **2019**, *84*, 11799-11812; c) M. O. Akram, A. Das, I. Chakrabarty, N. T. Patil, *Org. Lett.* **2019**, *21*, 8101-8105; d) R. M. Shanahan, A. Hickey, L. M. Bateman, M. E. Light, G. P. McGlacken, *J. Org. Chem.* **2020**, *85*, 2585-2596; e) D. S. Surry, S. L. Buchwald, *Angew. Chem. Int. Ed.* **2008**, *47*, 6338-6361; f) S. Koller, M. Blazejak, L. Hintermann, *Eur. J. Org. Chem.* **2018**, *14*, 1624-1633.
- [4] a) Z. Li, S.-L. Zhang, Y. Fu, Q.-X. Guo, L. Liu, *J. Am. Chem. Soc.* **2009**, *131*, 8815-8823; b) J. M. Dennis, N. A. White, R. Y. Liu, S. L. Buchwald, *ACS Catal.* **2019**, *9*, 3822-3830; c) Y. Sunesson, E. Lime, S. O. Nilsson Lill, R. E. Meadows, P.-O. Norrby, *J. Org. Chem.* **2014**, *79*, 11961-11969.
- [5] T. Gensch, F. J. Klauck, F. Glorius, *Angew. Chem. Int. Ed.* **2016**, *55*, 11287-11291.
- [6] a) T. Dohi, M. Ito, K. Morimoto, M. Iwata, Y. Kita, *Angew. Chem. Int. Ed.* **2008**, *47*, 1301-1304; b) M. Börjesson, T. Moragas, R. Martin, *J. Am. Chem. Soc.* **2016**, *138*, 7504-7507; c) T. Moragas, M. Gaydou, R. Martin, *Angew. Chem. Int. Ed.* **2016**, *55*, 5053-5057.

- [7] a) N. Qafisheh, S. Mukhopadhyay, Y. Sasson, *Adv. Synth. Catal.* **2002**, *344*, 1079-1083; b) A. Okada, T. Shibuguchi, T. Ohshima, H. Masu, K. Yamaguchi, M. Shibasaki, *Angew. Chem. Int. Ed.* **2005**, *44*, 4564-4567.
- [8] a) D. Zhao, W. Wang, S. Lian, F. Yang, J. Lan, J. You, *Chem. Eur. J.* **2009**, *15*, 1337-1340; b) B. Liegault, D. Lapointe, L. Caron, A. Vlassova, K. Fagnou, *J. Org. Chem.* **2009**, *74*, 1826-1834; c) M. Baghbanzadeh, C. Pilger, C. O. Kappe, *J. Org. Chem.* **2011**, *76*, 8138-8142; d) S. Marhadour, M.-A. Bazin, P. Marchand, *Tetrahedron Lett.* **2012**, *53*, 297-300; e) B. S. Schreib, M. Fadel, E. M. Carreira, *Angew. Chem. Int. Ed.* **2020**, *59*, 7818-7822; f) M. Lafrance, K. Fagnou, *J. Am. Chem. Soc.* **2006**, *128*, 16496-16497.
- [9] a) E. Paetzold, G. Oehme, *J. Mol. Catal. A: Chem.* **2000**, *152*, 69-76; b) N. E. Leadbeater, M. Marco, *J. Org. Chem.* **2003**, *68*, 5660-5667.
- [10] a) C. M. Starks, M. Halper, *Phase-transfer catalysis: fundamentals, applications, and industrial perspectives*, Springer Science & Business Media, **2012**; b) W. P. Weber, G. W. Gokel, *Phase transfer catalysis in organic synthesis, Vol. 4*, Springer Science & Business Media, **2012**.
- [11] C. M. Starks, *J. Am. Chem. Soc.* **1971**, *93*, 195-199.
- [12] E. V. Dehmlow, S. S. Dehmlow, *Phase transfer catalysis*, Wiley-VCH Verlag, Weinheim, **1993**.
- [13] F. A. Carey, R. J. Sundberg, *Advanced organic chemistry: part A: structure and mechanisms*, Springer Science & Business Media, **2007**.
- [14] C. J. Pedersen, *Science* **1988**, *241*, 536-540.
- [15] a) N. Jose, S. Sengupta, J. Basu, *J. Mol. Catal. A: Chem.* **2009**, *309*, 153-158; b) D. J. Sam, H. E. Simmons, *J. Am. Chem. Soc.* **1972**, *94*, 4024-4025; c) K. Nakamura, S. Nishiyama, S. Tsuruya, M. Masai, *J. Mol. Catal.* **1994**, *93*, 195-210.
- [16] G. Pozzi, S. Quici, R. H. Fish, *Adv. Synth. Catal.* **2008**, *350*, 2425-2436.
- [17] D. W. Kim, D.-S. Ahn, Y.-H. Oh, S. Lee, H. S. Kil, S. J. Oh, S. J. Lee, J. S. Kim, J. S. Ryu, D. H. Moon, *J. Am. Chem. Soc.* **2006**, *128*, 16394-16397.
- [18] J. W. Lee, H. Yan, H. B. Jang, H. K. Kim, S. W. Park, S. Lee, D. Y. Chi, C. E. Song, *Angew. Chem. Int. Ed.* **2009**, *48*, 7683-7686.
- [19] a) V. K. Aggarwal, E. Alonso, G. Fang, M. Ferrara, G. Hynd, M. Porcelloni, *Angew. Chem. Int. Ed.* **2001**, *40*, 1433-1436; b) B. S. Donslund, N. I. Jessen, J. B. Jakobsen, A. Monleón, R. P. Nielsen, K. A. Jørgensen, *Chem. Commun.* **2016**, *52*, 12474-12477; c) M. Makosza, M. Wawrzyniewicz, *Tetrahedron Lett.* **1969**, *10*, 4659-4662.

- [20] a) T. Kita, A. Georgieva, Y. Hashimoto, T. Nakata, K. Nagasawa, *Angew. Chem. Int. Ed.* **2002**, *41*, 2832-2834; b) S. K. Madhusudan, G. Agnihotri, D. S. Negi, A. K. Misra, *Carbohydr. Res.* **2005**, *340*, 1373-1377; c) R. Nouguier, M. Mchich, *Tetrahedron* **1988**, *44*, 2477-2481; d) E. Corey, F. Xu, M. C. Noe, *J. Am. Chem. Soc.* **1997**, *119*, 12414-12415; e) K. Maruoka, T. Ooi, *Chem. Rev.* **2003**, *103*, 3013-3028.
- [21] a) R. Pemha, D. E. Pegnyemb, P. Mosset, *Tetrahedron* **2012**, *68*, 2973-2983; b) S. Hanessian, M. Bayrakdarian, X. Luo, *J. Am. Chem. Soc.* **2002**, *124*, 4716-4721; c) E. V. Dehmlow, M. Lissel, *Tetrahedron* **1981**, *37*, 1653-1658.
- [22] a) A. Nelson, *Angew. Chem. Int. Ed.* **1999**, *38*, 1583-1585; b) T. Ooi, K. Maruoka, *Angew. Chem. Int. Ed.* **2007**, *46*, 4222-4266.
- [23] a) U. H. Dolling, P. Davis, E. J. Grabowski, *J. Am. Chem. Soc.* **1984**, *106*, 446-447; b) D. Hughes, U. Dolling, K. Ryan, E. Schoenewaldt, E. Grabowski, *J. Org. Chem.* **1987**, *52*, 4745-4752.
- [24] B. Lygo, P. G. Wainwright, *Tetrahedron Lett.* **1997**, *38*, 8595-8598.
- [25] a) M. Oestreich, *Angew. Chem. Int. Ed.* **2014**, *53*, 2282-2285; b) E. W. Werner, T.-S. Mei, A. J. Burckle, M. S. Sigman, *Science* **2012**, *338*, 1455-1458.
- [26] a) C. M. Avila, J. S. Patel, Y. Reddi, M. Saito, H. M. Nelson, H. P. Shunatona, M. S. Sigman, R. B. Sunoj, F. D. Toste, *Angew. Chem. Int. Ed.* **2017**, *56*, 5806-5811; b) E. Yamamoto, M. J. Hilton, M. Orlandi, V. Saini, F. D. Toste, M. S. Sigman, *J. Am. Chem. Soc.* **2016**, *138*, 15877-15880; c) S. Biswas, K. Kubota, M. Orlandi, M. Turberg, D. H. Miles, M. S. Sigman, F. D. Toste, *Angew. Chem. Int. Ed.* **2018**, *130*, 598-602; d) R. J. Phipps, F. D. Toste, *J. Am. Chem. Soc.* **2013**, *135*, 1268-1271.
- [27] a) N. Miyaura, A. Suzuki, *J. Chem. Soc., Chem. Commun.* **1979**, 866-867; b) N. Miyaura, A. Suzuki, *Chem. Rev.* **1995**, *95*, 2457-2483; c) A. Suzuki, *Proc. Jpn. Acad. Ser. B* **2004**, *80*, 359-371.
- [28] a) A. O. King, N. Okukado, E.-i. Negishi, *J. Chem. Soc., Chem. Commun.* **1977**, 683-684; b) L. Anastasia, E.-i. Negishi, *Org. Lett.* **2001**, *3*, 3111-3113; c) X. Zeng, M. Qian, Q. Hu, E. i. Negishi, *Angew. Chem. Int. Ed.* **2004**, *43*, 2259-2263; d) S. Baba, E. Negishi, *J. Am. Chem. Soc.* **1976**, *98*, 6729-6731.
- [29] a) D. Milstein, J. Stille, *J. Am. Chem. Soc.* **1978**, *100*, 3636-3638; b) J. Stille, B. Groh, *J. Am. Chem. Soc.* **1987**, *109*, 813-817.
- [30] a) E. i. Negishi, *Angew. Chem. Int. Ed.* **2011**, *50*, 6738-6764; b) V. F. Slagt, A. H. de Vries, J. G. De Vries, R. M. Kellogg, *Org. Process Res. Dev.* **2010**, *14*, 30-47.

- [31] K. Tamao, K. Sumitani, M. Kumada, *J. Am. Chem. Soc.* **1972**, *94*, 4374-4376.
- [32] a) Y. Hatanaka, T. Hiyama, *J. Org. Chem.* **1988**, *53*, 918-920; b) T. Hiyama, *J. Organomet. Chem.* **2002**, *653*, 58-61.
- [33] a) S. Tasler, B. H. Lipshutz, *J. Org. Chem.* **2003**, *68*, 1190-1199; b) J. W. Dankwardt, *Angew. Chem. Int. Ed.* **2004**, *43*, 2428-2432; c) S. Lou, G. C. Fu, *J. Am. Chem. Soc.* **2010**, *132*, 1264-1266.
- [34] a) S. Son, G. C. Fu, *J. Am. Chem. Soc.* **2008**, *130*, 2756-2757; b) M. A. Schade, A. Metzger, S. Hug, P. Knochel, *Chem. Commun.* **2008**, 3046-3048; c) D. Haas, J. M. Hammann, R. Greiner, P. Knochel, *ACS Catal.* **2016**, *6*, 1540-1552.
- [35] S.-I. Murahashi, *J. Organomet. Chem.* **2002**, *653*, 27-33.
- [36] M. G. Saulnier, J. F. Kadow, M. M. Tun, D. R. Langley, D. M. Vyas, *J. Am. Chem. Soc.* **1989**, *111*, 8320-8321.
- [37] N. Jabri, A. Alexakis, J. F. Normant, *Tetrahedron Lett.* **1983**, *24*, 5081-5084.
- [38] E. Negishi, S. R. Miller, *J. Org. Chem.* **1989**, *54*, 6014-6016.
- [39] a) R. F. Heck, *Palladium Reactions for Organic Syntheses, Vol. 19*, Academic Press: London, **1985**; b) R. F. Heck, *Org. React.* **2004**, *27*, 345-390; c) H. Dieck, F. Heck, *J. Organomet. Chem.* **1975**, *93*, 259-263.
- [40] L. Cassar, *J. Organomet. Chem.* **1975**, *93*, 253-257.
- [41] a) K. Sonogashira, Y. Tohda, N. Hagihara, *Tetrahedron Lett.* **1975**, *16*, 4467-4470; b) K. Sonogashira, *J. Organomet. Chem.* **2002**, *653*, 46-49; c) Francois Diederich, S. Peter J., *Metal-Catalyzed Cross-Coupling Reactions*, Wiley-VCH, Weinheim, **1998**.
- [42] a) A. F. Littke, G. C. Fu, *J. Org. Chem.* **1999**, *64*, 10-11; b) A. F. Littke, G. C. Fu, *J. Am. Chem. Soc.* **2001**, *123*, 6989-7000; c) M. Kawatsura, J. F. Hartwig, *J. Am. Chem. Soc.* **1999**, *121*, 1473-1478; d) A. Ehrentraut, A. Zapf, M. Beller, *Synlett* **2000**, *11*, 1589-1592; e) W. A. Herrmann, M. Elison, J. Fischer, C. Köcher, G. R. Artus, *Angew. Chem. Int. Ed.* **1995**, *34*, 2371-2374.
- [43] E.-i. Negishi, A. De Meijere, *Handbook of organopalladium chemistry for organic synthesis*, John Wiley & Sons, **2003**.
- [44] B. M. Trost, J. Dumas, M. Villa, *J. Am. Chem. Soc.* **1992**, *114*, 9836-9845.
- [45] R. Stephens, C. Castro, *J. Org. Chem.* **1963**, *28*, 3313-3315.
- [46] K. Okuro, M. Furuune, M. Enna, M. Miura, M. Nomura, *J. Org. Chem.* **1993**, *58*, 4716-4721.

- [47] a) R. Diercks, K. P. C. Vollhardt, *Angew. Chem. Int. Ed.* **1986**, *25*, 266-268; b) K. Nicolaou, C. Hwang, A. Smith, S. Wendeborn, *J. Am. Chem. Soc.* **1990**, *112*, 7416-7418; c) V. Fiandanese, D. Bottalico, C. Cardellicchio, G. Marchese, A. Punzi, *Tetrahedron* **2005**, *61*, 4551-4556.
- [48] a) N. Li, R. K. Lim, S. Edwardraja, Q. Lin, *J. Am. Chem. Soc.* **2011**, *133*, 15316-15319; b) N. E. Leadbeater, B. J. Tominack, *Tetrahedron Lett.* **2003**, *44*, 8653-8656.
- [49] a) G. Dyker, *Handbook of CH transformations: applications in organic synthesis*, Vol. 2, Wiley-VCH, **2005**; b) M. Zhang, *Adv. Synth. Catal.* **2009**, *351*, 2243-2270; c) R. Masuo, K. Ohmori, L. Hintermann, S. Yoshida, K. Suzuki, *Angew. Chem. Int. Ed.* **2009**, *48*, 3462-3465; d) L. Ackermann, R. Vicente, A. R. Kapdi, *Angew. Chem. Int. Ed.* **2009**, *48*, 9792-9826.
- [50] a) L. Ackermann, *Chem. Rev.* **2011**, *111*, 1315-1345; b) Y. Boutadla, D. L. Davies, S. A. Macgregor, A. I. Poblador-Bahamonde, *Dalton Trans.* **2009**, 5820-5831; c) D. Lapointe, K. Fagnou, *Chem. Lett.* **2010**, *39*, 1118-1126.
- [51] a) C. W. Fung, M. Khorramdel-Vahed, R. J. Ranson, R. M. Roberts, *J. Chem. Soc., Perkin Trans. 2* **1980**, 267-272; b) B. Biswas, M. Sugimoto, S. Sakaki, *Organometallics* **2000**, *19*, 3895-3908.
- [52] D. García-Cuadrado, A. A. Braga, F. Maseras, A. M. Echavarren, *J. Am. Chem. Soc.* **2006**, *128*, 1066-1067.
- [53] a) S. I. Gorelsky, D. Lapointe, K. Fagnou, *J. Am. Chem. Soc.* **2008**, *130*, 10848-10849; b) M. Lafrance, S. I. Gorelsky, K. Fagnou, *J. Am. Chem. Soc.* **2007**, *129*, 14570-14571; c) S. I. Gorelsky, D. Lapointe, K. Fagnou, *J. Org. Chem.* **2012**, *77*, 658-668.
- [54] a) L. Ackermann, R. Vicente, A. Althammer, *Org. Lett.* **2008**, *10*, 2299-2302; b) L. Ackermann, A. Althammer, S. Fenner, *Angew. Chem. Int. Ed.* **2009**, *48*, 201-204; c) S. Potavathri, K. C. Pereira, S. I. Gorelsky, A. Pike, A. P. LeBris, B. DeBoef, *J. Am. Chem. Soc.* **2010**, *132*, 14676-14681.
- [55] J. Yamaguchi, A. D. Yamaguchi, K. Itami, *Angew. Chem. Int. Ed.* **2012**, *51*, 8960-9009.
- [56] E. H. Cordes, R. B. Dunlap, *Acc. Chem. Res.* **1969**, *2*, 329-337.
- [57] Y. A. Dyadin, L. S. Aladko, *Mendeleev Commun.* **1995**, *6*, 239-240.
- [58] a) R. Hesse, K. K. Gruner, O. Kataeva, A. W. Schmidt, H. J. Knölker, *Chem. Eur. J.* **2013**, *19*, 14098-14111; b) S. Würtz, S. Rakshit, J. J. Neumann, T. Dröge, F. Glorius, *Angew. Chem. Int. Ed.* **2008**, *47*, 7230-7233; c) V. P. Kumar, K. K. Gruner, O. Kataeva, H. J. Knölker, *Angew. Chem. Int. Ed.* **2013**, *52*, 11073-11077.

- [59] a) D. Mandal, A. D. Yamaguchi, J. Yamaguchi, K. Itami, *J. Am. Chem. Soc.* **2011**, *133*, 19660-19663; b) A. D. Yamaguchi, D. Mandal, J. Yamaguchi, K. Itami, *Chem. Lett.* **2011**, *40*, 555-557; c) P. Xi, F. Yang, S. Qin, D. Zhao, J. Lan, G. Gao, C. Hu, J. You, *J. Am. Chem. Soc.* **2010**, *132*, 1822-1824.
- [60] N. P. Grimster, C. Gauntlett, C. R. Godfrey, M. J. Gaunt, *Angew. Chem. Int. Ed.* **2005**, *44*, 3125-3129.
- [61] A. García-Rubia, B. Urones, R. Gomez Arrayas, J. C. Carretero, *Angew. Chem. Int. Ed.* **2011**, *50*, 10927-10931.
- [62] a) H. Yi, P. Hu, S. A. Snyder, *Angew. Chem. Int. Ed.* **2020**, *59*, 2674-2678; b) H. Nagae, R. Aoki, S. n. Akutagawa, J. Kleemann, R. Tagawa, T. Schindler, G. Choi, T. P. Spaniol, H. Tsurugi, J. Okuda, *Angew. Chem. Int. Ed.* **2018**, *57*, 2492-2496; c) P. Kurcok, M. Śmiga, Z. Jedliński, *J. Polym. Sci., Part A: Polym. Chem.* **2002**, *40*, 2184-2189.
- [63] J. Crowe, T. Bradshaw, *Chemistry for the biosciences: the essential concepts*, Oxford University Press, **2014**.
- [64] J. E. Macintyre, *Dictionary of inorganic compounds*, CRC Press, **1992**.
- [65] L. Rast, *Additive-effects in Pd-catalyzed C-H transformations*, master thesis, Technical University of Munich (Garching bei München), **2019**.
- [66] D. J. Welsh, S. P. Jones, D. K. Smith, *Angew. Chem. Int. Ed.* **2009**, *48*, r4047-4051.
- [67] A. A. Kalathil, A. Kumar, B. Banik, T. A. Ruiter, R. K. Pathak, S. Dhar, *Chem. Commun.* **2016**, *52*, 140-143.
- [68] D. Załubiniak, M. Zakrzewski, P. Piątek, *Dalton Trans.* **2016**, *45*, 15557-15564.
- [69] R. J. Pakula, J. F. Berry, *Dalton Trans.* **2018**, *47*, 13887-13893.
- [70] a) A. Das, Y.-S. Chen, J. H. Reibenspies, D. C. Powers, *J. Am. Chem. Soc.* **2019**, *141*, 16232-16236; b) C. G. Espino, K. W. Fiori, M. Kim, J. Du Bois, *J. Am. Chem. Soc.* **2004**, *126*, 15378-15379.
- [71] R. J. Pakula, M. Srebro-Hooper, C. G. Fry, H. J. Reich, J. Autschbach, J. F. Berry, *Inorg. Chem.* **2018**, *57*, 8046-8049.
- [72] Y. Lou, M. Horikawa, R. A. Kloster, N. A. Hawryluk, E. Corey, *J. Am. Chem. Soc.* **2004**, *126*, 8916-8918.
- [73] P. Klein, *The Multi-Component-Catalyst (MCC) Principle: Designing Functional Catalyst Precursors for Reaction Development*, master thesis, Technical University of Munich (Garching bei München), **2016**.

- [74] a) C. StarEs, C. Liotta, *Phase Transfer Catalyst: Principles and Techniques*, Elsevier Inc., New York, **1978**; b) F. Montanari, D. Landini, F. Rolla, Phase-transfer catalyzed reactions in *Host Guest Complex Chemistry II*, Springer, **1982**, pp. 147-200; c) D. Landini, A. Maia, A. Rampoldi, *J. Org. Chem.* **1986**, *51*, 3187-3191.
- [75] C. M. Starks, C. L. Liotta, M. E. Halpern, *Phase-Transfer Catalysts in Phase-Transfer Catalysis*, Springer, **1994**, pp. 123-206.
- [76] a) J. Blum, I. Amer, A. Zoran, Y. Sasson, *Tetrahedron Lett.* **1983**, *24*, 4139-4142; b) J. Blum, I. Amer, K. P. C. Vollhardt, H. Schwarz, G. Hoehne, *J. Org. Chem.* **1987**, *52*, 2804-2813.
- [77] Y. Badrieh, J. Blum, H. Schumann, *J. Mol. Catal.* **1994**, *90*, 231-244.
- [78] A.-S. Castanet, F. Colobert, J.-R. Desmurs, T. Schlama, *J. Mol. Catal. A: Chem.* **2002**, *182*, 481-487.
- [79] P. Jakubec, A. Hawkins, W. Felzmann, D. J. Dixon, *J. Am. Chem. Soc.* **2012**, *134*, 17482-17485.
- [80] a) E. Corey, M. C. Noe, *J. Am. Chem. Soc.* **1993**, *115*, 12579-12580; b) E. Corey, M. C. Noe, S. Sarshar, *J. Am. Chem. Soc.* **1993**, *115*, 3828-3829.
- [81] S. Rossi, *Australian Medicines Handbook*, Taylor & Francis Group, United States of America, **2013**.
- [82] C. Bolchi, E. Valoti, L. Fumagalli, P. Ruggeri, V. Straniero, M. Pallavicini, *Org. Process Res. Dev.* **2014**, *18*, 976-979.
- [83] a) J. W. Lehman, *Operational organic chemistry: a laboratory course*, Allyn and Bacon New York, **1981**; b) M. Anbar, H. Taube, *J. Am. Chem. Soc.* **1958**, *80*, 1073-1077; c) J. Barry, G. Bram, G. Decodts, A. Loupy, P. Pigeon, J. Sansoulet, *Tetrahedron Lett.* **1982**, *23*, 5407-5408; d) J. H. Ramsden, R. S. Drago, R. Riley, *J. Am. Chem. Soc.* **1989**, *111*, 3958-3961; e) A. Perosa, P. Tundo, M. Selva, S. Zinovyev, A. Testa, *Org. Biomol. Chem.* **2004**, *2*, 2249-2252.
- [84] A. Ladenburg, O. Struve, *Chem. Ber.* **1877**, *10*, 43-49.
- [85] A. Simon, U. Uhlig, *Chem. Ber.* **1952**, *85*, 977-992.
- [86] M. Fabris, V. Lucchini, M. Noe, A. Perosa, M. Selva, *Chem. Eur. J.* **2009**, *15*, 12273-12282.
- [87] a) K. F. Zhang, Z. Y. Cao, G. Q. Zhang, L. S. Xiao, X. Z. Zhou, *Adv. Mater. Res.* **2013**, *781*, 263-271; b) L. E. Walker (Lonza LLC), US 6,784,307 B2, **2004**; c) D. E. Weisshaar, G. W. Earl, M. W. Amolins, K. L. Mickalowski, J. G. Norberg, B. D.

- Rekken, A. M. Burgess, B. D. Kaemingk, K. C. Behrens, *J. Surfactants Deterg.* **2012**, *15*, 199-205; d) R. H. G. Brinkhuis, J. A. J. Schutyser, P. J. Dolphijn, A. J. W. Buser, P. J. M. D. Elfrink, M. A. Gessner, M. D. Shalati (Allnex Netherlands BV), US 8,962,725 B2, **2015**.
- [88] a) R. Harner, J. Sydnor, E. Gilreath, *J. Chem. Eng. Data* **1963**, *8*, 411-412; b) J. Burgess, H. Press, **1978**.
- [89] a) A. Chanda, V. V. Fokin, *Chem. Rev.* **2009**, *109*, 725-748; b) Y. Hayashi, *Angew. Chem. Int. Ed.* **2006**, *45*, 8103-8104; c) B. H. Lipshutz, B. R. Taft, *Org. Lett.* **2008**, *10*, 1329-1332; d) B. H. Lipshutz, D. W. Chung, B. Rich, *Org. Lett.* **2008**, *10*, 3793-3796; e) B. H. Lipshutz, G. T. Aguinaldo, S. Ghorai, K. Voigtritter, *Org. Lett.* **2008**, *10*, 1325-1328; f) B. H. Lipshutz, A. R. Abela, *Org. Lett.* **2008**, *10*, 5329-5332.
- [90] a) G. Ngueta, *Eur. J. Clin. Nutr.* **2019**, 1-10; b) R. Rosal, A. Rodríguez, J. A. Perdigón-Melón, A. Petre, E. García-Calvo, M. J. Gómez, A. Agüera, A. R. Fernández-Alba, *Chemosphere* **2009**, *74*, 825-831; c) J. P. Telo, A. J. Vieira, *J. Chem. Soc., Perkin Trans. 2* **1997**, 1755-1758; d) K. Kigasawa, K. Ohkubo, H. Shimizu, T. Kohagizawa, R. Shoji, *Chem. Pharm. Bull.* **1974**, *22*, 2448-2451.
- [91] *This is Spinal Tap*, directed by R. Reiner, **1984** U.S.
- [92] H. Tomoda, T. Hirano, S. Saito, T. Mutai, K. Araki, *Bull. Chem. Soc. Jpn.* **1999**, *72*, 1327-1334.
- [93] a) J. W. Payne, J. R. Bettman, M. F. Luce, *Organ. Behav. Hum. Decis. Process.* **1996**, *66*, 131-152; b) M. E. Gallagher, *Stud. Comp. Int. Dev.* **2004**, *39*, 11-44; c) M. G. Kocher, M. Sutter, *J. Econ. Behav. Organ.* **2006**, *61*, 375-392; d) S. E. DeVoe, J. Pfeffer, *Organ. Behav. Hum. Decis. Process.* **2007**, *104*, 1-13; e) M. Jäckel, S. Wollscheid, *J. Leis. Res.* **2007**, *39*, 86-108.
- [94] G. Audi, F. Kondev, M. Wang, W. Huang, S. Naimi, *Chin. Phys. C* **2017**, *41*, 030001.
- [95] a) P. Hantraye, A. Brownell, D. Elmaleh, R. Spealman, U. Wüllner, G. Brownell, B. Madras, O. Isacson, *Neuroreport* **1992**, *3*, 265-268; b) R. M. Kwee, *Radiology* **2010**, *254*, 707-717; c) M. H. Umbehr, M. Müntener, T. Hany, T. Sulser, L. M. Bachmann, *Eur. Urol.* **2013**, *64*, 106-117; d) W. Chen, D. H. Silverman, S. Delaloye, J. Czernin, N. Kamdar, W. Pope, N. Satyamurthy, C. Schiepers, T. Cloughesy, *J. Nucl. Med.* **2006**, *47*, 904-911.

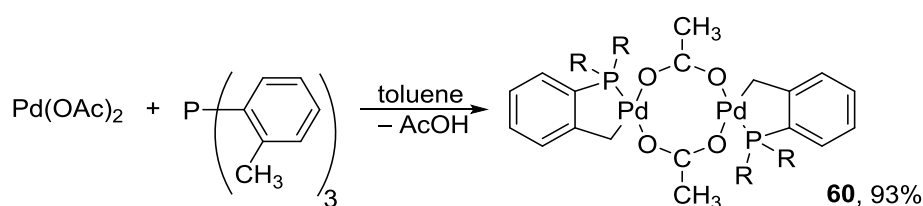
- [96] a) H. Doi, M. Goto, M. Suzuki, *Bull. Chem. Soc. Jpn.* **2012**, *85*, 1233-1238; b) H. Yang, P. G. Dormer, N. R. Rivera, A. J. Hoover, *Angew. Chem. Int. Ed.* **2018**, *57*, 1883-1887; c) H. Doi, *J. Labelled Compd. Radiopharm.* **2015**, *58*, 73-85.
- [97] T. W. Kwak, H. J. Shin, Y.-I. Jeong, M.-E. Han, S.-O. Oh, H.-J. Kim, D. H. Kim, D. H. Kang, *Drug Des. Dev. Ther.* **2015**, *9*, 2201.

**5 BENZYL, VINYL AND CYCLOHEPTATRIENYL PHOSPHONIUM SALTS:
MOLECULAR STOREHOUSE FOR AIR-SENSITIVE LIGANDS**

This chapter is divided in four main sections. In the beginning, the unifying subject, phosphines and their salts, is briefly presented (5.1). The first sub-chapter deals with benzyl and vinyl phosphonium salts (5.2). Their synthesis (5.2.1), isomerization (5.2.2), attempted release of free phosphine (5.2.3) as well as their application in catalysis (5.2.4) are depicted. Similarly, the specific case of cycloheptatrienyl (CHT) phosphonium salts are discussed in the third section of this chapter (5.3). Their synthesis and characterization by X-ray diffraction (5.3.1) reveals a susceptible electrocyclic rearrangement (5.3.3). CHT salts are subjected to different nucleophilic agents and conditions to testify their capability for ligand release (5.3.4). Direct comparison of quaternary cycloheptatrienyl salts with their free phosphine analogue permits us to evaluate their performance in catalysis (5.3.5). The conclusion and outlook (5.4) close this chapter. To present the full overview of this topic, results of the preceding master thesis have been included in the discussion.^[1]

5.1 Introduction

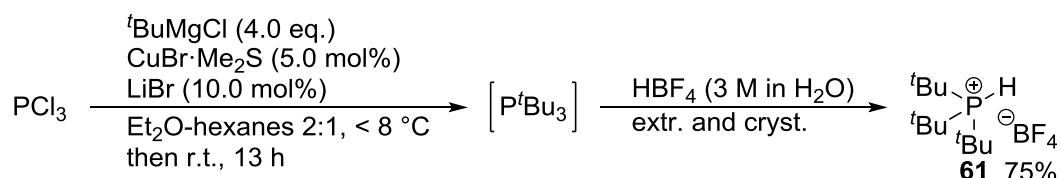
Ligand design is a central topic in today's homogeneous catalysis.^[2] Phosphines are among the most commonly used steering ligands. Triarylphosphines, and triphenylphosphine in particular, have been preferred for a long time due to their availability, stability and simple modification.^[3] Tri-*ortho*-tolylphosphine was among the first examples of a phosphine with increased steric hindrance, designed to suppress quaternization at phosphorus, and simple modification. It also displayed high activity in diverse Heck coupling reactions.^[4] Later, Herrmann and Beller showed that its superior reactivity is owed to the formation of a thermally robust palladacycle **60** (scheme 39).^[5]



Scheme 39. Formation of Herrmann-Beller catalyst from Pd(OAc)₂ and P(*o*-Tol)₃.^[5] R = *o*-Tol; Tol = tolyl.

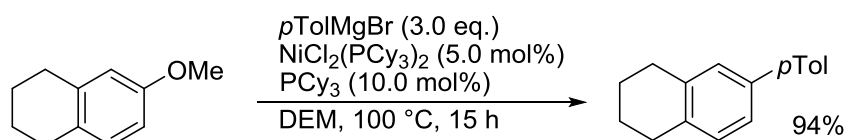
Even though trialkylphosphines have been neglected in the beginning, growing evidence proved their superior role due to electron-richness and bulky sterics. A major drawback of trialkylphosphines lies in their high sensitivity towards oxygen, with which they readily furnish the corresponding phosphine oxides. The broadly applicable *tert*-butyl phosphine derivatives^[6] suffer from fast radical chain oxidation^[7] in particular. The group of Fu purposed to circumvent this problem by protonation the free ligand with HBF₄, yielding air-stable quaternary,

protonated trialkylphosphonium salts.^[8] In combination with a weak base, the ligand is liberated from the salt and available for coordination to a metal center. The synthesis of tri-*tert*-butylphosphonium tetrafluoroborate (**61**) is representative of this approach and has been improved by Cramer and coworkers such that no air-sensitive intermediates need to be isolated (scheme 40).^[9] Use of a copper(I) salt as a catalyst in the alkylation of PCl_3 with Grignard reagent significantly increased the reaction rate.



Scheme 40. Synthesis of $(t\text{Bu})_3\text{P}\cdot\text{HBF}_4$ (**61**) by Cramer et al.^[9] extr. = extraction; cryst. = crystallization.

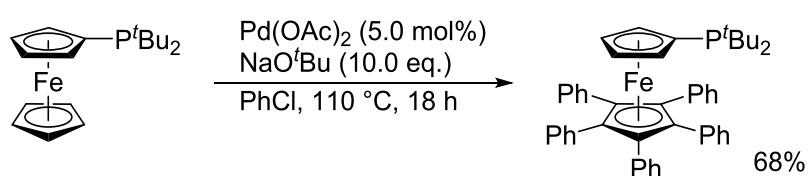
Next to tri-*tert*-butylphosphine, tricyclohexylphosphine has experienced widespread use.^[10] In combination with $\text{Pd}(\text{OAc})_2$, PCy_3 prevailed as best ligand in Suzuki-^[6a,10e] or Kumada-type^[10d] coupling reactions. The precatalyst $\text{PdCl}_2(\text{PCy}_3)_2$ enabled the reaction of highly activated aryl chlorides with arylboronic acids.^[11] Whereas a $\text{Pd}/\text{P}^t\text{Bu}_3$ catalyst system efficiently promotes Heck coupling of less activated aryl chlorides, Pd/PCy_3 seems to fail.^[12] The observed reluctance of $\text{Pd}(\text{PCy}_3)_2\text{HCl}$ to undergo reductive elimination to $\text{Pd}(\text{PCy}_3)_2$, thus regenerating $\text{Pd}(0)$, explains the low reactivity of Pd/PCy_3 in Heck reactions of aryl chlorides.^[13] In Suzuki coupling, ligand dependent chemoselectivity has been demonstrated with 4-chlorophenyl triflate.^[14] While $\text{Pd}/\text{P}^t\text{Bu}_3$, formed in situ from $\text{Pd}_2(\text{dba})_3$ and P^tBu_3 ,^[15] exclusively activates the C–Cl bond, reaction at the triflate moiety^[16] occurs with $\text{Pd}(\text{PCy}_3)_2$.^[6e,17] Computational studies by the group of Schoenebeck have revealed the rationale for the reversed regioselectivity.^[18] The monoligated Pd species reacts preferentially with C–Cl due to ease of distortion. However, dispersion effects favor the more nucleophilic intermediate, PdL_2 , whose reactivity is controlled by HOMO–LUMO interaction. In nickel-type chemistry, Dankwardt described the cross-coupling of Grignard reagents with aromatic alkyl ethers using $\text{NiCl}_2(\text{PCy}_3)_2$ and related derivatives as catalysts (scheme 41).^[19] Plenty of other examples have dealt with coupling reactions involving a Ni/PCy_3 (or Rh) catalyst system.^[20]



Scheme 41. Ni-catalyzed cross-coupling of Grignard reagents with aromatic alkyl ether according to Dankwardt.^[19]

Even though trialkylphosphines suffer from air-sensitivity, bulky derivatives seem to be stable in the solid state due to their crystallinity.^[21] With a melting point of >350 °C, triadamantylphosphine is stable in air for weeks, but readily oxidizes when exposed to air in solution. Under mild conditions, this bulky phosphine enabled the coupling of base sensitive polyhaloboron reagents with aryl bromides.^[22] Introduced by Beller et al.^[23], *n*-butyldiadamantylphosphine, known as cataCXium[®] A, proved practical in industrial catalysis.^[24] This mixed ligand permitted the C–H arylation of heterocycles with aryl chlorides,^[25] whereas You et al.^[26] had only succeeded with aryl bromides in their reaction. Other coupling reactions involving BuP(1-Ad)₂ include carbonylations^[27], stereospecific cross-coupling of organotrifluoroborates^[28], aminations^[29], and Heck coupling reactions^[23,30].

With the introduction of their ligand families, Buchwald in particular and Hartwig have revolutionized cross-coupling chemistry, not only in the amination of aryl halides.^[31] Whereas Hartwig relies on ferrocenyldialkylphosphines, Buchwald sticks to monodentate, bulky, and electron-rich dialkylbiarylphosphines. Interestingly, FcP^tBu₂ (Fc = ferrocenyl) in combination with Pd₂(dba)₃ only showed enhanced reactivity after an extended induction period.^[32] Observations from kinetics revealed an initial consumption of aryl bromide, with no product formation, pointing to a side-reaction taking place. Indeed, the ligand itself underwent perphenylation of the lower ferrocene ring furnishing the actual ligand of the active catalyst system, which displays high activity by virtue of its bulky nature (scheme 42).



Scheme 42. Ligand modification to QPhos in the aromatic C–O bond formation as described by Hartwig et al.^[32] Buchwald ligands exhibit a basic structure in which each substituent exhibits a distinct role (figure 31).^[33] **Alkyl groups** at the phosphorus atom increase electron density at phosphorus, enhancing the rate of oxidative addition. Bulky substituents likewise promote ligand dissociation, thus favoring generation of reactive [L₁Pd⁰] (L₁ = Buchwald ligand) species. Finally, the bulk of L in [L₁Pd⁰Ar(Nuc)] (Ar = aryl group, Nuc = nucleophile) aids in the reductive elimination of coupling product Ar–Nuc. The expansion of ligand size by introduction of the **lower ring** reduces the phosphine's propensity for oxidation. Due to stabilization of Pd–arene interactions, reductive elimination is preferred. While **para-substitution** of the lower ring usually emerges using more convenient synthesis procedures, **ortho-functionalization**

prevents cyclometallation. Steric bulk supports the formation of $[L_1Pd^0]$ species. Further **substitution of the upper ring** simulates the conformation of PR_2 over the bottom ring, hence abetting reductive elimination. Buchwald ligands are easily available on large scale (>10 kg) in a direct one-pot procedure.^[34] Conventional synthetic methods include the addition of an aryl Grignard or an aryllithium reagent to a benzyne intermediate generated in situ from the appropriate dihalobenzene. With the aid of CuCl catalysis, trapping of the biaryl Grignard intermediate with the corresponding dialkylchlorophosphine yields the desired phosphine. In figure 31 the most commonly used Buchwald ligands are depicted. With profound application in amination reactions^[35], fluorination of aryl (pseudo)halides^[36], or other reactions^[37], these ligands play an integral part in today's homogeneous catalysis. The most recent achievement of Buchwald et al. is the development of terphenyl ligand AlPhos that enables the fluorination of aryl (pseudo)halides at room-temperature.^[36d] Lately, AlPhos has also permitted the use of soluble, organic bases in C–N coupling reactions, as opposed to strong inorganic bases.^[38]

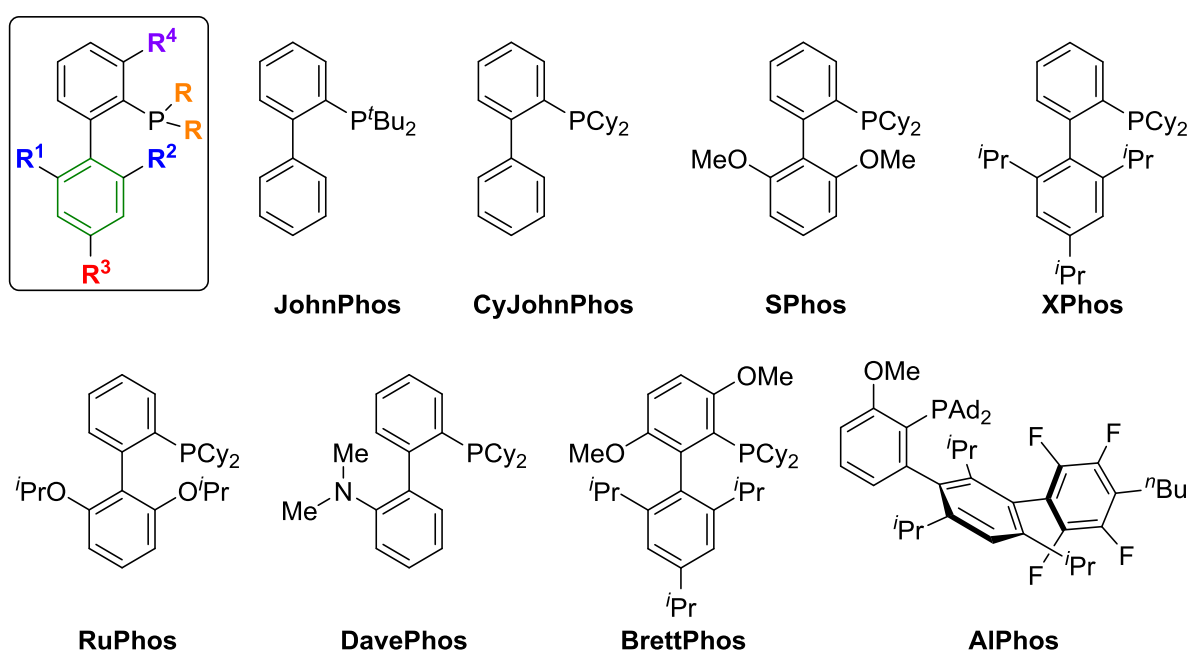


Figure 31. Selection of typical Buchwald ligands.^[33,36d] Ad = 1-adamantyl.

A third class of phosphine ligands was established by Stradiotto and coworkers who explored chelating P,N-^[39] or P,P-^[40] ligands (figure 32). Compared to the rather harsh conditions of Buchwald^[36f] and Hartwig^[41], the use of Mor-DalPhos allowed the coupling of aryl chlorides and tosylates with ammonia^[42] to proceed at room temperature. Shortly after, Stradiotto and coworkers reported additional application in the cross-coupling with hydrazine^[43], gold-catalyzed hydroamination of alkynes with dialkylamines^[44], as well as the mono- α -arylation of

acetone^[45]. The introduction of sterically demanding, yet electron poor bisphosphane PAd-DalPhos gave access to an air-stable Ni^{II}-precatalyst.^[46] The latter is capable of coupling a broad range of (hetero)aryl halides and sulfonates with plenty of amines, including gaseous ammonia. Variations in phosphorus substitution further extended nickel-catalyzed cross-coupling of aryl electrophiles with aliphatic alcohols^[47], sulfonamides^[48], and bulky primary alkylamines^[49].^[50]

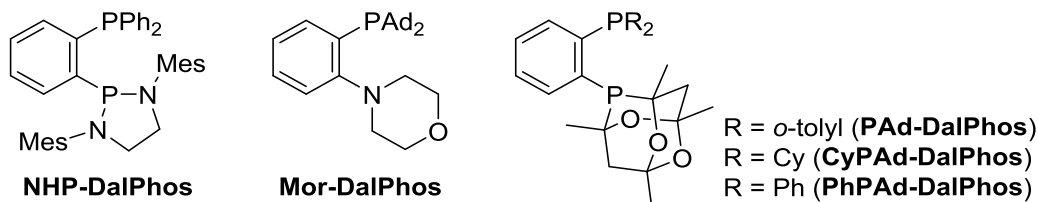


Figure 32. Examples of chelating P,N- and P,P-ligands described by Stradiotto et al. Mor = morpholine; NHP = N-heterocyclic phosphine.

Due to their big size and extended substitution pattern, the Buchwald, Hartwig and DalPhos ligands feature high stability towards oxygen. However, this does not apply to all ligands likewise, and the least so for trialkylphosphines or for many ligands in the dissolved state. Thus, Protonation of trialkylphosphines as introduced by the group of Fu^[8], was welcomed^[51] as facilitating the handling of air-sensitive phosphines. The suitability of protonated *tert*-phosphanes as ligand precursors appears evident. An even better protection of the phosphorus center is arguably provided by quaternization of phosphanes with alkyl electrophiles. Numerous quaternary phosphonium salts of the benzyl^[52], vinyl^[53], allyl^[54], and cycloheptatrienyl/norcaradienyl^[55] type exist, yet no reports depict their application as ligand precursors in catalysis. Quaternary phosphonium salts are mostly used as arylating^[56], or coupling reagent^[57] (e.g. PyBrOP[®],²⁸), next to uses as phase-transfer catalysts or ionic liquid reaction media^[60]. Pd- π -complexes of styryl phosphonium salts have been described in the literature.^[61] However, neither applications in catalysis nor the potential release of phosphine have been reported. The group of Fürstner already illustrated the synthesis of gold and rhodium ylide complexes derived from quaternary phosphonium salts^[53], and other groups^[62] have recently dealt with the application of phosphonium ylides as ligands in coupling chemistry.

Tropylium salts are readily available through different procedures.^[63] Among those salts, the perchlorate, hexafluorophosphate and tetrafluoroborate are easiest to handle, due to their

²⁸ PyBrOP[®] = bromotripyrrolidinophosphonium hexafluorophosphate. PyBOP[®], (benzotriazol-1-yloxy)tripyrrolidinophosphonium hexafluorophosphate was introduced by the group of Castro.

stability and non-hygroscopicity compared to the chloride, bromide or iodide.^[63b] The cycloheptatrienyl (CHT) motif permits π -coordination of metal atoms, and several complexes of Pd, Pt, Rh,... including CHT-phosphines or -imidazoles have so far been synthesized, bringing the phosphonium unit in close proximity to the metal center.^[64]

In this project, we want to pursue the isolation of air-stable P-alkylated quaternary phosphonium salts, based on standard tertiary phosphine ligands, and focusing on moderately labile unsaturated groups for quaternization, like benzyl, allyl, vinyl, and cycloheptatrienyl. For the tertiary phosphine platform, we looked towards cyclohexyl-type phosphines, as they have been much spotlighted in catalysis. Compared to a simple protonation (HPCy_3^+), quaternary salts are more stable since there is no danger of reversible proton loss at phosphorus. The ease with which the salts transfer phosphine to a metal precursor is a priori unknown but expected to depend on the structure of the alkyl group. Pre-complexation of the unsaturated phosphonium unit through π -coordination of the metal can be anticipated to play a key role in precatalyst activation.

5.2 Vinylic- and Benzylic- Tricyclohexylphosphonium Salts: Suitable Precursors for Active Catalyst Generation

The following chapter is divided in subsections. First, the synthesis as well as characterization of vinyl and benzyl phosphonium salts will be presented. The isomerization of allyl type salts delivers corresponding vinyl salts. A short excursion on the complexation of Pd to unsaturated phosphonium salts will be illustrated. The efficient release of free PCy₃ ligand from a styryl phosphonium salt will be investigated. Applications of vinyl- and benzyl-phosphonium salts in catalysis end this chapter.

5.2.1 Synthesis of vinylic- and benzylic-tricyclohexylphosphonium salts

In my master thesis, a range of vinylic and benzylic phosphonium salts has already been described (figure 33).^[1] Stirring of the corresponding halides with PCy₃ readily afforded benzyl salts **62** and **63**. In case of trityl chloride, steric crowding hindered substitution at the central C_{sp3}-carbon atom. Nucleophilic attack at the *para*-position of one of the phenyl groups was followed by 1,5-H shift affording **64** in 77% yield. A similar rearrangement had already been noticed in the reaction of PPh₃²⁹ or other phosphines with halo-triphenylmethanes.^[65] Whereas the PPh₃ derivative was available at comparably low temperatures (100 °C),^[61b] the synthesis of PCy₃ salt (**65**) took advantage of microwave assisted heating to 210 °C.

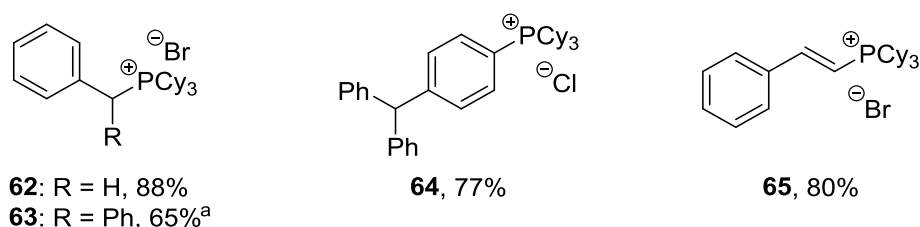


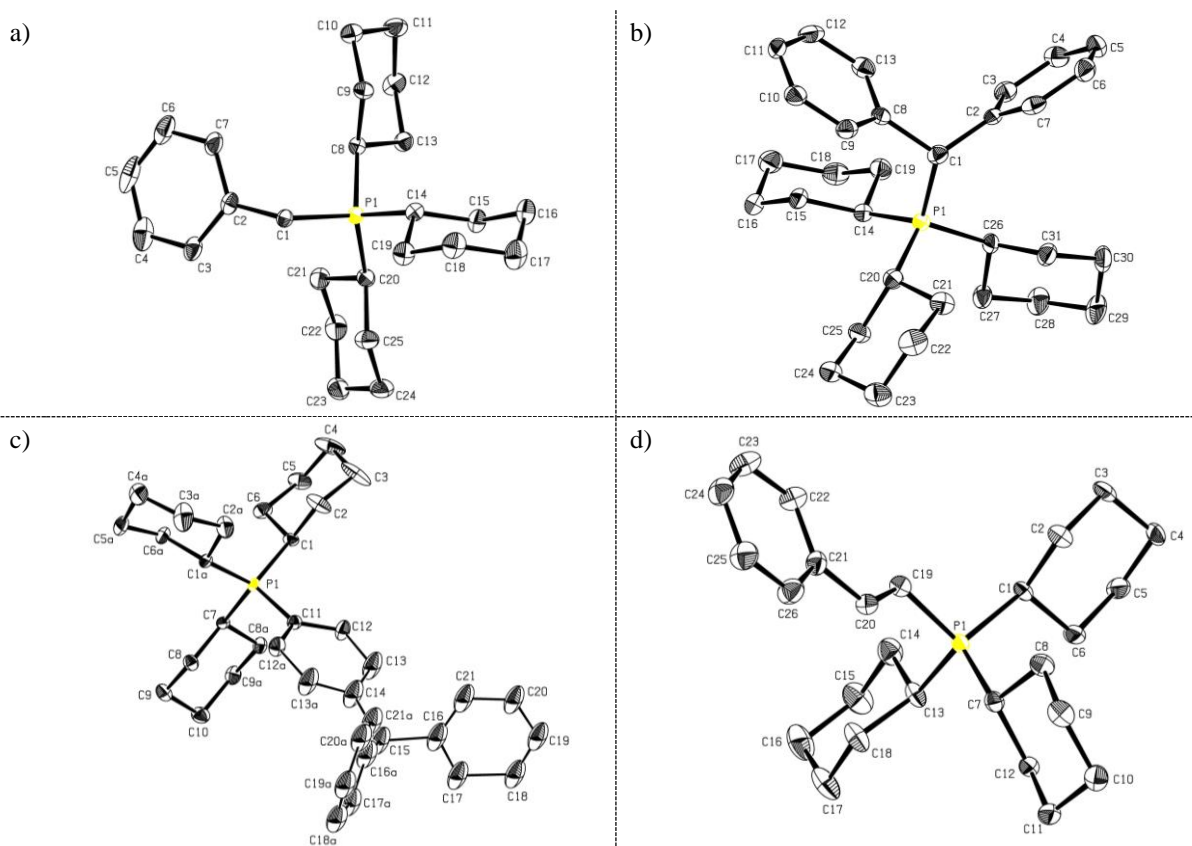
Figure 33. Available benzylic- and vinylic-phosphonium salts synthesized during my master thesis.^[1] ^aThe product contains impurities.

Suitable single crystals for X-ray diffraction were obtained by either slow diffusion of diethylether into a saturated solution of the salts in dichloromethane, or by direct overlaying of the latter phase with diethylether (table 22). Crystal data, as well as collected data for structure refinement are summarized in the appendix (8.3, table 64ff.). In each case, the phosphorus as well as benzylic carbon atoms show tetrahedral geometry, and the cyclohexyl groups adopt chair conformation. P–C_{Cy} bond distances lie within 1.80(6) and 1.84(1) Å, typical

²⁹ Reaction previously performed by Lukas Hintermann.

for C_{sp^3} -P bonds^[66], with the phosphonium unit as equatorial substituent. Benzyl-phosphorus bond distances are slightly longer, 1.84(1) Å for benzyl and 1.87(9) Å for benzhydryl. The latter occurs from either steric repulsion or the pronounced $+\sigma$ -effect, since C-P-C bond angles decrease with increasing size of the benzylic group. P- C_{sp^2} bond lengths are shorter, 1.80(3) Å for *para*-trityl and 1.78(6) Å for β -styryl salts, but still considerably longer than (R)HC⁻+PPh₃ ylide bonds (1.64(0)^[67] Å). Substituents of the vinylic double bond are arranged *trans* to each other. Within the limits of accuracy the salt's C=C bond length (1.34(1) Å) is similar to the one reported for styrene (1.32(5)^[68] Å) and shorter than those of styrene metal complexes^[68-69].

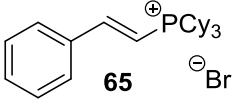
Table 22. X-ray crystal structures of benzylic and vinylic tricyclohexyl phosphonium salts: a) benzyl, b) benzhydryl, c) *p*-trityl, d) β -styryl. Ellipsoids are shown at 50% probability level. Hydrogen atoms, counter-ions as well as co-crystallized solvent molecules (CH₂Cl₂) are omitted for sake of clarity. Carbon atoms are depicted in grey, and phosphorus atoms in yellow.



Even though alkenyl phosphonium salt **65** had already been obtained in comparably high yield, we wanted to explore if we could further improve the reaction conditions (table 23). In the 1990's, the group of Stang reported the Pd-catalyzed synthesis of vinylic phosphonium salts from vinyl triflates and PPh₃.^[70] Later, Cheng et al. isolated β -styryl triphenylphosphonium salts from β -bromostyrenes and PPh₃ under Pd(PPh₃)₄ catalysis.^[61] Yet, no reports display the

isolation of related styryl tricyclohexylphosphonium salts. Previous investigations in our group including Pd(PPh₃)₄ as catalyst and NaOPiv as base/additive already afforded salt **65** in 80% yield at microwave-assisted heating (entry 1). Pd(OPiv)₂ as sole metal precursor and CMD additive diminished the yield (entry 2). Since reactions were usually performed at rather low scale, we wanted to increase reaction scale to confirm the results. At higher concentration (0.2 M), almost identical results were obtained at the 1.00 mmol scale (entry 3), entailing minor amounts of an unknown phosphorous impurity (δ_P 30.2, ~3.2 mol%), detected by ¹H- and ³¹P-NMR spectroscopy. The light yellowish color of the isolated solid might indicate the potential presence of a Pd complex. A spectral identification of the Pd species was not conducted. The use of NaBPPH₄ as additive led to virtually identical results without any substitution of the counterion from bromide to BPh₄ (entry 4). Aged Pd(dba)₂ precatalyst for those reactions was purified by the method of Ananikov et al.^[71]. Nevertheless, reduced amounts of styryl salt **65** were isolated (entry 5). Short heating of a Pd(PPh₃)₄/NaOPiv mixture for 15 minutes significantly improved the outcome of the ensuing phosphination with 95% isolated, and 97% spectral yield (entry 6). Further reduction of catalyst as well as additive loading halved the amount of salt (entry 7).

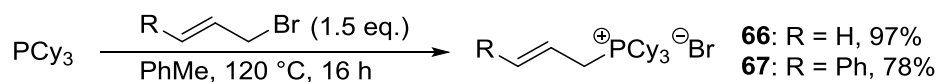
Table 23. Synthesis of (*E*)-tricyclohexyl(styryl)phosphonium bromide (**65**).^a precat. = precatalyst; t = time.

PCy_3 (1.0) + $\text{Br}-\text{CH}=\text{CH}-\text{Ph}$ (1.05)		$\xrightarrow[\text{PhMe, 210 }^\circ\text{C, } \mu\text{W, t}]{\text{Pd-precat., additive}}$		 65 Br^-
entry	Pd-precat. [mol%]	additive [mol%]	t [min]	yield [%]
1 ^b	Pd(PPh ₃) ₄ (5.0)	NaOPiv (10)	60	80
2 ^b	Pd(OPiv) ₂ (5.0)	NaOPiv (10)	60	55
3 ^c	Pd(PPh ₃) ₄ (5.0)	NaOPiv (10)	60	84 ^d (85)
4	Pd(PPh ₃) ₄ (5.0)	NaBPh ₄ (10)	60	(87)
5	Pd ₂ (dba) ₃ ·CHCl ₃ (2.5)	NaOPiv (10)	60	(53)
6	Pd(PPh ₃) ₄ (5.0)	NaOPiv (10)	15	95 ^d (97)
7	Pd(PPh ₃) ₄ (2.5)	NaOPiv (5)	15	(48)

^aReactions performed 500 μmol PCy₃ in toluene (4 mL) according to GP 5.2.3 (see 7.2.5.1); isolated yield. Spectral yield in brackets according to ¹H-NMR against internal standard, given in mol%. ^bReaction performed with 100 mg PCy₃ (357 μmol) in 5 mL toluene; entry extracted from my master thesis. ^cReaction performed with 1.00 mmol PCy₃ in 4 mL toluene. ^dContains minor amounts of a phosphorous species (δ_P 30.2).

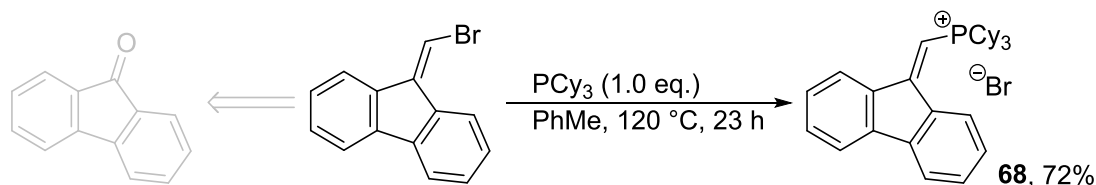
Next, we focused on vinyl- and allyl-type phosphonium salts. Allyl (**66**) and cinnamyl (**67**) tricyclohexylphosphonium salts were already known.^[52a] Heating of the corresponding allyl bromides and PCy₃ to 120 °C afforded both salts in good to excellent yields (scheme 43). The

desired products simply precipitated from the reaction mixture and were isolated via filtration. Cinnamyl bromide was prepared from HBr and cinnamyl alcohol in 97%³⁰ yield.^[72] It was used without further purification.



Scheme 43. Synthesis of allyl (**66**) and cinnamyl (**67**) tricyclohexylphosphonium bromide.

The group of Fürstner described the synthesis of singlet carbene ligands via deprotonation of fluorenylidene phosphonium salts.^[53] Among derivatives depicted, the PCy₃-based salt **68** took our attention. Wittig olefination^[73] of 9-fluorenone with (bromomethyl)triphenylphosphonium bromide³¹ delivered the required vinyl bromide in 69% yield. Heating with PCy₃ resulted in 72% of **68** (scheme 44). It is notable that this phosphination requires no catalyst, unlike the aforementioned one of styryl bromide. Presumably, the reaction proceeds via reversible deprotonation to a carbenoid species that reacts with neutral phosphane to phosphonium ylide, followed by reprotonation.



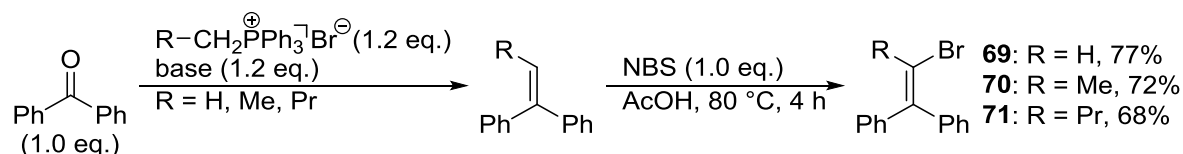
Scheme 44. Synthesis of fluorenylidene tricyclohexylphosphonium bromide (**68**) as described by the group of Fürstner.^[53] They immediately converted the crude product to the less coordinating BF₄⁻ derivative. The vinyl bromide is available via direct Wittig olefination of 9-fluorenone.^[73]

Since direct Wittig reaction with (bromomethyl)triphenylphosphonium bromide failed,³² a range of other vinyl bromides were prepared via two-step procedure including Wittig olefination^[75] followed by bromination^[76] with NBS in acetic acid (scheme 45). Olefin **69** was isolated in 77% yield. Since 1,1-diphenylethylene readily decomposes upon prolonged storage at room temperature, direct conversion of the latter is recommended. Methyl- (**70**) and propyl-substituted (**71**) derivatives were obtained in near identical yields. Both were accompanied by impurities occurring from incomplete or over-bromination which could not be separated.

³⁰ The product contains residual ethyl acetate (3 wt.%) and minor amounts of starting alcohol (8 wt.%).

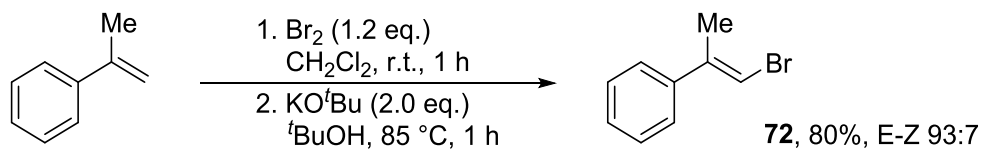
³¹ Synthesized according a procedure by the group of Drewes (see reference [74]) in 66% yield.

³² The failed reaction could also be owed to the employed base, KO^tBu. NaHMDS could have been more promising.



Scheme 45. Two-step synthesis of 2-bromo-1,1-diphenylethylenes. Wittig olefination: R = H:^[75a] a) KO^tBu, methyl triphenylphosphonium bromide, Et₂O, r.t., 15 min, b) benzophenone, Et₂O, 0 °C, 15 h; R = Me, Pr:^[75b] a) *n*-BuLi, alkyl (R = Me: ethyl, R = Pr: butyl) triphenylphosphonium bromide, THF, 0 °C, 2 h, b) benzophenone, 0 °C to r.t., 16 h. The bromination was conducted according to a procedure by Zhang et al.^[76] Yields indicated over two steps.

Commercially available α -methylstyrene was first brominated with Br₂. Small impurities from overbromination were detected in the ¹H-NMR spectrum. Nevertheless, direct conversion of the crude product with the strong base KO^tBu afforded the styryl bromide **72** in 80% yield over two steps; (*E*)-configuration being dominant. Minor amounts of regioisomeric 3-bromo-2-phenylpropene were inevitable.



Scheme 46. Two-step synthesis of 1-bromo-2-phenylpropene (**72**). Yield indicated over two steps. The product contains 3-bromo-2-phenylpropene (~1 mol%).

Olefins **69–72** were subjected to the previously established phosphination conditions for the synthesized styryl phosphonium salt **65** (table 24). The use of NaBPh₄ as additive in the synthesis of **65** afforded good results compared to NaOPiv. It has not yet been clarified which role NaBPh₄ plays in the described reaction. An in situ substitution of bromide to BPh₄⁻ would be imaginable when used in equimolar amounts which potentially increases the solubility of the reactants and product, but no exchange was observed at catalytic loading of NaBPh₄. Due to its superior crystallinity compared to NaOPiv, we decided to give it a try and employ the borate salt in the synthesis of other vinylic phosphonium salts. One should note that conditions using short heating time (table 23, entries 6 and 7) were established later than the results depicted in table 24 excluding entry 6. Pd-induced isomerization of the double bond hindered the complete conversion of vinyl bromide **72** (entries 1 and 2), affording low amounts of desired phosphonium salt. Catalyst deactivation by formation of a Pd–allyl species seems imaginable. 1,1-Diphenylethylenes feature a similar structural motif like fluorene derivative **68**. However, heating of the simplest alkenyl bromide **69** with PCy₃ in the absence of precatalyst and additive impeded any reaction (entry 3). Application of Pd(PPh₃)₄–NaBPh₄ conditions delivered the salt

in 75% spectroscopic yield (entry 4). In the crude $^1\text{H-NMR}$ spectrum, the already observed phosphorous impurity (δ_{H} 3.20-3.29, δ_{P} 30.2, 6.2 mol%) was present. Attempted crystallization of the salt entailed identical amounts of the impurity. The use of excess PCy_3 slightly improved the spectroscopic yield to 88% accompanied with 14 mol% Pd-PCy_3 species (entry 5). Filtration of a methanolic solution of the salt did not remove two additional phosphorous species (δ_{P} 30.2 (1.2 mol%), 33.6 (5.3 mol%)). Short heating times of 15 minutes led to significantly reduced phosphination yields (entry 6). In contrast to NaBPh_4 , NaOPiv already showed reduced amounts of side product (~5.0 mol% in total) in the crude NMR spectrum, delivering 58% of phosphonium salt after purification (entry 7). Substituted 1,1-diphenylethylenes **70** and **71** did not react with PCy_3 under any of the tested conditions (entries 8 and 9).

Table 24. Attempted synthesis of vinyl phosphonium salts.^a

		vinyl bromide (1.05 eq.) $\text{Pd}(\text{PPh}_3)_4$ (5.0 mol%) additive (10.0 mol%)				
PCy_3		PhMe, 210 °C, μW , t				
entry	vinyl bromide	precatalyst	additive	t [min]	product	yield [%]
1		$\text{Pd}(\text{PPh}_3)_4$	NaOPiv	80	73	(19) ^b
2	72	$\text{Pd}(\text{PPh}_3)_4$	NaBPh_4	60	73	(8) ^c
3 ^d		$\text{Pd}(\text{PPh}_3)_4$	-	20	74	-
4		$\text{Pd}(\text{PPh}_3)_4$	NaBPh_4	60	74	(75)
5 ^e	69	$\text{Pd}(\text{PPh}_3)_4$	NaBPh_4	60	74	66 ^f (88)
6		$\text{Pd}(\text{PPh}_3)_4$	NaBPh_4	15	74	46 ^f
7		$\text{Pd}(\text{PPh}_3)_4$	NaOPiv	60	74	58 ^g
8		$\text{Pd}(\text{PPh}_3)_4$	NaBPh_4	60	-	-
9		$\text{Pd}(\text{PPh}_3)_4$	NaBPh_4	60	-	-

^aReactions performed 500 μmol PCy_3 in toluene (4 mL) according to GP 5.2.3 (liquid ArBr) or 5.2.4 (solid ArBr) (see 7.2.5.1). Spectral yield in brackets according to $^1\text{H-NMR}$ against internal standard; isolated yield, given in mol%. ^b6% 2-phenylallyl isomer. ^c5% 2-phenylallyl isomer, 80% vinyl bromide. ^dReaction performed for 20 min at 190 °C without catalyst or additive in a microwave reactor. ^eReaction performed with 500 μmol vinyl bromide and 1.00 mmol PCy_3 . ^fThe product contains two additional phosphorous species (δ_{P} 30.2, 33.6). ^g0.9 mol% of phosphorous impurity (δ_{P} 30.2).

Suitable single crystals for X-ray analysis of tricyclohexyl(2,2-diphenylvinyl)phosphonium bromide (**73**, entry 6) were grown by slow diffusion of diethylether into a saturated solution of the salt in dichloromethane (figure 34). Crystal data, as well as collected data for structure

refinement are summarized in the appendix (8.3, table 88f.). One molecule of CH₂Cl₂ co-crystallized with the salt. The phosphorus atom is substituted in a tetrahedral fashion with cyclohexyl groups adopting chair conformation. P–C_{Cy} bond distances lie within 1.81(7) and 1.82(7) Å, typical for C_{sp3}-P bonds^[66], with the phosphonium unit in equatorial position. The P–C_{sp2} bond length (1.77(7) Å) is comparable to the one of the styryl salt **65** (1.78(6) Å). C=C bond lengths were identical (1.31(4) Å) for both salts. Phenyl groups are twisted to each other, oriented perpendicular to the C=C–P⁺ plane. The latter atoms span an angle of 134°, significantly wider than in styryl salt **65** (121°). Steric hindrance might be the reason for the considerably obtuse angle.

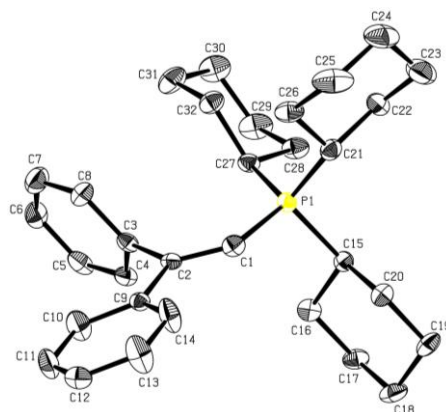
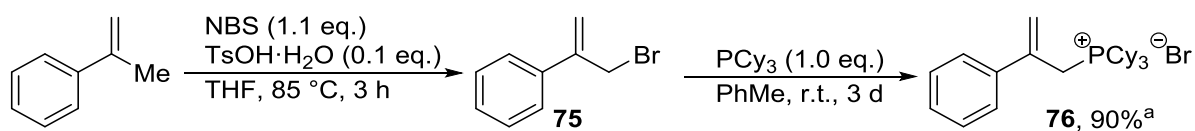


Figure 34. X-ray crystal structure of tricyclohexyl(2,2-diphenylvinyl)phosphonium bromide (**74**). Ellipsoids are shown at 50% probability level. Hydrogen atoms, counter-ion as well as co-crystallized solvent molecules (CH₂Cl₂) are omitted for sake of clarity. Carbon atoms are depicted in grey, and phosphorus atom in yellow.

As previously noted, the direct phosphination of 1-bromo-2-phenylpropene failed, delivering very low and equal amounts of the isomeric vinyl- and allyl phosphonium salts. Since already the substrate seems to be prone to isomerization, we envisaged the selective synthesis of the allylic phosphonium isomer (scheme 47). The group of Suginome had already reported the isolation of the latter as precursor for Wittig olefination.^[77] Allylic bromination of α -methylstyrene afforded the necessary allyl bromide **75** in 71%³³ yield following procedures of Gu^[78] and Mukherjee^[79]. Due to decomposition upon storage, **75** was quickly converted. Stirring for three days with PCy₃ in toluene gave 90% of **76** in >99% purity. Subsequent rearrangement to the vinyl derivative will be discussed in the upcoming section.

³³ a) (*E*)-1-bromo-2-phenylpropene (595 mg, 6%), b) (3-bromoprop-1-en-2-yl)benzene (3.78 g, 38%), c) mixture of both (a-b 25:75, 4.35 g, 44%). Mixed fraction c) was not further purified.



Scheme 47. Two-step procedure for the synthesis of phosphonium salt **76** following procedures by Gu^[78], Mukherjee^[79] and Suginome^[77]. ^a1.6 eq. of allyl bromide **75** were used.

5.2.2 Isomerization of allyl-type phosphonium salts

During the attempted phosphination of 1-bromo-2-phenyl-1-propene (**72**) we had noted the generation of both vinylic and allylic phosphonium salt, albeit in very low yield. It was not evident whether the isomerization occurred at the stage of the starting bromide or of the phosphonium salts, or what the relative stability of both phosphonium salts was. To study the isomerization equilibrium of allyl- versus vinyl-phosphonium salts in a fundamental manner, we first analyzed the isomerization behavior of our most simple allyl salt **66** under several conditions. Scanning of older literature reports revealed that diverse methods for the isomerization of allyl phosphonium salt **66** have already been reported. Filtration over basic Al₂O₃^[80] or stirring in basic^[81] media proved practical. To perform NMR scale experiments, we mixed allyl salt **66** in CDCl₃ with catalytic amounts of three amine bases: NEt₃, DABCO, and DBU (table 25).

Table 25. Base induced isomerization of allyl tricyclohexylphosphonium bromide (**66**).^a

entry	base [eq.]	t [d]	allyl [%]	vinyl [%]	H/D exchange
1	NEt ₃ (0.1)	5	93	7	yes
2	DABCO (0.3)	7	68	32	minor to none
3	DBU (0.1)	0.2	4	96	yes

^aReactions performed with <100 μmol allyl tricyclohexylphosphonium bromide in CDCl₃ (500 μL) according to GP 5.2.5 (see 7.2.5.1). The amount of educt was adjusted in a way that either 1.0 μL liquid or weighable amounts of solid (DABCO, 3.06 mg) could be added. Spectral yields according to ³¹P-NMR by integration of ³¹P-NMR signals (no internal standard), given in mol%. ³¹P-NMR shifts of detected species: δ_P 25.4 (vinyl), 29.7 (allyl).

The samples were monitored by ³¹P-NMR spectroscopy for several days and the species distribution (δ_P 25.4 (vinyl), 29.7 (allyl)) was analyzed. Analysis of the ¹H-NMR spectra further unveiled deuterium incorporation. The experiments were stopped if there was no further changes noticed. Minor amounts of vinyl salt (2 mol%) were already present from the synthesis of the allyl salt. The use of catalytic NEt₃ induced negligible generation of vinyl salt (entry 1). DABCO induced isomerization progressed very slowly (entry 2), yielding only 32% of

propenyl isomer after one week. In contrast, DBU delivered near quantitative amounts of propenyl isomer already after five hours (entry 3).³⁴

Whereas the deuterium incorporation-equilibrium is partly shifted to **66** when NEt₃ (0.1 eq.) was used, DBU (0.1 eq.) nearly fully exchanges propenyl protons at all positions after six days in CDCl₃ (figure 35).

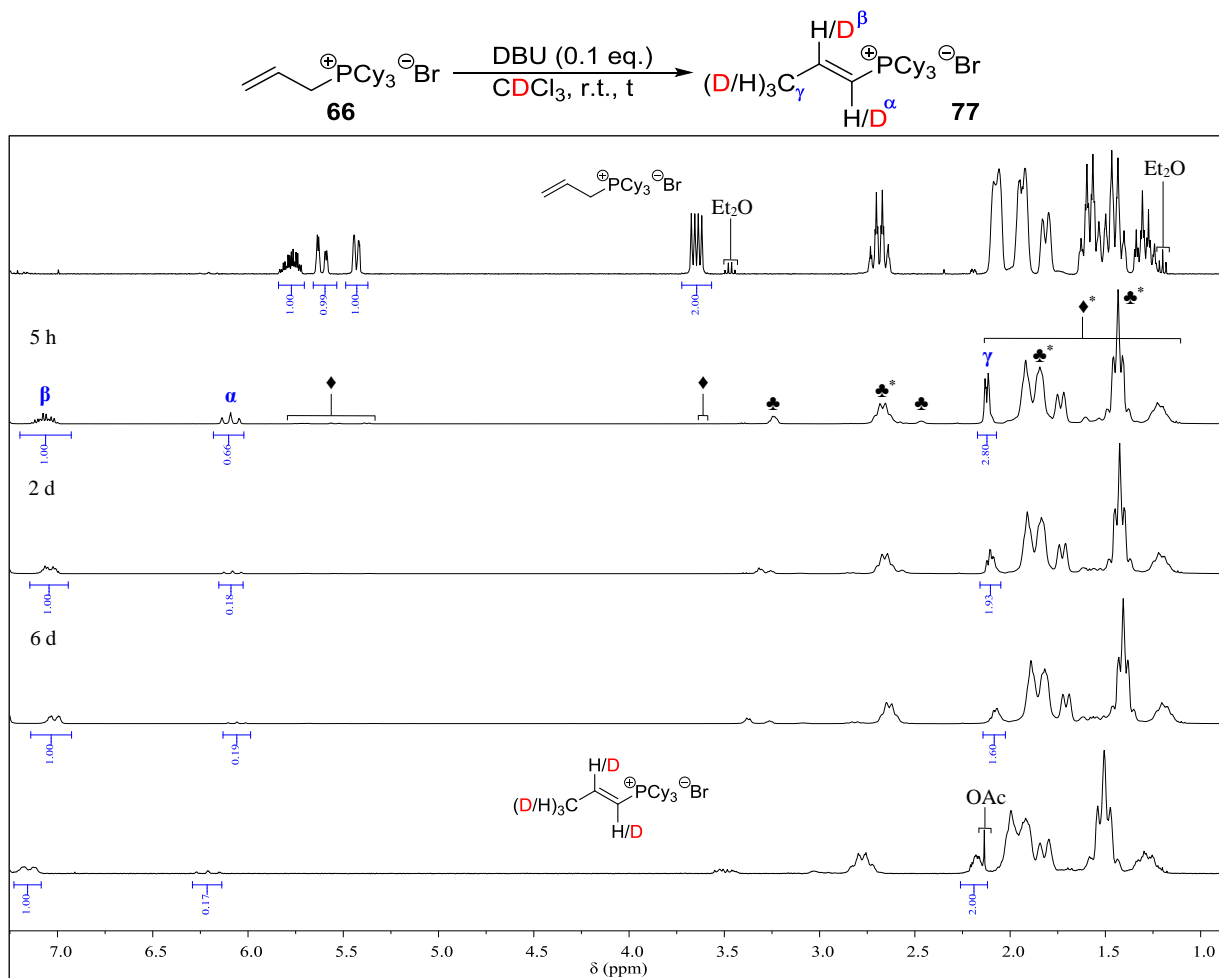


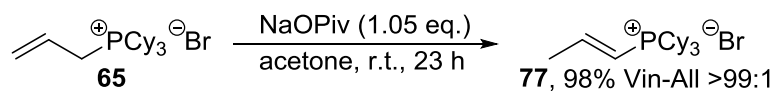
Figure 35. Stacked ¹H-NMR spectra (CDCl₃) of allyl tricyclohexylphosphonium bromide (**66**, top), the isomerization of allyl tricyclohexylphosphonium bromide (**65**) with DBU (0.1 eq.) after five hours (2nd), two days (3rd), six days (4th), and isolated, partially deuterated vinyl tricyclohexylphosphonium bromide (**77**, bottom). The bottom spectrum contains residual amounts of DBU·HOAc. Minor amounts of Et₂O occur from the starting material. Residual signals of the starting material are marked with ♦, those of DBU with ♣. *Signal overlayering.

This process is significantly accelerated by the addition of larger amounts (0.5, 1.0 or 1.5 eq.) of basic catalyst. The originally sharp signals of the vinyl group broaden as deuterium is

³⁴ The isomerization may be faster. Due to ‘traffic jam’ at the NMR machine, the first sample was only measured after four to five hours.

incorporation rises. The isomerization equilibrium is clearly shifted towards vinyl derivative. To further underline the ^2H -incorporation, we conducted the same experiment on larger scale (500 μmol). After completed rearrangement (2 days, Vin–All 98:2), the sample was quenched by addition of acetic acid (1 drop). The isolated crude material was analyzed via ^1H -, ^{31}P -, and ^2H -NMR methods. Besides product signals, those of DBU acetate could be observed. Next to minor amounts of starting allyl phosphonium salt (δ_{P} 31.9, 2.3 mol%), two additional phosphorous signals (δ_{P} 25.3 (82.5 mol%), 25.4 (15.2 mol%)) could be assigned to the vinyl salt **77**. With progressing deuterium incorporation, the broad signal at δ_{P} 25.3 belonging to partially deuterated **77** rises in intensity while the integral of the species at δ_{P} 25.4 decreases. Analysis of the ^2H -NMR spectrum confirmed partial deuteration of α -, β -, and γ - substituents (δ_{D} 2.15 (H_{γ}), 6.22 (H_{α}), 7.23 (H_{β})). Since both extremities (α , γ) of the vinyl unit are most electrophilic, deuterium was preferably incorporated at these positions. The actual degree of ^2H -incorporation could not be calculated due to overlay of reference signals with DBU.

By chance, we found that NaOPiv was an effective isomerization agent. Initially, we wanted to exchange the nonfunctional counter-ion bromide, with the functional CMD-additive pivalate via salt metathesis. Stirring of the allyl salt **65** with an equimolar amount of NaOPiv cleanly delivered vinyl salt **77** in 98% yield (scheme 48).

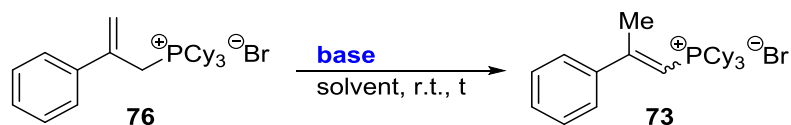


Scheme 48. Isomerization of allyl tricyclohexylphosphonium bromide (**65**) with NaOPiv to vinyl salt **77**. Vin = vinyl; All = allyl.

Keeping the above methods in mind, we transferred the rearrangement to our α -methylstyrene substituted phosphonium salt **76** to access the corresponding vinyl derivative **73** (table 26). We therefore mixed **76** with DBU, NaOPiv or NEt_3 and analyzed the experiments by ^1H -NMR spectroscopy either directly (NMR scale) or after work-up. Minor amounts of phosphine oxide (1.0 mol%) were detected but neglected for the product ratio calculations. In all cases, the (*E*)-vinyl isomer is clearly preferred due to lower steric hindrance in the product, the (*Z*)-isomer being present in 2-5 mol%. When storing a solution of the salt in CDCl_3 with catalytic amounts of DBU (0.1 eq.), ^1H -NMR analysis showed almost identical distribution of species after 30 minutes (entry 1) or one day (entry 2). The equilibrium even seems to be shifted to the starting material at prolonged reaction time. It might be possible that bromide ions react with chloroform, releasing chloride anions. The presence of the latter ions could induce further

isomerization to unwanted allylic phosphonium salt **76**. With progressing deuterium incorporation, a previously adjusted equilibrium can be shifted in turn.

Table 26. Isomerization of α -methylstyrene substituted phosphonium salt **73**.^a ac = acetone; exc. = excess.



entry	base [eq.]	solvent [mL]	t [h]	educt [%]	(<i>E</i>)- 77 [%]	(<i>Z</i>)- 77 [%]
1	DBU (0.1)	CDCl ₃ (0.5)	0.5	27	71	2
2	DBU (0.1)	CDCl ₃ (0.5)	24	33	63	4
3	NaOPiv (1.0)	DCM (2.0)	15	21	74	5
4	NaOPiv (1.0)	ac-DCM 1:1 (2.0)	24	12	83	5
5 ^b	NaOPiv (1.0)	DCM (2.0)	16	18	75	7
6	NEt ₃ (exc.)	MeCN (0.6)	18	27	70	3
7	NEt ₃ (exc.)	DCM (1.0)	18	30	67	3

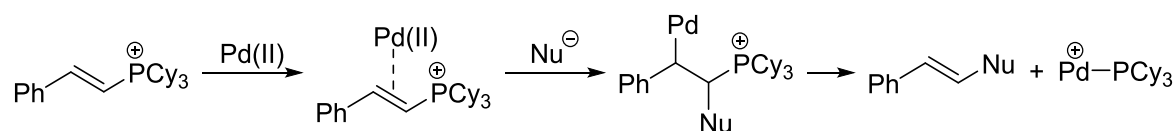
^aReactions performed with 67.0 μmol (NMR scale) or 100 μmol of phosphonium salt in the indicated solvent and volume according to GP 5.2.6a) or b) (see 7.2.5.1). Spectral yield according to ³¹P-NMR by integration of ³¹P-NMR signals (no internal standard), given in mol%. Minor amounts of phosphine oxide (1.5 mol%) were neglected. ³¹P-NMR shifts of detected species: δ 26.3 ((*Z*)-vinyl), 26.8 ((*E*)-vinyl), 30.5 (allyl). exc. refers to >10.0 eq. (here 35.9 eq.). ^bReaction conditions were applied to the isolated product of entry 4.

Equimolar amounts of NaOPiv in pure dichloromethane (entry 3) delivered virtually identical results to entry 1. Stirring in a 1:1 mixture with acetone (entry 4) led to slightly higher amounts of both vinyl isomers. Addition of a fresh portion of NaOPiv (0.3 eq.) increased the percentage of allyl substrate **75** at the cost of (*E*)-vinyl isomer (entry 5). Even though NEt₃ failed at catalytic loadings with allyl-PCy₃Br (**66**), we wanted to check if excess amounts of base favors the desired rearrangement. Adapted from Nesmeyanov et al.^[81d], allyl precursor **75** was subjected to NEt₃ (35.9 eq.) in acetonitrile (entry 6) or dichloromethane (entry 7). Unlike with NaOPiv, the reaction mixture can simply be evaporated to dryness. Crude products were directly analyzed by ¹H- and ³¹P-NMR spectroscopy. Both reaction media showed comparable results similar to those of entry 1. No quantitative shift of the equilibrium could be achieved. Future studies should involve raise in temperature to suppress any kinetically favored product. Under the conditions depicted in table 26, the state of equilibrium between allylic phosphonium salt **76** and vinylic derivative **73** was achieved. Even though **73** is more stable due to conjugation and a stronger C–P bond, steric repulsion most likely induces the humble preference for the formation of **77**. While **76** can be selectively prepared by quaternization without the use of base, the synthesis of phosphonium salt **73** from **76** under mild basic conditions affords a mixture of

isomers. It has not yet been clarified whether the isomerization suffers from the presence of bromide anions.

5.2.3 π -Complexation of alkenylphosphonium to Pd and release of free PCy₃ ligand

With the study of benzylic and vinylic phosphonium salts, we pursued one main objective: the design of a new reaction pathway to release air-sensitive phosphine from these air-stable compounds. We expect the formation of mono- or bis-ligated Pd–phosphine species (scheme 49) by combination of our salts with suitable Pd(II) precatalysts and nucleophiles. Oxidative addition of the C–P⁺ bond with subsequent β -elimination additionally appears reasonable for an alternative, efficient release pathway of active material.

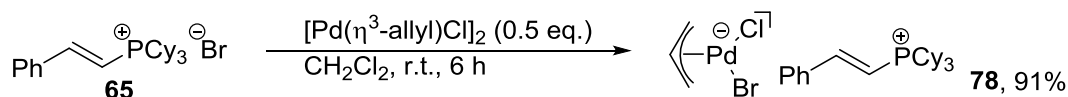


Scheme 49. Expected release of mono- or bis-ligated Pd–phosphine species. The bromide counter-ion was omitted for a better overview.

The group of Cheng has reported the synthesis of several η^2 -phosphonioalkene–Pd(0) complexes from alkenylphosphonium halides and palladium(0) species.^[61] These complexes were observed as catalyst intermediates in the Pd(0)-catalyzed reaction of PPh₃ with bromostyrene, and were also formed by stoichiometric reaction from bromostyrene and Pd(PAr₃)₄. Not only delivering the corresponding phosphonium salt, they might also act as potential precursors for phosphine release by the reverse reaction from the phosphonium salt back to Pd(0) and coordinated phosphine ligand. Before tackling the release of active species, we wanted to isolate PCy₃-based vinyl phosphonium Pd complexes to estimate their stability. Different Pd precursors including Pd(dba)₂³⁵, Pd(PhCN)₂Cl₂, Pd(cod)Cl₂, and [Pd(η^3 -allyl)Cl]₂ were chosen. Stirring of each complex with two equivalents of vinyl salt **65** in dichloromethane was awaited to deliver the desired compounds. In first instance, Pd(dba)₂ looked promising, since a clear orange solution was obtained. However, attempted crystallization of the crude product inside a glovebox entailed quantitative precipitation of Pd black, which confirms our assumption for the reduction of Pd(II) to Pd(0) displayed in scheme 49. No complexation was observed for Pd-nitrile or -cod precursors. Addition of salt **65** to a solution of [Pd(η^3 -allyl)Cl]₂ in dichloromethane afforded a yellow solid. The latter easily dissolves in chloroform whereas

³⁵ Old, not purified batch of Pd(dba)₂ was used.

educt **65** does not. Spectral analysis clearly revealed a considerable upfield shift of allyl as well as vinyl signals. Regarding our findings, we propose the formation of complex **78** in 91% yield (scheme 50). Bromide ions could have induced the cleavage of the chloride bridge in $[\text{Pd}(\eta^3\text{-allyl})\text{Cl}]_2$. A definite proof of structure by X-ray or elemental analysis has not yet been conducted, leaving us with our hypothesis. The complex salt **78** was not involved in the release of free phosphine, nor in catalysis.



Scheme 50. Complexation of vinyl salt **65** with $[\text{Pd}(\eta^3\text{-allyl})\text{Cl}]_2$.

As next step, we wanted to monitor the potential release of free PCy_3 by ^{31}P -NMR (figure 36). Our phosphonium salt **65** was subjected to a Pd(II) precatalyst and excess of strong base inside a screw cap NMR under argon. With the aid of an ultrasonic bath, the sample was mixed at either room temperature or 50 °C. The previous introduction of an internal standard (naphthalene) was expected to deliver quantification of any Pd- PCy_3 species in the ^1H -NMR. However, a quantitative statement could not be drawn due to low intensity of characteristic as well as overlaying of signals. We therefore limited our discussion to the observations in the ^{31}P -NMR. Even though suffering from low solubility, sonication of the suspension gradually intensifies the signal corresponding to our phosphonium salt **65**. Free tricyclohexylphosphine (δ_{P} 9.9) was observed after 90 minutes at 50 °C. Since the septum of the screw cap is slightly permeable, oxygen may diffuse leading to minor amounts of phosphine oxide (δ_{P} 48.2). After 30 minutes at 50 °C, two new doublets (δ_{P} 28.7 (d, $J = 2.6$ Hz), 36.0 (d, $J = 2.6$ Hz)) appeared while growing in intensity and remaining main component at prolonged heating. The group of Cheng described similar signal splitting and coupling for their η^2 -phosphonioalkene-Pd(0) complexes.^[61] Hence, we suppose the formation of a related Pd(0) complex, namely $[(\eta^2\text{-PhCH=CHPCy}_3)^+\text{Pd}(\text{PCy}_3)]\text{Br}$. Next to the Pd(0) complex, the well-known $\text{PdCl}_2(\text{PCy}_3)_2$ (δ_{P} 25.0) was detected. However, no $\text{Pd}(\text{PCy}_3)_2$ species (δ_{P} 39.2^[82]) was present in the ^{31}P -NMR. Solely, a tiny signal (δ_{P} 39.6) occurs at the corresponding region. The strong base, NaO'Bu, involved may deprotonate our phosphonium salt at the vinyl group, yielding an ylide. Under our conditions, two possible reaction pathways are imaginable. Polymerization as described by the group of Echavarren^[83] may be a reasonable explanation for the multitude of small signals. This hypothesis is further supported by the broad multiplets observed in the ^1H -NMR spectrum. It is also possible that the presence of strong base induced elimination of PCy_3

from the β -styryl tricyclohexylphosphonium salt (**65**), generating phenylacetylene, which tends to polymerize under the given conditions. In the $^1\text{H-NMR}$ spectrum of the attempted isomerization, no free phenylacetylene could be detected, but should be of interest for future investigations. The second possibility would consist of the generation of a ylide complex as reported by the group of Fürstner^[53] for fluorene-type phosphonium ylides. These complexes would most likely suffer from high temperatures, leading to major decomposition. Residual, comparably intense signals (δ_{P} 44.9, 45.6) cannot directly be assigned to any potential species. We suppose they arise from any complex degradation or intermediate involved in the release of free tricyclohexylphosphine. No attempts for the isolation of the main species were conducted but should be of interest for future research.

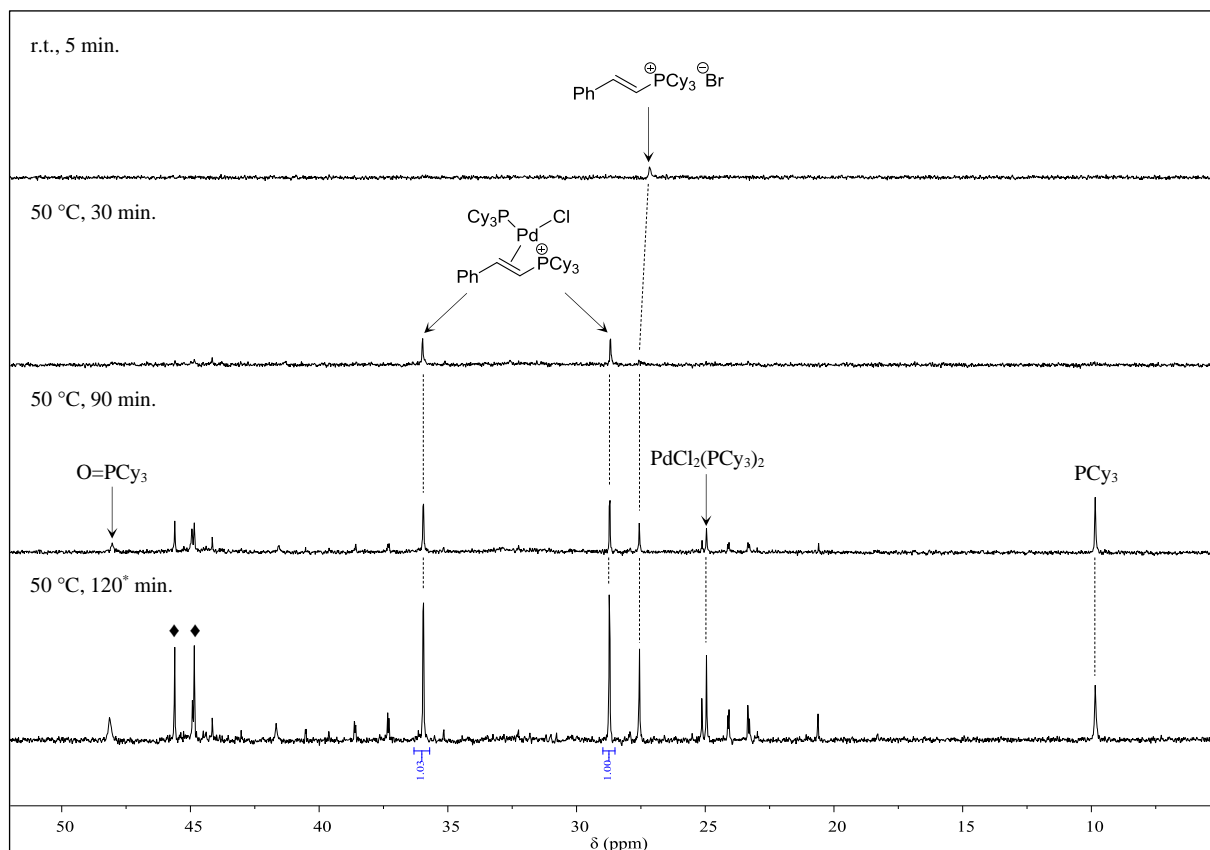
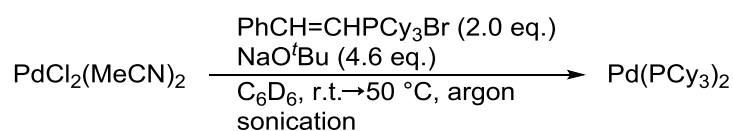
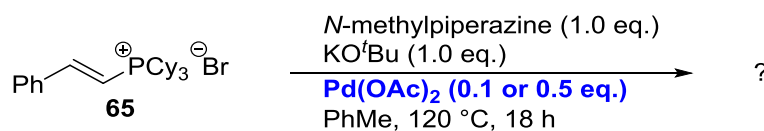


Figure 36. Stacked $^{31}\text{P-NMR}$ spectra ($[\text{D}_6]$ -benzene, cut-out) of attempted ligand release from the styryl salt **65** in the presence of $\text{PdCl}_2(\text{MeCN})_2$ and NaO^tBu . The sample was prepared inside a glovebox (see 7.2.5.6 for further details). Times indicated depict the total time of sonication at either room temperature or 50°C . Increase of temperature to 50°C was conducted after five minutes at ambient temperature. *The sample was sonicated for additional 30 minutes on the next day. Signals marked with \blacklozenge could not be assigned.

Subjecting our vinyl phosphonium salt **65** to related amination conditions described by Reddy et al.^[84] should further demonstrate the efficient release of free PCy₃ (scheme 51). After boiling of our salt for several hours with equimolar amounts of amine and KO^tBu in the presence of Pd precatalyst (0.1 or 0.5 eq.), reaction mixtures were filtered over Celite in air. Isolated solids were analyzed by ¹H- and ³¹P-NMR. While ¹H-NMR spectra were inconclusive due to strong overlapping of signals, a glance at ³¹P-NMR spectra allowed the differentiation of present species. Next to neglectable signals of Pd–phosphine species, tricyclohexylphosphine oxide was detected as major species for both catalyst loadings. Work-up was performed in air, any free PCy₃ suffered from oxidation, leaving no trace of phosphine. Residual amounts of phosphonium salt **65** were also observed.



Scheme 51. Attempted release of PCy₃ simulating amination conditions.

5.2.4 Vinyl and benzyl phosphonium salts in catalysis

Since the efficient generation of Pd species or free phosphine ligand was demonstrated in the last sub-chapter, we wanted to involve most of our phosphonium salts in state-of-the-art coupling chemistry. During my master thesis,^[11] we already included a range of salts in the Pd-catalyzed amination of chlorobenzene with *N*-methylpiperazine as described by Reddy et al.^[84] (table 27). Entries 1 and 2 display the results reported by Reddy et. al. for an ArCl–amine ratio of 1:1 or 1:2, respectively. At that time, reaction mixtures had been directly analyzed by q-NMR without aqueous work-up. More recent experiments used aqueous work-up with dilute, aqueous NaCl solution to remove residual base, leading to much sharper NMR spectra. Direct comparison of old and new experiments only reveals minor differences in yield (entries 4 and 5). The recovery of amine is not indicated given its solubility in water and relatively low boiling point³⁶. Thus, losses of the latter were inevitable. Unfunctional PdCl₂(MeCN)₂ was chosen as precatalyst to avoid any functionality owed to the Pd(0) precursor.

³⁶ Its characteristic smell could be perceived at the rotary evaporator as well as other glassware (separatory funnel, glass filter...) even after extensive rinsing with solvent (Et₂O).

Table 27. Pd-catalyzed amination of chlorobenzene with *N*-methylpiperazine with chlorobenzene, involvement of phosphonium salts.^a

entry	Pd-precatal.	additive	t [h]	yield [%]
1 ^{b,c}	PdCl ₂ (PCy ₃) ₂	-	12	64
2 ^b	PdCl ₂ (PCy ₃) ₂	-	12	88
3	PdCl ₂ (MeCN) ₂	-	12	<1
4	PdCl ₂ (PCy ₃) ₂	-	12	69
5 ^d	PdCl ₂ (PCy ₃) ₂	-	17	66
6	PdCl ₂ (MeCN) ₂	PCy ₃	12	77
7	PdCl ₂ (MeCN) ₂		12	43
8	PdCl ₂ (MeCN) ₂		12	30
9	PdCl ₂ (MeCN) ₂		12	40
10	PdCl ₂ (MeCN) ₂		17	66 ^d
11	PdCl ₂ (MeCN) ₂		17	64 ^d
12	PdCl ₂ (MeCN) ₂		12	70
13 ^b	PdCl ₂ (MeCN) ₂		17	64
14	PdCl ₂ (MeCN) ₂		17	44 ^d

^aReactions performed with 110 μ L amine (992 μ mol) in dry toluene (4 mL) according to GP 5.2.7 (see 7.2.5.1). Unless stated otherwise, crude mixtures were diluted with dichloromethane (15 mL), dried over MgSO₄, and subjected to q-NMR analysis after minor concentration of the solution; spectral yield according to ¹H-NMR with internal standard, given in mol%. ^bResults reported by Reddy et al.^[84] ^cAn ArCl–amine ratio of 1:1 was employed. ^dReaction mixtures subjected to aqueous work-up.

The combination of our salts with PdCl₂(MeCN)₂ yielded similar results as those observed for an ArCl–amine ratio of 1:1 reported by Reddy and Tanaka^[84] (table 27, entry 1, 64% of aryl amine). However, an ArCl–amine ratio of 1:2 was utilized in all our experiments. Leaving any phosphine ligand out stopped the reaction (entry 3). Pre-complexed PCy₃ in the form of PdCl₂(PCy₃)₂ delivered good results with both work-up techniques (entries 4 and 5). Best yields were obtained by the addition of free PCy₃ to the acetonitrile precatalyst (entry 6). Benzylic salts **62** and **63** arylated the amine in 43% (entry 7) and 30% (entry 8) yield, respectively. The rather low outcome of the benzhydryl salt **63** is probably owed to its impure nature. Trityl salt **64** reacted similar to the benzyl substituted one (entry 9). Cleavage of the PCy₃ is rather

challenging as it is directly bound to the phenyl ring. The addition of strong base to all three benzyl type phosphonium salt reactions led to a remarkable color change to wine red, most intense being observed for the trityl derivative **64**. Formation of a phosphorous ylide or trityl anion, which may coordinate the Pd center, is imaginable. Allyl salt **66** and its isomer **76** showed virtually identical yields within limits of accuracy (entries 10 and 11). Our styryl compound **65** resides among most efficient precursor (entries 12 and 13). Fluorene substituted phosphonium salt **68** described by the group of Fürstner^[53] performed on average similar to benzyl type salts (entry 14). Other phosphonium compounds, e.g. cinnamyl phosphonium salt **67**, were not involved but may be of interest for future studies.

5.3 Cycloheptatrienyl Phosphonium Salts: Synthesis, Reactivity and a Susceptible Rearrangement

In this chapter, we describe the tropylation of phosphines to give cycloheptatrienyl-phosphonium salt (CHT salt), mainly focusing on Buchwald ligands as starting materials. Their structure in solution as well as in the solid state will be analyzed. Attempts towards the isomerization of CHT phosphonium salts will be presented. Studies on the behavior of these salts when exposed to Pd complexes and/or nucleophile will be discussed. We postulate enhanced reactivity towards release of the phosphane from these phosphonium salts due to potential pre-coordination of the metal center to the CHT-unit. The last part of this chapter concentrates on application of CHT-phosphonium salts in catalysis.

5.3.1 Synthesis of cycloheptatrienyl phosphonium salts

Addition of free phosphine to a carbenium ion depicts the most straightforward way for the synthesis of phosphonium salts. Cycloheptatrienyl phosphonium salts are indeed readily formed from tropylium salts and free phosphane.^[55,85] Tropylium bromide or iodide would be alternative precursors for CHT-phosphonium units with halide counter-ions, which would be more versatile in anion exchange reactions. Yet, the tropylium halides suffer from high deliquescence as well as low stability upon storage.^[63b]

Cycloheptatrienyl hexafluorophosphate (Trop·PF₆) is hardly soluble in dichloromethane. However, upon addition of P-substituted P,P-dicyclohexylphosphines, quick dissolution of both reactants was observed. After filtration over Celite, the solutions were concentrated and the pure product salts precipitated with diethyl ether (table 28). In case no direct precipitation occurred, a rather slow crystallization of the ‘product phase’ could be induced by cooling. Even after intensive drying under reduced pressure and heating, some solvent remained attached to the products, which points to a tendency for solvate or clathrate formation. Initial experiments on tropylium salts have already been conducted during my master thesis.^[1] Namely, the reaction of tricyclohexyl-phosphine with Trop·PF₆ afforded 84% of the target salt (entry 1). We have now extended the synthesis procedure to cyclohexyl-type Buchwald ligands. Unsubstituted CyJohnPhos was efficiently tropyliated in 85% yield (entry 2). DavePhos was converted in good yield (entry 3). Similarly, quaternization of alkoxy phosphines SPhos and RuPhos was achieved (entries 4 and 5).

Table 28. Synthesis of cycloheptatrienyl phosphonium salts.^a struct. = structure; CHT = cycloheptatrienyl (red); NCD = norcaradienyl (green), Trop = tropylium.

entry	substrate	yield [%]	struct. in solution	solid state struct.	P-C1 _{Trop} bond length
1		84	CHT	CHT (KlePh5)	1.8306(17) Å
2		85	CHT	-	-
3		87	CHT	NCD (KlePh17)	1.782(2) Å
4		79	CHT	CHT (KlePh10)	1.828(2) Å
5		86	CHT	NCD (KlePh12)	1.7867(2) Å
6		85	CHT	NCD (KlePh11)	1.788(3) Å
7		86 ^b	CHT/NCD ^c	NCD (KlePh16)	1.7877(13) Å
8		93 ^d	CHT/NCD ^e	-	-
9		80 ^f	CHT	-	-

^aReactions performed with 250 μmol (or up to 1.00 mmol) phosphine in DCM (0.13-0.20 M) according to GP 5.3.1 (see 7.2.6.1). Isolated yield after drying in air. ^bThe product contains protonated species (8 wt.%). ^cCHT–NCD ~15:85 in [D₆]-acetone. ^dThe product contains protonated species (~8 wt.%), educt (~3 wt.%) as well as co-crystallized dichloromethane (~14 wt.%). ^eCHT–NCD ~15:85 in CDCl₃. ^fThe product contains protonated species (~9 wt.%).

In the case of SPhos, an increase in Trop·PF₆ equivalents to 2.0 yielded the product in over 90%. However, it was accompanied with protonated ligand (HPCy₂Ar·PF₆, 6.0 mol%) and Trop·PF₆. As our conventional reaction conditions resulted in pure products after single precipitation, we decided to stick to the initial procedure. Both ligands bearing isityl moieties, XPhos and BrettPhos, were functionalized in almost identical yields (entries 6 and 7). The latter was accompanied with a non-neglectable amount of protonated species, probably occurring from partial decomposition, deprotonation by free ligand or water in the system, or dynamic behavior in solution (see next paragraph for more discussion). In our group, one coworker focusses on the development of Buchwald type ligands based on naphthyl backbones.^[86] Both phosphines, KatPhos and CyAnPhos, were reacted with Trop·PF₆ in our conventional reaction set-up. Compared to BrettPhos, the structurally similar KatPhos was tropyliated in 93% yield (entry 8). Similar to the Buchwald ligand, greater amounts of protonated species as well as residual amounts of educt could not be separated from the target salt. The *m,m*-substituted ligand CyAnPhos was converted to the tropyliated derivative in 80% yield (entry 9), entailing protonated phosphine.

The cycloheptatrienyl (CHT, red) moiety is able to isomerize to the norcaradienyl (NCD, bicyclo[4.1.0]hepta-2,4-dien-7-yl, green) isomer.^[87] The CHT unit can either be arranged as axial or equatorial conformer. For NCD structures, an endo- and exo-isomer is possible, generating diastereomers. While CHT quickly isomerizes between both configurations, NCD prefers an exo-structure.^[87d] Cycloheptatriene derived salts, e.g. an imidazolidinium or spirocyclic substituted salt, are known for variable structures depending on their aggregate state.^[87d] In solution, several salts (table 28, entries 1-5) clearly show the presence of a CHT moiety. Isityl substituted compounds seem to shift the equilibrium to a NCD unit (entries 6-8). Solution NMR data of the XPhos salt still indicate the presence of a CHT structure. While alkene signals of the seven-membered ring appear broadened, no signal for H-1 of the CHT-unit is detected. These observations align with a dynamic equilibrium described by Daub et al.^[87e] and could initiate potential decomposition as observed for BrettPhos.³⁷ Concerning the C-H resonance adjacent to the P atom, a cyclo-propyl motif is predominant in the case of KatPhos and BrettPhos (entries 8 and 7). The missing *o,o'*-functionalization in CyAnPhos creates enough space for the existence of a CHT ring (entry 9). Considering the substitution

³⁷ Signal broadening due to rotational inhibition elicited by sterics cannot be excluded.

pattern of our salts, we conclude that in solution increased steric hindrance promotes decomposition of the salts to protonated ligand. The CHT-salts especially dissociate when mixed with alcohols. In [D₄]-methanol, quantitative formation of 7-([D₃]-methoxy)-cyclohepta-2,4,6-triene along with deuterated phosphonium salt is observed.

After analysis of the salt's structures in solution, we wanted to get a better insight in their solid-state structure. Crystallization by slow diffusion of diethylether into a saturated solution of our quaternary precursors in dichloromethane afforded suitable crystals for X-ray diffraction for most of our compounds (table 29). Crystal data, as well as collected data for structure refinement are summarized in the appendix (8.3, table 63ff.). To avoid any misunderstanding, the ad hoc numbering scheme used for both organic ligands is depicted in figure 37.

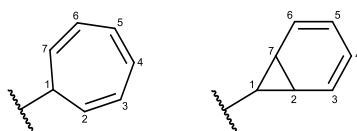


Figure 37. Numeration of CHT and NCD structures.

P–C_{1Trop} bond lengths³⁸ are listed in table 28. Less sterically hindered phosphonium salts, [(Trop)PCy₃]PF₆ and [(Trop)SPhos]PF₆, hold a CHT unit with boat conformation in the solid state. A NCD motif is observed with more crowded compounds. NCD salts crystallized in the exo conformation. Since the NCD ring is slightly less bulky than cyclohexyl, the bicycle is oriented towards the lower ring of the biphenyl. Whereas P–C_{1Trop} bond lengths of CHT containing salts range from 1.82(8)-1.83(0) Å, those of NCD are considerably shorter (1.78(2)-1.78(8) Å). The latter agree with bond lengths observed for [tBu₃P(NCD)][B(C₆F₅)₄] (1.79(1) Å) described by the group of Stephan.^[55b]

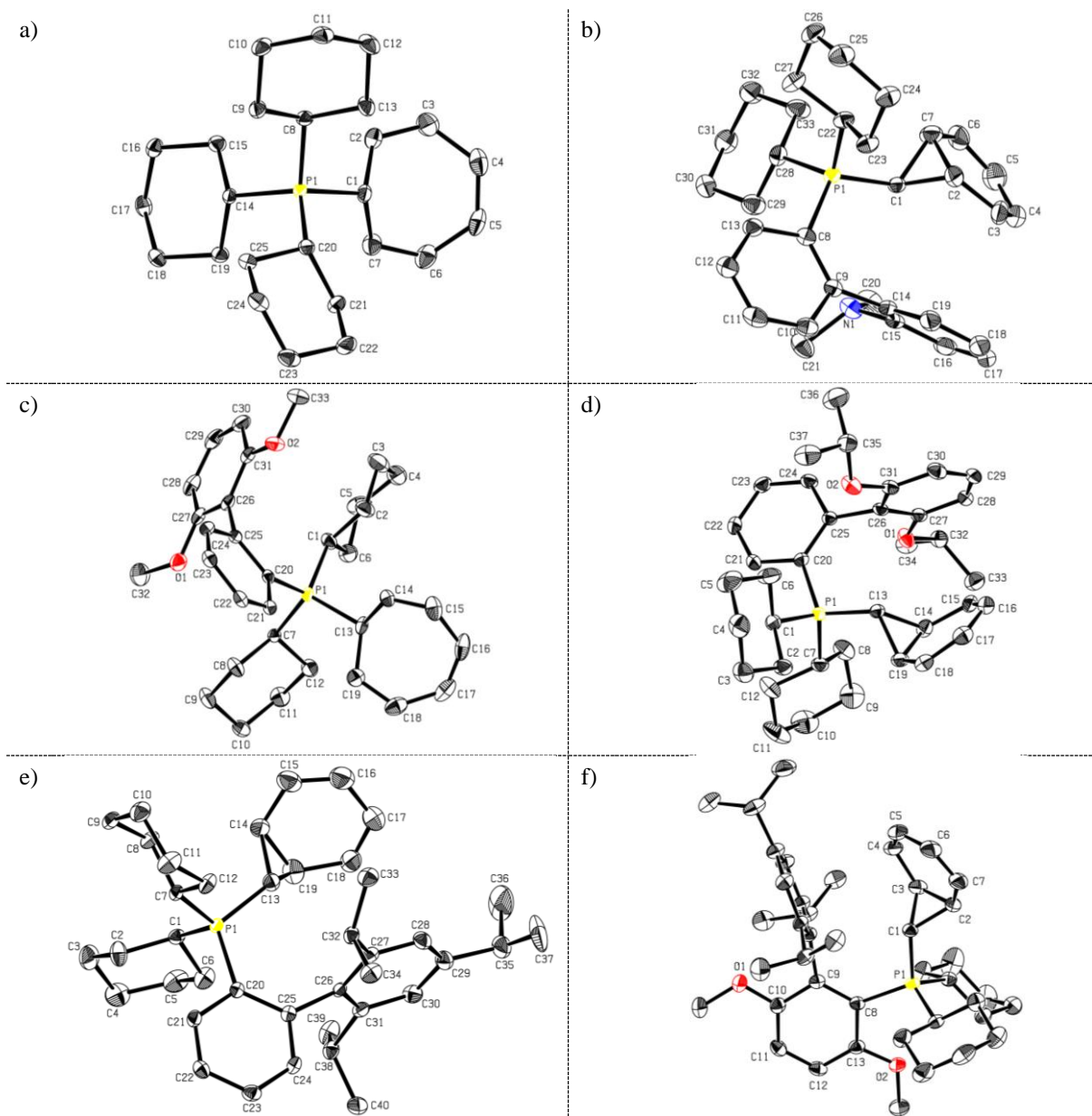
Cycloheptatrienes feature alternating bond lengths. Average distances range from 1.30(7)-1.34(3) Å for C=C bonds, 1.45(0)-1.47(4) Å for C_{sp2}–C_{sp2} bonds, and 1.51(6)-1.52(8) Å for C_{sp2}–C_{sp3} bonds. Depending on the structure, C₂–C₇³⁹ bond lengths of the tropylium core vary. The bicyclic NCD structure consists of a cyclopropane annulated with a cyclohexadiene. In cyclopropanes, C₂ and C₇ atoms are separated by 1.51(4) Å.^[87d] C₂–C₇ bond lengths of our NCD salts (1.50(6)-1.56(5) Å) are in accordance with the latter, Trop BrettPhos spanning the shortest one. Similar to work by Stezowski et al.^[87d], we suggest that the higher degree of strain

³⁸ For some X-ray structures, C1 carbon atoms of the tropylium ring are labeled as C13.

³⁹ For some X-ray structures, C₂ and C₇ carbon atoms of the tropylium ring are labeled as C14 and C19, respectively.

and substitution in the BrettPhos salt destabilizes the tropylated phosphine, leading to decomposition. In CHT compounds, C2–C7 distances are much longer (2.42(2)–2.43(5) Å) due to the seven-membered ring structure. Unfortunately, no suitable crystals of [(Trop)CyJohnPhos]PF₆, [(Trop)KatPhos]PF₆, and [(Trop)CyAnPhos]PF₆ for X-ray diffraction were obtained.

Table 29. X-ray crystal structures of phosphonium salts of tropylated ligands based on: a) PCy₃, b) DavePhos, c) SPhos, d) RuPhos, e) XPhos, and f) BrettPhos. Ellipsoids are shown at 50% probability level. Hydrogen atoms, PF₆ anions as well as several labels of [(Trop)BrettPhos]PF₆ are omitted for sake of clarity. Carbon atoms are depicted in grey, phosphorus atoms in yellow, nitrogen atoms in blue, and oxygen atoms in red.



So far, our focus lay on dicyclohexylphosphines. Considering their interest in catalysis,^[38b,88] we also wanted to study sterically more hindered di-*tert*-butylphosphines and MenJohnPhos derivatives (Men = menthyl) as established in our group (table 28).

Table 30. Attempted synthesis of other dialkyl cycloheptatrienyl phosphonium salts.^a T = temperature; t = time; Ar = 2-biphenyl; PO = phosphine oxide.

entry	R	solvent	T [°C]	t [h]	main product [%]
1		DCM	r.t.	1	[HP' Bu ₂ Ar][PF ₆] (54)
2		[D ₈]-THF	r.t. → 60	1 (r.t.) → 5 (60 °C)	educt (94)
3		[D ₆]-benzene	r.t. → 60	1 (r.t.) → 5 (60 °C)	educt (98)
4		[D ₃]-MeCN	r.t.	24	[HP' Bu ₂ Ar][PF ₆] (63) ^b
5 ^c		[D ₃]-MeCN	r.t.	0.5	educt (>99) ^d
6 ^e		[D ₃]-MeCN	r.t.	0.5	educt (>99) ^d
7		toluene	110	14	[HP' Bu ₂ Ar][PF ₆] (46) ^f
8		toluene ^g	90	16	[HP' Bu ₂ Ar][PF ₆] ^h
9		MeCN ⁱ	r.t.	1	[HP' Bu ₂ Ar][PF ₆] (49)
10		CDCl ₃	r.t.	1	educt (87) ^j
11 ^k		[D ₃]-MeCN	r.t.	1	[HP'(Men) ₂ Ar][PF ₆] (53) ^l
12		DCM	r.t.	5	[HP'(Men) ₂ Ar][PF ₆] (88) ^{h,m}
13		DCM	r.t.	18	[HP'(Men) ₂ Ar][PF ₆] (91) ^o

^aReactions performed in the indicated solvent (0.20 M) according to GP 5.3.1 (see 7.2.6.1). Scale of the reactions differ from 50.0 μmol to 1.00 mmol. Yield in brackets refers to either isolated material after precipitation, washing (Et₂O or pentane) and drying in air, or for reactions on NMR scale: yield determined by integration of ³¹P-NMR signals. ^b20% educt, 17% oxide species. Ratio changed over time. ^c1.0 eq. NEt₃ added. ^dQuantitative formation of CHT-ammonium salt. ^e1.0 eq. DBU added. ^f19% educt, 65% [HPR₂Ar][PF₆], 16% oxide species. ^gSolvent was degassed (20 min. bubbling of argon) prior use. ^hIsolated yield not determined; spectral ratio is given. ⁱDegassed, dry acetonitrile was used. ^j8% PO, 5% [HPR₂Ar][PF₆]. ^kAt r.t., the educt is hardly soluble. ^lSignals overlay in the ¹H-NMR spectrum. Broad signal at 37.9 ppm in the ³¹P-NMR spectrum might be assigned to a tropylated phosphine. ^m9% educt, 3% PO. ^o39% [HPR₂Ar][PF₆], 61% PO.

Application of our conventional synthesis procedure to JohnPhos yielded an off-white solid. Spectral analysis of the compound revealed the sole presence of protonated phosphine (entry 1). We were initially concerned that the remarkably high amount of [HP'**Bu**₂Ar][PF₆] (Ar = 2-biphenyl) might be owed to our solvent system, e.g. the presence of water. On NMR scale, integration of signals in the ³¹P-NMR allowed us to determine the ratios of species present. Starting from Trop·PF₆ and JohnPhos, no conversion was detected in [D₈]-THF or [D₆]-benzene (entries 2 and 3) even after raising the temperature to 60 °C. Neglecting the amount of

phosphine oxide (0.6%), two new, main signals (δ_P 29.8 (46.7%), 46.6 (31.9%)) arose in $[D_3]$ -MeCN (entry 4) next to residual educt (δ_P 17.5 (20.8%)) after immediate measurement of the sample.⁴⁰ The first one could be assigned to $[HP^tBu_2Ar][PF_6]$ (δ_P 29.8), the second one to a CHT-phosponium salt of JohnPhos (δ_P 46.6). Over time, the signal of the desired product decreased while the amount of $[HP^tBu_2Ar][PF_6]$ grew. Due to overlaying of signals in the 1H -NMR spectrum, Trop-HPF₆ was the sole side-product, which could clearly be identified. Similar to BrettPhos and analogues, the quaternization seems to be a reversible process driven by the formation of the least sterically hindered product, $[HP^tBu_2Ar][PF_6]$. To prevent phosphine ligand protonation, we envisaged the addition of bases. Unfortunately, neither NEt₃ (entry 5) nor DBU (entry 6) delivered the expected results. In both cases, cycloheptatrienyl hexafluorophosphate reacted with the base to R₃N-CHT, leaving the phosphine untouched apart from partial oxidation (<1%). Since Trop·PF₆ supposedly suffered from low solubility in benzene, we repeated the reaction in dry toluene (entries 7 and 8), raising the temperature to 110 °C and 90 °C, respectively. Unfortunately, the only isolated substance consisted in the protonated species. Identical results were obtained by stirring equimolar amounts of Trop·PF₆ and JohnPhos at room temperature in dry, degassed acetonitrile (entry 9).

Our group seeks for the synthesis of chiral menthyl phosphine ligands.^[89] Several derivatives of Buchwald ligands with menthyl instead of cyclohexyl groups, including MenJohnPhos, MenSPhos, but also ligands such as PhPMen₂ have been isolated to date. As the dimethylphosphines are prone to oxidation, we wanted to exemplarily convert the most simple one, JohnPhos, to its tropylylated phosphonium salt. Since limited amounts of ligand were available, initial experiments involved detection of species on NMR scale. Mixing both reactants in CDCl₃ mainly recovered the starting material (entry 10). A minor percentage could be attributed to $[HP(Men)_2Ar][PF_6]$ (5%) as well as phosphine oxide (8%).⁴¹ After one week, the sample showed an increase of both mentioned products. Even though MenJohnPhos and Trop·PF₆ are little soluble in acetonitrile, we followed the procedure by Stephan et al.^[55b] (entry 11). Next to familiar signals of (protonated) phosphine and oxide, a new, broad signal (δ 37.9 (39%)) arose in the ^{31}P -NMR spectrum. In correlation with the 1H -NMR spectrum, it could most likely be assigned to a tropylylated phosphonium salt. A precise statement on the

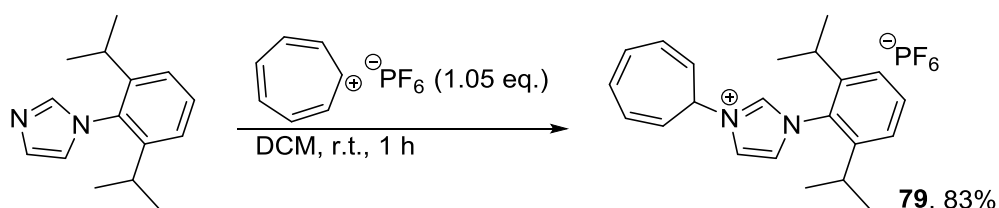
⁴⁰ Residual 20.8% were attributed to remaining educt phosphine.

⁴¹ ^{31}P -NMR shifts of detected species in CDCl₃: δ -22.2 (ArP(Men)₂), 0.8 ($[HP(Men)_2Ar][PF_6]$), 45.6 (OP(Men)₂Ar).

actual extent of phosphonium salt formation cannot be issued given that MenJohnPhos only completely dissolves in acetonitrile when heated. Large amounts of white solid were observed from the start of the reaction. Our conventional procedure in dichloromethane only afforded [HP(Men)₂Ar][PF₆] and phosphine oxide (entries 12 and 13). Prolonged stirring did actually not affect the outcome of the reaction (entry 13), but the gain in oxide resulted from removal of solvent at the rotary evaporator.

5.3.2 Cycloheptatrienyl imidazolium salt: a potential precursor for the synthesis of bidentate Pd complexes?

As result of a discussion with another group, they caught attention on our method for the tropylation of phosphines. Parts of their research focusses on the synthesis of bidentate carbocyclic/*N*-heterocyclic carbene ligands.^[64g,90] Functionalization of the imidazole core occurred directly at the metal complex site by introducing the appropriate nucleophile to a dinuclear Pd-CHT complex without isolation of the imidazolium salt. Two questions arose: is it possible to apply our method to the free imidazole? Will it be possible to isolate their Pd complex starting from our salt? Stirring of *N*-diisopropylphenylimidazole with a minor excess of Trop·PF₆ in dichloromethane afforded the desired salt as off-white solid in 83% yield (scheme 52). In solution, the C–H resonance of the tropylium unit clearly confirms the presence of a CHT structure. Compared to the phosphonium salts, CHT-signals⁴² are much more shifted downfield.



Scheme 52. Quaternization of *N*-(diisopropylphenyl)imidazole with Trop·PF₆ to imidazolium salt **79**.

Suitable crystals for X-ray diffraction were grown by slow diffusion of diethylether into a saturated solution of **79** in dichloromethane (figure 38). Crystal data, as well as collected data for structure refinement are summarized in the appendix (8.3, table 76f.). Similar to its appearance in solution, [(Trop)DippIm]PF₆ exhibits a cycloheptatrienyl structure in the solid state. Opposed to phosphonium salts, an endo-type configuration is observed. The N–C₁_{Trop} bond

⁴² All CHT-signals range over 6 ppm.

length (1.50(5) Å) is significantly shorter due to the nitrogen's hybridization, lying in the range of similar $N_{sp^2}-C_{sp^3}$ bond lengths^[91]. Concerning the CHT ring, bond lengths are alternating, with 1.33(9)-1.34(7) Å for C=C bonds, 1.43(3)-1.44(2) Å for $C_{sp^2}-C_{sp^2}$ bonds, and 1.49(9)-1.50(5) Å for $C_{sp^2}-C_{sp^3}$ bonds.

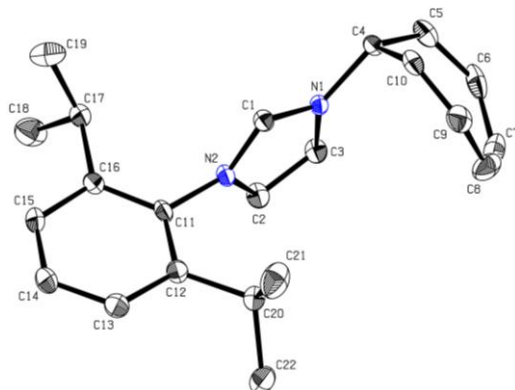
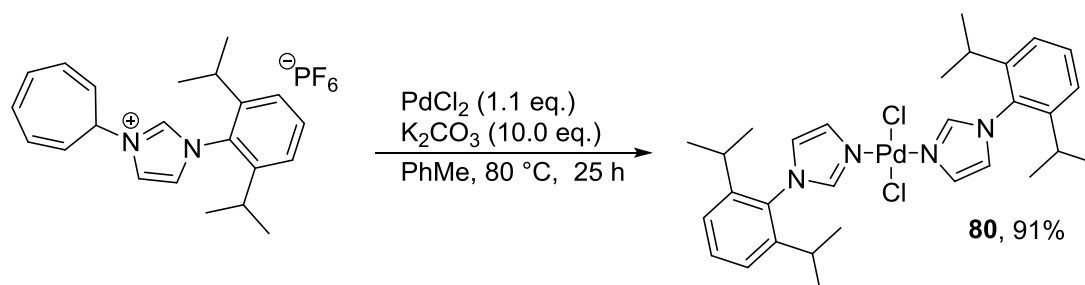


Figure 38. X-ray crystal structures of [(Trop)DippIm]PF₆ (**79**). Ellipsoids are shown at 50% probability level. Hydrogen atoms and PF₆ anion are omitted for sake of clarity. Carbon atoms are depicted in grey and nitrogen atoms in blue.

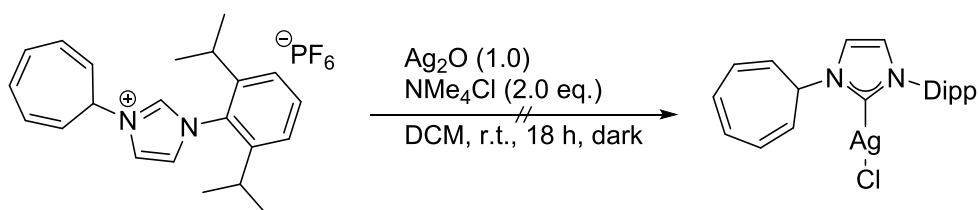
We wanted to investigate if the imidazolium salt is a potential precursor for the bidentate carbene ligand. Conventional Pd-carbene complex syntheses rely on the in situ deprotonation of the salt with direct coordination of Pd precatalyst, often PdCl₂.^[92] Following a similar protocol, we stirred the imidazolium salt **79** in the presence of PdCl₂ and K₂CO₃ at 80 °C. Purification of the crude material by flash column chromatography revealed loss of the seven membered ring. The ¹H-NMR signals of our crystalline, orange solid were significantly shifted compared to the unsubstituted imidazole. Regarding the color of the product as well as the presence of all signals in the NMR spectrum, we conclude the formation of the mononuclear Pd complex **80**. A direct synthesis attempt from the imidazole yielded identical results after crystallization.



Scheme 53. Attempted synthesis of a Pd-carbene complex.

Since the direct synthesis had failed, we envisaged an indirect approach via transmetalation from silver^[93] or copper^[94] carbene complex. A procedure by the Herrmann group involved the

incorporation of a bis(mesityl)imidazolium·BF₄.^[95] Chloride anions were introduced via the addition of NMe₄Cl. However, the addition of Pd precatalyst to the silver precursor did not lead to the desired carbene complex. Instead, the formation of a silver carbene palladate salt was observed. Following their procedure for the silver(I) carbene complex, we hoped to receive a similar compound with our unsymmetrical salt (scheme 54). During work-up, we already noticed large amounts of Ag⁰ as well as Ag₂O on top of the Celite pad. Loosing hope in the synthesis, spectral analysis of the filtrate corroborated the loss of the tropylium substituent. DippIm was the only detectable substance along with undefined decomposition adducts.



Scheme 54. Attempted synthesis of a silver(I) carbene complex. A dinuclear silver complex would also be imaginable. Dipp = diisopropylphenyl.

Regarding our findings, we guess that the tropylium unit is too labile due to its electrophilic C1–carbon atom. Any nucleophile, e.g. chloride, hydroxide or other, approaching releases the seven membered ring from the imidazole core. Once liberated, free amine might inhibit the formation of any carbene species. In the latter synthesis, an additional problem could occur from Ag₂O. Aged silver precursor might have suffered from partial decomposition. The reaction surely benefits from freshly prepared oxide.

5.3.3 Cycloheptatriene–norcaradiene: a susceptible rearrangement

Apart from two phosphonium salts, most of our cycloheptatrienyl phosphonium species rearranged to norcaradienyl species in the solid state. In solution, a CHT unit was predominant. NMR spectra of tropyliated XPhos, which show signals for both isomers, implied that they might be in equilibrium.^[96] It is not uncommon that a temperature dependency of the CHT–NCD distribution can be observed in suitable model systems.^[87e] We wanted to clarify whether we can shift the CHT–NCD equilibrium either thermodynamically or photochemically.

[(Trop)DavePhos]PF₆ exhibits a CHT structure in solution, a NCD one in the solid state. In the synthesis of the latter salt, cooling of the attempted precipitation mixture induced the slow crystallization of the ‘product phase’. Dissolution of these crystals in [D₆]-acetone showed a CHT structure as sole motif. Opposed to XPhos, DavePhos is perfectly soluble in [D₆]-acetone. A broad temperature range from –70 °C to +50 °C could be adjusted. To eliminate any residual

solvent occurring from its synthesis, azeotropic distillation with acetone was repeated several times (3X).⁴³ Both experiments (¹H and ³¹P) were recorded in 20 °C steps (figure 39). Due to the low ³¹P-NMR resolution of the machine, a relatively concentrated sample was prepared.

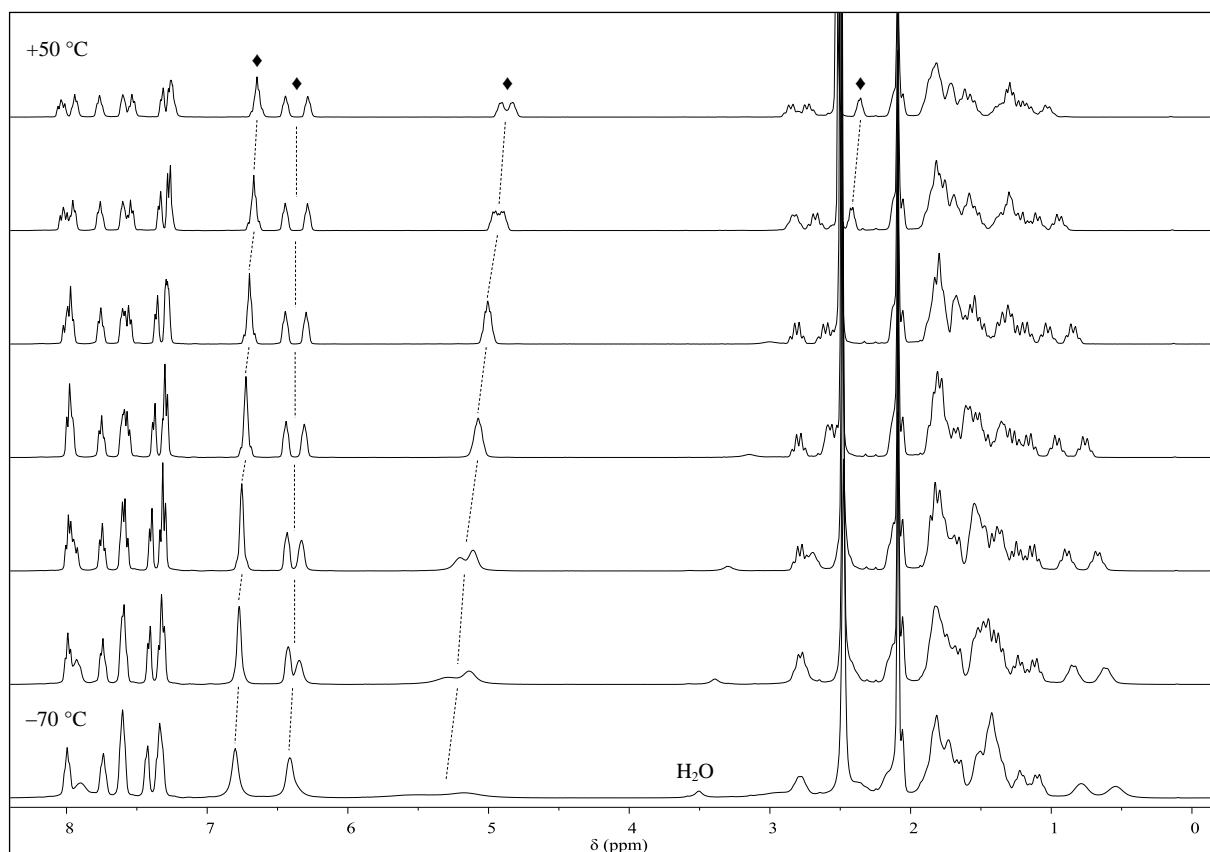
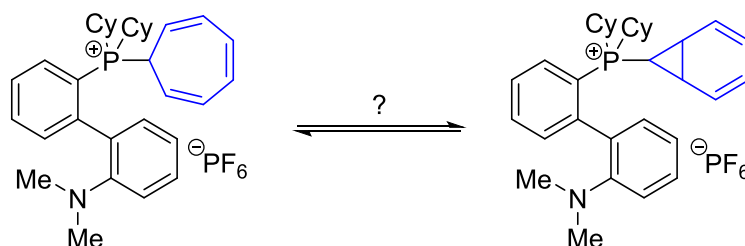


Figure 39. Variable temperature ¹H-NMR (T-NMR) spectra of [(Trop)DavePhos]⁺PF₆⁻ in [D₆]-acetone (0.12 M). NMR spectra were recorded at 400 Hz in 20 °C steps ranging from -70 °C to +50 °C. Signals of the cycloheptatrienyl unit were marked with ♦.

In none of the recorded ¹H-NMR spectra, the rise of a new NCD-C1 proton (expected at δ 0.0-0.4) can be observed. Signals of cycloheptatriene were shifted downfield and clearly broadened. At low temperatures, the rotational energy barrier is too high to be overcome, resulting in

⁴³ Even though the solid was dried for further twelve days under reduced pressure ($2.4 \cdot 10^{-2}$ mbar), acetone was still detected in the NMR. Anyway, it did not affect the outcome of the experiment.

splitting of signals. With raising temperature (+30 °C to +50 °C), coupling constants increase due to pronounced spin influence of the adjacent phosphorus atom. In the ^{31}P -NMR, only a weak signal shift ($\Delta(\delta)$ 0.3) could be perceived, being additionally broadened at -70 °C. Regarding our experiment, a CHT–NCD equilibrium shift can be excluded for [(Trop)DavePhos]PF₆. Since XPhos potentially exhibits a dynamic behavior in solution, future temperature NMR studies could be worth a try.

As photochemistry is a common tool for rearrangements^[97], we wanted to excite our salt with light to hopefully induce isomerization to the corresponding NCD compound. To determine if [(Trop)SPhos]PF₆ absorbs any light, we recorded UV/Vis of different dilutions in CHCl₃ (40.8 μM, 408 μM, 4.08 mM).⁴⁴ The most promising spectrum was obtained at a concentration of 408 μM (for spectrum see 8.4), showing an absorption maximum at 275 nm. Since we do not own any photoreactor, we contacted the group of Thorsten Bach, who is expert concerning photochemical rearrangements^[97g,98]. Using their photoreactors, we irradiated solutions of [(Trop)SPhos]PF₆ in CDCl₃ (40 mM)⁴⁵ at wavelengths ranging from 300 to 419 nm (table 31). Spectral analysis (^1H , ^{31}P) of the latter should indicate whether the isomerization took place or not.

Table 31. Irradiation of [(Trop)SPhos]PF₆ in CDCl₃.^a Ar = 2',6'-dimethoxybiphenyl-2-yl.

entry	wavelength λ	t [h]	$\delta(^{31}\text{P})^b$ [mol%]
1	300	4.5	19.0 (19), 41.5 (48)
2	350	4.5	19.0 (21), 30.8 (4), 41.5 (75)
3	366	2	19.0 (17), 30.8 (4), 41.5 (76)
4	419	16 ^c	19.0 (24), 34.6 (47), 41.5 (17)
5	350, 366	1 ^d	19.0 (14), 30.8 (4), 34.6 (17), 41.5 (65)

^aReactions performed with [(Trop)SPhos]PF₆ (14.2 mg, 22.0 μmol) in CDCl₃ (550 μL), following GP 5.3.2 (see 7.2.6.1). ^bIn the case of a wild mixture, main species are indicated; triplet of F₂P(O)OH or its anion was neglected. Number in brackets refers to mol% present. ^cClose to no conversion (~3%) after 2 hours at r.t. ^dIrradiated for 15 minutes at 350 nm (spectra measured; ratio: 18.9 (5), 30.8 (2), 34.6 (56), 41.5 (37)), additionally reacted at 366 nm (given ratios).

⁴⁴ Spectra were corrected by a blank measurement of the solvent.

⁴⁵ Any decrease in concentration would needlessly complicate execution of the reaction.

Starting with the shortest, and at the same time most energetic wavelength (300 nm), we irradiated our salt for four and a half hours at room temperature (entry 1). The triplet ($\delta -19.3$ ($J = 1016.3$ Hz)) belonging to $\text{F}_2\text{P}(\text{O})\text{OH}^{[99]}$ or its anion probably occurs from decomposition/hydrolysis of the PF_6 anion. Eight additional signals were present in the ^{31}P -NMR spectrum. The educt being fully consumed, one main signal ($\delta 41.5$) arose in the spectrum. Protonated phosphine ($\delta 19.0$) seems to be a prevalent side product in this reaction. Concerning ^1H -NMR, aromatic signals were significantly shifted downfield. The usual region for cycloheptatriene resembled to polymerized material. Despite, no NCD-C1 proton ($\delta < 0.5$) could be detected.

Yet, the newly emerging signal still rose our interest. By choosing longer wavelengths (350 nm), less side products occurred while the detected main species ($\delta 41.5$) was enriched (entry 2). Virtually identical results were achieved at 366 nm (entry 3). Leaving the ultraviolet light spectrum to 419 nm showed almost no conversion after one hour at room temperature (entry 4). Even after irradiation overnight, protonated phosphine was the major byproduct except for unreacted starting material. Short reaction times should clarify, if we could avoid protonation of the phosphine (entry 5). After 15 minutes at 350 nm, almost half of the salt was converted, our new species being predominant. Further irradiation of the sample at 366 nm⁴⁶ indicated that the progression of the reaction slowly approaches the results observed in entries 2 and 3. At this point, the reaction was stopped, since the amount of protonated species accompanied with the photochemical reaction could not be reduced.

Even though we can exclude any formation of a NCD species, we wanted to identify the main side product of the irradiation process. Merging entries 2 and 3, we attempted purification by flash column chromatography (DCM-MeOH 10:1). 2D spectral analysis (^1H , ^{31}P , HSQC, HMBC, APT, COSY) of the isolated compound revealed the actual structure. In a first instance, irradiation of the salt led to loss of the CHT group. In the excited state, the free SPhos ligand absorbed enough energy for the monodemethoxylation. The phosphorus atom seized its opportunity for ring closure to the tricyclic benzo[b]phosphindolium salt (figure 40). Due to observed P,C coupling of quaternary carbon atoms ($\delta 117.8$ (d, $J_{\text{P,C}} = 80.6$ Hz), 120.5 (d, $J_{\text{P,C}} = 79.7$ Hz, 1C), ^{13}C -NMR analysis supports our assumption.

⁴⁶ In the meantime, the 350 nm irradiation lamp was not in operation anymore.

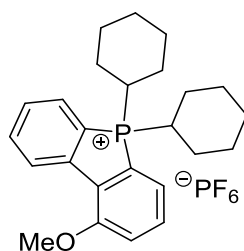
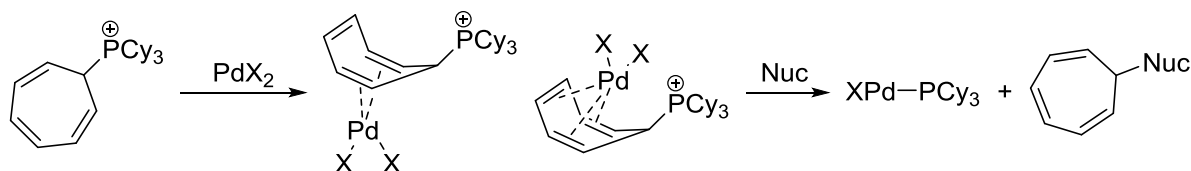


Figure 40. Main product emerging from irradiation of [(Trop)SPhos]PF₆. Counter-ion could either be F₂P(O)O⁻ (detected in the spectrum) or PF₆⁻. ³¹P-NMR spectra were only recorded from -40 ppm to +60 ppm for better resolution.

5.3.4 Reactivity of tropylium salts: transfer to Pd metal center

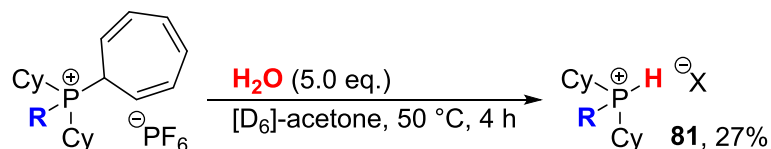
The reactivity of the tropyliated ligand phosphonium salts towards nucleophiles is of interest for their projected application as ligand precursor components in precatalysts. A pronounced coordination, either η^2 or η^3 of the CHT unit, to the metal center of a precursor complex is expected to enhance the reactivity of the CHT-phosphonium salt. Nucleophiles present in the reaction medium could attack the cycloheptatrienyl moiety at the C1-carbon atom, simultaneously releasing the phosphine. Following this hypothesis, we hoped to accelerate the generation of catalytically active Pd-phosphine species (scheme 55). Alternatively, π -coordinated electrophilic metal might induce a 1,2-hetero-metallation, followed by the β -elimination of metal and phosphane ligand. Finally, also the oxidative addition of the C-PR₃⁺ bond by a low-valent metal center as for example Pd(0) is conceivable.



Scheme 55. Potential coordination of tropylium salts to Pd with subsequent release of catalytically active Pd-phosphine species. PF₆⁻ counter-ion were omitted for sake of clarity. X = anion, e.g. halogen (chloride, bromide), acetate; Nuc = nucleophile (chloride, acetate, amine...).

In first instance, we wanted to verify whether our salts remain stable in the presence of aqueous media. If residual water affects our salts, we should be able to detect formation of protonated phosphine along with 1-hydroxycycloheptatriene or related solvent adducts. Water (ca. 5 eq.) was added to a solution of [(Trop)SPhos]PF₆ in CDCl₃ (see 7.2.6.1 for detailed procedure). After storing of the sample for 16 hours at room temperature, no decomposition was observed, in the ¹H- or ³¹P-NMR spectrum. Further monitoring of the emulsion for a whole week still did not show any changes. With low solubility in chloroform, the amount of water present in the

organic phase could have been too marginal for any decomposition to take place. Repetition of the analogous experiment in [D₆]-acetone at room temperature did not affect the educt at first. However, raising the temperature for four hours to 50 °C led to the formation of protonated phosphine (27%) according to ³¹P-NMR spectroscopy (scheme 56). The polar character of acetone accelerates the solvolysis and nucleophilic attack by water.^[100]



Scheme 56. Hydrolysis of [(Trop)SPhos]PF₆ in [D₆]-acetone. R = 2-(2',6'-dimethoxybiphenyl); X = PF₆ or OH.

The phosphines discussed in this chapter are useful ligands in catalytic amination reactions.^[6b,29a,29b,31,39b,44,101] With their nucleophilic character^[100], amines also constitute optimal reactants for efficient ligand release from the phosphonium salts. We subjected two of our phosphonium salts, SPhos and DavePhos, to different amines ranging from primary to tertiary (table 30). Since most phosphines are recrystallized in methanol, samples were purified by washing with cold alcohol. Due to their tendency for decomposition, we did not envisage the isolation nor quantification of cycloheptatrienyl amines but simply characterized them in the filtrate's crude NMR spectra. We chose 2-aminopyridine as secondary amine, since it exhibits very characteristic ¹H-NMR shifts. Stirring of [(Trop)SPhos]PF₆ with 2-aminopyridine in the presence of base afforded 75% of free phosphine (entry 1). *N*-(Cyclohepta-2,4,6-trien-1-yl)pyridin-2-amine constituted the major species of the filtrate. Next to 2-aminopyridine, residual troplated phosphonium salt and minor amounts of phosphine (oxide) were detected. In catalysis, reactions are often performed in toluene.^[102] Due to their ionic character, cycloheptatrienyl salts are less soluble in non-polar reaction media. However, mixing of [(Trop)DavePhos]PF₆ with 2-aminopyridine in toluene at 60 °C yielded near identical results (entry 2). The secondary amine, *N*-methylpiperazine, efficiently released DavePhos from its precursor (entry 3). Spectral analysis of the filtrate confirmed the formation of *N*-CHT-*N*'-methylpiperazine. In the case of tertiary amines, minor conversion was detected at room temperature (entry 4); heating to 50 °C slightly improved the yield (entry 5).

Table 32. Release of free phosphine from tropylium salts.^a PO = phosphine oxide.

entry	R	amine [eq.]	base [eq.]	solvent	T [°C]	t [h]	yield (Cy ₂ PR) [%]
1			K ₂ CO ₃ (2.4)	DCM	r.t.	13	75 ^b
2			K ₂ CO ₃ (2.0)	toluene	60	18	73 ^c
3			K ₂ CO ₃ (2.0)	DCM	r.t.	2	75 ^d
4 ^e		NEt ₃ (1.2)	-	CDCl ₃	r.t.	24	10 ^f
5 ^e		NEt ₃ (1.2)	-	CDCl ₃	50	16	20 ^g

^aReactions performed with tropylium salt (200 or 400 μmol) in the indicated solvent (0.2 M) according to GP 5.3.3 or 5.3.4 (NEt₃) (see 7.2.6.1); isolated yield of phosphine. ^bWork-up in air. Product composition: 96 mol% phosphine, 1 mol% educt, 2 mol% PO, 1 mol% other. ^cWork-up inside a glovebox. Product composition: 99 mol% phosphine, <1 mol% educt and PO each. Filtrates still contained minor amounts of free ligand as well as salt. ^dWork-up in air. Product composition: 98 mol% phosphine, 1 mol% educt, 1 mol% PO. ^eReaction performed on 50.2 μmol scale. ^fYield determined by integration of ³¹P-NMR signals: after 5 min. 5 mol% phosphine, 94 mol% educt, 1 mol% PO; after 24 h 10 mol% phosphine, 86 mol% educt, 4 mol% PO. ^gYield determined by integration of ³¹P-NMR signals: 20 mol% phosphine, 62 mol% educt, 18 mol% PO.

Primary as well as secondary amines proved to be ideal reaction partners for efficient phosphine release. Nevertheless, we wanted to investigate the direct transfer of ligand to palladium by detecting ligated Pd⁰ or Pd^{II} species. Short boiling (45 min.) of PdCl₂(MeCN)₂ with (CHT)PCy₃·PF₆ (2.0 eq.) in the presence of sodium acetate (2.0 eq.) partially converted the educt salt. According to ³¹P-NMR, PdCl₂(PCy₃)₂ was the major product (>50%) next to educt salt, decomposition adducts, and phosphine oxide. A precise quantification of the components was not possible, since PdCl₂(MeCN)₂ is moderately soluble in chloroform, and sparingly soluble in benzene.^[103] To get a better insight in the progression of the ligand transfer, we monitored the phosphine release via ³¹P-NMR analysis (figure 41). A screw cap NMR tube charged with Pd precatalyst, (CHT)PCy₃·PF₆, and excess of strong base was sonicated under the exclusion of air to imitate cross-coupling reaction conditions. Due to the very low solubility of our salt and the base in [D₆]-benzene, a suspension was observed during the entire reaction. Yet, after five minutes at room temperature, a new, small signal (δ 39.0) appeared in the

spectrum. Comparison with literature allowed the assignment to $\text{Pd}^0(\text{PCy}_3)_2$.^[82] With increasing time, and temperature (60 °C), the signal rose in intensity. No free ligand has been observed; direct coordination to Pd is preferred. Small amounts of $\text{PdCl}_2(\text{MeCN})_2$ (δ 25.1) were also detected. Sonication at 60 °C caused growing dissolution of the educt salt (δ 30.8). Partial decomposition of either starting material or complex led to the observed small impurities. Prolonged storing of the NMR sample (2 days) slowly advanced the dissociation of the Pd precatalyst, entailing the oxidation of free phosphine to its oxide due to diffusion of oxygen into the NMR tube. At the beginning of the reaction, we added naphthalene as internal standard for the quantification of generated Pd complex in the ^1H -NMR spectrum. However, strong overlapping of signals hindered an accurate measurement.⁴⁷

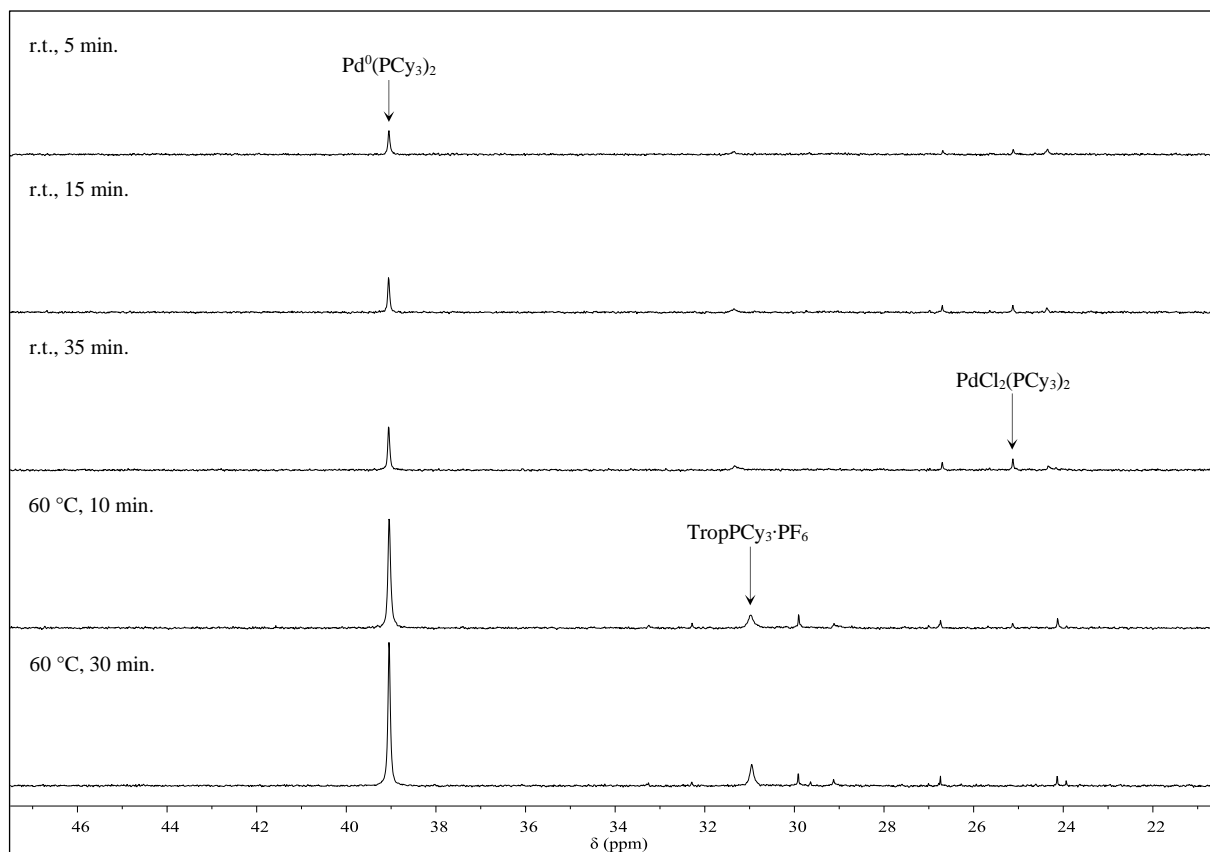
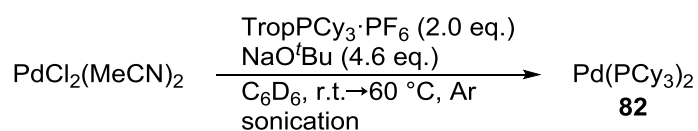


Figure 41. Stacked ^{31}P -NMR spectra ($[\text{D}_6]$ -benzene, cut-out) of phosphine transfer to Pd metal. The sample was prepared inside a glovebox (see 7.2.6.9 for details). Times indicated depict the total time of sonication at either room temperature or 60 °C. Increase of temperature to 60 °C was conducted after 35 min at ambient temperature.

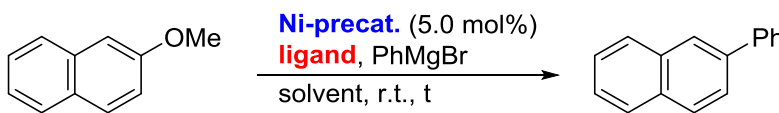
⁴⁷ Approximate integration of signals (PK-234-4) delivered 52% of Pd complex.

5.3.5 Cycloheptatrienyl phosphonium salts in catalysis: increase in efficiency?

We have efficiently demonstrated the fast release of free phosphine ligand from tropylium salts with immediate transfer to palladium metal. Palladium phosphine complexes have been confirmed by ^{31}P -NMR, which were reported to be active in catalysis.^[82,104]

In seeking potential applications of our CHT phosphonium salts, we came across the nickel-catalyzed cross-coupling of aryl Grignard reagents with aromatic alkyl ethers, which profits from the same type of ligand studied by us.^[19] The incorporation of Ni-PCy₃ precatalysts in 1:2 ratio proved to be crucial for the reaction. Regarding Dankwardt's substrate scope, 2-methoxynaphthalene should turn out as optimal starting material for q-NMR analysis. The characteristic shifts of the reaction components are well separated, simplifying spectral quantification. First screening experiments of Dankwardt included the use of THF as solvent at 60 °C. When CHT salt TropPCy₃·PF₆ was combined in co-catalytic amounts with metal precursor Ni(acac)₂, the reaction of PhMgBr with 2-MeONap showed moderate conversion to 2-phenylnaphthalene after 18 hours at room temperature (table 33, entry 1).

Table 33. Ni-catalyzed cross-coupling of PhMgBr with 2-methoxynaphthalene.^a Entries 2-5 were carried out as kinetic experiments, but best comparable yields are only depicted. precat. = precatalyst; acac = acetylacetonate; DEM = 1,1-diethoxymethane; dme = 1,2-dimethoxyethane.



entry	Ni-precatal.	ligand [mol%]	solvent	PhMgBr [eq.]	t [h]	ArOMe	yield
1 ^b	Ni(acac) ₂	TropPCy ₃ ·PF ₆ (20)	THF	3.2	18	52	45
2 ^{c,d}	NiCl ₂ (PCy ₃) ₂	PCy ₃ (10)	DEM-Et ₂ O (1:1)	1.5	2	4	89
3 ^e	NiCl ₂ (PCy ₃) ₂	PCy ₃ (10)	DEM-Et ₂ O (1:1)	1.5	4	9	86
4 ^e	NiCl ₂ (dme)	PCy ₃ (10)	DEM-Et ₂ O (1:1)	1.5	1	14	83
5 ^e	NiCl ₂ (dme)	TropPCy ₃ ·PF ₆ (10)	DEM-Et ₂ O (1:1)	1.5	5	100	0

^aReactions performed with 1.00 mmol 2-methoxynaphthalene in the indicated solvent (total volume 3 mL), according to GP 5.3.6 (see 7.2.6.1); Grignard reagent added as solution in THF, or Et₂O, respectively; spectral yield according to ^1H -NMR against internal standard, given in mol%. ^b0.25 M. ^c0.33 M. ^dReaction performed at 35 °C. ^e0.17 M.

The choice of solvent played a major role in the cross-coupling reaction.^[19] Non-polar ethers, such as diethoxymethane (DEM), Bu₂O, ⁱPr₂O, or ^tAmOMe (^tAm = tert-amyl, -CETMe₂) usually gave best results. Since DEM-Et₂O often proved superior, we stuck with a 1:1 mixture for further experiments. The amount of Grignard reagent was set to 1.5 equivalents when combining NiCl₂(PCy₃)₂ with additional PCy₃ (10.0 mol%), imitating the conditions described by Dankwardt. Initially, we wanted to monitor the reaction progress by withdrawing samples

after fixed time intervals. In first instance, the reaction progressed too fast (entry 2), showing 89% yield after two hours. Lowering of the temperature to room temperature along with dilution of the reaction medium provided better conditions for kinetic studies (entry 3). To exclusively scrutinize the influence of added ligand precursor, we changed the Ni precatalyst to the unfunctional etherate $\text{NiCl}_2(\text{dme})$. However, the latter significantly increased the rate of the reaction with virtually identical results after only one hour (entry 4), probably the consequence of worse solubility of $\text{NiCl}_2(\text{PCy}_3)_2$. It is also imaginable that the surplus of PCy_3 ligand in combination with $\text{NiCl}_2(\text{PCy}_3)_2$ blocked the active nickel center. No conversion at all was detected when $[(\text{Trop})\text{PCy}_3]\text{PF}_6$ was introduced as phosphine source in the established reaction conditions (entry 5). Two major issues might be responsible for the failed reaction. The salt might suffer from very low dissolution in the non-polar solvent mixture. Even though the Grignard solution did not exhibit any precipitation of inorganic decomposition adducts, degradation of the reagent cannot be excluded since no titration was conducted shortly before the reaction. Due to changes in our project priorities, we did not further investigate this type of Ni-catalyzed cross-coupling reaction.

Buchwald or related ligands have been extensively employed in Suzuki-Miyaura cross-coupling reactions.^[31a,33,105] In dioxane, complete conversion of 4-chloroanisole as one of the most demanding π -donor substrates with phenyl boronic acid has been observed after overnight reaction at 100 °C.^[31a,105b] At room temperature, higher catalyst loadings were indispensable. With the plethora of CHT salts synthesized, we wanted to examine whether our ligand precursors can keep up with the corresponding free phosphines. Hence, we subjected Buchwald ligands as well as our tropylium salts to similar reaction conditions reported in literature^[31a] (table 34). Instead of dioxane used in literature, we chose toluene. After stirring for five hours at 100 °C, reaction mixtures were directly analyzed by q-NMR from the reaction mixture. Losses in recovery might be due to partial volatility of 4-chloroanisole and anisole. In all cases, little or dehalogenated starting material was observed. Except for $[(\text{Trop})\text{CyJohnPhos}]\text{PF}_6$, our salts yielded the desired product in good to excellent yield. Free phosphines usually performed less efficient than our precursors. Solely CyJohnPhos afforded slightly enhanced reactivity (entry 1) compared to the quaternary salt (entry 2). CHT-alkylated DavePhos tremendously accelerated the reaction (entries 3 and 4). The dimethoxy substituted phosphine, SPhos (entry 5), slowed the reaction by 20% in contrast with its salt (entry 6). RuPhos delivered similar yields in either experiment (entries 7 and 8).

Table 34. Pd-catalyzed Suzuki cross-coupling of 4-chloroanisole with phenyl boronic acid using either tropyliated phosphonium salts or free phosphines.^a recov. = recovery; CHT = cycloheptatrienyl.

entry	ligand	state of phosphine ^b	educt [%]	anisole [%]	yield [%]	recov. [%]
1		free ligand	29	<1	69	98
2		CHT-salt	37	1	56	94
3 ^c		free ligand	-	-	93	-
3		free ligand	45	1	54	100
4		CHT-salt	3	<1	92	95
5		free ligand	28	1	71	100
6		CHT-salt	8	<1	86	94
7		free ligand	12	1	85	98
8		CHT-salt	5	<1	92	97
9		free ligand	19	2	79	100
10		CHT-salt	<1	<1	96	96
11		free ligand	18	<1	82	100
12		CHT-salt	<1	<1	95	95

^aReactions performed with 120 μ L (985 μ mol) 4-chloroanisole in toluene (2 mL), according to GP 5.3.7 (see 7.2.6.1); spectral yield according to ¹H-NMR with internal standard, given in mol%. ^bFree refers to commercially available free phosphine ligand; CHT-salt to synthesized tropylium salts. ^cReaction conditions reported by Buchwald et al.^[31a]; 4-chloroanisole (2.00 mmol, 1.0 eq.), PhB(OH)₂ (1.5 eq.), K₃PO₄ (2.0 eq.), Pd(OAc)₂ (0.5 mol%), DavePhos (0.75 mol%) at 100 °C in dioxane (6 mL) until completion as judged by GC analysis.

Sterically bulky XPhos afforded good results (entry 9). However, [(Trop)XPhos]PF₆ speeded the coupling up by 20%, giving near quantitative yield of the biaryl (entry 10). Virtually identical results as for XPhos were obtained for BrettPhos (entries 11 and 12). Interestingly, other screening experiments of our group revealed quantitative conversion after only one hour. Biggest difference lay in the involved base. Whereas powdery⁴⁸ K₃PO₄ was weighed inside a glove-box and used for all manipulations depicted in table 34, previous reactions performed in

⁴⁸ The solid was dried for at least two hours at 300 °C under reduced pressure (0.8-1.2 mbar) and stored inside a glove-box.

our group relied on salt stored in a Schlenk flask. The already slightly clumpy base was weighed in air, allowing further uptake of water. The latter seems to exhibit a crucial role in catalyst pre-activation.^[105a,105d,106] We suggest working under completely anhydrous conditions impeded Pd^{II} reduction in case where the free phosphines were applied. Except for [(Trop)CyJohnPhos]PF₆, our precursors underlined their superior role for catalyst activation. The cross-coupling reaction displayed in table 34 might also profit from a Pd–ligand ratio of 1:1. Under the reaction conditions employed, our tropylium salts could have released lower amounts of free phosphine, thus approaching a 1:1 metal to ligand ratio. Further investigations should focus on varying the Pd–ligand ratio to clarify the reasons for the superior reactivity of our tropylium salts compared to the free Buchwald ligands.

5.4 Conclusion and outlook

A range of allylic, benzylic and alkenyl tricyclohexylphosphonium salts has been synthesized (figure 42). While allylic and benzylic were available by simple stirring of PCy₃ with the appropriate halides in dichloromethane, styryl salts **65** and **69** required microwave assisted heating in the presence of Pd(0) precatalyst and a salt additive. The latter were accompanied with minor amounts of an yet unknown phosphorous impurity. Increased steric hindrance or the absence of an α -CH bond blocked any conversion of 2-substituted (Me, Pr) 2-bromo-1,1-diphenylethylenes. Several of the new phosphonium salts were characterized by X-ray analysis as well as standard NMR methods.

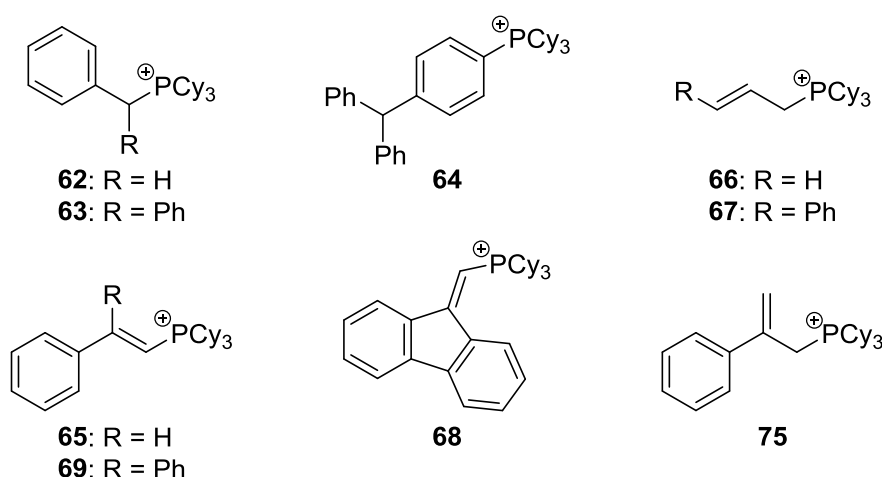


Figure 42. Isolated tricyclohexylphosphonium salts. Counter-ions (bromide, chloride) were omitted for sake of chloride.

Since attempts towards synthesizing an α -methylstyrene phosphonium salt gave a low amount of the desired product along with its allyl isomer, we had a closer look on the isomerization of

allyl type phosphonium salts. Sodium pivalate as well as DBU turned out to be efficient reagents for quantitative rearrangement of allyl tricyclohexylphosphonium bromide to its propenyl derivative. The reaction with DBU in deuterated chloroform also led to near full incorporation of deuterium at propenyl extremities. However, isomerization of tricyclohexyl(2-phenylallyl)-phosphonium bromide (**75**) only provides an equilibrium mixture of allylic and alkenylic phosphonium salt (figure 43).

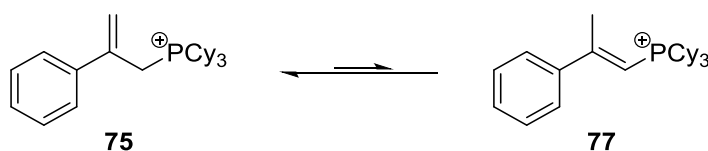


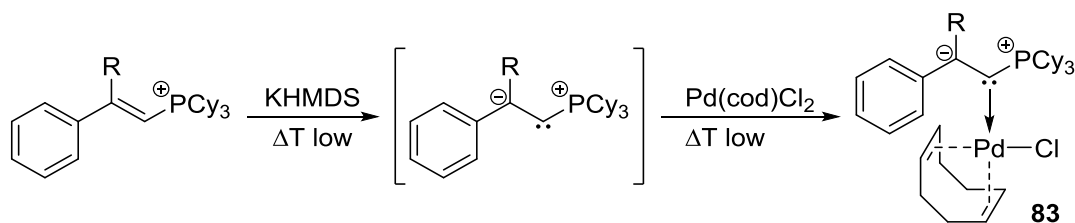
Figure 43. Observed equilibrium in the rearrangement of phosphonium salt **75** to **77**. Counter-ions (bromide) were omitted for sake of clarity.

Most of our unsaturated phosphonium salts were evaluated as ligand precursors in the Pd-catalyzed amination of chlorobenzene with *N*-methylpiperazine reported by Reddy et al.^[84]. Whereas allyl and styryl phosphonium salts performed similarly to the well-known PdCl₂(PCy₃)₂ precatalyst (66%), benzyl and fluorenyl type compounds led to lower yields (<45%). A characteristic color change to wine red at beginning of the reaction might indicate the formation of ylidic species in case of benzylic phosphonium salts.

To verify the potential ligand release from our unsaturated precursors, the styryl phosphonium salt **65** was heated with Pd precatalyst in the presence of strong base or a nucleophile. In the ³¹P-NMR spectrum, one could observe that the vinyl-PCy₃ bond was cleaved, releasing free phosphine. Next to minor amounts of phosphine oxide, signals belonging to a mixed alkenyl tricyclohexylphosphonium-Pd complex were detected as main species. The presence of PdCl₂(PCy₃)₂ was also confirmed. High concentrations of strong base led to the formation of Pd black. In the ³¹P-NMR spectrum, a large amount of small phosphorous signals was detected. The temporary presence of an ylide due to deprotonation followed by polymerization^[83] might be imaginable. Broad signals observed in the ¹H-NMR spectrum support the hypothesis of polymerization. Since the conditions have not yet been optimized, less harsh conditions could ameliorate the enrichment of free ligand in solution, thus generating an active catalyst in the presence of palladium. A major issue might be the low solubility of salt **65** in non-polar solvent, such as benzene, toluene, or THF, requiring elevated temperatures for any release to take place. An increase in solubility could be obtained by substitution of the counterion from bromide to TRISPHAT (phosphorous(V) tris(tetrachlorocatecholate)phat) using ion-exchange. Variations

of base/nucleophile (weak vs. strong) and Pd precatalyst (Pd^0 vs. Pd^{II} source) could further promote the efficient release of free ligand. Strong base should also be avoided to prevent unwanted decomposition.

Future studies could focus on the isolation of a PCy_3 -ylide–Pd complex to verify its potential activity in catalysis. Mono- and diphenylethylene phosphonium salts would be convenient precursors, since their structural motif might stabilize intermediates due to π - or σ -effects. Substitution of halide counter-ions by less coordinating ones (BF_4^- , PF_6^- , or other) might be useful to prevent any unwanted side-reactions. Deprotonation should be attempted at low temperature (-78°C) with non-nucleophilic amide base (alkali HMDS) instead of $n\text{-BuLi}$ ^[107]. Subsequent addition of $\text{Pd}(\text{cod})\text{Cl}_2$ might yield the desired complex **83** (scheme 57). Once in hand, stability studies would provide further insight in the potential release of free PCy_3 ligand.



Scheme 57. Proposed reaction sequence for the formation of carbene complex **83**. Bromide ions were omitted and should be replaced by a less coordinating anion prior deprotonation.

Phosphination of bromoalkenes failed with several substrates. Under Pd catalysis, the group of Stang was able to isolate substituted PPh_3 -based vinyl phosphonium salts from vinyl triflates, including the 2-phenyl-1-propen-1-yl derivative.^[70] Similar PCy_3 -based salts from corresponding pseudo-halides would be worth a try. Steric crowding around the C_{sp^3} atom of trityl chloride hindered the formation of the desired salt. Tri-*para*-substituted triphenylmethanes could block any unwanted phosphination of phenyl groups, possibly favoring the attack of the central carbon atom. Unfunctional anions of our salts could be substituted by ions exerting a distinctive role, thus leading to multifunctional precursors. Besides stored ligand and Pd(II) reducing agent, one could add CMD, base or other functionality. Widespread use of these phosphonium salts in catalysis is yet to come.

A specific class of phosphonium salts for use as ligand precursor was presented in the form of CHT-phosphonium salts derived from ligand and tropylium salts. Whereas tropylation of most common cyclohexyl based Buchwald ligands worked smoothly, other derivatives could not be converted, entailing quantitative formation of protonated phosphine. Crowded phosphines, e.g.

BrettPhos, KatPhos, and CyAnPhos, showed minor amounts of the latter side-product. Increasing bulk around the phosphorus atom proved crucial for the synthesis. In most cases, the cycloheptatrienyl species was predominant in solution. In case of BrettPhos and KatPhos tropylium salts, an equilibrium between a CHT- and NCD-species (CHT/NCD 15:85) seems to be present but could not be influenced. Except for CyJohnPhos, KatPhos and CyAnPhos, suitable crystals for X-ray diffraction were grown by slow diffusion of diethylether into a saturated solution of salts. Analysis of structures revealed the susceptibility of CHT-salts towards rearrangement. A norcaradienyl motif was observed in particular with bulky phosphonium salts. Even though an [(NCD)P^tBu₃]PF₆ salt has been reported, JohnPhos as well as Men₂JohnPhos (Men = menthyl) only afforded the protonated phosphine, which might be due to increased steric hindrance of substituents. The synthetic procedure of tropylium alkylation was further extended to one imidazole, where the resulting imidazolium salt did not rearrange to an NCD salt in the solid state. Attempts for the synthesis of a desired Pd carbene complex failed, causing loss of the CHT unit.

With the aid of variable temperature NMR, we studied the behavior of one ligand derived tropylium phosphonium salt in solution, namely [(Trop)DavePhos]PF₆. Apart from broadening of signals as consequence of slow rotation at low temperatures, no formation of a NCD phosphonium salt was detected. Since photochemistry is known for rearrangement^[98,108] reactions, we envisaged structural modification of our salt, [(Trop)SPhos]PF₆, induced by photochemical excitation. Irradiation at either 350 or 366 nm enriched the newly formed species as major product along with minor amounts of protonated phosphine. Spectral analysis of isolated material excluded any rearrangement of the seven membered ring but reasoned the generation of a tricyclic benzo[b]phosphindolium salt (figure 44).

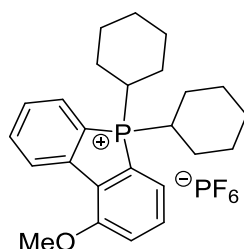


Figure 44. Main product emerging from irradiation of [(Trop)SPhos]PF₆. Counter-ion could either be F₂P(O)O⁻ (detected in the spectrum) or PF₆⁻. ³¹P-NMR spectra were only recorded from -40 ppm to +60 ppm for better resolution.

The stability of [(Trop)SPhos]PF₆ as well as potential for efficient ligand release was analyzed by subjecting them to different conditions. Under aqueous conditions, [(Trop)SPhos]PF₆ partially decomposed to its protonated analogue when heated in acetone. Primary and secondary amines easily generated substituted cycloheptatriene along with free phosphine ligand. The tertiary amine, NEt₃, only showed minor conversion. Direct transfer of the PCy₃ unit from the cationic phosphonium salt to Pd metal was verified by ³¹P-NMR spectroscopy.

In Ni-catalyzed Kumada cross-coupling^[19] of PhMgBr with 2-methoxynaphthalene, we combined [(Trop)PCy₃]PF₆ with NiCl₂(dme) at room temperature to verify the feasibility of our tropylium salts as free phosphine precursors in catalysis. However, a low amount of 2-phenylnaphthalene was obtained. The low conversion could be owed to poor solubility of the salt or previous decomposition of the Grignard reagent. Astonishing results were obtained in the Pd-catalyzed Suzuki coupling of 4-chloroanisole with phenyl boronic acid. In most cases, our quaternary salts proved superior to the free phosphine when combined with Pd(OAc)₂. A direct comparison between our tropylium salts and the results obtained in literature cannot be made, since DavePhos in dioxane solution^[31a] was the only condition reported. Our cross-coupling reactions were performed in toluene and showed almost identical reactivity to the one reported for DavePhos^[31a]. We suggest that the cycloheptatrienyl motif supports catalyst pre-activation.^[105a,105d,106b,106c]

The steric bulk near the phosphine seems to have an influence on the CHT/NCD-distribution in solution and in the solid state. In most cases no NCD structure was observed in solution. Whereas an NCD structure was predominant in solution with bulky BrettPhos and KatPhos tropylium salts, minor steric bulk already induced rearrangement to the NCD-conformation with most tropylium salts when crystallizing. However, it is unclear why the latter motif is not preferred in solution or why no tropylated phosphine was obtained with ^tBu₂P- or Men₂P-ligands. Further attempts for the crystallization of [(Trop)CyJohnPhos]PF₆, [(Trop)KatPhos]PF₆ and [(Trop)CyAnPhos]PF₆ would clarify their structure in the solid state, thus giving more insight in the relationship between steric bulk and structure of the tropylium unit. Since [(Trop)XPhos]PF₆ seemed to present a dynamic behavior in solution, variable temperature NMR might induce enrichment of either one rearrangement species. In that manner, one or both species could be detected in the NMR spectra and indicate a shift in equilibrium. The choice of solvent could have crucial impact on their distribution. Solvent dependent decomposition of cycloheptatrienyl salts would deliver useful information for

application in catalysis. Pre-activation of Pd induced by our salts will surely find serious attention in catalysis, especially when aqueous conditions are undesirable. Substitution of unfunctional anion or the combination with Pd metal would increase the degree of functionality of our salts. Superior reactivity compared to simple, free phosphines would be attributed, leaving plenty of room for the discovery of unprecedented coupling chemistry.

5.5 References

- [1] P. Klein, *The Multi-Component-Catalyst (MCC) Principle: Designing Functional Catalyst Precursors for Reaction Development*, master thesis, Technical University of Munich (Garching bei München), **2016**.
- [2] S. L. Buchwald, D. Milstein, *Ligand Design in Metal Chemistry: Reactivity and Catalysis*, John Wiley & Sons, **2016**.
- [3] a) P. Fitton, E. A. Rick, *J. Organomet. Chem.* **1971**, *28*, 287-291; b) A. Sekiya, N. Ishikawa, *J. Organomet. Chem.* **1976**, *118*, 349-354; c) D. Milstein, J. Stille, *J. Am. Chem. Soc.* **1979**, *101*, 4992-4998; d) J. W. Labadie, J. Stille, *J. Am. Chem. Soc.* **1983**, *105*, 6129-6137.
- [4] a) C. B. Ziegler Jr, R. F. Heck, *J. Org. Chem.* **1978**, *43*, 2941-2946; b) A. Spencer, *J. Organomet. Chem.* **1983**, *258*, 101-108.
- [5] W. A. Herrmann, C. Brossmer, K. Öfele, C. P. Reisinger, T. Priermeier, M. Beller, H. Fischer, *Angew. Chem. Int. Ed.* **1995**, *34*, 1844-1848.
- [6] a) A. F. Littke, G. C. Fu, *Angew. Chem. Int. Ed.* **1998**, *37*, 3387-3388; b) J. F. Hartwig, M. Kawatsura, S. I. Hauck, K. H. Shaughnessy, L. M. Alcazar-Roman, *J. Org. Chem.* **1999**, *64*, 5575-5580; c) G. Mann, C. Incarvito, A. L. Rheingold, J. F. Hartwig, *J. Am. Chem. Soc.* **1999**, *121*, 3224-3225; d) K. H. Shaughnessy, P. Kim, J. F. Hartwig, *J. Am. Chem. Soc.* **1999**, *121*, 2123-2132; e) A. F. Littke, C. Dai, G. C. Fu, *J. Am. Chem. Soc.* **2000**, *122*, 4020-4028; f) A. F. Littke, G. C. Fu, *J. Am. Chem. Soc.* **2001**, *123*, 6989-7000; g) M. Nishiyama, T. Yamamoto, Y. Koie, *Tetrahedron Lett.* **1998**, *39*, 617-620.
- [7] S. A. Buckler, *J. Am. Chem. Soc.* **1962**, *84*, 3093-3097.
- [8] M. R. Netherton, G. C. Fu, *Org. Lett.* **2001**, *3*, 4295-4298.
- [9] T. Saget, N. Cramer, *Synthesis* **2011**, *15*, 2369-2371.
- [10] a) A. J. Blacker, M. L. Clarke, M. S. Loft, J. M. Williams, *Org. Lett.* **1999**, *1*, 1969-1971; b) M. R. Netherton, C. Dai, K. Neuschütz, G. C. Fu, *J. Am. Chem. Soc.* **2001**, *123*, 10099-10100; c) R. B. Bedford, C. S. Cazin, S. L. Hazelwood, *Chem. Commun.* **2002**, 2608-2609; d) A. C. Frisch, N. Shaikh, A. Zapf, M. Beller, *Angew. Chem. Int. Ed.* **2002**, *41*, 4056-4059; e) J. H. Kirchhoff, C. Dai, G. C. Fu, *Angew. Chem. Int. Ed.* **2002**, *41*, 1945-1947; f) M. R. Netherton, G. C. Fu, *Angew. Chem. Int. Ed.* **2002**, *41*, 3910-3912.
- [11] W. Shen, *Tetrahedron Lett.* **1997**, *38*, 5575-5578.
- [12] A. F. Littke, G. C. Fu, *J. Org. Chem.* **1999**, *64*, 10-11.

- [13] G. C. Fu, *Acc. Chem. Res.* **2008**, *41*, 1555-1564.
- [14] A. De Meijere, S. Bräse, M. Oestreich, *Metal catalyzed cross-coupling reactions and more*, John Wiley & Sons, **2013**.
- [15] a) J. P. Stambuli, M. Bühl, J. F. Hartwig, *J. Am. Chem. Soc.* **2002**, *124*, 9346-9347; b) J. P. Stambuli, C. D. Incarvito, M. Bühl, J. F. Hartwig, *J. Am. Chem. Soc.* **2004**, *126*, 1184-1194; c) M. Yamashita, J. F. Hartwig, *J. Am. Chem. Soc.* **2004**, *126*, 5344-5345.
- [16] F. Barrios-Landeros, B. P. Carrow, J. F. Hartwig, *J. Am. Chem. Soc.* **2009**, *131*, 8141-8154.
- [17] a) E. Galardon, S. Ramdeehul, J. M. Brown, A. Cowley, K. K. Hii, A. Jutand, *Angew. Chem. Int. Ed.* **2002**, *41*, 1760-1763; b) G. Espino, A. Kurbangalieva, J. M. Brown, *Chem. Commun.* **2007**, 1742-1744.
- [18] F. Schoenebeck, K. Houk, *J. Am. Chem. Soc.* **2010**, *132*, 2496-2497.
- [19] J. W. Dankwardt, *Angew. Chem. Int. Ed.* **2004**, *43*, 2428-2432.
- [20] a) Z. Y. Tang, Q. S. Hu, *Adv. Synth. Catal.* **2004**, *346*, 1635-1637; b) Z.-Y. Tang, Q.-S. Hu, *J. Am. Chem. Soc.* **2004**, *126*, 3058-3059; c) M. Jankowska, O. Shuvalova, N. Bespalova, M. Majchrzak, B. Marciniak, *J. Organomet. Chem.* **2005**, *690*, 4492-4497; d) P. Leowanawat, N. Zhang, A.-M. Resmerita, B. M. Rosen, V. Percec, *J. Org. Chem.* **2011**, *76*, 9946-9955; e) P. Leowanawat, N. Zhang, M. Safi, D. J. Hoffman, M. C. Fryberger, A. George, V. Percec, *J. Org. Chem.* **2012**, *77*, 2885-2892; f) J. Malineni, R. L. Jezorek, N. Zhang, V. Percec, *Synthesis* **2016**, *48*, 2808-2815; g) S.-Q. Zhang, B. L. Taylor, C.-L. Ji, Y. Gao, M. R. Harris, L. E. Hanna, E. R. Jarvo, K. Houk, X. Hong, *J. Am. Chem. Soc.* **2017**, *139*, 12994-13005.
- [21] L. Chen, P. Ren, B. P. Carrow, *J. Am. Chem. Soc.* **2016**, *138*, 6392-6395.
- [22] a) L. Chen, D. R. Sanchez, B. Zhang, B. P. Carrow, *J. Am. Chem. Soc.* **2017**, *139*, 12418-12421; b) L. Chen, H. Francis, B. P. Carrow, *ACS Catal.* **2018**, *8*, 2989-2994.
- [23] A. Ehrentraut, A. Zapf, M. Beller, *Synlett* **2000**, *11*, 1589-1592.
- [24] a) M. Beller, C. Fuhrmann, A. Zapf, A. Ehrentraut (Evonik Operations GmbH), US 7,148.176 B2, **2006**; b) S. Klaus, H. Neumann, A. Zapf, D. Strübing, S. Hübner, J. Almena, T. Riermeier, P. Groß, M. Sarich, W. R. Krahnert, *Angew. Chem. Int. Ed.* **2006**, *45*, 154-158; c) A. G. Sergeev, A. Spannenberg, M. Beller, *J. Am. Chem. Soc.* **2008**, *130*, 15549-15563.
- [25] H. A. Chiong, O. Daugulis, *Org. Lett.* **2007**, *9*, 1449-1451.

- [26] D. Zhao, W. Wang, S. Lian, F. Yang, J. Lan, J. You, *Chem. Eur. J.* **2009**, *15*, 1337-1340.
- [27] a) X. F. Wu, H. Neumann, M. Beller, *ChemCatChem* **2010**, *2*, 509-513; b) H. Neumann, A. Brennfürer, P. Groß, T. Riermeier, J. Almena, M. Beller, *Adv. Synth. Catal.* **2006**, *348*, 1255-1261; c) H. Neumann, A. Brennfürer, M. Beller, *Chem. Eur. J.* **2008**, *14*, 3645-3652; d) A. Brennfürer, H. Neumann, M. Beller, *Angew. Chem. Int. Ed.* **2009**, *48*, 4114-4133.
- [28] G. A. Molander, S. R. Wisniewski, *J. Am. Chem. Soc.* **2012**, *134*, 16856-16868.
- [29] a) F. Rataboul, A. Zapf, R. Jackstell, S. Harkal, T. Riermeier, A. Monsees, U. Dingerdissen, M. Beller, *Chem. Eur. J.* **2004**, *10*, 2983-2990; b) A. Tewari, M. Hein, A. Zapf, M. Beller, *Tetrahedron* **2005**, *61*, 9705-9709; c) T. Schulz, C. Torborg, S. Enthaler, B. Schaeffner, A. Dumrath, A. Spannenberg, H. Neumann, A. Boerner, M. Beller, *Chem. Eur. J.* **2009**, *15*, 4528-4533.
- [30] a) P. Hermange, T. M. Gøgsig, A. T. Lindhardt, R. H. Taaning, T. Skrydstrup, *Org. Lett.* **2011**, *13*, 2444-2447; b) M. Stephan, J. Panther, F. Wilbert, P. Ozog, T. J. Müller, *Eur. J. Org. Chem.* **2020**, *14*, 2086-2092.
- [31] a) D. W. Old, J. P. Wolfe, S. L. Buchwald, *J. Am. Chem. Soc.* **1998**, *120*, 9722-9723; b) B. C. Hamann, J. F. Hartwig, *J. Am. Chem. Soc.* **1998**, *120*, 7369-7370.
- [32] Q. Shelby, N. Kataoka, G. Mann, J. Hartwig, *J. Am. Chem. Soc.* **2000**, *122*, 10718-10719.
- [33] R. Martin, S. L. Buchwald, *Acc. Chem. Res.* **2008**, *41*, 1461-1473.
- [34] S. Kaye, J. M. Fox, F. A. Hicks, S. L. Buchwald, *Adv. Synth. Catal.* **2001**, *343*, 789-794.
- [35] a) P. Ruiz-Castillo, S. L. Buchwald, *Chem. Rev.* **2016**, *116*, 12564-12649; b) F. Inoue, M. Kashihara, M. R. Yadav, Y. Nakao, *Angew. Chem. Int. Ed.* **2017**, *56*, 13307-13309; c) R. Dorel, C. P. Grugel, A. M. Haydl, *Angew. Chem. Int. Ed.* **2019**, *58*, 17118-17129.
- [36] a) T. J. Maimone, P. J. Milner, T. Kinzel, Y. Zhang, M. K. Takase, S. L. Buchwald, *J. Am. Chem. Soc.* **2011**, *133*, 18106-18109; b) H. G. Lee, P. J. Milner, S. L. Buchwald, *Org. Lett.* **2013**, *15*, 5602-5605; c) H. G. Lee, P. J. Milner, S. L. Buchwald, *J. Am. Chem. Soc.* **2014**, *136*, 3792-3795; d) A. C. Sather, H. G. Lee, V. Y. De La Rosa, Y. Yang, P. Müller, S. L. Buchwald, *J. Am. Chem. Soc.* **2015**, *137*, 13433-13438; e) A. C. Sather, S. L. Buchwald, *Acc. Chem. Res.* **2016**, *49*, 2146-2157; f) D. S. Surry, S. L. Buchwald, *J. Am. Chem. Soc.* **2007**, *129*, 10354-10355.

- [37] a) Y. Yang, S. L. Buchwald, *J. Am. Chem. Soc.* **2013**, *135*, 10642-10645; b) E. J. Cho, T. D. Senecal, T. Kinzel, Y. Zhang, D. A. Watson, S. L. Buchwald, *Science* **2010**, *328*, 1679-1681; c) M. R. Yadav, M. Nagaoka, M. Kashihara, R.-L. Zhong, T. Miyazaki, S. Sakaki, Y. Nakao, *J. Am. Chem. Soc.* **2017**, *139*, 9423-9426.
- [38] a) J. M. Dennis, N. A. White, R. Y. Liu, S. L. Buchwald, *J. Am. Chem. Soc.* **2018**, *140*, 4721-4725; b) J. M. Dennis, N. A. White, R. Y. Liu, S. L. Buchwald, *ACS Catal.* **2019**, *9*, 3822-3830.
- [39] a) R. J. Lundgren, K. D. Hesp, M. Stradiotto, *Synlett* **2011**, *17*, 2443-2458; b) C. A. Wheaton, J.-P. J. Bow, M. Stradiotto, *Organometallics* **2013**, *32*, 6148-6161; c) R. J. Lundgren, A. Sapping-Kumankumah, M. Stradiotto, *Chem. Eur. J.* **2010**, *16*, 1983-1991.
- [40] A. V. Gatien, C. M. Lavoie, R. N. Bennett, M. J. Ferguson, R. McDonald, E. R. Johnson, A. W. Speed, M. Stradiotto, *ACS Catal.* **2018**, *8*, 5328-5339.
- [41] Q. Shen, J. F. Hartwig, *J. Am. Chem. Soc.* **2006**, *128*, 10028-10029.
- [42] R. J. Lundgren, B. D. Peters, P. G. Alsabeh, M. Stradiotto, *Angew. Chem. Int. Ed.* **2010**, *49*, 4071-4074.
- [43] R. J. Lundgren, M. Stradiotto, *Angew. Chem. Int. Ed.* **2010**, *49*, 8686-8690.
- [44] K. D. Hesp, M. Stradiotto, *J. Am. Chem. Soc.* **2010**, *132*, 18026-18029.
- [45] K. D. Hesp, R. J. Lundgren, M. Stradiotto, *J. Am. Chem. Soc.* **2011**, *133*, 5194-5197.
- [46] C. M. Lavoie, P. M. MacQueen, N. L. Rotta-Loria, R. S. Sawatzky, A. Borzenko, A. J. Chisholm, B. K. Hargreaves, R. McDonald, M. J. Ferguson, M. Stradiotto, *Nat. Commun.* **2016**, *7*, 1-11.
- [47] P. M. MacQueen, J. P. Tassone, C. Diaz, M. Stradiotto, *J. Am. Chem. Soc.* **2018**, *140*, 5023-5027.
- [48] R. T. McGuire, C. M. Simon, A. A. Yadav, M. J. Ferguson, M. Stradiotto, *Angew. Chem. Int. Ed.* **2020**, *59*, 8952-8956.
- [49] J. P. Tassone, E. V. England, P. M. MacQueen, M. J. Ferguson, M. Stradiotto, *Angew. Chem. Int. Ed.* **2019**, *58*, 2485-2489.
- [50] J. S. Clark, R. T. McGuire, C. M. Lavoie, M. J. Ferguson, M. Stradiotto, *Organometallics* **2018**, *38*, 167-175.
- [51] a) M. Baghbanzadeh, C. Pilger, C. O. Kappe, *J. Org. Chem.* **2011**, *76*, 8138-8142; b) S. Marhadour, M.-A. Bazin, P. Marchand, *Tetrahedron Lett.* **2012**, *53*, 297-300; c) B.

- Liegault, D. Lapointe, L. Caron, A. Vlassova, K. Fagnou, *J. Org. Chem.* **2009**, *74*, 1826-1834; d) C. A. Fleckenstein, H. Plenio, *Chem. Eur. J.* **2007**, *13*, 2701-2716.
- [52] a) H. J. Bestmann, O. Kratzer, *Chem. Ber.* **1962**, *95*, 1894-1901; b) H. J. Bestmann, R. Dötzer, *Synthesis* **1989**, *3*, 204-205.
- [53] M. Alcarazo, R. M. Suárez, R. Goddard, A. Fürstner, *Chem. Eur. J.* **2010**, *16*, 9746-9749.
- [54] T. Yamamoto, O. Saito, A. Yamamoto, *J. Am. Chem. Soc.* **1981**, *103*, 5600-5602.
- [55] a) I. V. Shevchenko, V. P. Kukhar', O. I. Kolodyazhnyi, *J. Gen. Chem. USSR (Engl. Transl.)* **1989**, *59*, 424-425, 477-478; b) M. H. Holthausen, J. M. Bayne, I. Mallov, R. Dobrovetsky, D. W. Stephan, *J. Am. Chem. Soc.* **2015**, *137*, 7298-7301; c) I. V. Shevchenko, V. P. Kukhar', O. I. Kolodyazhnyi, *J. Gen. Chem. USSR (Engl. Transl.)* **1990**, *60*, 1544-1547, 1730-1735.
- [56] L. K. Hwang, Y. Na, J. Lee, Y. Do, S. Chang, *Angew. Chem. Int. Ed.* **2005**, *44*, 6166-6169.
- [57] a) F.-A. Kang, Z. Sui, W. V. Murray, *J. Am. Chem. Soc.* **2008**, *130*, 11300-11302; b) V. P. Mehta, S. G. Modha, E. V. Van der Eycken, *J. Org. Chem.* **2010**, *75*, 976-979; c) A. Sharma, D. Vachhani, E. Van der Eycken, *Org. Lett.* **2012**, *14*, 1854-1857; d) X. Zhang, A. McNally, *Angew. Chem. Int. Ed.* **2017**, *56*, 9833-9836.
- [58] E. Frérot, J. Coste, A. Pantaloni, M.-N. Dufour, P. Jouin, *Tetrahedron* **1991**, *47*, 259-270.
- [59] J. Coste, D. Le-Nguyen, B. Castro, *Tetrahedron Lett.* **1990**, *31*, 205-208.
- [60] a) J. McNulty, A. Capretta, J. Wilson, J. Dyck, G. Adjabeng, A. Robertson, *Chem. Commun.* **2002**, 1986-1987; b) H. Cao, L. McNamee, H. Alper, *Org. Lett.* **2008**, *10*, 5281-5284; c) J. Zhu, M. Pérez, D. W. Stephan, *Angew. Chem. Int. Ed.* **2016**, *55*, 8448-8451.
- [61] a) J.-P. Duan, F.-L. Liao, S.-L. Wang, C.-H. Cheng, *Organometallics* **1997**, *16*, 3934-3940; b) C.-C. Huang, J.-P. Duan, M.-Y. Wu, F.-L. Liao, S.-L. Wang, C.-H. Cheng, *Organometallics* **1998**, *17*, 676-682.
- [62] a) T. Scherpf, C. Schwarz, L. T. Scharf, J. A. Zur, A. Helbig, V. H. Gessner, *Angew. Chem. Int. Ed.* **2018**, *57*, 12859-12864; b) P. Weber, T. Scherpf, I. Rodstein, D. Lichte, L. T. Scharf, L. J. Gooßen, V. H. Gessner, *Angew. Chem. Int. Ed.* **2019**, *58*, 3203-3207.

- [63] a) K. Conrow, *Org. Synth.* **1973**, *5*, 1138; b) H. J. Dauben Jr, F. A. Gadecki, K. M. Harmon, D. L. Pearson, *J. Am. Chem. Soc.* **1957**, *79*, 4557-4558; c) J. Crivello, *Synth. Commun.* **1973**, *3*, 9-12.
- [64] a) M. Herberhold, W. Milius, S. Eibl, *Z. Anorg. Allg. Chem.* **1999**, *625*, 341-346; b) M. Herberhold, A. Pfeifer, W. Milius, *Z. Anorg. Allg. Chem.* **2002**, *628*, 2919-2929; c) M. Herberhold, T. Schmalz, W. Milius, B. Wrackmeyer, *J. Organomet. Chem.* **2002**, *641*, 173-184; d) M. Herberhold, T. Schmalz, W. Milius, B. Wrackmeyer, *Inorg. Chim. Acta* **2002**, *334*, 10-16; e) M. Herberhold, N. Akkus, W. Milius, *Z. Anorg. Allg. Chem.* **2003**, *629*, 2458-2464; f) B. Wrackmeyer, B. Ullmann, R. Kempe, M. Herberhold, *Z. Anorg. Allg. Chem.* **2005**, *631*, 2629-2634; g) C. Jandl, K. Öfele, F. E. Kühn, W. A. Herrmann, A. Pöthig, *Organometallics* **2014**, *33*, 6398-6407.
- [65] a) H. Hoffmann, P. Schellenbeck, *Chem. Ber.* **1966**, *99*, 1134-1142; b) G. Bidan, M. Genies, *Tetrahedron Lett.* **1978**, *19*, 2499-2502; c) P. Huszthy, G. Izsó, *J. Chem. Soc., Perkin Trans* **1989**, *2*, 1513; d) P. Huszthy, M. Kajtár-Peredy, K. Lempert, J. Hegedüs-Vajda, *J. Chem. Soc., Perkin Trans. 2* **1992**, 347-353.
- [66] H. Scordia, R. Kergoat, M. M. Kubicki, J. E. Guerchais, P. L'Haridon, *Organometallics* **1983**, *2*, 1681-1687.
- [67] E. Ebsworth, T. E. Fraser, D. W. Rankin, *Chem. Ber.* **1977**, *110*, 3494-3500.
- [68] Z. Guan, Metal catalysts in olefin polymerization in *Topics in Organometallic Chemistry, Vol. 26*, Springer, Berlin, **2009**.
- [69] a) W. J. Evans, T. A. Ulibarri, J. W. Ziller, *J. Am. Chem. Soc.* **1990**, *112*, 219-223; b) G. Erker, K. Kropp, J. L. Atwood, W. E. Hunter, *Organometallics* **1983**, *2*, 1555-1561.
- [70] R. J. Hinkle, P. J. Stang, M. H. Kowalski, *J. Org. Chem.* **1990**, *55*, 5033-5036.
- [71] S. S. Zaleskiy, V. P. Ananikov, *Organometallics* **2012**, *31*, 2302-2309.
- [72] K. Singh, S. J. Staig, J. D. Weaver, *J. Am. Chem. Soc.* **2014**, *136*, 5275-5278.
- [73] G. C. Paul, J. J. Gajewski, *Synthesis* **1997**, *5*, 524-526.
- [74] S. E. Drewes, N. D. Emslie, M. Hemingway, *Synth. Commun.* **1990**, *20*, 1671-1679.
- [75] a) M. L. Conner, M. K. Brown, *J. Org. Chem.* **2016**, *81*, 8050-8060; b) M. Brown, R. Kumar, J. Rehbein, T. Wirth, *Chem. Eur. J.* **2016**, *22*, 4030-4035.
- [76] G. Zhang, R.-X. Bai, C.-H. Li, C.-G. Feng, G.-Q. Lin, *Tetrahedron* **2019**, *75*, 1658-1662.
- [77] T. Ohmura, K. Masuda, I. Takase, M. Suginome, *J. Am. Chem. Soc.* **2009**, *131*, 16624-16625.

- [78] X. T. Li, Q. S. Gu, X. Y. Dong, X. Meng, X. Y. Liu, *Angew. Chem. Int. Ed.* **2018**, *57*, 7668-7672.
- [79] C. B. Tripathi, S. Mukherjee, *Angew. Chem. Int. Ed.* **2013**, *52*, 8450-8453.
- [80] L. Horner, I. Ertel, H. D. Ruprecht, O. Bělovský, *Chem. Ber.* **1970**, *103*, 1582-1588.
- [81] a) Y. V. Svyaschenko, B. B. Barnych, D. M. Volochnyuk, N. V. Shevchuk, A. N. Kostyuk, *J. Org. Chem.* **2011**, *76*, 6125-6133; b) M. Z. Ovakimyan, G. Gasparyan, M. Movsisyan, M. Grigoryan, *Russ. J. Gen. Chem.* **2013**, *83*, 136-137; c) M. Grigoryan, *Russ. J. Gen. Chem.* **2014**, *84*, 501-504; d) N. A. Nesmeyanov, V. Mikul'shina, V. Kharitonov, P. Petrovskii, O. Reutov, *Bull Acad. Sci. USSR, Div. Chem. Sci.* **1989**, *38*, 1076-1079.
- [82] E. A. Mitchell, M. C. Baird, *Organometallics* **2007**, *26*, 5230-5238.
- [83] A. M. Castaño, A. M. Echavarren, J. López, A. Santos, *J. Organomet. Chem.* **1989**, *379*, 171-175.
- [84] N. P. Reddy, M. Tanaka, *Tetrahedron Lett.* **1997**, *38*, 4807-4810.
- [85] a) S. M. Kruse, S. K. Hurst, *Tetrahedron Lett.* **2015**, *56*, 6319-6322; b) D. G. Gilheany, N. T. Thompson, B. J. Walker, *Tetrahedron Lett.* **1987**, *28*, 3843-3844.
- [86] K. Reinhardt, *New Syntheses of Chiral P-Menthylphosphane-Ligands and Syntheses of Benzo-annelated Ligands of the Buchwald Type*, master thesis, Technical University of Munich (Garching bei München), **2017**.
- [87] a) W. Betz, J. Daub, *Chem. Ber.* **1974**, *107*, 2095-2114; b) W. Betz, J. Daub, K. M. Rapp, *Liebigs Ann. Chem.* **1974**, *1974*, 2089-2109; c) M. Baldwin, F. McLafferty, D. M. Jerina, *J. Am. Chem. Soc.* **1975**, *97*, 6169-6174; d) W. Bauer, J. Daub, G. Maas, M. Michna, K. M. Rapp, J. J. Stezowski, *Chem. Ber.* **1982**, *115*, 99-118; e) J. Daub, H. D. Lüdemann, M. Michna, R. M. Strobl, *Chem. Ber.* **1985**, *118*, 620-633; f) K. i. Takeuchi, M. Arima, K. Okamoto, *Tetrahedron Lett.* **1981**, *22*, 3081-3084; g) G. Maier, *Angew. Chem. Int. Ed.* **1967**, *79*, 446-458; h) S. W. Staley, M. A. Fox, A. Cairncross, *J. Am. Chem. Soc.* **1977**, *99*, 4524-4526.
- [88] a) I. Coldham, D. Leonori, *Org. Lett.* **2008**, *10*, 3923-3925; b) J. Moon, M. Jang, S. Lee, *J. Org. Chem.* **2009**, *74*, 1403-1406; c) D. M. Ferguson, J. R. Bour, A. J. Canty, J. W. Kampf, M. S. Sanford, *J. Am. Chem. Soc.* **2017**, *139*, 11662-11665; d) M. H. Aukland, F. J. Talbot, J. A. Fernández-Salas, M. Ball, A. P. Pulis, D. J. Procter, *Angew. Chem. Int. Ed.* **2018**, *57*, 9785-9789.

- [89] S. Koller, J. Gatzka, K. M. Wong, P. J. Altmann, A. Pöthig, L. Hintermann, *J. Org. Chem.* **2018**, *83*, 15009-15028.
- [90] a) K. Mantas-Öktem, K. Öfele, A. Pöthig, B. Bechlars, W. A. Herrmann, F. E. Kühn, *Organometallics* **2012**, *31*, 8249-8256; b) C. Jandl, A. Pöthig, *Chem. Commun.* **2017**, 53, 2098-2101.
- [91] a) A. J. Arduengo III, R. L. Harlow, M. Kline, *J. Am. Chem. Soc.* **1991**, *113*, 361-363; b) N. Kuhn, M. Steimann, K. Sweidan, *Z. Naturforsch. B* **2005**, *60*, 123-124; c) L. Delaude, A. Demonceau, J. Wouters, *Eur. J. Inorg. Chem.* **2009**, *13*, 1882-1891; d) S. Kronig, E. Theuergarten, D. Holschumacher, T. Bannenberg, C. G. Daniliuc, P. G. Jones, M. Tamm, *Inorg. Chem.* **2011**, *50*, 7344-7359.
- [92] M. G. Organ, S. Calimsiz, M. Sayah, K. H. Hoi, A. J. Lough, *Angew. Chem. Int. Ed.* **2009**, *48*, 2383-2387.
- [93] a) H. M. Wang, I. J. Lin, *Organometallics* **1998**, *17*, 972-975; b) K. S. Coleman, H. T. Chamberlayne, S. Turberville, M. L. Green, A. R. Cowley, *Dalton Trans.* **2003**, 2917-2922; c) S. Warsink, P. Hauwert, M. A. Siegler, A. L. Spek, C. J. Elsevier, *Appl. Organomet. Chem.* **2009**, *23*, 225-228.
- [94] M. R. Furst, C. S. Cazin, *Chem. Commun.* **2010**, *46*, 6924-6925.
- [95] W. A. Herrmann, S. K. Schneider, K. Öfele, M. Sakamoto, E. Herdtweck, *J. Organomet. Chem.* **2004**, *689*, 2441-2449.
- [96] a) R. Hoffmann, *Tetrahedron Lett.* **1970**, *11*, 2907-2909; b) O. A. McNamara, A. R. Maguire, *Tetrahedron* **2011**, *67*, 9-40.
- [97] a) H. E. Zimmerman, D. J. Schuster, *J. Am. Chem. Soc.* **1961**, *83*, 4486-4488; b) M. Pomerantz, *J. Am. Chem. Soc.* **1967**, *89*, 694-696; c) H. E. Zimmerman, P. Hackett, D. F. Juers, J. M. McCall, B. Schroeder, *J. Am. Chem. Soc.* **1971**, *93*, 3653-3662; d) W. G. Dauben, M. Kellogg, J. Seeman, N. D. Vietmeyer, P. H. Wendschuh, *Pure Appl. Chem.* **1973**, *33*, 197-216; e) H. E. Zimmerman, D. R. Diehl, *J. Am. Chem. Soc.* **1979**, *101*, 1841-1857; f) M. B. Rubin, *J. Am. Chem. Soc.* **1981**, *103*, 7791-7792; g) H. P. Latscha, U. Kazmaier, H. A. Klein, *Photochemie in Organische Chemie*, Springer, **2002**, pp. 377-381.
- [98] a) M. M. Maturi, A. Pöthig, T. Bach, *Aust. J. Chem.* **2015**, *68*, 1682-1692; b) M. Leverenz, C. Merten, A. Dreuw, T. Bach, *J. Am. Chem. Soc.* **2019**, *141*, 20053-20057.
- [99] H. Brunner, T. Kurosawa, M. Muschiol, T. Tsuno, G. b. Balázs, M. Bodensteiner, *Organometallics* **2013**, *32*, 4904-4911.

- [100] J. Clayden, N. Greeves, S. Warren, *Organic Chemistry*, OUP Oxford, Oxford, **2012**.
- [101] X. Huang, K. W. Anderson, D. Zim, L. Jiang, A. Klapars, S. L. Buchwald, *J. Am. Chem. Soc.* **2003**, *125*, 6653-6655.
- [102] a) N. Miyaura, S. L. Buchwald, Cross-coupling reactions: a practical guide in *Top. Curr. Chem.*, Vol. 219, Springer, Berlin, **2002**; b) F. Diederich, P. J. Stang, *Metal-catalyzed cross-coupling reactions*, John Wiley & Sons, **2008**.
- [103] V. V. Grushin, C. Bensimon, H. Alper, *Inorg. Chem.* **1994**, *33*, 4804-4806.
- [104] a) A. W. Fraser, J. E. Besaw, L. E. Hull, M. C. Baird, *Organometallics* **2012**, *31*, 2470-2475; b) E. A. Mitchell, P. G. Jessop, M. C. Baird, *Organometallics* **2009**, *28*, 6732-6738; c) D. M. Norton, E. A. Mitchell, N. R. Botros, P. G. Jessop, M. C. Baird, *J. Org. Chem.* **2009**, *74*, 6674-6680.
- [105] a) J. P. Wolfe, S. L. Buchwald, *Angew. Chem. Int. Ed.* **1999**, *38*, 2413-2416; b) R. Pratap, D. Parrish, P. Gunda, D. Venkataraman, M. K. Lakshman, *J. Am. Chem. Soc.* **2009**, *131*, 12240-12249; c) T. Kinzel, Y. Zhang, S. L. Buchwald, *J. Am. Chem. Soc.* **2010**, *132*, 14073-14075; d) C. M. So, C. P. Lau, F. Y. Kwong, *Angew. Chem. Int. Ed.* **2008**, *47*, 8059-8063.
- [106] a) N. C. Bruno, S. L. Buchwald, *Org. Lett.* **2013**, *15*, 2876-2879; b) B. P. Fors, P. Krattiger, E. Strieter, S. L. Buchwald, *Org. Lett.* **2008**, *10*, 3505-3508; c) A. H. Dardir, P. R. Melvin, R. M. Davis, N. Hazari, M. Mohadjer Beromi, *J. Org. Chem.* **2018**, *83*, 469-477.
- [107] G. Märkl, W. Bauer, *Tetrahedron Lett.* **1993**, *34*, 2915-2918.
- [108] a) R. Alonso, T. Bach, *Angew. Chem. Int. Ed.* **2014**, *53*, 4368-4371; b) K.-H. Rimboeck, A. Poethig, T. Bach, *Synthesis* **2015**, *47*, 2869-2884; c) M. M. Maturi, M. Wenninger, R. Alonso, A. Bauer, A. Pöthig, E. Riedle, T. Bach, *Chem. Eur. J.* **2013**, *19*, 7461-7472; d) M. H. Umbehr, M. Müntener, T. Hany, T. Sulser, L. M. Bachmann, *Eur. Urol.* **2013**, *64*, 106-117; e) R. J. Pakula, M. Srebro-Hooper, C. G. Fry, H. J. Reich, J. Autschbach, J. F. Berry, *Inorg. Chem.* **2018**, *57*, 8046-8049; f) M. Grübel, I. Bosque, P. J. Altmann, T. Bach, C. R. Hess, *Chem. Sci.* **2018**, *9*, 3313-3317.

6 DUAL METAL CATALYSIS: COMBINING HYDROGEN AUTO TRANSFER AND HECK COUPLING

This chapter is subdivided in four main parts. Examples of dehydrogenation and Heck enamine coupling as well as combinations of both will be outlined (6.1). Dual metal catalysis enabled the use of trialkylamines as donors in Heck-type coupling (6.2). Several experiments involving substrate, precatalyst, and other factor screening will be delineated (6.2.1-6.2.3). A plausible mechanism will be proposed (6.2.4). Literature precedents allowed us to analyze the coupling of styrenes with chloropyrimidines (6.3). The conclusion and outlook end this chapter (6.4).

6.1 Introduction

Activation of hydrogen has fascinated chemists for several decades. The most prominent example depicts the hydrogenation of nitrogen through the Haber-Bosch process, generating ammonia.^[1] The use of metal precatalysts is indispensable to lower the necessary energy for hydrogen activation. On a homogeneous level, Wilkinson^[2] and Crabtree^[3] delivered astonishing results hydrogenating aliphatic alkenes (figure 45). Since then, more and more active catalysts^[4] have evolved, also concerning heterogeneous^[5] and enantioselective^[6] hydrogenation.

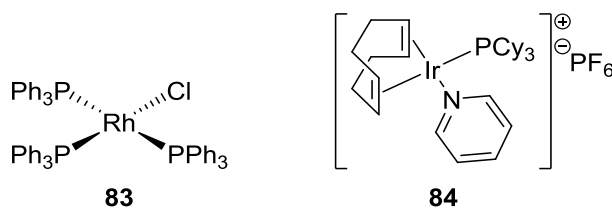
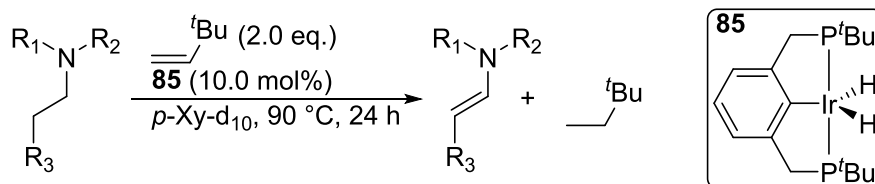


Figure 45. Left: Wilkinson's catalyst^[2b] (**83**), right: Crabtree's catalyst^[3a,3b] (**84**).

The reversed step of the above process is designated as dehydrogenation, formally oxidizing substrates by eliminating H₂.^[7] Hydrogen elimination with concomitant release of free hydrogen gas is called acceptorless dehydrogenation.^[8] Besides alkanes^[9], alcohols are prominent starting materials for dehydrogenation. Opposed to mostly stoichiometric methods from organic chemistry (Cr-oxides^[10], TEMPO^[11]...), catalytic oxidation via H₂ abstraction^[12] constitutes a more atom-economic method. Dehydrogenation of primary and secondary amines is less common, since the resulting imines are prone to nucleophilic attack by residual amine. Still, selective, catalytic dehydrogenation of amines to nitriles^[13] or imines^[14] has been achieved. The question arose whether the product imines are formed by a direct CH–NH or α,β -CH–CH dehydrogenation with subsequent isomerization. By blocking both β -positions with methyl groups, the group of Jensen was still able to conduct the desired conversion, pointing to the first possibility.^[14] However, just a few years later Goldman et al. were able to generate

enamines from tertiary amines using the identical PCP-Ir-pincer complex **85** in the presence of *tert*-butylethylene (TBE) as hydrogen acceptor (scheme 58).^[15]



Scheme 58. Transfer-dehydrogenation of tertiary amines catalyzed by the PCP-Ir-pincer complex **85** described by Goldman et al.^[15] Xy = xylene.

Dehydrogenation of primary alcohols delivers electrophilic carbonyl compounds which can undergo follow-up reactions with other nucleophiles, typically alcohols or amines (figure 46).^[8] Two pathways can be differentiated. After addition of a nucleophile to carbonyl, a second equivalent of hydrogen can be abstracted, generating ester^[16]/lactone^[16c,16d,17] or amide^[18]/lactam^[17,19], respectively (pathway a)). In the case of amines, elimination of water can follow the formation of intermediate hemiaminal (pathway b)), rendering imines.^[20] Subsequent inter- or intramolecular cyclization followed by dehydrogenation or base-promoted elimination is often encountered, giving access to pyrazines^[21] or pyrroles.^[22] The selective synthesis of acetals from alcohols has also been described.^[23]

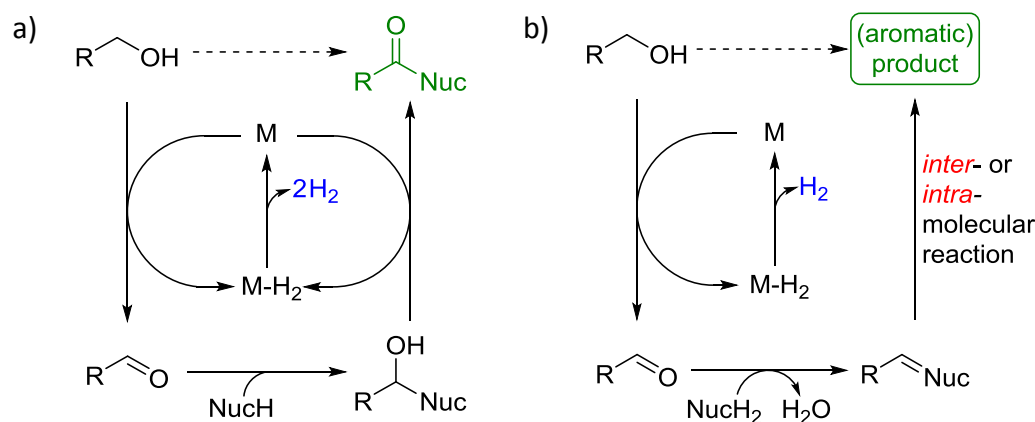


Figure 46. Potential pathways for acceptorless, dehydrogenative coupling of alcohols.^[8] Nuc = nucleophile; M = metal.

The release of free hydrogen gas or its addition to a sacrificial acceptor do not constitute the only potential reaction routes.^[8] Competing with pathway b) in figure 46, the metal-hydride species is capable of hydrogenating the intermediate generated from nucleophilic addition (figure 47). Since abstracted H₂ is returned to the catalytic cycle, the process is known as borrowing hydrogen reaction, also referred to as hydrogen auto-transfer (HAT). The sole side-product is water, and thus the whole transformation pictures a role model of green chemistry.

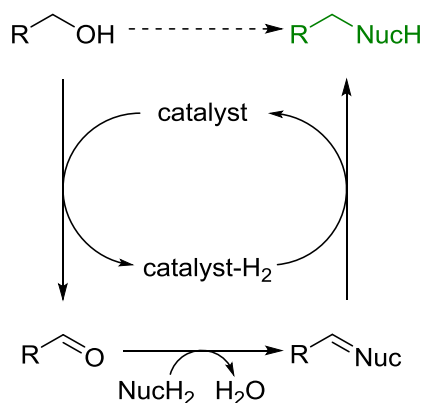
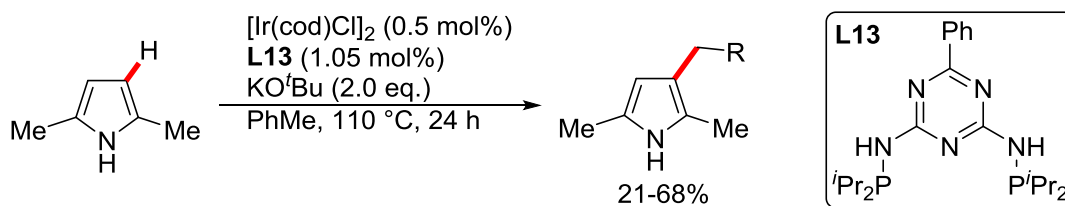


Figure 47. Borrowing hydrogen reaction or hydrogen auto-transfer (HAT).^[8] Nuc = nucleophile.

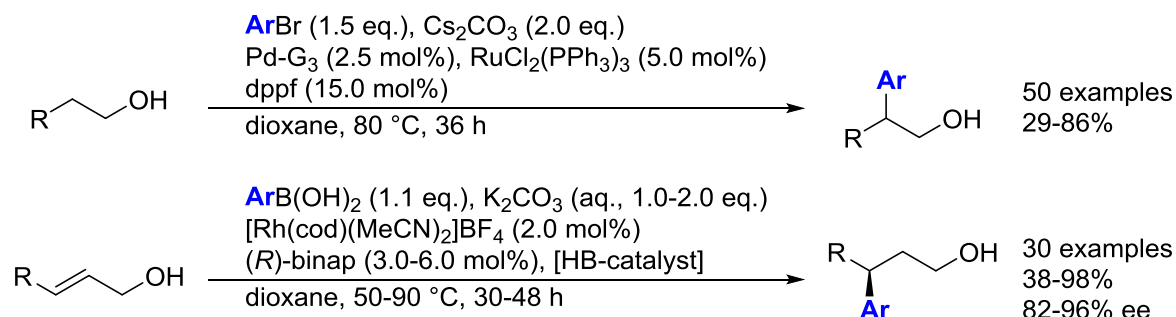
HAT chemistry starting from alcohols that does not require toxic reagents such as alkyl halides^[24] delivers a convenient method for the alkylation of nucleophiles.^[25] Through the borrowing hydrogen concept, the direct amination of alcohols with ammonia^[26] or the synthesis of oxazolidin-2-ones^[27] have been accessible. Alkylation may also occur at acidified C_{sp3}-H centers via their activation as carbanions, but besides also at C_{sp2}-atoms of electron rich arenes, e.g. indoles^{[28], [25c]}. The group of Li achieved the regioselective alkylation of (hetero)arenes employing [RhCp*Cl₂]₂ as catalyst in substrates containing heterocyclic directing groups.^[29] Besides alcohols,^[30] amines^[31] can act as alkylation agents. Metal-free versions of HAT-alkylations utilizing alkali base as catalyst enable the required H-transfer through a Cannizzarro-type mechanism^{[32], [33]}. Early work concerning C-alkylation of pyrroles has been performed by Hans-Fischer^[34], which was revived and further outlined in our group^[35] using either alkali base or a PNP-Ir-pincer complex as catalysts (scheme 59).



Scheme 59. Catalytic C-alkylation of pyrroles described by Koller et al.^[35] Minor amounts of dialkylated pyrrole (0-4%) were detected for 2,5-dimethylpyrroles. 2,4-Dimethylpyrroles usually delivered better conversion, also entailing larger amounts of dialkylated product. R = electron-rich or -poor arene.

Dual metal catalysis is an emerging field in current research and takes advantage of either metal-selective coupling^[36] or photoredox^[37] chemistry. Lately, the group of Dydio was able to functionalize inherently unreactive sites of primary alcohols.^[38] Ru-catalyzed dehydrogenation of primary alcohols to the corresponding aldehyde followed by Pd-assisted arylation of the base-generated enolate are key elements of the reaction (scheme 60, top). Additionally, allyl

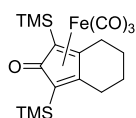
alcohols were efficiently converted to hydroarylated adducts with γ -selectivity using a Rh-precatalyst in conjunction with either Ru or Fe hydrogen borrowing catalyst (scheme 60, bottom). The presence of ancillary, chiral ligand, (*R*)-binap, even yielded enantiomerically enriched products.



Scheme 60. Pd/Ru-catalyzed β -arylation of primary alcohols (top) and γ -selective hydroarylation of allylic alcohols (bottom) described by the group of Dydio.^[38] Ar = electron-rich or -poor (hetero)arene; Pd-G₃ = Buchwald 3rd generation precatalyst complex, di- μ -mesylbis[2'-amino-*N*][1,1'-biphenyl]-2-yl-*C*dipalladium(II); dppf = 1,1'-bis(diphenylphosphino)ferrocene; binap = 2,2'-bis-diphenylphosphino-1,1'-binaphthyl; [HB-catalyst] = hydrogen-borrowing catalyst, either RuH₂(PPh₃)₄ (10.0 mol%) or [Fe]-carbonyl complex⁴⁹ (7.5 mol%). Trimethylamine-*N*-oxide (11.3 mol%) was additionally added to reaction mixtures involving the [Fe]-carbonyl complex.

Considering these interesting results, the question arose whether similar reactivity can be extended to other substrate classes. As mentioned before, amines may serve as convenient starting materials for dehydrogenation.^[14,31] Intermediary imines are prone to subsequent conversion ((de)hydrogenation, cyclization or other) depending on the conditions chosen. A suitable substitution pattern may induce tautomerization^[40] to the corresponding enamine, which would be amenable as alkene C–H-donor for Heck-type coupling. Above all, enamines have been common feedstocks for the synthesis of indoles^[41] or pyrroles^[42].^[43] Since Goldman and coworkers reported the successful synthesis of enamines from tertiary amines,^[15] we envisioned that unexplored reactivity was still to be investigated with this kind of substrates. Direct arylation of enamines followed by hydrogenation would give access to potentially biologically active amines, including phenylethylamines,^[44] in a one-pot procedure. As last part of this thesis, we wanted to tackle this challenge by starting with simple tertiary amines. Given

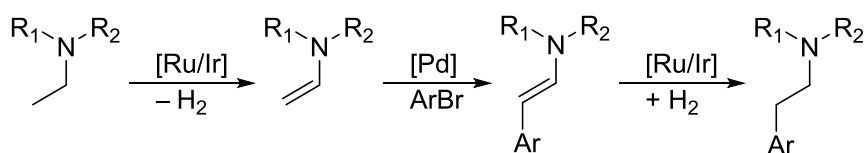
⁴⁹ [Fe] = Knölker's iron complex



that Heck coupling will play a key role of the planned reaction, we also wanted to analyze the direct Pd-catalyzed coupling of styrene derivatives with chloropyrimidines to sharpen our Heck skills. The only precedents for this transformation were related to coupling of iodo-heterocycles^[45], and the reaction examples delivered rather low yields of heteroarylated alkene.

6.2 Harnessing Trialkylamines as Donors in Heck cross-coupling via a Hydrogen Auto Transfer Process

Inspired by the work of Dydio^[38], we asked ourselves whether we could exploit a bimetallic catalyst system to convert tertiary amines into enamine donors for Heck-type coupling (scheme 61).



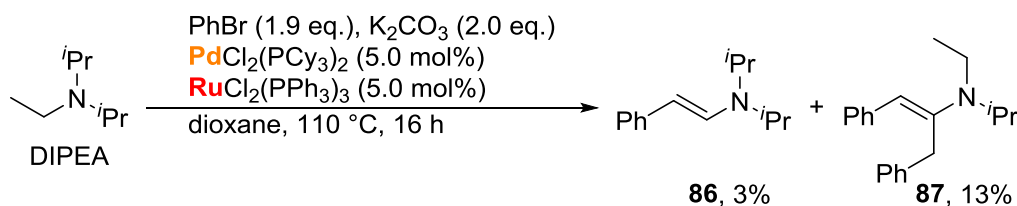
Scheme 61. Expected reaction sequence in the activation of tertiary amines. R₁, R₂ = Me, Et, ⁱPr, or other. Ar = arene.

The incorporation of either Ru- or Ir-based precatalysts is expected to permit dehydrogenation of ethyl (or longer) alkyl chains of amines. In interplay with a Pd catalyst, the generated olefin should be amenable to Heck coupling. Subsequent hydrogenation of the enamine double bond would deliver the arylated amine. If released hydrogen gas will not be returned to the catalytic cycle, either a sacrificial hydrogen donor will be needed, or released hydrogen gas will remain untouched. In the latter case, enamines will be obtained as reaction product.

6.2.1 Coincidence or getting started?

Dydio and coworkers employed RuCl₂(PPh₃)₃ as well as Buchwald's 3rd generation Pd precatalyst together with dppf ligand.^[38] Since the Pd-G3 precursor was not yet available in our group, we initially chose PdCl₂(PCy₃)₂ as coupling catalyst based on its broad applicability^[46]. Due to increased steric hindrance, Hünig's base^[47] (*N,N*-diisopropylethylamine; hereafter referred to as DIPEA) was expected to be an ideal substrate for dehydrogenation of its ethyl moiety. With their PCP-Ir-pincer complex, Goldman and coworkers^[15] had claimed exclusive dehydrogenation of the less substituted alkyl chain, supporting our plan. Sticking to the Ru-precursor of Dydio^[38] and excess amounts of bromobenzene as arylating agent, we conducted our first experiment under the conditions depicted in scheme 62. After the indicated time, we filtered the reaction mixture and removed residual solvent in vacuum. Quantification of the

starting material was omitted, since most of the amine is removed azeotropically. Even though no free amine could be observed, two interesting sets of signals could be detected. In the ^1H -NMR spectrum of the crude material, one was assigned one to the arylated (*E*)-olefin **86** (δ 5.36 (d), 6.88 (d)). By trituration of the crude product with hexanes⁵⁰, an enriched extract was obtained and could be analyzed by 2D-NMR. Thus, the major reaction product was identified as **87** (scheme 62), which implies that the Ru-catalyst surprisingly had dehydrogenated one isopropyl group, and that the resulting enamine had undergone twofold arylation.

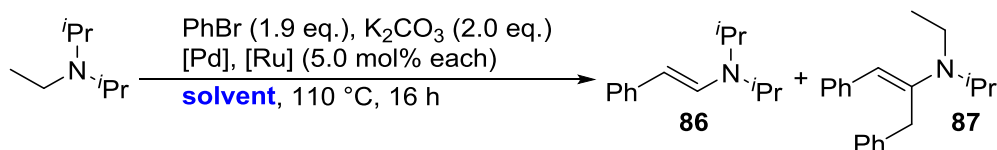


Scheme 62. Initial experiment towards dehydrogenative coupling of tertiary amines. Reaction performed with 500 μmol DIPEA according to GP 6.2.1 (see 7.2.7.1 for details).

To further simplify work-up, reaction mixtures were filtered over Celite, and the crudes were analyzed by q-NMR (^1H) against an internal standard. Decomposition of the tertiary amine to either a primary or a secondary one may have taken place, but could not have been detected, due to the rather low boiling points of those products, explaining the low recovery. Since a little of the desired reaction was taking place, we continued our investigation by screening solvents (table 35). Opposed to dioxane (entry 1), apolar toluene completely blocked any reaction even at higher temperatures (entry 2), showing only recovered starting material. The same goes for diethyl carbonate (entry 3) and 1,2-dichloroethane (entry 4), the latter showing reduced amounts of unreacted DIPEA. While DMSO diminished the generation of side-products, this dipolar aprotic solvent minimally increased the quantity of desired olefin **86** (entry 5). Virtually identical portions of both products were found in acetonitrile (entry 6). Comparable results were obtained in DMF (entry 7). The tertiary amide solvent DMAc led to slightly enhanced reactivity (entry 8), affording 20% of desired coupling product **86**. In comparison to DMF and DMAc, NMP produced intermediate amounts of enamines **86** and **87** (entry 9). For reasons of practicability, also regarding ^1H -NMR analysis, further screening was conducted in DMF.

⁵⁰ We chose hexanes to avoid extraction of any catalyst.

Table 35. Dual metal-catalyzed dehydrogenative coupling of DIPEA with PhBr; **solvent** screening.^a Catalyst loading refers to mol% of metal, not formula units. n.d. = not determined. DEC = diethoxy carbonate; DCE = dichloroethane.

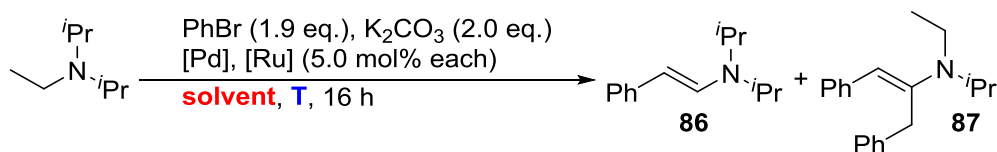


entry	[Pd]	[Ru]	solvent	DIPEA [%]	86 [%]	87 [%]
1	PdCl ₂ (PCy ₃) ₂	RuCl ₂ (PPh ₃) ₃	dioxane	n.d. ^b	3	13
2 ^c	PdCl ₂ (PCy ₃) ₂	RuCl ₂ (PPh ₃) ₃	PhMe	80	0	0
3	PdCl ₂ (PCy ₃) ₂	RuCl ₂ (PPh ₃) ₃	DEC	81	0	0
4	PdCl ₂ (PCy ₃) ₂	RuCl ₂ (PPh ₃) ₃	1,2-DCE	48	0	0
5	PdCl ₂ (PCy ₃) ₂	RuCl ₂ (PPh ₃) ₃	DMSO	61	5	<1
6	PdCl ₂ (PCy ₃) ₂	RuCl ₂ (PPh ₃) ₃	MeCN	53	12	10
7	PdCl ₂ (PCy ₃) ₂	RuCl ₂ (PPh ₃) ₃	DMF	56	11	9
8	PdCl ₂ (PCy ₃) ₂	RuCl ₂ (PPh ₃) ₃	DMAc	43	20	12
9	PdCl ₂ (PCy ₃) ₂	RuCl ₂ (PPh ₃) ₃	NMP	45	15	11

^aReactions performed with 500 μmol DIPEA (87.0 μL) in the indicated solvent (2 mL) according to GP 6.2.1a) (see 7.2.7.1); spectral yield according to ¹H-NMR with internal standard, given in mol%. ^bResidual DIPEA was azeotropically removed. ^cReaction performed at 140 °C.

Temperature is an important factor in catalysis. Whereas selectivity is often promoted by low temperature^[48], unreactive functionalities are frequently activated at high temperatures^[49]. Even though our reaction failed in toluene at 140 °C, we wanted to know whether selectivity and reactivity could be controlled by the temperature (table 36).

Table 36. Dual metal-catalyzed dehydrogenative coupling of DIPEA with PhBr; **temperature** screening in high boiling **solvents**.^a Catalyst loading refers to mol% of metal, not formula units. n.d. = not determined.



entry	[Pd]	[Ru]	solvent	T [°C]	DIPEA [%]	86 [%]	87 [%]
1	PdCl ₂ (PCy ₃) ₂	RuCl ₂ (PPh ₃) ₃	DMSO	140	44	12	3
2	PdCl ₂ (PCy ₃) ₂	RuCl ₂ (PPh ₃) ₃	DMF	140	n.d. ^b	14	11
3	PdCl ₂ (PCy ₃) ₂	RuCl ₂ (PPh ₃) ₃	DMAc	80	88	0	0
4	PdCl ₂ (PCy ₃) ₂	RuCl ₂ (PPh ₃) ₃	DMAc	140	36	12	10
5 ^c	PdCl ₂ (PCy ₃) ₂	RuCl ₂ (PPh ₃) ₃	DMAc	140	21	10	9

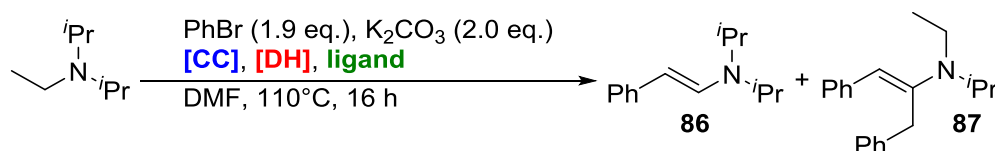
^aReactions performed with 500 μmol DIPEA (87.0 μL) in the indicated solvent (2 mL) according to GP 6.2.1a) (see 7.2.7.1); spectral yield according to ¹H-NMR with internal standard, given in mol%.

^bSignals of DIPEA overlaid too much for accurate integration. ^cReaction performed in a 10 mL Schlenk tube; other experiments were performed in an 8 mL screw capped vial.

At 110 °C, a little dehydrogenative coupling product was observed in DMSO. Increasing the temperature to 140 °C improved the yield of olefin **86** to 12% with preferred selectivity over **87** (entry 1). No significant changes were detected in DMF (entry 2). No reaction took place at 80 °C in DMAc (entry 3). Higher temperatures (140 °C) lowered the amount of both species irrespective of the reaction vessel involved (entries 4 and 5). Both an increase or a reduction of temperature did not considerably ameliorate the dehydrogenative coupling of DIPEA with PhBr.

Either one of the employed precatalysts might be too unreactive for the desired transformation. Therefore, we performed systematic variations of the coupling or dehydrogenation precatalyst (table 37). The dehydrogenation catalyst was changed first, followed by the cross-coupling precursor. The previous best result is depicted in entry 1.

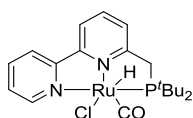
Table 37. Dual metal-catalyzed dehydrogenative coupling of DIPEA with PhBr; **ligand**, **[CC]** and **[DH]** precatalyst screening.^a **[CC]** = cross-coupling precatalyst. **[DH]** = dehydrogenation precatalyst; Cp* = pentamethylcyclopentadienyl; Cp = cyclopentadiene; dppf = 1,1'-bis(diphenylphosphino)ferrocene.



entry	[CC] [mol%]	[DH] [mol%]	ligand [mol%]	DIPEA	86 [%]	87 [%]
1	PdCl ₂ (PCy ₃) ₂ (5.0)	RuCl ₂ (PPh ₃) ₃ (5.0)	-	56	11	9
2	PdCl ₂ (PCy ₃) ₂ (5.0)	CpRuCl(PPh ₃) ₂ (5.0)	-	72	5	7
3	PdCl ₂ (PCy ₃) ₂ (5.0)	RuHCl(CO)(PPh ₃) ₃ (5.0)	-	53	12	2
4	PdCl ₂ (PCy ₃) ₂ (5.0)	[RuCl ₂ (<i>p</i> -cymene)] ₂ (2.5)	-	35	14	21
5	PdCl ₂ (PCy ₃) ₂ (5.0)	Milstein <i>N,N,P</i> -Ru ⁵¹ (5.0)	-	38	15	22
6	PdCl ₂ (PCy ₃) ₂ (5.0)	[Cp*IrCl ₂] ₂ (2.5)	-	12	26	18
7	NiCl ₂ (PCy ₃) ₂ (5.0)	RuCl ₂ (PPh ₃) ₃ (5.0)	-	79	0	0
8	IPr-PEPPSI (5.0)	RuCl ₂ (PPh ₃) ₃ (5.0)	-	41	14	10
9	Pd(OAc) ₂ (5.0)	RuCl ₂ (PPh ₃) ₃ (5.0)	S-Phos (15.0)	89	0	0
10	Pd-G3 (2.5)	RuCl ₂ (PPh ₃) ₃ (5.0)	dppf (15.0)	53	8	8
11	Pd(dba) ₂ ·CHCl ₃ (5.0)	RuCl ₂ (PPh ₃) ₃ (5.0)	dppf (15.0)	66	5	3

^aReactions performed with 500 μmol DIPEA (87.0 μL) in DMF (2 mL) according to GP 6.2.1a) (see 7.2.7.1); spectral yield according to ¹H-NMR with internal standard, given in mol%.

⁵¹ *N,N,P*-Ru pincer^c



Use of a related CpRu complex hampered the reaction (entry 2). Replacing RuCl₂(PPh₃)₃ with a hydrido-Ru-complex lowered the amount of diarylated allyl species **87** (entry 3). The *p*-cymene RuCl₂ complex significantly promoted the dehydrogenation of the isopropyl moiety and increased the proportion of **87** (entry 4). Milstein's *N,N,P*-Ru-Pincer complex^[50] afforded virtually identical results (entry 5). Interestingly, [Cp*IrCl₂]₂ shifted the selectivity to the desired olefin (**86**), and almost 50% of products **86** and **87** (entry 6). Exchanging of the cross-coupling catalyst with a similar Ni derivative blocked the reaction (entry 7). IPr-PEPPSI is an effective precatalyst in a wide range of reactions^[51] and was introduced by Organ and coworkers^[52]. Yet, this precursor delivered almost identical results (entry 8) to our initial conditions (entry 1). Buchwald's widely applied Pd(OAc)₂-SPhos system^[53] failed (entry 9). The group of Dydio had combined Buchwald's 3rd generation Pd-precatalyst with dppf as ligand.^[38] To those conditions, Pd-G3 was synthesized via a two-step procedure in 82% overall yield.^[54] However, Dydio's promising combination for his β-arylation reaction turned out to be ineffective in our reaction (entry 10). The use of a Pd(0) precursor complex even lowered the product yield (entry 11). We suppose that the additional ligand blocks free coordination sites at the metal center, disfavoring any approach of substrates. Given the effective suppression of side-product, the catalyst combination of entry 3 was involved in further screening experiments, besides the conventional RuCl₂(PPh₃)₃ dehydrogenation catalyst.

The group of Dydio had stirred their coupling mixtures for 36 h at 80 °C (scheme 60).^[38] Dilution of reaction mixtures usually slows the conversion in a catalytic reaction, similar to a decrease in temperature. To substantiate whether our reaction require more time to run to completion, we extended the reaction time (table 38). However, either running the reaction for one, two or three days at 110 °C did not affect the outcome of the arylation (entries 1-3). Dehydrogenative coupling does not always involve the release of hydrogen gas. Sacrificial hydride acceptors can be added to the reaction mixture to consume any generated H₂, and this may suppress unwanted side-reactions. The addition of 1,4-benzoquinone in combination with either Ru-precatalyst retarded the catalytic reaction, also in DMAc (entries 4 and 5). In contrast, the unwanted olefin **87** was preferred in the presence of styrene as hydrogen acceptor (entry 6). No proof of actual hydrogenation of styrene was attempted. Detection of released hydrogen should be of interest for future research. Interestingly, the reaction can be performed in air with no loss in yield (entry 7). We still prepared to conduct all investigations under argon to avoid any hydrolysis of enamines to the corresponding carbonyl compounds.

Table 38. Dual metal-catalyzed dehydrogenative coupling of DIPEA with PhBr; **additive** and **time** screening.^a Catalyst loading refers to mol% of metal, not formula units. BQ = benzoquinone; n.d. = not determined.

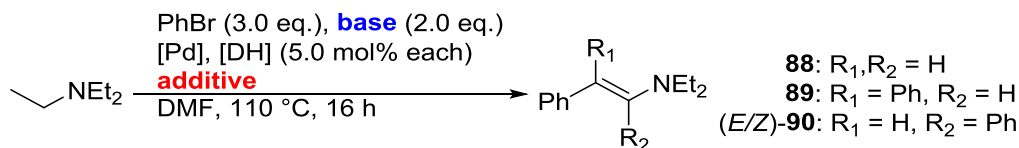
entry	[Pd]	[Ru]	additive	t [h]	DIPEA [%]	86 [%]	87 [%]
1 ^b	PdCl ₂ (PCy ₃) ₂	RuHCl(CO)(PPh ₃) ₃	-	24	47	10	4
2 ^b	PdCl ₂ (PCy ₃) ₂	RuHCl(CO)(PPh ₃) ₃	-	48	50	13	6
3 ^b	PdCl ₂ (PCy ₃) ₂	RuHCl(CO)(PPh ₃) ₃	-	72	49	11	6
4	PdCl ₂ (PCy ₃) ₂	RuCl ₂ (PPh ₃) ₃	1,4-BQ	16	24	2	3
5 ^c	PdCl ₂ (PCy ₃) ₂	RuHCl(CO)(PPh ₃) ₃	1,4-BQ	16	32	6	2
6	PdCl ₂ (PCy ₃) ₂	RuCl ₂ (PPh ₃) ₃	styrene	16	52	0	17
7 ^d	PdCl ₂ (PCy ₃) ₂	RuCl ₂ (PPh ₃) ₃	-	16	n.d. ^e	10	11

^aReactions performed with 500 μmol DIPEA (87.0 μL) in DMF (2 mL) according to GP 6.2.1a) (see 7.2.7.1); spectral yield according to ¹H-NMR with internal standard, given in mol%. ^bReaction performed in 1 mL DMF. ^cReaction performed in DMAc (2 mL). ^dReaction performed in air. ^eResidual DIPEA was removed at the rotary evaporator.

6.2.2 Changing the amine – reduction of complexity or not?

Since DIPEA bears different alkyl chains at nitrogen, competitive dehydrogenation leads to the formation of unwanted side-product. Substitution of the tertiary amine with a symmetric one would eliminate this regioselectivity issue. Hence, we focused our attention on triethylamine, even though Goldman et al.^[15] had reported mere average conversion of the amine to the desired enamine (25-65%). Application of the so far best reaction conditions from the previous screening to the new substrate NEt₃ is depicted in table 39. The first catalyst combination involved Cp*Ir-dimer and PdCl₂(PCy₃)₂ (entry 1). Next to the signals of the desired olefin **88** (δ 5.15 (d), 6.76 (d)), three additional singlets were observed in the alkenyl region. The (*Z*)-isomer of **88** was noticed, however. After aqueous work-up, 2D-NMR as well as GC-MS analysis revealed the presence of diarylated enamines **89** and **90**, whose signals belonged to the three detected singlets in the crude reaction mixture (δ 5.49 (*E*)-**90**, 5.62 (*Z*)-**90**, 6.35 (**89**), see 7.2.7.5 for NMR details), with (*E*)-**90** being generally preferred over its (*Z*)-isomer. The (*E*/*Z*)-ratio for **90** in most cases amounted to 9:1 or 10:1 (*E*/*Z*) and will not be indicated. Even though the following experiments were subjected to aqueous work-up, aldehydes were not usually noticed in the ¹H-NMR spectra of crude mixtures (<1%). The recovery of tertiary amine is not indicated, since residual amounts of the starting amine were washed away with water.

Table 39. Dual metal-catalyzed dehydrogenative coupling of NEt₃ with PhBr; previous (DIPEA) best conditions, **base** and **additive** screening. ^a Catalyst loading refers to mol% of metal, not formula units. [DH] = dehydrogenation precatalyst.



entry	[Pd]	[DH]	base	additive [eq.]	88	89	(E/Z)-90
1	PdCl ₂ (PCy ₃) ₂	[Cp*IrCl ₂] ₂	K ₂ CO ₃	-	25	<1	6
2	PdCl ₂ (PCy ₃) ₂	[Cp*IrCl ₂] ₂	KO ^t Bu	-	21	<1	2
3	PdCl ₂ (PCy ₃) ₂	RuCl ₂ (PPh ₃) ₃	K ₂ CO ₃	-	8	3	15
4	PdCl ₂ (PCy ₃) ₂	RuCl ₂ (PPh ₃) ₃	Ag ₂ CO ₃	-	0	0	0
5	PdCl ₂ (PCy ₃) ₂	Milstein ⁵¹	K ₂ CO ₃	-	7	5	21
6	IPr-PEPPSI	[Cp*IrCl ₂] ₂	K ₂ CO ₃	-	30	<1	7
7 ^b	IPr-PEPPSI	[Cp*IrCl ₂] ₂	K ₂ CO ₃	-	26 ^b	4 ^b	18 ^b
8	IPr-PEPPSI	[Cp*IrCl ₂] ₂	K ₃ PO ₄	-	32	2	10
9	IPr-PEPPSI	[Cp*IrCl ₂] ₂	K ₂ CO ₃	NBu ₄ DiPP (0.1)	11	3	11
10	IPr-PEPPSI	[Cp*IrCl ₂] ₂	K ₂ CO ₃	norbornene (2.0)	0	0	0
11	-	[Cp*IrCl ₂] ₂	K ₂ CO ₃	-	<1	0	0

^aReactions performed with 500 μmol DIPEA (87.0 μL) in DMF (2 mL) according to GP 6.2.1a) (see 7.2.7.1); spectral yield according to ¹H-NMR with internal standard, given in mol%. ^bReaction performed in DMAc.

Use of strong *tert*-butoxide base did not affect the outcome of the reaction (entry 2). Substitution of the dehydrogenation precatalyst to RuCl₂(PPh₃)₃ preferred the formation of diarylated **(E/Z)-90** (entry 3). Introduction of the halide abstractor base Ag₂CO₃ completely blocked the reaction (entry 4). Milstein's *N,N,P*-Ru-pincer complex favored **(E/Z)-90** (entry 5). While IPr-PEPPSI delivered virtually identical results to PdCl₂(PCy₃)₂ in DMF (entry 6), performing the reaction in DMAc increased the amount of **(E/Z)-90** side-product (entry 7). Phosphate base did not influence the selectivity or reactivity (entry 8). Our defunction onium carboxylate NBu₄DiPP lowered the amount of alkene **88**, while slightly promoting diarylation to **(E/Z)-90** (entry 9). Competitive coordination of metal centers with additional reactants and additive seems to impede the reaction. Similar results were obtained when adding phosphine ligand (see 6.2.1, table 37). Goldman and coworkers had observed that substitution of *tert*-butylethane with norbornene as hydrogen acceptor gave almost quantitative conversion of triethylamine, providing 75% of di-dehydrogenated product.^[15] In our case, the dehydrogenative coupling entirely stopped when norbornene was tried (entry 10). Leaving the cross-coupling precatalyst out expectedly stopped the coupling step (entry 11). Given the good reactivity as well as

comparably high selectivity, we mostly stuck to the IPr-PEPPSI/[Cp*IrCl₂]₂ precatalyst system of entry 6 for the next screening phase.

Although not shown, low amounts of phenyl bromide and biaryl were noticed in all q-NMR analyses for table 39. Notably, a signal belonging to benzene was additionally observed. We supposed that any released hydrogen gas could reduce aryl bromide in the presence of metal precatalysts, thereby consuming part of the reactant. Variation of equivalents (NEt₃ and PhBr) should clarify if reactivity or selectivity might be affected (table 40).

Table 40. Dual metal-catalyzed dehydrogenative coupling of NEt₃ with PhBr; **NEt₃** and **PhBr** equivalents screening.^a Catalyst loading refers to mol% of metal, not formula units.

entry	[Pd]	[Ir]	NEt₃ [eq.]	PhBr [eq.]	88 [%]	89 [%]	(<i>E/Z</i>)- 90 [%]
1	PdCl ₂ (PCy ₃) ₂	[Cp*IrCl ₂] ₂	2.0	1.0	<1	0	<1
2	IPr-PEPPSI	[Cp*IrCl ₂] ₂	1.0	3.0	11	7	40
3 ^b	IPr-PEPPSI	[Cp*IrCl ₂] ₂	1.0	3.0	24	3	15
4 ^c	IPr-PEPPSI	[Cp*IrCl ₂] ₂	1.0	3.0	17	9	32
5	IPr-PEPPSI	[Cp*IrCl ₂] ₂	1.0	4.0	12	8	38
6	IPr-PEPPSI	[Cp*IrCl ₂] ₂	1.0	10.0	6	11	46

^aReactions performed with 500 μmol NEt₃ (70.0 μL) in DMF (2 mL) according to GP 6.2.1b) (see 7.2.7.1); spectral yield according to ¹H-NMR with internal standard, given in mol%. ^bReaction stopped after six hours at 110 °C. ^cReaction performed in DMAc (2 mL).

Indeed, setting the aryl bromide as limiting component delivered insignificant quantities of **88** or (*E/Z*)-**90** (entry 1). On the contrary, use of 3.0 equivalents of PhBr significantly increased the overall conversion to alkenyl compounds (entry 2), with diarylation being preferred. Stopping the reaction after only six hours afforded lower amounts of **89** and (*E/Z*)-**90**, leaving more of the desired olefin **88** behind, due to decelerated diarylation (entry 3). Performing the reaction in dimethyl-acetamide slightly improved the coupling selectivity (entry 4). An increase to 4.0 equivalents of ArBr entailed even larger portions of (*E/Z*)-**90** at the cost of monoarylated olefin **88** (entry 5). Approaching the status of a co-solvent, excessive incorporation of PhBr (10.0 eq.) exclusively gave rise to mainly diarylated alkenes **89** and (*E/Z*)-**90** (entry 6). Unlike in the catalysis studied by Goldman and coworkers^[15], neither di-dehydrogenated vinylamine nor subsequently arylated derivative were detected.

Since product generation did not profit from using more than 3.0 equivalents of aryl bromide, we continued with a 1:3 substrate ratio. While K₂CO₃ seemed effective, we also tried other

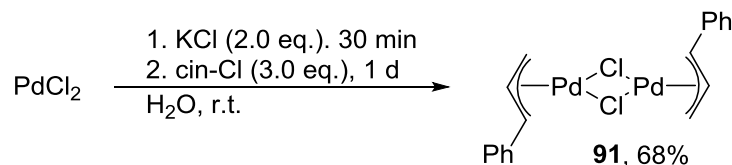
carbonate bases in the reaction (table 41). Whereas Cs₂CO₃ (entry 1) and KHCO₃ (entry 2) cleanly improved the selectivity to the desired olefin **88**, overall reaction was hampered. Na₂CO₃ most likely suffered from reduced solubility^[55] and only delivered 7% of **88** (entry 3). Introduction of Ag₂O as additive inhibited the reaction (entry 4) and also gave rise to the formation of a silver mirror. As with benzoquinone in its potential role as oxidant or hydride acceptor, other quinones, such as Me₂-BQ (entry 5), Cl₄-BQ (entry 6), or DDQ (entry 7) proved inefficient.

Table 41. Dual metal-catalyzed dehydrogenative coupling of NEt₃ with PhBr; **base** screening.^a Catalyst loading refers to mol% of metal, not formula units. BQ = benzoquinone; DDQ = 2,3-dichloro-5,6-dicyano-1,4-benzoquinone.

entry	[Pd]	[Ir]	base	additive [eq.]	88 [%]	89 [%]	(E/Z)- 90 [%]
1	IPr-PEPPSI	[Cp*IrCl ₂] ₂	Cs ₂ CO ₃	-	17	0	1
2	IPr-PEPPSI	[Cp*IrCl ₂] ₂	KHCO ₃	-	12	0	3
3	IPr-PEPPSI	[Cp*IrCl ₂] ₂	Na ₂ CO ₃	-	7	0	<1
4	IPr-PEPPSI	[Cp*IrCl ₂] ₂	K ₂ CO ₃	Ag ₂ O (1.5)	2	0	0
5	IPr-PEPPSI	[Cp*IrCl ₂] ₂	K ₂ CO ₃	2,6-Me ₂ BQ (0.5)	<1	<1	1
6	IPr-PEPPSI	[Cp*IrCl ₂] ₂	K ₂ CO ₃	Cl ₄ -BQ (0.5)	0	0	0
7	IPr-PEPPSI	[Cp*IrCl ₂] ₂	K ₂ CO ₃	DDQ (0.5)	<1	<1	<1

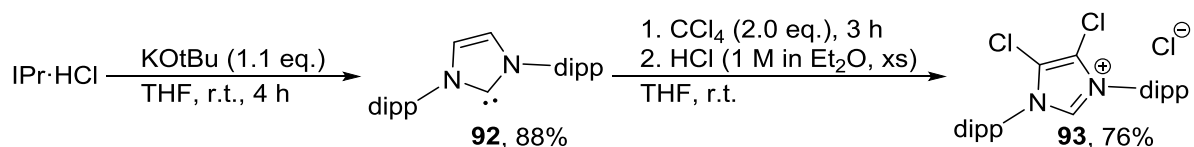
^aReactions performed with 500 μmol NEt₃ (70.0 μL) in DMF (2 mL) according to GP 6.2.1b) (see 7.2.7.1); spectral yield according to ¹H-NMR with internal standard (1,3,5-trimethoxybenzene), given in mol%.

A plethora of Organ's IPr-PEPPSI derivatives is currently available. Given the good performance of IPr-PEPPSI, we focused on the synthesis of a few other precatalysts in the hope of enriching the amount of desired coupling product **88**. Starting from PdCl₂, we isolated the cinnamyl dimer **91** in 68% following a procedure by the group of Nolan^[56] (scheme 63). The reaction was performed in the dark to avoid any decomposition of the allyl reagent due to light.



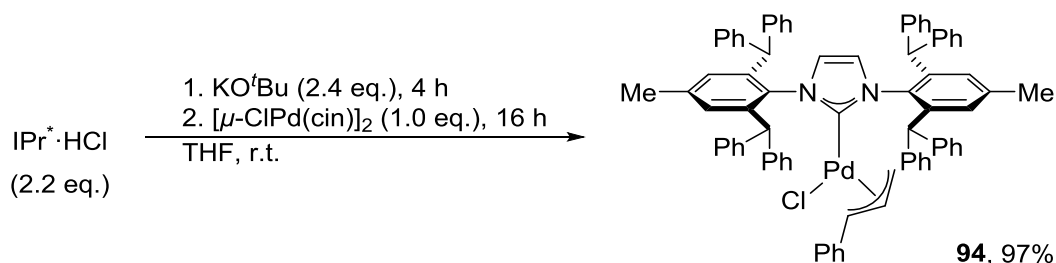
Scheme 63. Synthesis of [μ-CIPd(cin)]-dimer according to a procedure by the group of Nolan^[56]. cin = cinnamyl. Conducting all manipulation under strictly inert and dry conditions, the free carbene ligand, IPr (**92**), was synthesized in 88% yield according to reports by Nolan et al.^[57] (scheme 64). The ligand was stored inside a glovebox for further use. Chlorination of the imidazole backbone

was enabled by toxic CCl_4 following a procedure by Organ et al.^[51c]. Precipitation of the imidazolium salt was induced by the addition of ethereal HCl excess, affording $\text{IPr}^{\text{Cl}}\cdot\text{HCl}$ (**93**) in 76% yield.



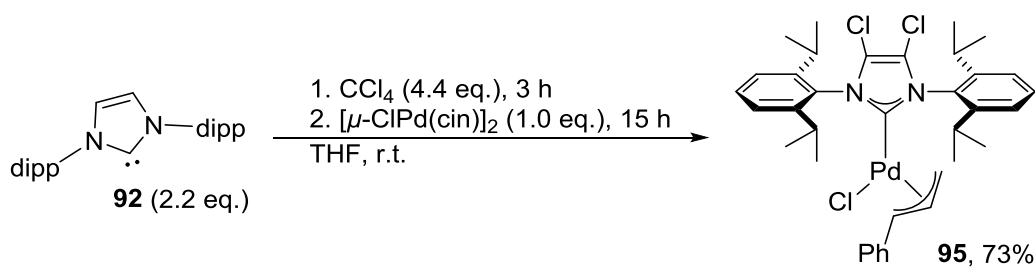
Scheme 64. Two-step synthesis of $\text{IPr}^{\text{Cl}}\cdot\text{HCl}$. The free carbene ligand, IPr (**92**) was isolated according to the group of Nolan^[57]. Subsequent chlorination of the imidazole backbone was performed following reports from Organ et al.^[51c]. dipp = 2,6-diisopropylphenyl; xs = excess.

Nolan's protocol for allyl type complex syntheses relied on the isolation of intermediate carbene ligands.^[56] However, Sigman and coworkers previously proved either way is possible: starting from deprotonated ligand or in situ from imidazolium salt in the presence of strong base.^[58] We used both methods, depending on the complex to be generated. Following more recent reports of Nolan^[59], $[\text{Pd}(\text{IPr}^*)(\text{cin})\text{Cl}]$ (**94**) was available in almost quantitative yield starting from the corresponding imidazolium salt (scheme 65). The latter was previously synthesized by Dr. L. Zhai in our group. This kind of Pd-allyl complexes is easily purified by flash column chromatography.



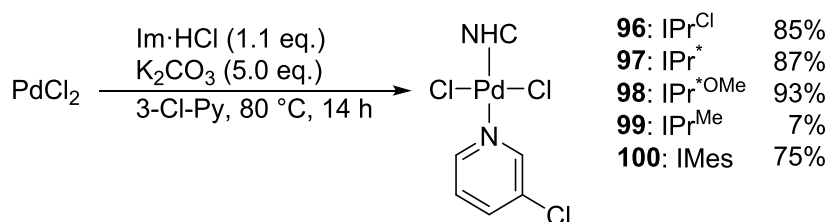
Scheme 65. Synthesis of $[\text{Pd}(\text{IPr}^*)(\text{cin})\text{Cl}]$ (**94**) starting from $\text{IPr}^*\cdot\text{HCl}$ according to a procedure by Nolan.^[59] cin = cinnamyl.

We also attempted to synthesize a more electron-deficient precatalyst based on the $\text{IPr}^{\text{Cl}}\text{-NHC}$ ligand. Opposed to Nolan and coworkers^[60] who isolated each reactant individually, we envisaged an one-pot procedure starting from the free IPr carbene (**92**). A solution of the latter was combined with CCl_4 . Complete chlorination of the backbone was achieved after only three hours at room temperature. After addition of $[\mu\text{-ClPd(cin)}]_2$, purification by flash column chromatography gave 73% of $[\text{Pd}(\text{IPr}^{\text{Cl}})(\text{cin})\text{Cl}]$ (**95**) as yellow crystalline solid (scheme 66).



Scheme 66. One-pot synthesis of [Pd(IPr^{Cl})(cin)Cl] (**95**) starting from the free IPr carbene (**92**). cin = cinnamyl.

Next to these cinnamyl complexes, we wanted to further extend our selection to other PEPPSI precatalysts **96-100**. The latter were easily available following a procedure by Organ et al.^[52] (scheme 67). Except for IPr^{Me}-PEPPSI (**99**), all complexes were obtained in good to excellent yield and purity. The main reason for the very low yield of **99** is due to the incorporation of IPr^{Me}·HOTf instead of the chloride salt. Since major amounts of imidazolium salt were recovered, we supposed that the triflate one either suffered from low solubility or lack of chloride ions to generate complex **99**. Synthesis attempts via our established method depicted in chapter 3.2.1 were not conducted.

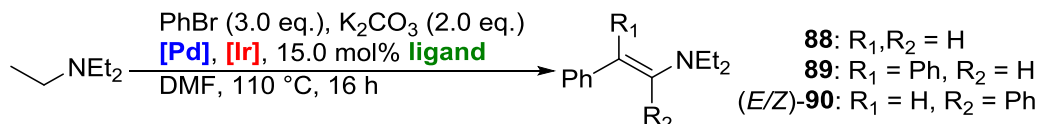


Scheme 67. Synthesis of PEPPSI derivatives. IPr^{Me}·HOTf was used for the synthesis of IPr^{Me}-PEPPSI (**99**).

Having several Pd cross-coupling precatalysts in our deposit, we started screening of catalysts as well as their loading (table 42). Dilution of previously established conditions involving IPr-PEPPSI and [Cp^{*}IrCl₂]₂ precatalysts (entry 1) slightly shifted the selectivity to the desired coupling product **88** (entry 2). To avoid wasting solvent, further experiments kept the initial concentration as in entry 1. Additional free carbene ligand partly lowered the reactivity (entry 3). Even in the change of dehydrogenation catalyst, a little diarylated (*E/Z*)-**90** as well as equal amounts of olefins **88** and **89** were formed (entry 4). Supposedly, IPr-PEPPSI dehydrogenates tertiary amine to a certain extent. There are some literature reports describing Pd(OTf)₂ or Pd on carbon for the efficient (α,β)-dehydrogenation of cyclic alcohols, imidazolines, ketones or aldehydes.^[61] In addition to releasing hydrogen gas, the Ir-catalyst might also be involved in reduction or oxidation of Pd, or intermetallic interactions with Pd. Increasing the Ir-loading to 5.0 mol% led to enhanced formation of the monoarylated alkene **88** (entry 5), still entailing

virtually identical quantities of diarylation. However, reduction to 1.0 mol% [Ir] promoted the generation of (*E/Z*)-**90** isomers (entry 6).

Table 42. Dual metal-catalyzed dehydrogenative coupling of NEt₃ with PhBr; **ligand**, [Pd] and [Ir] precatalyst screening. ^a cin = cinnamyl.



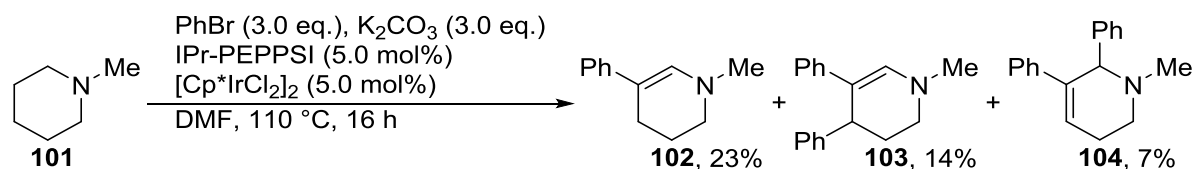
entry	[Pd] ^b [mol%]	[Ir] ^c [mol%]	ligand	88 [%]	89 [%]	(<i>E/Z</i>)- 90 [%]
1	IPr-PEPPSI	[Cp*IrCl ₂] ₂	-	11	7	40
2 ^d	IPr-PEPPSI	[Cp*IrCl ₂] ₂	-	23	6	24
3	IPr-PEPPSI	[Cp*IrCl ₂] ₂	IPr	15	5	31
4	IPr-PEPPSI	-	-	2	2	8
5	IPr-PEPPSI	[Cp*IrCl ₂] ₂ (5.0)	-	24	3	25
6	IPr-PEPPSI	[Cp*IrCl ₂] ₂ (1.0)	-	7	5	31
7 ^d	IPr-PEPPSI (10.0)	[Cp*IrCl ₂] ₂	-	19	7	28
8	IPr-PEPPSI (2.5)	[Cp*IrCl ₂] ₂	-	18	6	29
9	IPr-PEPPSI (1.0)	[Cp*IrCl ₂] ₂	-	25	2	14
10 ^e	IPr-PEPPSI (1.0)	[Cp*IrCl ₂] ₂	-	16	5	34
11	IPr ^{Cl} -PEPPSI	[Cp*IrCl ₂] ₂	-	17	6	35
12	IPr [*] -PEPPSI	[Cp*IrCl ₂] ₂	-	20	5	29
13	IPr ^{*OMe} -PEPPSI	[Cp*IrCl ₂] ₂	-	12	7	38
14	IMes-PEPPSI	[Cp*IrCl ₂] ₂	-	18	5	28
15	IPent-PEPPSI	[Cp*IrCl ₂] ₂	-	18	5	30
16	IPr ^{Me} -PEPPSI	[Cp*IrCl ₂] ₂	-	25	4	27
17	[Pd(IPr [*])(cin)Cl]	[Cp*IrCl ₂] ₂	-	32	1	7
18	[Pd(IPr [*])(cin)Cl] (1.0)	[Cp*IrCl ₂] ₂	-	22	4	22
19	[Pd(IPr ^{Cl})(cin)Cl]	[Cp*IrCl ₂] ₂	-	31	3	10
20	PdCl ₂ (PCy ₃) ₂ (5.0)	[Cp*IrCl ₂] ₂	PCy ₃	0	0	0
21	Pd(OAc) ₂ (5.0)	[Cp*IrCl ₂] ₂	P ^t Bu ₃ ·HBF ₄	0	0	0
22 ^f	Pd(OAc) ₂ (5.0)	[Cp*IrCl ₂] ₂	P ^t Bu ₃ ·HBF ₄	0	0	0

^aReactions performed with 500 μmol NEt₃ (70.0 μL) in DMF (2 mL) according to GP 6.2.1b) (see 7.2.7.1); spectral yield according to ¹H-NMR with internal standard, given in mol%. ^bUnless stated otherwise, 5.0 mol% of Pd precatalyst used. ^cUnless stated otherwise, 2.5 mol% of Ir-dimer used. ^dReaction performed in 5 mL DMF. ^eStirring for 40 hours at 110 °C. ^fUse of KO^tBu instead of K₂CO₃.

Neither raising the Pd-loading to 10.0 mol% in dilute solution (entry 7), nor lowering [Pd] to 2.5 mol% had a noticeable effect (entry 8). Low amounts of Pd (1.0 mol%) preferred the monoarylated species **88** (entry 9), reducing the overall reactivity. Prolonged stirring of the reaction mixture induced further arylation of the olefin **88** already present (entry 10). Despite of a plethora of PEPPSI-precatalysts tested, virtually identical amounts of products **88**, **89**, and

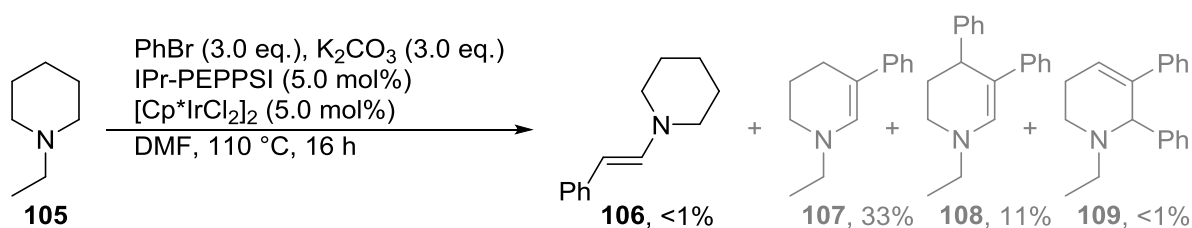
(*E/Z*)-**90** were detected (entries 11-15), and they were only slightly more selective than IPr-PEPPSI (entry 1). IPr^{Me}-PEPPSI was the only complex that stood out from its siblings (entry 16), displaying slightly enhanced formation of **88**. Somewhat disappointed by the PEPPSI precatalysts, we hoped for more success with our cinnamyl precursors. Indeed, incorporation of [Pd(IPr^{*})(cin)Cl] almost exclusively delivered the desired coupling product **88** at the cost of overall conversion to desired products (entry 17). Reduction of catalyst loading to 1.0 mol% improved the consumption of reactants but afforded identical amounts of **89** and (*E/Z*)-**90** (entry 18). Similar results were obtained with electron-deficient [Pd(IPr^{Cl})(cin)Cl] (entry 19). While the addition of ligands such as S-Phos or dppf hampered the reaction, we hoped that trialkylphosphines, often used in cross-coupling chemistry, might show a positive effect. While the reaction worked without (table 39, entry 1), it was completely blocked by extra PCy₃ (entry 20). Combination of Pd(OAc)₂ with P^tBu₃, released in situ from ^tBu₃P·HBF₄ by base prevented any dehydrogenative coupling from taking place (entries 21 and 22).

The highest yield achieved so far relied on the IPr-PEPPSI/[Cp^{*}IrCl₂]₂ catalyst system. Since screening efforts did not exceed certain levels of product yield, we started changing the amine substrate. By using *N*-methylpiperidine (**101**) as starting material, we hoped to suppress unwanted side-products occurring from diarylation. Subjecting **101** to our conditions delivered a mixture of three main isomers **102**, **103** and **104**, however (scheme 68).



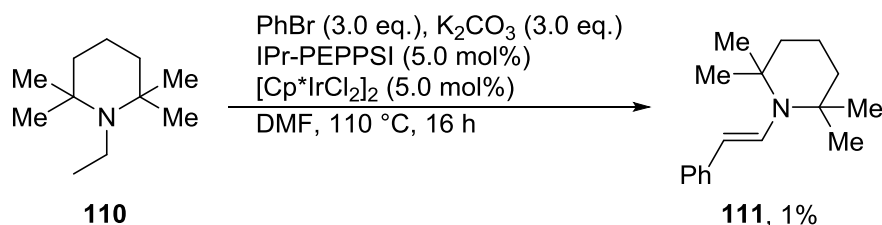
Scheme 68. Dual metal-catalyzed dehydrogenative coupling of *N*-methylpiperidine (**102**) with PhBr. Minor amounts of triarylated piperidine (1%) were detected.

With *N*-ethylpiperidine (**105**) as substrate, Goldman and coworkers^[15] had observed the exclusive dehydrogenation of the ethyl group with their catalyst. They found a complete lack in reactivity of the six-membered ring, also case of methyl derivative **101**. Using our procedure, the unwanted dehydrogenation of the free alkyl chain was observed (scheme 69), however as for *N*-methylpiperidine (**101**), our catalyst-system preferably dehydrogenated α,β -positions in the ring, affording the desired olefin **106** in <1% yield, but 33% of **107**. Diarylated species **108** and **109** resulted from allylic activation by Pd.



Scheme 69. Dual metal-catalyzed dehydrogenative coupling of *N*-ethylpiperidine (**105**) with PhBr. The dehydrogenative coupling of the ethyl group afforded <1%. Residual amounts of amine (23%) were detected.

By blocking both ring positions next to nitrogen, we hoped to prevent dehydrogenation of the heterocycle. The tetramethyl-substituted piperidine derivative **110** was prepared in 79% yield following a procedure by the group of Berke. Sadly, almost no conversion was detected in a catalytic standard run (scheme 71). Our dehydrogenative couplings with piperidines proceeded unlike the reaction of Goldman et al.^[15], leaving us with NEt₃ as most successful substrate.



Scheme 70. Dual metal-catalyzed dehydrogenative coupling of *N*-ethyl-2,2,6,6-tetramethylpiperidine (EtTMP, **110**) with PhBr. Residual amounts of amine (46%) were detected.

6.2.3 Diversifying the aryl bromide – influence of the substitution pattern

Substrate variations in the amine part had only led to unwanted as well as unexpected arylation reactions so far. In terms of phenyl bromide, while the reaction mostly lacked selectivity, the overall yield was satisfactory. Cross-coupling reactions often depend on involved substrates. The reactivity of aryl electrophiles decreases in the row I > Br > Cl (> F).^[62] Substitution patterns at the benzene ring exhibiting electronic properties certainly influence the latter. Similarly, increased steric bulk around the reactive electrophilic site retards its conversion.

To facilitate conversion of unreactive substrates, chemists take advantage of highly active catalysts, as those employed in table 42. Since no decisive changes in selectivity or reactivity had been achieved, we sought to diversify the aryl halide, while focusing on the IPr-PEPPSI/[Cp*IrCl₂]₂ catalyst-system (table 43). While less reactive chlorobenzene stopped the reaction (entry 1), iodobenzene afforded 22% of the desired olefin **88** along with 10% (*E/Z*)-**90** (entry 2). Large amounts of biphenyl were also detected, due to homocoupling of PhI.

Table 43. Dual metal-catalyzed dehydrogenative coupling of NEt₃ with ArX.^a Catalyst loading refers to mol% of metal, not formula units.

$\text{NEt}_3 \xrightarrow[\text{DMF, 110 } ^\circ\text{C, 16 h}]{\text{ArX (3.0 eq.), K}_2\text{CO}_3 \text{ (2.0 eq.)}, [\text{Pd}], [\text{Ir}] \text{ (5.0 mol\% each)}} \text{Ar}-\text{C}(\text{R}_1)=\text{C}(\text{NEt}_2)-\text{C}(\text{R}_2)$

112: R₁, R₂ = H
113: R₁ = Ar, R₂ = H
(E/Z)-114: R₁ = H, R₂ = Ar

entry	ArX	[Pd]	[Ir]	112 [%]	113 [%]	(E/Z)- 114 [%]
1		IPr-PEPPSI	[Cp*IrCl ₂] ₂	2	0	<1
2		IPr-PEPPSI	[Cp*IrCl ₂] ₂	22	<1	10
3 ^b		IPr-PEPPSI	[Cp*IrCl ₂] ₂	3	0	0
4 ^c		IPr-PEPPSI	[Cp*IrCl ₂] ₂	11	1	6
5		IPr-PEPPSI	[Cp*IrCl ₂] ₂	2	7	44
6		IPr-PEPPSI	[Cp*IrCl ₂] ₂	0	3	53
7		IPr-PEPPSI	[Cp*IrCl ₂] ₂	3	0	<1
8		IPr-PEPPSI	[Cp*IrCl ₂] ₂	0	0	47
9		IPr-PEPPSI	[Cp*IrCl ₂] ₂	8	6	40
10		IPr-PEPPSI	[Cp*IrCl ₂] ₂	15	0	0
11		IPr-PEPPSI	[Cp*IrCl ₂] ₂	0	0	0
12		IPr-PEPPSI	[Cp*IrCl ₂] ₂	47	0	11
13 ^d		IPr-PEPPSI	[Cp*IrCl ₂] ₂	49	0	10
14 ^e		IPr-PEPPSI	[Cp*IrCl ₂] ₂	54	0	14
15		IPr-PEPPSI	[Cp*IrCl ₂] ₂	12 ^d	0 ^d	0 ^d
16		IPr-PEPPSI	[Cp*IrCl ₂] ₂	24 ^d	0 ^d	0 ^d
17 ^f		PdCl ₂ (PCy ₃) ₂	RuCl ₂ (PPh ₃) ₃	<1	0	-

^aReactions performed with 500 μmol NEt₃ (70.0 μL) in DMF (2 mL) according to GP 6.2.1b) (see 7.2.7.1); spectral yield according to ¹H-NMR with internal standard, given in mol%. ^bReaction performed with 2.5 mol% IPr-PEPPSI. ^cNBu₄Br (3.0 eq.) was added. Reaction performed with 5.0 mol% IPr-PEPPSI. ^dReaction performed with 4.0 eq. K₃PO₄. ^eReaction performed with 4.0 K₂CO₃. ^fReaction performed with 524 μmol DIPEA (87.0 μL) in DMF (2 mL) following GP 6.2.1b) (7.2.7.1); 2.0 eq. ArBr were added. ^fYield refers to observed diarylated allyl side-product occurring from dehydrogenation of an isopropyl group.

Phenyl triflate showed little conversion when used alone (entry 3), but the addition of NBu₄Br as bromide source led to slightly enhanced reactivity (entry 4), although still less than with PhBr. Electron-rich arenes including *p*-TolBr (entry 5) and *p*-bromoanisole (entry 6) almost exclusively gave a mixture of diarylated olefins **113** and (*E/Z*)-**114**. 1-Bromo-4-*tert*-butylbenzene retarded the dehydrogenative coupling, yielding only 3% of alkene **112** (entry 7). Diarylation was preferred with *p*-(*N,N*-dimethyl)aminophenyl bromide (entry 8). The same goes for *m,m*-xylyl aryl bromide (entry 9). Sterically hindered bromomesitylene solely resulted in 15% of coupling product **112** (entry 10). However, 2-bromobiphenyl failed to react (entry 11). Surprisingly, 1-bromonaphthalene showed very good selectivity, delivering 47% of target material **112** as well as 11% of (*E/Z*)-**114** (entry 12). Steric repulsion, may have prevented the β-diarylation of the alkene, producing olefin **112**. While the addition of 4.0 equivalents of K₃PO₄ gave similar results (entry 13), use of 4.0 eq. K₂CO₃ slightly increased the overall reactivity and yield (entry 14). Further substitution of the naphthyl moiety with a 2-methoxy group inhibited all diarylation (entry 15), entailing 12% of monoarylation product **112**. The large anthracene derivative afforded even higher amounts (24%) of the latter, with no trace of side-products (entry 16). Electron-deficient aryl bromides were not used in the dehydrogenative coupling of NEt₃, since a previously performed experiment involving DIPEA and *p*-bromobenzonitrile in the presence of Pd- and Ru-precatalysts had not shown any yield (entry 17).

Given the promising results with 1-bromonaphthalene, a final screening effort relied on this electrophile. To avoid wasting inorganic base, we decided not to increase the amount of K₂CO₃, but stuck to 2.0 equivalents. Further dilution of reaction mixtures was also omitted.

Having applied nearly every Ir- and Ru-precatalyst available in our storage, we had not yet focused on Rh-type precursors noted for their effective (de)hydrogenation^[2,63] activity (table 44). Unfunctionalized [RhCl(cod)]₂ showed similar selectivity compared to the Ir-dimer (entry 1). However, the amount of **115-117** formed decreased. Wilkinson's catalyst, RhCl(PPh₃)₃, afforded almost identical amounts of olefins **115** and (*E/Z*)-**117** and no olefin **116** at low catalyst loading (entry 2). Higher quantities of catalyst slightly diminished the overall yield (entry 3). Use of RhH(CO)(PPh₃)₃ gave similar results.

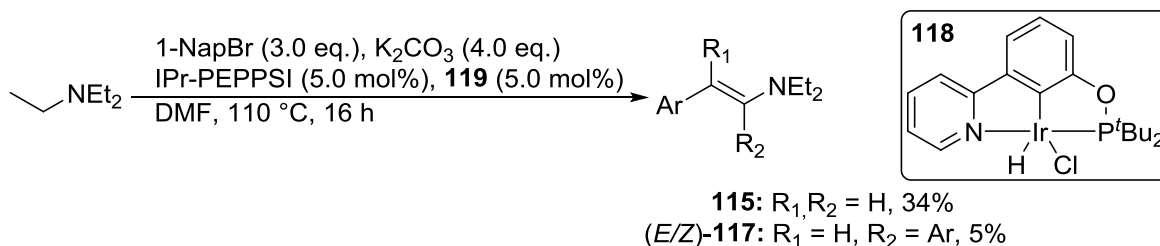
Table 44. Dual metal-catalyzed dehydrogenative coupling of NEt₃ with 1-NapBr; further [DH] screening.^a Nap = naphthyl; Ar = 1-Nap; cod = 1,5-cyclooctadiene.

entry	[Pd]	[DH]	115 [%]	116 [%]	(E/Z)-117 [%]
1	IPr-PEPPSI	[RhCl(cod)] ₂ (2.5)	23	0	7
2	IPr-PEPPSI	RhCl(PPh ₃) ₃ (2.5)	18	0	5
3	IPr-PEPPSI	RhCl(PPh ₃) ₃ (5.0)	14	0	3
4	IPr-PEPPSI	RhH(CO)(PPh ₃) ₃ (2.5)	19	0	5
5	IPr-PEPPSI	RhH(CO)(PPh ₃) ₃ (5.0)	13	0	3

115: R₁, R₂ = H
116: R₁ = Ar, R₂ = H
(E/Z)-117: R₁ = H, R₂ = Ar

^aReactions performed with 500 μmol NEt₃ (70.0 μL) in DMF (2 mL) according to GP 6.2.1b) (see 7.2.7.1); spectral yield according to ¹H-NMR with internal standard, given in mol%.

In our glovebox, we came across Ir-precatalyst **118** depicted in scheme 71. The complex has previously been reported by the group of Zheng who employed it in the α-arylation of unactivated esters using alcohols.^[64] In our dehydrogenative coupling, reduced conversion to enamines along with marginal better selectivity was observed. Again, no β-diarylated alkene **116** was observed.

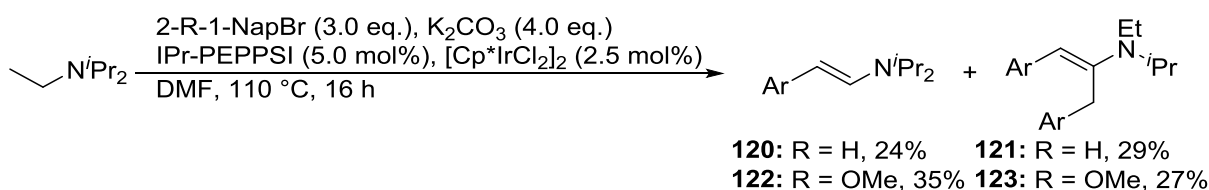


Scheme 71. Attempted dehydrogenative coupling of NEt₃ with 1-NapBr using the *N,C,P*-Ir-pincer complex **119**, previously prepared by Dr. M. Blazejak in our group.^[65] The reaction afforded 34% of **115** and 5% of **117**. Ar = 1-Nap.

Preliminary best conditions (table 37, entry 6)⁵² for the dehydrogenative coupling of DIPEA had delivered 26% of the desired olefin **86** besides 18% of side-product **87**. While selectivity and reactivity have been stepwise improved for triethylamine, we envisaged subjecting DIPEA to our newly determined conditions (scheme 72). The reaction of DIPEA with 1-bromonaphthalene resulted in 24% of desired product **120**, entailing 29% of diarylated enamine **121**. Compared to NEt₃, virtually identical results were obtained. Each of the amine substrates holds its own advantage. Whereas concurring dehydrogenation of other alkyl groups

⁵² PhBr (1.9 eq.), K₂CO₃ (2.0 eq.), PdCl₂(PCy₃)₂ (5.0 mol%), [Cp*IrCl₂]₂ (2.5 mol%), DMF, 110 °C, 16 h.

is not possible in the case of NEt₃, the isopropyl groups in DIPEA block over-arylation of the target product **120**. Diarylation was impeded by involving 1-bromo-2-methoxynaphthalene when starting from triethylamine. Even though large quantities (34%) of the desired olefin **122** were detected with DIPEA, we still observed 27% of undesired side-product **123**.



Scheme 72. Application of the optimized catalytic conditions for dehydrogenative coupling of DIPEA with aryl bromides. 1-Bromo-naphthalene and 1-bromo-2-methoxynaphthalene were used as electrophiles. Nap = naphthyl.

6.2.4 Proposed mechanism

Based on the observations so far, we want to propose a plausible mechanism for the coupling of NEt₃ (**A**) with ArBr (**B**) (figure 48). We suppose that no intermetallic interactions occur, which simplifies the analysis. The [DH] catalyst based on Ir, Ru, or Rh dehydrogenates the tertiary amine **A**, entailing a metal–hydride species [DH]H₂ and enamine **A'**. Release of hydrogen gas or hydrogenolysis of ArBr (**B**) regenerates the [DH] precatalyst. Oxidative addition of aryl bromide **B** to previously activated Pd metal (reduction with H₂, base or other from Pd^{II}) affords species **124**. Approach of the olefinic substrate generates π -complex **125**. Insertion of the enamine into the Pd–carbon bond in a syn addition step leads to the formation of σ -complex **126**. In the case of a *cis*-configuration, strain is relieved by rotation to the *trans*-isomer **126**. Via β -hydride elimination a new Pd–alkene complex **127** is formed. Release of the desired coupling product **88** yields Pd–hydride complex **128**. The presence of stoichiometric base, such as K₂CO₃, induces reductive elimination of HBr, which reacts with the base. KBr as well as KHCO₃ (or CO₂ and H₂O) emerge. The latter process furnishes L₂Pd⁰ ready for the next turnover. For diarylation, alkene **88** would reinsert into the Pd-species **124** and repeat the catalytic cycle. The C–H arylation cycle is essentially the one established from Heck coupling of enamines.^[41,42b,66] A threefold coupling was never observed. Dehydrogenative coupling of other substrates, e.g. DIPEA, *N*-(*m*)ethylpiperidine, or EtTMP, is expected to follow the same reaction path no matter which alkyl group is activated.

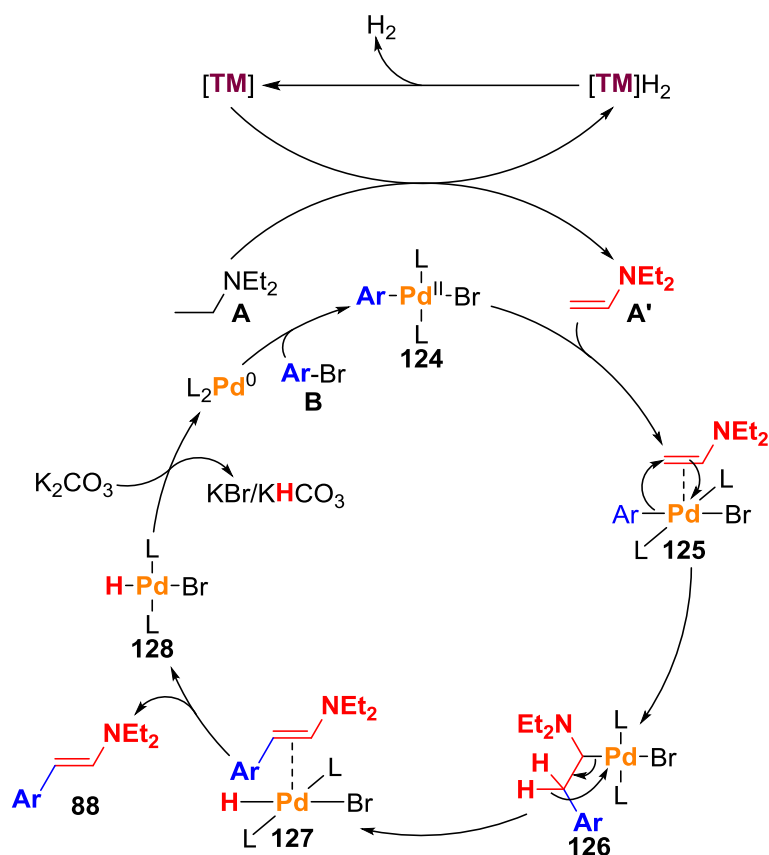
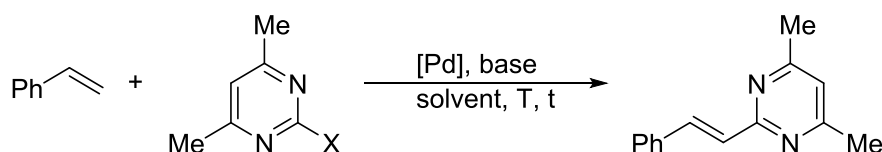


Figure 48. Proposed mechanism of the dehydrogenative coupling of NEt_3 (A) with ArBr (B). Pd-catalyst was either activated by reduction with hydrogen gas, base or other. [DH] = dehydrogenation precatalyst (Ir, Ru, or Rh); L = NHC, phosphine or other.

6.3 Heck Cross-Coupling of Styrenes with Pyrimidyl Chlorides

Little is known so far about the Heck cross-coupling of alkenes with pyrimidyl chlorides. The sole precedents one stumbles upon in literature have been described by the group of Yamanaka.^[45] In the presence of Pd catalyst, several olefins and iodo pyrimidines reacted in hot triethylamine, barely exceeding 55% yield of coupling product. While aryl iodides are generally easiest to couple, several methods for the homocoupling^[67] of pyrimidine halides have been reported, illustrating interesting motifs in biheterocyclic ligands for complex synthesis.^[68] Chemists seek to identify the cheapest and most efficient way for the synthesis of target compounds. Not only by cost but also by availability, aryl chlorides represent the most convenient starting materials for coupling chemistry. They sometimes also constitute intermediates in the synthesis of the corresponding iodides.^[67b] For pyrimidyl chlorides, several convenient procedures starting either from amino^[69] or hydroxy^[67b,70] derivatives are available.

Regarding the results obtained by Yamanaka and coworkers^[45], we sought to extend the coupling profile to pyrimidyl chlorides as cheap analogue (scheme 73). In the following, a coherent screening effort is summarized in individual tables.



Scheme 73. Heck coupling of pyrimidyl halides with styrene. Yamanaka et al. reacted pyrimidyl iodides with alkenes, including styrene, in the presence of different Pd precatalysts and NEt_3 as solvent/base.^[45] X = halide.

We started with a simple catalyst system as depicted in table 45 including inorganic base (K_2CO_3) and $\text{Pd}(\text{OAc})_2$. In all cases, the recovery was very low, undoubtedly owed to polymerization of styrene. Neglectable quantities of homocoupling adduct along with residual amounts of aryl chloride were observed. Most of the latter hydrolyzed during work-up and was removed with the aqueous phase. We therefore decided to not indicate the amount of recovered aryl chloride or of its homocoupling derivative. Interestingly, the reaction already delivered 31% of coupling product in DMF (entry 1). Related dipolar aprotic solvent, NMP (entry 2), as well as less polar solvents, toluene (entry 3) and dioxane (entry 4) slowed the reaction down, providing only 10% olefinic pyrimidine. While other inorganic bases (entries 5 and 6) nearly stopped the reaction, the use of Ag_2CO_3 solely led to the formation of a polymeric species whose precise structure was not determined (entry 7).

Table 45. Heck coupling of styrene with 2-chloro-4,6-dimethylpyrimidine (ArCl); **solvent** and **base** screening.^a

entry	ArCl	solvent	base	styrene [%]	yield [%]
1		DMF	K_2CO_3	26	31
2		NMP	K_2CO_3	53	10
3		PhMe	K_2CO_3	<1	10
4		dioxane	K_2CO_3	5	10
5		DMF	K_3PO_4	53	2
6		DMF	Cs_2CO_3	11	<1
7		DMF	Ag_2CO_3	~39 ^b	0 ^b

^aReactions performed with 524 μmol styrene (60.0 μL) in the indicated solvent (1 mL) according to GP 6.3.1 (see 7.2.8.1); spectral yield according to $^1\text{H-NMR}$ with internal standard, given in mol%. ^bPolymeric species observed, overlaying with most aromatic signals. No product observed.

Sticking with the best conditions of table 45, we envisaged Pd-precatalyst as well as temperature screening as next step (table 46). In first instance, we involved the well-known IPr-PEPPSI, effective in a broad field of catalysis^[51a,51b,71], in our cross-coupling reaction (entry 1). Despite its usually reliable performance, reduced reactivity was detected. With Pd(OAc)₂, lowering of the temperature to 90 °C almost stopped the coupling (entry 2). Even though the starting material suffered less from decomposition, hardly any styryl pyrimidine formed at 110 °C (entry 3). Since temperatures above 120 °C delivered virtually identical results (entries 4 and 5; table 45, entry 1), we chose 120 °C for further screening due to improved recovery of styrene. The presence of Pd(PPh₃)₄ considerably retarded the reaction (entry 6), showing almost no conversion nor decomposition of the starting alkene.

Table 46. Heck coupling of styrene with 2-chloro-4,6-dimethylpyrimidine (ArCl); **temperature** and **Pd-precatalyst** screening.^a precat. = precatalyst.

entry	ArCl	Pd-precatalyst	T [°C]	styrene [%]	yield [%]
1		IPr-PEPPSI	130	42	17
2		Pd(OAc) ₂	90	32	3
3		Pd(OAc) ₂	110	58	14
4		Pd(OAc) ₂	120	37	28
5		Pd(OAc) ₂	150	18	24
6		Pd(PPh ₃) ₄	120	70	1

^aReactions performed with 524 μmol styrene (60.0 μL) in the indicated solvent (1 mL) according to GP 6.3.1 (see 7.2.8.1); spectral yield according to ¹H-NMR with internal standard, given in mol%.

Additional catalyst-components (additives) potentially improve the outcome of a reaction. On that account, we wanted to verify whether increased functionality of the catalyst-system leads to enhanced reactivity (table 47). The first three entries were performed prior to the temperature screening, hence still conducted at 130 °C. Like Pd(PPh₃)₄, S-Phos decelerated the cross-coupling activity of Pd(OAc)₂ in DMF (entry 1) and NMP (entry 2). Addition of the difunctional onium carboxylate salt, NBu₄DiPP (**47**), did not affect the outcome of the reaction (entry 3). However, the electron deficient pyridone returned to initially detected yields of the unfunctionalized catalyst system (entry 4). Although electron-poor pyridones are convenient CMD additives in C_{sp2}- and C_{sp3}-coupling chemistry^[72], the combination of Pd(OAc)₂ with pyridone alone disappointed in turn (entry 5). We tested two of our difunctional salts,

NBu₄DiPP (**47**) and NBu₄OPiv (**49**) in the cross-coupling (entries 6 and 7). Luckily enough, both compounds improved the reaction in similar manner. Retaining to our screening procedure delineated in chapter 2.2, experiments of table 47 may be considered as (small) 1x3 screening matrix. Once again, these results underline the necessity to know which catalyst-components are expected to be successful in a specific reaction.

Table 47. Heck coupling of styrene with 2-chloro-4,6-dimethylpyrimidine (ArCl); **additive** screening.^a DiPP = diisopropyl propionate; Py-2-OH = pyridin-2-ol.

entry	ArCl	additive	T [°C]	styrene [%]	yield [%]
1		S-Phos	130	63	8
2 ^b		S-Phos	130	50	12
3		S-Phos	130	40	12
4		NBu ₄ DiPP	130	12	26
		S-Phos			
		NBu ₄ DiPP			
5		5-Cl-2-NO ₂ -Py-2-OH	120	49	14
6		NBu ₄ DiPP	120	37	41
7		NBu ₄ OPiv	120	30	47

^aReactions performed with 524 μmol styrene (60.0 μL) in the indicated solvent (1 mL) according to GP 6.3.1 (see 7.2.8.1); spectral yield according to ¹H-NMR with internal standard, given in mol%. ^bReaction performed in NMP (1 mL).

A range of other solvents as well as inorganic bases were available in our laboratory (table 48). For reasons of practicability⁵³, we involved NBu₄DiPP (**47**) as difunctional onium carboxylate in the following experiments. Dipolar, aprotic solvent dimethylacetamide afforded the olefinic pyrimidine in 33% yield (entry 1). In dimethylsulfoxide, the coupling almost stopped (entry 2). Due to temperatures above its boiling point, most of acetonitrile was observed at the top of the Schlenk tube, delivering low conversion (entry 3). Excess amounts of acetate base impeded the arylation (entry 4). Increasing the equivalents of K₂CO₃ marginally affected the expected cross-coupling.

⁵³ Reminder: NBu₄DiPP is much less hygroscopic than its pivalate brother. Weighing is much more convenient with the propionate salt **47**.

Table 48. Heck coupling of styrene with 2-chloro-4,6-dimethylpyrimidine (ArCl); **solvent** and **base** screening.^a DMAc = dimethylacetamide.

entry	ArCl	solvent	base	styrene [%]	yield [%]
1		DMAc	K ₂ CO ₃	39	33
2		DMSO	K ₂ CO ₃	48	5
3		MeCN	K ₂ CO ₃	50	11
4		DMF	NaOAc	45	3
5 ^b		DMF	K ₂ CO ₃	34	38

^aReactions performed with 524 μmol styrene (60.0 μL) in the indicated solvent (1 mL) according to GP 6.3.1 (see 7.2.8.1); spectral yield according to ¹H-NMR with internal standard, given in mol%. ^bReaction performed with 3.0 eq. base.

Used in a wide plethora of coupling chemistry^[73], cataCXium® A, ⁿBuAd₂P, consists of a convenient ligand in catalysis. In our case, the theory of retarded reaction due to coordinating phosphine to Pd was further confirmed by the addition of cataCXium® A as ligand (table 49, entry 1).

Table 49. Heck coupling of styrene with 2-chloro-4,6-dimethylpyrimidine (ArCl); **additive**, **Pd-precat.** and **ArCl** screening.^a precat. = precatalyst; DiPP = diisopropyl propionate; Ad = adamantyl.

entry	ArCl	Pd-precat. [mol%]	additive [eq.]	styrene [%]	yield [%]
1		Pd(OAc) ₂ (5.0)	NBu ₄ DiPP (0.1) ⁿ BuAd ₂ P (0.1)	54	<1
2		Pd(OAc) ₂ (5.0)	NBu ₄ DiPP (0.1) AgOAc (2.0)	9	2
3		Pd(OAc) ₂ (5.0)	PivOH (0.2)	39	29
4		Pd(OAc) ₂ (10.0)	NBu ₄ DiPP (0.2)	37	42
5		PdCl ₂ (PCy ₃) ₂ (5.0)	NBu ₄ OPiv (0.1)	60	<1
6 ^b		Pd(OAc) ₂ (5.0)	NBu ₄ OPiv (0.1)	38	42
7		Pd(OAc) ₂ (5.0)	NBu ₄ DiPP (0.1)	46	<1

^aReactions performed with 524 μmol styrene (60.0 μL) in the indicated solvent (1 mL) according to GP 6.3.1 (see 7.2.8.1); spectral yield according to ¹H-NMR with internal standard, given in mol%. ^bReaction performed with 2.0 eq. ArCl.

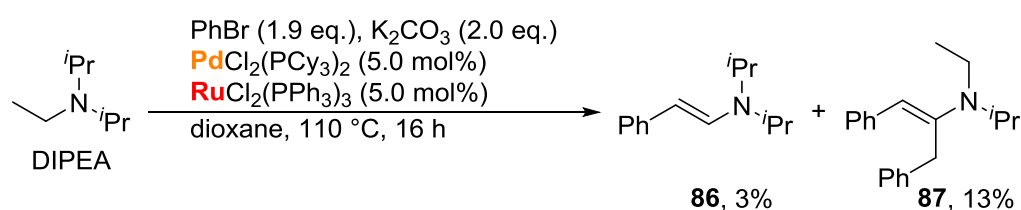
Commonly employed as salt^[74] or generated in situ^[75] in C_{sp3}-coupling chemistry, detailed protocols report the significant lowering of transition states in the presence of AgOAc due to intermetallic interactions of Pd and Ag ions.^[76] Incorporation of AgOAc in the coupling of

styrene with pyrimidyl chlorides promoted the decomposition of the involved starting materials (entry 2) as evidenced by the formation of a silver mirror. Negligible amounts of coupling product were detected. Use of pivalic acid showed almost identical yield as in the monofunctional catalyst system (entry 3 vs. table 45, entry 1). Increase of catalyst loading to 10.0 mol% did not alter the conversion (entry 4). Changing the Pd-precatalyst to PdCl₂(PCy₃)₂ in combination with NBu₄OPiv completely stopped the reaction (entry 5), probably owing to coordinated phosphine ligand. Since screening of catalyst-components did not lead to any further amelioration, we attempted two different conditions in terms of the aryl chloride. Installation of two equivalents of the previously implemented pyrimidine derivative merely raised the amount of aryl chloride recovered (entry 6). Less activated, unsubstituted pyrimidine did not react at all (entry 7).

Initial steps were made virtually imitating the results obtained for iodopyrimidines as described by Yamanaka et al.^[45], but plenty of possibilities are yet to be discovered. At this point, screening was abandoned, with table 47, entry 6 representing the best result.

6.4 Conclusion and Outlook

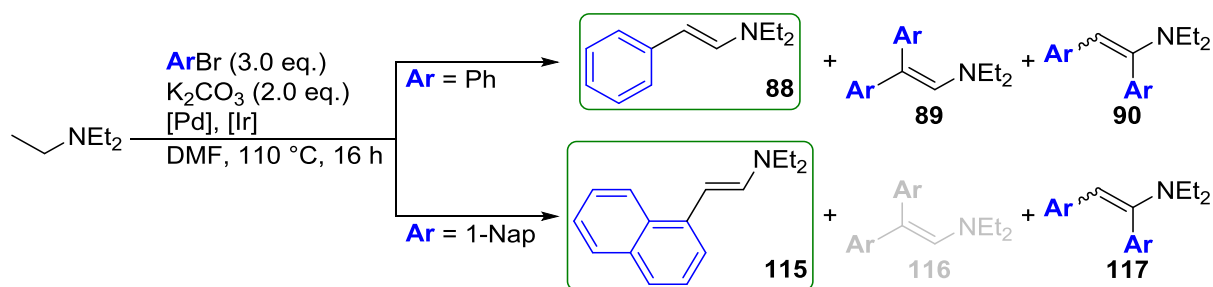
In the first part of this chapter dehydrogenative coupling starting from tertiary amines and ArBr to give arylated enamines was attempted. First experiments involved DIPEA and bromobenzene as reactants, and a PdCl₂(PCy₃)₂–RuCl₂(PPh₃)₃ catalyst system (scheme 74). Concurring dehydrogenation of alkyl groups, ethyl vs. *iso*-propyl, entailed non neglectable amounts of allyl species **87**.



Scheme 74. Initial experiment towards dehydrogenative coupling of tertiary amines.

By changing the amine to symmetric triethylamine, the observed side-reaction was not possible. Three additional diarylated alkenes were observed, including α - and β -functionalization of the desired enamine **88**. Combination of IPr-PEPPSI with [Cp*IrCl₂]₂ in the presence of 3.0 eq. PhrBr led to almost 60% conversion to olefinic products (scheme 75). Whereas a variation of PEPPSI catalysts did not significantly influence the outcome of the reaction, NHC–Pd–cinnamyl complexes enriched the desired monoarylated alkene **88**. Addition of sacrificial

hydrogen acceptors or oxidants blocked the reaction. Even though Goldman and coworkers^[15] did not observe dehydrogenation of cyclic alkyl group with their Ir-pincer, our dehydrogenative coupling solely occurred inside the 6-membered rings. Use of EtTMP (**111**) as substrate impeded the transformation. Screening of aryl halides showed no reaction with chlorobenzene, reduced reactivity with iodobenzene, and minor conversion with phenyl triflate. Whereas electron-rich aryl bromides promote over-arylation, increase in steric bulk (MesBr) suppressed the latter, only producing the desired target material. Best results were obtained when 1-NapBr was used as starting amine, giving 54% of aryl enamine **115** and 14% of diarylation adduct **117** (scheme 75). Application of our best conditions to DIPEA ameliorated the reactivity, still entailing large amounts of side-product **87**.

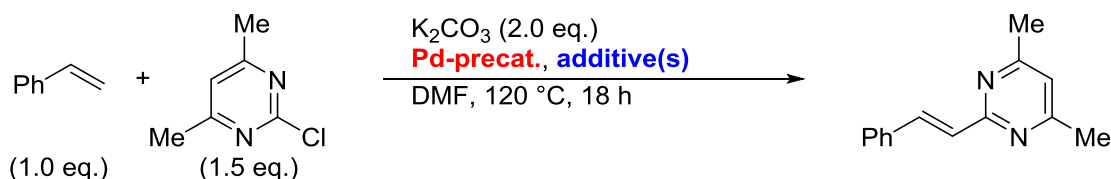


Scheme 75. Optimized catalytic conditions for dehydrogenative coupling of NEt_3 with aryl bromides. [Pd] = IPr-PEPSI (5.0 mol%); [Ir] = $[\text{Cp}^*\text{IrCl}_2]_2$ (2.5 mol%); Nap = naphthyl. The corresponding target product is circled in green.

The incorporation of soluble, unfunctionalized Pd-precatalyst could eliminate any concurrent coordination of metal centers. To understand unknown reactivity and selectivity, other electron-rich and -poor aryl bromides could be introduced in the reaction. Over-arylation could be suppressed by using sterically hindered *N,N*-di-*tert*-butyl-*N*-ethyl-amine as substrate. Tertiary, phenyl-substituted ethylamines could be interesting starting materials for an intramolecular reaction, potentially yielding indoles.

Overall, we have established a novel transformation delivering β -arylated enamines directly from tertiary amines and ArBr under dual-metal catalysis. Our method overcomes the need for the extensive preparation of alkenyl bromides, which in turn would have to be aminated in a second step to afford enamines. Even though our scope of aryl halides has yet been limited to bromides, the dehydrogenative coupling is of potential interest in the synthesis of pharmaceuticals or natural products, especially if it were possible to return released hydrogen gas back into the catalytic cycle. In that manner, β -aryl-*N,N*-dialkylamines could be prepared in a multistep-1-pot-reaction.

The second part of this chapter dealt with the Heck coupling of styrene with chloropyrimidines (scheme 76). A ‘naked’ catalyst based on Pd(OAc)₂ with no added donor ligand already afforded 31% of (*E*)-4,6-dimethyl-2-styrylpyrimidine. Any addition of phosphine or NHC ligand suppressed the arylation. The screening was mostly performed at 120 °C to prevent styrene decomposition and homocoupling of aryl chloride occurring at higher temperature. To our delight, the difunctional onium carboxylates, NBu₄OPiv or NBu₄DiPP, significantly enhanced the desired coupling, yielding 47% of arylated olefin.



Scheme 76. Heck coupling of 2-chloro-4,6-dimethylpyrimidine with styrene.

In the Heck coupling of styrene with 2-chloro-4,6-dimethylpyrimidine, we have efficiently extended the leaving group scope to heteroaryl chlorides as cheap analogue compared to the corresponding iodide. The reaction profited from PTC and CMD effects evocated by our difunctional onium carboxylates.

6.5 References

- [1] a) F. Haber, R. Le Rossignol (BASF SE), US971501A, **1910**; b) F. Haber, R. Le Rossignol (BASF SE), US1202995A, **1916**.
- [2] a) D. Evans, J. Osborn, F. Jardine, G. Wilkinson, *Nature* **1965**, *208*, 1203-1204; b) J. A. Osborn, F. Jardine, J. F. Young, G. Wilkinson, *J. Chem. Soc. A. inorg. phys. theor.* **1966**, 1711-1732.
- [3] a) R. H. Crabtree, G. E. Morris, *J. Organomet. Chem.* **1977**, *135*, 395-403; b) R. H. Crabtree, H. Felkin, G. E. Morris, *J. Organomet. Chem.* **1977**, *141*, 205-215; c) R. H. Crabtree, M. W. Davis, *J. Org. Chem.* **1986**, *51*, 2655-2661.
- [4] a) G. Bond, P. Sermon, *Gold Bull.* **1973**, *6*, 102-105; b) T. Ueno, M. Suzuki, T. Goto, T. Matsumoto, K. Nagayama, Y. Watanabe, *Angew. Chem. Int. Ed.* **2004**, *43*, 2527-2530; c) S. C. Bart, E. J. Hawrelak, E. Lobkovsky, P. J. Chirik, *Organometallics* **2005**, *24*, 5518-5527.
- [5] a) S. Ikeda, S. Ishino, T. Harada, N. Okamoto, T. Sakata, H. Mori, S. Kuwabata, T. Torimoto, M. Matsumura, *Angew. Chem. Int. Ed.* **2006**, *45*, 7063-7066; b) J. W. Veldsink, M. J. Bouma, N. H. Schön, A. A. Beenackers, *Catal. Rev.* **1997**, *39*, 253-318; c) B. Desai, C. O. Kappe, *J. Comb. Chem.* **2005**, *7*, 641-643.
- [6] a) A. Lightfoot, P. Schnider, A. Pfaltz, *Angew. Chem. Int. Ed.* **1998**, *37*, 2897-2899; b) R. Waymouth, P. Pino, *J. Am. Chem. Soc.* **1990**, *112*, 4911-4914; c) M. R. Friedfeld, M. Shevlin, G. W. Margulieux, L.-C. Campeau, P. J. Chirik, *J. Am. Chem. Soc.* **2016**, *138*, 3314-3324.
- [7] H. A. Wittcoff, B. G. Reuben, J. S. Plotkin, *Industrial organic chemicals*, John Wiley & Sons, **2012**.
- [8] C. Gunanathan, D. Milstein, *Science* **2013**, *341*.
- [9] a) T. Aoki, R. H. Crabtree, *Organometallics* **1993**, *12*, 294-298; b) G. Rosini, A. Goldman, C. Jensen, W. Kaska, *Chem. Commun.* **1997**, 2273-2274; c) A. Goldman, *Chem. Commun.* **1999**, 655-656.
- [10] a) K. E. Harding, L. M. May, K. F. Dick, *J. Org. Chem.* **1975**, *40*, 1664-1665; b) B. S. Bal, K. S. Kochhar, H. W. Pinnick, *J. Org. Chem.* **1981**, *46*, 1492-1493.
- [11] J. M. Hoover, B. L. Ryland, S. S. Stahl, *J. Am. Chem. Soc.* **2013**, *135*, 2357-2367.
- [12] a) A. Dobsen, S. D. Robinson, *J. Organomet. Chem.* **1975**, *87*, C52-C53; b) D. Morton, D. J. Cole-Hamilton, *J. Chem. Soc., Chem. Commun.* **1987**, 248-249; c) G. Lighthart, R.

- Meijer, M. Donners, J. Meuldijk, J. Vekemans, L. Hulshof, *Tetrahedron Lett.* **2003**, *44*, 1507-1509; d) J. Zhang, M. Gandelman, L. J. Shimon, H. Rozenberg, D. Milstein, *Organometallics* **2004**, *23*, 4026-4033; e) S. Musa, I. Shaposhnikov, S. Cohen, D. Gelman, *Angew. Chem. Int. Ed.* **2011**, *50*, 3533-3537; f) J. Zhang, E. Balaraman, G. Leitius, D. Milstein, *Organometallics* **2011**, *30*, 5716-5724.
- [13] K.-N. T. Tseng, A. M. Rizzi, N. K. Szymczak, *J. Am. Chem. Soc.* **2013**, *135*, 16352-16355.
- [14] X.-Q. Gu, W. Chen, D. Morales-Morales, C. M. Jensen, *J. Mol. Catal. A: Chem.* **2002**, *189*, 119-124.
- [15] X. Zhang, A. Fried, S. Knapp, A. S. Goldman, *Chem. Commun.* **2003**, 2060-2061.
- [16] a) Y. Blum, Y. Shvo, *J. Organomet. Chem.* **1985**, *282*, C7-C10; b) J. Zhang, G. Leitius, Y. Ben-David, D. Milstein, *J. Am. Chem. Soc.* **2005**, *127*, 10840-10841; c) S.-I. Murahashi, K.-i. Ito, T. Naota, Y. Maeda, *Tetrahedron Lett.* **1981**, *22*, 5327-5330; d) S. Murahashi, T. Naota, K. Ito, Y. Maeda, H. Taki, *J. Org. Chem.* **1987**, *52*, 4319-4327.
- [17] M. Peña-López, H. Neumann, M. Beller, *ChemCatChem* **2015**, *7*, 865-871.
- [18] a) V. R. Pattabiraman, J. W. Bode, *Nature* **2011**, *480*, 471-479; b) C. Gunanathan, Y. Ben-David, D. Milstein, *Science* **2007**, *317*, 790-792; c) H. Zeng, Z. Guan, *J. Am. Chem. Soc.* **2011**, *133*, 1159-1161.
- [19] Y. Zheng, X. Nie, Y. Long, L. Ji, H. Fu, X. Zheng, H. Chen, R. Li, *Chem. Commun.* **2019**, *55*, 12384-12387.
- [20] a) B. Gnanaprakasam, J. Zhang, D. Milstein, *Angew. Chem. Int. Ed.* **2010**, *49*, 1468-1471; b) M. A. Esteruelas, N. Honczek, M. Oliván, E. Oñate, M. Valencia, *Organometallics* **2011**, *30*, 2468-2471; c) A. Maggi, R. Madsen, *Organometallics* **2012**, *31*, 451-455; d) G. Zhang, S. K. Hanson, *Org. Lett.* **2013**, *15*, 650-653.
- [21] a) B. Gnanaprakasam, E. Balaraman, Y. Ben-David, D. Milstein, *Angew. Chem. Int. Ed.* **2011**, *50*, 12240-12244; b) P. Daw, A. Kumar, N. A. Espinosa-Jalapa, Y. Diskin-Posner, Y. Ben-David, D. Milstein, *ACS Catal.* **2018**, *8*, 7734-7741.
- [22] a) N. D. Schley, G. E. Dobereiner, R. H. Crabtree, *Organometallics* **2011**, *30*, 4174-4179; b) D. Srimani, Y. Ben-David, D. Milstein, *Angew. Chem. Int. Ed.* **2013**, *52*, 4012-4015; c) S. Qu, Y. Dang, C. Song, M. Wen, K.-W. Huang, Z.-X. Wang, *J. Am. Chem. Soc.* **2014**, *136*, 4974-4991; d) P. Daw, Y. Ben-David, D. Milstein, *J. Am. Chem. Soc.*

- 2018**, *140*, 11931-11934; e) S. P. Midya, V. G. Landge, M. K. Sahoo, J. Rana, E. Balaraman, *Chem. Commun.* **2018**, *54*, 90-93.
- [23] a) C. Gunanathan, L. J. Shimon, D. Milstein, *J. Am. Chem. Soc.* **2009**, *131*, 3146-3147; b) E. Kossoy, Y. Diskin-Posner, G. Leitius, D. Milstein, *Adv. Synth. Catal.* **2012**, *354*, 497-504.
- [24] a) R. Johnstone, D. Payling, C. Thomas, *J. Chem. Soc. C Org.* **1969**, 2223-2224; b) S. J. Tremont, H. U. Rahman, *J. Am. Chem. Soc.* **1984**, *106*, 5759-5760.
- [25] a) Y. Tsuji, K. T. Huh, Y. Ohsugi, Y. Watanabe, *J. Org. Chem.* **1985**, *50*, 1365-1370; b) G. Guillena, D. J. Ramon, M. Yus, *Chem. Rev.* **2010**, *110*, 1611-1641; c) T. Irrgang, R. Kempe, *Chem. Rev.* **2018**, *119*, 2524-2549.
- [26] a) C. Gunanathan, D. Milstein, *Angew. Chem. Int. Ed.* **2008**, *47*, 8661-8664; b) D. Pingen, C. Müller, D. Vogt, *Angew. Chem. Int. Ed.* **2010**, *49*, 8130-8133; c) S. Imm, S. Bähn, M. Zhang, L. Neubert, H. Neumann, F. Klasovsky, J. Pfeffer, T. Haas, M. Beller, *Angew. Chem. Int. Ed.* **2011**, *50*, 7599-7603.
- [27] M. Peña-López, H. Neumann, M. Beller, *Angew. Chem. Int. Ed.* **2016**, *55*, 7826-7830.
- [28] a) A. E. Putra, K. Takigawa, H. Tanaka, Y. Ito, Y. Oe, T. Ohta, *Eur. J. Org. Chem.* **2013**, *28*, 6344-6354; b) S. H. Siddiki, K. Kon, K. i. Shimizu, *Chem. Eur. J.* **2013**, *19*, 14416-14419; c) S. Bartolucci, M. Mari, A. Bedini, G. Piersanti, G. Spadoni, *J. Org. Chem.* **2015**, *80*, 3217-3222.
- [29] J. Xia, Z. Huang, X. Zhou, X. Yang, F. Wang, X. Li, *Org. Lett.* **2018**, *20*, 740-743.
- [30] S. Bähn, S. Imm, K. Mevius, L. Neubert, A. Tillack, J. M. Williams, M. Beller, *Chem. Eur. J.* **2010**, *16*, 3590-3593.
- [31] a) S. Imm, S. Bähn, A. Tillack, K. Mevius, L. Neubert, M. Beller, *Chem. Eur. J.* **2010**, *16*, 2705-2709; b) S. Lerch, L. N. Unkel, M. Brasholz, *Angew. Chem. Int. Ed.* **2014**, *53*, 6558-6562.
- [32] C. G. Swain, A. L. Powell, W. A. Sheppard, C. R. Morgan, *J. Am. Chem. Soc.* **1979**, *101*, 3576-3583.
- [33] a) L. J. Allen, R. H. Crabtree, *Green Chem.* **2010**, *12*, 1362-1364; b) R. Cano, M. Yus, D. J. Ramón, *Tetrahedron Lett.* **2013**, *54*, 3394-3397; c) Q. Xu, J. Chen, H. Tian, X. Yuan, S. Li, C. Zhou, J. Liu, *Angew. Chem. Int. Ed.* **2014**, *53*, 225-229.

- [34] a) H. Fischer, E. Bartholomäus, *Chem. Ber.* **1912**, *45*, 466-471; b) H. Fischer, E. Bartholomäus, *Chem. Ber.* **1912**, *45*, 1979-1986; c) H. Fischer, K. Eismayer, *Chem. Ber.* **1914**, *47*, 1820-1828.
- [35] S. Koller, M. Blazejak, L. Hintermann, *Eur. J. Org. Chem.* **2018**, *14*, 1624-1633.
- [36] a) L. K. Ackerman, M. M. Lovell, D. J. Weix, *Nature* **2015**, *524*, 454-457; b) A. M. Olivares, D. J. Weix, *J. Am. Chem. Soc.* **2018**, *140*, 2446-2449; c) L. Huang, L. K. Ackerman, K. Kang, A. M. Parsons, D. J. Weix, *J. Am. Chem. Soc.* **2019**, *141*, 10978-10983; d) S. Mishra, A. Aponick, *Angew. Chem. Int. Ed.* **2019**, *58*, 9485-9490.
- [37] a) M. Jouffroy, D. N. Primer, G. A. Molander, *J. Am. Chem. Soc.* **2016**, *138*, 475-478; b) H. Yue, C. Zhu, M. Rueping, *Angew. Chem. Int. Ed.* **2018**, *57*, 1371-1375; c) W. Yu, L. Chen, J. Tao, T. Wang, J. Fu, *Chem. Commun.* **2019**, *55*, 5918-5921.
- [38] D. Lichosyt, Y. Zhang, K. Hurej, P. Dydio, *Nat. Catal.* **2019**, *2*, 114-122.
- [39] H. J. Knölker, E. Baum, H. Goesmann, R. Klaus, *Angew. Chem. Int. Ed.* **1999**, *38*, 2064-2066.
- [40] E. Breitmaier, G. Jung, *Organische Chemie: Grundlagen, Verbindungsklassen, Reaktionen, Konzepte, Molekülstruktur, Naturstoff*, Georg Thieme Verlag, **2009**.
- [41] a) Z. Shi, F. Glorius, *Angew. Chem. Int. Ed.* **2012**, *51*, 9220-9222; b) H. H. Nguyen, M. J. Kurth, *Org. Lett.* **2013**, *15*, 362-365.
- [42] a) S. Rakshit, F. W. Patureau, F. Glorius, *J. Am. Chem. Soc.* **2010**, *132*, 9585-9587; b) R. Grigg, V. Savic, *Chem. Commun.* **2000**, 873-874; c) L. Wang, L. Ackermann, *Org. Lett.* **2013**, *15*, 176-179.
- [43] Y. Aoyagi, T. Mizusaki, A. Ohta, *Tetrahedron Lett.* **1996**, *37*, 9203-9206.
- [44] a) P. H. Connell, *Br. Med. J.* **1957**, *1*, 582; b) B. M. Angrist, S. Gershon, *Biol. Psychiatry* **1970**; c) P. Kalix, *Annu. Rev. Pharmacol. Toxicol.* **1992**, *70*, 77-86.
- [45] a) T. Sakamoto, H. Arakida, K. Edo, H. Yamanaka, *Heterocycles* **1981**, *16*, 965-968; b) T. Sakamoto, H. Arakida, K. Edo, H. Yamanaka, *Chem. Pharm. Bull.* **1982**, *30*, 3647-3656.
- [46] a) N. P. Reddy, M. Tanaka, *Tetrahedron Lett.* **1997**, *38*, 4807-4810; b) C. Yi, R. Hua, *Tetrahedron Lett.* **2006**, *47*, 2573-2576; c) M. Li, R. Hua, *Appl. Organomet. Chem.* **2008**, *22*, 397-401; d) A. Jutand, Mechanisms of the Mizoroki–Heck reaction in *The Mizoroki–Heck Reaction, Vol. 1*, John Wiley & Sons, Ltd., Chichester, United Kingdom, **2009**, pp. 1-50.
- [47] S. Hünig, M. Kiessel, *Chem. Ber.* **1958**, *91*, 380-392.

- [48] a) E. J. Corey, G. H. Posner, *J. Am. Chem. Soc.* **1968**, *90*, 5615-5616; b) R. Palkovits, M. Antonietti, P. Kuhn, A. Thomas, F. Schüth, *Angew. Chem. Int. Ed.* **2009**, *48*, 6909-6912; c) A. Wittstock, V. Zielasek, J. Biener, C. Friend, M. Bäumer, *Science* **2010**, *327*, 319-322; d) J. Li, H. Chang, L. Ma, J. Hao, R. T. Yang, *Catal. Today* **2011**, *175*, 147-156.
- [49] a) C. J. Li, *Angew. Chem. Int. Ed.* **2003**, *42*, 4856-4858; b) O. P. Pereshivko, V. A. Peshkov, E. V. Van der Eycken, *Org. Lett.* **2010**, *12*, 2638-2641; c) S. L. Helmbrecht, J. Schlüter, M. Blazejak, L. Hintermann, *Eur. J. Org. Chem.* **2020**, 2062-2076.
- [50] E. Balaraman, B. Gnanaprakasam, L. J. Shimon, D. Milstein, *J. Am. Chem. Soc.* **2010**, *132*, 16756-16758.
- [51] a) M. G. Organ, M. Abdel-Hadi, S. Avola, I. Dubovyk, N. Hadei, E. A. B. Kantchev, C. J. O'Brien, M. Sayah, C. Valente, *Chem. Eur. J.* **2008**, *14*, 2443-2452; b) C. Valente, M. E. Belowich, N. Hadei, M. G. Organ, *Eur. J. Org. Chem.* **2010**, *23*, 4343-4354; c) M. Pompeo, R. D. Froese, N. Hadei, M. G. Organ, *Angew. Chem. Int. Ed.* **2012**, *51*, 11354-11357; d) L. Benhamou, C. Besnard, E. P. Kündig, *Organometallics* **2014**, *33*, 260-266.
- [52] C. J. O'Brien, E. A. B. Kantchev, C. Valente, N. Hadei, G. A. Chass, A. Lough, A. C. Hopkinson, M. G. Organ, *Chem. Eur. J.* **2006**, *12*, 4743-4748.
- [53] T. E. Barder, S. D. Walker, J. R. Martinelli, S. L. Buchwald, *J. Am. Chem. Soc.* **2005**, *127*, 4685-4696.
- [54] N. C. Bruno, M. T. Tudge, S. L. Buchwald, *Chem. Sci.* **2013**, *4*, 916-920.
- [55] O. Kunbing, X. Zhenfeng, *Acta Chimica Sinica -Chinese Edition* **2013**, *71*, 13-25.
- [56] N. Marion, O. Navarro, J. Mei, E. D. Stevens, N. M. Scott, S. P. Nolan, *J. Am. Chem. Soc.* **2006**, *128*, 4101-4111.
- [57] L. Jafarpour, E. D. Stevens, S. P. Nolan, *J. Organomet. Chem.* **2000**, *606*, 49-54.
- [58] D. R. Jensen, M. S. Sigman, *Org. Lett.* **2003**, *5*, 63-65.
- [59] A. Chartoire, M. Lesieur, L. Falivene, A. M. Slawin, L. Cavallo, C. S. Cazin, S. P. Nolan, *Chem. Eur. J.* **2012**, *18*, 4517-4521.
- [60] F. Izquierdo, C. Zinser, Y. Minenkov, D. B. Cordes, A. M. Slawin, L. Cavallo, F. Nahra, C. S. Cazin, S. P. Nolan, *ChemCatChem* **2018**, *10*, 601-611.
- [61] a) Y. Amemiya, D. D. Miller, F.-L. Hsu, *Synth. Commun.* **1990**, *20*, 2483-2489; b) T. Diao, T. J. Wadzinski, S. S. Stahl, *Chem. Sci.* **2012**, *3*, 887-891; c) J. Zhou, G. Wu, M. Zhang, X. Jie, W. Su, *Chem. Eur. J.* **2012**, *18*, 8032-8036; d) T. Diao, D. Pun, S. S.

- Stahl, *J. Am. Chem. Soc.* **2013**, *135*, 8205-8212; e) D. Pun, T. Diao, S. S. Stahl, *J. Am. Chem. Soc.* **2013**, *135*, 8213-8221.
- [62] G. A. Molander, *Science of Synthesis: Cross-Coupling and Heck Type Reactions 1*, Thieme, Philadelphia, US, **2013**.
- [63] T. Stephenson, S. Morehouse, A. R. Powell, J. Heffer, G. Wilkinson, *J. Chem. Soc.* **1965**, 3632-3640.
- [64] L. Guo, X. Ma, H. Fang, X. Jia, Z. Huang, *Angew. Chem. Int. Ed.* **2015**, *54*, 4023-4027.
- [65] M. Blazejak, *Mikrowellenassistierte Katalytische Synthesemethoden am Beispiel der Hydroalkyoxilyerung, Transferhydrierung und Wasserstoffautotransfer-Alkylierung*, PhD thesis, Technical University of Munich (Garching bei München), **2015**.
- [66] a) K. Yamazaki, Y. Nakamura, Y. Kondo, *J. Chem. Soc., Perkin Trans. 1* **2002**, 2137-2138; b) S. Würtz, S. Rakshit, J. J. Neumann, T. Dröge, F. Glorius, *Angew. Chem. Int. Ed.* **2008**, *47*, 7230-7233.
- [67] a) P. F. Schwab, F. Fleischer, J. Michl, *J. Org. Chem.* **2002**, *67*, 443-449; b) G. Vlád, I. T. Horváth, *J. Org. Chem.* **2002**, *67*, 6550-6552; c) L. Bouilly, A. Turck, N. Plé, M. Darabantu, *J. Heterocycl. Chem.* **2005**, *42*, 1423-1428.
- [68] a) G. H. Allen, R. P. White, D. P. Rillema, T. J. Meyer, *J. Am. Chem. Soc.* **1984**, *106*, 2613-2620; b) M. P. Garcia, J. L. Millan, M. A. Esteruelas, L. A. Oro, *Polyhedron* **1987**, *6*, 1427-1431; c) C. Janiak, L. Uehlin, H.-P. Wu, P. Klüfers, H. Piotrowski, T. G. Scharmann, *J. Chem. Soc., Dalton Trans.* **1999**, 3121-3131.
- [69] a) R. R. Adams, F. C. Whitmore, *J. Am. Chem. Soc.* **1945**, *67*, 735-738; b) B.-L. Wang, Y.-X. Shi, Y. Ma, X.-H. Liu, Y.-H. Li, H.-B. Song, B.-J. Li, Z.-M. Li, *J. Agric. Food Chem.* **2010**, *58*, 5515-5522; c) B. Wang, Y. Shi, Y. Zhan, L. Zhang, Y. Zhang, L. Wang, X. Zhang, Y. Li, Z. Li, B. Li, *Chin. J. Chem.* **2015**, *33*, 1124-1134.
- [70] a) N. Hirano, H. Inoue, T. Nagahara, T. Ohyama, M. Kaino, K. Hayashi, S. Hara, R. Suzuki (Toray Industries Inc.), US7566724B2, **2009**; b) K. Bhasin, E. Arora, A. S. Grover, H. Singh, S. Mehta, A. K. Bhasin, C. Jacob, *J. Organomet. Chem.* **2013**, *732*, 137-141.
- [71] M. G. Organ, M. Abdel-Hadi, S. Avola, N. Hadei, J. Nasielski, C. J. O'Brien, C. Valente, *Chem. Eur. J.* **2007**, *13*, 150-157.
- [72] a) P. Wang, P. Verma, G. Xia, J. Shi, J. X. Qiao, S. Tao, P. T. Cheng, M. A. Poss, M. E. Farmer, K.-S. Yeung, *Nature* **2017**, *551*, 489-493; b) Y.-Q. Chen, Z. Wang, Y. Wu,

- S. R. Wisniewski, J. X. Qiao, W. R. Ewing, M. D. Eastgate, J.-Q. Yu, *J. Am. Chem. Soc.* **2018**, *140*, 17884-17894; c) R.-Y. Zhu, Z.-Q. Li, H. S. Park, C. H. Senanayake, J.-Q. Yu, *J. Am. Chem. Soc.* **2018**, *140*, 3564-3568; d) G. Xia, J. Weng, L. Liu, P. Verma, Z. Li, J.-Q. Yu, *Nat. Chem.* **2019**, *11*, 571-577.
- [73] a) S. Klaus, H. Neumann, A. Zapf, D. Strübing, S. Hübner, J. Almena, T. Riermeier, P. Groß, M. Sarich, W. R. Krahnert, *Angew. Chem. Int. Ed.* **2006**, *45*, 154-158; b) H. Neumann, A. Brennführer, P. Groß, T. Riermeier, J. Almena, M. Beller, *Adv. Synth. Catal.* **2006**, *348*, 1255-1261; c) T. Schareina, A. Zapf, W. Mägerlein, N. Müller, M. Beller, *Tetrahedron Lett.* **2007**, *48*, 1087-1090; d) H. A. Chiong, O. Daugulis, *Org. Lett.* **2007**, *9*, 1449-1451; e) X. F. Wu, H. Neumann, M. Beller, *ChemCatChem* **2010**, *2*, 509-513; f) J. Schranck, A. Tlili, H. Neumann, P. G. Alsabeh, M. Stradiotto, M. Beller, *Chem. Eur. J.* **2012**, *18*, 15592-15597.
- [74] W. G. Whitehurst, J. H. Blackwell, G. N. Hermann, M. J. Gaunt, *Angew. Chem. Int. Ed.* **2019**, *58*, 9054-9059.
- [75] H. Lin, X. Pan, A. L. Barsamian, T. M. Kamenecka, T. D. Bannister, *ACS Catal.* **2019**, *9*, 4887-4891.
- [76] a) M. Anand, R. B. Sunoj, H. F. Schaefer III, *J. Am. Chem. Soc.* **2014**, *136*, 5535-5538; b) W. Feng, T. Wang, D. Liu, X. Wang, Y. Dang, *ACS Catal.* **2019**, *9*, 6672-6680.

7 EXPERIMENTAL SECTION

7.1 General remarks

7.1.1 Reagents and chemicals

Unless otherwise specified, all reagents and solvents were obtained from commercial suppliers or the university's chemical store and were used without further purification. Technical quality solvents for column chromatography, crystallizations or work-up procedures were distilled prior use. Water used in reaction or work-up procedures consisted of deionized water from the tap.

Solvents for water-free reactions were filtered over aluminum oxide (Sigma Aldrich, neutral, Brockmann I), degassed by argon bubbling via a cannula for 15 minutes and stored over molecular sieves (3 Å or 4 Å). The residual water content was determined by Karl-Fischer-titration, using a coulometric Karl-Fischer titration apparatus from Schott Instruments Titroline KF trace.^[1] Acetonitrile was dried over molecular sieves (4 Å) in solvent purifier (MBraun MB-SPS). The solvents listed below (table 50) were purchased as 'extra-dry' from commercial suppliers with a water content below 50 ppm.

Table 50. Purchased dry solvents.

solvent	purity [%]	information	supplier
DMAc	99.5	extra dry over molecular sieve 4 Å, AcroSeal™, ACROS Organics™	Fisher Scientific
DMF	99.8	extra dry over molecular sieve 4 Å, AcroSeal™, ACROS Organics™	Fisher Scientific
DMSO	≥99.9	anhydrous	Sigma Aldrich
MeOH	99.9	extra dry, AcroSeal™, ACROS Organics™	Fisher Scientific

Zinc dust for catalytic zincation was pre-treated to obtain a reproducible quality also with the usual 'aged' samples present in many laboratories: zinc powder (150 g; BASF) was stirred in aqueous HCl (0.5 M, 150 mL) for two hours, filtered through a glass filter, the zinc on the filter washed with H₂O (100 mL), EtOH (2 x 100 mL) and Et₂O (3 x 100 mL) and pre-dried on the filter by sucking air with a water-jet vacuum (fast flow) for 15 minutes. The zinc powder was transferred into a 100 mL Schlenk flask and dried in vacuum (0.01 mbar) at 40 °C for three hours, when it presented itself as free-flowing powder. Vacuum drying was continued overnight at room temperature. The powder was stored under argon until further use.

PdCl₂(MeCN)₂ was prepared by a literature procedure and stored in a Schlenk tube under argon.^[2] Larger amounts were stored in a glovebox.

NiCl₂(dme) was prepared by the *Inorganic Syntheses* procedure and stored in a Schlenk tube under argon.^[3] Larger amounts were stored in a glovebox.

Inorganic bases (potassium carbonate, cesium carbonate, potassium phosphate) were finely ground and pre-dried for two days at 150 °C in an oven (20% ventilation). The solids were further dried in vacuum (0.8-1.2 mbar) at 300 °C for at least two hours using a tube furnace (type LOSA) from HTM Reetz GmbH. Potassium bicarbonate was dried for three days at 60 °C in an oven (20% ventilation). The hygroscopic bases were stored either in a Schlenk flask or inside a glovebox under argon.

Alkali pivalates were prepared by neutralizing a solution of pivalic acid in ethanol with the according hydroxide bases.^[4] Removal of the solvent under reduced pressure (45 °C, 7 mbar) followed by washing with diethylether and drying (r.t., <1.0·10⁻¹ mbar) afforded pure salts.

Molecular sieves (3 Å and 4 Å) were dried for five hours in vacuum (0.8-1.2 mbar) at 400 °C and stored under argon.

Celite[®] (545, treated with sodium carbonate, flux calcined) was purchased by Fisher Scientific (H33152) and used as filter aid either on a suction filter or in a Pasteur pipette.

7.1.2 Work techniques

Air and moisture sensitive reactions were carried out under Argon (Westfalen, 4.6) using Standard Schlenk techniques.^[5]

Screw capped vials (8 mL, VWR, 548-0821) with silicon/PTFE screw PP caps (VWR, 548-0863) were used as reaction vials, if stated. For reactions under argon, the vials were introduced into a glovebox, filled with all starting materials and solvent(s), closed and stirred with/without heating outside the glovebox.

Heating and cooling. Oil baths were filled with silicon oil (Guessing, silicon oil M100). Schlenk tubes were heated in an alumina block. Freezing mixtures of 0 °C were obtained by mixing ice and water. Temperatures below 0 °C were reached with appropriate mixtures (-15 °C: NaCl-ice 1:3 or -78 °C: dry ice saturated isopropanol or acetone). Temperatures were controlled with a digital contact thermometer.

Microwave assisted reactions were conducted in an Anton Paar 300 microwave synthesis reactor (specifications: max. power: 850 W, max. temperature: 300 °C, max. pressure: 30bar) with a MAS 24 auto-sampler. Borosilicate glasses (10 mL or 20 mL) were used as reaction vials, which

were sealed with a PEEK-cap and a PTFE-coated silicon septum. The temperature was measured via an external infrared thermometer and calibrated with an internal ruby thermometer. A typical temperature and pressure profile of a microwave assisted reaction is depicted in the appendix (8.5).

Flash column chromatography was performed on silica gel 60 (Acros, 35-70 μm) as stationary phase with the eluent mixtures given for the corresponding procedures. Compressed air (0.1-0.3 bar) was used for flash elution.

Photochemical reactions were carried out in a NMR tube in a Rayonet RPR-100 photochemical reactor (Southern New England Ultra Violet Company, Branford, CT, USA). The set-up consisted of 16 fluorescence lamps (8 W, λ_{max} . 300^[6], 350^[7], 366^[6] or 419^[8] nm) orientated in a cylindrical fashion with the sample placed in the middle of the chamber. The chamber was cooled to room temperature with the aid of ventilation to assure no overheating.

Sampling for kinetic studies was conducted as follows (table 51). The desired temperature was adjusted at least one hour before the start of the reaction to avoid any fluctuation. To assure homogeneous distribution in the solution, the internal standard was best added at the beginning of the reaction.⁵⁴ A screw cap vial was charged with water (3 mL) and organic solvent (3 mL), e.g. Et₂O or EtOAc (step 1).⁵⁵ After retrieval of a sample from the reaction ($\sim 250 \mu\text{L}$)⁵⁶, it was added to the extraction mixture. The vial was closed with a cap (no septum), shaken for ten seconds and left alone to allow phases to separate (step 2). A second screw cap (silicon/PTFE septum) vial was charged with MgSO₄ (~ 250 mg) and a stirring bar. It was placed in close to proximity to the extraction vial (step 3). Parts of the organic phase ($\sim 2/3$) were transferred to the MgSO₄ vial with the aid of a Pasteur pipette (step 4). The organic phase was stirred for approx. two minutes (~ 800 rpm) at room temperature (step 5) before the solvent was removed under reduced pressure (water-jet pump, slow flow, ca. 500 mbar) with the aid of a cannula (\varnothing 0.90 mm, color code yellow, step 6). The vial was evacuated for another minute (water-jet pump, fast flow, ca. 20 mbar) with the aid of a cannula (\varnothing 0.90 mm, color code yellow) to get rid of residual organic solvent (step 7). The vial was slowly vented by puncturing the septum (cannula, \varnothing 0.90 mm, color code yellow, step 8).⁵⁷ Solid stuck to the walls was gently scratched off with a Pasteur pipette (step 9). The walls were rinsed with deuterated solvent (700 μL), e.g. CDCl₃, (step 10)

⁵⁴ It was made sure to add enough solvent, so the reaction cannot run dry.

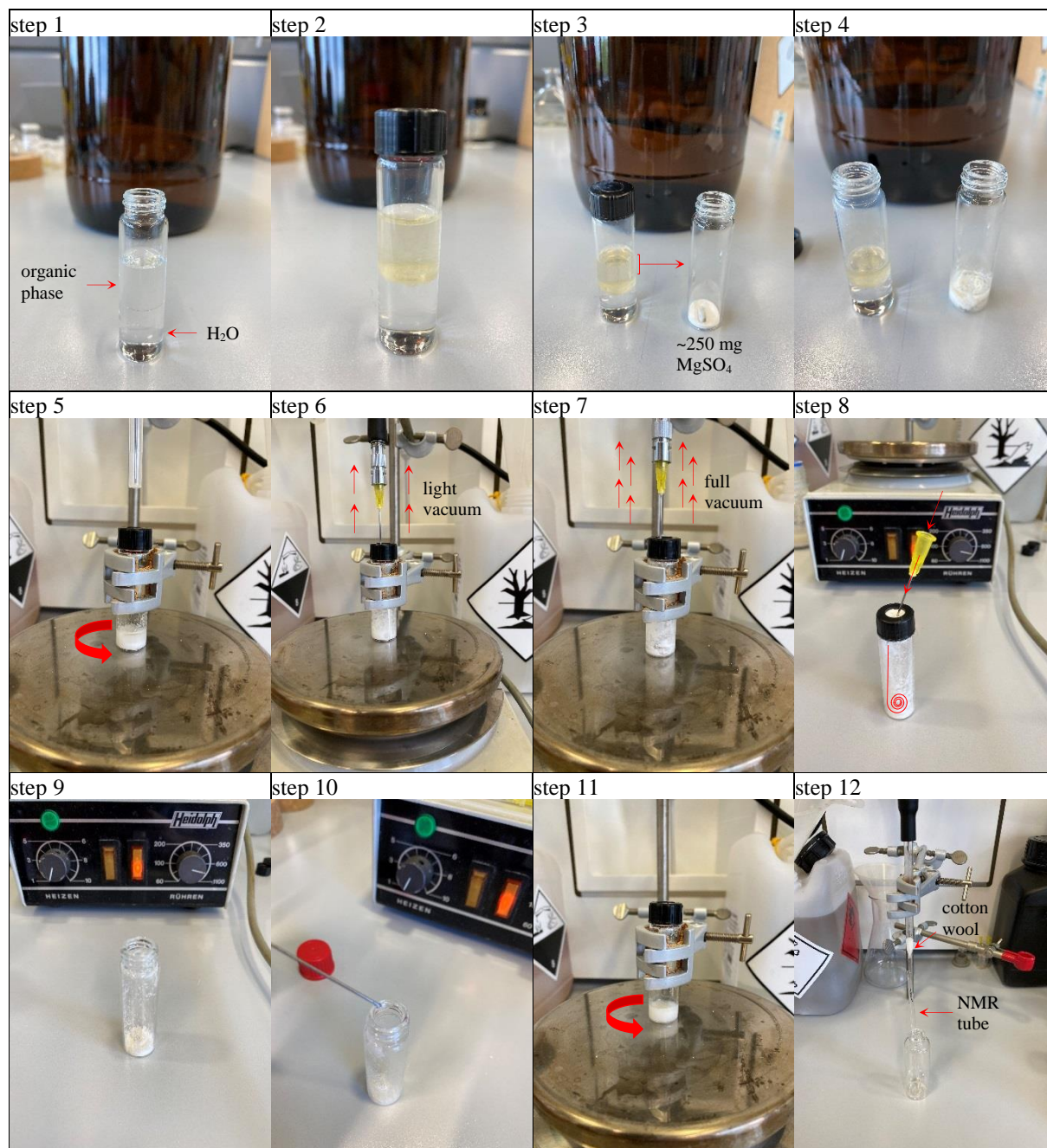
⁵⁵ An organic solvent with density smaller than water simplifies the work-up process.

⁵⁶ The volume withdrawn does not have to be the same for each sampling.

⁵⁷ An angle of 45°-60° is recommended to prevent excessive twirling of the solid.

and the suspension was stirred for two minutes at room temperature (~800 rpm, step 11).⁵⁸ The whole mixture was filtered over cotton wool fitted in a Pasteur pipette (150 mm) into a NMR tube (step 12).

Table 51. Step-by-step guide for kinetic study sampling. Example with Et₂O as organic phase.



⁵⁸ The solvent was added from a safe distance (~2 cm) to the vial to exclude any contamination of the syringe.

7.1.3 Analytics

Elemental analyses were carried out by the analytical core laboratories of the catalytic research center at Technical University of Munich. A *CHNS*-analyzer realizes the chemical digestion of a substance by oxidative combustion at elevated temperatures (ca. 1000 °C). Via a helium stream emerging CO₂, H₂O, N₂ and SO₂ gases are fed into a separate and measuring system. The separation follows general gas chromatographic principles. Gases are detected by a thermal conductivity cell and the percentage of C, H, N and S are calculated.

Qualitative thin-layer chromatography (TLC) was performed on silica-coated glass plates (Merck, silica gel 60 F₂₅₄). Compounds were detected under UV light ($\lambda = 254$ or 366 nm) and by staining with Mostain solution (10.0 g (NH₄)₆[Mo₇O₂₄]·4 H₂O, 200 mg Ce(SO₄)₂·4 H₂O, 12 mL H₂SO₄ (conc.) in 190 mL water) and gently heating with a heat-gun (approx. 100 °C).

X-Ray diffraction. Grown single crystals were measured at the analytical core labs of the catalytic research center of the TUM by Dr. Alexander Pöthig, Dr. Philipp Altmann or myself. Data were collected on a single crystal X-ray diffractometer equipped with a CMOS detector (Photon 100), a rotating anode TXS and a Helios mirror optic using the APEX3 software package or a single crystal x-ray diffractometer equipped with a CMOS detector (Photon 100), an IMS microsource with MoK α radiation ($\lambda = 0.71073$ Å) and a Helios optic using the APEX3 software package or a single crystal X-ray diffractometer equipped with a CCD detector (APEXII), a fine-focus sealed tube with MoK α radiation ($\lambda = 0.71073$ Å) and a Triumph optic monochromator using the APEX3 software package.^[9] Measurements were performed on single crystals coated with perfluorinated ether. The crystals were fixed on top of a kapton micro sampler and frozen under a stream of cold nitrogen. A matrix scan was used to determine the initial lattice parameters. Reflections were corrected for Lorentz and polarization effects, scan speed, and background using SAINT.^[10] Absorption correction, including odd and even ordered spherical harmonics was performed using.^[11] Space group assignment was based upon systematic absences, E statistics, and successful refinement of the structure. The structures were solved using SHELXT with the aid of successive difference Fourier maps, and were refined against all data using SHELXL in conjunction with SHELXLE.^[12] Hydrogen atoms were calculated in ideal positions as follows: Methyl hydrogen atoms were refined as part of rigid rotating groups, with a C–H distance of 0.98 Å and $U_{\text{iso(H)}} = 1.5 \cdot U_{\text{eq(C)}}$. Other H atoms were placed in calculated positions and refined using a riding model, with methylene and aromatic C–H distances of 0.99 Å and 0.95 Å, respectively, and other C–H distances of 1.00 Å, all with $U_{\text{iso(H)}} = 1.2 \cdot U_{\text{eq(C)}}$.

Non-hydrogen atoms were refined with anisotropic displacement parameters. Full-matrix least-squares refinements were carried out by minimizing $\sum w(F_o^2 - F_c^2)^2$ with the SHELXL weighting scheme.^[12a] Neutral atom scattering factors for all atoms and anomalous dispersion corrections for the non-hydrogen atoms were taken from *International Tables for Crystallography*.^[13] Images of the crystal structures were generated with Mercury and PLATON.^[14] CCDC 1946096-1946098 contain the supplementary crystallographic data for X-ray crystal structures of chapter 3. These data are provided free of charge by The Cambridge Crystallographic Data Centre.

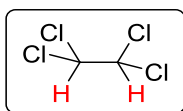
NMR spectroscopy. NMR spectra were recorded at 300 K either on a Bruker AVHD-300, AVHD-400, AVHD-500 or AVHD-500cr. Variable temperature NMR spectra were recorded on a Bruker DRX400. Proton NMR spectra were recorded with a delay $d_1 = 20$ s between the pulses. Chemical shifts are reported in parts per million (ppm) relative to the residual signal of the deuterated solvent or the residual signal of tetramethylsilane (table 52). Attached proton test (¹³C-APT NMR) allowed the assignment of carbon signals; methine (CH) and methyl (CH₃) signals are positive, quaternary (C_{quat}) and methylene (CH₂) signals are negative.^[15] The ¹⁹F- and ³¹P-NMR spectra are machine-referenced to CFC1₃, respectively H₃PO₄ (85%), as external standards.^[16] If necessary, spectral width (sw) of ³¹P-NMR spectra was reduced to 100 ppm (O₁P = usually 10 ppm, depending on product signals $\neq 0$ ppm). ¹¹B-NMR were recorded without reference. The broad signal rises from the used borosilicate NMR tubes.^[17] Multiplicities are abbreviated as follows: s - singlet, d - doublet, t - triplet, q - quartet, quint. - quintet, sext. - sextet, sept. - septet, m - multiplet, br - broad signal. Coupling constants (*J*) are indicated in Hertz (Hz). Apparent multiplets that occur as a result of accidental equality of coupling constants those of magnetically non-equivalent protons are marked as virtual (*virt.*).

Table 52. Respective chemical shifts of the residual signal(s) of deuterated solvents in ¹H- and ¹³C-NMR spectra.

solvent	¹ H-shift [ppm]	¹³ C-shift [ppm]
CDCl ₃	7.26 (s)	77.2 (t)
[D ₆]-acetone	2.06 (quint.)	29.8 (sept.), 206.3 (s)
[D ₃]-acetonitrile	1.94 (quint.)	1.3 (sept.), 118.3 (s)
[D ₂]-dichloromethane	5.32 (t)	54.0 (quint.)
[D ₆]-dimethylsulfoxide	2.50 (quint.)	39.5 (sept.)
[D ₆]-benzene	7.16 (s)	128.1 (t)
[D ₄]-methanol	3.31 (quint.)	49.0 (sept.)
tetramethylsilane	0.00 (s)	0.0 (s)

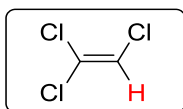
Quantitative NMR (q-NMR) analysis was carried out as follows. The crude reaction mixture was homogeneously dissolved in an appropriate solvent (CDCl_3 or dichloromethane, if suitable). An internal standard (see below) was added via Hamilton μL syringe (or as weighed amount of solid) and the solution was homogenized by swirling. In case of a non-deuterated solvent, a sample of the reaction mixture (ca. 50 μL) was added to an NMR tube containing CDCl_3 (450 μL) and was mixed by shaking. If CDCl_3 was used, a sample of the reaction mixture (500 μL) was transferred to an empty NMR tube without further dilution. A proton NMR ($d_1 = 20$ s, 16 scans) was measured.^[18]

The yield of the reaction is determined by comparison of the integral of the internal standard with the integral of characteristic signals of the reaction product(s) and starting material(s) in the ^1H -NMR spectra. The exemplary analysis of a q-NMR spectrum is depicted in the appendix (8.5).



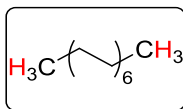
1,1,2,2-tetrachloroethane:

^1H -NMR (500 MHz, CDCl_3): δ 5.91 (s, 2H).



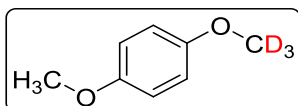
1,1,2-trichloroethylene:

^1H -NMR (500 MHz, CDCl_3): δ 6.45 (s, 1H).



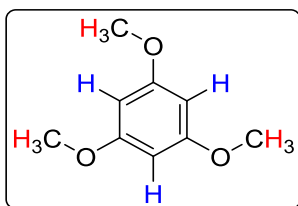
tetradecane:

^1H -NMR (500 MHz, CDCl_3): δ 0.85 (t, $J = 6.5$ Hz, 6H).



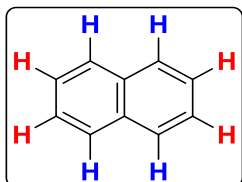
1-methoxy-4-([D₃]-methoxy)benzene:^[19]

^2H -NMR (61 MHz, CHCl_3): δ 3.63 (s, 3H).⁵⁹



1,3,5-trimethoxybenzene:

^1H -NMR (500 MHz, CDCl_3): δ 3.75 (s, 9H), 6.08 (s, 3H).



naphthalene:

^1H -NMR (400 MHz, CDCl_3): δ 7.47 (m, 4H), 7.84 (m, 4H).

⁵⁹ For quantification of both ^1H and ^2H .

UV/Vis spectroscopy was performed on a Perkin Elmer Lambda 35 UV/Vis spectrometer in the analytical core laboratories of the Technical University of Munich. Spectra were recorded using a Hellma precision cell made of quartz Suprasil with a pathway of 1 cm. Solvents and concentrations are given for each spectrum.

High resolution mass spectrometry (HRMS) were carried out by the analytical core labs at Technical University of Munich. ESI-HRMS were recorded on a Thermo Fisher Scientific LTQ FT Ultra ion trap with a Fourier Transform Ion Cyclotron Resonance (FT-ICR) MS detector.

HPLC: Analytical HPLC was performed using an auto-sampler 3800, a manager 5000 and a pump 1000 of the Smartline series from Knauer. UV-active substances were detected by a diode array detector K-2800 of the WellChrom series. Caffeine reaction mixtures (injection volume 20 μ L) were separated using a silica gel column (Kromasil 100 Si – 5 μ), which was cooled to 20 °C, as stationary phase and a *tert*-butylmethylether/methanol mixture (TBME-MeOH 40:1) as eluent. The retention times are 2.57 minutes for 8-phenylcaffeine and 12.88 minutes for caffeine. The flow rate was kept constant at 1.5 mL/min and the pressure never outstripped 65 bar. The mixtures were analyzed at 274 nm. See general procedure 3.7 (7.2.3.1) for sample drawing of caffeine arylation reactions. As reference measurement equimolar amounts of caffeine and 8-phenylcaffeine (300 μ mol, 600 μ mol and 900 μ mol) were dissolved in dichloromethane in a volumetric flask (100 mL). One milliliter of the prepared solution was diluted with dichloromethane in another volumetric flask (10 mL) and the final mixture was analyzed via HPLC under the conditions described above. The obtained injection amounts of substance, as well as average peak areas, are summarized in table 53.

Table 53. Injected amounts of substance ($n_{inj.}$) of caffeine and 8-phenylcaffeine and their average peak area. Average peak areas were received by calculating the mean of the collected area of four measurements.

compound	$n_{inj.}$ [nmol]	average peak area [-]
caffeine	6	30.3946
caffeine	12	59.0916
caffeine	18	90.4098
phenylcaffeine	6	24.9539
phenylcaffeine	12	48.3602
phenylcaffeine	18	72.5619

The above reported values were plotted in two separate graphs (injection amount vs. average peak area) and a trend line was drawn (see 8.2 figure 49 and figure 50). A linear correlation was determined. By using the trend line equations, the amount of substance of caffeine ($n_{Caff.}$)

and phenylcaffeine ($n_{\text{Phcaff.}}$) present in a reaction mixture (after one, two, three, ... hour(s)) can be calculated via equations 1.1 and 1.2. The factor 1/16 represents the applied dilution during the sample drawing and $x_{\text{Caff.}}$ (or $x_{\text{Phcaff.}}$) the or phenylcaffeine. The outcome equals the amount of substance of caffeine, respectively phenylcaffeine, in mmol.

$$n_{\text{caff.}} = \frac{1}{16} \cdot y_{\text{caff.}} = \frac{1}{16} \cdot (0.1998 \cdot x_{\text{caff.}} + 0.0176) \quad 1.1$$

$$n_{\text{Phcaff.}} = \frac{1}{16} \cdot y_{\text{Phcaff.}} = \frac{1}{16} \cdot (0.252 \cdot x_{\text{Phcaff.}} - 0.2553) \quad 1.2$$

With the peak areas converted to amounts of substance of caffeine, the conversion of each reaction can be calculated following equation 1.3. Unless otherwise specified, the initial amount of caffeine (n_0) present in the arylations is always equal to 1.50 mmol. The yield of phenylcaffeine after 20 hours reaction time can be determined by insertion of the amount of substance of phenylcaffeine detected after into equation 1.4.

$$\text{conversion [\%]} = \frac{n_{\text{caff.}}}{n_0} \cdot 100 = \frac{n_{\text{caff.}}}{1.50 \text{ mmol}} \cdot 100 \quad 1.3$$

$$\text{yield [\%]} = \frac{n_{\text{Phcaff.}}}{n_0} \cdot 100 = \frac{n_{\text{Phcaff.}}}{1.50 \text{ mmol}} \cdot 100 \quad 1.4$$

7.2 Synthesis procedures

Experimental data of each chapter will be depicted in this section. General procedures (GP) of individual topics will be listed in the beginning of each subject. Numeration of the latter will be conducted as follows: number of corresponding chapter in the main discussion, followed by a dot and the count of the mentioned procedure, e.g. 2.1.4 refers to general procedure 4 of chapter 2.1.

7.2.1 Generation of Organozinc Reagents by Nickel-Diazadiene-Complex Catalyzed Zinc Insertion into Aryl Sulfonates

7.2.1.1 General synthesis procedures

General procedure 1.1 – Synthesis of aryl sulfonates in aqueous base

This procedure was adapted from Lei and coworkers.^[20] An aqueous sodium hydroxide solution (15%, 3.3 eq.) was added to a solution of a phenol (1.0 eq.) in THF (1.7 M). At 0 °C, a solution of TsCl (1.2 eq.) in THF (0.9 M) was added dropwise and the suspension was stirred for 24 hours at room temperature. The reaction mixture was transferred with EtOAc (4 mL/mmol) to a separatory funnel and the phases were separated. The organic phase was washed with water (2 x 2.5 mL/mmol) and a saturated aqueous solution of NaCl (1 mL/mmol), dried over MgSO₄, filtered and the solvent was removed under reduced pressure (45 °C, 7 mbar). Washing with hexanes or purification by CC and drying under reduced pressure ($<1.0 \cdot 10^{-1}$ mbar) afforded the pure product.

General procedure 1.2 – Metalation followed by iodolysis – analytical scale with q-NMR quantification

A pre-dried ($2 \cdot 10^{-2}$ mbar, heat-gun) Schlenk tube was charged with zinc powder (262 mg, 4.00 mmol, 4.0 eq.), which was dried under vacuum ($2 \cdot 10^{-2}$ mbar) and stirring with a heat-gun. 1,2-Dibromoethane (98%, 17.6 μ L, 37.6 mg, 200 μ mol, 0.2 eq.) was added and the walls were rinsed with dry DMF (1 mL) (heat and gas evolution were observed). After stirring at 60 °C for 20 minutes, the reaction mixture was cooled down to room temperature for five minutes in a water bath. NiCl₂(dme) (11.0 mg, 50.0 μ mol, 5 mol%) and IPr-MeDAD (40.5 mg, 100 μ mol, 10 mol%) were added and the walls were rinsed with dry DMF (1 mL). The brownish-green suspension was stirred for 30 minutes at room temperature. Finally, the aryl tosylate (1.00 mmol, 1.0 eq.) was added, the walls were rinsed with dry DMF (1 mL) and the reaction mixture was stirred for 20 hours at room temperature. Then it was cooled to 0 °C before adding

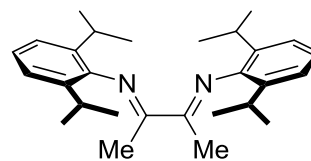
iodine (1.02 g, 4.00 mmol, 4.0 eq.) and stirring for ten minutes at 0 °C. A saturated aqueous solution of NH₄Cl (10 mL) and solid sodium sulfite (approx. 500 mg) were added and the reaction mixture was stirred until most of the brown color faded. The aqueous phase was extracted with diethylether (10 mL and 3 × 5 mL) (or ethyl acetate in the case of non-volatile products). The combined organic phase was washed with a saturated aqueous solution of NH₄Cl (2 × 20 mL) and NaCl (20 mL), dried over MgSO₄, filtered and the solvent was removed under reduced pressure (40 °C, 700 mbar for volatile products, 200 mbar for non-volatile ones). The crude product was analyzed by q-NMR using either 1,1,2,2-tetrachloroethane (50.0 μL, 473.6 μmol) or trichloroethene (200 μL, 2.22 mmol) as internal standard according to the general procedure (see 7.1.3).

General procedure 1.3 – Metalation followed by iodolysis on preparative scale

A pre-dried ($2 \cdot 10^{-2}$ mbar, heat-gun) Schlenk tube was charged with zinc powder (523 mg, 8.00 mmol, 4.0 eq.), which was dried under vacuum ($2 \cdot 10^{-2}$ mbar) and stirring with a heat-gun. 1,2-Dibromoethane (98%, 35.2 μL, 75.1 mg, 400 μmol, 0.2 eq.) was added and the walls were rinsed with dry DMF (2 mL) (heat and gas evolution were observed). After stirring at 60 °C for 20 minutes, the reaction mixture was cooled down to room temperature for five minutes in a water bath. NiCl₂(dme) (22.0 mg, 100 μmol, 5 mol%) and **L2** (80.9 mg, 200 μmol, 10 mol%) were added and the walls were rinsed with dry DMF (2 mL). The brownish-green suspension was stirred for 30 minutes at room temperature. Finally, the aryl tosylate (2.00 mmol, 1.0 eq.) was added, the walls were rinsed with DMF (2 mL) and the reaction mixture was stirred for 20 hours at room temperature. Unless otherwise stated, it was cooled to 0 °C before adding iodine (2.03 g, 8.00 mmol, 4.0 eq.) and stirring for ten minutes at 0 °C. A saturated aqueous solution of NH₄Cl (10 mL) and solid sodium sulfite (approx. 1 g) were added and the reaction mixture was stirred until most of the brown color faded. Et₂O (10 mL or ethyl acetate in the case of non-volatile products) was added and the suspension was filtered. Additionally, the pad of Celite was rinsed with the used extracting solvent (3 × 5 mL). The organic phase was separated, washed with a saturated aqueous solution of NH₄Cl (2 × 20 mL) and NaCl (20 mL), dried over MgSO₄, filtered and the solvent was removed under reduced pressure (40 °C, 700 mbar, 150 mbar for non-volatile products). Purification by flash CC afforded the desired products.

7.2.1.2 Synthesis of standard ligand IPr-MeDAD

Diacetyl-bis(2,6-diisopropylphenylimine) or N,N'-(butane-2,3-diyl-idene)-bis(2,6-diisopropylaniline) or IPr-MeDAD (CAS 74663-77-7, PK-SP-14, L2).

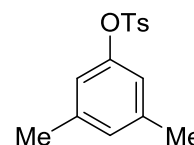


The ligand was prepared according to the original procedure of tom Dieck et al.^[21] Diacetyl (5.40 mL, 62.1 mmol, 1.0 eq.) was added dropwise to a solution of 2,6-diisopropylaniline (23.2 g, 131 mmol, 2.1 eq.), formic acid (600 μ L, catalytic) in methanol (45 mL). The reaction mixture was stirred for three hours at room temperature. The solid was filtered off and washed with ice-cold methanol (3 x 20 mL). After storing of the filtrate at -25 $^{\circ}$ C overnight, the yellow crystals were filtered and washed with cold methanol (-25 $^{\circ}$ C, 3 x 10 mL). The two fractions were combined and dried in a ventilated oven at 60 $^{\circ}$ C overnight, affording yellow crystals (18.3 g, 73%).

1 H-NMR (400 MHz, $[D_6]$ -benzene, PK-SP-14-F1): δ 1.18 (*virt.* t, J = 6.8 Hz, 24H), 2.16 (s, 6H), 2.88 (sept., J = 6.8 Hz, 4H), 7.09-7.14 (m, 2H), 7.17-7.20 (m, 4H). **13 C-NMR** (75 MHz, $[D_6]$ -benzene, PK-SP-14-F1): δ 16.6, 22.8, 23.3, 29.1, 123.6, 124.5, 135.3, 146.8, 168.5. The analytical data matched those reported in literature.^[21]

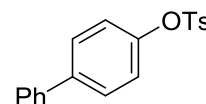
7.2.1.3 Synthesis of aryl sulfonates

3,5-Dimethylphenyltosylate (CAS 95127-25-6, PK-328). 3,5-Dimethylphenol (3.05 g, 25.0 mmol, 1.0 eq.), *p*-TsCl (5.72 g, 30.0 mmol, 1.2 eq.) and aqueous sodium hydroxide (15%, 19 mL, 3.3 eq.) in THF (50 mL) were reacted according to general procedure 1.1. Purification by washing with hexanes (2 x 20 mL) and drying under reduced pressure (r.t., $<1.0 \cdot 10^{-1}$ mbar) afforded a white solid (6.46 g, 94%).



1 H-NMR (400 MHz, $CDCl_3$, PK-328-N): δ 2.23 (*virt.* q, J = 0.7 Hz, 6H), 2.45 (s, 3H), 6.57-6.64 (m, 2H), 6.84-6.89 (m, 1H), 7.28-7.34 (m, 2H), 7.69-7.76 (m, 2H). **13 C-NMR** (101 MHz, $CDCl_3$, PK-328-N): δ 21.3, 21.8, 119.9, 128.6, 128.8, 129.7, 132.9, 139.6, 145.2, 149.6. The analytical data matched those reported in literature.^[22]

4-Biphenyltosylate (CAS 76996-40-2, PK-329). 4-Phenylphenol (4.26 g, 25.0 mmol, 1.0 eq.), *p*-TsCl (5.72 g, 30.0 mmol, 1.2 eq.) and aqueous sodium



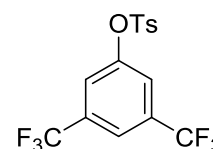
hydroxide (15%, 19 mL, 3.3 eq.) in THF (50 mL) were reacted according to general procedure 1.1. Before aqueous work-up, the suspension was filtered, the collected solid (5.82 g, 17.9 mmol, 72%) washed with EtOAc (50 mL) and hexanes (50 mL) and dried under reduced pressure (r.t., $<1.0 \cdot 10^{-1}$ mbar). Purification by washing with hexanes (2 x 20 mL) of the crude

material yielded from extraction and drying under reduced pressure (r.t., $<1.0 \cdot 10^{-1}$ mbar) afforded a white, crystalline solid (2.09 g, 26%). Total yield: 7.91 g, 98%.

$^1\text{H-NMR}$ (400 MHz, CDCl_3 , PK-329-2-N): δ 2.45 (s, 3H), 7.01-7.10 (m, 2H), 7.29-7.38 (m, 3H), 7.39-7.46 (m, 2H), 7.46-7.54 (m, 4H), 7.71-7.81 (m, 2H). **$^{13}\text{C-NMR}$** (101 MHz, CDCl_3 , PK-329-2-N): δ 21.9, 122.8, 127.2, 127.8, 128.4, 128.7, 129.0, 129.9, 132.6, 139.9, 140.3, 145.5, 149.1. The analytical data matched those reported in literature.^[23]

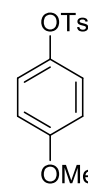
3,5-Bis(trifluoromethyl)phenyltosylate (CAS 1416330-87-4, PK-330).

3,5-Bis(trifluoromethyl)phenol (3.45 g, 15.0 mmol, 1.0 eq.), *p*-TsCl (3.43 g, 18.0 mmol, 1.2 eq.) and aqueous sodium hydroxide (15%, 11 mL, 3.3 eq.) in THF (30 mL) were reacted according to general procedure 1.1. Purification by CC (EtOAc-hexanes 1:30) and drying under reduced pressure (r.t., $<1.0 \cdot 10^{-1}$ mbar) afforded a white, crystalline solid (1.57 g, 27%).



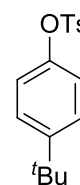
TLC: $R_f = 0.15$ (EtOAc-hexanes 1:30) [UV]. **$^1\text{H-NMR}$** (400 MHz, CDCl_3 , PK-330-A): δ 2.48 (s, 3H), 7.35-7.41 (m, 2H), 7.42-7.46 (m, 2H), 7.70-7.76 (m, 2H), 7.77-7.80 (m, 1H). **$^{13}\text{C-NMR}$** (101 MHz, CDCl_3 , PK-330-N): δ 21.9, 121.0 (t, $J = 3.9$ Hz), 121.2, 123.4-123.5 (m), 123.9, 128.7, 130.3, 131.5, 133.4 (d, $J = 34.6$ Hz), 146.7, 150.1. The analytical data matched those reported in literature.^[23]

4-Methoxyphenyltosylate (CAS 38891-91-0, PK-331). 4-Methoxyphenol (3.10 g, 25.0 mmol, 1.0 eq.), *p*-TsCl (5.72 g, 30.0 mmol, 1.2 eq.) and aqueous sodium hydroxide (15%, 19 mL, 3.3 eq.) in THF (50 mL) were reacted according to general procedure 1.1. Purification by washing with hexanes (2 x 20 mL) and drying under reduced pressure (r.t., $<1.0 \cdot 10^{-1}$ mbar) afforded a white solid (6.79 g, 98%).



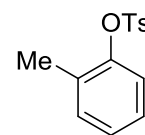
$^1\text{H-NMR}$ (400 MHz, CDCl_3 , PK-331-N): δ 2.44 (s, 3H), 3.76 (s, 3H), 6.73-6.80 (m, 2H), 6.85-6.91 (m, 2H), 7.28-7.33 (m, 2H), 7.66-7.72 (m, 2H). **$^{13}\text{C-NMR}$** (101 MHz, CDCl_3 , PK-331-N): δ 21.8, 55.7, 114.6, 123.5, 128.7, 129.8, 132.5, 143.2, 145.3, 158.3. The analytical data matched those reported in literature.^[20]

4-tert-Butylphenyltosylate (CAS 7598-28-9, PK-332). 4-*tert*-Butylphenol (3.76 g, 25.0 mmol, 1.0 eq.), *p*-TsCl (5.72 g, 30.0 mmol, 1.2 eq.) and aqueous sodium hydroxide (15%, 19 mL, 3.3 eq.) in THF (50 mL) were reacted according to general procedure 1.1. Purification by washing with hexanes (2 x 20 mL) and drying under reduced pressure (r.t., $<1.0 \cdot 10^{-1}$ mbar) afforded a white solid (7.31 g, 96%).



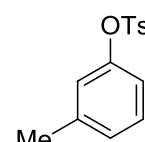
¹H-NMR (400 MHz, CDCl₃, PK-332-N): δ 1.28 (s, 9H), 2.45 (s, 3H), 6.86-6.93 (m, 2H), 7.25-7.30 (m, 2H), 7.30-7.33 (m, 2H), 7.70-7.75 (m, 2H). **¹³C-NMR** (101 MHz, CDCl₃, PK-332-N): δ 21.8, 31.5, 34.7, 121.8, 126.6, 128.6, 129.8, 132.9, 145.3, 147.5, 150.2. The analytical data matched those reported in literature.^[20]

2-Methylphenyltosylate (CAS 599-75-7, PK-344). 2-Methylphenol (5.41 g, 50.0 mmol, 1.0 eq.), *p*-TsCl (11.5 g, 60.0 mmol, 1.2 eq.) and aqueous sodium hydroxide (15%, 38 mL, 3.3 eq.) in THF (100 mL) were reacted according to general procedure 1.1. Purification by washing with hexanes (2 x 30 mL) and drying under reduced pressure (r.t., $<1.0 \cdot 10^{-1}$ mbar) afforded a white solid (10.8 g, 82%).



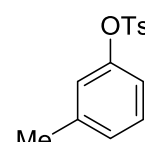
¹H-NMR (500 MHz, CDCl₃, PK-344-N): δ 2.08 (s, 3H), 2.46 (s, 3H), 6.96-7.02 (m, 1H), 7.08-7.18 (m, 3H), 7.32 (d, $J = 8.1$ Hz, 2H), 7.71-7.77 (m, 2H). **¹³C-NMR** (101 MHz, CDCl₃, PK-344-13C): δ 16.4, 21.8, 122.4, 127.0, 127.1, 128.5, 129.9, 131.7, 131.7, 133.4, 145.4, 148.5. The analytical data matched those reported in literature.^[20]

3-Methylphenyltosylate (CAS 3955-72-4, PK-345). 3-Methylphenol (5.41 g, 50.0 mmol, 1.0 eq.), *p*-TsCl (11.5 g, 60.0 mmol, 1.2 eq.) and aqueous sodium hydroxide (15%, 38 mL, 3.3 eq.) in THF (100 mL) were reacted according to general procedure 1.1. Purification by CC (EtOAc-hexanes 1:10) and drying under reduced pressure (r.t., $<1.0 \cdot 10^{-1}$ mbar) afforded a yellowish oil (13.0 g, 99%), which solidified upon cooling in the fridge.



¹H-NMR (400 MHz, CDCl₃, PK-345-N): δ 2.29 (s, 3H), 2.45 (s, 3H), 6.67-6.76 (m, 1H), 6.82-6.90 (m, 1H), 7.02-7.07 (m, 1H), 7.14 (t, $J = 7.9$ Hz, 1H), 7.28-7.33 (m, 2H), 7.68-7.76 (m, 2H). **¹³C-NMR** (101 MHz, CDCl₃, PK-345-N): δ 21.4, 21.8, 119.3, 123.1, 127.9, 128.6, 129.3, 129.8, 132.8, 140.1, 145.3, 149.7. The analytical data matched those reported in literature.^[20]

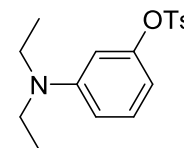
4-Methylphenyltosylate (CAS 3899-96-5, PK-346). 4-Methylphenol (5.41 g, 50.0 mmol, 1.0 eq.), *p*-TsCl (11.5 g, 60.0 mmol, 1.2 eq.) and aqueous sodium hydroxide (15%, 38 mL, 3.3 eq.) in THF (100 mL) were reacted according to general procedure 1.1. Purification by washing with hexanes (2 x 30 mL) and drying under reduced pressure (r.t., $<1.0 \cdot 10^{-1}$ mbar) afforded a white solid (12.0 g, 91%).



¹H-NMR (400 MHz, CDCl₃, PK-345-N): δ 2.29 (s, 3H), 2.45 (s, 3H), 6.67-6.76 (m, 1H), 6.82-6.90 (m, 1H), 7.02-7.07 (m, 1H), 7.14 (t, $J = 7.9$ Hz, 1H), 7.28-7.33 (m, 2H), 7.68-7.76 (m, 2H). **¹³C-NMR** (101 MHz, CDCl₃, PK-345-N): δ 21.4, 21.8, 119.3, 123.1, 127.9, 128.6,

129.3, 129.8, 132.8, 140.1, 145.3, 149.7. The analytical data matched those reported in literature.^[20]

3-*N,N*-Diethylaminophenyltosylate (CAS 2259293-70-2, PK-KF-03). 3-*N,N*-Diethylaminophenol (4.13 g, 25.0 mmol, 1.0 eq.), *p*-TsCl (5.72 g, 30.0 mmol, 1.2 eq.) and aqueous sodium hydroxide (15%, 19 mL, 3.3 eq.) in THF (50 mL)

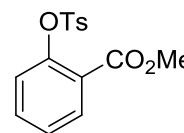


were reacted according to general procedure 1.1. Purification by flash column chromatography (EtOAc-hexanes 1:10) and drying under reduced pressure (r.t., $<1.0 \cdot 10^{-1}$ mbar) afforded a white solid (13.5 g, 88%).

TLC: $R_f = 0.34$ (EtOAc-hexanes 1:10) [UV]. **¹H-NMR** (400 MHz, CDCl₃, PK-KF-03-Fraktion5): δ 1.05 (t, $J = 7.1$ Hz, 6H), 3.23 (q, $J = 7.1$ Hz, 4H), 6.14-6.24 (m, 2H), 6.45-6.52 (m, 1H), 7.00-7.08 (m, 1H), 7.26-7.35 (m, 2H), 7.70-7.78 (m, 2H). **¹³C-NMR** (101 MHz, CDCl₃, PK-KF-03-13C): δ 12.4, 21.7, 44.5, 105.5, 108.4, 110.2, 128.7, 129.7, 129.9, 133.0, 145.1, 148.9, 151.2. This compound is known to literature, but no analytical data is available.

Methyl 2-(((4-methylphenyl)sulfonyl)oxy)benzoate (51207-44-4, PK-KF-02).

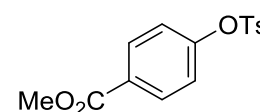
This compound was synthesized following a slightly modified procedure from the group of Khan.^[24] Methyl 4-hydroxybenzoate (3.81 g, 25.0 mmol, 1.0 eq.)



was dissolved in pyridine (4 mL). At 0 °C, *p*-TsCl (6.36 g, 33.3 mmol, 1.3 eq.) was slowly added. The milky suspension was stirred for 2.5 hours at 0 °C before being kept in the fridge (4 °C) overnight. The suspension was diluted with water (20 mL) and neutralized with aqueous HCl (2 M). After transferring to a separatory funnel, the aqueous phase was extracted with EtOAc (2 x 50 mL). The combine organic extract was washed with a saturated aqueous solution of NaCl (20 mL), dried over MgSO₄, filtered and the solvent was removed under reduced pressure (40 °C, 30 mbar). After washing with hexanes (3 x 25 mL) and drying in air (r.t., overnight), a colorless crystalline solid (4.92 g, 64%) was obtained.

¹H-NMR (400 MHz, CDCl₃, PK_KF_02_N): δ 2.45 (s, 3H), 3.80 (s, 3H), 7.10 (dd, $J = 8.2, 1.1$ Hz, 1H), 7.29-7.37 (m, 3H), 7.47 (ddd, $J = 8.2, 7.4, 1.8$ Hz, 1H), 7.68-7.76 (m, 2H), 7.88 (dd, $J = 7.8, 1.8$ Hz, 1H). **¹³C-NMR** (101 MHz, CDCl₃, PK_KF_01_N): δ 21.9, 52.5, 124.1, 125.7, 127.2, 128.7, 129.8, 132.1, 132.8, 133.4, 145.6, 148.0, 165.2. The analytical data matched those reported in the literature.^[25]

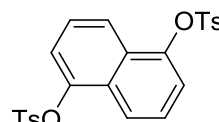
Methyl 4-(((4-methylphenyl)sulfonyl)oxy)benzoate (51207-43-3, PK-KF-17). This compound was synthesized following a slightly modified procedure from the group of Khan.^[24] Methyl 4-hydroxybenzoate (7.61 g,



50.0 mmol, 1.0 eq.) was dissolved in pyridine (8 mL). At 0 °C, *p*-TsCl (12.7 g, 66.5 mmol, 1.3 eq.) was slowly added. The milky suspension was stirred for 30 minutes at 0 °C before being kept in the fridge (4 °C) overnight.⁶⁰ The suspension was diluted with water (20 mL) and neutralized with aqueous HCl (2 M). After transferring to a separatory funnel, the aqueous phase was extracted with EtOAc (2 x 50 mL). The combine organic extract was washed with a saturated aqueous solution of NaCl (20 mL), dried over MgSO₄, filtered and the solvent was removed under reduced pressure (40 °C, 30 mbar). After washing with hexanes (3 x 50 mL) and drying in air (r.t., overnight), a colorless crystalline solid (13.5 g, 88%) was obtained.

¹H-NMR (400 MHz, CDCl₃, PK_KF_17_N): δ 2.45 (s, 3H), 3.90 (s, 3H), 7.02-7.12 (m, 2H), 7.29-7.37 (m, 2H), 7.65-7.74 (m, 2H), 7.94-8.02 (m, 2H). ¹³C-NMR (101 MHz, CDCl₃, PK_KF_01_N): δ 21.9, 52.5, 122.5, 128.6, 129.1, 130.0, 131.4, 132.3, 145.9, 153.1, 166.1. The analytical data matched those reported in the literature.^[24]

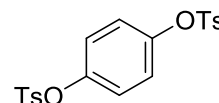
Naphthyl-1,5-ditosylate (CAS 151710-15-5, PK-KF-06). 1,5-Dihydroxy-naphthalene (8.01 g, 50.0 mmol, 1.0 eq.), *p*-TsCl (22.9 g, 120 mmol, 2.4 eq.) and aqueous sodium hydroxide (15%, 76 mL, 6.6 eq.) in THF



(170 mL) were reacted according to general procedure 1.1. Washing with water (3 x 20 mL), acetone (50 mL) and hexanes (100 mL) followed by drying in an oven (50 °C) overnight afforded a pale white solid (13.3 g, 57%). The product contained tetrahydrofuran (0.7 wt.%).

¹H-NMR (400 MHz, CDCl₃, PK-KF-06-N): δ 2.43 (s, 6H), 7.19 (dd, *J* = 7.6, 0.9 Hz, 2H), 7.24-7.37 (m, 8H), 7.73-7.80 (m, 4H), 7.80-7.86 (m, 2H). ¹³C-NMR (101 MHz, CDCl₃, PK-KF-06-N): δ 21.9, 119.4, 121.2, 126.1, 128.6, 128.9, 130.0, 132.7, 145.7, 145.8. The analytical data matched those reported in the literature.^[26]

Benzene-1,5-ditosylate (CAS 2581-43-3, PK-KF-16). Hydroquinone (5.51 g, 50.0 mmol, 1.0 eq.), *p*-TsCl (22.9 g, 120 mmol, 2.4 eq.) and



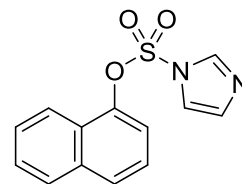
aqueous sodium hydroxide (15%, 76 mL, 6.6 eq.) in THF (170 mL) were reacted according to general procedure 1.1. Before aqueous work-up, the suspension was filtered. The collected solid was washed with water (3 x 25 mL), EtOH (2 x 25 mL) and hexanes (3 x 25 mL) and dried under reduced pressure (r.t., $1.0 \cdot 10^{-1}$ mbar), yielding a first fraction of white crystalline solid (6.46 g, 31%). The crude product obtained from extraction was washed with water (3 x 25 mL), EtOH (2 x 25 mL) and hexanes (3 x 25 mL) and dried under reduced pressure (r.t., $1.0 \cdot 10^{-1}$

⁶⁰ The reaction mixture solidified after stirring for 30 minutes at 0 °C.

mbar). A second fraction of white crystalline solid (4.53 g, 22%) was isolated. Total yield: 11.0 g, 53%.

¹H-NMR (400 MHz, CDCl₃, PK_KF_16_N_F1): δ 2.46 (s, 6H), 6.90 (s, 4H), 7.27-7.35 (m, 4H), 7.62-7.72 (m, 4H). **¹³C-NMR** (101 MHz, CDCl₃, PK_KF_16_N_F1): δ 21.9, 123.7, 128.6, 130.0, 132.1, 145.8, 148.0. The analytical data matched those reported in the literature.^[20]

2-Imidazole-1-sulfonatenaphthalene (CAS 1139705-28-4, PK-388). The procedure was adapted from the group of Albaneze-Walker.^[27] A suspension of 1-naphthol (364 mg, 2.52 mmol, 1.0 eq.), 1,1'-sulfonyldiimidazole (1.00 g, 5.05 mmol, 2.0 eq.) and CsCO₃ (411 mg,

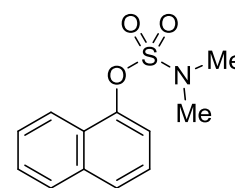


1.26 mmol, 0.5 eq.) in THF (35 mL) was stirred for 24 hours at room temperature. The solvent of the greenish suspension was removed under reduced pressure (45 °C, 320 mbar). After cooling to 0 °C, EtOAc (20 mL) and a saturated aqueous solution of NH₄Cl (15 mL) were added, yielding an orange-yellow two-phase mixture. The phases were separated and the aqueous phase was extracted with EtOAc (2 x 40 mL). The organic phase was washed with water (50 mL), a saturated aqueous solution of NaCl (40 mL), dried over MgSO₄, filtered and the solvent was removed under reduced pressure (45 °C, 100 mbar). Purification by CC (EtOAc-hexanes 1:2) afforded a light pinkish solid (630 mg, 91%).

TLC: R_f = 0.25 (EtOAc-hexanes 1:3) [UV]. **¹H-NMR** (500 MHz, CDCl₃, PK-388-A): δ 7.00 (dd, J = 7.7, 1.0 Hz, 1H), 7.10 (dd, J = 1.7, 0.8 Hz, 1H), 7.29 (t, J = 1.5 Hz, 1H), 7.40 (t, J = 8.0 Hz, 1H), 7.49-7.59 (m, 2H), 7.73-7.92 (m, 4H). **¹³C-NMR** (101 MHz, CDCl₃, PK-388-13C): δ 117.9, 118.6, 120.6, 125.2, 126.5, 127.5, 127.8, 128.2, 128.8, 131.5, 135.0, 137.6, 145.4. The analytical data matched those reported in literature.^[27]

***N,N*-Dimethylamino-1-sulfamoylnaphthalene (CAS 1144-13-4, PK-389).**

The procedure was adapted from the group of Spillane.^[28] 1-Naphthol (1.44 g, 10.0 mmol, 2.0 eq.) and benzyltriethylammonium chloride (45.8 mg,

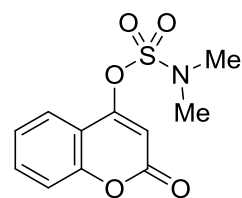


201 μ mol, 4 mol%) were added to a 25 mL round-bottom flask. The flask was sealed with a septum, evacuated (r.t., $<1.0 \cdot 10^{-1}$ mbar) and backfilled with argon three times. Toluene (2.5 mL) and aqueous sodium hydroxide (30%, 2.5 mL) were added and the mixture was stirred at room-temperature. A solution of sulfamoyl chloride (719 mg) in toluene (2.5 mL) was added dropwise and the yellowish-green two-phase system was stirred for seven hours at 50 °C. The reaction mixture was transferred with diethyl ether (15 mL) to a separatory funnel leading to three-phase system. To further decrease polarity, hexanes (10 mL) were added and

phases were separated. The organic phase was washed with aqueous sodium hydroxide (2 M, 20 mL), water (3 x 20 mL, until the water phase was neutral) and a saturated aqueous solution of NaCl (20 mL), dried over MgSO₄, filtered and the solvent was removed under reduced pressure (45 °C, 25 mbar). The yellowish oil crystallized promptly. After pulverizing and drying under reduced pressure (r.t., <1.0·10⁻¹ mbar), an off-white solid (1.07 g, 85%) was obtained.

¹H-NMR (400 MHz, CDCl₃, PK-389-N-2): δ 3.06 (s, 6H), 7.45 (t, *J* = 7.9 Hz, 1H), 7.50-7.62 (m, 3H), 7.76 (dd, *J* = 8.2, 1.0 Hz, 1H), 7.85-7.90 (m, 1H), 8.15-8.21 (m, 1H). **¹³C-NMR** (101 MHz, CDCl₃, PK-389-N-2): δ 39.0, 117.9, 121.6, 125.5, 126.8, 126.9, 127.3, 128.1, 135.0, 146.2. The analytical data matched those reported in literature.^[29]

***N,N*-Dimethylamino-1-sulfamoylnaphthalene** (CAS 1803035-97-3, **PK-401**). DMAP (61.1 mg, 500 μmol, 0.1 eq.) and 4-Hydroxycoumarin

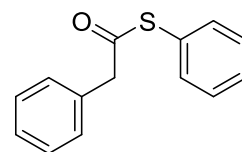


(811 mg, 5.00 mmol, 1.0 eq.) were suspended in dichloromethane (50 mL). Triethylamine (3.4 mL) was added. After the remaining white solid dissolved, *N,N*-dimethylaminosulfamoyl chloride (1.08 mL, 1.44 g, 10.0 mmol, 2.0 eq.) was added dropwise at room temperature. The clear, yellow solution was stirred for two and a half hours at room temperature. The reaction mixture was transferred with dichloromethane (20 mL) to a separatory funnel. The organic phase was washed with water (2 x 120 mL), a saturated aqueous solution of NaCl (100 mL), dried over MgSO₄, filtered and the solvent was removed under reduced pressure (45 °C, 500 mbar). Purification by CC (EtOAc-hexanes 1:10 → 1:2 → 1:1) afforded a yellowish oil (410 mg, 30%).

TLC: *R*_f = 0.28 (EtOAc-hexanes 1:2) [UV]. **¹H-NMR** (400 MHz, CDCl₃, PK-401-B): δ 3.14 (s, 6H), 6.52 (s, 1H), 7.30-7.36 (m, 1H), 7.34-7.41 (m, 1H), 7.61 (ddd, *J* = 8.6, 7.3, 1.6 Hz, 1H), 7.72 (dd, *J* = 7.9, 1.6 Hz, 1H). **¹³C-NMR** (101 MHz, CDCl₃, PK-401-B): δ 39.1, 102.2, 115.1, 117.3, 122.6, 124.6, 133.3, 153.7, 158.4, 161.1. This compound is known to literature, but no analytical data is available.

7.2.1.4 Synthesis of electrophiles

Phenylacetic acid *S*-thiophenylester (CAS 18245-74-4, **PK-378**). The procedure was adapted from the group of Yadav.^[30] **Caution:** prepare an aqueous solution of NaOCl (approx. 3-5%) to eliminate bad smell of glassware. Phenylacetyl chloride (3.86 g, 25.0 mmol, 1.0 eq.) was dissolved in toluene (40 mL). Activated zinc dust (1.64 g, 25.1 mmol, 1.0 eq.) was added. The suspension was stirred for ten

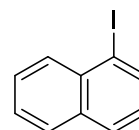


minutes at room temperature before a solution of thiophenol (2.60 mL) in toluene (50 mL) was added dropwise. After 30 minutes at room temperature, the reaction mixture was transferred with diethylether (100 mL) to a separatory funnel. The organic phase was washed with a saturated aqueous solution of NaHCO₃ (150 mL), water (150 mL), a saturated aqueous solution of NaCl (100 mL), dried over MgSO₄, filtered and the solvent was removed under reduced pressure (45 °C, 25 mbar). Purification by CC (pentane-Et₂O 100:0 → 20:1 → 10:1 → 5:1) afforded a white, slightly smelling solid (4.02 g, 70%).

TLC: $R_f = 0.33$ (pentane-Et₂O 20:1) [UV]. **¹H-NMR** (400 MHz, CDCl₃, PK-378-C): δ 3.91 (s, 2H), 7.28 – 7.40 (m, 10H). **¹³C-NMR** (101 MHz, CDCl₃, PK-378-C): δ 50.3, 127.7, 127.9, 128.9, 129.3, 129.5, 129.8, 133.5, 134.6, 195.4. The analytical data matched those reported in literature.^[31]

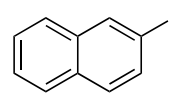
7.2.1.5 Zincation-iodination products from aryl tosylates (table 4)

Example procedure for 1-naphthyl tosylate – preparative scale (CAS 90-14-2, PK-305, 3). A pre-dried ($2 \cdot 10^{-2}$ mbar, heat-gun) Schlenk tube was charged with zinc powder (523 mg, 8.00 mmol, 4.0 eq.), which was dried under vacuum ($2 \cdot 10^{-2}$ mbar) and stirring with a heat-gun. 1,2-Dibromoethane (98%, 35.2 μ L, 75.1 mg, 400 μ mol, 0.2 eq.) was added and the walls were rinsed with dry DMF (2 mL) (heat and gas evolution were observed). After stirring at 60 °C for 20 minutes, the reaction mixture was cooled down to room temperature for five minutes in a water bath. NiCl₂(dme) (22.0 mg, 100 μ mol, 5 mol%) and IPr-MeDAD (80.9 mg, 200 μ mol, 10 mol%) were added and the walls were rinsed with dry DMF (2 mL). The brownish-green suspension was stirred for 30 minutes at room temperature. Finally, the 1-naphthyl tosylate (597 mg, 2.00 mmol, 1.0 eq.) was added, the walls were rinsed with dry DMF (2 mL) and the reaction mixture was stirred for 20 hours at room temperature. Next, it was cooled to 0 °C before adding iodine (2.03 g, 8.00 mmol, 4.0 eq.) and stirring for ten minutes at 0 °C. A saturated aqueous solution of NH₄Cl (10 mL) and solid sodium sulfite (ca. 1 g) were added and the reaction mixture was stirred until most of the brown color had faded. Et₂O (10 mL) was added and the suspension was filtered. Additionally, the pad of Celite was rinsed with Et₂O (3 \times 5 mL). The organic phase was separated, washed with a saturated aqueous solution of NH₄Cl (2 \times 20 mL) and NaCl (20 mL), dried over MgSO₄, filtered and the solvent was removed under reduced pressure (40 °C, 700 mbar). Purification by CC (pentane) afforded a yellowish oil (485 mg, 96%, ArI-ArH 98:2).



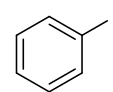
TLC: $R_f = 0.72$ (pentane) [UV]. **$^1\text{H NMR}$** (500 MHz, CDCl_3 , PK-304-A2): δ 7.18 (*virt. t*, $^3J \approx 7.8$ Hz, 1H), 7.49-7.54 (m, 1H), 7.54-7.60 (m, 1H), 7.77 (d, $^3J = 8.0$ Hz, 1H), 7.80-7.87 (m, 1H), 8.04-8.13 (m, 2H). **$^{13}\text{C-NMR}$** (101 MHz, CDCl_3 , PK-304-A2-13C): δ 99.7, 126.9, 127.0, 127.9, 128.7, 129.1, 132.3, 134.3, 134.5, 137.6. The analytical data matched those reported in the literature.^[32]

2-Iodonaphthalene (CAS 612-55-5, PK-382). 2-Naphthyl tosylate (597 mg, 2.00 mmol, 1.0 eq.), activated zinc dust (523 mg, 8.00 mmol, 4.0 eq.), 1,2-dibromoethane (98%, 35.2 μL , 75.1 mg, 400 μmol , 0.2 eq.), $\text{NiCl}_2(\text{dme})$ (22.0 mg, 100 μmol , 5 mol%), IPr-MeDAD (80.9 mg, 200 μmol , 10 mol%) and iodine (2.03 g, 8.00 mmol, 4.0 eq.) in DMF (6 mL) were reacted according to 1.3. Purification by CC (pentane) afforded a pale yellow solid (485 mg, 96%, ArI-ArH = 95:5).



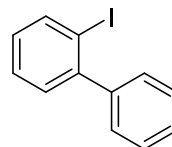
TLC: $R_f = 0.65$ (pentane) [UV]. **$^1\text{H-NMR}$** (400 MHz, CDCl_3 , PK-382-A): δ 7.44-7.52 (m, 2H), 7.56 (d, $^3J = 8.7$ Hz, 1H), 7.66-7.75 (m, 2H), 7.75-7.82 (m, 1H), 8.21-8.26 (m, 1H). **$^{13}\text{C-NMR}$** (101 MHz, CDCl_3 , PK-382-A): δ 91.6, 126.6, 126.8, 126.9, 128.0, 129.6, 132.2, 134.5, 135.1, 136.8. The analytical data matched those reported in the literature.^[33]

Iodobenzene (CAS 591-50-4, PK-314). Phenyl tosylate (497 mg, 2.00 mmol, 1.0 eq.), activated zinc dust (523 mg, 8.00 mmol, 4.0 eq.), 1,2-dibromoethane (98%, 35.2 μL , 75.1 mg, 400 μmol , 0.2 eq.), $\text{NiCl}_2(\text{dme})$ (22.0 mg, 100 μmol , 5 mol%), IPr-MeDAD (80.9 mg, 200 μmol , 10 mol%) and iodine (2.03 g, 8.00 mmol, 4.0 eq.) in DMF (6 mL) were reacted according to 1.3. Purification by CC (pentane) afforded a colorless oil (347 mg, 85%).



TLC: $R_f = 0.89$ (pentane) [UV]. **$^1\text{H-NMR}$** (400 MHz, CDCl_3 , PK-314-N): δ 7.07-7.15 (m, 2H), 7.30-7.36 (m, 1H), 7.66-7.75 (m, 2H). **$^{13}\text{C-NMR}$** (101 MHz, CDCl_3 , PK-314-N): δ 94.5, 127.6, 130.4, 137.6. Analytical data matched those reported in the literature.^[34]

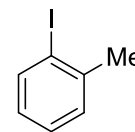
2-Iodobiphenyl (CAS 2113-51-1, PK-320). 2-Biphenyl tosylate (649 mg, 2.00 mmol, 1.0 eq.), activated zinc dust (523 mg, 8.00 mmol, 4.0 eq.), 1,2-dibromoethane (98%, 35.2 μL , 75.1 mg, 400 μmol , 0.2 eq.), $\text{NiCl}_2(\text{dme})$ (22.0 mg, 100 μmol , 5 mol%), IPr-MeDAD (80.9 mg, 200 μmol , 10 mol%) and iodine (2.03 g, 8.00 mmol, 4.0 eq.) in DMF (6 mL) were reacted according to general procedure 1.3. Purification by CC (pentane) afforded colorless oil (550 mg, 98%).



TLC: $R_f = 0.62$ (pentane) [UV]. **$^1\text{H-NMR}$** (400 MHz, CDCl_3 , PK-320-N): δ 7.03 (*virt. td*, $^3J = 7.8$, $^4J \approx 1.8$ Hz, 1H), 7.29-7.45 (m, 7H), 7.96 (dd, $^3J = 8.0$, $^4J = 1.2$ Hz, 1H). **$^{13}\text{C-NMR}$**

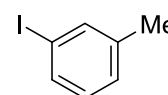
(101 MHz, CDCl₃, PK-320-N): δ 98.8, 127.8, 128.1, 128.2, 128.9, 129.4, 130.2, 139.6, 144.4, 146.8. The analytical data matched those reported in the literature.^[34]

1-Iodo-2-methylbenzene (CAS 615-37-2, PK-357). 2-Methylphenyl tosylate (525 mg, 2.00 mmol, 1.0 eq.), activated zinc dust (523 mg, 8.00 mmol, 4.0 eq.), 1,2-dibromoethane (98%, 35.2 μ L, 75.1 mg, 400 μ mol, 0.2 eq.), NiCl₂(dme) (22.0 mg, 100 μ mol, 5 mol%), IPr-MeDAD (80.9 mg, 200 μ mol, 10 mol%) and iodine (2.03 g, 8.00 mmol, 4.0 eq.) in DMF (6 mL) were reacted according to general procedure 1.3. Purification by CC (pentane) afforded a pinkish oil (413 mg, 95%).



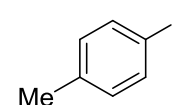
TLC: R_f = 0.84 (pentane) [UV]. **¹H-NMR** (400 MHz, CDCl₃, PK-357-A): δ 2.43 (s, 3H), 6.82-6.90 (m, 1H), 7.21-7.27 (m, 2H), 7.80 (d, ³ J = 7.8 Hz, 1H). **¹³C-NMR** (101 MHz, CDCl₃, PK-357-A): δ 28.3, 101.3, 127.5, 128.3, 129.9, 139.1, 141.5. The analytical data matched those reported in the literature.^[35]

1-Iodo-3-methylbenzene (CAS 615-95-6, PK-364). 3-Methylphenyl tosylate (525 mg, 2.00 mmol, 1.0 eq.), activated zinc dust (523 mg, 8.00 mmol, 4.0 eq.), 1,2-dibromoethane (98%, 35.2 μ L, 75.1 mg, 400 μ mol, 0.2 eq.), NiCl₂(dme) (22.0 mg, 100 μ mol, 5 mol%), IPr-MeDAD (80.9 mg, 200 μ mol, 10 mol%) and iodine (2.03 g, 8.00 mmol, 4.0 eq.) in DMF (6 mL) were reacted according to general procedure 1.3. Purification by CC (pentane) afforded a colorless oil (368 mg, 85%).



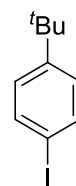
TLC: R_f = 0.81 (pentane) [UV]. **¹H-NMR** (400 MHz, CDCl₃, PK-364-A): δ 2.30 (s, 3H), 6.98 (virt. t, ³ J = 7.8 Hz, 1H), 7.13 (d, ³ J = 7.8 Hz, 1H), 7.49 (d, ³ J = 7.8 Hz, 1H), 7.55 (s, 1H). **¹³C-NMR** (101 MHz, CDCl₃, PK-364-A): δ 21.2, 94.5, 128.5, 130.1, 134.6, 138.2, 140.4. The analytical data matched those reported in the literature.^[35]

1-Iodo-4-methylbenzene (CAS 624-31-7, PK-358). 4-Methylphenyl tosylate (525 mg, 2.00 mmol, 1.0 eq.), activated zinc dust (523 mg, 8.00 mmol, 4.0 eq.), 1,2-dibromoethane (98%, 35.2 μ L, 75.1 mg, 400 μ mol, 0.2 eq.), NiCl₂(dme) (22.0 mg, 100 μ mol, 5 mol%), IPr-MeDAD (80.9 mg, 200 μ mol, 10 mol%) and iodine (2.03 g, 8.00 mmol, 4.0 eq.) in DMF (6 mL) were reacted according to general procedure 1.3. Purification by CC (pentane) afforded a colorless oil (392 mg, 90%).



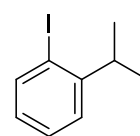
TLC: R_f = 0.89 (pentane) [UV]. **¹H-NMR** (400 MHz, CDCl₃, PK-358-A2): δ 2.29 (s, 4H), 6.88-6.97 (m, 2H), 7.52-7.60 (m, 2H). **¹³C-NMR** (101 MHz, CDCl₃, PK-358-A2): δ 21.2, 90.3, 131.3, 137.4, 137.6. The analytical data matched those reported in the literature.^[35]

4-tert-Butyl-1-iodobenzene (CAS 35779-04-5, PK-356) 4-tert-Butylphenyl tosylate (609 mg, 2.00 mmol, 1.0 eq.), activated zinc dust (523 mg, 8.00 mmol, 4.0 eq.), 1,2-dibromoethane (98%, 35.2 μ L, 75.1 mg, 400 μ mol, 0.2 eq.), NiCl₂(dme) (43.9 mg, 200 μ mol, 10 mol%), IPr-MeDAD (162 mg, 400 μ mol, 20 mol%) and iodine (2.03 g, 8.00 mmol, 4.0 eq.) in DMF (6 mL) were reacted according to general procedure 1.3. Purification by CC (pentane) afforded a colorless oil (396 mg, 76%).



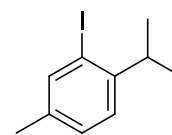
TLC: R_f = 0.75 (pentane) [UV]. **¹H-NMR** (400 MHz, CDCl₃, PK-356-A3): δ 1.29 (s, 9H), 7.10-7.16 (m, 2H), 7.58-7.64 (m, 2H). **¹³C-NMR** (101 MHz, CDCl₃, PK-356-A3): δ 31.3, 34.7, 90.8, 127.7, 137.2, 151.0. The analytical data matched those reported in the literature.^[36]

1-Iodo-2-isopropylbenzene (CAS 19099-54-8, PK-390). 2-Isopropylphenyl tosylate (586 mg, 2.00 mmol, 1.0 eq.), activated zinc dust (523 mg, 8.00 mmol, 4.0 eq.), 1,2-dibromoethane (98%, 35.2 μ L, 75.1 mg, 400 μ mol, 0.2 eq.), NiCl₂(dme) (43.9 mg, 200 μ mol, 10 mol%), IPr-MeDAD (162 mg, 400 μ mol, 20 mol%) and iodine (2.03 g, 8.00 mmol, 4.0 eq.) in DMF (6 mL) were reacted according to general procedure 1.3. Purification by CC (pentane) afforded a pinkish oil (393 mg, 80%).



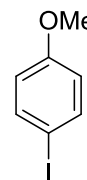
TLC: R_f = 0.80 (pentane) [UV]. **¹H-NMR** (400 MHz, CDCl₃, PK-390-A): δ 1.23 (d, ³ J = 6.8 Hz, 6H), 3.19 (sept, ³ J = 6.8 Hz, 1H), 6.87 (ddd, ³ J = 7.8, 7.1, ⁴ J = 1.8 Hz, 1H), 7.24 (dd, ³ J = 7.8, ⁴ J = 1.8 Hz, 1H), 7.28–7.33 (m, 1H), 7.82 (dd, J = 7.8, 1.3 Hz, 1H). **¹³C-NMR** (101 MHz, CDCl₃, PK-390-A): δ 23.2, 38.2, 101.3, 126.1, 127.8, 128.7, 139.7, 150.5. The analytical data matched those reported in the literature.^[37]

2-Iodo-1-isopropyl-4-methylbenzene (CAS 4395-81-7, PK-366) 2-Isopropyl-4-methylphenyl tosylate (609 mg, 2.00 mmol, 1.0 eq.), activated zinc dust (523 mg, 8.00 mmol, 4.0 eq.), 1,2-dibromoethane (98%, 35.2 μ L, 75.1 mg, 400 μ mol, 0.2 eq.), NiCl₂(dme) (43.9 mg, 200 μ mol, 10 mol%), IPr-MeDAD (162 mg, 400 μ mol, 20 mol%) and iodine (2.03 g, 8.00 mmol, 4.0 eq.) in DMF (6 mL) were reacted according to general procedure 1.3. Purification by CC (pentane) afforded a colorless oil (399 mg, 77%).



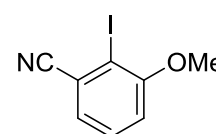
TLC: R_f = 0.86 (pentane) [UV]. **¹H-NMR** (400 MHz, CDCl₃, PK-366-A): δ 1.21 (d, ³ J = 6.8 Hz, 6H), 2.24-2.28 (m, 3H), 3.15 (sept, ³ J = 6.8 Hz, 1H), 7.11-7.13 (m, 2H), 7.64-7.68 (m, 1H). **¹³C-NMR** (101 MHz, CDCl₃, PK-366-A): δ 20.4, 23.3, 37.7, 101.2, 125.6, 129.5, 137.6, 140.0, 147.5. This compound is known to literature, but no analytical data is available.

1-Iodo-4-methoxybenzene (CAS 696-62-8, PK-355). 4-Methoxyphenyl tosylate (557 mg, 2.00 mmol, 1.0 eq.), activated zinc dust (523 mg, 8.00 mmol, 4.0 eq.), 1,2-dibromoethane (98%, 35.2 μ L, 75.1 mg, 400 μ mol, 0.2 eq.), NiCl₂(dme) (22.0 mg, 100 μ mol, 5 mol%), IPr-MeDAD (80.9 mg, 200 μ mol, 10 mol%) and iodine (2.03 g, 8.00 mmol, 4.0 eq.) in DMF (6 mL) were reacted according to general procedure 1.3. Purification by CC (pentane) afforded an off-white solid (389 mg, 83%).



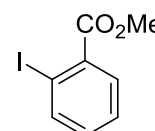
TLC: R_f = 0.21 (pentane) [UV]. **¹H NMR** (400 MHz, CDCl₃, PK-355-A): δ 3.77 (s, 3H), 6.64-6.71 (m, 2H), 7.52-7.58 (m, 2H). **¹³C NMR** (101 MHz, CDCl₃, PK-355-A): δ 55.5, 82.8, 116.5, 138.3, 159.6. The analytical data matched those reported in the literature.^[38]

2-Iodo-3-methoxybenzonitrile (CAS 490039-70-8, PK-315). 2-Cyano-6-methoxyphenyl tosylate (607 mg, 2.00 mmol, 1.0 eq.), activated zinc dust (523 mg, 8.00 mmol, 4.0 eq.), 1,2-dibromoethane (98%, 35.2 μ L, 75.1 mg, 400 μ mol, 0.2 eq.), NiCl₂(dme) (22.0 mg, 100 μ mol, 5 mol%), IPr-MeDAD (80.9 mg, 200 μ mol, 10 mol%) and iodine (2.03 g, 8.00 mmol, 4.0 eq.) in DMF (6 mL) were reacted according to general procedure 1.3. Purification by CC (pentane-Et₂O 10:1 \rightarrow 5:1 \rightarrow 2:1) afforded an off-white solid (443 mg, 86%).



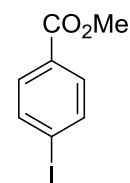
TLC: R_f = 0.22 (pentane-Et₂O 10:1) [UV]. **¹H-NMR** (400 MHz, CDCl₃, PK-315-d): δ 3.93 (s, 3H), 7.00 (dd, ³J = 8.4, ⁴J = 1.3 Hz, 1H), 7.23 (dd, ³J = 7.7, ⁴J = 1.3 Hz, 1H), 7.41 (dd, ³J = 8.4, ⁴J = 7.7 Hz, 1H). **¹³C-NMR** (101 MHz, CDCl₃, PK-315-d): δ 56.9, 91.2, 114.6, 119.5, 122.3, 126.5, 130.1, 159.3. The analytical data matched those reported in the literature.^[39]

Methyl 2-iodobenzoate (CAS 610-97-9, PK-KF-14). Methyl-2-(tosyloxy)benzoate (613 mg, 2.00 mmol, 1.0 eq.), activated zinc dust (523 mg, 8.00 mmol, 4.0 eq.), 1,2-dibromoethane (98%, 35.2 μ L, 75.1 mg, 400 μ mol, 0.2 eq.), NiCl₂(dme) (43.9 mg, 200 μ mol, 10 mol%), IPr-MeDAD (162 mg, 400 μ mol, 20 mol%) and iodine (2.03 g, 8.00 mmol, 4.0 eq.) in DMF (6 mL) were reacted according to general procedure 1.3. Purification by CC (EtOAc-hexanes 1:40) afforded a light-yellow oil (501 mg, 96%).



TLC: R_f = 0.14 (EtOAc-hexanes 1:40) [UV]. **¹H-NMR** (400 MHz, CDCl₃, PK-KF-14-B-2): δ 3.94 (s, 3H), 7.15 (virt. td, ³J = 7.7, ⁴J \approx 1.7 Hz, 1H), 7.40 (virt. td, ³J = 7.7, ⁴J \approx 1.1 Hz, 1H), 7.80 (dd, ³J = 7.8, ⁴J = 1.7 Hz, 1H), 8.00 (dd, ³J = 7.8, ⁴J = 1.1 Hz, 1H). **¹³C-NMR** (101 MHz, CDCl₃, PK-KF-14-B-2): δ 52.6, 94.2, 128.0, 131.1, 132.8, 135.3, 141.5, 167.1. The analytical data matched those reported in the literature.^[40]

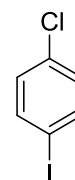
Methyl 4-iodobenzoate (CAS 619-44-3, PK-KF-23). Methyl-4-(tosyloxy)benzoate (613 mg, 2.00 mmol, 1.0 eq.), activated zinc dust (523 mg, 8.00 mmol, 4.0 eq.), 1,2-dibromoethane (98%, 35.2 μ L, 75.1 mg, 400 μ mol, 0.2 eq.), NiCl₂(dme)



(43.9 mg, 200 μ mol, 10 mol%), IPr-MeDAD (162 mg, 400 μ mol, 20 mol%) and iodine (2.03 g, 8.00 mmol, 4.0 eq.) in DMF (6 mL) were reacted according to general procedure 1.3. Purification by CC (DCM-hexanes 1:10) afforded a light-yellow oil (391 mg, 75%).

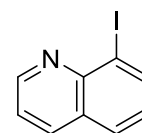
TLC: R_f = 0.11 (DCM-hexanes 1:10) [UV]. **¹H-NMR** (400 MHz, CDCl₃, PK-KF-23-AB): δ 3.91 (s, 3H), 7.72-7.77 (m, 2H), 7.78-7.82 (m, 2H). **¹³C-NMR** (101 MHz, CDCl₃, PK-KF-23-AB): δ 52.4, 100.8, 129.8, 131.2, 137.9, 166.7. The analytical data matched those reported in the literature.^[41]

1-Chloro-4-iodobenzene (CAS 637-87-6, PK-372). 4-Chlorophenyl-*p*-toluene sulfonate (565 mg, 2.00 mmol, 1.0 eq.), activated zinc dust (523 mg, 8.00 mmol, 4.0 eq.), dibromoethane (98%, 35.2 μ L, 75.1 mg, 400 μ mol, 0.2 eq.), NiCl₂(dme)



(22.0 mg, 100 μ mol, 5 mol%), IPr-MeDAD (80.9 mg, 200 μ mol, 10 mol%) and iodine (2.03 g, 8.00 mmol, 4.0 eq.) in DMF (6 mL) were reacted according to general procedure 1.3. Purification by CC (pentane) afforded a pinkish oil (365 mg, 77%, IC₆H₄Cl-C₆H₄I₂-PhI 91:6:3). **TLC:** R_f = 0.84 (pentane) [UV]. **¹H-NMR** (400 MHz, CDCl₃, PK-372-A): δ 7.06-7.11 (m, 2H), 7.57-7.64 (m, 2H). **¹³C-NMR** (101 MHz, CDCl₃, PK-372-A): δ 91.3, 130.7, 134.4, 138.9, 139.5. The analytical data matched those reported in the literature.^[42]

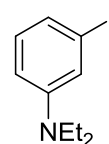
8-Iodoquinoline (CAS 1006-47-9, PK-KF-15) Quinolin-8-yl tosylate (599 mg, 2.00 mmol, 1.0 eq.), activated zinc dust (523 mg, 8.00 mmol, 4.0 eq.), 1,2-dibromoethane (98%, 35.2 μ L, 75.1 mg, 400 μ mol, 0.2 eq.), NiCl₂(dme)



(43.9 mg, 200 μ mol, 10 mol%), IPr-MeDAD (162 mg, 400 μ mol, 20 mol%) and iodine (2.03 g, 8.00 mmol, 4.0 eq.) in DMF (6 mL) were reacted according to general procedure 1.3. Purification by CC (EtOAc-hexanes 1:100) followed by Kugelrohr distillation (160-180 °C, 9 mbar) afforded a yellowish oil (283 mg, 56%).

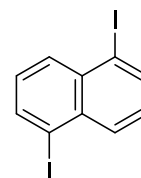
TLC: R_f = 0.19 (EtOAc-hexanes 1:100) [UV]. **¹H-NMR** (400 MHz, CDCl₃, PK-KF-15-dest): δ 7.28 (*virt.* t, ³*J* = 7.7 Hz, 1H), 7.46 (dd, ³*J* = 8.2, 4.2 Hz, 1H), 7.83 (dd, ³*J* = 8.1, ⁴*J* = 1.3 Hz, 1H), 8.11 (dd, ³*J* = 8.2, ⁴*J* = 1.7 Hz, 1H), 8.37 (dd, ³*J* = 7.4, ⁴*J* = 1.3 Hz, 1H), 9.03 (dd, ³*J* = 4.3, ⁴*J* = 1.7 Hz, 1H). **¹³C-NMR** (101 MHz, CDCl₃, PK-KF-15-dest): δ 103.6, 122.1, 127.9, 129.0, 129.0, 137.0, 140.3, 147.3, 151.6. The analytical data matched those reported in the literature.^[43]

***N,N*-Diethyl-3-iodoaniline** (CAS 72375-64-5, **PK-KF-19**). 3-*N,N*-Diethylaminophenyl tosylate (639 mg, 2.00 mmol, 1.0 eq.), activated zinc dust (523 mg, 8.00 mmol, 4.0 eq.), 1,2-dibromoethane (98%, 35.2 μ L, 75.1 mg, 400 μ mol, 0.2 eq.), NiCl₂(dme) (22.0 mg, 100 μ mol, 5 mol%), IPr-M^cDAD (80.9 mg, 200 μ mol, 10 mol%) and iodine (609 mg, 2.40 mmol, 1.2 eq.) in DMF (6 mL) were reacted according to general procedure 1.3. Purification by CC (EtOAc-hexanes 1:100) afforded a yellowish oil (528 mg, 96%).



TLC: R_f = 0.14 (EtOAc-hexanes 1:100) [UV]. **¹H-NMR** (400 MHz, CDCl₃, PK-KF-19-B): δ 1.14 (t, ³ J = 7.1 Hz, 6H), 3.31 (q, ³ J = 7.1 Hz, 4H), 6.56-6.66 (m, 1H), 6.89 (t, ³ J = 7.9 Hz, 1H), 6.92-6.99 (m, 2H). **¹³C-NMR** (101 MHz, CDCl₃, PK-KF-19-B): δ 12.6, 44.4, 96.0, 111.0, 120.5, 124.3, 130.7, 149.1. The analytical data matched those reported in the literature.^[44]

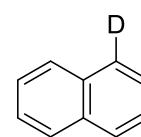
1,5-Diiodonaphthalene (CAS 27715-4-2, **PK-KF-24**) 1,5-Naphthyl ditosylate (937 mg, 2.00 mmol, 1.0 eq.), activated zinc dust (1.04 g, 16.0 mmol, 8.0 eq.), 1,2-dibromoethane (98%, 70.4 μ L, 150 mg, 800 μ mol, 0.4 eq.), NiCl₂(dme) (65.9 mg, 300 μ mol, 15 mol%), IPr-M^cDAD (243 mg, 600 μ mol, 30 mol%) and iodine (4.06 g, 16.0 mmol, 8.0 eq.) in NMP (6 mL) were reacted according to general procedure 1.3. Purification by CC (hexanes) afforded a pale yellow solid (665 mg, 88%).



TLC: R_f = 0.71 (hexanes) [UV]. **¹H-NMR** (400 MHz, CDCl₃, PK-KF-24-A): δ 7.27 (*virt.* t, ³ J = 7.8 Hz, 3H), 8.10-8.16 (m, 4H). **¹³C-NMR** (101 MHz, CDCl₃, PK-KF-24-A): δ 99.8, 128.6, 133.8, 134.8, 138.7. The analytical data matched those reported in the literature.^[45]

7.2.1.6 Reactions of ArZnOTs with electrophiles – reaction products (table 5)

Reaction with D₂O: ***1-(²H)-naphthalene*** (CAS 875-62-7, **PK-302**). 1-Naphthyl tosylate (597 mg, 2.00 mmol, 1.0 eq.), activated zinc dust (523 mg, 8.00 mmol, 4.0 eq.), 1,2-dibromoethane (98%, 35.2 μ L, 75.1 mg, 400 μ mol, 0.2 eq.), NiCl₂(dme) (22.0 mg, 100 μ mol, 5 mol%) and IPr-M^cDAD (80.9 mg, 200 μ mol, 10 mol%) in DMF (6 mL) were reacted according to general procedure 1.3. After catalytic zincation, the reaction mixture was cooled to 0 °C and D₂O (2 mL) was added. After stirring for 15 minutes at 0 °C and 30 minutes at room temperature, a saturated aqueous solution of NH₄Cl (10 mL) and Et₂O (10 mL) were added and the suspension was filtered. The organic phase was separated, washed with a saturated aqueous solution of NH₄Cl (2 \times 20 mL) and NaCl (20 mL), dried over

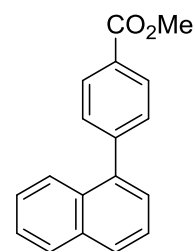


MgSO₄, filtered and the solvent was removed under reduced pressure (40 °C, 700 mbar). Purification by CC (pentane) afforded a white solid (234 mg, 91%, 95% D at C-1).

TLC: $R_f = 0.70$ (pentane) [UV]. **¹H-NMR** (500 MHz, CDCl₃, PK-302-1H): δ 7.44-7.50 (m, 4H), 7.82-7.86 (m, 3H). **²H NMR** (61 MHz, CHCl₃, PK-302-2H) δ 7.93 (br s, 1D). **¹³C-NMR** (101 MHz, CDCl₃, PK-302-13C): δ 125.8, 126.0 (3C), 127.7 (t, ² $J_{C,D} = 24.2$ Hz), 128.0, 128.0 (2C), 133.5, 133.6. The analytical data matched those reported in the literature.^[46]

Negishi coupling: methyl 4-(naphthalen-1-yl)benzoate (CAS 229467-26-9, PK-318).

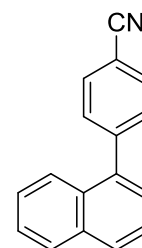
1-Naphthyl tosylate (597 mg, 2.00 mmol, 1.0 eq.), activated zinc dust (523 mg, 8.00 mmol, 4.0 eq.), 1,2-dibromoethane (98%, 35.2 μ L, 75.1 mg, 400 μ mol, 0.2 eq.), NiCl₂(dme) (22.0 mg, 100 μ mol, 5 mol%) and IPr-MeDAD (80.9 mg, 200 μ mol, 10 mol%) in DMF (6 mL) were reacted according to general procedure 1.3. After catalytic zincation, a second pre-dried ($3 \cdot 10^{-2}$ mbar, heat-gun) Schlenk tube was charged with Pd(OAc)₂ (6.7 mg, 20.0 μ mol, 2 mol%), S-Phos (24.6 mg, 40.0 μ mol, 4 mol%) and methyl *p*-iodobenzoate (262 mg, 1.00 mmol, 1.0 eq.) in DMF (3 mL). After stirring for five minutes at room temperature, the above naphthylzinc tosylate solution (4.5 mL) was added dropwise and the brownish reaction mixture was stirred for one hour at room temperature. After quenching with a saturated aqueous solution of NH₄Cl (10 mL) and Et₂O (10 mL), the suspension was filtered. The organic phase was separated, washed with a saturated aqueous solution of NH₄Cl (2 \times 20 mL), aqueous HCl (6 M, 20 mL), water (20 mL) and a saturated aqueous solution of NaCl (20 mL), dried over MgSO₄, filtered and the solvent removed under reduced pressure (40 °C, 190 mbar). Purification by CC (pentane-Et₂O 50:1 \rightarrow 10:1) afforded an off-white solid (250 mg, 95%).



TLC: $R_f = 0.34$ (pentane-Et₂O 20:1) [UV]. **¹H-NMR** (400 MHz, CDCl₃, PK-318-N2): δ 3.97 (s, 3H), 7.39-7.47 (m, 2H), 7.48-7.55 (m, 2H), 7.55-7.59 (m, 2H), 7.81-7.93 (m, 3H), 8.14-8.19 (m, 2H). **¹³C-NMR** (101 MHz, CDCl₃, PK-318-N2): δ 52.3, 125.5, 125.7, 126.1, 126.5, 127.1, 128.4, 128.5, 129.2, 129.7, 130.3, 131.4, 133.9, 139.3, 145.7, 167.2. The analytical data matched those reported in the literature.^[47]

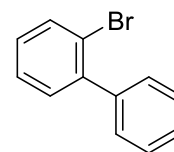
Negishi coupling: 4-(naphthalen-1-yl)benzonitrile (CAS 27331-37-9, PK-319).

1-Naphthyl tosylate (597 mg, 2.00 mmol, 1.0 eq.), activated zinc dust (523 mg, 8.00 mmol, 4.0 eq.), 1,2-dibromoethane (98%, 35.2 μ L, 75.1 mg, 400 μ mol, 0.2 eq.), NiCl₂(dme) (22.0 mg, 100 μ mol, 5 mol%) and IPr-MeDAD (80.9 mg,



200 μmol , 10 mol%) in DMF (6 mL) were reacted according to general procedure 1.3. After catalytic zincation, a second pre-dried ($3 \cdot 10^{-2}$ mbar, heat-gun) Schlenk tube was charged with $\text{Pd}(\text{OAc})_2$ (6.7 mg, 20.0 μmol , 2 mol%), S-Phos (24.6 mg, 40.0 μmol , 4 mol%) and *p*-bromobenzonitrile (182 mg, 1.00 mmol, 1.0 eq.) in DMF (3 mL). After stirring for five minutes at room temperature, the above naphthylzinc tosylate solution (4.5 mL) was added dropwise and the brownish reaction mixture was stirred for one hours at room temperature. After addition of a saturated aqueous solution of NH_4Cl (10 mL) and Et_2O (10 mL), the resulting suspension was filtered. The organic phase was separated, washed with a saturated aqueous solution of NH_4Cl (2×20 mL), aqueous HCl (6 M, 20 mL), water (20 mL) and a saturated aqueous solution of NaCl (20 mL), dried over MgSO_4 , filtered and evaporated under reduced pressure (40 $^\circ\text{C}$, 190 mbar). Purification by CC (pentane- Et_2O 20:1) afforded an off-white solid (215 mg, 94%). **TLC:** $R_f = 0.29$ (pentane- Et_2O 20:1) [UV]. **$^1\text{H-NMR}$** (400 MHz, CDCl_3 , PK-319-N): δ 7.40 (dd, $^3J = 7.0$, $^4J = 1.3$ Hz, 1H), 7.46 (*virt.* ddd, $^3J = 8.3$, 7.0, $^4J = 1.3$ Hz, 1H), 7.50-7.57 (m, 2H), 7.57-7.65 (m, 3H), 7.75-7.81 (m, 3H), 7.90-7.95 (m, 2H). **$^{13}\text{C-NMR}$** (101 MHz, CDCl_3 , PK-319-N): δ 111.3, 119.1, 125.3, 125.5, 126.3, 126.8, 127.2, 128.7, 128.9, 131.0, 131.1, 132.3, 133.9, 138.3, 145.8. The analytical data matched those reported in the literature.^[48]

Bromination with *N*-bromosuccinimide: 2-bromo-1,1'-biphenyl (CAS



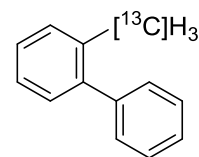
2052-07-5, PK-322). 2-Biphenyl tosylate (649 mg, 2.00 mmol, 1.0 eq.), activated zinc dust (523 mg, 8.00 mmol, 4.0 eq.), 1,2-dibromoethane (98%, 35.2 μL , 75.1 mg, 400 μmol , 0.2 eq.), $\text{NiCl}_2(\text{dme})$ (22.0 mg, 100 μmol , 5 mol%) and IPr-MeDAD (80.9 mg, 200 μmol , 10 mol%) in DMF (6 mL) were reacted according to general procedure 1.3. After catalytic zincation, the reaction mixture was cooled to 0 $^\circ\text{C}$ and *N*-bromosuccinimide (1.42 g, 8.00 mmol, 4.0 eq.) was added. After stirring for ten minutes at 0 $^\circ\text{C}$, a saturated aqueous solution of NH_4Cl (10 mL) and solid sodium sulfite (1.20 g) were added and the reaction mixture was stirred until most of the brown color had faded. Et_2O (10 mL) was added and the suspension was filtered. The organic phase was separated, washed with a saturated aqueous solution of NH_4Cl (2×20 mL) and NaCl (20 mL), dried over MgSO_4 , filtered and the solvent was removed under reduced pressure (40 $^\circ\text{C}$, 700 mbar). Purification by CC (pentane) afforded a yellow oil (445 mg, 96%).

TLC: $R_f = 0.64$ (pentane) [UV]. **$^1\text{H-NMR}$** (400 MHz, CDCl_3 , PK-322-N): δ 7.20 (ddd, $^3J = 8.0$, 6.8, $^4J = 2.3$ Hz, 1H), 7.31-7.46 (m, 7H), 7.65-7.69 (m, 1H). **$^{13}\text{C-NMR}$** (101 MHz,

CDCl₃ PK-322-N): δ 122.8, 127.5, 127.7, 128.1, 128.8, 129.5, 131.4, 133.2, 141.3, 142.7. The analytical data matched those reported in the literature.^[49]

Methylation (and ¹³C labeling) by Negishi coupling: 2-(¹³C)-methyl-1,1'-

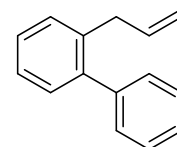
biphenyl (CAS 2399432-56-3, PK-375). 2-Biphenyl tosylate (649 mg, 2.00 mmol, 1.0 eq.), activated zinc dust (523 mg, 8.00 mmol, 4.0 eq.), 1,2-dibromoethane (98%, 35.2 μ L, 75.1 mg, 400 μ mol, 0.2 eq.), NiCl₂(dme) (22.0 mg, 100 μ mol, 5 mol%) and IPr-^{Me}DAD (80.9 mg, 200 μ mol, 10 mol%) in DMF (6 mL) were reacted according to general procedure 1.3. After catalytic zincation, Pd(OAc)₂ (13.5 mg, 60.0 μ mol, 3 mol%) and S-Phos (49.3 mg, 120 μ mol, 6 mol%) were added to the reaction mixture and the walls were rinsed with DMF (600 μ L). Next ¹³C-MeI (190 μ L, 433 mg, 3.03 mmol, 1.5 eq.) was added dropwise and the suspension was stirred for two hours at room temperature. To complete the reaction, another portion of ¹³C-MeI (70.0 μ L, 160 mg, 1.00 mmol, 1.1 eq.) was added dropwise and the reaction mixture was stirred 30 minutes at room temperature. The reaction was quenched with a saturated aqueous solution of NH₄Cl (10 mL) and aqueous HCl (6 M, 4 mL). The suspension was filtered over a pad of Celite (2 cm) and the remaining solid was rinsed with EtOAc (3 \times 5 mL). The organic phase was separated, washed with a saturated aqueous solution of NH₄Cl (2 \times 20 mL) and NaCl (20 mL). After drying over MgSO₄ and filtration, the solvent was removed under reduced pressure (40 $^{\circ}$ C, 150 mbar). Purification by CC (pentane) afforded a colorless oil (317 mg, 94%; Ar¹³CH₃-ArH 87:13).



TLC: R_f = 0.52 (pentane) [UV]. **¹H-NMR** (400 MHz, CDCl₃, PK-375-A2): δ 2.27 (d, ² $J_{H,C}$ = 126.8 Hz, 3H), 7.22-7.29 (m, 4H), 7.30-7.37 (m, 3H), 7.38-7.47 (m, 2H). **¹³C-NMR** (101 MHz, CDCl₃, PK-375-A2): δ 20.6, 125.9, 126.9, 127.4, 128.2, 129.3, 129.9 (d, J = 2.6 Hz), 130.4 (d, J = 3.4 Hz), 135.3, 135.7, 142.1 (dd, J = 3.1, 1.9 Hz). **HRMS** (EI): m/z [M] calcd for [¹²C₁₂¹³CH₁₂]: 169.0967; found 169.0963. This compound is known to literature, but no analytical data is available.

Allylation with allyl bromide: 2-allyl-1,1'-biphenyl (CAS 41658-35-9, PK-376).

2-Biphenyl tosylate (649 mg, 2.00 mmol, 1.0 eq.), activated zinc dust (523 mg, 8.00 mmol, 4.0 eq.), 1,2-dibromoethane (98%, 35.2 μ L, 75.1 mg, 400 μ mol, 0.2 eq.), NiCl₂(dme) (22.0 mg, 100 μ mol, 5 mol%) and IPr-^{Me}DAD (80.9 mg, 200 μ mol, 10 mol%) in DMF (6 mL) were reacted according to general procedure 1.3. After catalytic zincation, Pd(OAc)₂ (13.5 mg, 60.0 μ mol, 3 mol%) and S-Phos (49.3 mg, 120 μ mol,

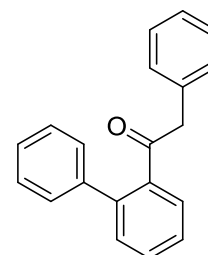


6 mol%) were added to the reaction mixture and the walls were rinsed with DMF (500 μ L). Allyl bromide (350 μ L, 490 mg, 4.05 mmol, 2.0 eq.) was added dropwise at 0 $^{\circ}$ C and the suspension was stirred for one day at room temperature. To assure completion of the reaction, more allyl bromide (350 μ L, 490 mg, 4.05 mmol, 2.0 eq.) was added dropwise at 0 $^{\circ}$ C and the suspension allowed to warm to room temperature over a period of one day. After cooling to 0 $^{\circ}$ C, a saturated aqueous solution of NH_4Cl (10 mL) and ethyl acetate (10 mL) were added. The suspension was filtered over a pad of Celite (2 cm) and the solid was rinsed with ethyl acetate (3 \times 5 mL). The organic phase was separated, washed with a saturated aqueous solution of NH_4Cl (2 \times 20 mL) and NaCl (20 mL), dried over MgSO_4 , filtered and the solvent was removed under reduced pressure (40 $^{\circ}$ C, 120 mbar). Purification by CC (pentane) afforded a colorless oil (356 mg, 92%; ArAllyl-ArH 96:4).

TLC: R_f = 0.52 (pentane) [UV]. **$^1\text{H-NMR}$** (400 MHz, CDCl_3 , PK-376-A): δ 3.34 (virt. dt, 3J = 6.4, $^4J \approx 1.7$ Hz, 2H), 4.92 (virt. dq, 3J = 17.1, $^4J \approx 1.7$ Hz, 1H), 4.98-5.04 (m, 1H), 5.89 (ddt, 3J = 17.1, 10.1, 4J = 6.4 Hz, 1H), 7.22-7.43 (m, 9H). **$^{13}\text{C-NMR}$** (101 MHz, CDCl_3 , PK-376-A): δ 37.6, 115.9, 126.2, 127.0, 127.5, 128.2, 129.4, 129.8, 130.2, 137.4, 137.9, 141.8, 142.1. Analytical data matched those reported in the literature.^[50]

Desulfurative acylation with thioesters: 1-([1,1'-biphenyl]-2-yl)-2-phenylethanone (CAS 229970-97-2, PK-357).

2-Biphenyl tosylate (649 mg, 2.00 mmol, 1.0 eq.), activated zinc dust (523 mg, 8.00 mmol, 4.0 eq.), 1,2-dibromoethane (98%, 35.2 μ L, 75.1 mg, 400 μ mol, 0.2 eq.), $\text{NiCl}_2(\text{dme})$ (22.0 mg, 100 μ mol, 5 mol%) and IPr-MeDAD (80.9 mg, 200 μ mol,

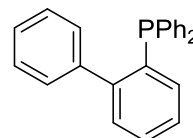


10 mol%) in DMF (6 mL) were reacted according to general procedure 1.3. After catalytic zincation, a second pre-dried ($3 \cdot 10^{-2}$ mbar, heat-gun) Schlenk tube was charged with $\text{Pd}(\text{OAc})_2$ (22.5 mg, 100 μ mol, 10 mol%), S-Phos (82.1 mg, 200 μ mol, 20 mol%) and phenyl thioacetic acid *S*-phenyl ester (228 mg, 1.00 mmol, 1.0 eq.) in DMF (1 mL). After stirring for five minutes at room temperature, the above biphen-2-ylzinc tosylate solution (4.5 mL) was added dropwise and the brownish reaction mixture was stirred five hours at room temperature. The reaction was quenched with 25% aqueous NH_3 (10 mL) and ethyl acetate (10 mL), stirred and the suspension filtered. The organic phase was separated, washed with aqueous NH_3 (25%, 20 mL), an aqueous solution of NaOH (2 M, 2 \times 20 mL), water (20 mL), aqueous HCl (6 M, 20 mL), water (20 mL) and a saturated solution of NaCl (20 mL). After drying over MgSO_4 and filtration, the solvent

was removed under reduced pressure (40 °C, 25 mbar). Purification by CC (EtOAc-hexanes 1:50 → 1:30) afforded a yellow viscous oil (195 mg, 72%).

TLC: $R_f = 0.18$ (EtOAc-hexanes 1:50) [UV]. **$^1\text{H-NMR}$** (500 MHz, CDCl_3 , PK-357-d): δ 3.54 (s, 2H), 6.83-6.91 (m, 2H), 7.15-7.22 (m, 3H), 7.35-7.47 (m, 8H), 7.48-7.52 (m, 1H). **$^{13}\text{C-NMR}$** (75 MHz, CDCl_3 , PK-357-d): δ 49.7, 126.9, 127.6, 128.1, 128.2, 128.4, 129.0, 129.1, 129.7, 130.2, 130.7, 134.2, 140.1, 140.7, 140.8, 205.2. This compound is known to literature, but no analytical data is available.

Phosphination with PPh_2Cl : [1,1'-biphenyl]-2-ylidiphenylphosphane (CAS 13885-09-1, PK-380).

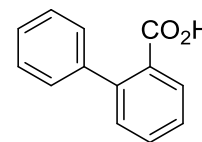


A pre-dried ($2 \cdot 10^{-2}$ mbar, heat-gun) Schlenk tube was charged with zinc powder (523 mg, 8.00 mmol, 4.0 eq.), which was dried under vacuum ($2 \cdot 10^{-2}$ mbar) and stirring with a heat-gun. 1,2-Dibromoethane (98%, 38.3 μL , 76.7 mg, 400 μmol , 0.2 eq.) was added and the walls were rinsed with dry THF (2 mL) (heat and gas evolution were observed). After stirring at 60 °C for 20 minutes, the reaction mixture was cooled down to room temperature for five minutes in a water bath. $\text{NiCl}_2(\text{dme})$ (43.9 mg, 200 μmol , 10 mol%) and IPr-MeDAD (162 mg, 400 μmol , 20 mol%) were added and the walls were rinsed with dry THF (2 mL). The brownish-green suspension was stirred for 30 minutes at room temperature. Finally, the 2-biphenyl tosylate (649 mg, 2.00 mmol, 1.0 eq.) was added, the walls were rinsed with dry THF (2 mL) and the reaction mixture was stirred for 20 hours at room temperature. Zinc dust was allowed to settle down for 30 minutes. In a second pre-dried ($2 \cdot 10^{-2}$ mbar, heat-gun) Schlenk tube PPh_2Cl (110.2 mg, 499 μmol , 1.0 eq.) was dissolved in dry THF (1.5 mL). The above synthesized ArZnOTs (2.4 mL, 1.6 eq.) was added dropwise to the latter after filtration over a PTFE-syringe filter (0.2 μm pore size). $\text{CuCl} \cdot 2\text{LiCl}^{61}$ (1 M in THF, 500 μL , 500 μmol , 1.0 eq.) was added and the brown reaction mixture was stirred for 18 hours at room temperature. Under argon, aqueous ammonia (25%, 10 mL), $\text{Na}_2(\text{EDTA}) \cdot 2\text{H}_2\text{O}$ and EtOAc (10 mL) were added subsequently at 0 °C. The two-phase system was transferred to a separatory funnel and the organic phase was diluted with EtOAc (25 mL). Phases were separated and the organic phase was washed with aqueous ammonia (25%, 2 x 20 mL), water (20 mL) and a saturated aqueous solution of NaCl (20 mL), dried over MgSO_4 , filtered and the solvent was removed under reduced pressure (45 °C, 25 mbar). The crude product was dissolved

⁶¹ CuCl and LiCl (1:2) were dried at 150 °C for three hours under reduced pressure ($< 2 \cdot 10^{-1}$ mbar) and dissolved in THF (1 M) by stirring for 16 hours at room temperature.

in CDCl₃, trichloroethane (200 μL, 2.22 mmol) was added, and the mixture was homogenized by swiveling of the flask. An aliquot (500 μL) was transferred to a NMR tube and ¹H- (20 s delay) as well as ³¹P-NMR (sw = 300 ppm, O₁P = 100 ppm) spectra were recorded. However, the reaction only showed minor conversion and the crude material was discarded.

Zincation under CO₂ atmosphere: biphenyl-2-carboxylic acid (CAS 947-84-2, PK-395). Exemplarily one attempted synthesis procedure is depicted.



2-Biphenyl tosylate (649 mg, 2.00 mmol, 1.0 eq.), activated zinc dust (523 mg, 8.00 mmol, 4.0 eq.), 1,2-dibromoethane (98%, 35.2 μL, 75.1 mg, 400 μmol, 0.2 eq.), NiCl₂(dme) (22.0 mg, 100 μmol, 5 mol%) and IPr-^{Me}DAD (80.9 mg, 200 μmol, 10 mol%) in DMF (6 mL) were reacted according to general procedure 1.3. After addition of the tosylate and stirring for one hour at room temperature, CO₂ was added via a CO₂ filled balloon (approx. 25 mL) and the reaction mixture was stirred for 19 hours at room temperature. A GC-MS sample revealed no conversion to the carboxylic acid as well as minor conversion of the aryl tosylate. Therefore, the reaction was discarded. Other catalyst systems (NiCl₂(dme)+neocuproine 1:2) showed similar results.

7.2.2 The Multifunctional Component Catalyst (MFCC) Principle: Definitions, Screening, and Application

7.2.2.1 General synthesis procedures

The following experiments were performed in headspace vials. With the aid of the appropriate crimping tool, reaction vessels were closed with a butyl rubber septum and an aluminum flip-flop flange cap. Additives present in all experiments of a matrix, HiLo precatalyst mixtures as well as bromobenzene were added as solutions in the indicated solvent. The content was not determined via NMR. Reaction mixtures were flushed with inert gas via a cannula (\varnothing 0.90 mm, color code yellow) by evacuation ($<1.0 \cdot 10^{-1}$ mbar, r.t.) and refilling with argon thrice. Heating was conducted in aluminum blocks. Vials were reopened with the opposite crimping tool.

General procedure 2.1 – 2D matrix screening – arylation of caffeine (general)

In air, a headspace vial was charged with caffeine (97.1 mg, 500 μ mol, 1.0 eq.), catalyst (25.0 μ mol, 5.0 mol%), additive(s) (50.0 μ mol, 10.0 mol% each) and pre-dried K_3PO_4 (212 mg, 1.00 mmol, 2.0 eq.).⁶² The vessel was closed and flushed with argon as indicated in the preface. Solutions of remaining additive(s) (10.0 mol% each) and PhBr (1.5 eq.) in dry DMF were added. The total volume should add up to 1.5 mL. After stirring for five minutes at room temperature, the suspension was heated for 2.5 hours to 100 °C (400 rpm).

a) *flash column chromatography*. At room temperature, reaction mixtures were diluted with DCM–MeOH (10:1, 2 mL) and filtered over a short pad of SiO_2 (~3 cm), eluting with the latter mixture (50 mbar). After removal of the solvent under reduced pressure (45 °C, 10 mbar), a q-NMR (1,3,5-trimethoxybenzene) was conducted according to the general procedure for q-NMR analysis (7.1.3).

b) *fast extraction*. At room temperature, the internal standard, 1,3,5-trimethoxybenzene, was directly weighed to the vial. A saturated aqueous solution of NaCl (2 mL) and EtOAc (3 mL) were added. The vessel was closed as indicated above and shaken until homogeneous distribution was obtained (1-2 min.). A sample was withdrawn for q-NMR analysis (7.1.3).

General procedure 2.2 – 2D matrix screening – arylation of caffeine (HiLo setting)

Preparation of HiLo precatalyst solutions. A pre-dried Schlenk tube ($<1.0 \cdot 10^{-1}$ mbar, heat gun) was charged with three metal precatalysts ($PdCl_2(MeCN)_2$, $NiCl_2(dme)$, $CoBr_2$). The metal on

⁶² In the case of air-sensitive or hygroscopic reagents, weighing should be performed inside a glovebox.

Hi setting (5.0 mol%) will be added on 250 μmol scale, others at Lo loading (0.5 mol%) on 25.0 μmol scale. The walls were rinsed with dry DMF (5 mL) and the mixture was stirred at room temperature until a finely dispersed suspension or solution was obtained (~10 min.). Samples (0.5 mL) for reactions were withdrawn while stirring at room temperature (800 rpm). In air, a headspace vial was charged with caffeine (97.1 mg, 500 μmol , 1.0 eq.), additive(s) (10.0 mol% each) and pre-dried K_3PO_4 (212 mg, 1.00 mmol, 2.0 eq.).⁶² The vessel was closed and flushed with argon as indicated in the preface. Solutions of remaining additive(s) (10.0 mol% each), HiLo precatalyst solution (0.5 mL) and PhBr (1.5 eq.) in dry DMF were added. The total volume should add up to 1.5 mL. After stirring for five minutes at room temperature, the suspension was heated for 2.5 hours to 100 °C (400 rpm). At room temperature, the internal standard, 1,3,5-trimethoxybenzene, was directly weighed to the vial. A saturated aqueous solution of NaCl (2 mL) and EtOAc (3 mL) were added. The vessel was closed as indicated above and shaken until homogeneous distribution was obtained (1-2 min.). A sample was withdrawn for q-NMR analysis (7.1.3).

7.2.1.1 Exemplary procedures

Table 8, $E_{1,2}$, according to general procedure 2.1 (PK-702): In air, a headspace vial was charged with caffeine (97.1 mg, 500 μmol , 1.0 eq.), $\text{PdCl}_2(\text{MeCN})_2$ (6.49 mg, 25.0 μmol , 5.0 mol%), $\text{NBu}_4\cdot\text{HSO}_4$ (17.0 mg, 50.0 μmol , 10.0 mol%) and pre-dried K_3PO_4 (212 mg, 1.00 mmol, 2.0 eq.). The vessel was closed and flushed with argon as indicated in the preface. Solutions of PivOH (0.1 M, 0.5 mL, 50.0 μmol , 10.0 mol%) and PhBr (0.75 M, 1.0 mL, 1.50 mmol, 1.5 eq.) in dry DMF were added. After stirring for five minutes at room temperature, the suspension was heated for 2.5 hours to 100 °C (400 rpm). At room temperature, 1,3,5-trimethoxybenzene (30.3 mg, 180.2 μmol) was directly weighed to the vial. A saturated aqueous solution of NaCl (2 mL) and EtOAc (3 mL) were added. The vessel was closed as indicated above and shaken until homogeneous distribution was obtained (1-2 min.). A sample was withdrawn for q-NMR analysis (7.1.3, NMR file: PK-702-q, AVHD500).

Table 9, $E_{2,3}$, according to general procedure 2.2 (PK-693): *Preparation of HiLo precatalyst solution (Ni Hi, Pd and Co Lo)*. A pre-dried Schlenk tube ($<1.0\cdot 10^{-1}$ mbar, heat gun) was charged with $\text{NiCl}_2(\text{dme})$ (54.9 mg, 250 μmol), $\text{PdCl}_2(\text{MeCN})_2$ (6.49 mg, 25.0 μmol), and CoBr_2 (5.47 mg, 25.0 μmol). The walls were rinsed with dry DMF (5 mL) and the mixture was stirred at room temperature until a finely dispersed suspension or solution was obtained

(~10 min.). Samples for reactions were withdrawn while stirring at room temperature (800 rpm).

In air, a headspace vial was charged with caffeine (97.1 mg, 500 μmol , 1.0 eq.), NBu_4HSO_4 (17.0 mg, 50.0 μmol , 10.0 mol%), PivOH (5.1 mg, 50.0 μmol , 10.0 mol%), and pre-dried K_3PO_4 (212 mg, 1.00 mmol, 2.0 eq.). The vessel was closed and flushed with argon as indicated in the preface. Solutions of 2-pyridone (0.1 M, 50.0 μmol , 10.0 mol%), HiLo precatalyst solution (0.5 mL) and PhBr (1.5 M, 0.5 mL, 1.50 mmol, 1.5 eq.) in dry DMF were added. After stirring for five minutes at room temperature, the suspension was heated for 2.5 hours to 100 $^\circ\text{C}$ (400 rpm). At room temperature, 1,3,5-trimethoxybenzene (42.7 mg, 253.9 μmol) was directly weighed to the vial. A saturated aqueous solution of NaCl (2 mL) and EtOAc (3 mL) were added. The vessel was closed as indicated above and shaken until homogeneous distribution was obtained (1-2 min.). A sample was withdrawn for q-NMR analysis (7.1.3, NMR file: PK-693-q, AVHD500).

7.2.3 Multifunctional Catalyst Component Precursors: The NHC-Pd-Pivalate System

7.2.3.1 General synthesis procedures

General procedure 3.1– Synthesis of IPr-PEPPSI from (IPrH)₂[Pd₂Cl₆]

A headspace vial was charged with (IPrH)₂[Pd₂Cl₆] (1.0 eq.) and base. The walls were rinsed with the indicated solvent. The suspension was stirred at room temperature until complete dissolution was reached. 3-Chloropyridine was added and the resulting suspension was stirred for one day at the indicated temperature. At room temperature, the suspension was diluted with DCM (2 mL) and filtered over a short pad of SiO₂ (~3 cm), eluting with DCM to complete recovering of the complex. The solvent was removed under reduced pressure (45 °C, 7 mbar). A yellowish solid was usually obtained. Trituration with pentane (1 x 6 mL, 1 x 4 mL) and drying under reduced pressure (r.t., <1.0·10⁻¹ mbar) afforded IPr-PEPPSI as pale yellow solid.

General procedure 3.2 – Comparison of imidazolium ¹H-NMR shifts

A NMR tube was tared on an analytical balance (0.01 mg accuracy). Imidazolium salt (12.45 μmol) was weighed directly in the NMR tube.⁶³ The salt was dissolved in the indicated solvent (500 μL, CDCl₃ or [D₆]-acetone) and a proton NMR (d₁ = 20 s, 16 scans, AVHD500) was recorded as soon as possible.

General procedure 3.3 – Suzuki-coupling of *p*-chloroanisole and *p*-toluene boronic acid

The reaction was performed according to a procedure by the group of Jin.^[51] (IPrH)₂[Pd₂Cl₆] (60.24 mg, 50.0 μmol, 0.5 mol%), *p*-toluene boronic acid (163.2 mg, 1.20 mmol, 1.2 eq.) and KO^tBu (134.7 mg, 1.20 mmol, 1.2 eq.) were fitted in a Schlenk tube. After threefold evacuation (1.5·10⁻¹ mbar) and backfilling with argon, *p*-chloroanisole⁶⁴ (142.6 mg, 1.00 mmol, 1.0 eq.) was added. The walls were rinsed with the indicated solvent and the Schlenk tube was closed with a Teflon sleeve and glass stopper. The suspension was stirred for 19 hours at room temperature (600 rpm) before addition of water (7 mL). In the case of copious amounts of black solid, the reaction mixture was filtered over a short pad of Celite, rinsing the latter with Et₂O (3 x 2 mL), and transferred to a separatory funnel. Phases were separated and the aqueous phase was extracted with Et₂O (3 x 20 mL). The combined organic phase was dried over MgSO₄, filtered and the solvent was removed under reduced pressure (45 °C, 6 mbar). A q-NMR

⁶³ A maximum deviation of 0.01 mg was maintained for all weighing processes.

⁶⁴ The electrophile was added via a tared syringe. The difference in mass after addition was used for yield determination/calculation.

(tetrachloroethane: 100 μL , 947.3 μmol) was conducted according to the general procedure for q-NMR analysis (7.1.3).

General procedure 3.4 – α -Arylation of 3-pentanone

The reaction was performed according to a slightly modified procedure by Lu and co-workers.^[52] In a 10 mL Schlenk tube, which was dried under vacuum ($1.2 \cdot 10^{-1}$ mbar) with a heat-gun, palladium catalyst (0.5 mol% in case of dimer, 1.0 mol% in case of monomer), if needed, additive (2.0 mol%) and KO^tBu (2.0 eq.) were added. The tube was evacuated ($1.4 \cdot 10^{-1}$ mbar) and backfilled with argon three times. After addition of toluene (1 mL/mmol) and stirring for two minutes at room temperature, 3-pentanone (2.0 eq.) and 4-chloroanisole (1.0 eq.), were added. The yellow suspension was stirred for three hours at 80 °C (600 rpm) before adding water (2 mL) at room temperature. Next, the reaction mixture was filtered over Celite to remove Pd(0). After dilution with diethyl ether (25 mL/mmol) and water (25 mL/mmol), the organic phase was separated and the aqueous phase was extracted with diethyl ether (2 x 15 mL/mmol). The combined organic phase was dried over MgSO₄, filtered and the solvent was removed under reduced pressure (45 °C, 60 mbar). A q-NMR (tetrachloroethane: 50.0 μL , 473.6 μmol ; 100 μL , 947.3 μmol) was conducted according to the general procedure for q-NMR analysis (7.1.3).

General procedure 3.5 – Heck coupling of aryl bromides with *tert*-butyl acrylate

The reaction was performed according to a procedure by the group of Lu.^[53] Pd-precatalyst (2 mol% referred to Pd) and K₂CO₃ (276 mg, 2.00 mmol, 2.0 eq.) were fitted in a 10 mL Schlenk tube which was evacuated ($1.2 \cdot 10^{-1}$ mbar) and backfilled with argon thrice. Aryl bromide (1.00 mmol, 1.0 eq.) and *tert*-butyl acrylate (175 μL , 1.20 mmol, 1.2 eq.) were added. The walls were rinsed with NMP (400 μL). After stirring at room temperature for one minute, the reaction mixture was stirred for 18 hours at 140 °C (600 rpm). The reaction was allowed to cool to room temperature before adding water (2 mL) and Et₂O (2 mL). Filtration over a short pad of Celite and rinsing of the latter with Et₂O (3 x 2 mL) removed any amount of insoluble (mostly black) solid. The crude material was diluted with water (25 mL) and Et₂O (45 mL) and transferred to a separatory funnel. Phases were separated. The organic phase was washed with water (25 mL) and an aqueous solution of NaCl (25 mL), dried over MgSO₄, filtered and the solvent was removed under reduced pressure (45 °C, 500 mbar). A q-NMR (trichloroethylene: 50.0 μL , 555.6 μmol or tetrachloroethane: 100 μL , 947.3 μmol) was conducted according to the general procedure for q-NMR analysis (7.1.3).

General procedure 3.6 – Domino Sonogashira/hydroalkoxylation – kinetic study

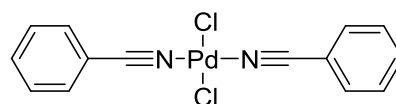
The reaction was performed according to a slightly modified procedure by Peris and coworkers.^[54] A 20 mL Schlenk tube was charged with 2-bromobenzyl alcohol (187.0 mg, 1.00 mmol, 1.0 eq.), Pd(OAc)₂ (2.25 mg, 10.0 μmol, 1.0 mol%), ligand salt (2.0 mol%), K₃PO₄ (637 mg, 3.00 mmol, 3.0 eq.) and 1,4-dimethoxybenzene (71.42 mg, 516.9 μmol) as internal standard. After evacuating ($1.8 \cdot 10^{-1}$ mbar) and backfilling with argon thrice, dry DMSO (5.6 mL) and phenylacetylene (160 μL, 149 mg, 1.45 mmol, 1.5 eq.) were added. The reaction mixture was stirred at 80 °C (600 rpm). Samples (100 – 250 μL) of the brown reaction mixture were added to a vial containing an aqueous HCl solution (2 M, 3 mL) and diethyl ether (3 mL) after 10, 20, 30, 50, and 70 minutes respectively (see 7.1.2 for pictured details). After shaking for ten seconds, the organic phase was transferred to a second vial containing MgSO₄ (150-250 mg). After drying over MgSO₄, the solvent was removed under reduced pressure (water-jet pump, ca. 20 mbar) with the aid of a cannula (Ø 0.90 mm, color code yellow). The walls were rinsed with CDCl₃ (700 μL) and the crude mixture was stirred for two minutes at room temperature. The suspension was filtered over cotton wool into a NMR tube. An ¹H-NMR (delay = 20 s, 16 scans) was measured.^[18] The yield of the reaction was determined by comparison of the integral of the internal standard with the integral of characteristic signals of the reaction product(s) and starting material(s) in the ¹H-NMR spectra.

General procedure 3.7 – Arylation of caffeine

K₃PO₄ (637 mg, 3.00 mmol, 2.0 eq.) was added to a Schlenk tube and dried for 15 minutes in high vacuum ($2 \cdot 10^{-2}$ mbar) with a heat-gun. Caffeine (291 mg, 1.50 mmol, 1.0 eq.), bromobenzene (236 μL, 353 mg, 2.25 mmol, 1.5 eq.), PdCl₂(MeCN)₂ (19.5 mg, 75.0 μmol, 5.0 mol%) and additive (10 mol%) were added under argon and the walls were washed with *N,N*-dimethylformamide (5 mL). The reaction mixture was stirred for five minutes at room temperature, followed by heating for six hours to 100 °C (600 rpm). Samples for kinetic studies were drawn as follows. Stirring of the reaction mixture was stopped one minute before sample drawing. Via a Hamilton syringe a defined volume of the solution (100 μL) was retrieved every hour and diluted with dichloromethane in a volumetric flask (25 mL). The flask was shaken until a homogeneous phase was obtained. Next a sample was taken and measured instantly. For the calculation of the amount of substance present in the reaction mixture, see 7.1.3.

7.2.3.2 Synthesis of multifunctional metal precatalysts

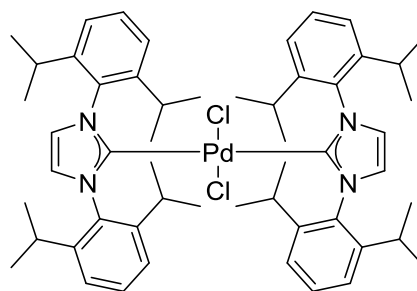
Pd(PhCN)₂Cl₂ (CAS 14220-64-5, PK-516, 34). This compound was synthesized according to a slightly modified



procedure by the group of Munakata.^[55] Benzonitrile (30 mL) was degassed for 20 minutes by bubbling argon via a cannula. Palladium(II) chloride (1.00 g, 5.64 mmol, 1.0 eq.) was added and the suspension was stirred for one hour at 100 °C. The orange suspension was quickly filtered over a pad of Celite and the pad was rinsed with benzonitrile (1 x 10 mL, 2 x 5 mL). After cooling to room temperature, the filtrate was added to pentane (300 mL), which caused precipitation of a yellow orange solid. Filtration, washing with pentane (3 x 100 mL) and drying in air afforded a first batch of yellow orange precatalyst (1.13 g, 50%). The Celite pad (including unreacted PdCl₂) was transferred to Schlenk flask containing degassed benzonitrile (26 mL). The suspension was stirred for an additional hour at 100 °C, quickly filtered and the residue rinsed with benzonitrile (10 mL). After addition to pentane (300 mL), filtration, washing with pentane (3 x 50 mL) and drying in air, a second batch of yellow orange solid (620 mg, 31%) was obtained. Total yield: 1.75 g, 81%.

¹H-NMR (300 MHz, [D₆]-benzene, PK-516-R): δ 6.60-6.69 (m, 4H), 6.76-6.84 (m, 2H), 6.93-7.01 (m, 4H). An additional signal set for mono coordinated Pd complex can be observed in the NMR. This compound is known to literature, but no reference NMR is available.

(IPr)₂PdCl₂ (CAS 852523-60-5, PK-601, 38).^[56] IPr-HCl (223 mg, 525 μmol, 2.1 eq.), palladium(II) chloride (44.3 mg, 250 μmol, 1.0 eq.) and K₂CO₃ (346 mg, 2.50 mmol, 10.0 eq.) were added to a 20 mL Schlenk tube, which afterwards was evacuated (3.1 · 10⁻¹ mbar) and backfilled with argon three times. The walls were rinsed



with toluene (2.5 mL) and the suspension was stirred for 17 hours at 80 °C. After cooling to room temperature, the yellow brown reaction mixture was diluted with dichloromethane (2 mL) and passed through a short pad of silica, eluting with dichloromethane until no further complex was collected. The solvent was removed under reduced pressure (45 °C, 8 mbar) and the residue was washed with pentane (2 x 4 mL). Drying for five hours under reduced pressure (r.t., 2.2 · 10⁻¹ mbar) afforded a yellow solid (197 mg, 83%).

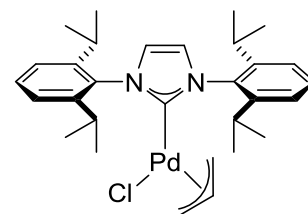
¹H-NMR (400 MHz, CDCl₃, PK-601-A2): δ 0.87 (d, *J* = 6.8 Hz, 24H, CH₃), 0.93 (d, *J* = 6.8 Hz, 24H, CH₃), 2.90 (sept., *J* = 6.8 Hz, 8H, CH(CH₃)₂), 6.71 (s, 4H, NCHCH), 7.07 (d, *J* = 7.8 Hz,

8H, H_{Ar}), 7.35 (t, $J = 7.8$ Hz, 4H, H_{Ar}). $^{13}\text{C-NMR}$ (101 MHz, CDCl_3 , PK-601-A2): δ 23.0, 26.2, 28.3, 123.8, 124.2, 129.3, 136.5, 146.6, 172.8. The analytical data matched those reported in the literature.^[56]

[Pd(allyl)Cl]₂ (CAS 12012-95-2, PK-552, 36). This compound was synthesized according to a procedure by the group of Nolan.^[57] Water (125 mL) was added to a Schlenk flask (3 x evacuated, $1.0 \cdot 10^{-1}$ mbar, and backfilled with argon), the flask was closed with a septum and argon was bubbled for 30 minutes through the water. Palladium(II) chloride (887 mg, 5.00 mmol, 1.0 eq.) and KCl (746 mg, 10.0 mmol, 2.0 eq.) were added under argon flow and the suspension was stirred for one hour at room temperature. Allyl chloride (1.25 mL, 15.3 mmol, 3.1 eq.) was added to the red solution and the reaction mixture was stirred in the dark for one day at room temperature. The orange suspension was transferred to a separatory funnel and extracted with dichloromethane (4 x 50 mL). The organic phase was dried over MgSO_4 , filtered and the solvent was removed under reduced pressure (45 °C, 7 mbar). The obtained solid was dissolved in dichloromethane (5 mL) and precipitation was caused by addition of pentane (25 mL). Filtration, washing with pentane (3 x 25 mL) and drying under reduced pressure (45 °C, 7 mbar) afforded a yellow solid (874 mg, 96%).

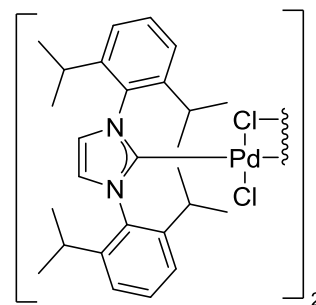
$^1\text{H-NMR}$ (400 MHz, CDCl_3 , PK-552-FS): δ 3.05 (dt, $J = 12.1, 0.7$ Hz, 4H), 4.12 (dt, $J = 6.7, 0.7$ Hz, 4H), 5.47 (tt, $J = 12.1, 6.7$ Hz, 2H). $^{13}\text{C-NMR}$ (101 MHz, CDCl_3 , PK-552-FS): δ 63.1, 111.3. The analytical data matched those reported in the literature.^[58]

[(IPr)Pd(allyl)Cl] (CAS 478980-03-9, PK-553, 37). This compound was synthesized according to a procedure by the group of Sigman.^[59] IPr-HCl (1.71 g, 4.01 mmol, 2.1 eq.), [Pd(allyl)Cl]₂ (700 mg, 1.91 mmol, 1.0 eq.) and KO^tBu (514 mg, 4.58 mmol, 2.4 eq.) were added to a Schlenk tube, which afterwards was evacuated ($1.5 \cdot 10^{-1}$ mbar) and backfilled with argon three times. The walls were rinsed with dry THF (10 mL) and the brown suspension was stirred for 19 hours at room temperature. After transferring to a round bottom flask, the solvent was removed under reduced pressure (45 °C, 8 mbar). Filtration over a short pad of silica, eluting with Et_2O and drying under reduced pressure (r.t., $8.7 \cdot 10^{-2}$ mbar) afforded a fluffy off-white solid (2.13 g, 98%). The product contained diethylether (0.7 wt.%) and tetrahydrofuran (0.4 wt.%).



¹H-NMR (400 MHz, CDCl₃, PK-553-A): δ 1.08 (d, $J = 6.8$ Hz, 6H, CH₃), 1.18 (d, $J = 6.8$ Hz, 6H, CH₃), 1.33 (d, $J = 6.8$ Hz, 6H, CH₃), 1.39 (d, $J = 6.8$ Hz, 6H, CH₃), 1.56-1.59 (m, 1H, H_{All}),⁶⁵ 2.77 (d, $J = 13.6$ Hz, 1H, H_{All}), 2.86 (sept., $J = 6.8$ Hz, 2H, CH(CH₃)₂), 3.01-3.06 (m, 1H, H_{All}), 3.12 (sept., $J = 6.8$ Hz, 2H, CH(CH₃)₂), 3.90 (dd, $J = 7.5, 2.2$ Hz, 1H, H_{All}), 4.73-4.88 (m, 1H, H_{All}), 7.15 (s, 2H, NCHCH), 7.25-7.29 (m, 4H, H_{Ar}), 7.42 (t, $J = 7.8$ Hz, 2H, H_{Ar}). **¹³C-NMR** (101 MHz, CDCl₃, PK-553-A): δ 22.9, 23.1, 25.9, 26.7, 28.7, 28.7, 49.6, 72.7, 114.3, 123.9, 124.0, 124.3, 130.0, 136.0, 146.1, 146.3. The analytical data matched those reported in the literature.^[59]

[(IPr)Pd(μ -Cl)Cl]₂ (CAS 444910-17-2, PK-561, 35). This compound was synthesized according to a procedure by the group of Sigman.^[59] A Schlenk tube containing [(IPr)Pd(allyl)Cl] (286 mg, 500 μ mol, 1.0 eq.) was evacuated ($1.9 \cdot 10^{-1}$ mbar) and backfilled with argon three times. An ethereal solution of HCl (1 M in Et₂O, 5 mL) was added and the suspension was stirred for one hour at room

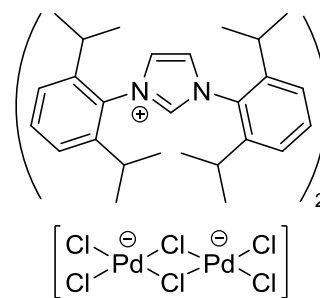


temperature. Gas evolution could be observed immediately after addition. The solvent was slowly removed with the aid of a water-jet vacuum pump before drying for 30 minutes at elevated water flow (ca. 20 mbar). The solid was dissolved in chloroform, transferred to a flask and the solvent was removed under reduced pressure (40 °C, 8 mbar). Washing with Et₂O (1 x 3 mL, 1 x 2 mL) and drying under reduced pressure (r.t., $8.3 \cdot 10^{-2}$ mbar) afforded a bright orange solid (261 mg, 92%).

¹H-NMR (500 MHz, CDCl₃, PK-561-R): δ 1.00 (br d, $J = 36.1$ Hz, 24H, CH₃), 1.31 (br d, $J = 53.1$ Hz, 24H, CH₃), 2.60 (br s, 4H, CH(CH₃)₂), 2.86 (br s, 4H, CH(CH₃)₂), 6.98 (s, 4H, NCHCH), 7.22-7.41 (m, 8H, H_{Ar}), 7.54 (t, $J = 7.8$ Hz, 4H, H_{Ar}). **¹³C-NMR** (75 MHz, CDCl₃, PK-516-13C): δ 23.4, 26.4, 28.8, 124.4, 125.4, 130.5, 134.4, 146.4-146.7 (m), 148.1. The analytical data matched those reported in the literature.^[60]

⁶⁵ Signal overlays with water (HDO) from the deuterated solvent.

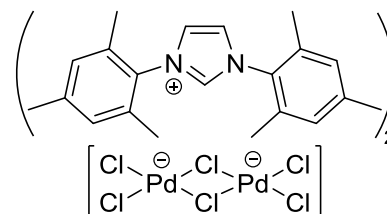
(*IPrH*)₂[Pd₂Cl₆] (**PK-534, 16**). Palladium(II) chloride (887 mg, 5.00 mmol, 1.0 eq.) and IPr·HCl (2.13 g, 5.00 mmol, 1.0 eq.) were suspended in acetone (37.5 mL) and stirred for one day at room temperature. The dark-red solution was filtered over a short pad of Celite, the pad was rinsed with acetone (3 x 4 mL) and the solvent was removed under reduced pressure (45 °C, 200 mbar), affording



a dark-red oil. After triturating with diethylether (15 mL) and scratching with a spatula, a red solid crystallized. The crystalline material was filtered off and washed with diethylether (2 x 10 mL) and pentane (2 x 15 mL). Drying under vacuum (r.t., 9.8·10⁻² mbar) afforded a red crystalline solid (2.98 g, 99%). Suitable single crystals for X-ray analysis (KlePh1) were grown by slow diffusion of diethylether into a saturated solution of the product in ethanol.

¹H-NMR (300 MHz, [D₆]-acetone, PK-534-R): δ 1.27 (d, *J* = 6.8 Hz, 12H, CH₃), 1.33 (d, *J* = 6.8 Hz, 12H, CH₃), 2.61 (sept., *J* = 6.8 Hz, 4H, CH(CH₃)₂), 7.55 (d, *J* = 7.7 Hz, 3H, H_{Ar}), 7.72 (*virt. t.*, *J* = 7.7 Hz, 2H, H_{Ar}), 8.47 (d, *J* = 1.6 Hz, 2H, N(CH)₂N), 9.83 (t, *J* = 1.6 Hz, 1H, NCHN). ¹³C-NMR (75 MHz, [D₆]-acetone, PK-006-N): δ 23.9, 24.7, 29.9, 125.7, 127.6, 131.1, 133.1, 139.5, 146.1. **Analysis** calcd for C₅₄H₇₄Cl₆N₄Pd₂ C 53.84, H 6.19, N 4.65; found C 53.83, H 6.36, N 4.51.

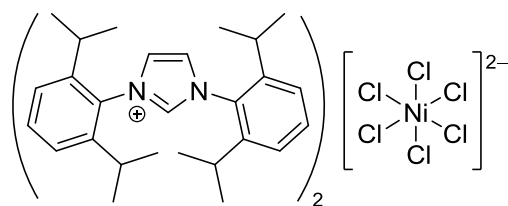
(*IMesH*)₂[Pd₂Cl₆] (**PK-040, 17**). Palladium(II) chloride (35.5 mg, 200 μmol, 1.0 eq.) and IMes·HCl (68.2 mg, 200 μmol, 1.0 eq.) were suspended in acetone (2 mL) and stirred for one day at room temperature. The red solution was



filtered over Celite, the pad was rinsed with acetone (3 x 2 mL) and the solvent was removed under reduced pressure (45 °C, 200 mbar), affording a red solid. After washing with diethylether (3 x 2 mL) and drying under vacuum (r.t., 8.5·10⁻² mbar) a dark-red solid (96.4 mg, 93%) was obtained. Suitable single crystals for X-ray analysis (KlePh2) were grown by slow diffusion of diethylether into a saturated solution of (IMesH)₂[PdCl₄] in ethanol.

¹H-NMR (500 MHz, [D₆]-acetone, PK-040-N): δ 2.26 (s, 12H, *o*-CH₃), 2.42 (s, 6H, *p*-CH₃), 7.24 (s, 4H, H_{Ar}), 8.21 (d, *J* = 1.6 Hz, 2H, NCHCH), 9.62 (t, *J* = 1.6 Hz, 1H, NCHN). ¹³C-NMR (75 MHz, [D₆]-acetone, PK-040-N): δ 17.7, 21., 126.1, 130.6, 132.0, 135.5, 139.3, 142.2. **Analysis** calcd for C₄₂H₅₀Cl₆N₄Pd₂ C 48.67, H 4.86, N 5.41; found 48.35, H 4.99, N 5.66.

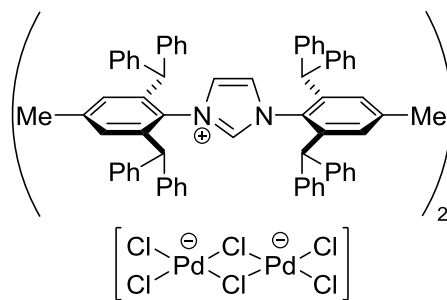
(*IPrH*)₂[NiCl₆] (**PK-490**). NiCl₂·6H₂O (23.8 mg, 100 μmol, 1.0 eq.) and IPr·HCl (42.5 mg, 100 μmol, 1.0 eq.) were suspended in acetone (1 mL) and stirred for nine hours at room temperature. The light blue



solution was filtered over a short pad of Celite, the pad was rinsed with acetone (3 x 3 mL) and the solvent was removed under reduced pressure (45 °C, 7 mbar). A light blue solid (51.6 mg, >100%) was obtained. Due to high deliquescence, the solid should be stored under argon. The depicted structure is only supposed but not verified by elemental analysis or X-ray diffraction. Further applications were not conducted

¹H-NMR (500 MHz, [D₆]-acetone, PK-490-R): δ 1.19 (d, *J* = 6.7 Hz, 12H, CH₃), 1.43 (d, *J* = 6.7 Hz, 12H, CH₃), 2.21 (sept., *J* = 6.7 Hz, 4H, CH(CH₃)₂), 6.29-6.95 (m, 2H, NCHCH), 7.44-7.52 (m, 4H, H_{Ar}), 7.61-7.73 (m, 2H, H_{Ar}), 8.84-9.09 (m, 1H, NCHN).

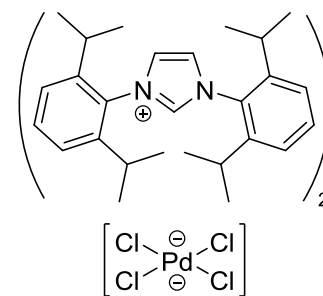
(*IPr*H*)[Pd₂Cl₆] (**PK-897, 20**). Palladium(II) chloride (88.6 mg, 500 μmol, 1.0 eq.) and IPr*·HCl (475 mg, 500 μmol, 1.0 eq.) were suspended in dichloromethane (4 mL) and stirred for 20 hours at room temperature. The red solution was filtered over Celite, the pad was rinsed with dichloromethane (3 x 1 mL) and the solvent was



removed under reduced pressure (45 °C, 8 mbar), affording a dark red solid. After washing with pentane (3 x 5 mL) and drying under reduced pressure (r.t., 2.7·10⁻² mbar), a red solid (535 mg, 95%) was obtained. Suitable single crystals for X-ray analysis (KlePh19) were obtained by slow diffusion of diethylether into a saturated solution of the product in dichloromethane. The product contains dichloromethane (1 wt.%)

¹H-NMR (400 MHz, CDCl₃, PK-897-R2): δ 2.30 (s, 6H, CH₃), 5.27 (s, 4H, CH(Ph)₂), 5.34 (s, 2H, NCHCH), 6.68-6.89 (m, 12H, H_{Ar}), 7.03-7.24 (m, 16H, H_{Ar}), 7.27-7.41 (m, 16H, H_{Ar}), 11.14 (br s, 1H, NCHN). ¹³C-NMR (101 MHz, CDCl₃, PK-892-N2): δ 22.3, 51.5, 123.4, 126.9, 127.1, 128.6, 128.9, 129.4, 130.1, 130.4, 131.3, 140.6, 141.3, 141.7, 142.0, 143.1. **Analysis** calcd for C₁₃₈H₁₁₄Cl₆N₄Pd₂ C 73.54, H 5.10, N 2.49; found 73.03, H 5.04, N 2.51.

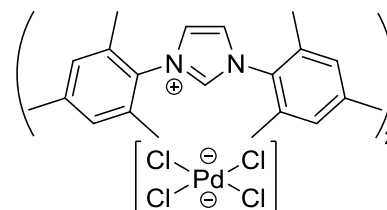
(IPrH)₂[PdCl₄] (PK-011, 18). Palladium(II) chloride (88.8 mg, 500 μmol, 1.0 eq.) and IPr·HCl (425 mg, 1.00 mmol, 2.0 eq.) were suspended in acetone (5 mL) and stirred for two days at room temperature. The resulting red solution was filtered over Celite, the pad was rinsed with acetone (3 x 2 mL) and the solvent was removed under reduced pressure (45 °C, 200 mbar), affording a pale red solid.



After washing with diethylether (10 mL) and pentane (10 mL) and drying under vacuum (r.t., $9.8 \cdot 10^{-2}$ mbar), a light red solid (497 mg, 97%) was obtained.

¹H-NMR (300 MHz, [D₆]-acetone, PK-011-N): δ 1.27 (d, $J = 6.8$ Hz, 24H, CH₃), 1.31 (d, $^3J = 6.8$ Hz, 24H, CH₃), 2.61 (sept., $J = 6.8$ Hz, 8H, CH(CH₃)₂), 7.51 (d, $J = 7.7$ Hz, 8H, H_{Ar}), 7.67 (*virt. t.*, $J = 7.7$ Hz, 4H, H_{Ar}), 8.47 (d, $J = 1.6$ Hz, 4H, NCHCH), 10.61 (t, $J = 1.6$ Hz, 2H, NCHN). **¹³C-NMR** (75 MHz, [D₆]-acetone, PK-011-N): δ 23.9, 24.8, 29.9, 125.5, 127.4, 131.4, 132.8, 140.5, 146.2. **Analysis** calcd for C₅₄H₇₄Cl₄N₄Pd C 63.13, H 7.26, N 5.45; found C 62.74, H 7.38, N 5.26.

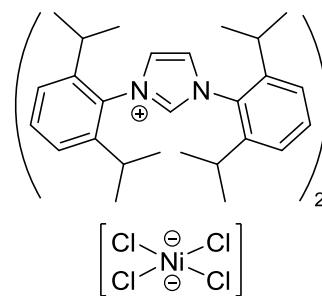
(IMesH)₂[PdCl₄] (PK-041, 19). Palladium(II) chloride (35.5 mg, 200 μmol, 1.0 eq.) and IMes·HCl (136 mg, 400 μmol, 2.0 eq.) were suspended in acetone (2.5 mL) and stirred for two days at room temperature. The resulting red



solution was filtered over Celite, the pad was rinsed with acetone (3 x 2 mL) and the solvent was removed under reduced pressure (45 °C, 200 mbar), affording a light red oil. After triturating with pentane (7 mL) and scratching with a spatula, a light red solid crystallized. The crystalline material was filtered off and washed with diethylether (10 mL) and pentane (10 mL). Drying under vacuum ($9.8 \cdot 10^{-2}$ mbar) afforded a light red crystalline solid (169 mg, 99%). Single crystals for X-ray analysis (KlePh2) were grown by slow diffusion of diethylether into a saturated solution of the product in ethanol. However, the material crystallized turned out to be (IMesH)₂[Pd₂Cl₆], as shown by the crystal structure analysis.

¹H-NMR (500 MHz, [D₆]-acetone, PK-041-N): δ 2.23 (s, 12H, *o*-CH₃), 2.37 (s, 6H, *p*-CH₃), 7.14 (s, 4H, H_{Ar}), 8.20 (d, $J = 1.6$ Hz, 2H, NCHCH), 10.29 (t, $J = 1.6$ Hz, 1H, NCHN). **¹³C-NMR** (75 MHz, [D₆]-acetone, PK-041-N): δ 17.8, 21.2, 126.0, 130.4, 132.2, 135.5, 140.2, 141.7. **Analysis** calcd for C₄₂H₅₀Cl₄N₄Pd C 57.51, H 5.98, N 6.39; found C 57.72, H 5.92, N 6.32.

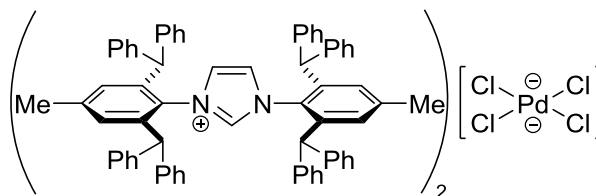
(*IPrH*)₂[NiCl₄] (**PK-491**). NiCl₂·6H₂O (23.8 mg, 100 μmol, 1.0 eq.) and *IPr*·HCl (85.0 mg, 200 μmol, 2.0 eq.) were suspended in acetone (1 mL) and stirred for nine hours at room temperature. The dark blue solution was filtered over Celite, the pad was rinsed with acetone (3 x 3 mL) and the solvent was removed under reduced pressure (45 °C, 7 mbar). A dark blue solid (103 mg, 105%) was obtained.



The high yield is due to the deliquescence of the solid which should be stored under argon. Further analysis as well as applications were not conducted.

¹H-NMR (500 MHz, [D₆]-acetone, PK-491-R): δ 1.19 (d, *J* = 6.8 Hz, 12H, CH₃), 1.42 (d, *J* = 6.8 Hz, 12H, CH₃), 2.25 (sept., *J* = 6.8 Hz, 4H, CH(CH₃)₂), 6.84 (s, 2H, NCHCH), 7.48 (d, *J* = 7.8 Hz, 4H, H_{Ar}), 7.67 (t, *J* = 7.8 Hz, 2H, H_{Ar}), 9.21 (s, 1H, NCHN). The catalyst salt is already reported in the literature, but spectroscopic data differs from ours.^[61]

(*IPr*H*)[Pd₂Cl₆] (**PK-898, 2I**). Palladium(II) chloride (44.3 mg, 250 μmol, 1.0 eq.) and *IPr**·HCl (475 mg, 500 μmol, 2.0 eq.) were suspended in dichloromethane (4 mL) and



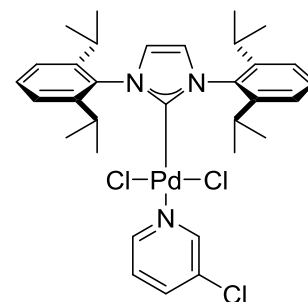
stirred for 48 hours at room temperature. The suspension was filtered over a suction filter and the remaining solid was washed with dichloromethane (3 x 2 mL) and pentane (3 x 3 mL). After drying in air, a light pink solid (472 mg, 91%) was obtained. Slow diffusion of diethylether into a saturated solution of the product in chloroform afforded suitable single crystals for X-ray analysis of (*IPr*H*)₂[Pd₂Cl₆].

¹H-NMR (500 MHz, [D₆]-dimethylsulfoxide, PK-898-DMSO): δ 2.23 (s, 6H, CH₃), 4.90 (s, 4H, CH(Ph)₂), 6.80-6.90 (m, 8H, H_{Ar}), 6.90-6.96 (m, 8H, H_{Ar}), 6.97 (s, 4H, H_{Ar}), 7.18-7.34 (m, 24H, H_{Ar}), 10.77 (t, *J* = 1.6 Hz, 1H, NCHN). ¹³C-NMR (101 MHz, (D₆)-dimethylsulfoxide, PK-898 13C DMSO): δ 21.3, 50.9, 125.3, 127.1, 127.3, 128.7, 128.8, 128.8, 129.0, 129.6, 130.0, 140.0, 141.3, 141.5, 141.7. ¹H-NMR (500 MHz, CDCl₃, PK-898-CDCl₃): δ 2.23 (s, 6H, CH₃), 5.29 (s, 4H, CH(Ph)₂), 5.40 (d, *J* = 1.3 Hz, 2H, NCHCH), 6.70-6.84 (m, 12H), 7.04-7.22 (m, 16H, H_{Ar}), 7.22-7.38 (m, 16H, H_{Ar}), 12.07 (s, 1H, NCHN)⁶⁶. ¹³C-NMR (101 MHz, CDCl₃, PK-898 13C CDCl₃): δ 22.1, 51.4, 123.4, 127.0, 128.6, 128.8, 129.4, 130.2, 130.3, 131.1,

⁶⁶ Partial H/D exchange with the deuterated solvent.

140.7, 141.6, 142.0, 142.9. **Analysis** calcd for C₁₃₈H₁₁₄Cl₄N₄Pd C 79.82, H 5.53, N 2.70; found 78.44, H 5.53, N 2.72.

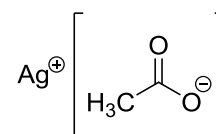
IPr-PEPPSI (CAS 2387902-68-1, PK-551, 22). Palladium(II) chloride (177 mg, 1.00 mmol, 1.0 eq.) and IPrHCl (425 mg, 1.00 mmol, 1.0 eq.) were suspended in acetone (4 mL) and stirred for one day at room temperature, providing a dark-red solution. Next, K₂CO₃ (207 mg, 1.5 mmol, 1.5 eq.) and 3-Cl-pyridine (240 μL, 287 mg, 2.52 mmol, 2.5 eq.) were added and the orange suspension



was stirred for one day at 40 °C. After cooling to room temperature, the orange suspension was diluted with dichloromethane (4 mL), passed through a short pad of silica gel eluting with dichloromethane until the product was completely recovered. After removing the solvent under reduced pressure (45 °C, 8 mbar), the remaining solid was washed with pentane (3 x 10 mL) and dried under vacuum (8.7·10⁻² mbar). A pale-yellow solid (634 mg, 93%) was obtained.

¹H-NMR (400 MHz, CDCl₃, PK-551-A): δ 1.12 (d, *J* = 6.8 Hz, 12H, CH₃), 1.48 (d, ³*J* = 6.8 Hz, 12H, CH₃), 3.16 (sept., *J* = 6.8 Hz, 4H, CH(CH₃)₂), 7.07 (ddd, *J* = 8.2, 5.5, 0.5 Hz, 1H, H_{py}), 7.14 (s, 2H, NCHCH), 7.35 (d, *J* = 7.8 Hz, 4H, H_{Ar}), 7.47-7.52 (m, 2H), 7.55 (ddd, *J* = 8.2, 2.4, 1.4 Hz, 1H, H_{py}), 8.52 (dd, ³*J* = 5.5, 1.4 Hz, 1H,), 8.60 (dd, *J* = 2.4, 0.5 Hz, 2H,).
¹³C-NMR (101 MHz, CDCl₃, PK-551-A2): δ 23.4, 26.5, 28.9, 124.2, 124.5, 125.3, 130.5, 132.1, 135.1, 137.6, 146.8, 149.5, 150.6, 153.6. The analytical data matched those reported in the literature.^[62]

Ag(OAc) (CAS 563-63-3, KH-17, 31). In the dark, silver carbonate (10.0 g, 36.3 mmol, 1.0 eq.) was suspended in toluene (50 mL). Acetic acid (6.6 mL, 108 mmol, 3.0 eq.) was added and the suspension was stirred for three hours

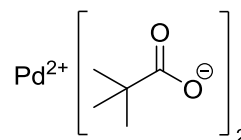


at room temperature under the exclusion of light. The white precipitate was filtered off, washed with diethylether (3 x 50 mL) and dried under reduced pressure (r.t., <1.0·10⁻¹ mbar).⁶⁷ A white fluffy solid (11.9 g, 98%) was obtained. The solid was stored in a brown glass covered with aluminium foil at a dark place (under the hood).

Analysis calcd for C₂H₃AgO₂ C 14.39, H 1.81; found C 14.33, H 1.73. This compound is known to literature.^[63]

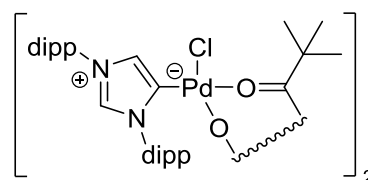
⁶⁷ The flask was covered in aluminum foil to prevent decomposition of the salt.

Pd(OPiv)₂ (CAS 106224-36-6, *LK-16*, **32**). PdCl₂ (71.1 mg, 401 μmol, 1.0 eq.) and KCl (62.8 mg, 842 μmol, 2.1 eq.) were dissolved in water (6 mL). After stirring for 30 minutes at room temperature, NaOPiv (109 mg, 880 μmol, 2.2 eq.) and Et₂O (6 mL) were added. The two-phase mixture was stirred for 20 minutes at room temperature before the organic phase was separated to a second flask with the aid of a syringe. The aqueous phase was extracted twice with Et₂O (6 mL) following the described procedure. After the final extraction, AgOPiv⁶⁸ (37.0 mg, 177 μmol, 0.4 eq.) was added to the second flask and the dark orange suspension was stirred for one hour at room temperature under exclusion of light. Filtration over a short plug of silica⁶⁹ (6 cm, Et₂O) and removal of the solvent under reduced pressure (45 °C, 8 mbar) afforded Pd(OPiv)₂ (55.3 mg, 45%) as orange, crystalline solid.



Analysis calcd for C₁₀H₁₈O₄Pd C 38.91, H 5.88; found C 39.00, H 5.91. This compound is a known compound.^[64]

(^mIPr)₂Pd₂Cl₂(μ-OPiv)₂ (*PK-117*, **33**). A suspension of palladium(II) chloride (177 mg, 1.00 mmol, 1.0 eq.) and IPr·HCl (425 mg, 1.00 mmol, 1.0 eq.) in acetone (10 mL) was stirred for one day at room temperature. The red solution was filtered through a cotton plug to remove residual palladium and the solvent was concentrated (approx. 7 mL, 45 °C, 450 mbar). Next, sodium pivalate (372 mg, 3.00 mmol, 3.0 eq.) and acetone (5 mL) were added and the suspension was stirred for four hours at room temperature. The resulting dark yellow suspension was filtered through a plug of Celite, the solids washed with acetone (3 x 5 mL) and the filtrate evaporated under reduced pressure (45 °C, min. pressure 8 mbar). A dark yellow solid was collected. Dissolution in dichloromethane (15 mL) followed by filtration through a plug of Celite to remove further insoluble palladium rests and evaporation to dryness (45 °C, 8 mbar) afforded a bright yellow solid (347 mg, 55% over two steps). Suitable single crystals for X-ray analysis (KlePh3) were grown by slow evaporation of a saturated solution of the product in dichloromethane.



¹H-NMR (400 MHz, [D₂]-dichloromethane, PK-117-13C): δ 0.89 (s, 18H, C(CH₃)₃), 1.02-1.09 (m, 18H, CH(CH₃)₂), 1.12 (d, *J* = 6.7 Hz, 6H, CH(CH₃)₂), 1.15 (d, *J* = 6.7 Hz, 6H, CH(CH₃)₂),

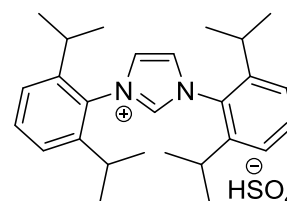
⁶⁸ Previously synthesized during my master thesis.

⁶⁹ Only collected the first colored band.

1.29 (d, $J = 6.7$ Hz, 6H, $\text{CH}(\text{CH}_3)_2$), 1.34 (d, $J = 6.5$ Hz, 6 H, $\text{CH}(\text{CH}_3)_2$), 1.81 (d, $J = 6.5$ Hz, 6H, $\text{CH}(\text{CH}_3)_2$), 2.29 (sept., $J = 6.7$ Hz, 2H, $\text{CH}(\text{CH}_3)_2$), 2.55-2.73 (m, 4H, $\text{CH}(\text{CH}_3)_2$), 3.33 (sept., $J = 6.7$ Hz, 2H, $\text{CH}(\text{CH}_3)_2$), 7.24 (d, $J = 7.8$ Hz, 2H, H_{Ar}), 7.28-7.35 (m, 4H, H_{Ar}), 7.48 (t, $J = 7.8$ Hz, 2H, H_{Ar}), 7.53-7.61 (m, 4H, H_{Ar}), 7.69 (d, $J = 1.9$ Hz, 2H, H_{Im}), 7.82 (d, $J = 1.9$ Hz, 2H, H_{Im}). $^{13}\text{C-NMR}$ (101 MHz, $[\text{D}_2]$ -dichloromethane, PK-117-13C): δ 23.7, 23.8, 24.3, 24.6, 24.9, 25.8, 25.9, 27.3, 28.4, 28.8, 28.9, 29.1, 29.3, 40.4, 124.6, 124.8, 125.1, 127.1, 128.7, 130.6, 131.4, 131.7, 134.9, 135.1, 145.5, 146.8, 146.9, 188.5. **Analysis** calcd for $\text{C}_{64}\text{H}_{90}\text{Cl}_2\text{N}_4\text{O}_4\text{Pd}_2$ C 60.85, H 7.18, N 4.44; found C 60.85, H 7.32, N 4.53.

7.2.3.3 Synthesis of imidazolium salts

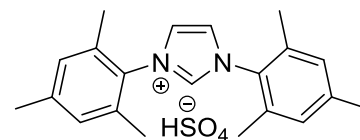
***IPr-HSO₄* (LR-016, 23).** A suspension of *p*-formaldehyde (1.75 g, 58.4 mmol, 1.1 eq.) and IPr-DAD (20.0 g, 53.1 mmol, 1.0 eq.) in ethyl acetate (520 mL) was heated to 70 °C. Upon addition of an ethereal solution of sulfuric acid (1 M in Et₂O, 53.1 mL, 53.1 mmol, 1.0 eq.)



over 15 minutes, the yellow suspension turned reddish. After stirring for one hour at 70 °C, a white precipitate formed. Next, the suspension was stirred for 15 minutes at 0 °C. The solid was filtered and washed with diethyl ether (3 x 20 mL). Drying for 16 hours at 100 °C in an oven afforded a pale beige to white powder (22.6 g, 87%).

$^1\text{H-NMR}$ (500 MHz, $[\text{D}_6]$ -acetone, PK-046-N): δ 1.25 (d, $J = 6.9$ Hz, 12H, $\text{CH}(\text{CH}_3)_2$), 1.30 (d, $^3J = 6.8$ Hz, 12H, $\text{CH}(\text{CH}_3)_2$), 2.60 (sept., $J = 6.9$ Hz, 4H, $\text{CH}(\text{CH}_3)_2$), 7.51 (d, $J = 7.8$ Hz, 4H, H_{Ar}), 7.67 (*virt.* t, $J = 7.8$ Hz, 2H, H_{Ar}), 8.50 (d, $J = 1.6$ Hz, 2H, NCHCH), 9.88 (t, $J = 1.6$ Hz, 1H, NCHN). $^{13}\text{C-NMR}$ (75 MHz, $[\text{D}_6]$ -acetone, PK-046-N): δ 23.9, 24.6, 125.5, 127.8, 131.3, 132.8, 139.6, 146.2. **Analysis** calcd for $\text{C}_{26}\text{H}_{35}\text{N}_2\text{O}_4\text{S}$ C 66.21, H 7.48, N 5.94, S 6.80; found C 66.66, H 7.89, N 5.76 S 6.31.

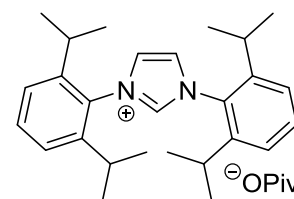
***IMes-HSO₄* (LR-020XVII).** A suspension of *p*-formaldehyde (41.3 mg, 1.38 mmol, 1.1 eq.) and IMes-DAD (366 mg, 1.25 mmol, 1.0 eq.) in dioxane (12.5 mL) was heated to 70 °C.



Upon addition of an ethereal solution of sulfuric acid (1 M in Et₂O, 1.25 mL, 1.25 mmol, 1.0 eq.) over 15 minutes, the yellow suspension turned from reddish to brownish. After stirring for one hour at 70 °C, a white precipitate formed. Next, the suspension was stirred for 15 minutes at 0 °C. The solid was filtered and washed with ethyl acetate (10 mL), followed by diethyl ether (2 x 10 mL). Drying for 16 hours at 100 °C in an oven afforded a pale beige to white powder (478 mg, 95%).

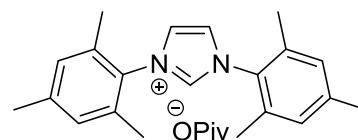
¹H-NMR (400 MHz, [D₆]-dimethylsulfoxide, PK-IMesHSO₄): δ 2.13 (s, 12H, *o*-CH₃), 2.36 (s, 6H, *p*-CH₃), 7.21 (s, 4H, H_{Ar}), 8.29 (d, *J* = 1.6 Hz, 2H, NCHCH), 9.66 (t, *J* = 1.6 Hz, 1H, NCHN). **¹³C-NMR** (101 MHz, [D₆]-dimethylsulfoxide, PK-IMesHSO₄): δ 16.9, 20.6, 124.8, 129.4, 131.0, 134.3, 138.5, 140.6. **Analysis** calcd for C₂₁H₂₆N₂O₄S C, 62.66; H 6.51, N 6.96, S 7.97; found C 62.39, H 6.83, N 6.90 S 7.86.

***IPr*·HOPiv (PK-048, 24)**. Potassium pivalate (295 mg, 2.10 mmol, 1.05 eq.) and IPr·HCl (851 mg, 2.00 mmol, 1.0 eq.) were suspended in acetone (35 mL) and stirred for 15 hours at room temperature. The reaction mixture was filtered through a short pad of Celite to remove potassium chloride and the remaining solid was washed with acetone (3 x 5 mL). After evaporation of the solvent under reduced pressure (45 °C, 8 mbar), the collected solid was washed with diethylether (2 x 15 mL) and dried under vacuum (r.t., 8.7·10⁻² mbar), affording a white, crystalline solid (917 mg, 94%).



¹H-NMR (500 MHz, [D₆]-acetone, PK-048-R): δ 1.00 (s, 9H, C(CH₃)₃), 1.29 (d, *J* = 6.8 Hz, 12H, CH(CH₃)₂), 1.30 (d, *J* = 6.8 Hz, 12H, CH(CH₃)₂), 2.59 (sept., *J* = 6.8 Hz, 4H, CH(CH₃)₂), 7.49 (d, *J* = 7.8 Hz, 4H, H_{Ar}), 7.65 (*virt.* t, *J* = 7.8 Hz, 2H, H_{Ar}), 8.41 (s, 2H, NCHCH). **¹H-NMR** (300 MHz, [D₆]-dimethylsulfoxide, PK-048-N): δ 1.00 (s, 9H, C(CH₃)₃), 1.16 (d, *J* = 6.8 Hz, 12H, CH(CH₃)₂), 1.26 (d, *J* = 6.8 Hz, 12H, CH(CH₃)₂), 2.35 (sept., *J* = 6.8 Hz, 5H, CH(CH₃)₂), 7.53 (d, *J* = 7.8 Hz, 4H, H_{Ar}), 7.69 (*virt.* t, *J* = 7.8 Hz, 2H, H_{Ar}), 8.57 (d, *J* = 1.4 Hz, 2H, NCHCH), 10.24 (t, *J* = 1.4 Hz, 1 H, NCHN). **¹H-NMR** (500 MHz, CDCl₃, PK-837-IPrHOPiv-CDCl₃): δ 0.99 (s, 9H, C(CH₃)₃), 1.21 (d, *J* = 6.9 Hz, 12H, CH(CH₃)₃), 1.29 (d, *J* = 6.8 Hz, 12H, CH(CH₃)₃), 2.48 (sept., *J* = 6.8 Hz, 4H, CH(CH₃)₃), 7.34 (d, *J* = 7.8 Hz, 4H, H_{Ar}), 7.56 (t, *J* = 7.8 Hz, 2H, H_{Ar}), 8.48 (s, 2H, NCHCH), 9.39 (s, 1H, NCHN)⁷⁰. **¹³C-NMR** (75 MHz, [D₆]-dimethylsulfoxide, PK-048-N): δ 23.1, 24.1, 28.1, 28.6, 38.1, 124.6, 126.2, 130.1, 131.8, 139.4, 144.8, 179.8. **¹³C-NMR** (126 MHz, (D₆)-acetone, PK-837-IPrHOPiv-cr): δ 23.9, 24.7, 24.7, 39.3, 125.2, 126.9, 131.7, 132.4, 142.7 (t, *J*_{C,D} = 33.1 Hz), 146.2, 181.3. **Analysis** calcd for C₃₂H₄₆N₂O₂·1.5 H₂O C 74.23, H 9.54, N 5.41; found C 74.00, H 9.17, N 5.44.

***IMes*·HOPiv (PK-054, 25)**. Potassium pivalate (61.7 mg, 440 μmol, 1.0 eq.) and IMes·HCl (150 mg, 440 μmol, 1.0 eq.) were suspended in acetone (6 mL) and stirred for 15 hours at

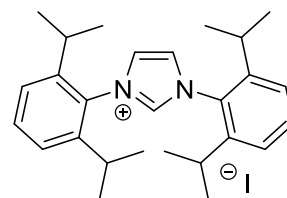


⁷⁰ The area integral of this signal decreases with time due to partial H/D exchange with [D₆]-acetone.

room temperature. The reaction mixture was filtered through a short pad of Celite to remove potassium chloride and the remaining solid was washed with acetone (3 x 2 mL). After evaporation of the solvent under reduced pressure (45 °C, 8 mbar), the collected solid was washed with diethylether (2 x 2 mL) and dried under vacuum (r.t., $8.7 \cdot 10^{-2}$ mbar), affording an off-white yellowish solid (106 mg, 59%). Minor impurities by the starting material can be detected in the NMR. No analytical pure product could be isolated.

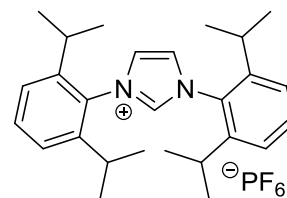
¹H-NMR (500 MHz, [D₆]-acetone, PK-054-N): δ 0.91 (s, 9H, C(CH₃)₃), 2.24 (s, 12H, *o*-CH₃), 2.36 (s, 9H, *p*-CH₃), 7.14 (d, $J = 1.2$ Hz, 4H, H_{Ar}), 8.12 (s, 2H, NCHCH). **¹H-NMR** (500 MHz, [D₆]-dimethylsulfoxide, PK-054-2D): δ 0.90 (s, 9H, C(CH₃)₃), 2.12 (s, 12H, *o*-CH₃), 2.35 (s, 6H, *p*-CH₃), 7.20 (s, 4H, H_{Ar}), 8.29 (d, $J = 1.4$ Hz, 2H, NCHCH), 9.93 (t, $J = 1.4$ Hz, 1H, NCHN). **¹³C-NMR** (75 MHz, [D₆]-dimethylsulfoxide, PK-054-N): δ 16.9, 20.6, 28.8, 38.4, 124.8, 129.3, 131.0, 134.3, 138.9, 140.5, 179.8. Analysis calcd for C₃₂H₄₆N₂O₂·2 H₂O C 70.56, H 8.65, N 6.33; found C 69.47, H 8.12, N 6.30.

IPr·HI (CAS 524742-02-7, PK-830, 26). IPr·HCl (850 mg, 2.00 mmol, 1.0 eq.) and KI (332 mg, 2.00 μ mol, 1.0 eq.) were suspended in acetone (20 mL). After stirring for seven hours at room temperature, the reaction mixture was filtered, the filter rinsed with acetone (3 x 5 mL) and the solvent was removed under reduced pressure (45 °C, 8 mbar). Further drying for one hour under reduced pressure (45 °C, 8 mbar) afforded a white solid (975 mg, 94%).



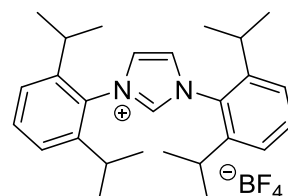
¹H-NMR (500 MHz, [D₆]-dimethylsulfoxide, PK-830-N): δ 1.16 (d, $J = 6.8$ Hz, 12H, CH₃), 1.26 (d, $J = 6.8$ Hz, 12H, CH₃), 2.35 (sept., $J = 6.8$ Hz, 4H, CH(CH₃)₂), 7.53 (d, $J = 7.8$ Hz, 4H, H_{Ar}), 7.69 (t, $J = 7.8$ Hz, 2H, H_{Ar}), 8.56 (d, $J = 1.6$ Hz, 2H, NCHCH), 10.16 (t, $J = 1.6$ Hz, 1H, NCHN). **¹³C-NMR** (75 MHz, [D₆]-acetone, PK-830-N) δ 23.8, 24.7, 29.9, 125.5, 127.3, 131.2, 132.9, 140.3, 146.1. The analytical data matched those reported in the literature.^[65]

IPr·HPF₆ (CAS 897038-14-1, PK-828, 27). IPr·HCl (850 mg, 2.00 mmol, 1.0 eq.) and potassium hexafluorophosphate (387 mg, 2.10 mmol, 1.05 eq.) were suspended in acetone (20 mL). After stirring for three hours at room temperature, the reaction mixture was filtered, the filter rinsed with acetone (3 x 5 mL) and the solvent was removed under reduced pressure (45 °C, 8 mbar). Further drying for two hours under reduced pressure (45 °C, 8 mbar) afforded a snow-white solid (1.06 g, 99%).



¹H-NMR (400 MHz, [D₆]-acetone, PK-828): δ 1.26 (d, *J* = 6.9 Hz, 12H, CH₃), 1.31 (d, *J* = 6.9 Hz, 12H, CH₃), 2.60 (sept., *J* = 6.9 Hz, 4H, CH(CH₃)₂), 7.55 (d, *J* = 7.8 Hz, 4H, H_{Ar}), 7.71 (t, *J* = 7.8 Hz, 2H, H_{Ar}), 8.44 (d, *J* = 1.6 Hz, 2H, NCHCH), 9.80 (t, *J* = 1.6 Hz, 1H, NCHN). **³¹P-NMR** (162 MHz, [D₆]-acetone, PK-828): δ -144.2 (sept., *J* = 707.4 Hz). **¹³C-NMR** (101 MHz, [D₆]-acetone, PK-828) δ 23.8, 24.6, 29.9, 125.7, 127.5, 131.1, 133.1, 139.5, 146.2. The analytical data matched those reported in the literature.^[66]

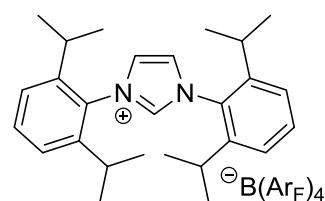
IPr-HBF₄ (CAS 286014-25-3, PK-833, 28). IPr·HCl (850 mg, 2.00 mmol, 1.0 eq.) was dissolved in water (20 mL).⁷¹ An aqueous solution of NaBF₄ (231 mg, 2.10 μmol, 1.05 eq. in 1 mL H₂O) was added dropwise. A white solid immediately precipitated. The suspension was stirred for 15 minutes at room temperature. After filtration, washing with water (3 x 5 mL) and drying for 14 hours in an oven (no ventilation) at 100 °C, a white solid (916 mg, 96%) was obtained.



¹H-NMR (500 MHz, [D₆]-acetone, PK-834-IPrHBF₄): δ 1.26 (d, *J* = 6.9 Hz, 12H, CH₃), 1.31 (d, *J* = 6.9 Hz, 12H, CH₃), 2.60 (sept., *J* = 6.9 Hz, 4H, CH(CH₃)₂), 7.55 (d, *J* = 7.8 Hz, 4H, H_{Ar}), 7.70 (t, *J* = 7.8 Hz, 2H, H_{Ar}), 8.43 (d, *J* = 1.7 Hz, 2H, NCHCH), 9.89 (d, *J* = 1.7 Hz, 1H, NCHN). **¹¹B-NMR** (96 MHz, [D₆]-acetone, PK-833-N) δ -0.9. **¹³C-NMR** (75 MHz, [D₆]-acetone, PK-833-N) δ 23.8, 24.6, 29.9⁷², 125.6, 127.4, 131.1, 133.0, 139.7, 146.1. The analytical data matched those reported in the literature.^[67]

IPr-HB(Ar_F)₄ (Ar_F = 3,5-bis(trifluoromethyl)phenyl, PK-829, 29).

IPr·HCl (213 mg, 500 μmol, 1.0 eq.) and NaB(Ar_F)₄ (465 mg, 525 μmol, 1.05 eq.) were suspended in acetone (5 mL). After stirring for three hours at room temperature, the reaction mixture was filtered, the filter rinsed with acetone (3 x 3 mL) and the solvent was removed under reduced pressure (45 °C, 8 mbar). Further drying for two hours under reduced pressure (45 °C, 8 mbar) afforded a white solid (598 mg, 95%).



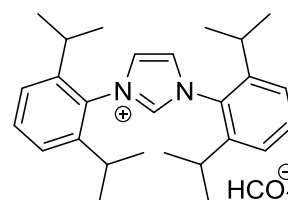
¹H-NMR (400 MHz, [D₆]-acetone, PK-829): δ 1.26 (d, *J* = 6.8 Hz, 12H, CH₃), 1.31 (d, *J* = 6.8 Hz, 12H, CH₃), 2.61 (sept, *J* = 6.8 Hz, 4H, CH(CH₃)₂), 7.55 (d, *J* = 7.8 Hz, 4H, H_{Ar}), 7.65-7.74 (m, 6H, H_{Ar}), 7.75-7.83 (m, 8H, H_{BArF}), 8.46 (d, *J* = 1.6 Hz, 2H, NCHCH), 9.91 (t,

⁷¹ Gentle heating with a heat-gun accelerates the dissolution of the salt.

⁷² This signal overlays with the deuterated solvent.

$J = 1.6$ Hz, 1H, NCHN). **^{19}F -NMR** (376 MHz, $[\text{D}_6]$ -acetone, PK-829) $\delta -63.3$. **^{11}B -NMR** (96 MHz, $[\text{D}_6]$ -acetone, PK-829-R): $\delta -6.6$. **^{13}C -NMR** (101 MHz, $[\text{D}_6]$ -acetone, PK-829) δ 23.8, 24.6, 29.9, 118.3-118.7 (m, p -CH), 125.4 (q, $J_{\text{C,F}} = 271.8$ Hz, CF_3), 125.7, 127.4, 130.0 (qq, $J_{\text{C,F}} = 31.7$ Hz, $J_{\text{C,B}} = 2.9$ Hz, m - C_{quat}), 131.2, 133.1, 135.6 (br s), 139.7, 146.2, 162.6 (q, $J_{\text{C,B}} = 49.9$ Hz, C_{quat}). No CAS available. The analytical data matched those reported in the literature.^[68]

***IPr*- HCO_3** (CAS 1663476-15-0, PK-836, 30).^[69] IPr-HCl (850 mg, 2.00 mmol, 1.0 eq.) was added to a pre-dried Schlenk tube (1.8 · 10⁻¹ mbar, heat-gun). Inside a glovebox, pre-dried KHCO_3 (211 mg, 2.10 mmol, 1.05 eq.) was added and the walls were rinsed with dry

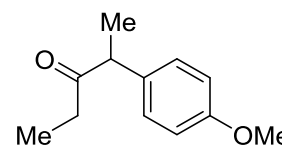


methanol (2 mL). The suspension was stirred for 16 hours at room temperature before being filtered over Celite under argon. The solvent was removed under reduced pressure (r.t., <1.0 · 10⁻¹ mbar). In air, the solid was dissolved in acetone (6 mL) and filtered over a syringe filter (0.2 μm , PTFE). After removal of the solvent under reduced pressure (45 °C, 8 mbar), washing with diethylether (3 x 3 mL) and drying in an oven (50 °C) for two hours, a white solid (666 mg, 74%) was obtained.

^1H -NMR (400 MHz, $[\text{D}_4]$ -methanol, PK-836-wash-MeOD): δ 1.26 (d, $J = 6.9$ Hz, 12H, $\text{CH}(\text{CH}_3)_3$), 1.33 (d, $J = 6.9$ Hz, 12H, $\text{CH}(\text{CH}_3)_3$), 2.48 (sept., $J = 6.9$ Hz, 4H, $\text{CH}(\text{CH}_3)_3$), 7.52 (d, $J = 7.8$ Hz, 4H, H_{Ar}), 7.68 (t, $J = 7.8$ Hz, 2H, H_{Ar}), 8.27 (s, 2H, NCHCH)⁷³. C2-proton is not observed due H/D exchange with the deuterated solvent. **^{13}C -NMR** (126 MHz, $[\text{D}_4]$ -methanol, PK-836-wash-13C): δ 23.9, 24.8, 30.4, 126.0, 127.1 (t, $^2J_{\text{C,D}} = 15.3$ Hz, NCDCH), 127.4, 127.5, 131.5 (d, $J = 3.2$ Hz, NCDCH), 133.4, 140.5 (br s), 146.5, 161.4 (HCO_3^-). Fast equilibration of $\text{HCO}_3^-/\text{CO}_2^-$ result in a single signal in the ^{13}C -NMR spectrum.^[70] Additional signals (δ 127.3, 129.5, 140.3) occurring from partial decomposition can be observed in the ^{13}C -NMR. This compound is known to literature, but no reference spectra are available.

7.2.3.4 α -Arylation of 3-pentanone with 4-Cl-anisole

2-(4-Methoxyphenyl)pentan-3-one (CAS 84736-54-9, PK-566). 3-Pentanone (215 μL , 174 mg, 2.02 mmol, 2.0 eq.), 4-chloroanisole (122 μL , 143 mg, 1.00 mmol, 1.0 eq.), KO^tBu (226 mg, 2.01 mmol,



⁷³ Partial H/D exchanges with the deuterated solvent.

2.0 eq.) and (IPrH)₂[Pd₂Cl₆] (6.02 mg, 5.00 μmol, 0.5 mol%) in toluene (1 mL) were reacted according to general procedure 3.4. After purification by flash CC (EtOAc-hexanes 1:50), the mono-arylated product (154 mg, 801 μmol, 80%) was obtained as colourless oil.

TLC: $R_f = 0.13$ (EtOAc-hexanes 1:50) [UV, Mostain]. **¹H-NMR** (300 MHz, CDCl₃, PK-566-A): δ 0.96 (t, $J = 7.3$ Hz, 3H, CH₂CH₃), 1.36 (d, $J = 7.0$ Hz, 3H, CHCH₃), 2.26-2.48 (m, 2H, CH₂CH₃), 3.71 (q, $J = 7.0$ Hz, 1H, CHCH₃), 3.79 (s, 3H, OCH₃), 6.82-6.90 (m, 2H, H_{Ar}), 7.09-7.17 (m, 2H, H_{Ar}). **¹³C NMR** (75 MHz, CDCl₃, PK-566-A-13C): δ 8.2, 17.7, 34.2, 52.0, 55.4, 114.4, 129.0, 133.1, 158.8, 212.0. The analytical data matched those reported in the literature.^[52]

7.2.3.5 Exemplary procedures

Table 11, entry 3, according to general procedure 3.3 (PK-550). The reaction was performed according to a procedure by the group of Jin.^[51] (IPrH)₂[Pd₂Cl₆] (60.24 mg, 50.0 μmol, 0.5 mol%), *p*-toluene boronic acid (163.2 mg, 1.20 mmol, 1.2 eq.) and KO^tBu (134.7 mg, 1.20 mmol, 1.2 eq.) were fitted in a Schlenk tube. After threefold evacuation ($1.5 \cdot 10^{-1}$ mbar) and backfilling with argon, *p*-chloroanisole⁷⁴ (142.6 mg, 1.00 mmol, 1.0 eq.) was added. The walls were rinsed with 2-PrOH and the Schlenk tube was closed with a Teflon sleeve and glass stopper. The suspension was stirred for 19 hours at room temperature (600 rpm) before addition of water (7 mL). The reaction mixture was filtered over a short pad of Celite, rinsing the latter with Et₂O (3 x 2 mL), and transferred to a separatory funnel. Phases were separated and the aqueous phase was extracted with Et₂O (3 x 20 mL). The combined organic phase was dried over MgSO₄, filtered and the solvent was removed under reduced pressure (45 °C, 6 mbar). A q-NMR (tetrachloroethane: 100 μL, 947.3 μmol) was conducted according to the general procedure for q-NMR analysis (7.1.3, NMR file: PK-550-q, AVHD400).

Table 13, entry 1, according to general procedure 3.5 (PK-599). The reaction was performed according to a procedure by the group of Lu.^[53] (IMesH)₂[Pd₂Cl₆] (10.36 mg, 10.0 μmol, 1.0 mol%) and K₂CO₃ (276 mg, 2.00 mmol, 2.0 eq.) were fitted in a 10 mL Schlenk tube which was evacuated ($1.2 \cdot 10^{-1}$ mbar) and backfilled with argon thrice. 2-Bromomesitylene (150 μL, 995 μmol, 1.0 eq.) and *tert*-butyl acrylate (175 μL, 1.20 mmol, 1.2 eq.) were added. The walls were rinsed with NMP (400 μL). After stirring at room temperature for one minute, the reaction

⁷⁴ The electrophile was added via a tared syringe. The difference in mass after addition was used for yield determination/calculation.

mixture was stirred for 18 hours at 140 °C (600 rpm). The reaction was allowed to cool to room temperature before adding water (2 mL) and Et₂O (2 mL). Filtration over a short pad of Celite and rinsing of the latter with Et₂O (3 x 2 mL) removed any amount of insoluble (mostly black) solid. The crude material was diluted with water (25 mL) and Et₂O (45 mL) and transferred to a separatory funnel. Phases were separated. The organic phase was washed with water (25 mL) and an aqueous solution of NaCl (25 mL), dried over MgSO₄, filtered and the solvent was removed under reduced pressure (45 °C, 500 mbar). A q-NMR (tetrachloroethane: 100 μL, 947.3 μmol) was conducted according to the general procedure for q-NMR analysis (7.1.3, NMR file: PK-599-q, AVHD500).

7.2.4 Difunctional Onium Carboxylate Additives for Catalytic Coupling

7.2.4.1 General synthesis procedures

General procedure 4.1 – Synthesis of methyltrioctylammonium (MTOA) carboxylates

MTOA methyl carbonate (1.1 eq.) and acid (1.0 eq.) were weighed into a round-bottom flask. The reaction mixture was stirred for two hours at 50 °C until gas evolution ceased. After cooling to room temperature, the stirring bar was washed with Et₂O before being removed. The solvents (Et₂O and generated MeOH) as well as CO₂ were removed under reduced pressure (50 °C, 8 mbar, 2 h).

General procedure 4.2 – Arylation of caffeine in DMF

Caffeine (97.1 mg, 500 μmol, 1.0 eq.), PdCl₂(MeCN)₂ (6.49 mg, 25.0 μmol, 5.0 mol%), and additive salt (10.0 mol%) were added to a pre-dried ($2 \cdot 10^{-2}$ mbar, heat-gun) Schlenk tube, which was introduced into a glovebox. K₃PO₄ (212 mg, 1.00 mmol, 2.0 eq.) and bromobenzene (Hamilton syringe, 79.0 μL, 750 μmol, 1.5 eq.) were added and the walls were rinsed with dry DMF (1.5 mL). After five minutes at room temperature outside the glovebox, the suspension was stirred for either 2.5 or 13 hours at 100 °C (pre-heated aluminum block, 600 rpm). At room temperature, the reaction mixture was filtered over a short pad of silica (5 cm), eluting with a DCM-MeOH mixture (10:1, 75-100 mL) until no further reaction components were recovered. After removal of the solvent under reduced pressure (50 °C, 15 mbar), a q-NMR (1,3,5-trimethoxybenzene: 168.19 g/mol) was conducted according to the general procedure for q-NMR analysis (7.1.3).

General procedure 4.3 – Arylation of caffeine in DMF – HPLC sampling

K₃PO₄ (637 mg, 3.00 mmol, 2.0 eq.) was added to a Schlenk tube and dried for 15 minutes in high vacuum ($2 \cdot 10^{-2}$ mbar) with a heat-gun. Caffeine (291 mg, 1.50 mmol, 1.0 eq.), bromobenzene (236 μL, 353 mg, 2.25 mmol, 1.5 eq.), PdCl₂(MeCN)₂ (19.5 mg, 75.0 μmol, 5.0 mol%) and additive (10.0 mol%) were added under argon and the walls were washed with *N,N*-dimethylformamide (5 mL). The reaction mixture was stirred for five minutes at room temperature, followed by heating for six hours to 100 °C (600 rpm). Samples for kinetic studies were drawn as follows. Stirring of the reaction mixture was stopped one minute before sample drawing. Via a Hamilton syringe a defined volume of the solution (100 μL) was retrieved every hour and diluted with dichloromethane in a volumetric flask (25 mL). The flask was shaken

until a homogeneous phase was obtained. Next a sample was taken and measured instantly. For the calculation of the amount of substance present in the reaction mixture, see 7.1.3.

General procedure 4.4 – Arylation of caffeine in water

Caffeine (97.1 mg, 500 μmol , 1.0 eq.), $\text{PdCl}_2(\text{MeCN})_2$ (6.49 mg, 25.0 μmol , 5.0 mol%), and dry K_3PO_4 (212 mg, 1.00 mmol, 2.0 eq.) were added to a Schlenk tube, which was evacuated ($<1.0 \cdot 10^{-1}$ mbar) and backfilled with argon thrice. Additive salt (10.0 mol%) and bromobenzene (Hamilton syringe, 79.0 μL , 750 μmol , 1.5 eq.) were added and the walls were rinsed with degassed⁷⁵ water (1.5 mL). After five minutes at room temperature, the suspension was stirred for 13 hours at 100 °C (pre-heated aluminum block, 600 rpm). At room temperature, the reaction mixture was transferred with DCM (50 mL) to a separatory funnel. A saturated aqueous solution of NaCl (25 mL) was added, phases were separated and the water phase was extracted with DCM (2 x 25 mL). The combined organic extract was dried over Na_2SO_4 , filtered and the solvent was removed under reduced pressure (50 °C, 7 mbar). A q-NMR (1,3,5-trimethoxybenzene: 168.19 g/mol) was conducted according to the general procedure for q-NMR analysis (7.1.3).

General procedure 4.5 – Arylation of benzene

The procedure was adapted from the group of Fagnou et al.^[71] $\text{Pd}(\text{OAc})_2$ (3.37 mg, 15.0 μmol , 3.0 mol%), DavePhos (5.90 mg, 15.0 μmol , 3.0 mol%), and NBu_4DiPP (60.0 mg, 150 μmol , 0.3 eq.) were placed in a Schlenk tube, which was evacuated ($<1.0 \cdot 10^{-1}$ mbar) and backfilled with argon thrice. If solid, aryl bromide (1.0 eq.) was added. The Schlenk tube was transferred into a glovebox and K_2CO_3 (173 mg, 1.25 mmol, 2.5 eq.) was added. Outside the glovebox, aryl bromide (if liquid, Hamilton syringe, 1.0 eq.) was added. The walls were rinsed with benzene (2.5 mL) and DMAc (2.9 mL). After five minutes at room temperature, the suspension was stirred for 15 hours at 120 °C (600 rpm). The cooled, brown suspension was transferred to a separatory funnel and diluted with Et_2O (50 mL). The organic phase was washed with water (3 x 25 mL), a saturated aqueous solution of NaCl (25 mL), dried over MgSO_4 , filtered and the solvent was removed under reduced pressure (45 °C, 500 mbar).⁷⁶ A q-NMR (1,3,5-trimethoxybenzene: 168.19 g/mol) was conducted according to the general procedure for q-NMR analysis (7.1.3).

⁷⁵ Water was degassed for 30 minutes by injection of argon via a cannula.

⁷⁶ Residual benzene was not removed to avoid any potential, azeotropic distillation of reactants.

General procedure 4.6 – Arylation of other heterocycles

The procedure was adapted from Fagnou et al.^[72] and Kappe et al.^[73]. Heterocycle (if solid, 1.0-1.5 eq.), Pd(OAc)₂ (4.49 mg, 20.0 μmol, 2.0 mol%), and NBu₄DiPP (120 mg, 300 μmol, 0.3 eq.) were placed in a Schlenk tube, which was evacuated ($2.1 \cdot 10^{-1}$ mbar) and backfilled with argon thrice. Inside a glovebox, PCy₃ (11.2 mg, 40.0 μmol, 4.0 mol%) and K₂CO₃ (207 mg, 1.50 mmol, 1.5 eq.) were added. Outside the glovebox, aryl bromide (Hamilton syringe, 1.0 eq.) and heterocycle (if liquid, Hamilton syringe, 1.5 eq.) were added and the walls were rinsed with dry DMAc (2 mL). After five minutes at room temperature, the suspension was stirred for the indicated time at 100 °C (preheated aluminum block, 600 rpm). The cooled reaction mixture was transferred to a separatory funnel and diluted with EtOAc (50 mL). The organic phase was washed with water (3 x 25 mL), a saturated aqueous solution of NaCl (1 x 25 mL), dried over MgSO₄, filtered and the solvent was removed under reduced pressure (45 °C, 50 mbar).⁷⁷ A q-NMR (1,3,5-trimethoxy-benzene: 168.19 g/mol) was conducted according to the general procedure for q-NMR analysis (7.1.3).

General procedure 4.7 – Arylation of 2-phenylimidazo[1,2-a]pyridine

The procedure was adapted from Marching et al.^[74] 2-Phenylimidazo[1,2-a]pyridine (194 mg, 1.00 mmol, 1.0 eq.), Pd-catalyst (20.0 μmol, 2.0 mol%), and additive salt (0.1-0.3 eq.) were placed in a Schlenk tube. Inside a glovebox, K₂CO₃ (207 mg, 1.50 mmol, 1.5 eq.) and if stated PCy₃ (11.2 mg, 40.0 μmol, 4.0 mol%) were added. Outside the glovebox, aryl bromide (Hamilton syringe, 1.2 eq.) was added and the walls were rinsed with dry DMAc (4 mL). After five minutes at room temperature, the reaction mixture was stirred for 18 hours at the indicated temperature (600 rpm). The suspension was transferred to a separatory funnel and diluted with EtOAc (50 mL). The organic phase was washed with water (3 x 25 mL), a saturated solution of NaCl (1 x 25 mL), dried over MgSO₄, filtered and the solvent was removed under reduced pressure (45 °C, 100 mbar). A q-NMR (1,3,5-trimethoxy-benzene: 168.19 g/mol) was conducted according to the general procedure for q-NMR analysis (7.1.3).

General procedure 4.8 – Arylation of 2-phenylimidazo[1,2-a]pyridine – kinetic study

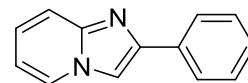
The procedure was adapted from Marching et al.^[74] 2-Phenylimidazo[1,2-a]pyridine (194 mg, 1.00 mmol, 1.0 eq.), Pd-catalyst (20.0 μmol, 2.0 mol%), 1,3,5-trimethoxybenzene (internal standard weighed on an analytical balance with 0.01 mg accuracy) and additive salt (0.1-0.3 eq.)

⁷⁷ Except for NaCl washing, phases separate very slowly.

were placed in a Schlenk tube. Inside a glovebox, K_2CO_3 (207 mg, 1.50 mmol, 1.5 eq.) and if stated PCy_3 (11.2 mg, 40.0 μ mol, 4.0 mol%) were added. Outside the glovebox, 4-bromotoluene (Hamilton syringe, 150 μ L, 1.24 mmol, 1.2 eq.) was added, the walls were rinsed with dry DMAc (4 mL) and the Schlenk tube was closed with a septum. After five minutes at room temperature, the reaction mixture was stirred at the indicated temperature (600 rpm). Samples were withdrawn after 5, 15, 30, 45, 60, and 90 minutes as follows (see 7.1.2 for pictured details): an aliquot (~150 μ L) was added to a screw cap vial containing water (4 mL) and Et_2O (4 mL). The vial was shaken for ten seconds and the organic phase was transferred to a second vial containing $MgSO_4$ (150-250 mg). After drying over $MgSO_4$, the solvent was removed under reduced pressure (water-jet pump, ca. 20 mbar) with the aid of a cannula (\varnothing 0.90 mm, color code yellow). The walls were rinsed with $CDCl_3$ (700 μ L) and the crude mixture was stirred for three minutes at room temperature. The suspension was filtered over cotton wool into an NMR tube. An 1H -NMR spectrum (delay = 20 s, 16 scans) was measured.^[18] The yield of the reaction was determined by comparison of the integral of the internal standard with the integral of characteristic signals of the reaction product(s) and starting material(s) in the 1H -NMR spectra.

7.2.4.2 Synthesis of precursors

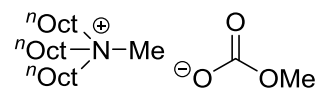
2-Phenylimidazo[1,2-a]pyridine (CAS 4105-21-9, PK-251, 59). The procedure was adapted from Tomoda et al.^[75] ω -Bromo acetophenone (94%, 6.35 g, 30.0 mmol, 1.0 eq.) and 2-aminopyridine (2.82 g, 30.0 mmol, 1.0 eq.) in dioxane-water (2:1, 45 mL) were refluxed for 30 minutes at 110 °C. After stepwise addition of Na_2CO_3 (4.77 g, 45.0 mmol, 1.5 eq.) at room temperature, the suspension was stirred for another 22 hours at 110 °C. Concentrated HCl (24 mL) was added to the cooled reaction mixture and insoluble solid was filtered off. The filtrate was basified with aqueous sodium hydroxide (6 M, 50 mL), and was extracted with DCM (4 x 50 mL). The combined organic extract was dried over $MgSO_4$, filtered and the solvent was removed under reduced pressure (45 °C, 7 mbar). Purification by flash column chromatography (EtOAc-hexanes 1:5 \rightarrow 1:2 \rightarrow 1:1 \rightarrow 2:1 \rightarrow 3:1 \rightarrow 1:0), followed by recrystallization (toluene-hexanes 1:2, 130 mL) and drying under reduced pressure (r.t., $<1.0 \cdot 10^{-1}$ mbar) afforded off-white needles (3.94 g, 64%).



TLC: R_f = 0.17 (EtOAc-hexanes 1:2) [UV]. **1H -NMR** (500 MHz, $CDCl_3$, PK-251-D1): δ 6.76 (td, J = 6.7, 1.0 Hz, 1H), 7.16 (ddd, J = 9.0, 6.7, 1.2 Hz, 1H), 7.30-7.37 (m, 1H), 7.40-7.49 (m, 2H), 7.59-7.66 (m, 1H), 7.85 (s, 1H), 7.93-7.99 (m, 2H), 8.10 (dt, J = 6.7, 1.2 Hz, 1H).

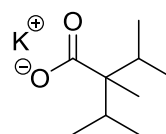
¹³C-NMR (75 MHz, CDCl₃, PK-251-13C): δ ¹³C NMR (75 MHz, CDCl₃) δ 108.1, 112.3, 117.4, 124.6, 125.6, 126.0, 127.9, 128.7, 133.8, 145.6, 145.7. The analytical data matched those reported in the literature.^[75]

Methyltrioctylammonium (MTOA) methyl carbonate (CAS 488711-07-5, PK-1054, 54). The procedure was adapted from Perosa and coworkers.^[76] Inside a glovebox, a 30 mL microwave reaction vessel was charged with trioctylamine (2.65 g, 7.50 mmol, 1.0 eq.), dimethyl carbonate (4.9 mL, 58.5 mmol, 7.8 eq.) and dry methanol (3.3 mL). The vial was closed with a PEEK-cap including a PTFE-coated silicon septum. Outside the glovebox, the biphasic reaction mixture was heated for six hours⁷⁸ to 150 °C with the aid of a microwave reactor. After cooling to room temperature, the colorless solution was transferred with Et₂O (3 x 5 mL) to a round-bottom flask. Removal of the solvent and drying under reduced pressure (4 h, 45 °C, 7 mbar) afforded a yellow-orange oil (3.28 g, 98%). The product contained methanol (~1 mol%), unreacted trioctylamine (~1 mol%) and methyltrioctylammonium hydrogen carbonate salt (9 mol%), adding to approximately 90% purity.



¹H-NMR (400 MHz, [D₆]-dimethylsulfoxide, PK-1054-N): δ 0.83-0.92 (m, 9H), 1.12-1.36 (m, 30H), 1.54-1.66 (m, 6H), 2.94 (s, 3H), 3.14-3.24 (m, 6H), 3.16 (s, 3H). **¹³C-NMR** (101 MHz, [D₆]-dimethylsulfoxide, PK-1054-N): δ 13.9, 21.3, 22.0, 25.8, 28.4, 28.5, 31.2, 47.5 (N(CH₃)), 50.8 (OCH₃), 60.5 (C₁), 155.5 (C=O). The analytical data matched those reported in the literature.^[76]

Potassium 2-isopropyl-2,3-dimethylbutanoate (PK-994). 2-Isopropyl-2,3-dimethylbutanoic acid (475 mg, 3.00 mmol, 1.0 eq.) was dissolved in *i*PrOH (10 mL) and three drops of phenolphthalein in *i*PrOH (0.74%) were added. A solution of KOH in *i*PrOH (0.23 M) was added until the solution turned light pink (total volume added: 13.2 mL). After stirring for ten minutes at room temperature, the solvent was removed under reduced pressure (45 °C, 50 mbar). The obtained solid was further dried in vacuo (1 h, 60 °C, 7 mbar), before being washed with Et₂O (3 x 10 mL). Drying for twelve hours in an oven (10% ventilation) at 60 °C afforded a white solid (568 mg, 96%). In contrast to the free acid, the isolated salt did not dissolve in chloroform.



¹H-NMR (300 MHz, [D₄]-methanol, PK-994-N): δ 0.86 (d, *J* = 6.8 Hz, 6H), 0.92 (s, 3H), 0.93 (d, *J* = 6.8 Hz, 6H), 1.95 (sept., *J* = 6.8 Hz, 2H). **¹³C-NMR** (75 MHz, CDCl₃, PK-994-13C): δ

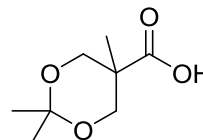
⁷⁸ The maximal reaction time is limited for microwave heating; the total reaction time was split in two.

15.9, 18.5, 19.4, 33.7, 54.5, 184.2. This product is not known to literature, but further analysis of the solid was not conducted.

7.2.4.3 Synthesis of carboxylic acids

2,2,5-Trimethyl-1,3-dioxane-5-carboxylic acid (CAS 16837-14-2, PK-912,

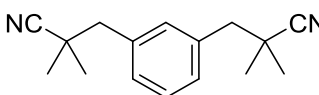
45). This procedure was adapted from the group of Dhar.^[77] 2,2-Bis(hydroxymethyl)propionic acid (20.1 g, 150 mmol, 1.0 eq.) and 2,2-



dimethoxypropane (29.0 mL, 236 mmol, 1.6 eq.) were suspended in acetone (80 mL). After addition of *p*-toluene sulfonic acid monohydrate (1.63 g, 8.55 mmol, 6 mol%), the reaction mixture was stirred for one day at room temperature. The yellow solution was neutralized with an ethanolic mixture of aqueous ammonia (50:50, 6.3 mL) before the solvent was replaced by dichloromethane (350 mL). The organic phase was washed with water (2 x 80 mL), a saturated aqueous solution of NaCl (3 x 100 mL), dried over MgSO₄, filtered and the solvent was removed under reduced pressure (45 °C, 8 mbar). Further azeotropic distillation with toluene (2 x 30 mL) afforded a crystalline, impure solid (16.0 g). Purification by crystallization⁷⁹ (hexanes-Et₂O 9:1, 200 mL) yielded a white, micro-crystalline solid (12.6 g, 48%).

¹H-NMR (400 MHz, CDCl₃, PK-912-N-13C): δ 1.21 (s, 3H), 1.44 (d, *J* = 12.7 Hz, 6H), 3.69 (d, *J* = 11.9 Hz, 2H), 4.19 (d, *J* = 11.9 Hz, 2H). ¹³C-NMR (101 MHz, CDCl₃, PK-912-N-13C): δ 18.5, 22.0, 25.5, 41.9, 66.1, 98.5, 179.9. The analytical data matched those reported in the literature.^[77]

***α,α,α',α'*-Tetramethyl-1,3-benzenedipropionitrile (esp-diCN, CAS 69774-36-3, PK-913).** This procedure was adapted from Berry et



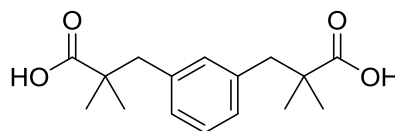
al.^[78] A pre-dried Schlenk flask ($1.3 \cdot 10^{-1}$ mbar) was charged with solid LDA (2.75 g, 25.6 mmol, 2.05 eq.). At -78 °C, THF (44 mL) was added and the reaction mixture was stirred for five minutes until all solids dissolved. Isobutyronitrile (2.30 mL, 25.6 mmol, 2.05 eq.) was added and the orange solution was stirred for 50 minutes at -78 °C. A solution of *α,α'*-dibromo-*m*-xylene (97%, 3.40 g, 12.5 mmol, 1.0 eq.) in THF (12 mL) was added dropwise over a period of 15 minutes. The mixture was stirred for ten minutes at -78 °C before stirring for 15 hours at room temperature. Water (35 mL) and EtOAc (75 mL) were added and the phases were separated. The organic phase was washed with water (30 mL), a saturated aqueous solution of

⁷⁹ Note: a small amount of solid remains insoluble while crystallization. Product losses may occur due to sublimation.

NaCl (30 mL), dried over MgSO₄, filtered and the solvent was removed under reduced pressure (45 °C, 100 mbar). The yellow oil was diluted in EtOAc (4 mL) and filtered over a short pad of silica (9 cm), eluting with EtOAc until no further product was collected. The solvent was removed under reduced pressure (45 °C, 7 mbar). The obtained solid was dissolved in EtOAc (8 mL), hexanes (150 mL) were added and the solution was stored for three days at -25 °C. The crystals were filtered off, pulverized and washed with hexanes (3 x 10 mL). After drying under reduced pressure (45 °C, 8 mbar), a white solid (1.75 g, 58%) was obtained. The filtrate was stored for one day at -25 °C, affording more white, crystalline solid (704 mg, 23%). Total yield: 2.45 g, 81%.

¹H-NMR (400 MHz, CDCl₃, PK-913-cryst): δ 1.36 (s, 12H), 2.82 (s, 4H), 7.17 – 7.25 (m, 3H), 7.32 (dd, *J* = 8.2, 6.8 Hz, 1H). ¹³C-NMR (101 MHz, CDCl₃, PK-913-cryst): δ 26.7, 33.7, 46.7, 124.8, 128.6, 129.4, 132.3, 136.0. The analytical data matched those reported in the literature.^[79]

***α,α,α',α'*-Tetramethyl-1,3-benzenedipropionic acid (*H*₂*esp*, CAS 819050-88-9, PK-914, 46).** This procedure was adapted from Berry et al.^[78]. A 25 mL Schlenk flask charged with esp-



diCN (1.44 g, 6.00 mmol, 1.0 eq.) and KOH (1.90 g, 33.9 mmol, 5.7 eq.) evacuated ($2.5 \cdot 10^{-1}$ mbar) and backfilled with argon three times. Ethylene glycol (7.5 mL) was added and a reflux condenser with an argon balloon was fitted on the flask. The two-phase mixture was stirred for 16 hours at 180 °C.⁸⁰ After cooling to room temperature, the yellowish solution was transferred with chloroform (20 mL) and water (20 mL) to a separatory funnel. Aqueous HCl (6 M, 12 mL) was added and the organic layer was collected. The aqueous phase was extracted with EtOAc (2 x 65 mL). The combined organic phase was washed with water (2 x 25 mL), a saturated aqueous solution of NaCl, dried over MgSO₄, filtered and the solvent was removed under reduced pressure (45 °C, 190 mbar). The yellow oil was diluted with EtOAc (4 mL) and passed through a short pad of silica, eluting with EtOAc until no further product was collected. The solvent was removed under reduced pressure (45 °C, 100 mbar). The obtained solid was dissolved in EtOAc (8 mL) and hexanes (125 mL) were added. After storing at -25 °C for one day, solids were filtered off and washed with hexanes (3 x 15 mL). After drying in air, a colorless, micro-crystalline solid (1.64 g, 98%) was obtained.

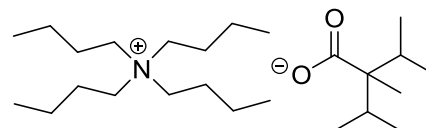
⁸⁰ First heating for one hour at 170 °C.

¹H-NMR (400 MHz, CDCl₃, PK-914-N): δ 1.17 (s, 12H), 2.84 (s, 4H), 6.94-7.07 (m, 3H), 7.18 (t, $J = 7.5$ Hz, 1H), 11.70 (br s, 1H). **¹³C-NMR** (101 MHz, CDCl₃, PK-914-N): δ 24.6, 43.7, 46.1, 127.7, 128.8, 131.8, 137.5, 184.4. The analytical data matched those reported in the literature.^[79]

7.2.4.4 Synthesis of difunctional onium carboxylates

Tetrabutylammonium 2-isopropyl-2,3-dimethylbutanoate

(**PK-KH-01**, 47). 2-isopropyl-2,3-dimethylbutanoic acid (3.00 g, 19.0 mmol, 1.0 eq.) and a grain of phenolphthalein

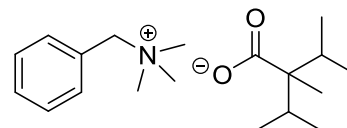


(ca. 0.5 mg) were dissolved in ⁱPrOH (20 mL). An aqueous solution of tetrabutylammonium hydroxide (40 wt.%) was added until the solution turned light pink (total volume added: 12.4 mL). After stirring for one hour at room temperature, the solvent was removed under reduced pressure (45 °C, 100 mbar). Residual alcohol as well as most of the water was removed by two-fold azeotropic distillation with toluene (20 mL). After cooling in the fridge for one day (less is also tolerable), the solid dissolved in hot toluene (4 mL), over-layered with hexanes (4 mL) and stores in the fridge overnight. The crystals (4.75 g, 63%) were filtered off, washed with hexanes (2 x 10 mL) and dried under reduced pressure (<1.0·10⁻¹ mbar). A second crystallization afforded a colorless, crystalline solid (2.29 g, 30%). Total yield: 7.04 g, 93%. The solid is little hygroscopic. Suitable single crystals for X-ray analysis (KlePh18) were grown by slow diffusion of hexanes into a saturated solution of the salt in toluene.

¹H-NMR (500 MHz, [D₆]-benzene, PK-KH-01-cryst): δ 0.92 (t, $J = 7.3$ Hz, 12H), 1.23-1.33 (m, 14H), 1.33-1.43 (m, 8H), 1.46 (s, 3H), 1.48 (d, $J = 6.8$ Hz, 6H), 2.48 (sept., $J = 6.8$ Hz, 2H) 3.09-3.30 (m, 8H). **¹³C-NMR** (75 MHz, [D₆]-benzene, PK-KH-01-cryst-13C): δ 14.0, 17.0, 19.1, 20.1, 20.2, 24.4, 33.5, 53.2, 58.7, 178.6.

Benzyl trimethylammonium 2-isopropyl-2,3-dimethylbutanoate

(**PK-890**, 48). 2-isopropyl-2,3-dimethylbutanoic acid (791 mg, 5.00 mmol, 1.0 eq.) was dissolved in ⁱPrOH (5 mL) and three



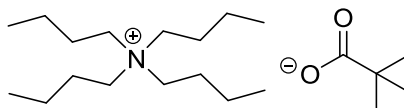
drops of phenolphthalein in ⁱPrOH (0.74 wt.%) were added. A methanolic solution of benzyl trimethylammonium hydroxide (40%) was added until the solution turned light pink (total volume added: 3.35 mL). After stirring for five minutes at room temperature, the solvent was removed under reduced pressure (45 °C, 65 mbar). Residual alcohol as well as most of the water was removed by two-fold azeotropic distillation with toluene (1 x 5 mL, 1 x 10 mL). The obtained white solid was suspended in hexanes (10 mL), filtered and washed with hexanes

(3 x 10 mL). After drying under reduced pressure (45 °C, 7 mbar) a white, crystalline solid (1.47 g, 95%) was obtained.

¹H-NMR (300 MHz, CDCl₃, PK-890-N): δ 0.88 (d, *J* = 6.8 Hz, 6H), 0.97 (s, 3H), 0.98 (d, *J* = 6.8 Hz, 6H), 2.00 (sept., *J* = 6.8 Hz, 2H), 3.44 (s, 9H), 4.95 (s, 2H), 7.39-7.55 (m, 3H), 7.55-7.65 (m, 2H). **¹³C-NMR** (75 MHz, CDCl₃, PK-890-N): δ 16.1, 18.5, 19.4, 32.9, 34.9, 53.0, 69.7, 128.0, 129.3, 130.8, 133.2, 180.9.

***Tetrabutylammonium pivalate* (CAS 25255-91-8, PK-626,**

49). Pivalic acid (2.04 g, 20.0 mmol, 1.0 eq.) and a grain of phenolphthalein (ca. 0.5 mg) were dissolved in *i*PrOH

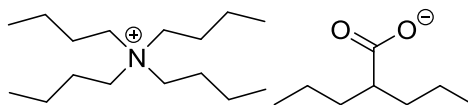


(20 mL). An aqueous solution of tetrabutylammonium hydroxide (40 wt.%) was added until the solution turned light pink (total volume added: 13.1 mL). After stirring for one hour at room temperature, the solvent was removed under reduced pressure (50 °C, 40 mbar). Residual alcohol as well as most of the water was removed by two-fold azeotropic distillation with toluene (10 mL). After cooling to 0 °C, the crystalline solid was washed with hexanes (1 x 10 mL, 3 x 5 mL) and dried in air. The crude product, containing approx. one equivalent of water, was suspended in a toluene-hexanes (2:1, 60 mL) mixture and hexanes were removed under reduced pressure (45 C, 300 mbar) until all solids dissolved. Upon storing of the solution in the fridge for one week (less is also tolerable) colorless crystals formed. Filtration, washing with hexanes (2 x 15 mL) and drying under reduced pressure ($3.3 \cdot 10^{-1}$ mbar) afforded a light purple, hygroscopic solid (6.42 g, 93%).

¹H-NMR (300 MHz, [D₆]-benzene, PK-626-N): δ 0.94 (t, *J* = 7.2 Hz, 12H), 1.23-1.54 (m, 16H), 1.68 (s, 9H), 3.20-3.33 (m, 8H). **¹³C-NMR** (75 MHz, [D₆]-benzene, PK-626-N): δ 14.1, 20.2, 24.6, 30.4, 40.1, 58.8, 181.6. The analytical data matched those reported in the literature.^[80]

***Tetrabutylammonium valproate* (PK-1009, 50).**

Valproate (722 mg, 5.01 mmol, 1.0 eq.) was dissolved



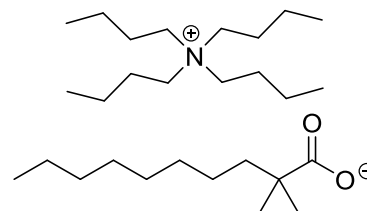
in *i*PrOH (5 mL) and three drops of phenolphthalein in *i*PrOH (0.74 wt.%) were added. An aqueous solution of tetrabutylammonium hydroxide (40%) was added until the solution turned light pink (total volume added: 3.4 mL). After stirring for 15 minutes at room temperature, the solvent was removed under reduced pressure (45 °C, 8 mbar). Residual alcohol as well as most of the water was removed by azeotropic distillation with toluene (2 x 15 mL, 1 x 20 mL). After drying under reduced pressure (55 °C, 7 mbar, 3 hours) a white solid (1.87 g, 97%) was

obtained. The product still contains toluene (0.2 wt.%). Due to its highly hygroscopic nature, the salt was stored in a glovebox to facilitate weighing in.

¹H-NMR (300 MHz, CDCl₃, PK-1009-N): δ 0.87 (t, *J* = 7.1 Hz, 6H), 0.99 (t, *J* = 7.3 Hz, 12H), 1.24-1.52 (m, 14H), 1.52-1.73 (m, 10H), 2.08-2.22 (m, 1H), 3.37-3.49 (m, 8H). **¹³C-NMR** (75 MHz, CDCl₃, PK-1009-N): δ 13.8, 14.7, 19.9, 21.5, 24.3, 36.3, 49.7, 59.0, 181.4.

Tetrabutylammonium 2,2-dimethyldecanoate (PK-927, 51).

2,2-Dimethyldecanoic acid (1.00 g, 5.00 mmol, 1.0 eq.) was dissolved in *i*PrOH (5 mL) and three drops of phenolphthalein in *i*PrOH (0.74 wt.%) were added. An aqueous solution of

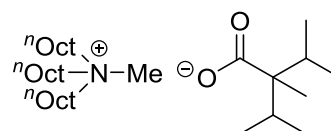


tetrabutylammonium hydroxide (40%) was added until the solution turned light pink (total volume added: 3.28 mL). After stirring for 15 minutes at room temperature, the solvent was removed under reduced pressure (45 °C, 90 mbar). Residual alcohol as well as most of the water was removed by azeotropic distillation with toluene (3 x 6 mL, 2 x 15 mL). After drying under reduced pressure (45 °C, 8 mbar) an orange, viscous oil (2.23 g, 101%) was obtained. The product contains toluene (0.6 wt.%).

¹H-NMR (300 MHz, CDCl₃, PK-927-R2): δ 0.82-0.92 (m, 3H), 0.99 (t, *J* = 7.3 Hz, 12H), 1.11 (s, 6H), 1.25 (s, 12H), 1.44 (sext., *J* = 7.3 Hz, 10H), 1.58-1.75 (m, 8H), 3.28-3.49 (m, 8H). **¹³C-NMR** (75 MHz, CDCl₃, PK-927-R2): δ 13.8, 14.2, 19.9, 22.8, 24.3, 25.7, 26.9, 29.6, 30.0, 30.9, 32.1, 42.4, 43.1, 59.0, 183.0.

Methyltrioctylammonium (MTOA) 2-isopropyl-2,3-dimethylbutanoate (PK-1066).

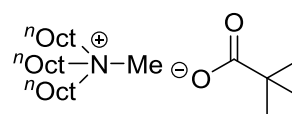
MTOA methyl carbonate (444 mg, 1.00 mmol, 1.1 eq.) and 2-isopropyl-2,3-dimethylbutanoic acid



(143 mg, 904 μmol, 1.0 eq.) were reacted according to general procedure 4.1. Drying under reduced pressure (50 °C, 8 mbar, 2 h) afforded a yellow-orange oil (510 mg, 107%). The higher yield is due to hydrogen carbonate salt (8 wt.%) as well as trioctylamine (1 wt.%) impurity.

¹H-NMR (300 MHz, [D₆]-dimethylsulfoxide, PK-1079-N): δ 0.63-0.97 (m, 24H), 1.11-1.41 (m, 30H), 1.15-1.38 (m, 6H), 1.79 (sept., *J* = 6.8 Hz, 2H), 2.96 (s, 3H), 3.12-3.32 (m, 6H). **¹³C-NMR** (75 MHz, [D₆]-dimethylsulfoxide, PK-1079-N): δ 13.9, 16.0, 18.1, 19.1, 21.3, 22.0, 25.8, 28.4, 28.5, 31.1, 32.1, 47.4, 51.3, 60.4, 176.2.

Methyltrioctylammonium (MTOA) pivalate (PK-1066). MTOA methyl carbonate (444 mg, 1.00 mmol, 1.1 eq.) and pivalic acid (92.5 mg, 906 μmol, 1.0 eq.) were reacted according to general



procedure 4.1. Gas and heat evolution was already observed at room temperature. Drying under reduced pressure (50 °C, 8 mbar, 2 h) afforded a yellow-orange oil (461 mg, 109%). The higher yield is due to hydrogen carbonate salt (8 wt.%) as well as trioctylamine (1 wt.%) impurity.

¹H-NMR (300 MHz, [D₆]-dimethylsulfoxide, PK-1066-N): δ 0.81-0.92 (m, 9H), 0.93 (s, 9H), 1.15-1.40 (m, 30H), 1.46-1.72 (m, 6H), 2.96 (s, 3H), 3.08-3.37 (m, 6H). **¹³C-NMR** (75 MHz, [D₆]-dimethylsulfoxide, PK-1066-N): δ 13.9, 21.3, 22.0, 25.8, 28.4, 28.5, 29.0, 31.1, 38.4, 47.4, 60.4, 179.4.

Methyltrioctylammonium (MTOA) valproate (PK-1081).

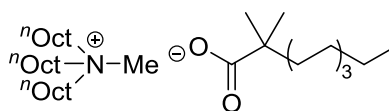
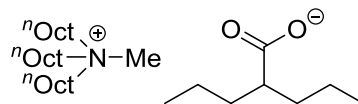
MTOA methyl carbonate (444 mg, 1.00 mmol, 1.1 eq.) and valproate (131 mg, 908 μmol, 1.0 eq.) were reacted according to general procedure 4.1. Drying under reduced pressure (50 °C, 8 mbar, 2 h) afforded a yellow-orange oil (494 mg, 106%). The higher yield is due to hydrogen carbonate salt (8 wt.%) as well as trioctylamine (1 wt.%) impurity.

¹H-NMR (300 MHz, [D₆]-dimethylsulfoxide, PK-1081-N): δ 0.74-0.94 (m, 15H), 1.01-1.48 (m, 40H), 1.53-1.75 (m, 6H), 1.85 (tt, *J* = 9.2, 5.2 Hz, 1H), 2.98 (s, 3H), 3.09-3.42 (m, 6H). **¹³C-NMR** (75 MHz, [D₆]-dimethylsulfoxide, PK-1079-N): δ 13.9, 14.4, 20.7, 21.3, 22.0, 25.8, 28.4, 28.5, 31.1, 35.8, 47.4, 48.1, 60.4, 177.4.

Methyltrioctylammonium (MTOA) 2,2-dimethyldecanoate

(PK-1065). MTOA methyl carbonate (444 mg, 1.00 mmol, 1.09 eq.) and 2,2-dimethyldecanoic acid (184 mg, 919 μmol, 1.0 eq.) were reacted according to general procedure 4.1. Drying under reduced pressure (50 °C, 8 mbar, 2 h) afforded a yellow-orange oil (550 mg, 105%). The higher yield is due to hydrogen carbonate (7 wt.%) salt as well as trioctylamine (1 wt.%) impurity.

¹H-NMR (400 MHz, [D₆]-dimethylsulfoxide, PK-1065-N): δ 0.81-0.91 (m, 18H), 1.05-1.67 (m, 44H), 1.37-1.67 (m, 6H) 2.94 (s, 3H), 3.12-3.28 (m, 6H). **¹³C-NMR** (75 MHz, [D₆]-dimethylsulfoxide, PK-1065-N): δ 13.9 (4C)⁸¹, 21.3, 22.0, 22.1, 25.1, 25.8, 26.9, 28.4, 28.5, 28.8, 29.3, 30.3, 31.2, 31.4, 41.8, 42.0, 47.4, 60.4, 178.9.



⁸¹ Two signals (terminal CH₃ groups) overlay.

7.2.4.5 Exemplary procedures

Table 17, entry 6, according to general procedure 4.2 (PK-1041). Caffeine (97.1 mg, 500 μmol , 1.0 eq.), $\text{PdCl}_2(\text{MeCN})_2$ (6.49 mg, 25.0 μmol , 5.0 mol%), and NBu_4DiPP (20.0 mg, 50.0 μmol , 10.0 mol%) were added to a pre-dried ($2 \cdot 10^{-2}$ mbar, heat-gun) Schlenk tube, which was introduced into a glovebox. K_3PO_4 (212 mg, 1.00 mmol, 2.0 eq.) and bromobenzene (Hamilton syringe, 79.0 μL , 750 μmol , 1.5 eq.) were added and the walls were rinsed with dry DMF (1.5 mL). After five minutes at room temperature outside the glovebox, the suspension was stirred for either 2.5 hours at 100 $^\circ\text{C}$ (pre-heated aluminum block, 600 rpm). At room temperature, the reaction mixture was filtered over a short pad of silica (5 cm), eluting with a DCM-MeOH mixture (10:1, 100 mL) until no further reaction components were recovered. After removal of the solvent under reduced pressure (50 $^\circ\text{C}$, 15 mbar), a q-NMR (1,3,5-trimethoxybenzene: 168.19 g/mol, 37.2 mg, 221.2 μmol) was conducted according to the general procedure for q-NMR analysis (7.1.3, NMR file: PK-1041-q, AVHD400).

Table 18, entry 1, according to general procedure 4.4. (PK-1084). Caffeine (97.1 mg, 500 μmol , 1.0 eq.), $\text{PdCl}_2(\text{MeCN})_2$ (6.49 mg, 25.0 μmol , 5.0 mol%), and dry K_3PO_4 (212 mg, 1.00 mmol, 2.0 eq.) were added to a Schlenk tube, which was evacuated ($<1.0 \cdot 10^{-1}$ mbar) and backfilled with argon thrice. Methyltrioctylammonium pivalate (27.8 mg, 59.2 μmol , 12.0 mol%) and bromobenzene (Hamilton syringe, 79.0 μL , 750 μmol , 1.5 eq.) were added and the walls were rinsed with degassed⁸² water (1.5 mL). After five minutes at room temperature, the suspension was stirred for 13 hours at 100 $^\circ\text{C}$ (pre-heated aluminum block, 600 rpm). At room temperature, the reaction mixture was transferred with DCM (50 mL) to a separatory funnel. A saturated aqueous solution of NaCl (25 mL) was added, phases were separated and the water phase was extracted with DCM (2 x 25 mL). The combined organic extract was dried over Na_2SO_4 , filtered and the solvent was removed under reduced pressure (50 $^\circ\text{C}$, 7 mbar). A q-NMR (1,3,5-trimethoxy-benzene: 168.19 g/mol, 33.2 mg, 197.4 μmol) was conducted according to the general procedure for q-NMR analysis (7.1.3, NMR file: PK-1084-q, AVHD400).

Table 19, entry 2, according to general procedure 4.5 (PK-1018). The procedure was adapted from the group of Fagnou.^[71] $\text{Pd}(\text{OAc})_2$ (3.37 mg, 15.0 μmol , 3.0 mol%), DavePhos (5.90 mg, 15.0 μmol , 3.0 mol%), and NBu_4DiPP (60.0 mg, 150 μmol , 0.3 eq.) were placed in a Schlenk

⁸² Water was degassed for 30 minutes by injection of argon via a cannula.

tube, which was evacuated ($<1.0 \cdot 10^{-1}$ mbar) and backfilled with argon thrice. The Schlenk tube was transferred into a glovebox and K_2CO_3 (173 mg, 1.25 mmol, 2.5 eq.) was added. Outside the glovebox, 4-bromoanisole (63.0 μL , 503 μmol , 1.0 eq.) was added. The walls were rinsed with benzene (2.5 mL) and DMAc (2.9 mL). After five minutes at room temperature, the suspension was stirred for 15 hours at 120 °C (600 rpm). The cooled, brown suspension was transferred to a separatory funnel and diluted with Et_2O (50 mL). The organic phase was washed with water (3 x 25 mL), a saturated aqueous solution of NaCl (25 mL), dried over MgSO_4 , filtered and the solvent was removed under reduced pressure (45 °C, 500 mbar).⁸³ A q-NMR (1,3,5-trimethoxy-benzene: 168.19 g/mol, 28.3 mg, 168.3 μmol) was conducted according to the general procedure for q-NMR analysis (7.1.3, NMR file: 1018-q, AVHD500).

Table 20, entry 1, according to general procedure 4.6 (PK-998). The procedure was adapted from the group of Fagnou^[72] and Kappe^[73]. $\text{Pd}(\text{OAc})_2$ (4.49 mg, 20.0 μmol , 2.0 mol%), and NBu_4DiPP (120 mg, 300 μmol , 0.3 eq.) were placed in a Schlenk tube, which was evacuated ($2.1 \cdot 10^{-1}$ mbar) and backfilled with argon thrice. Inside a glovebox, PCy_3 (11.2 mg, 40.0 μmol , 4.0 mol%) and K_2CO_3 (207 mg, 1.50 mmol, 1.5 eq.) were added. Outside the glovebox, 4-bromoanisole (Hamilton syringe, 125 μL , 1.00 mmol, 1.0 eq.) and 1-methylimidazole (121 μL , 1.50 mmol, 1.5 eq.) were added and the walls were rinsed with dry DMAc (2 mL). After five minutes at room temperature, the suspension was stirred for 18 hours at 100 °C (preheated aluminum block, 600 rpm). The cooled reaction mixture was transferred to a separatory funnel and diluted with EtOAc (50 mL). The organic phase was washed with water (3 x 25 mL), a saturated aqueous solution of NaCl (1 x 25 mL), dried over MgSO_4 , filtered and the solvent was removed under reduced pressure (45 °C, 50 mbar).⁸⁴ A q-NMR (1,3,5-trimethoxy-benzene: 168.19 g/mol, 34.9 mg, 207.5 μmol) was conducted according to the general procedure for q-NMR analysis (7.1.3, NMR file: PK-998-q, AVHD500).

Table 21, entry 3, according to general procedure 4.7 (PK-1001). The procedure was adapted from Marching et al.^[74] 2-Phenylimidazo[1,2-a]pyridine (194 mg, 1.00 mmol, 1.0 eq.), $\text{Pd}(\text{OAc})_2$ (4.49 mg, 20.0 μmol , 2.0 mol%), and NBu_4DiPP (120 mg, 300 μmol , 0.3 eq.) were placed in a Schlenk tube. Inside a glovebox, K_2CO_3 (207 mg, 1.50 mmol, 1.5 eq.) and PCy_3 (11.2 mg, 40.0 μmol , 4.0 mol%) were added. Outside the glovebox, 4-bromotoluene (Hamilton

⁸³ Residual benzene was not removed to avoid any potential, azeotropic distillation of reactants.

⁸⁴ Except for NaCl washing, phases separate very slowly.

syringe, 99%, 147 μ L, 1.20 mmol, 1.2 eq.) was added and the walls were rinsed with dry DMAc (4 mL). After five minutes at room temperature, the reaction mixture was stirred for 18 hours at 100 °C (600 rpm). The suspension was transferred to a separatory funnel and diluted with EtOAc (50 mL). The organic phase was washed with water (3 x 25 mL), a saturated solution of NaCl (1 x 25 mL), dried over MgSO₄, filtered and the solvent was removed under reduced pressure (45 °C, 100 mbar). A q-NMR (1,3,5-trimethoxy-benzene: 168.19 g/mol, 35.3 mg, 209.9 μ mol) was conducted according to the general procedure for q-NMR analysis (7.1.3, NMR file: PK-1001-q, AVHD500).

7.2.5 Vinyl and Benzyl PCy₃-Based Phosphonium Salts: Suitable Precursors for Active Catalyst Generation

7.2.5.1 General synthesis procedures

General procedure 5.2.1 – Wittig olefination with benzophenone an *n*-BuLi

This procedure was adapted from Wirth et al.^[81] In a pre-dried Schlenk flask ($<1.0 \cdot 10^{-1}$ mbar, heat-gun), alkylphosphonium bromide (36.0 mmol, 1.2 eq.) was suspended in THF (60 mL). At 0 °C, a solution of *n*-BuLi (2.5 M in hexanes, 14.4 mL, 36.0 mmol, 1.2 eq.) was added dropwise. After complete addition, the suspension was stirred for two hours at 0 °C. A solution of benzophenone (5.47 g, 30.0 mmol, 1.0 eq.) in THF (30 mL) was added dropwise. After stirring for 30 minutes at 0 °C, the suspension was stirred for 16 hours at room temperature. At 0 °C, a saturated aqueous solution of NH₄Cl (30 mL) and diethylether (30 mL) were added. Phases were separated and the aqueous phase was extracted with diethylether (2 x 50 mL). The combined organic extract was washed with water (2 x 50 mL), a saturated solution of NaCl (1 x 50 mL), dried over MgSO₄, filtered and the solvent was removed under reduced pressure (50 °C, 300 mbar). The crude product was filtered and washed with hexanes (2 x 25 mL) to remove insoluble triphenylphosphine oxide. The washing phase was evaporated to dryness. Purification by flash column chromatography afforded the pure product.

General procedure 5.2.2 – Synthesis of quaternary alkyl tricyclohexylphosphonium salts

Under argon, tricyclohexylphosphine (280 mg, 1.00 mmol, 1.0 eq.) was dissolved in degassed dichloromethane (2 mL/mmol). While stirring, benzyl halide (1.00 mmol, 1.0 eq.) was added and the walls were rinsed with dichloromethane (2-3 mL/mmol). The reaction mixture was stirred for 15 hours at room temperature. After concentration of the solution to approx. 1-1.5 mL, the addition of diethylether (5 mL) caused precipitation of the product. The solid was filtered off and washed with diethylether (3 x 3 mL). Drying under reduced pressure (16 h, r.t., $<1.0 \cdot 10^{-1}$ mbar) afforded the pure product.

General procedure 5.2.3 – Microwave assisted synthesis of vinyl tricyclohexylphosphonium salts (liquid aryl bromide)

Inside a glovebox, tricyclohexylphosphine (1.0 eq.) and Pd precatalyst (5.0 mol%) were added. The walls were rinsed with toluene (2 mL/mmol). After closing the vial with a septum⁸⁵, the

⁸⁵ A NS14 septum was used and turned the other way around to close to microwave vial.

vessel was transferred outside the glovebox. Argon counterflow was ensured with the aid of a cannula (\varnothing 0.90 mm, color code yellow). Additive (10.0 mol%) was added. If liquid (or subliming solid), aryl bromide (1.0-1.3 eq.) was added at once (solid) or dropwise⁸⁶ (liquid). Walls were rinsed with toluene (2 mL/ mmol) and the vial was closed with a PEEK-cap and a PTFE-coated silicon septum. The reaction mixture was stirred for five minutes at room temperature and afterwards heated in an Anton Paar microwave reactor at the indicated temperature and time. At room temperature and in air, the suspension was diluted with dichloromethane (4 mL/mmol) and filtered over a short pad of Celite, eluting with dichloromethane (3 x 2 mL). The solvent was removed under reduced pressure (45 °C, 50 mbar). Dissolution of the obtained solid in a minimum amount of dichloromethane (~2 mL/mmol) followed by addition of diethylether (20 mL/mmol) led to the formation of copious amounts of precipitate. The latter was filtered over a glass filter, washed with Et₂O (3 x 3 mL/mmol) and dried by suction of air with a water-jet pump (fast flow) for 30 minutes. The solid was dissolved in a minimum amount of methanol and filtered over a short pad of Celite to remove insoluble Pd complex, eluting with methanol until no product was recovered. Removal of the solvent and drying under reduced pressure (2 h, 50 °C, 7 mbar) afforded the desired product.

General procedure 5.2.4 – Microwave assisted synthesis of vinyl tricyclohexylphosphonium salts (solid aryl bromide)

If not prone to sublimation, aryl bromide (1.05 eq.) and additive (10.0 mol%) were added in air to a microwave reaction tube which was transferred inside a glovebox. Tricyclohexylphosphine (1.0 eq.) and Pd precatalyst (5.0 mol%) were added. The walls were rinsed with toluene (4 mL/mmol). After closing the vial with a PEEK-cap and a PTFE-coated silicon septum, the vessel was transferred outside the glovebox. The reaction mixture was stirred for five minutes at room temperature and afterwards heated in an Anton Paar microwave reactor at the indicated temperature and time. At room temperature and in air, the suspension was diluted with dichloromethane (4 mL/mmol) and filtered over a short pad of Celite, eluting with dichloromethane (3 x 2 mL). The solvent was removed under reduced pressure (45 °C, 50 mbar). Dissolution of the obtained solid in a minimum amount of dichloromethane (~2 mL/mmol) followed by addition of diethylether (20 mL/mmol) led to the formation of copious amounts of precipitate. The latter was filtered over a glass filter, washed with Et₂O (3 x 3 mL/mmol) and dried by suction of air with a water-jet pump (fast flow) for 30 minutes. The solid was dissolved in a minimum amount of

⁸⁶ The dropwise addition allowed a more accurate weighing of aryl bromide.

methanol and filtered over a short pad of Celite to remove insoluble Pd complex, eluting with methanol until no product was recovered. Removal of the solvent and drying under reduced pressure (2 h, 50 °C, 7 mbar) afforded the desired product.

General procedure 5.2.5 – Isomerization of allyl tricyclohexylphosphonium bromide

A NMR tube was tared on an analytical balance (0.01 mg accuracy). Allyl tricyclohexylphosphonium bromide (NEt₃: 28.90 mg, 72.00 μmol; DABCO: 36.53 mg, 91.00 μmol; DBU: 26.88 mg, 66.96 μmol; 1.0 eq.) was dissolved in CDCl₃ (500 μL) directly in the NMR tube. For DABCO involving reactions, the base (3.06 mg, 27.30 μmol, 0.3 eq.) was added prior dissolution, liquid bases (NEt₃: 1.0 μL, 6.7 μmol, 0.1 eq.; DBU: 1.0 μL, 7.2 μmol, 0.1 eq.) were added afterwards. The tube was closed with a rubber cap and shaken. ¹H-NMR (d₁ = 20 s, 16 scans) and ³¹P-NMR (sw = 100 ppm, O₁P = 50 ppm) spectra were recorded periodically.

General procedure 5.2.6 – Isomerization of α-methylstyrene substituted phosphonium salt

a) NMR scale. A NMR tube was tared on an analytical balance (0.01 mg accuracy). Tricyclohexyl(2-phenylallyl)phosphonium bromide (32.00 mg, 67.00 μmol, 1.0 eq.) was dissolved in CDCl₃ (500 μL) directly in the NMR tube. DBU (1.0 μL, 7.2 μmol, 0.1 eq.) was added. The tube was closed with a rubber cap and shaken. ¹H-NMR (d₁ = 20 s, 16 scans) and ³¹P-NMR (sw = 100 ppm, O₁P = 50 ppm) spectra were recorded periodically.

b) Flask scale. Tricyclohexyl(2-phenylallyl)phosphonium bromide (47.8 mg, 100 μmol, 1.0 eq.) was dissolved or suspended in the indicated solvent (mixture).⁸⁷ Base (NaOPiv: 12.4 mg, 100 μmol, 1.0 eq. or NEt₃: 500 μL, 3.59 mmol, 35.9 eq.) was added and the suspension was stirred for at least 15 hours at room temperature. For NEt₃ reactions, the solvents were removed with the aid of a water-jet pump (slow flow (~500 mbar) in the beginning, fast flow (~20 mbar) when 'dry'). The crude product was analyzed by ¹H- (d₁ = 20 s, 16 scans) and ³¹P-NMR (sw = 100 ppm, O₁P = 50 ppm). Reactions involving NaOPiv were filtered over a short pad of Celite and the solvent was removed under reduced pressure (45 °C, 8 mbar). The crude product was washed with pentane (3 x 3 mL) and dried under reduced pressure (1 h, 50 °C, 8 mbar). ¹H- (d₁ = 20 s, 16 scans) and ³¹P-NMR (sw = 100 ppm, O₁P = 50 ppm) spectra were recorded.

General procedure 5.2.7 – Amination of chlorobenzene

The amination of chlorobenzene was adapted from Reddy et al.^[82]. Under argon, a pre-dried Schlenk tube (<1.0·10⁻¹ mbar, heat-gun) was charged with sodium *tert*-butoxide (139 mg,

⁸⁷ Note: Reactions involving NEt₃ as base were performed in a 10 mL Schlenk tube.

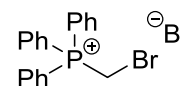
1.39 mmol, 1.4 eq.), palladium source (2.0 mol%), and PCy₃-source (4.0 mol%). The walls were rinsed with dry, degassed toluene (2 mL). The Schlenk tube was evacuated ($<1.0 \cdot 10^{-1}$ mbar, r.t.) and backfilled with argon thrice. *N*-methylpiperazine (110 μ L, 992 μ mol, 1.0 eq.), and chlorobenzene (201 μ L, 1.98 mmol, 2.0 eq.) were added and the walls were rinsed with dry, degassed toluene (2 mL). After stirring for five minutes at room temperature, the reaction mixture was heated for the indicated time to 120 °C (600 rpm).

a) Drying over MgSO₄ (old method). The solution was allowed to cool to room temperature and diluted with dichloromethane (15 mL). The organic phase was dried over MgSO₄, filtered and concentrated under reduced pressure (>700 mbar) to remove dichloromethane. If insoluble rests were visible, dichloromethane was again added until a homogeneous solution was obtained. A q-NMR (1,1,2,2-tetrachloroethane: 53.0 μ L, 502 μ mol) was conducted according to the general procedure for q-NMR analysis (7.1.3).

b) Aqueous work-up (new method). The solution was allowed to cool to room temperature and transferred to a separatory funnel. After dilution with Et₂O (30 mL), the organic phase was washed with an aqueous, dilute NaCl solution (H₂O–sat. aq. NaCl 1:1, 2 x 25 mL), and a saturated aqueous solution of NaCl (25 mL). The ethereal phase was dried over MgSO₄, filtered and the solvent was removed under reduced pressure (45 °C, 200 mbar). A q-NMR (1,1,2,2-tetrachloroethane: 200 μ L, 1.895 mmol) was conducted according to the general procedure for q-NMR analysis (7.1.3).

7.2.5.2 Synthesis of precursors

(Bromomethyl)triphenylphosphonium bromide (CAS 1034-49-7, PK-442).



The procedure was adapted from Drewes et al.^[83]. At room temperature, dibromomethane (4.20 mL, 60.1 mmol, 2.1 eq.) was added to a solution of triphenylphosphine (7.50 g, 28.6 mmol, 1.0 eq.) in toluene⁸⁸ (50 mL). The colorless solution was heated for one day to 123 °C. After cooling to 0 °C, the suspension was filtered; the collected solid was washed with toluene (2 x 10 mL) and pentane (2 x 25 mL), and dried under reduced pressure (r.t., 16 h, $<1.0 \cdot 10^{-1}$ mbar).⁸⁹ A first fraction of white solid (4.66 g, 37%) was obtained. Meanwhile, another portion of dibromomethane (4.20 mL, 60.1 mmol, 2.1 eq.) was added to the filtrate which was heated for one day to 123 °C. Cooling to 0 °C, filtration followed by washing with

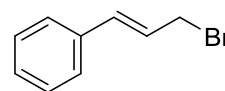
⁸⁸ No dry toluene was used.

⁸⁹ The toluene washing phase was collected in the filtration of the first filtration.

toluene (2 x 50 mL) and pentane (50 mL), and drying under reduced pressure (r.t., 16 h, $<1.0 \cdot 10^{-1}$ mbar) afforded more white, crystalline solid (3.52 g, 28%). Total yield: 8.18 g, 66%.

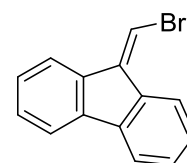
$^1\text{H-NMR}$ (300 MHz, CDCl_3 , PK-442-2): δ 5.90 (d, $J_{\text{P,H}} = 5.8$ Hz, 2H), 7.64-7.76 (m, 6H), 7.76-7.86 (m, 3H), 7.90-8.03 (m, 6H). **$^{13}\text{C-NMR}$** (101 MHz, CDCl_3 , PK-442-R): δ 18.6 (d, $J_{\text{P,C}} = 54.3$ Hz, CH_2), 117.1 (d, $J_{\text{P,C}} = 88.9$ Hz), 130.5 (d, $J_{\text{P,C}} = 13.0$ Hz), 134.5 (d, $J_{\text{P,C}} = 10.2$ Hz), 135.6 (d, $J_{\text{P,C}} = 3.1$ Hz). **$^{31}\text{P-NMR}$** (122 MHz, CDCl_3 , PK-422-2): δ 21.9 (s, minor isomer, 6.7 mol%), 24.0 (s, major, 93.3 mol%). Impurities were detected in the $^1\text{H-NMR}$ (δ 3.33 (d, $J = 13.2$ Hz, 3H), 7.54-8.02 (m, 15H)) and $^{31}\text{P-NMR}$ (δ 19.4⁹⁰ (2.3 mol%), 22.0 (6.0 mol%)) spectra. One species could be assigned to methyl triphenylphosphonium bromide ($\delta_{\text{P}} 22.0$).^[84] The analytical data matched those reported in literature.^[85]

Cinnamyl bromide (CAS 4392-24-9, PK-447). The procedure was adapted from Weaver et al.^[86] At 0 °C, aqueous hydrogen bromide (48%, 50 mL) was added to cinnamyl alcohol (3.00 g, 22.4 mmol, 1.0 eq.). After stirring for three hours at room temperature, saturated aqueous solution of NaHCO_3 (250 mL) and Na_2CO_3 (90 mL) were slowly added until gas evolution ceased. The aqueous phase was extracted with EtOAc (1 x 150 mL, 1 x 100 mL). The combined organic extract was washed with water (100 mL), a saturated aqueous solution of NaCl (100 mL), dried over Na_2SO_4 , filtered and the solvent was removed under reduced pressure (40 °C, 40 mbar). A yellowish oil (4.25 g, 97%) was obtained and used without further purification. The product contained ethyl acetate (3 wt.%) and minor amounts of starting material (8 wt.%).



$^1\text{H-NMR}$ (300 MHz, CDCl_3 , PK-447-R): δ 4.16 (dd, $J = 7.7, 1.0$ Hz, 1H), 6.39 (dt, $J = 15.6, 7.7$ Hz, 1H), 6.65 (d, $J = 15.6$ Hz, 1H), 7.20-7.47 (m, 5H). The analytical data matched those reported in literature.^[86]

9-(Bromomethylene)-9H-fluorene (CAS 4612-64-0, PK-TE-09). The procedure was adapted from Gajewksi et al.^[87] In a pre-dried Schlenk tube ($<1.0 \cdot 10^{-1}$ mbar, heat-gun), (bromomethyl)triphenyl-phosphonium bromide (480 mg, 1.10 mmol, 1.1 eq.) was suspended in THF (3 mL). After dropwise addition of a NaHMDS solution (1 M in THF, 1.10 mL, 1.1 eq.) at -60 °C (dry ice-acetone, not saturated), the yellow suspension was stirred for 40 minutes at the same temperature. A solution of 9-fluorenone (180 mg, 1.00 mmol, 1.0 eq.) in THF (500 μL) was added dropwise. The

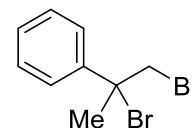


⁹⁰ Only observed in the first fraction of solid.

suspension was allowed to warm to room temperature and stirred for 20 hours at ambient temperature. Water (30 mL) was added and aqueous phase was extracted with diethylether (3 x 20 mL). The combined organic extract was dried over MgSO₄, filtered and the solvent was removed under reduced pressure (40 °C, 8 mbar). Purification by flash column chromatography (hexanes) afforded a yellow solid (179 mg, 69%). The product contains 1,1,2,2-tetrachloroethane (2 wt.%) from previous q-NMR analysis.

TLC: $R_f = 0.49$ (hexanes) [UV, Mostain]. **¹H-NMR** (400 MHz, CDCl₃, PK-TE-09-W): δ 7.27 (dt, $J = 7.5, 1.1$ Hz, 1H), 7.31-7.40 (m, 3H), 7.43 (td, $J = 7.5, 1.1$ Hz, 1H), 7.55 (dt, $J = 7.5, 0.9$ Hz, 1H), 7.68 (ddt, $J = 16.0, 7.5, 0.9$ Hz, 2H), 8.57 (dt, $J = 7.5, 0.9$ Hz, 1H). **¹³C-NMR** (101 MHz, CDCl₃, PK-TE-09-W2): δ 105.9, 119.9, 120.0, 120.3, 125.8, 127.4, 127.4, 128.8, 129.6, 136.7, 138.5, 139.0, 139.3, 141.6. The analytical data matched those reported in literature.^[87]

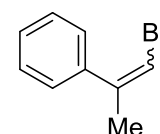
(1,2-Dibromopropan-2-yl)benzene (CAS 36043-44-4, PK-BC-04). The procedure was adapted from Lodder et al.^[88] At 0 °C, bromine (1.19 mL, 23.4 mmol, 1.2 eq.) was added dropwise to a solution of α -methylstyrene



(2.36 g, 20.0 mmol, 1.0 eq.) in dichloromethane (30 mL). The reddish solution was stirred for one hour at room temperature. Residual bromine was quenched with the addition of a saturated aqueous solution of Na₂SO₃ (30 mL) and the aqueous phase was extracted with dichloromethane (3 x 30 mL). The combined organic extract was dried over MgSO₄, filtered and the solvent was removed under reduced pressure (40 °C, 150 mbar). A light yellow oil (6.00 g, 108%) was obtained. The product contained minor impurities from over-bromination^[89] but was used without purification in the next step, elimination to 1-bromo-2-phenylpropene.

¹H-NMR (300 MHz, CDCl₃, PK-BC-04-R): δ 2.32 (s, 3H), 4.14 (d, $J = 10.2$ Hz, 1H), 4.33-4.39 (m, 1H), 7.24-7.44 (m, 3H), 7.50-7.64 (m, 2H). **¹³C-NMR** (75 MHz, CDCl₃, PK-BC-04-R): δ 30.1, 43.6, 63.9, 126.7, 128.6, 128.6, 142.0. The analytical data matched those reported in literature.^[90]

(E/Z)-1-bromo-2-phenylpropene (CAS 16917-35-4, PK-BC-05, 72). The procedure was adapted from the Lodder et al.^[88] (1,2-Dibromopropan-2-yl)benzene (6.00 g, 21.5 mmol, 1.0 eq.)⁹¹ was dissolved in ^tBuOH (100 mL).

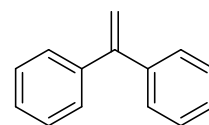


⁹¹ Impurities of the starting material were not considered.

KO^tBu (4.83 g, 43.0 mmol, 2.0 eq.) was added and the reaction mixture was stirred for one hour at 85 °C.⁹² Water (150 mL) was added and the aqueous phase was extracted with diethyl ether (3 x 75 mL). The combined organic extract was washed with an aqueous solution of NaOH (1 M, 20 mL), water (3 x 20 mL), dried over MgSO₄, filtered and the solvent was removed under reduced pressure (45 °C, 100 mbar). A yellowish oil (3.13 g, 80% over 2 steps, E–Z 93:7). The product contains minor amounts of diethylether (0.6 wt.%). Other small impurities (~1 wt.%) stems from 3-bromo-2-phenylpropene^[91]. Since the attempted synthesis of a vinyl phosphonium salt failed, it was not further purified.

(E)-isomer: ¹H-NMR (500 MHz, CDCl₃, PK-BC-05-wash): δ 2.22 (d, *J* = 1.3 Hz, 3H), 6.44 (d, *J* = 1.3 Hz, 1H), 7.28-7.38 (m, 6H). **(Z)-isomer:** ¹H-NMR (500 MHz, CDCl₃, PK-BC-05-wash): δ 2.12 (d, *J* = 1.5 Hz, 3H), 6.23 (d, *J* = 1.5 Hz, 1H), 7.27-7.38 (m, 5H). The analytical data matched those reported in the literature.^[88,92]

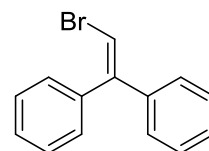
1,1-Diphenylethylene or ethene-1,1-diyldibenzene (CAS 530-48-3, PK-674). The procedure was adapted from Brown et al.^[93]



A pre-dried Schlenk flask (1.5·10⁻¹ mbar, heat-gun) was charged with methyl triphenylphosphonium bromide (10.7 g, 30.0 mmol, 1.2 eq.). The flask was evacuated (1.7·10⁻¹ mbar) and refilled with argon thrice. Walls were rinsed with dry diethylether (100 mL) and KO^tBu (3.36 g, 30.0 mmol, 1.2 eq.) was slowly added in eight portions. The reaction mixture was stirred for 15 minutes at room temperature. At 0 °C, benzophenone (4.56 g, 25.0 mmol, 1.0 eq.) was added over a period of 15 minutes. After stirring for 15 hours at room temperature, the white suspension was filtered over a short pad of Celite, eluting with diethylether (3 x 25 mL). Purification by column chromatography (hexanes) afforded a colorless oil (3.70 g, 82%). The product decomposes over time!

¹H-NMR (400 MHz, CDCl₃, PK-674-A): δ 5.46 (s, 2H), 7.26-7.41 (m, 10H). ¹³C-NMR (101 MHz, CDCl₃, PK-674-A): δ 114.3, 127.7, 128.2, 128.3, 141.5, 150.1. The analytical data matched those reported in literature.^[93]

(2-Bromoethene-1,1-diyl)dibenzene or **2-bromo-1,1-diphenylethylene** (CAS 13249-58-6, PK-732, 69). The procedure was adapted from Feng et al.^[94]



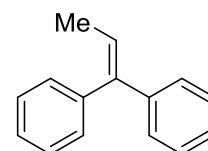
1,1-Diphenylethylene (2.39 g, 13.3 mmol, 1.0 eq.) and *N*-bromosuccinimide (2.41 g, 13.5 mmol, 1.0 eq.) were suspended in acetic acid (50 mL). The

⁹² No cooling was adjusted inside a reflux condenser, since ^tBuOH would solidify.

suspension was stirred for four hours at 80 °C. After cooling to room temperature, water (100 mL) was added and the aqueous phase was extracted with diethylether (2 x 50 mL). The combined organic extract was washed with an aqueous solution of NaOH (2 M, 2 x 50 mL), water (1 x 50 mL), a saturated aqueous solution of NaCl (1 x 50 mL), dried over MgSO₄, filtered, and the solvent was removed under reduced pressure (45 °C, 300 mbar). Purification by flash column chromatography (hexanes) afforded a white, crystalline solid (3.24 g, 94%). **TLC:** $R_f = 0.35$ (hexanes) [UV]. **¹H-NMR** (300 MHz, CDCl₃, PK-732-A2): δ 6.77 (s, 1H), 7.16-7.25 (m, 2H), 7.26-7.34 (m, 5H), 7.34-7.46 (m, 3H). **¹³C-NMR** (75 MHz, CDCl₃, PK-732-A2): δ 105.3, 127.8, 128.1, 128.3, 128.4, 128.6, 129.8, 139.2, 140.9, 147.0. The analytical data matched those reported in literature.^[94]

1,1-Diphenylpropylene or prop-1-ene-1,1-diylidibenzene (CAS 778-66-5,

PK-KH-05). Benzophenone (5.47 g, 30.0 mmol, 1.0 eq.), ethyltri-

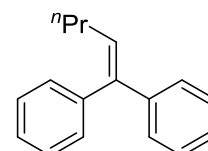


phenylphosphonium bromide (13.4 g, 36.0 mmol, 1.2 eq.), and *n*-BuLi (14.4 mL, 36.0 mmol, 1.2 eq.) in THF (90 mL) were reacted according to general procedure 5.2.1. Purification by flash column chromatography (pentane) afforded a white solid (5.61 g, 96%).

TLC: $R_f = 0.65$ (pentane) [UV]. **¹H-NMR** (400 MHz, CDCl₃, PK-KH-05-N): δ 1.76 (d, $J = 7.0$ Hz, 3H), 6.17 (q, $J = 7.0$ Hz, 1H), 7.15-7.34 (m, 8H), 7.34-7.42 (m, 2H). **¹³C-NMR** (101 MHz, CDCl₃, PK-KH-05-N): δ 15.8, 124.3, 126.9, 127.0, 127.3, 128.2, 128.3, 130.2, 140.2, 142.6, 143.1. The analytical data matched those reported in literature.^[95]

1,1-Diphenylpentylene or pent-1-ene-1,1-diylidibenzene (CAS 1530-11-6,

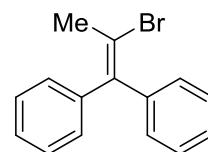
PK-KH-04). Benzophenone (5.47 g, 30.0 mmol, 1.0 eq.), butyl-



triphenylphosphonium bromide (14.4 g, 36.0 mmol, 1.2 eq.), and *n*-BuLi (14.4 mL, 36.0 mmol, 1.2 eq.) in THF (90 mL) were reacted according to general procedure 5.2.1. Purification by flash column chromatography (pentane) afforded a white solid (6.51 g, 98%).

TLC: $R_f = 0.58$ (pentane) [UV]. **¹H-NMR** (400 MHz, CDCl₃, PK-KH-05-N): δ 0.90 (t, $J = 7.4$ Hz, 3H), 1.47 (dt, $J = 14.8, 7.4$ Hz, 2H), 2.09 (q, $J = 7.4$ Hz, 2H), 6.09 (t, $J = 7.4$ Hz, 1H), 7.13-7.33 (m, 8H), 7.33-7.41 (m, 2H). **¹³C-NMR** (101 MHz, CDCl₃, PK-KH-04-N): δ 14.0, 23.3, 32.0, 126.9, 126.9, 127.3, 128.2, 128.3, 130.1, 130.3, 140.5, 141.7, 143.1. The analytical data matched those reported in literature.^[81]

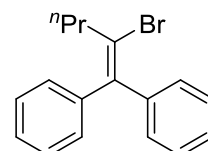
2-Bromo-1,1-diphenylpropene or (2-bromoprop-1-ene-1,1-diyl)dibenzene



(CAS 781-32-8, PK-KH-07, 70). The procedure was adapted from Feng et al.^[94] 1,1-Diphenylpropene (2.00 g, 10.3 mmol, 1.0 eq.) and *N*-bromosuccinimide (1.93 g, 10.8 mmol, 1.1 eq.) were suspended in acetic acid (50 mL). The suspension was stirred for four hours at 80 °C. After cooling to room temperature, diethylether (75 mL) was added. Phases were separated. The organic extract was washed with an aqueous solution of NaOH (2 M, 2 x 50 mL), water (1 x 50 mL), a saturated aqueous solution of NaCl (1 x 50 mL), dried over MgSO₄, filtered, and the solvent was removed under reduced pressure (50 °C, 500 mbar). Since the crude product exhibit a strong acetic acid smell, the crude product was once again diluted with diethylether (70 mL). The organic layer was washed with an aqueous solution of NaOH (6 M, 2 x 50 mL), water (1 x 50 mL), a saturated aqueous solution of NaCl (1 x 50 mL), dried over MgSO₄, filtered, and the solvent was removed under reduced pressure (50 °C, 500 mbar). Purification by flash column chromatography (hexanes) afforded two fractions of a white solid: a) 865 mg (31%) contained 8.0 mol% (5.4 wt.%) starting material, b) 1.28 g (46%, >99% purity). Total yield: 2.10 g, 75%.

TLC: $R_f = 0.27$ (hexanes) [UV, Mostain]. **¹H-NMR** (300 MHz, CDCl₃, PK-KH-07-B2): δ 2.43 (s, 3H), 7.13-7.36 (m, 10H). **¹H-NMR** (500 MHz, [D₄]-methanol, PK-KH-07-methanol): δ 2.39 (s, 3H), 7.16-7.35 (m, 10H). **¹³C-NMR** (75 MHz, [D₄]-methanol, PK-KH-07-B2-13C): δ 27.6, 121.8, 128.1, 128.4, 129.0, 129.4, 130.1, 130.2, 142.1, 143.4, 144.6. The analytical data matched those reported in literature.^[96]

2-Bromo-1,1-diphenylpentene or (2-bromopent-1-ene-1,1-diyl)dibenzene

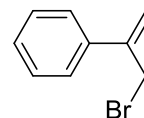


(CAS 22133-86-4, PK-KH-08, 71). The procedure was adapted from Feng et al.^[94] 1,1-Diphenylpentene (2.00 g, 9.00 mmol, 1.0 eq.) and *N*-bromosuccinimide (1.68 g, 9.45 mmol, 1.1 eq.) were suspended in acetic acid (50 mL). The suspension was stirred for 5.5 hours at 80 °C. Since the reaction was not yet complete (TLC, SiO₂, hexanes), another portion of *N*-bromosuccinimide (160 mg, 899 μ mol, 0.1 eq.) was added to the yellowish solution. Stirring was continued for two hours at 80 °C. After cooling to room temperature, diethylether (75 mL) was added. Phases were separated. The organic extract was washed with an aqueous solution of NaOH (6 M, 2 x 50 mL), water (1 x 50 mL), a saturated aqueous solution of NaCl (1 x 50 mL), dried over MgSO₄, filtered, and the solvent was removed under reduced pressure (50 °C, 500 mbar). Purification by flash column chromatography (hexanes) afforded a yellowish oil (1.87 g, 69%). The product contains impurities of

overbromination, elimination and minor amounts of starting material, counting to 15 mol% in total. The product was still involved in the synthesis of vinyl phosphonium salts.

TLC: $R_f = 0.45$ (hexanes) [UV, Mostain]. **$^1\text{H-NMR}$** (300 MHz, CDCl_3 , PK-KH-08-C): δ 0.91 (t, $J = 7.4$ Hz, 3H), 1.62-1.81 (m, 2H), 2.55 (t, $J = 7.4$ Hz, 2H), 7.14-7.46 (m, 10H). **$^{13}\text{C-NMR}$** (75 MHz, CDCl_3 , PK-KH-08-K2-13C): δ 13.2, 22.4, 40.4, 127.2, 127.3, 127.8, 128.1, 128.5, 128.9, 129.2, 130.4, 141.2, 142.1, 143.4. The compound is known to literature, but no analytical data is available.^[97]

(3-bromoprop-1-en-2-yl)benzene (CAS 3360-54-1, PK-863, 74). The procedure was adapted from Gu et al.^[98] and Mukherjee et al.^[91]. A suspension of α -methylstyrene (5.91 g, 50.0 mmol, 1.0 eq.), *N*-bromosuccinimide (9.35 g, 52.5 mmol, 1.1 eq.), and $\text{TsOH}\cdot\text{H}_2\text{O}$ (953 mg, 5.01 mmol, 0.1 eq.) in THF (150 mL) was heated for three hours to 85 °C. Since TLC (SiO_2 , hexanes) revealed incomplete reaction, another portion of *N*-bromosuccinimide (934 mg, 5.00 mmol, 0.1 eq.) was added and the suspension was stirred for one hour at 85 °C. After cooling to room temperature, the solvent was removed under reduced pressure (45 °C, 300 mbar). Hexanes (150 mL) were added. The organic layer was washed with water (3 x 40 mL), a saturated solution of NaCl (1 x 40 mL), dried over MgSO_4 , filtered and the solvent was removed under reduced pressure (45 °C, 100 mbar). Purification by flash column chromatography (hexanes) afforded three fraction of colorless oils: a) (*E*)-1-bromo-2-phenylpropene (595 mg, 6%), b) (3-bromoprop-1-en-2-yl)benzene (3.78 g, 38%), c) mixture of both (a-b 25:75, 4.35 g, 44%).⁹³ The product is prone to decomposition upon prolonged storage! The pure fraction already showed decomposition in the NMR spectra after half a day and was directly used in the next step. The compound is irritant to eyes.

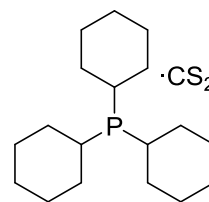


TLC: $R_f = 0.35$ (hexanes) [UV]. **$^1\text{H-NMR}$** (300 MHz, CDCl_3 , PK-863-B): δ 1.54 (s, 1H), 4.39 (br s, 2H), 5.41-5.62 (m, 2H), 7.29-7.43 (m, 3H), 7.43-7.55 (m, 2H). **$^{13}\text{C-NMR}$** (75 MHz, CDCl_3 , PK-863-B): δ 34.3, 117.3, 126.3, 128.4, 128.7, 137.8, 144.4. The analytical data matched those reported in literature.^[91,98]

⁹³ Separation was not 100% successful due to failed (broad) layering of the crude product on the SiO_2 pad. Purification was not repeated, since the amount of isolated pure fraction was sufficient for the planned follow-up reaction.

Tricyclohexylphosphine carbon disulfide adduct (CAS 2636-88-6, PK-TE-

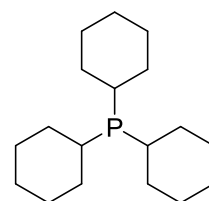
13). The procedure was adapted from Heyn et al.^[99] A 250 mL Schlenk flask was charged with magnesium turnings (Merck, (8.05817, 'cheap & good'), 4.25 g, 175 mmol, 3.5 eq.) and was evacuated ($<1.0 \cdot 10^{-1}$ mbar) and



backfilled with argon thrice. Magnesium turnings were wetter with 1,2-Dibromoethane (70.0 μ L, 809 μ mol, 0.2 eq.). At 40 °C, a solution of chlorocyclohexane (20.8 mL, 175 mmol, 3.5 eq.) in degassed Et₂O (58 mL) was added dropwise. After complete addition, the reaction mixture was refluxed for two hours at 45 °C before dilution with degassed TBME (8.3 mL). In second argon filled 250 mL Schlenk flask, phosphorus trichloride (4.20 mL, 48.0 mmol, 1.0 eq.) was dissolved in degassed TBME (23 mL). At -15 °C, the prepared Grignard solution was added dropwise to the PCl₃ solution.⁹⁴ A white solid precipitated. The suspension was diluted with TMBE (10 mL) and Et₂O (20 mL), and stirred⁹⁵ for 16 hours at room temperature. Slow addition of a degassed, aqueous solution of NH₄Cl (7%, 50 mL) affords a yellow, two-phase system. Under argon, phases were separated with the aid of a Teflon cannula and the organic phase was dried over MgSO₄. The organic layer was transferred to a third, argon flushed flask via Whatman filtration. After removal of the solvent under reduced pressure (r.t., $<1.0 \cdot 10^{-1}$ mbar) to approx. 80 mL, carbon disulfide (4.20, 69.0 mmol, 1.4 eq.) was added causing the precipitation of a red solid. The latter was filtered in air, washed with cold portions of Et₂O (2 x 10 mL) and dried under reduced pressure (r.t., $<1.0 \cdot 10^{-1}$ mbar). A red, crystalline solid (9.98 g, 62%) was obtained. The solid was used as received in the next step (release of free tricyclohexylphosphine).

Tricyclohexylphosphine (CAS 2622-14-2, PK-TE-13). The procedure was

adapted from Heyn et al.^[99] In a 250 mL Schlenk flask fitted with a distillation unit PCy₃·CS₂ (9.90 g, 27.8 mmol, 1.0 eq.) was suspended in degassed ethanol (150 mL). After heating for 30 minutes to 90 °C, occasional argon



flow facilitated removal of carbon disulfide from the suspension.⁹⁶ As soon as CS₂ was completely removed, a solution was obtained. At that time, the temperature was raised to 100 °C to remove residual ethanol. Recrystallization in degassed ethanol (15 mL) at 70 °C and drying

⁹⁴ Caution: PCl₃ reacts violently!!

⁹⁵ Voluminous amounts of white solid impeded regular stirring. The suspension was more or less left standing for 16 hours at room temperature.

⁹⁶ A bubbler (filled with silicon oil) is fitted at the end of the distillation unit.

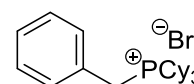
under reduced pressure (2 h, 40 °C, $<1.0 \cdot 10^{-1}$ mbar) afforded a light yellowish solid (6.33 g, 81%).

$^1\text{H-NMR}$ (300 MHz, CDCl_3 , PK-PCy3-Theresa): δ 1.17-1.54 (m, 15H), 1.63-1.90 (m, 12H), 1.92-2.07 (m, 6H). **$^{13}\text{C-NMR}$** (101 MHz, $[\text{D}_6]$ -benzene, PK-TE-13-W): δ 27.0 (d, $J_{\text{P,C}} = 0.9$ Hz), 28.1 (d, $J_{\text{P,C}} = 9.1$ Hz), 31.7 (d, $J_{\text{P,C}} = 12.6$ Hz), 32.3 (d, $J_{\text{P,C}} = 18.8$ Hz). **$^{31}\text{P-NMR}$** (122 MHz, CDCl_3 , PK-PCy3-Theresa): δ 10.0. The analytical data matched those reported in literature.^[100]

7.2.5.3 Synthesis of phosphonium salts

***Benzyltricyclohexylphosphonium bromide* (CAS 57441-10-8, PK-167, 62).**

This compound was prepared during my master thesis.

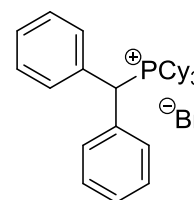


Tricyclohexylphosphine (280 mg, 1.00 mmol, 1.0 eq.) and benzyl bromide (119 μL , 171 mg, 1.00 mmol, 1.0 eq.) in dichloromethane (5 mL) were reacted at room temperature according to general procedure 5.2.2. Drying under reduced pressure (16 h, r.t., $<1.0 \cdot 10^{-1}$ mbar) afforded a white crystalline solid (395 mg, 88%). Suitable single crystals for X-ray analysis (KlePh7) were grown by layering a saturated solution of the product in dichloromethane with diethylether.

$^1\text{H-NMR}$ (400 MHz, CDCl_3 , PK-167-R): δ 1.17-1.33 (m, 3H), 1.33-1.57 (m, 12H), 1.73-1.84 (m, 3H), 1.84-1.95 (m, 6H), 1.95-2.07 (m, 6H), 2.67-2.81 (m, 3H), 4.30 (d, $J = 14.1$ Hz, 2H), 7.31-7.40 (m, 3H), 7.42-7.48 (m, 2H). **$^{13}\text{C-NMR}$** (101 MHz, CDCl_3 , PK-167-N): δ 23.4 (d, $J_{\text{P,C}} = 40.9$ Hz), 25.6 (d, $J_{\text{P,C}} = 1.6$ Hz), 26.7 (d, $J_{\text{P,C}} = 11.7$ Hz), 27.3 (d, $J_{\text{P,C}} = 4.1$ Hz), 31.1 (d, $J_{\text{P,C}} = 38.6$ Hz), 128.5 (d, $J_{\text{P,C}} = 3.2$ Hz), 129.4 (d, $J_{\text{P,C}} = 2.6$ Hz), 129.6, 130.5 (d, $J_{\text{P,C}} = 4.9$ Hz). **$^{31}\text{P-NMR}$** (162 MHz, CDCl_3 , PK-167-R): $\delta = 29.3$. **Analysis** calcd for $\text{C}_{25}\text{H}_{40}\text{BrP}$ C 66.51, H 8.93, P 6.86; found C 66.08, H 9.02, P 6.86. The analytical data matched those reported in the literature.^[101]

***Benzhydryltricyclohexylphosphonium bromide* (PK-168, 63).**

This compound was prepared during my master thesis. Tricyclohexylphosphine (280 mg, 1.00 mmol, 1.0 eq.) and benzhydryl bromide (247 mg, 1.00 mmol, 1.0 eq.) in dichloromethane (5 mL) were reacted at room temperature



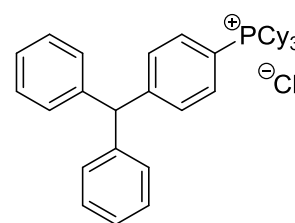
according to general procedure 5.2.2. After drying under reduced pressure (16 h, r.t., $<1.0 \cdot 10^{-1}$ mbar), an off-white solid (341 mg, 65%) was collected. No analytical pure product could be isolated. In the $^{31}\text{P-NMR}$ spectra, several other phosphorous species (δ 19.5 (3.0 mol%), 28.2 (0.7 mol%), 33.5 (HPCy_3Br , 6.5 mol%)) were detected. The product contains diethylether (~ 4.5 mol%) Crystallization of the product entailed 0.5 eq. of dichloromethane even after

extensive drying under reduced pressure (r.t., $<1.0 \cdot 10^{-1}$ mbar). Suitable single crystals for X-ray analysis (KlePh8) were grown by layering a saturated solution of the product in dichloromethane with diethylether.

$^1\text{H-NMR}$ (400 MHz, CDCl_3 , PK-168-R): δ 1.10-1.29 (m, 3H), 1.29-1.48 (m, 12H), 1.76 (d, $J = 13.5$ Hz, 3H), 1.81-1.95 (m, 6H), 1.95-2.06 (m, 6H), 2.84 (q, $J = 11.4$ Hz, 3H), 6.22 (d, $J = 18.0$ Hz, 1H), 7.31-7.38 (m, 2H), 7.41 (t, $J = 7.2$ Hz, 4H), 7.79-7.86 (m, 4H). **$^{13}\text{C-NMR}$** (101 MHz, CDCl_3 , PK-168-R): δ 25.7, 27.1 (d, $J_{\text{P,C}} = 11.5$ Hz), 28.0 (d, $J_{\text{P,C}} = 4.4$ Hz), 33.2 (d, $J_{\text{P,C}} = 34.8$ Hz), 45.8 (d, $J_{\text{P,C}} = 34.3$ Hz), 128.8 (d, $J_{\text{P,C}} = 2.2$ Hz), 129.5, 130.7 (d, $J_{\text{P,C}} = 5.6$ Hz), 134.2 (d, $J_{\text{P,C}} = 4.0$ Hz). **$^{31}\text{P-NMR}$** (162 MHz, CDCl_3 , PK-168-R): δ 29.8. **Analysis** calcd for $\text{C}_{31}\text{H}_{44}\text{BrP} \cdot 2.5 \text{H}_2\text{O}$ C 65.03, H 8.63, P 5.41; found C 65.00, H 8.36, P 5.61. **HRMS** (ESI) calcd for $\text{C}_{31}\text{H}_{44}\text{P}^+$ 447.3175, found 447.3174.

(4-Benzhydrylphenyl)tricyclohexylphosphonium chloride (PK-154,

64). This compound was prepared during my master thesis. Tricyclohexylphosphine (280 mg, 1.00 mmol, 1.0 eq.) and trityl chloride (279 mg, 1.00 mmol, 1.0 eq.) in dichloromethane (5 mL) were reacted at room temperature according to general procedure

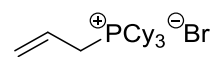


5.2.2. Drying under reduced pressure (16 h, r.t., $<1.0 \cdot 10^{-1}$ mbar) afforded a white powder (430 mg, 77%). Suitable single crystals for X-ray analysis (KlePh9) were grown by slow diffusion of diethylether into a saturated solution of the product in dichloromethane.

$^1\text{H-NMR}$ (400 MHz, CDCl_3 , PK-154-N): δ 1.16-1.27 (m, 3H), 1.38-1.50 (m, 6H), 1.53-1.67 (m, 6H), 1.77-1.93 (m, 9H), 1.99-2.11 (m, 6H), 3.24 (q, $J = 12.3$ Hz, 3H), 5.59 (s, 1H), 7.08-7.14 (m, 4H), 7.22-7.27 (m, 2H), 7.29-7.35 (m, 4H), 7.50 (dd, $J = 8.2, 2.7$ Hz, 2H), 7.95-8.05 (m, 2H). **$^{13}\text{C-NMR}$** (101 MHz, CDCl_3 , PK-154-N): δ 25.8, 26.6 (d, $J_{\text{P,C}} = 12.2$ Hz), 27.2 (d, $J_{\text{P,C}} = 3.4$ Hz), 29.9 (d, $J_{\text{P,C}} = 41.1$ Hz), 57.1, 111.3 (d, $J_{\text{P,C}} = 74.7$ Hz), 127.0, 128.8, 129.5, 131.4 (d, $J_{\text{P,C}} = 11.1$ Hz), 133.8 (d, $J_{\text{P,C}} = 7.5$ Hz), 142.3, 150.9 (d, $J_{\text{P,C}} = 3.1$ Hz). **$^{31}\text{P-NMR}$** (162 MHz, CDCl_3 , PK-154-N): δ 29.8. **Analysis** calcd for $\text{C}_{31}\text{H}_{44}\text{BrP} \cdot 2.5 \text{H}_2\text{O}$ C 65.03, H 8.63, P 5.41; found C 65.00, H 8.36, P 5.61. **HRMS** (ESI) calcd for 523.3488, found 523.3486.

Allyl tricyclohexylphosphonium bromide (CAS 79251-36-8, PK-451,

PK-877, 66). The compound was prepared according to a slightly modified

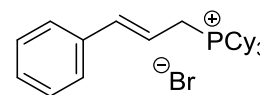


procedure for alkyl tricyclohexylphosphonium salts described by Bestmann et al.^[102] Inside a glovebox, a 20 mL Schlenk tube was charged with tricyclohexylphosphine (280 mg, 1.00 mmol, 1.0 eq.) and transferred outside the glovebox. The walls were rinsed with dry, degassed toluene

(2 mL). After dropwise addition of allyl bromide (125 μ L, 1.45 mmol, 1.5 eq.) at room temperature, the yellowish solution was stirred for 16 hours at 120 $^{\circ}$ C. The two-phase mixture was stored inside a freezer (-25 $^{\circ}$ C) for one hour leading to solidification of one phase. The suspension was filtered in air. Washing with Et₂O (3 x 2 mL, 1 x 4 mL) and drying in air afforded a white solid (391 mg, allyl-vinyl 98:2, 97%). The product contains minor amounts of diethylether (0.4 wt.%). Prolonged drying under reduced pressure (3 h, 45 $^{\circ}$ C, 7 mbar) did not diminish the amount of diethylether.

¹H-NMR (300 MHz, CDCl₃, PK-877-N): δ 1.19-1.75 (m, 15H), 1.76-2.24 (m, 15H), 2.61-2.79 (m, 3H), 3.66 (ddt, $J = 14.6, 7.2, 1.1$ Hz, 2H), 5.44 (ddd, $J = 9.8, 2.7, 1.1$ Hz, 1H), 5.56-5.68 (m, 1H), 5.70-5.88 (m, 1H). **³¹P-NMR** (122 MHz, CDCl₃, PK-877-N): δ 25.4 (s, vinyl species, 2.4 mol%) 29.7 (s, allyl species, 97.6 mol%). This compound is known to literature, but no analytical data is available.

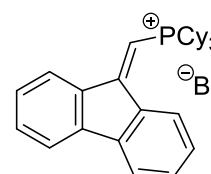
Cinnamyl tricyclohexylphosphonium bromide (CAS 80922-19-6, PK-450, 67). The procedure was adapted from Bestmann et al.^[102] Inside a



glovebox, a 20 mL Schlenk tube was charged with tricyclohexylphosphine (280 mg, 1.00 mmol, 1.0 eq.) and transferred outside the glovebox. The walls were rinsed with dry, degassed toluene (2 mL). After addition of cinnamyl bromide (89%, 286 mg, 1.45 mmol, 1.5 eq.) at room temperature, the solution was stirred for 16 hours at 120 $^{\circ}$ C. The precipitated solid was filtered off, washed with Et₂O (3 x 3 mL), and dried in air. A white solid (371 mg, 78%) was obtained. The product contains minor amounts of toluene (0.3 wt.%).

¹H-NMR (400 MHz, CDCl₃, PK-450-R): δ 1.29 (qt, $J = 12.9, 3.4$ Hz, 3H), 1.45 (qt, $J = 12.9, 3.4$ Hz, 7H), 1.61 (qt, $J = 12.6, 3.4$ Hz, 7H), 1.77-1.85 (m, 3H), 1.88-2.03 (m, 6H), 2.06-2.17 (m, 7H), 2.72 (qt, $J = 12.6, 2.7$ Hz, 3H), 3.88 (ddd, $J = 14.6, 7.8, 0.9$ Hz, 2H), 6.02 (dtd, $J = 15.6, 7.8, 4.2$ Hz, 1H), 6.94 (dd, $J = 15.6, 4.2$ Hz, 1H), 7.27-7.41 (m, 5H). **³¹P-NMR** (162 MHz, CDCl₃, PK-450-R): δ 30.7. This compound is known to literature, but no analytical data is available.

((9H-Fluoren-9-ylidene)methyl)tricyclohexylphosphonium bromide (PK-TE-10, 68). The procedure was adapted from the group of Fürstner.^[103]



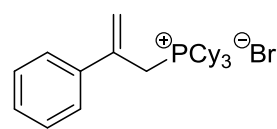
Under argon, a solution of tricyclohexylphosphine (186 mg, 663 μ mol, 1.0 eq.) and 9-(bromomethylene)-9H-fluorene (170 mg, 663 μ mol, 1.0 eq.)

in degassed toluene (9 mL) was heated for 23 hours at 120 $^{\circ}$ C. The yellow solid was filtered

off and washed with toluene (3 x 3 mL). Drying under reduced pressure (2 h, 45 °C, 7 mbar) afforded a yellow solid (257 mg, 72%).

¹H-NMR (400 MHz, [D₂]-dichloromethane, PK-TE-10): δ 1.23-1.39 (m, 3H), 1.47-1.72 (m, 12H), 1.72-1.97 (m, 9H), 2.06-2.22 (m, 6H), 3.39 (qt, $J = 12.2, 2.9$ Hz, 3H), 6.73 (d, $J = 9.7$ Hz, 1H), 7.38 (td, $J = 7.5, 1.0$ Hz, 1H), 7.47 (*virt. t.*, $J = 7.5$ Hz, 1H), 7.50-7.58 (m, 2H), 7.65 (d, $J = 7.4$ Hz, 1H), 7.68-7.75 (m, 1H), 7.84-7.92 (m, 1H), 8.25 (d, $J = 7.7$ Hz, 1H). **¹³C-NMR** (101 MHz, [D₂]-dichloromethane, PK-TE-10): δ 26.0, 27.0 (d, $J = 12.5$ Hz), 28.4 (d, $J = 3.9$ Hz), 33.8 (d, $J = 41.4$ Hz), 97.3 (d, $J = 75.1$ Hz), 120.5, 121.5, 123.8 (d, $J = 0.9$ Hz), 125.7, 128.9, 129.3, 132.5, 133.2, 144.2, 160.1. **³¹P-NMR** (162 MHz, [D₂]-dichloromethane, PK-TE-10): δ 27.9. The analytical data matched those reported in the literature.

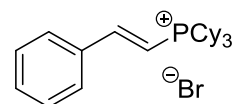
***Tricyclohexyl(2-phenylallyl)phosphonium bromide* (CAS, PK-865, 76).** The compound was prepared according to a procedure for the triphenylphosphonium salt described by the group of Suginome.^[104]



Inside a glovebox, a 20 mL Schlenk tube was charged with tricyclohexylphosphine (280 mg, 1.00 mmol, 1.0 eq.) and transferred outside the glovebox. The walls were rinsed with degassed toluene (2 mL). (3-bromoprop-1-en-2-yl)benzene (312 mg, 1.58 mmol, 1.6 eq.) was added leading to immediate precipitation of white solid. After stirring for three days at room temperature, the solid was filtered off, washed with toluene (4 mL) and Et₂O (3 x 4 mL), and dried in air. A white solid (430 mg, 90%) was obtained. The product contains minor amounts of toluene (0.7 wt.%).

¹H-NMR (400 MHz, CDCl₃, PK-865-R): δ 1.07-1.35 (m, 9H), 1.45-1.62 (m, 6H), 1.62-2.11 (m, 15H), 2.41-2.58 (m, 3H), 4.28 (d, $J = 15.0$ Hz, 2H), 5.52 (d, $J = 4.3$ Hz, 1H), 5.72 (d, $J = 4.3$ Hz, 1H), 7.32-7.48 (m, 3H), 7.51-7.64 (m, 2H). **¹³C-NMR** (75 MHz, CDCl₃, PK-865-N): δ 23.8 (d, $J_{P,C} = 40.4$ Hz), 25.6 (d, $J_{P,C} = 1.7$ Hz), 26.7 (d, $J_{P,C} = 11.8$ Hz), 27.3 (d, $J_{P,C} = 4.0$ Hz), 31.1 (d, $J_{P,C} = 38.5$ Hz), 122.5 (d, $J_{P,C} = 9.8$ Hz), 127.1, 128.8, 129.1, 138.8 (d, $J_{P,C} = 9.2$ Hz), 140.3 (d, $J_{P,C} = 1.9$ Hz). **³¹P-NMR** (162 MHz, CDCl₃, PK-865-R): δ 30.5.

***(E)-Tricyclohexyl(styryl)phosphonium bromide* (PK-850, 65).** Tricyclohexylphosphine (140 mg, 500 μ mol, 1.0 eq.), ω -bromostyrene (115 mg, 628 μ mol, 1.3 eq.), Pd(PPh₃)₄ (29 mg, 25.0 μ mol, 5.0 mol%), and NaOPiv (6.2 mg, 50.0 μ mol, 10 mol%) in dry, degassed toluene (4 mL) were reacted for 15 minutes at 210 °C in an Anton Paar microwave reactor according to general procedure 5.2.3. Drying in an oven for 16 hours at 100 °C afforded an off-white solid (217 mg, 94%). Suitable crystals for X-ray analysis

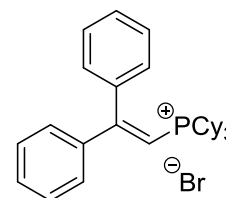


(KlePh4) were grown by slow diffusion of diethylether into a saturated solution of the product in dichloromethane. The product contains methanol (~0.2 mol%) and an unknown PCy₃ species (δ_P 30.2 in [D₄]-methanol, ~1.1-3.3 mol% depending on amount of PCy₃ groups present).

¹H-NMR (300 MHz, [D₄]-methanol, PK-850-R): δ 1.26-1.72 (m, 15H), 1.72-1.87 (m, 3H), 1.87-2.10 (m, 12H), 2.68-2.92 (m, 3H), 6.59 (dd, $J = 17.7, 15.7$ Hz, 1H), 7.41-7.55 (m, 3H), 7.65 (*virt. t.*, $J = 17.7$ Hz, 1H), 7.72-7.81 (m, 2H). **¹³C-NMR** (101 MHz, CDCl₃, PK-102-13C): δ 26.1 (d, $J_{P,C} = 1.6$ Hz), 27.0 (d, $J_{P,C} = 12.3$ Hz), 27.4 (d, $J_{P,C} = 3.6$ Hz), 31.0 (d, $J_{P,C} = 43.0$ Hz), 101.9 (d, $J_{P,C} = 77.0$ Hz), 129.3, 129.5, 132.0, 135.0 (d, $J_{P,C} = 17.0$ Hz), 154.9. **³¹P-NMR** (122 MHz, [D₄]-methanol, PK-850-R): δ 27.9. **Analysis** calcd for C₂₆H₄₀BrP C 67.38, H 8.70, P 6.68; found C 66.78, H 8.72, P 6.66. **HRMS** (ESI) calcd for 383.2862, found 383.2862.

Tricyclohexyl(2,2-diphenylvinyl)phosphonium bromide (PK-KH-24, 74).

Tricyclohexylphosphine (280 mg, 1.00 mmol, 1.0 eq.), 2-bromo-1,1-diphenylethylene (286 mg, 1.10 mmol, 1.1 eq.), Pd(PPh₃)₄ (58 mg, 50.0 μ mol, 5.0 mol%), and NaOPiv (12.5 mg, 100 μ mol, 10.0 mol%) in

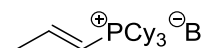


dry, degassed toluene (4 mL) were reacted for one hour at 210 °C in an Anton Paar microwave reactor according to general procedure 5.2.4. Drying in an oven at 50 °C for 16 hours afforded an off-white solid (314 mg, 58%). Suitable crystals for X-ray analysis (HinKr1) were grown by slow diffusion of diethylether into a saturated solution of the product in dichloromethane. The product contains an unknown PCy₃ species (δ_P 30.1 in CDCl₃, ~1.1-3.4 mol% depending on the amount of PCy₃ groups present).

¹H-NMR (400 MHz, CDCl₃, PK-KH-24-crzst⁹⁷): δ 1.17-1.39 (m, 9H), 1.41-1.66 (m, 6H), 1.65-2.11 (m, 15H), 2.58 (qt, $J = 12.5, 2.8$ Hz, 3H), 6.74 (d, $J = 12.4$ Hz, 1H), 7.23-7.31 (m, 2H), 7.34-7.44 (m, 3H), 7.48-7.62 (m, 5H). **¹³C-NMR** (101 MHz, CDCl₃, PK-KH-24-crzst⁹⁷): δ 25.3, 26.3 (d, $J_{P,C} = 12.3$ Hz), 27.4 (d, $J_{P,C} = 3.7$ Hz), 31.9 (d, $J_{P,C} = 41.9$ Hz), 102.1 (d, $J_{P,C} = 73.4$ Hz), 128.5, 128.6, 128.8, 129.8, 130.7, 137.5 (d, $J_{P,C} = 4.9$ Hz), 140.0 (d, $J_{P,C} = 15.8$ Hz), 165.8. **³¹P-NMR** (162 MHz, CDCl₃, PK-KH-24-crzst⁹⁷): δ 28.1.

7.2.5.4 Isomerization of allyl-type phosphonium salts

(E)-Tricyclohexyl(prop-1-en-1-yl)phosphonium bromide (CAS 79251-35-7



(acetate salt), PK-463, 77). Allyl tricyclohexylphosphonium bromide (50.0 mg, 125 μ mol,

⁹⁷ Original file misnamed; correct name is PK-KH-24-cryzt.

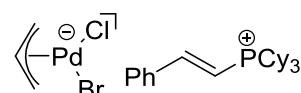
1.0 eq.) and NaOPiv (16.5 mg, 133 μ mol, 1.06 eq.) were suspended in acetone (2.5 mL). The reaction mixture was stirred for 23 hours at room temperature. The suspension was filtered over a short pad of Celite, eluting with acetone (3 x 2 mL). The solvent was removed under reduced pressure (45 °C, 9 mbar), affording a white solid (49.0 mg, 98%).

$^1\text{H-NMR}$ (400 MHz, CDCl_3 , PK-463-R): δ 1.19-1.38 (m, 3H), 1.42-1.59 (m, 12H), 1.76-2.11 (m, 15H), 2.20 (dt, $J = 6.5, 2.0$ Hz, 3H), 2.69-2.87 (m, 3H), 6.20 (ddd, $J = 19.1, 17.3, 2.0$ Hz, 1H), 7.17 (tq, $J = 17.3, 6.5$ Hz, 1H). $^{31}\text{P-NMR}$ (162 MHz, CDCl_3 , PK-463-R): δ 25.4 (s, vinyl isomer, 99.0 mol%), 29.8 (allyl isomer, 1.0 mol%). The product contains acetone (4.8 wt.%). The acetate salt is known to literature but no reference data could be found.

7.2.5.5 Synthesis of Pd-precatalysts

$\text{Pd}_2(\text{dba})_3 \cdot \text{CHCl}_3$ (CAS 52522-40-4, PK-TE-12) – purification of $\text{Pd}(\text{dba})_2$ (dba = dibenzylideneacetone). This procedure was adapted from the group of Ananikov.^[105] Purities of Pd-dba samples were determined by consulting their calculations. Aged $\text{Pd}(\text{dba})_2$ (43%, 1.00 g, 1.74 mmol) was dissolved in chloroform. Remaining Pd black was separated by filtration over a short pad of Celite, eluting with chloroform (2 x 10 mL). The solvent was removed under reduced pressure (≤ 40 °C, 300 mbar). After dissolution of the purple solid in a minimum amount of chloroform, acetone (4 x amount of CHCl_3) was added. The mixture was stored for 16 hours at -25 °C (freezer). Crystals were filtered off, washed with cold acetone (5 °C, 3 x 5 mL) and dried under reduced pressure (16 h, r.t., $< 1.0 \cdot 10^{-1}$ mbar). A dark purple solid (89% purity, 411 mg, 46%) was obtained. NMR files: PK-TE-12-R, PK-TE-12-R2, PK-TE-12-W, PK-TE-12-W2.

$[(\eta^3\text{-allyl})\text{PdClBr}][(\text{trans-PhCHCHPCy}_3^+)]$ (PK-TE-06, 78). A pre-dried ($< 1.0 \cdot 10^{-1}$ mbar, heat-gun) 10 mL Schlenk tube was charged with $[(\eta^3\text{-allyl})\text{PdCl}]_2$ (18.3 mg, 50.0 μ mol, 1.0 eq.)⁹⁸ and (*E*)-tricyclohexyl(styryl)-phosphonium bromide (46.3 mg, 100 μ mol, 2.0 eq.). Walls were rinsed with dry, degassed dichloromethane (1 mL) and the yellow solution was stirred for six hours at room temperature. Inside a glovebox, the reaction mixture was filtered over a short pad of Celite, eluting with dichloromethane (3 x 1 mL). The solvent was removed under reduced pressure with the aid of an external vacuum pump ($< 1.0 \cdot 10^{-1}$ mbar). The yellow solid was washed with diethylether (3 x 1 mL) and hexanes (3 x 1 mL), and dried under reduced pressure (r.t., $< 1.0 \cdot 10^{-1}$ mbar). A



⁹⁸ The Pd-allyl dimer was previously synthesized as part of a different subject (7.2.3.2).

yellow solid (63.0 mg, 91%) was obtained. The solid is stable as solid and in solution in air. The product contains diethylether (0.3 wt.%) and dichloromethane (1.2 wt.%). The structure of the complex has not yet been verified by X-ray or elemental analysis, but ¹H-NMR signals are clearly shifted, and the complex is soluble in chloroform. In comparison, the phosphonium salt precursor is hardly soluble in chloroform.

¹H-NMR (400 MHz, CDCl₃, PK-TE-air): δ 1.21-1.38 (m, 3H), 1.48-1.71 (m, 12H), 1.77-1.88 (m, 3H), 1.88-2.03 (m, 6H), 2.03-2.19 (m, 6H), 2.83-3.01 (m, 5H), 4.06 (d, *J* = 6.6 Hz, 2H), 5.34 (tt, *J* = 12.0, 6.6 Hz, 1H), 6.89 (dd, *J* = 17.8, 15.8 Hz, 1H), 7.40-7.51 (m, 3H), 7.65 (*virt. t.*, *J* = 17.8 Hz, 1H), 7.86-7.96 (m, 2H). **³¹P-NMR** (162 MHz, CDCl₃, PK-TE-06-W): δ 27.7.

7.2.5.6 Release of free PCy₃ ligand from a styryl phosphonium salt

PK-240. A screw cap NMR tube was charged with PdCl₂(MeCN)₂ (6.5 mg, 25.0 μmol, 1.0 eq.), (*E*)-tricyclohexyl(styryl)phosphonium bromide (23.2 mg, 50.0 μmol, 2.0 eq.), and naphthalene⁹⁹ (6.3 mg, 53.1 μmol). Inside a glovebox, NaO^tBu (11.0 mg, 114 μmol, 4.6 eq.) was added and the walls of the tube were rinsed with [D₆]-benzene (700 μL). The tube was closed with an appropriate cap and removed from the glovebox. After sonication for five minutes at room temperature, a ³¹P-NMR (sw = 700 ppm, O₁P = 100 ppm, AVHD300, filename: PK-240-0) spectrum was recorded. Sonication was continued as indicated in figure 36 (5.2.3, AVHD300, filenames: PK-240-1,...).

7.2.5.7 Exemplary procedure

Table 27, entry 9, according to general procedure 5.2.7 (PK-467). The amination of chlorobenzene was adapted from Reddy et al.^[82]. Under argon, a pre-dried Schlenk tube (<1.0·10⁻¹ mbar, heat-gun) was charged with sodium *tert*-butoxide (139 mg, 1.39 mmol, 1.4 eq.), PdCl₂(MeCN)₂ (5.2 mg, 19.8 μmol, 2.0 mol%), and tricyclohexylstyrylphosphonium bromide (**65**, 18.4 mg, 40.0 μmol, 4.0 mol%). The walls were rinsed with dry, degassed toluene (2 mL). The Schlenk tube was evacuated (<1.0·10⁻¹ mbar, r.t.) and backfilled with argon thrice. *N*-methylpiperazine (110 μL, 992 μmol, 1.0 eq.), and chlorobenzene (201 μL, 1.98 mmol, 2.0 eq.) were added and the walls were rinsed with dry, degassed toluene (2 mL). After stirring for five minutes at room temperature, the reaction mixture was heated for 17 hours to 120 °C (600 rpm). The solution was allowed to cool to room temperature and transferred to a separatory

⁹⁹ Note: Naphthalene could have been left out, since integration of ¹H-NMR signals failed.

funnel. After dilution with Et₂O (30 mL), the organic phase was washed with an aqueous, dilute NaCl solution (H₂O–sat. aq. NaCl 1:1, 2 x 25 mL), and a saturated aqueous solution of NaCl (25 mL). The ethereal phase was dried over MgSO₄, filtered and the solvent was removed under reduced pressure (45 °C, 200 mbar). A q-NMR (1,1,2,2-tetrachloroethane: 200 μL, 1.895 mmol) was conducted according to the general procedure for q-NMR analysis (7.1.3, NMR file: PK-467-q, AVHD500).

7.2.6 Cycloheptatrienyl Phosphonium Salts: Synthesis, Reactivity and a Susceptible Rearrangement

7.2.6.1 General synthesis procedures

General procedure 5.3.1 – Synthesis of quaternary Buchwald ligand tropylium salts

In air, Buchwald ligand (1.0 eq.) and tropylium hexafluorophosphate (Trop·PF₆, 1.05-1.1 eq.) were added to a Schlenk tube. The atmosphere was exchanged three times by evacuation and backfilling with argon. The walls were rinsed with dry dichloromethane (0.13-0.20 M) and the suspension was stirred until disappearance of the solids.¹⁰⁰ After one hour, the solution was filtered over a short pad of Celite (~ 0.5 cm) in air. Evaporation of the solvent under reduced pressure (45 °C, min. pressure 7 mbar) afforded the crude product. Unless otherwise stated, the obtained solid (or oil) was dissolved (or diluted in case of an oil) in a minimum amount of dichloromethane (2 mL/mmol). Diethylether (10 mL/mmol) was added to cause precipitation or crystallization. The solid was isolated by filtration and washed with diethylether (3 x 2 mL). Drying in air overnight yielded the pure salt.

General procedure 5.3.2 – Irradiation of [(Trop)SPhos]PF₆

[(Trop)SPhos]PF₆ (14.2 mg, 22.0 μmol) was weighed in a conventional NMR tube. Inside a glovebox, dry, degassed CDCl₃ (550 μL) was added. The sample was inserted in a photoreactor and irradiated for the indicated time at room temperature at the indicated wavelength. For analysis, ¹H-NMR (d₁ = 20 s, 16 scans) and ³¹P-NMR (sw = 100 ppm, O₁P = 10 ppm) spectra were recorded.

General procedure 5.3.3 – Reactivity towards primary or secondary amines

A Schlenk tube was charged with tropyliated phosphine (1.0 eq.) and amine (if solid, 1.0-1.2 eq.). Inside a glovebox, K₂CO₃ (2.0-2.4 eq.) was added. The walls were rinsed with the indicated solvent (5 mL/mmol). Outside the glovebox, amine (if liquid, 2.0 eq.) was added. The suspension was stirred for the indicated time at either room temperature or 50 °C. The suspension was filtered over a short pad of Celite, eluting with dichloromethane (3 x 1 mL). After removal of the solvent under reduced pressure (~2 h, 50 °C, 8 mbar), the solid was suspended in methanol (-25 °C, 1 mL). Filtration, washing with methanol (-25 °C, 3 x 1 mL) and drying under reduced pressure (~1 h, 45 °C, 8 mbar) or in air afforded the product.

¹⁰⁰ Note: tropylium hexafluorophosphate is nearly insoluble in dichloromethane.

General procedure 5.3.4 – Reactivity of [(Trop)SPhos]PF₆ towards NEt₃

A NMR tube was charged with [(Trop)SPhos]PF₆ (32.5 mg, 50.2 μmol, 1.0 eq.). CDCl₃ (500 μL) was added and the tube was shaken until complete dissolution of the solid was reached. Triethylamine (Hamilton syringe, 8.4 μL, 60.2 μmol, 1.2 eq.) was added. The NMR tube was either stored at room temperature or at 50 °C in an oil bath for the indicated time. ¹H- (d₁ = 20 s, 16 scans) and ³¹P-NMR (sw = 100 ppm, O₁P = 10 ppm) spectra were recorded.

General procedure 5.3.5 – Preparation of PhMgBr in THF or Et₂O

A pre-dried (<1.0·10⁻¹ mbar, heat-gun) Schlenk flask was charged with magnesium turnings (Merck (8.05817), 1.47 g, 60.0 mmol, 1.2 eq.) which were overlaid with dry solvent (10 mL). A portion (~1/8) of a solution of bromobenzene (5.35 mL, 50.0 mmol, 1.0 eq.) in dry solvent (40 mL) was added at once. The start of the reaction was indicated by evolution of heat and clouding of the suspension.¹⁰¹ Residual amounts of aryl bromide were added dropwise assuring gentle boiling of the reaction mixture without any external heating. After complete addition, the brown suspension was stirred for 40 minutes at room temperature. The reagent's concentration was determined via titration with salicylaldehyde phenylhydrazone following a procedure by the group of Jones.^[106]

General procedure 5.3.6 – Ni-catalyzed coupling of 2-methoxynaphthalene with PhMgBr

This procedure was partially adapted from Dankwardt.^[107] A pre-dried Schlenk tube (<1.0 · 10⁻¹ mbar, heat-gun) was charged with Ni-precatalyst (5.0 mol%), 2-methoxynaphthalene (158 mg, 1.00 mmol, 1.0 eq.). If needed (kinetic study), tetradecane (250 μL, 960.2 μmol) was added in an argon counterflow. The walls were rinsed with solvent (THF, DEM-Et₂O 1:1) and the Schlenk tube was closed with a septum. While stirring at room temperature, previously prepared Grignard solution (in THF or Et₂O, according to general procedure 5.3.5) was added in one portion.¹⁰² The total solvent volume should add up to 3 mL. The dark brown suspension was stirred for the indicated time at room temperature (600 rpm). For kinetic studies, samples were withdrawn as follows (see 7.1.2 for pictured details). An aliquot (~200 μL) was added to a screw cap vial containing aqueous HCl (2 M, 2 mL) and Et₂O (2 mL). The vial was shaken for ten seconds and the organic phase was transferred to a second vial containing MgSO₄ (150-

¹⁰¹ Partial amounts of bromobenzene can first be added as non-diluted reagent but the mixture should quickly be diluted after start of the reaction.

¹⁰² Concentrations after addition of Grignard reagent: THF (0.25 M), DEM-Et₂O (1:1, either 0.33 M or 0.17 M).

250 mg). After drying over MgSO_4 , the solvent was removed under reduced pressure (water-jet pump, fast flow, ca. 20 mbar) with the aid of a cannula ($\text{\O} 0.90$ mm, color code yellow). The walls were rinsed with CDCl_3 (700 μL) and the crude mixture was stirred for three minutes at room temperature. The suspension was filtered over cotton wool into a NMR tube. A ^1H -NMR (delay = 20 s, 16 scans) spectrum was measured.

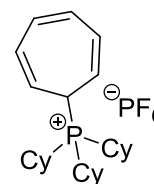
General procedure 5.3.7 – Pd-catalyzed Suzuki coupling of 4-Cl-anisole with $\text{PhB}(\text{OH})_2$

A 20 mL Schlenk tube¹⁰³ was charged with $\text{Pd}(\text{OAc})_2$ (2.21 mg, 9.85 μmol , 1.0 mol%), phenyl boronic acid (180 mg, 1.48 mmol, 1.5 eq.), and ligand (19.7 μmol , 2.0 mol%). The tube was transferred inside a glovebox. Dry K_3PO_4 (418 mg, 1.97 mmol, 2.0 eq.) and 4-chloroanisole (120 μL , 985 μmol , 1.0 eq.) were added and the walls were rinsed with dry toluene (2 mL). The Schlenk tube was closed with a glass stopper and teflon sleeve and removed from the glovebox. After stirring for five minutes at room temperature, the suspension was heated for five hours to 100 $^\circ\text{C}$ (pre-heated aluminum block, 600 rpm). The reaction mixture was cooled to room temperature. Dibenzyl ether (Hamilton syringe, 50.0 μL , 263.0 μmol) was added as internal standard. Stirring was continued for five minutes at room temperature before a q-NMR was conducted following the general procedure for q-NMR analysis (7.1.3).

7.2.6.2 Synthesis of quaternary cycloheptatriene salts

Cyclohepta-2,4,6-trienyltricyclohexylphosphonium hexafluorophosphate

($[(\text{Trop})\text{PCy}_3]\text{PF}_6$, **PK-236**). Tricyclohexylphosphine (280 mg, 1.00 mmol, 1.0 eq.) and $\text{Trop}\cdot\text{PF}_6$ (236 mg, 1.00 mmol, 1.0 eq.) in dichloromethane (5 mL)



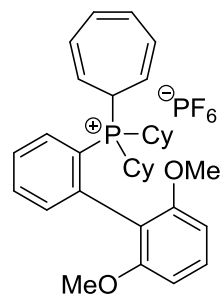
were reacted according to general procedure 5.3.1. Drying under reduced pressure (1 d, r.t., $<1.0\cdot 10^{-1}$ mbar) afforded a white solid (434 mg, 84%). Suitable single crystals for X-ray analysis (KlePh5) were grown by slow diffusion of diethylether into a saturated solution of the salt at room temperature. The product contains minor amounts of diethylether (0.4 wt%).

^1H -NMR (300 MHz, CDCl_3 , PK-236-R): δ 1.18-1.38 (m, 3H), 1.39-1.68 (m, 12H), 1.71-2.11 (m, 15H), 2.20 (dt, $J = 12.7, 6.5$ Hz, 1H), 2.58-2.81 (m, 3H), 5.27-5.39 (m, 2H), 6.42-6.64 (m, 2H), 6.81 (t, $J = 3.2$ Hz, 2H). ^{13}C -NMR (75 MHz, CDCl_3 PK-062-N): δ 25.3 (d, $J_{\text{P,C}} = 1.6$ Hz), 26.4 (d, $J_{\text{P,C}} = 11.7$ Hz), 27.5 (d, $J_{\text{P,C}} = 4.3$ Hz), 29.7 (d, $J_{\text{P,C}} = 50.7$ Hz), 30.7 (d, $J_{\text{P,C}} = 38.4$ Hz),

¹⁰³ A 20 mL Schlenk tube was chosen to assure homogeneous mixing of all components.

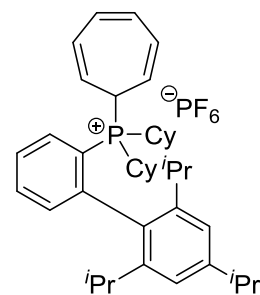
110.2 (d, $J_{P,C} = 2.2$ Hz), 129.0 (d, $J_{P,C} = 12.4$ Hz), 131.5. $^{31}\text{P-NMR}$ (122 MHz, CDCl_3 , PK-236-R): δ -144.3 (sept., $J_{P,F} = 712.0$ Hz, PF_6), 29.9 (s, single/major isomer). **Analysis** calcd for $\text{C}_{25}\text{H}_{40}\text{F}_6\text{P}_2$ C 58.13, H 7.81, F 22.07, P 11.99; found C 58.26, H 8.06, F 21.50, P 11.33. **HRMS** (ESI) calcd for $\text{C}_{25}\text{H}_{40}\text{P}^+$ 371.2862, found 371.2862. Free phosphine (CAS 2622-14-2): $^{31}\text{P-NMR}$ (162 MHz, CDCl_3): δ 9.2.^[108]

Cyclohepta-2,4,6-trienyldicyclohexyl-(2',6'-dimethoxybiphenyl)-2-ylphosphonium hexafluorophosphate (*[(Trop)SPhos]PF₆*, **PK-261**,). SPhos (205 mg, 500 μmol , 1.0 eq.) and Trop·PF₆ (124 mg, 525 μmol , 1.05 eq.) in dichloromethane (4 mL) were reacted according to general procedure 5.3.1. Drying in air afforded an off-white solid (254 mg, 79%). Suitable single crystals for X-ray analysis (KlePh10) were grown by overlaying a saturated solution of the salt in dichloromethane with diethylether and cooling to 0 °C.



$^1\text{H-NMR}$ (500 MHz, CDCl_3 , PK-261-N): δ 1.15-1.28 (m, 6H), 1.36-1.49 (m, 4H), 1.69-1.97 (m, 10H), 2.19-2.23 (m, 1H), 2.56 (q, $J_{P,H} = 12.5$ Hz, 2H), 3.70 (s, 6H), 4.89 (q, $J = 8.5$ Hz, 2H), 6.34-6.35 (m, 2H), 6.67-6.76 (m, 4H), 7.28-7.31 (m, 1H), 7.46 (t, $J = 8.5$ Hz, 1H), 7.67 (t, $J = 7.4$ Hz, 1H), 7.74 (t, $J = 7.4$ Hz, 1H), 7.82 (dd, $J = 11.6, 8.5$ Hz, 1H). $^{13}\text{C-NMR}$ (101 MHz, CDCl_3 , PK-261-N): δ 25.3 (d, $J_{P,C} = 1.4$ Hz, CH_2), 26.6 (d, $J_{P,C} = 12.8$ Hz, CH_2), 26.7 (d, $J_{P,C} = 12.8$ Hz, CH_2), 27.6 (d, $J_{P,C} = 4.1$ Hz, CH_2), 28.0 (d, $J_{P,C} = 4.1$ Hz, CH_2), 29.2 (d, $J_{P,C} = 54.8$ Hz, CH), 34.1 (d, $J_{P,C} = 40.1$ Hz, CH), 56.2 (CH_3), 103.2-103.4 (br m, CH), 105.1 (CH), 115.7 (C_{quat}), 116.7 (d, $J_{P,C} = 54.1$ Hz, C_{quat}), 116.9 (C_{quat}), 127.5 (d, $J_{P,C} = 11.8$ Hz, CH_2), 128.6 (d, $J_{P,C} = 11.1$ Hz, CH_2), 130.6 (CH_2), 131.6 (CH_2), 134.2 (d, $J_{P,C} = 2.9$ Hz, CH_2), 134.8 (d, $J_{P,C} = 8.0$ Hz, CH_2), 135.9 (d, $J_{P,C} = 10.8$ Hz, CH_2), 141.1 (d, $J_{P,C} = 6.3$ Hz, C_{quat}), 157.6 (C_{quat}). $^{31}\text{P-NMR}$ (162 MHz, CDCl_3 , PK-261-N): δ -144.3 (sept., $J_{P,F} = 712.0$ Hz, PF_6), 19.0 (s, protonated species, 2.5 mol%), 34.6 (s, major isomer, 97.5 mol%). Free phosphine (CAS 657408-07-6): $^{31}\text{P-NMR}$ (162 MHz, CDCl_3): δ -8.0.^[109]

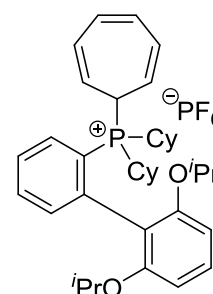
Cyclohepta-2,4,6-trienyldicyclohexyl-(2',4',6'-triisopropylbiphenyl)-2-ylphosphonium hexafluorophosphate (*[(Trop)XPhos]PF₆*, **PK-262**). XPhos (238 mg, 500 μmol , 1.0 eq.) and Trop·PF₆ (124 mg, 525 μmol , 1.05 eq.) in dichloromethane (4 mL) were reacted according to general procedure 5.3.1. Drying in air afforded a white solid (302 mg, 85%). Suitable single crystals for X-ray analysis (KlePh11) were grown by



overlaying a saturated solution of the salt in dichloromethane with diethylether and cooling to 0 °C. The product contains diethylether (0.6 wt.%) due to co-crystallization.

¹H-NMR¹⁰⁴ (500 MHz, [D₂]-dichloromethane, PK-262-CD₂Cl₂): δ 0.97 (d, *J* = 6.7 Hz, 6H), 1.05-1.38 (m, 18H), 1.38-2.04 (m, 14H), 2.31 (sept., *J* = 6.7 Hz, 2H), 2.58 (q, *J* = 12.3 Hz, 2H), 2.97 (sept., *J* = 6.7 Hz, 1H), 4.14 (br s, 2H), 6.14 (br s, 2H), 6.40 (br s, 2H), 7.12 (s, 2H), 7.32 (t, *J* = 5.6 Hz, 1H), 7.67-7.88 (m, 3H). **¹³C-NMR**¹⁰⁴ (101 MHz, [D₂]-dichloromethane, PK-262-CD₂Cl₂): δ 22.7 (CH₃), 24.2 (CH₃), 25.6 (d, *J*_{P,C} = 1.9 Hz, CH₂), 26.3 (CH₃), 27.0 (d, *J*_{P,C} = 3.5 Hz, CH₂), 27.1 (d, *J*_{P,C} = 3.5 Hz, CH₂), 28.0 (d, *J*_{P,C} = 3.8 Hz, CH₂), 28.4 (d, *J*_{P,C} = 3.8 Hz, CH₂), 31.6 (CH), 34.5 (d, *J*_{P,C} = 41.3 Hz, CH), 34.9 (CH), 116.1 (C_{quat.}), 116.5 (d, *J*_{P,C} = 71.4 Hz, C_{quat.}), 122.8 (CH), 127.3-127.7 (m, CH), 128.6-128.9 (m, CH), 129.2 (d, *J*_{P,C} = 11.4 Hz, CH), 134.1 (d, *J*_{P,C} = 3.1 Hz, CH), 134.3 (d, *J*_{P,C} = 1.9 Hz, CH), 134.2-134.4 (m, CH), 136.8 (d, *J*_{P,C} = 11.1 Hz, CH), 146.7 (C_{quat.}), 146.8 (C_{quat.}), 151.2 (C_{quat.}). **³¹P-NMR** (162 MHz, [D₂]-dichloromethane, PK-262-CD₂Cl₂): δ -144.4 (sept., *J*_{P,F} = 712.0 Hz, PF₆), 16.0 (s, protonated species, 1.5 mol%), 33.9 (s, major isomer, 98.5 mol%). Free phosphine (CAS 564483-18-7): **³¹P-NMR** (121 MHz, [D₆]-benzene): δ -11.5.^[110]

Cyclohepta-2,4,6-trienyldicyclohexyl-(2',6'-diisopropoxybiphenyl)-2-ylphosphonium hexafluorophosphate (*[(Trop)RuPhos]PF₆*, **PK-266**). RuPhos (233 mg, 500 μmol, 1.0 eq.) and Trop·PF₆ (124 mg, 525 μmol, 1.05 eq.) in dichloromethane (3 mL) were reacted according to general procedure 5.3.1. Drying in air afforded a white solid (301 mg, 86%). Suitable single crystals for X-ray analysis (KlePh12) were grown by slow diffusion of diethylether into a saturated solution of the salt in dichloromethane.



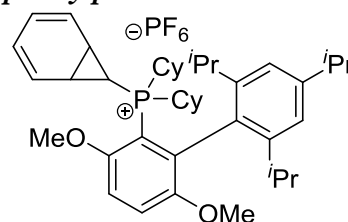
¹H-NMR (500 MHz, CDCl₃, PK-266-N): δ 1.02 (d, *J* = 6.0 Hz, 6H), 1.14-1.36 (m, 6H), 1.18 (d, *J* = 6.0 Hz, 6H), 1.37-1.52 (m, 4H), 1.69-1.76 (m, 2H), 1.76-1.92 (m, 7H), 1.92-2.01 (m, 2H), 2.60-2.80 (m, 2H), 4.38-4.59 (m, 4H), 6.12-6.24 (m, 2H), 6.42-6.53 (m, 2H), 6.62 (d, *J* = 8.4 Hz, 2H), 7.08-7.16 (m, 1H), 7.32 (t, *J* = 8.4 Hz, 1H), 7.64-7.75 (m, 2H), 7.79-7.91 (m, 1H). **¹³C-NMR** (101 MHz, CDCl₃, PK-266-N): δ 21.9 (CH₃), 22.4 (CH₃), 25.0 (d, *J*_{P,C} = 55.6 Hz, CH) 25.4 (d, *J*_{P,C} = 1.4 Hz, CH₂), 26.3 (d, *J*_{P,C} = 9.2 Hz, CH₂), 26.4 (d, *J*_{P,C} = 9.2 Hz, CH₂), 27.5 (d, *J*_{P,C} = 3.9 Hz, CH₂), 27.8 (d, *J*_{P,C} = 3.7 Hz, CH₂), 33.6 (d,

¹⁰⁴ Due to H/D-exchange, the C1-proton of the tropylium unit is not observed. Long C–D relaxation time together with potential overlay of signals impede the assignment of the C1-carbon even with the aid of cryo-NMR (PK-262-13C-cryo).

$J_{P,C} = 41.5$ Hz, CH), 71.5 (CH), 107.3 (CH), 117.0 (d, $J_{P,C} = 73.8$ Hz, $C_{quat.}$), 120.1 (d, $J_{P,C} = 2.5$ Hz, $C_{quat.}$), 127.1 (d, $J_{P,C} = 10.4$ Hz, CH), 128.4 (d, $J_{P,C} = 11.6$ Hz, CH), 128.9 (CH), 130.8 (CH), 133.2 (d, $J_{P,C} = 9.0$ Hz, CH), 133.5 (d, $J_{P,C} = 3.1$ Hz, CH), 135.1 (d, $J_{P,C} = 10.9$ Hz, CH), 142.2 (d, $J_{P,C} = 5.8$ Hz, $C_{quat.}$), 156.6 ($C_{quat.}$). $^{31}\text{P-NMR}$ (162 MHz, CDCl_3 , PK-266-N): δ -144.2 (sept., $J_{P,F} = 712.0$ Hz, PF_6), 20.7 (s, protonated species, 1.6 mol%), 33.6 (s, major isomer, 98.4 mol%). Free phosphine (CAS 787618-22-8): $^{31}\text{P-NMR}$ (121 MHz, $[\text{D}_6]$ -benzene): δ -8.8.^[111]

Norcaradienyldicyclohexyl-(3,6-dimethoxy-2',4',6'-triisopropylbiphenylphosphonium hexa-

fluorophosphate ($[(\text{Trop})\text{BrettPhos}]\text{PF}_6$, PK-433). BrettPhos (134 mg, 250 μmol , 1.0 eq.) and Trop $\cdot\text{PF}_6$ (64.9 mg, 275 μmol , 1.1 eq.) in dichloromethane (2 mL) were reacted according to general procedure 5.3.1. Drying under reduced pressure ($<1.0 \cdot$



10^{-1} mbar) afforded a white solid (166 mg, 86%). Suitable single crystals for X-ray analysis (KlePh16) were grown by overlaying a solution of the salt in dichloromethane (0.1 M) with diethylether (4.5 x volume of dichloromethane) and storing at -25 $^{\circ}\text{C}$ for several days. The product contains diethylether (3 wt.%) due to co-crystallization as well as protonated species (8 wt.%).

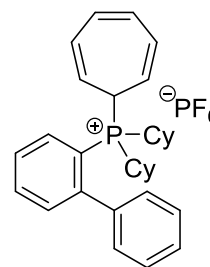
Norcaradienyl species (major isomer):¹⁰⁵ $^1\text{H-NMR}$ (400 MHz, $[\text{D}_6]$ -acetone, PK-433-Aceton): δ 0.27-0.31 (m, 1H), 0.86-1.04 (m, 7H), 1.23 (d, $J = 6.8$ Hz, 6H), 1.27-1.78 (m, 20H), 1.82-1.95 (m, 5H), 2.45 (sept. $J = 6.9$ Hz, 2H), 2.72-2.90 (m, 4H), 2.97 (sept., $J = 6.9$ Hz, 1H), 3.60 (s, 3H), 4.25 (s, 3H), 5.67-5.71 (m, 2H), 5.88 (dd, $J = 7.0, 2.7$ Hz, 2H), 7.18 (s, 2H), 7.47 (dd, $J = 9.1, 5.9$ Hz, 1H) 7.54 (d, $J = 9.1$ Hz, 1H). $^{31}\text{P-NMR}$ (162 MHz, $[\text{D}_6]$ -acetone, PK-433-Aceton): δ -144.2 (sept., $J_{P,F} = 712.0$ Hz, PF_6), 19.5 (s, protonated species, 7.6 mol%), 40.0 (s, major isomer, 80.1 mol%), 40.8 (s, minor isomer, 12.4 mol%).

Protonated species: $^1\text{H-NMR}$ (300 MHz, $[\text{D}_4]$ -methanol, PK-344-MeOH): δ 1.01 (d, $J = 6.7$ Hz, 6H), 1.21-1.51 (m, 20H), 1.59-1.94 (m, 10H), 1.94-2.15 (m, 2H), 2.35 (sept., $J = 6.7$ Hz, 2H), 2.67-2.89 (m, 2H), 2.98 (sept., $J = 6.8$ Hz, 1H), 3.72 (s, 3H), 4.04 (s, 3H), 7.20 (s, 2H), 7.34 (dd, $J = 9.2, 5.9$ Hz, 1H), 7.53 (d, $J = 9.2$ Hz, 1H). $^{31}\text{P-NMR}$ (122 MHz, $[\text{D}_4]$ -methanol, PK-344-MeOH): δ -144.6 (sept., $J_{P,F} = 712.0$ Hz, PF_6), 18.3 (t, $J_{P,D} = 70.4$ Hz,

¹⁰⁵ Due to low solubility and observed partial decomposition, no $^{13}\text{C-NMR}$ could be measured.

protonated species, 92.1 mol%), 39.7 (s, major isomer, 8.7 mol%).¹⁰⁶ Free phosphine (CAS 1070663-78-3): ³¹P-NMR (162 MHz, CDCl₃): δ 1.6.^[112]

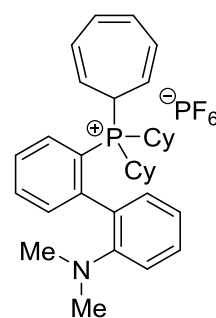
Cyclohepta-2,4,6-trienyldicyclohexyl-2-biphenylphosphonium hexafluoro-phosphate (*[(Trop)CyJohnPhos]PF₆*, **PK-661**). CyJohnPhos (351 mg, 1.00 mmol, 1.0 eq.) and Trop·PF₆ (248 mg, 1.05 mmol, 1.05 eq.) in dichloromethane (5 mL) were reacted according to general procedure 5.3.1. Drying in air afforded a white, crystalline solid (498 mg, 85%). The product contains diethylether (1 wt.%) and dichloromethane (3 wt.%) due to co-crystallization.



¹H-NMR (300 MHz, CDCl₃, PK-661-N): δ 1.10-1.27 (m, 6H), 1.41-1.57 (m, 4H), 1.70-1.91 (m, 10H), 2.02-2.20 (m, 2H), 2.31-2.44 (dt, *J* = 12.0, 6.4 Hz, 1H), 5.12-5.28 (m, 2H), 6.44-6.63 (m, 2H), 6.79 (t, *J* = 2.8 Hz, 2H), 7.19-7.31 (m, 2H), 7.46-7.62 (m, 4H), 7.69-7.75 (m, 1H), 7.78-7.84 (m, 1H), 7.94 (dd, *J* = 12.1, 7.8 Hz, 1H). ¹³C-NMR (75 MHz, CDCl₃, PK-661-N): δ 25.1 (d, *J*_{P,C} = 1.9 Hz, CH₂), 26.5 (d, *J*_{P,C} = 8.3 Hz, CH₂), 26.6 (d, *J*_{P,C} = 8.4 Hz, CH₂), 27.8 (d, *J*_{P,C} = 4.0 Hz, CH₂), 28.5 (d, *J*_{P,C} = 4.1 Hz, CH₂), 30.4 (d, *J*_{P,C} = 54.4 Hz, CH), 35.5 (d, *J*_{P,C} = 39.8 Hz, CH), 107.3-107.5 (m, CH), 113.5 (d, *J*_{P,C} = 71.1 Hz, C_{quat.}), 128.7 (d, *J*_{P,C} = 11.0 Hz, CH), 128.8 (CH), 129.3 (CH), 129.4 (d, *J*_{P,C} = 11.0 Hz, CH), 130.0 (CH), 131.3 (CH), 134.5 (d, *J*_{P,C} = 7.9 Hz, CH), 134.6 (CH), 134.8 (d, *J*_{P,C} = 7.7 Hz, CH), 139.5 (d, *J*_{P,C} = 2.7 Hz, C_{quat.}), 147.1 (d, *J*_{P,C} = 7.7 Hz, C_{quat.}). ³¹P-NMR (122 MHz, CDCl₃, PK-661-N): δ -144.3 (sept., *J*_{P,F} = 712.0 Hz, PF₆), 18.5 (s, protonated species, 1.5 mol%), 36.5 (s, major isomer, 98.5 mol%). Free phosphine (CAS 247940-06-3): ³¹P-NMR (121 MHz, CDCl₃): δ -12.7.^[113]

Cyclohepta-2,4,6-trienyldicyclohexyl-(2'-(dimethylamino)biphenyl)-2-yl-phosphonium hexafluorophosphate (*[(Trop)DavePhos]PF₆*, **PK-662**).

DavePhos (394 mg, 1.00 mmol, 1.0 eq.) and Trop·PF₆ (248 mg, 1.05 mmol, 1.05 eq.) in dichloromethane (5 mL) were reacted according to general procedure 5.3.1. Drying in air afforded a white, crystalline solid (546 mg, 87%). Suitable single crystals for X-ray analysis (KlePh17) were grown by slow diffusion of diethylether into a saturated solution of the salt in dichloromethane. The product contains diethylether (1 wt.%) and dichloromethane (2 wt.%) due to co-crystallization.

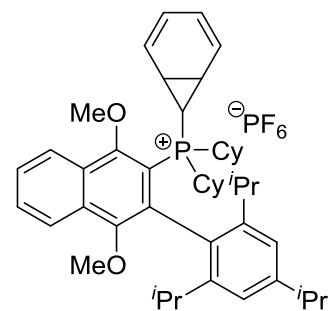


¹⁰⁶ NMR name different due to typing error at the NMR machine.

¹H-NMR (300 MHz, CDCl₃, PK-662-N): δ 0.74-2.03 (m, 20H), 2.25 (dt, *J* = 9.5, 6.2 Hz, 1H), 2.37-2.52 (m, 1H), 2.45 (s, 6H), 2.66 (qt, *J* = 13.0, 3.1 Hz, 1H), 4.74-4.82 (m, 1H), 4.87-4.92 (m, 1H), 6.24-6.29 (m, 1 H), 6.40-6.45 (m, 1H), 6.59-6.77 (m, 2H), 7.08-7.23 (m, 3H), 7.44-7.51 (m, 2H), 7.68-7.85 (m, 3H). **¹³C-NMR** (75 MHz, CDCl₃, PK-662-N): δ 25.1 (d, *J*_{P,C} = 1.3 Hz, CH₂), 25.2 (d, *J*_{P,C} = 1.5 Hz, CH₂), 25.9 (d, *J*_{P,C} = 12.4 Hz, CH₂), 26.6 (d, *J*_{P,C} = 12.6 Hz, CH₂), 26.8 (d, *J*_{P,C} = 11.6 Hz), 27.0 (d, *J*_{P,C} = 12.0 Hz, CH₂), 27.4 (d, *J*_{P,C} = 4.1 Hz, CH₂), 27.8 (d, *J*_{P,C} = 4.1 Hz, CH₂), 28.4 (d, *J*_{P,C} = 3.7 Hz, CH₂), 28.5 (d, *J*_{P,C} = 4.8 Hz, CH₂), 28.9 (d, *J*_{P,C} = 55.3 Hz, CH), 33.3 (d, *J*_{P,C} = 26.7 Hz, CH), 33.8 (d, *J*_{P,C} = 26.9 Hz, CH), 44.2 (CH₃), 99.5-100.3 (m, CH), 114.1 (d, *J*_{P,C} = 73.3 Hz, C_{quat.}), 118.9 (CH), 123.8 (CH), 127.5 (d, *J*_{P,C} = 3.1 Hz, CH), 127.7 (d, *J*_{P,C} = 2.8 Hz, CH), 128.8 (d, *J*_{P,C} = 11.1 Hz, CH), 130.2 (CH), 130.4 (CH), 130.8 (CH), 132.2 (CH), 133.6 (d, *J*_{P,C} = 1.7 Hz, C_{quat.}), 134.7 (d, *J*_{P,C} = 3.0 Hz, CH), 135.4 (d, *J*_{P,C} = 7.8 Hz, CH), 136.0 (d, *J*_{P,C} = 11.1 Hz, CH), 146.8 (d, *J*_{P,C} = 6.9 Hz, C_{quat.}), 151.1 (C_{quat.}). **³¹P-NMR** (122 MHz, CDCl₃, PK-662-N): δ -144.3 (sept., *J*_{P,F} = 712.0 Hz, PF₆), 20.2 (s, protonated species, 1.6 mol%), 35.2 (s, major isomer, 98.4 mol%). **³¹P-NMR** (203 MHz, [D₄]-methanol, PK-662-meoh): δ -144.6 (sept., *J*_{P,F} = 712.0 Hz, PF₆), 17.6 (t, *J*_{P,D} = 74.2 Hz, protonated species, 7.2 mol%), 35.3 (s, major isomer, 92.8 mol%). **³¹P-NMR** (122 MHz, [D₆]-acetone, PK-662-Aceton): δ -144.2 (sept., *J*_{P,F} = 712.0 Hz, PF₆), 35.6 (s, major isomer). Free phosphine (CAS 213697-53-1): **³¹P-NMR** (121 MHz, CDCl₃): δ -8.7.^[114]

Norcaradienyldicyclohexyl-(3-(2',4',6'-triisopropylphenyl)-1,4-dimethoxynaphthalen-2-yl)phosphonium hexafluorophosphate (**[(Trop)KatPhos]PF₆**, **PK-670**).

KatPhos (147 mg, 250 μmol, 1.0 eq.) and Trop-PF₆ (62.0 mg, 263 mmol, 1.05 eq.) in dichloromethane (1.3 mL) were reacted according to general procedure 5.3.1. The crude product was washed with diethylether



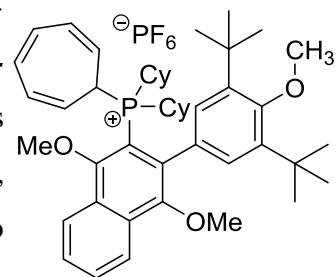
(3 x 2 mL). Drying under reduced pressure (1 h, 45 °C, 8 mbar) afforded an off-white solid (191 mg, 93%). The product contains protonated species (~8 wt.%), educt (~3 wt.%) as well as co-crystallized dichloromethane (~14 wt.%). Further purification by precipitation from dichloromethane did not increase the purity of the product. The salt decomposes over time.

Norcaradienyl species (major isomer):¹⁰⁷ ¹H-NMR (400 MHz, CDCl₃, PK-670-N): δ 0.49 (br s, 1H), 0.88-2.09 (m, 63H), 2.13-3.07 (m, 10H), 3.24 (br s, 3H), 4.42 (br s, 3H), 5.64 (br s, 1H), 5.78 (br s, 1H), 7.12 (br s, 2H), 7.69-7.83 (m, 2H), 8.03-8.14 (m, 2H), 8.17-8.34 (m, 2H). ³¹P-NMR (162 MHz, CDCl₃, PK-670-N): δ -144.3 (sept., $J_{P,F}$ = 712.0 Hz, PF₆), 0.4 (s, educt, 3.9 mol%), 21.2 (s, protonated species, 9.0 mol%), 39.1 (s, major NCD-isomer, 73.4 mol%), 40.0 (br s, minor CHT-isomer, 13.7 mol%).

Protonated species:¹⁰⁸ ¹H NMR (400 MHz, [D₄]-methanol, PK-670-N2-MeOD) δ 1.11-1.23 (m, 9H), 1.23-1.57 (m, 23H), 1.60-1.97 (m, 9H), 2.15-2.28 (m, 2H), 2.43 (sept., J = 6.8 Hz, 2H), 3.02 (sept., J = 6.8 Hz, 1H), 3.70 (s, 3H), 4.42 (s, 3H), 7.28 (s, 2H), 7.84 (dddd, J = 23.2, 8.2, 6.9, 1.3 Hz, 2H), 8.24-8.32 (m, 1H), 8.35-8.42 (m, 1H). ³¹P-NMR (162 MHz, CDCl₃, PK-670-N): δ -144.6 (sept., $J_{P,F}$ = 712.0 Hz, PF₆), 18.2 (t, J = 68.8 Hz, protonated species, 93.8 mol%), 39.5 (s, major NCD-isomer, 6.2 mol%). Free phosphine: ³¹P-NMR (162 MHz, [D₆]-benzene, KR-119-f2): δ -0.3.

Cyclohepta-2,4,6-trienyldicyclohexyl(3-(3',5'-di-tert-butyl-4'-methoxyphenyl)-1,4-dimethoxynaphthalen-2-yl)phosphonium hexafluorophosphate (*[(Trop)CyAnPhos]PF₆*, PK-1019).

CyAnPhos (224 mg, 353 μ mol, 1.0 eq.) and Trop·PF₆ (91.8 mg, 389 μ mol, 1.05 eq.) in dichloromethane (1.7 mL) were reacted according to general procedure 5.3.1. The crude product was washed with diethylether (1 x 15 mL, 3 x 3 mL). Drying under reduced pressure (2 h, 50 °C, 7 mbar) afforded a white solid (236 mg, 80%). The product contains protonated species (~9 wt.%) as well as co-crystallized diethylether (~2 wt.%). The salt partially decomposes when heated with chloroform. A color change to brown is perceived.



¹H-NMR (400 MHz, CDCl₃, PK-966-N2-CDCl₃): δ 1.12-1.34 (m, 9H), 1.38-1.64 (m, 18H), 1.45 (s, 9 H), 1.64-2.00 (m, 12H), 2.40 (*virt.* q, $J_{P,H}$ = 6.2 Hz, 1H), 2.61 (q, $J_{P,H}$ = 12.6 Hz, 2H), 3.27 (s, 3H), 3.77 (s, 3H), 4.27 (s, 3H), 4.86 (*virt.* q, J = 8.6 Hz, 2H), 6.26-6.37 (m, 2H), 6.68

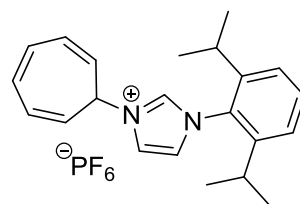
¹⁰⁷ ¹H-NMR shifts were extracted from the obtained mixture of isomers/reaction products. Shifts of the CHT-species could not be extracted. ¹³C-NMR was too unconcentrated to differentiate carbon atoms. As it was also recorded at a later time, the product suffered from decomposition over time, showing the protonated species as major isomer.

¹⁰⁸ NMR spectra were recorded after additional purification by precipitation from dichloromethane. In the ¹H-NMR spectrum, diethylether (46 mol%) and dichloromethane (13 mol%) are visible even after extensive drying of the isolated product. The sample also did not completely dissolve, e.g. KatPhos is insoluble in methanol.

(*virt.* t, $J = 3.3$ Hz, 2H), 7.25 (s, 2H), 7.67-7.84 (m, 2H), 8.18 (dd, $J = 16.8, 8.2$ Hz, 2H). **$^1\text{H-NMR}$** (300 MHz, $[\text{D}_6]$ -acetone, PK-1019-R): δ 1.16-1.44 (m, 8H), 1.50 (s, 18H), 1.55-1.97 (m, 12H), 1.97-2.23 (m, 5H), 2.35 (q, $J = 6.4$ Hz, 1H), 2.72-2.91 (m, 2H), 3.30 (s, 3H), 3.85 (s, 3H), 4.36 (s, 3H), 4.72-4.93 (m, 2H), 6.28-6.47 (m, 2H), 6.59-6.73 (m, 2H), 7.47 (s, 2H), 7.81 (ddd, $J = 8.3, 6.8, 1.3$ Hz, 1H), 7.89 (ddd, $J = 8.3, 6.8, 1.3$ Hz, 1H), 8.27 (dd, $J = 8.3, 1.3$ Hz, 1H), 8.34 (d, $J = 8.4$ Hz, 1H). **$^{13}\text{C-NMR}$** (101 MHz, CDCl_3 , PK-966-N2- CDCl_3): δ 25.2 (d, $J_{\text{P,C}} = 1.2$ Hz, CH_2), 26.7 (*virt.* t, $J_{\text{P,C}} = 12.9$ Hz, CH_2), 28.2 (d, $J_{\text{P,C}} = 4.0$ Hz, CH_2), 28.7 (d, $J_{\text{P,C}} = 4.0$ Hz, CH_2), 32.1 (CH_3), 32.1 (CH), 36.2 (s, C_{quat}), 36.2 (d, $J_{\text{P,C}} = 40.6$ Hz, CH), 60.7 (CH_3), 65.1 (CH_3), 65.4 (CH_3), 103.1 (d, $J_{\text{P,C}} = 72.0$ Hz, C_{quat}), 123.8 (CH), 124.0 (d, $J_{\text{P,C}} = 10.9$ Hz, CH), 126.7 (C_{quat}), 126.7 (d, $J_{\text{P,C}} = 13.0$ Hz, CH), 128.3 (CH), 128.6 (CH), 129.1 (d, $J_{\text{P,C}} = 1.6$ Hz, C_{quat}), 129.3 (C_{quat}), 130.1 (CH), 130.8 (CH), 130.9 (CH), 132.3 (d, $J_{\text{P,C}} = 6.2$ Hz, C_{quat}), 132.8 (d, $J_{\text{P,C}} = 2.2$ Hz, C_{quat}), 144.5 (C_{quat}), 152.2 (d, $J_{\text{P,C}} = 13.2$ Hz, C_{quat}), 160.9 (C_{quat}), 161.0 (C_{quat}). **$^{31}\text{P-NMR}$** (122 MHz, CDCl_3 , PK-966-N2- CDCl_3): δ -144.4 (sept., $J_{\text{P,F}} = 712.0$ Hz, PF_6), 21.2 (br s, protonated species, 11.2 mol%), 38.8 (s, major isomer, 88.8 mol%). **$^{31}\text{P-NMR}$** (122 MHz, $[\text{D}_6]$ -acetone, PK-1019-R): δ 20.5 (br s, protonated species, 8.3 mol%), 39.4 (s, major isomer, 91.7 mol%).

Protonated species: **$^1\text{H-NMR}$** (300 MHz, $[\text{D}_4]$ -methanol, PK-966-MeOD): δ 1.18-1.46 (m, 12H), 1.50 (s, 18H), 1.66-2.15 (m, 12H), 2.70-2.94 (m, 2H), 3.62 (s, 3H), 3.82 (s, 3H), 4.34 (s, 3H), 7.25 (s, 2H), 7.74-7.96 (m, 2H), 8.28-8.37 (m, 2H). **$^{31}\text{P-NMR}$** (122 MHz, $[\text{D}_4]$ -methanol, PK-966-MeOD): δ 19.6 (t, $J_{\text{P,D}} = 68.2$ Hz, protonated species, 91.6 mol%), 38.9 (s, major isomer, 8.4 mol%). Free phosphine: **$^{31}\text{P-NMR}$** (121 MHz, $[\text{D}_6]$ -benzene, KR-236-1): δ -0.1.

***N*-Cyclohepta-2,4,6-trienyl-*N'*-diisopropylphenylimidazolium hexafluorophosphate (Trop dippIm $\cdot\text{PF}_6$, PK-385, 79).** *N*-Diisopropylphenyl-imidazole (1.14 g, 5.00 mmol, 1.0 eq.) and Trop $\cdot\text{PF}_6$ (1.24 g, 5.25 mmol, 1.05 eq.) in dichloromethane (15 mL)



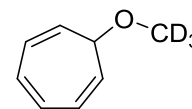
were reacted according to general procedure 5.3.1. Drying in air afforded an off-white solid (1.93 g, 83%). The product contains diethylether (0.5 wt.%) and dichloromethane (0.5 wt.%).

$^1\text{H-NMR}$ (400 MHz, $[\text{D}_2]$ -dichloromethane, PK-385-N): δ 1.12 (d, $J = 6.8$ Hz, 7H), 1.14 (d, $J = 6.8$ Hz, 8H), 2.10 (sept., $J = 6.8$ Hz, 2H), 6.05 (t, $J = 7.9$ Hz, 1H), 6.21 (t, $J = 8.8$ Hz, 2H), 6.75-6.92 (m, 4H), 7.12 (*virt.* t, $J = 1.9$ Hz, 1H), 7.32 (d, $J = 7.9$ Hz, 2H), 7.44 (*virt.* t, $J = 1.9$ Hz, 1H), 7.56 (t, $J = 7.9$ Hz, 1H), 7.90 (*virt.* t, $J = 1.9$ Hz, 1H). **$^{31}\text{P-NMR}$** (162 MHz, $[\text{D}_2]$ -dichloromethane, PK-385-N): δ -144.5 (sept., $J = 712$ Hz, PF_6). **$^{13}\text{C-NMR}$** (75 MHz,

[D₂]-dichloromethane, PK-385-13C): δ 24.3, 24.5, 29.0, 56.6, 119.6, 123.2, 124.6, 125.2, 130.3, 131.9, 132.4, 132.5, 136.0, 145.9.

7.2.6.3 Observed decomposition product of the CHT moiety

7-([D₃]-methoxy)-cyclohepta-2,4,6-triene. This side-product was often detected due to decomposition of a tropylium substituted salt in [D₄]-methanol.

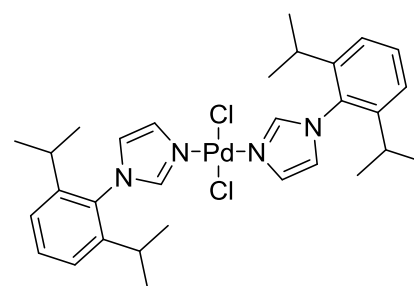


¹H-NMR (400 MHz, [D₄]-methanol, PK-966-N2-MeOD): δ 3.37 (tt, J = 4.5, 1.5 Hz, 1H), 5.41-5.56 (m, 2H), 6.16 (dddd, J = 9.4, 3.7, 2.6, 1.5 Hz, 2H), 6.65-6.67 (m, 2H). ¹³C-NMR (101 MHz, [D₄]-methanol, PK-966-N2-MeOD): δ 79.2 (CH), 124.3 (CH), 126.1 (CH), 132.0 (CH). Methoxy group not observed due to low concentration and very low signal (triplet) intensity. The analytical data matched those reported in the literature.^[115]

7.2.6.4 Conversion of Trop dippIm with metal precursors

Bis-*N*'-(*N*'-diisopropylphenyl)imidazolyl palladium(II) chloride (PK-384, 80). The procedure is similar to the one

reported by the group of Organ.^[116] As a different outcome of the reaction was expected, equivalents are not optimal. A 25 mL round-bottom flask was charged with Trop dippIm·PF₆ (150 mg, 323 μ mol, 1.0 eq.), PdCl₂ (52.0 mg,

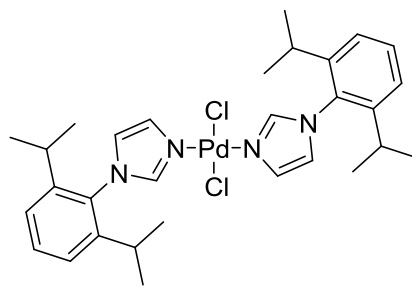


294 μ mol, 1.8 eq.), and K₂CO₃ (406 mg, 2.94 mmol, 18.0 eq.). The flask was closed with a septum, evacuated ($<1.0 \cdot 10^{-1}$ mbar) and backfilled with argon thrice. The walls were rinsed with dry toluene (5 mL). After five minutes at room temperature, the suspension was stirred for 25 hours at 80 °C. The yellow suspension was diluted with dichloromethane (10 mL) and filtered over a short pad of silica (~3 cm) eluting with dichloromethane (15 mL). After removal of the solvent under reduced pressure (40 °C, 55 mbar), the solid was washed with pentane (3 x 2 mL). Drying under reduced pressure (~2 h, 40 °C, 7 mbar) afforded a bright orange solid (93.3 mg, 91%). The isolated salt contains minor impurities of dippIm (0.7 wt.%).

¹H-NMR (400 MHz, CDCl₃, PK-384-FS-CDCl₃): δ 1.12 (d, J = 6.9 Hz, 12H), 1.16 (d, J = 6.9 Hz, 12H), 2.34 (sept., J = 6.9 Hz, 4H), 6.83 (virt. t, J = 1.3 Hz, 2H), 7.25 (d, J = 7.8 Hz, 4H), 7.46 (t, J = 7.8 Hz, 2H), 7.69 (virt. t, J = 1.3 Hz, 2H), 8.12 (virt. t, J = 1.3 Hz, 2H). ¹³C-NMR (101 MHz, CDCl₃, PK-384-FS-CDCl₃): δ 24.4, 24.6, 28.4, 121.1, 124.2, 130.2, 130.7, 132.0, 140.7, 146.3.

Bis-N-(N'-diisopropylphenyl)imidazolyl palladium(II) chloride – direct synthesis approach (PK-776, 80).

The procedure is similar to the one reported by the group of Organ.^[116] A pre-dried Schlenk tube ($2.1 \cdot 10^{-1}$ mbar) was charged with PdCl₂ (355 mg, 2.00 mmol, 1.0 eq.) and *N*-dippIm (959 mg, 4.20 mmol, 2.1 eq.). Inside a glovebox,



K₂CO₃ (2.76 g, 20.0 mmol, 10.0 eq.) was added and the walls were rinsed with dry, degassed toluene (5 mL). Outside the glovebox, the suspension was stirred for five minutes at room temperature before being heated for 16 hours at 80 °C. The suspension was filtered over Celite and the pad was rinsed with dichloromethane (3 x 15 mL).¹⁰⁹ Most of the solvent was removed under reduced pressure (40 °C, 150 mbar). The flask containing the crude product was left open inside a fume hood to allow evaporation of residual toluene. On the next day, large red crystals had formed, and the supernatant was transferred to a second flask. The solid was washed with toluene (4 mL) and pentane (2 x 4 mL). Drying under reduced pressure (1 h, 40 °C, 7 mbar) afforded red crystals (1.04 g, 82%). The filtrate was evaporated to dryness and washed with Et₂O (4 x 4 mL). Drying under reduced pressure (40 °C, 8 mbar) yielded a second fraction of red solid (114 mg, 9%). Total yield: 1.25 g, 91%.

¹H-NMR (300 MHz, CDCl₃, PK-776-cryst): δ 1.12 (d, $J = 6.8$ Hz, 6H), 1.16 (d, $J = 6.8$ Hz, 12H), 2.34 (sept., $J = 6.8$ Hz, 4H), 6.76-6.90 (m, 2H), 7.25 (d, $J = 7.8$ Hz, 4H), 7.46 (d, $J = 7.8$ Hz, 2H), 7.64-7.76 (m, 2H), 8.06-8.19 (m, 2H). ¹³C-NMR (101 MHz, CDCl₃, PK-384-FS-CDCl₃): δ 24.3, 24.6, 28.3, 121.0, 124.1, 130.2, 130.7, 131.9, 140.7, 146.2.

7.2.6.5 Variable temperature NMR study

A J-Young NMR tube was charged with [(Trop)DavePhos]PF₆ (36.6 mg, 58.1 μ mol), transferred into a glovebox, and closed with its special cap. Outside the glovebox, the NMR tube was cooled to -78 °C with the aid of a dry ice saturated acetone bath. In an argon counterflow, dry, degassed [D₆]-acetone (450 μ L) was slowly added. After complete addition, the J-Young tube was closed and shaken until dissolution of the solid was reached.¹¹⁰ The cooled sample was transferred to a pre-cooled (-70 °C) Bruker NMR machine (DRX400). ¹H-NMR as well as ³¹P-NMR spectra (standard parameters were recorded at temperatures ranging

¹⁰⁹ While cooling to room temperature, red crystals emerged.

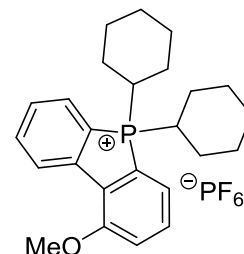
¹¹⁰ Cooling and shaking were performed in a continuous alternation to assure the sample will not heat up.

from $-70\text{ }^{\circ}\text{C}$ to $+50\text{ }^{\circ}\text{C}$ in $20\text{ }^{\circ}\text{C}$ steps. Homogeneous tempering was achieved by holding the temperature for five minutes before measurement.

7.2.6.6 Irradiation of [(Trop)SPhos]PF₆

5,5-Dicyclohexyl-1-methoxy-5H-benzo[b]phosphindol-5-ium hexafluorophosphate or phosphorodifluoridate (PK-1036 and PK-1046).

[(Trop)SPhos]PF₆ (14.2 mg, 22.0 μmol) in CDCl₃ (550 μL) was reacted once for 4.5 hours at 350 nm and two hours at 366 nm (PK-1046) according to general procedure 5.3.2. Purification of merged experiments



by flash column chromatography (DCM-MeOH 10:1) afforded a colorless, glassy solid (7.5 mg)¹¹¹.

TLC: $R_f = 0.24$ (DCM-MeOH 10:1) [UV]. **¹H-NMR** (400 MHz, CDCl₃, PK-1036-1046-BC): δ 0.98-1.35 (m, 4H), 1.48-1.63 (m, 4H), 1.64-1.82 (m, 6H), 1.88-2.06 (m, 6H), 3.81-3.96 (m, 2H), 4.09 (s, 3H), 7.34 (d, $J = 8.4$ Hz, 1H), 7.54-7.68 (m, 2H), 7.76 (tt, $J = 7.8, 1.5$ Hz, 1H), 7.92 (virt. t, $J = 7.8$ Hz, 1H), 8.30 (virt. t, $J = 8.1$ Hz, 1H), 8.52 (dd, $J = 8.1, 2.6$ Hz, 1H). **¹³C-NMR** (101 MHz, CDCl₃, PK-1036-1046-BC): δ 25.4 (d, $J_{P,C} = 1.8$ Hz, CH₂), 25.8 (d, $J_{P,C} = 14.0$ Hz, CH₂), 26.3 (d, $J_{P,C} = 6.8$ Hz, CH₂), 26.4 (d, $J_{P,C} = 6.8$ Hz, CH₂), 31.1 (d, $J_{P,C} = 39.2$ Hz, CH), 56.0 (CH₃), 117.8 (d, $J_{P,C} = 80.6$ Hz, C_{quat.}), 117.8 (d, $J_{P,C} = 2.5$ Hz, CH), 120.5 (d, $J_{P,C} = 79.7$ Hz, C_{quat.}), 124.8 (d, $J_{P,C} = 9.2$ Hz, CH), 127.9 (d, $J_{P,C} = 8.6$ Hz, CH), 129.5 (d, $J_{P,C} = 11.2$ Hz, CH), 132.0 (d, $J_{P,C} = 12.9$ Hz, CH), 132.5 (CH), 132.9 (d, $J_{P,C} = 9.6$ Hz, CH), 135.3 (d, $J_{P,C} = 2.3$ Hz, CH), 144.9 (d, $J_{P,C} = 14.3$ Hz, C_{quat.}), 157.7 (d, $J_{P,C} = 11.7$ Hz, C_{quat.}). **³¹P-NMR**¹¹² (162 MHz, CDCl₃, PK-1036-1046-BC) δ -14.1 (t, $J = 957.9$ Hz, F₂P(O)O⁻ or F₂P(O)OH), 42.03.

7.2.6.7 Attempted hydrolysis of [(Trop)SPhos]PF₆

In CDCl₃ (PK-1029). A J-Young tube was charged with [(Trop)SPhos]PF₆ (32.3 mg, 50.0 μmol , 1.0 eq.). Inside a glovebox, dry, degassed CDCl₃ (500 μL) was added. ¹H- ($d_1 = 20$ s, 16 scans) and ³¹P-NMR (sw = 100 ppm, O₁P = 10 ppm) spectra were recorded. Water (Hamilton syringe, 5.00 μL , 278 μmol , 5.6 eq.) was added. ¹H- ($d_1 = 20$ s, 16 scans) and ³¹P-NMR (sw = 100 ppm, O₁P = 10 ppm) spectra were recorded after 30 minutes and 16 hours at

¹¹¹ No percentage given since the anion distribution, F₂P(O)O⁻ or PF₆⁻, is unclear.

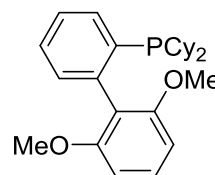
¹¹² ³¹P-NMR was only recorded from -40 to $+60$ ppm for better resolution. Signal of F₂P(O)O⁻ is comparably small.

room temperature. After storing of the sample for one week at room temperature, no color change has been perceived. Solely, an emulsion has been observed. No decomposition was detected.

In [D₆]-acetone (PK-1096). A conventional NMR tube was charged with [(Trop)SPhos]PF₆ (32.3 mg, 50.0 μmol, 1.0 eq.). After addition of [D₆]-acetone (500 μL) in air, the sample was shaken until homogeneous dissolution of the salt. Water (Hamilton syringe, 5.00 μL, 278 μmol, 5.6 eq.) was added. ¹H- (d₁ = 20 s, 16 scans) and ³¹P-NMR (sw = 700 ppm, O₁P = 100 ppm) spectra were recorded. No decomposition was detected. The sample was heated for four hours at 50 °C before recording ¹H- (d₁ = 20 s, 16 scans) and ³¹P-NMR (sw = 700 ppm, O₁P = 100 ppm) spectra.

7.2.6.8 Reactivity of tropylated phosphines towards amines

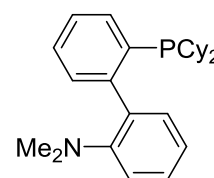
S-Phos or 2-dicyclohexylphosphino-2',6'-dimethoxybiphenyl (CAS 657408-07-6, PK-1053). [(Trop)SPhos]PF₆ (129 mg, 200 μmol, 1.0 eq.), 2-aminopyridine (22.6 mg, 240 μmol, 1.2 eq.), and K₂CO₃ (66.4 mg, 480 μmol, 2.4 eq.) in dichloromethane (1 mL) were reacted for 13 hours at



room temperature according to general procedure 5.3.3. Drying in air afforded a light yellow solid (61.2 mg, 75%). The product contained minor amounts of methanol (0.6 wt.%).

¹H-NMR (400 MHz, CDCl₃, PK-1053-FS): δ 0.95-1.31 (m, 10H), 1.54-1.73 (m, 10H), 1.73-1.84 (m, 2H), 3.67 (s, 6H), 6.58 (d, *J* = 8.4 Hz, 2H), 7.14-7.21 (m, 1H), 7.27-7.36 (m, 2H), 7.39 (t, *J* = 7.4 Hz, 1H), 7.53-7.61 (m, 1H). ¹³C-NMR (101 MHz, CDCl₃, PK-1053-FS): δ 26.7, 27.5 (d, *J*_{P,C} = 7.6 Hz), 27.7 (d, *J*_{P,C} = 11.9 Hz), 29.2 (d, *J*_{P,C} = 9.2 Hz), 30.1 (d, *J*_{P,C} = 16.8 Hz), 34.1 (d, *J*_{P,C} = 13.8 Hz), 55.4, 103.3, 120.1 (d, *J*_{P,C} = 7.2 Hz), 126.3, 128.7 (d, *J*_{P,C} = 59.0 Hz), 131.7 (d, *J*_{P,C} = 6.1 Hz), 132.5 (d, *J*_{P,C} = 3.7 Hz), 136.1 (d, *J*_{P,C} = 17.8 Hz), 143.1 (d, *J*_{P,C} = 32.0 Hz), 157.5-157.7 (m). ³¹P-NMR (162 MHz, CDCl₃, PK-1053-FS): δ -9.1.¹¹³

DavePhos or 2-dicyclohexylphosphino-2'-(*N,N*-dimethylamino)biphenyl (CAS 213697-53-1, PK-1015). [(Trop)DavePhos]PF₆ (126 mg, 200 μmol, 1.0 eq.), *N*-methylpiperazine (44.5 μL, 402 μmol, 2.0 eq.), and K₂CO₃ (55.4 mg, 400 μmol, 2.0 eq.) in dichloromethane (1 mL) were reacted for



¹¹³ According to ³¹P-NMR, minor amounts of tropylium salt (0.9 mol%) as well as phosphine oxide (1.5 mol%) are present. The latter might occur from non-aerobic work-up.

two hours at room temperature according to general procedure 5.3.3. Drying under reduced pressure (16 h, r.t., $6.5 \cdot 10^{-2}$ mbar) afforded a white solid (58.6 mg, 75%).

$^1\text{H-NMR}$ (400 MHz, CDCl_3 , PK-1015-FS): δ 0.71-1.39 (m, 10H), 1.42-1.83 (m, 11H), 1.94-2.10 (m, 1H)¹¹⁴, 2.44 (s, 6H), 6.91-7.10 (m, 3H), 7.26-7.35 (m, 3H), 7.35-7.42 (m, 1H), 7.55 (d, $J = 7.4$ Hz, 1H). **$^{31}\text{P-NMR}$** (162 MHz, CDCl_3 , PK-1015-FS): δ -9.8.¹¹⁵

7.2.6.9 Transfer of phosphine to Pd metal from TropPCy₃·PF₆: a NMR study

PK-234. A screw cap NMR tube was charged with $\text{PdCl}_2(\text{MeCN})_2$ (6.5 mg, 25.0 μmol , 1.0 eq.), TropPCy₃·PF₆ (25.8 mg, 50.0 μmol , 2.0 eq.), and naphthalene (6.2 mg, 48.4 μmol) as internal standard. Inside a glovebox, NaO^tBu (11.0 mg, 114 μmol , 4.6 eq.) and [D₆]-benzene (500 μL) were added. The tube was closed with an appropriate cap and removed from the glovebox. After sonication for five minutes at room temperature, a $^{31}\text{P-NMR}$ (sw = 700 ppm, O₁P = 100 ppm, filenames: PK-234-1, -2, -3...) spectrum was recorded. Sonication was continued as indicated in figure 41 (5.3.4). Integration of $^1\text{H-NMR}$ signals (AVHD500, PK-234-4) revealed the presence of 52% of $\text{Pd}(\text{PCy}_3)_2$. The indication is not accurate, since strong overlapping of signals was observed.

7.2.6.10 Exemplary procedures

Table 34, entry 6, according to general procedure 5.3.7 (PK-1067). A 20 mL Schlenk tube¹¹⁶ was charged with $\text{Pd}(\text{OAc})_2$ (2.21 mg, 9.85 μmol , 1.0 mol%), phenyl boronic acid (180 mg, 1.48 mmol, 1.5 eq.), and [(Trop)S-Phos]PF₆ (12.7 mg, 19.7 μmol , 2.0 mol%). The tube was transferred inside a glovebox. Dry K_3PO_4 (418 mg, 1.97 mmol, 2.0 eq.) and 4-chloroanisole (120 μL , 985 μmol , 1.0 eq.) were added and the walls were rinsed with dry toluene (2 mL). The Schlenk tube was closed with a glass stopper and teflon sleeve and removed from the glovebox. After stirring for five minutes at room temperature, the suspension was heated for five hours to 100 °C (pre-heated aluminum block, 600 rpm). The reaction mixture was cooled to room temperature. Dibenzyl ether (Hamilton syringe, 50.0 μL , 263.0 μmol) was added as internal standard. Stirring was continued for five minutes at room temperature before the mixture was analyzed following the general procedure for q-NMR (7.1.3, NMR file PK-1067-q AVHD500).

¹¹⁴ Signal belongs to the C1_{Cy} proton. The other proton overlays with the multiplet (δ 1.42-1.83).

¹¹⁵ According to $^{31}\text{P-NMR}$, minor amounts of tropylium salt (1.0 mol%) as well as phosphine oxide (1.3 mol%) are present. The latter might occur from non-aerobic work-up.

¹¹⁶ A 20 mL Schlenk tube was chosen to assure homogeneous mixing of all components.

7.2.7 Accessing Trialkylamines as Donors in Heck cross-coupling via a Hydrogen Auto Transfer Process

7.2.7.1 General synthesis procedure

General procedure 6.2.1 – Coupling of trialkylamines with aryl bromides

Unless otherwise stated, a screw cap vial was charged with Pd- and Ir-, Ru- or Rh-precatalyst (5 mol% based on metal). The vial was introduced into a glovebox. Base (2.0 eq.), aryl bromide (3.0 eq.) and amine (1.0 eq.) were added in the indicated order. The walls were rinsed with dry solvent (4 mL/mmol), the vial was closed with a screw cap and the suspension was stirred for 16 hours at 110 °C in a pre-heated metal block outside the glovebox.

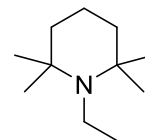
a) At room temperature, the suspension was filtered over a short pad of Celite (in a Pasteur pipette), eluting with CHCl₃ (3 x 0.5 mL). 1,3,5-Trimethoxybenzene (20.0-35.0 mg) was added as internal standard and the contents of the flask was dissolved in CDCl₃ (800 μL). A sample (500 μL) was transferred to a NMR tube and a ¹H-NMR spectrum (d₁ = 20 s, 16 scans) was recorded.

b) At room temperature, the suspension was filtered over a short pad of Celite (in a Pasteur pipette) directly into a separatory funnel. The pad was rinsed with Et₂O (3 x 2 mL) and the filtrate was diluted with additional Et₂O (50 mL). The organic phase was washed with water (3 x 25 mL), a saturated aqueous solution of NaCl (1 x 25 mL), dried over MgSO₄, filtered and the solvent was removed under reduced pressure (45 °C, 500 mbar). 1,3,5-Trimethoxybenzene (20.0-35.0 mg) was added as internal standard and the contents of the flask was dissolved in CDCl₃ (800 μL). A sample (500 μL) was transferred to a NMR tube and a ¹H-NMR spectrum (d₁ = 20 s, 16 scans) was recorded.

7.2.7.2 Synthesis of trialkyl amines

N-Ethyl-2,2,6,6-tetramethylpiperidine (*EtTMP*, CAS 32163-58-9, PK-952, 105).

This procedure was adapted from the group of Berke.^[117] 2,2,6,6-Tetramethylpiperidine (4.94 g, 35.0 mmol, 1.0 eq.) and K₂CO₃ (6.05 g, 43.8 mmol, 1.3 eq.) were suspended in acetonitrile (8.75 mL). The reaction mixture was stirred for four hours at 85 °C before adding ethyl iodide (3.4 mL, 42.0 mmol, 1.2 eq.). After stirring for 19 hours at 85 °C, the suspension was filtered, the filter was rinsed with EtOAc (3 x 10 mL) and the solvent was removed under reduced pressure (45 °C, 90 mbar). Purification by CC

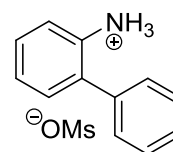


(EtOAc-hexanes 1:20 → 1:10) afforded a colorless, viscous oil (4.70 g, 79%) which solidified upon cooling.

¹H-NMR (300 MHz, [D₆]-benzene, PK-952-A2): δ 1.01 (s, 12H), 1.10 (t, *J* = 7.0 Hz, 3H), 1.35-1.52 (m, 6H), 2.40 (q, *J* = 7.0 Hz, 2H). **¹³C-NMR** (75 MHz, [D₆]-benzene, PK-952-A2): δ 18.2, 21.4, 27.7 (br s), 38.4, 41.6, 54.6. The analytical data matched those reported in the literature.^[118]

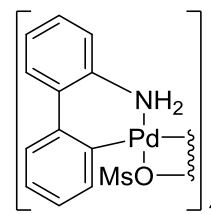
7.2.7.3 Synthesis of Pd precatalysts

2-Ammoniumbiphenyl mesylate (CAS 1445085-50-6, PK-1010). This compound was synthesized according to a procedure by the group of Buchwald.^[119] Methanesulfonic acid (537 mg, 5.59 mmol, 1.1 eq.) in Et₂O (3 mL) was slowly added to a solution of 2-aminobiphenyl (846 mg, 5.00 mmol, 1.0 eq.) in diethylether (18 mL). The suspension was stirred for 30 minutes at room temperature. Filtration, washing with diethylether (3 x 5 mL) and drying under reduced pressure (1.5·10⁻¹ mbar) afforded a pinkish solid (1.29 mg, 97%).



¹H-NMR (500 MHz, [D₄]-methanol, PK-1010-N): δ 2.68 (s, 3H), 7.37-7.68 (m, 9H). **¹³C-NMR** (75 MHz, [D₄]-methanol, PK-772-N): δ 39.5, 124.9, 129.1, 129.9, 130.1, 130.3, 130.3, 130.6, 133.0, 137.6, 138.5. The analytical data matched those reported in the literature.^[119]

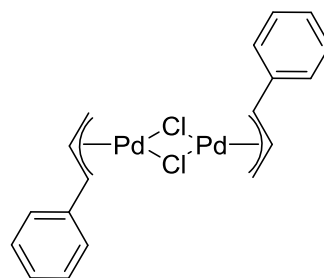
μ-OMs dimer (CAS 1435520-65-2, PK-773). This compound was synthesized according to a procedure by the group of Buchwald.^[119] A Schlenk tube containing palladium acetate (225 mg, 1.00 mmol, 1.0 eq.) and 2-ammoniumbiphenyl mesylate (265 mg, 1.00 mmol, 1.0 eq.) was evacuated (1.4·10⁻¹ mbar) and backfilled with argon three times. The walls were rinsed with anhydrous toluene (4 mL) and the suspension was stirred for 45 minutes at 50 °C. Filtration, washing with toluene (5 mL) and diethylether (3 x 5 mL) and drying under reduced pressure (9.7·10⁻² mbar) afforded a tan solid (313 mg, 85%). The product contains diethylether (1 wt.%).



¹H-NMR (500 MHz, [D₃]-acetonitrile, PK-773-N) δ 2.56 (s, 6H), 6.28 (br s, 4H, NH₂), 7.03-7.10 (m, 2H), 7.12-7.22 (m, 4H), 7.23-7.31 (m, 4H), 7.37 (d, *J* = 6.8 Hz, 2H), 7.46 (d, *J* = 7.6 Hz, 2H), 7.55-7.64 (m, 2H). **¹³C-NMR** (75 MHz, [D₃]-acetonitrile, PK-773-13C) δ 40.0, 121.5, 126.2, 127.1, 127.3, 128.1, 128.8, 128.9, 136.5, 137.4, 137.8, 139.8, 140.2. The analytical data matched those reported in literature.^[119]

***Palladium(π -cinnamyl) chloride dimer* ($[\mu\text{-ClPd}(\text{cin})]_2$ CAS**

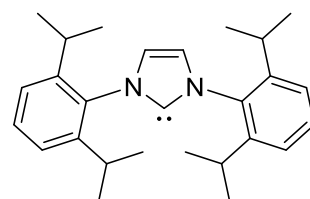
12131-44-1, PK-884, 91). This compound was synthesized according to a procedure by Nolan and coworkers.^[57] Water (125 mL) was added to a Schlenk flask (3 x evacuated, $1.2 \cdot 10^{-1}$ mbar, and backfilled with argon), the flask was closed with a septum and argon was bubbled for 30 minutes through the water.



Palladium(II) chloride (887 mg, 5.00 mmol, 1.0 eq.) and KCl (746 mg, 10.0 mmol, 2.0 eq.) were added under argon flow and the suspension was stirred for one hour at room temperature. Cinnamyl chloride (2.10 mL, 15.0 mmol, 3.0 eq.) was added to the red solution and the reaction mixture was stirred in the dark for one day at room temperature. The orange suspension was transferred to a separatory funnel and extracted with dichloromethane (3 x 50 mL). The organic phase was dried over MgSO_4 , filtered over a pad of Celite, the pad was rinsed with dichloromethane (2 x 25 mL) and the solvent was removed under reduced pressure (45 °C, 100 mbar). The obtained solid was dissolved in dichloromethane (5 mL) and precipitation was caused by addition of pentane (30 mL). Filtration, washing with pentane (3 x 25 mL) and drying in air afforded a yellow orange solid (793 mg, 68%). The product contains dichloromethane (4 mol%).

$^1\text{H-NMR}$ (300 MHz, CDCl_3 , PK-884-N): δ 2.93-3.13 (m, 1H), 3.96 (dd, $J = 6.8, 0.9$ Hz, 1H), 4.62 (d, $J = 11.4$ Hz, 1H), 5.80 (td, $J = 11.7, 6.8$ Hz, 1H), 7.14-7.40 (m, 4H), 7.40-7.59 (m, 2H). **$^{13}\text{C-NMR}$** (75 MHz, CDCl_3 , PK-884-N): δ 59.6, 82.0, 106.1, 128.1, 128.6, 129.2, 137.1. This compound is known to literature but no analytical data is available.

IPr (CAS 244187-81-3, PK-518, 92). This compound was synthesized according to a procedure by Nolan and coworkers.^[120] A pre-dried ($1.0 \cdot 10^{-1}$ mbar, heat-gun) 250 mL Schlenk flask was charged with $\text{IPr}\cdot\text{HCl}$ (6.50 g, 15.3 mmol, 1.0 eq.). In a glovebox,



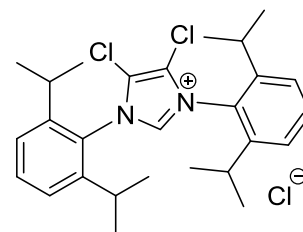
KO^tBu (1.86 g, 16.7 mmol, 1.1 eq.) was added and the walls were rinsed with degassed, dry THF (60 mL). After stirring for four hours at room temperature, the solvent was removed under reduced pressure ($1.0 \cdot 10^{-1}$ mbar) and the obtained solid was dried for two hours *in vacuo*. The residue was suspended in dry toluene (70 mL), heated to 70 °C and filtered over a pre-dried pad of Celite¹¹⁷ (3 cm). The flask as well as the pad of Celite were rinsed with additional dry toluene

¹¹⁷ Celite was pre-dried for 17 hours at 130 °C in an oven (40% ventilation) and additionally dried under reduced pressure ($5.0 \cdot 10^{-2}$ mbar) with a heat-gun.

(70 °C, 15 mL in total). After removal of the solvent under reduced pressure ($5 \cdot 10^{-2}$ mbar, water bath) and drying *in vacuo* afforded a white solid (5.20 g, 88%). The solid is sensitive to air and moisture and was stored in a glovebox.

$^1\text{H-NMR}$ (300 MHz, $[\text{D}_6]$ -benzene, PK-518-R): δ 1.15 (d, $J = 6.9$ Hz, 12H), 1.25 (d, $J = 6.9$ Hz, 12H), 2.91 (sept., $J = 6.9$ Hz, 4H), 6.58 (s, 2H), 7.10-7.15 (m, 3H), 7.26 (dd, $J = 8.5, 6.8$ Hz, 2H). **$^{13}\text{C-NMR}$** (75 MHz, $[\text{D}_6]$ -benzene, PK-518-R): δ 23.6, 24.8, 28.8, 121.6, 123.7, 129.0, 139.0, 146.3, 220.7. The analytical data matched those reported in the literature.^[121]

IPr^{Cl}-HCl (CAS 905931-87-5, PK-906, 93). This compound was synthesized according to a procedure by the group of Organ.^[122] In a glovebox, a pre-dried Schlenk tube ($1.0 \cdot 10^{-1}$ mbar, heat-gun) was charged with IPr (972 mg, 2.50 mmol, 1.0 eq.). Under argon counter-flow, the walls were rinsed with dry THF (12 mL) and the yellow

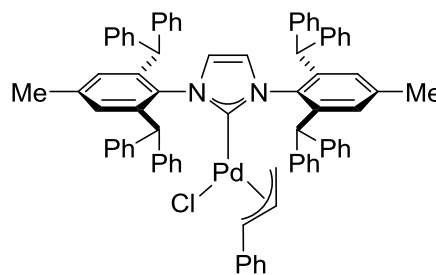


solution was stirred for five minutes at room temperature before adding CCl_4 (485 μL , 5.00 mmol, 2.0 eq.) dropwise (one minute). After stirring for three hours at room temperature, $^1\text{H-NMR}$ analysis (C_6D_6 , 400 μL , PK-906-3h, AVHD500)¹¹⁸ of an aliquot (ca. 50 μL) revealed complete conversion of the starting material. A solution of HCl (1 M, 5 mL) in diethylether was added dropwise to the vigorously stirring red/pinkish solution, leading to the precipitation of a voluminous white solid. Filtration after five minutes at room temperature, washing with diethylether (3 x 10 mL) and drying in an oven at 60 °C (no ventilation) afforded a white solid (1.06 g, 86%).

$^1\text{H-NMR}$ (500 MHz, $[\text{D}_3]$ -acetonitrile, PK-906-FS): δ 1.18 (d, $J = 6.8$ Hz, 12H), 1.28 (d, $J = 6.8$ Hz, 12H), 2.46 (sept., $J = 6.8$ Hz, 2H), 7.52 (d, $J = 7.9$ Hz, 4H), 7.72 (t, $J = 7.9$ Hz, 2H), 10.06 (br s, 1H). **$^{13}\text{C-NMR}$** (101 MHz, $[\text{D}_3]$ -acetonitrile, PK-906-13C): δ 23.3, 25.0, 29.9, 123.7, 126.2, 127.9, 134.0, 139.1, 147.1. The analytical data matched those reported in the literature.^[122]

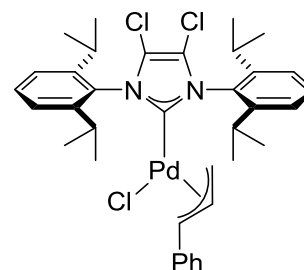
¹¹⁸ The NMR tube was evacuated ($3.5 \cdot 10^{-1}$ mbar) and backfilled with argon three times.

[Pd(IPr^{*})(cin)Cl] (CAS 1380314-24-8, PK-887, 94). This compound was synthesized according to a procedure by Nolan and coworkers.^[123] IPr^{*}·HCl (522 mg, 550 μmol, 2.2 eq.) was added to a pre-dried Schlenk flask (1.1·10⁻¹ mbar, heat-gun). KOtBu (67.3 mg, 600 μmol, 2.4 eq.) was added and the flask was evacuated (9.6 ·10⁻² mbar) and backfilled with argon three times. The walls were rinsed with THF (46 mL) and the suspension was stirred for four hours at room temperature. [μ-ClPd(cin)]₂ (130 mg, 250 μmol, 1.0 eq.) was added. After 16 hours at room temperature, the solvent was removed under reduced pressure (45 °C, 8 mbar) on a rotary evaporator. The residue was dissolved in a minimum amount of dichloromethane and passed through a short pad of silica (8 cm), eluting with dichloromethane until no further product was collected. The solvent was removed under reduced pressure (45 °C, 8 mbar). Dissolution in dichloromethane (5 mL) followed by precipitation with pentane (40 mL), washing with pentane (3 x 3 mL) and drying in air afforded a first batch of catalyst (481 mg, 82%) as light yellow solid. The filtrate was concentrated, dissolved in dichloromethane (4 mL) and overlaid with pentane (10 mL). After one day in the fridge, the crystals (87.8 mg, 15%) were filtered off, washed with hexanes (3 x 3 mL) and dried under reduced pressure (45 °C, 8 mbar). The product contained pentane (1 wt.%).



¹H-NMR (500 MHz, [D₂]-dichloromethane, PK-887-N2): δ 1.18 (d, *J* = 11.4 Hz, 1H), 2.25 (s, 6H), 2.58 (d, *J* = 6.8 Hz, 1H), 4.52 (d, *J* = 13.0 Hz, 1H), 4.96-5.07 (m, 1H), 5.26 (s, 2H), 5.80 (s, 2H), 5.93 (s, 2H), 6.77-6.87 (m, 8H), 6.90 (d, *J* = 3.3 Hz, 4H), 7.06-7.15 (m, 12H), 7.16-7.50 (m, 25H). ¹³C-NMR (75 MHz, [D₂]-dichloromethane, PK-887-N2): δ 22.0, 47.8, 52.0, 91.4, 109.5, 123.9, 126.9, 126.9, 127.0, 127.6, 128.1, 128.6, 128.9, 129.0, 129.7, 130.5, 130.6, 131.1, 136.4, 138.5, 139.1, 141.6, 142.0, 144.1, 144.2, 145.1, 145.2, 183.6. The analytical data matched those reported in the literature.^[123]

[Pd(IPr^{Cl})(cin)Cl] (CAS 2170714-93-7, PK-907, 95).^[124] In a glovebox, a pre-dried Schlenk tube (1.9·10⁻¹ mbar, heat-gun) was charged with IPr (428 mg, 1.10 mmol, 2.2 eq.). The walls were rinsed with THF (5 mL) and CCl₄ (215 μL, 2.22 mmol, 4.4 eq.) was added dropwise at room temperature. After stirring for three hours at room temperature, ¹H-NMR analysis (C₆D₆, 400 μL, PK-907-3h, AVHD500)^[118] of an aliquot (50 μL) revealed complete consumption of the starting material. [μ-ClPd(cin)]₂ (259 mg, 500 μmol,

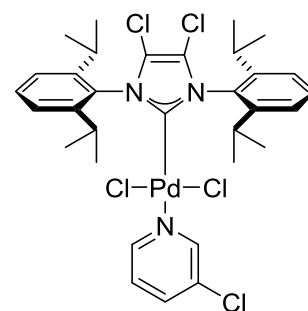


1.0 eq.) was added, the walls were rinsed with THF (2 mL) and brown suspension was stirred for 15 hours at room temperature. The solvent was removed under reduced pressure ($1.1 \cdot 10^{-1}$ mbar) and the obtained solid was dried for 30 minutes *in vacuo*. The crude product was dissolved in dichloromethane (4 mL) and filtered over a short pad of silica (5 cm) covered with Celite (0.5 cm), eluting with dichloromethane until no further complex was collected. Removal of the solvent under reduced pressure (45 °C, 500 mbar), washing with hexanes (1 x 5 mL, 3 x 2 mL) and drying in air afforded a light yellow, crystalline solid (525 mg, 73%). In solution an allylic and a linear species (allylic-linear 91.7:8.3) can be observed.

Allylic species: $^1\text{H-NMR}$ (400 MHz, $[\text{D}_6]$ -benzene, PK-907-13C): δ 1.09 (d, $J = 6.8$ Hz, 12H), 1.28-1.53 (m, 12H), 2.97-3.33 (m, 5H), 4.19 (d, $J = 12.6$ Hz, 1H), 4.89-5.03 (m, 1H), 6.94-6.99 (m, 3H), 6.99-7.14 (m, 6H), 7.13-7.21 (m, 2H). $^{13}\text{C-NMR}$ (101 MHz, $[\text{D}_6]$ -benzene, PK-907-13C): δ 24.4, 25.2 (d, $J = 9.4$ Hz), 29.0, 48.5, 90.7, 108.8, 120.2, 124.8 (br s), 127.0, 128.2, 128.3, 131.2, 133.6, 138.1, 147.4, 191.1.

Linear species:¹¹⁹ $^1\text{H-NMR}$ (400 MHz, $[\text{D}_6]$ -benzene, PK-907-13C): δ 1.05 (d, $J = 6.9$ Hz, 6H), 1.23 (d, $J = 6.7$ Hz, 6H), 1.38 (d, $J = 6.7$ Hz, 6H), 1.80 (d, $J = 11.8$ Hz, 10H), 2.41 (d, $J = 13.3$ Hz, 1H), 2.97-3.03 (m, 2H), 4.22-4.34 (m, 1H), 5.66 (d, $J = 8.2$ Hz, 1H), 6.82-6.92 (m, 4H). $^{13}\text{C-NMR}$ (101 MHz, $[\text{D}_6]$ -benzene, PK-907-13C): δ 23.7, 24.4, 25.1, 25.4, 28.9, 51.9, 90.9, 106.4, 120.0, 124.6 (d, $J = 5.3$ Hz), 126.3, 127.9, 131.0, 133.2, 136.9, 147.1 (d, $J = 10.4$ Hz), 191.0. Missing carbon atom overlayers with the deuterated solvent. The analytical data matched those reported in the literature.^[124]

***IPr^{Cl}-PEPSI* (CAS 1435347-20-8, PK-922, 96).** This compound was synthesized according to a slightly modified procedure by the group of Organ.^[122] $\text{IPr}^{\text{Cl}}\cdot\text{HCl}$ (543 mg, 1.10 mmol, 1.1 eq.), K_2CO_3 (691 mg, 5.00 mmol, 5.0 eq.) and PdCl_2 (177 mg, 1.00 mmol, 1.0 eq.) were added to a 20 mL Schlenk tube. The system was evacuated ($2.1 \cdot 10^{-1}$ mbar) and backfilled with argon three times. The walls were rinsed with 3-Cl-pyridine (4 mL). After stirring for 18 hours at 80 °C, the orange/brown suspension was cooled to room temperature, diluted with dichloromethane (5 mL) and filtered over a short pad of silica (3 cm) covered with Celite, eluting with dichloromethane until no further complex was collected. The solvent was removed under

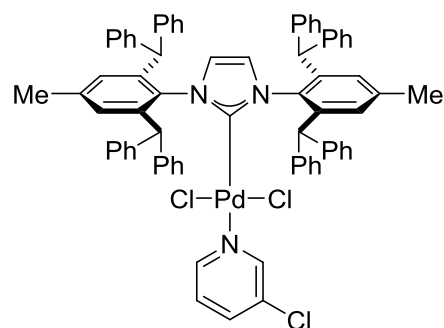


¹¹⁹ Only characteristic signals indicated. Most signals overlay with the allylic species.

reduced pressure (50 °C, 7 mbar). The residue was dissolved in minimum amount of dichloromethane, overlaid with hexanes and stored in the fridge for four days. After filtration, washing with hexanes (3 x 4 mL) and drying in an oven (60 °C, no ventilation) overnight, a first batch of orange block-shaped crystals (474 mg, 63%) was obtained. A second crystallization afforded further orange complex (164 mg, 22%). Total yield: 638 mg, 85%.

¹H-NMR (400 MHz, CDCl₃, PK-922-cryst): δ 1.19 (d, *J* = 6.7 Hz, 12H), 1.47 (d, *J* = 6.7 Hz, 12H), 3.05 (sept., *J* = 6.7 Hz, 4H), 7.07 (dd, *J* = 8.2, 5.6 Hz, 1H), 7.40 (d, *J* = 7.8 Hz, 4H), 7.52-7.61 (m, 3H), 8.48 (dd, *J* = 5.6, 1.3 Hz, 1H), 8.56 (d, *J* = 2.3 Hz, 1H). **¹³C-NMR** (101 MHz, CDCl₃, PK-922-13C): δ 24.8, 25.5, 29.0, 120.8, 124.5, 124.9, 131.4, 132.1, 132.2, 137.7, 147.8, 149.6, 150.6, 157.8. The analytical data matched those reported in the literature.^[122]

***IPr*^{*}-PEPPSI (CAS 1399234-94-6, PK-891, 97)**. This compound was synthesized according to a procedure by Nolan and coworkers.^[125] *IPr*^{*}·HCl (522 mg, 550 μmol, 1.1 eq.), K₂CO₃ (346 mg, 2.50 mmol, 5.0 eq.) and PdCl₂ (88.7 mg, 500 μmol, 1.0 eq.) were added to a 25 mL round bottom flask. The walls were rinsed with 3-Cl-pyridine



(2 mL). After stirring for 14 hours at 80 °C, the orange suspension was cooled to room temperature, diluted with dichloromethane (5 mL) and filtered over a short pad of silica (6 cm) covered with Celite, eluting with dichloromethane until no further complex was collected. The solvent was removed under reduced pressure (45 °C, 8 mbar) and the residue was washed with pentane (3 x 25 mL). The solid was dissolved in dichloromethane (5 mL), overlaid with pentane (10 mL) and stored in the fridge for four hours. After filtration, washing with a mixture of CH₂Cl₂-pentane (1:4, 3 x 5 mL) and drying in an oven (65 °C, no ventilation) overnight, a fluffy, light-yellow solid (523 mg, 87%) was obtained. The product contained pentane (1 wt.%).

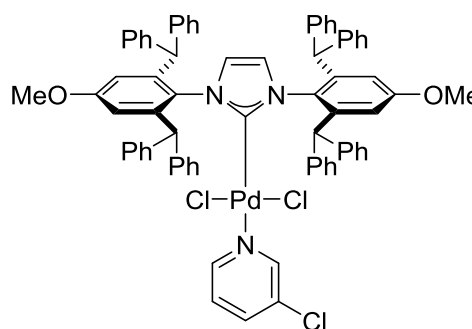
¹H-NMR (400 MHz, [D₆]-benzene, PK-891-cryst-2nd-2): δ 1.76 (s, 6H), 5.16 (s, 2H) 6.07 (dd, *J* = 8.2, 5.5 Hz, 1H), 6.62 (dq, *J* = 8.2, 1.3 Hz, 1H), 6.80-6.86 (m, 4H), 6.86-6.93 (m, 12H), 7.00-7.08 (m, 12H), 7.13 (d, *J* = 3.7 Hz, 12H), 7.86-7.95 (m, 8H), 9.03 (dd, *J* = 5.5, 1.3 Hz, 1H), 9.43 (d, *J* = 2.4 Hz, 1H). **¹³C-NMR** (101 MHz, [D₆]-benzene, PK-891-cryst-2): δ 21.3, 51.6, 124.3, 124.4, 126.5, 126.6, 128.5, 130.1, 131.2, 131.3, 132.2, 136.1, 137.5, 139.2, 143.0, 144.9, 145.1, 149.9, 150.9, 152.3. Some signals overlay with the deuterated solvent. **¹³C-NMR** (75 MHz, CDCl₃, PK-891-13C) δ 21.9, 51.0, 124.3, 124.7, 126.2, 127.9, 128.3, 129.6, 130.6,

131.1, 132.6, 135.5, 138.1, 138.5, 141.7, 144.0, 144.7, 149.6, 150.0, 151.1. The analytical data matched those reported in the literature.^[125]

IPr^{*OMe}-PEPPSI (CAS 2242624-59-3, PK-921, 98).

This compound was synthesized according to a slightly modified procedure by Browne and coworkers.^[126]

*IPr^{*OMe}·HCl* (1.08 g, 1.10 mmol, 1.1 eq.), K_2CO_3 (691 mg, 5.00 mmol, 5.0 eq.) and $PdCl_2$ (177 mg, 1.00 mmol, 1.0 eq.) were added to a 20 mL Schlenk tube. The system was evacuated ($2.1 \cdot 10^{-1}$ mbar) and

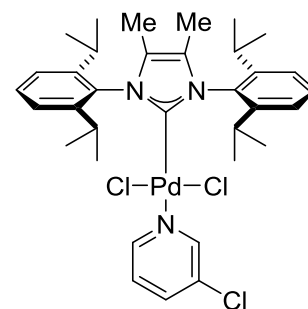


backfilled with argon three times. The walls were rinsed with 3-Cl-pyridine (4 mL). After stirring for 18 hours at 80 °C, the yellow suspension was cooled to room temperature, diluted with dichloromethane (5 mL) and filtered over a short pad of silica (3 cm) covered with Celite, eluting with dichloromethane until no further complex was collected. The solvent was removed under reduced pressure (50 °C, 7 mbar). The residue was dissolved in minimum amount of dichloromethane, overlaid with hexanes and stored in the fridge for four days. After filtration, washing with hexanes (3 x 4 mL) and drying in an oven (60 °C, no ventilation) overnight, a light-yellow solid (690 mg, 56%) was obtained. A second crystallization afforded further yellow complex (462 mg, 37%) with minor impurities, which can be removed by further crystallization. The product contained dichloromethane (2 wt.%) and hexanes (4 wt.%).

¹H-NMR (400 MHz, $CDCl_3$, PK-921-cryst): δ 3.50 (s, 6H), 4.82 (s, 2H), 6.32 (s, 4H), 6.48 (s, 4H), 6.76 (d, $J = 7.2$ Hz, 8H), 6.95-7.11 (m, 12H), 7.11-7.28 (m, 13H), 7.32 (dd, $J = 8.2, 5.5$ Hz, 1H), 7.43 (d, $J = 7.2$ Hz, 8H), 7.79 (d, $J = 8.1$ Hz, 1H), 9.04 (d, $J = 5.5$ Hz, 1H), 9.17 (d, $J = 1.3$ Hz, 1H). **¹³C-NMR** (75 MHz, $CDCl_3$, PK-921-13C): δ 51.2, 55.0, 115.6, 124.3, 124.8, 126.3, 126.4, 128.0, 128.3, 129.5, 130.6, 130.9, 132.6, 138.1, 143.8, 143.9, 144.3, 149.9, 150.3, 150.9, 159.0. The analytical data matched those reported in the literature.^[126]

IPr^{Me}-PEPPSI (CAS 905459-29-2, PK-951, 99). This compound

was synthesized according to a slightly modified procedure by the group of Organ.^[122] *IPr^{Me}·HOTf* (624 mg, 1.10 mmol, 1.1 eq.), K_2CO_3 (691 mg, 5.00 mmol, 5.0 eq.) and $PdCl_2$ (177 mg, 1.00 mmol, 1.0 eq.) were added to a 20 mL Schlenk tube. The system was evacuated ($2.0 \cdot 10^{-1}$ mbar) and backfilled with argon three times. The

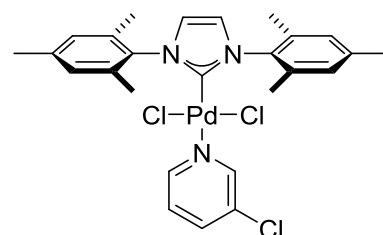


walls were rinsed with 3-Cl-pyridine (4 mL). After stirring for 16 hours at 80 °C, the

orange/brown suspension was cooled to room temperature, diluted with dichloromethane (5 mL) and filtered over a short pad of silica (3 cm) covered with Celite, eluting with dichloromethane until no further complex was collected. The solvent was removed under reduced pressure (50 °C, 7 mbar). The residue was washed with ethanol (3 x 5 mL), Et₂O (3 x 5 mL) and pentane (3 x 5 mL). After drying in an oven (60 °C, no ventilation) overnight, a yellow solid (48.7 mg, 7%) was obtained.

¹H-NMR (300 MHz, [D₂]-dichloromethane, PK-950=wash): δ 1.09 (d, *J* = 6.6 Hz, 12H), 1.43 (d, *J* = 6.6 Hz, 12H), 1.93 (s, 6H), 3.08 (sept., *J* = 6.6 Hz, 4H), 7.12 (ddd, *J* = 8.2, 5.5, 0.5 Hz, 1H), 7.36-7.44 (m, 4H), 7.54 (dd, *J* = 8.4, 7.0 Hz, 2H), 7.62 (ddd, *J* = 8.2, 2.4, 1.4 Hz, 1H), 8.57 (dd, *J* = 5.5, 1.4 Hz, 1H), 8.65 (dd, *J* = 2.4, 0.5 Hz, 1H). The file name is due to a typing error at the NMR machine. **¹³C-NMR** (101 MHz, [D₂]-dichloromethane, PK-950-wash-13C): δ 11.4, 25.4, 25.6, 29.0, 124.9, 125.2, 129.9, 130.6, 132.2, 134.2, 138.1, 148.3, 150.0, 150.3, 150.8. Additional signals (PK-950-wash-13C, ¹H-NMR: δ 1.51 (d), ¹³C-NMR: δ 26.4) can be detected after prolonged storing of an NMR sample. The analytical data matched those reported in the literature.^[122]

IMes-PEPPSI (CAS 905459-29-2, PK-951, 100). This compound was synthesized according to a procedure by the group of Organ.^[62] IMes·HCl (375 mg, 1.10 mmol, 1.1 eq.), K₂CO₃ (691 mg, 5.00 mmol, 5.0 eq.) and PdCl₂ (177 mg, 1.00 mmol, 1.0 eq.) were added to a 20 mL Schlenk tube. The



system was evacuated ($2.0 \cdot 10^{-1}$ mbar) and backfilled with argon three times. The walls were rinsed with 3-Cl-pyridine (4 mL). After stirring for 16 hours at 80 °C, the orange/brown suspension was cooled to room temperature, diluted with dichloromethane (5 mL) and filtered over a short pad of silica (3 cm) covered with Celite, eluting with dichloromethane until no further complex was collected. The solvent was removed under reduced pressure (50 °C, 8 mbar). The residue was dissolved in minimum amount of dichloromethane, overlaid with hexanes and stored in the fridge for five days. Filtration, washing with hexanes (3 x 4 mL) and drying in an oven (60 °C, no ventilation) overnight yielded yellow crystals (446 mg, 75%).

¹H-NMR (300 MHz, CDCl₃, PK-951-N): δ 2.35 (s, 12H), 2.38 (s, 6H), 7.00-7.12 (m, 7H), 7.56 (ddd, *J* = 8.2, 2.4, 1.3 Hz, 1H), 8.50 (dd, *J* = 5.5, 1.3 Hz, 1H), 8.59 (dd, *J* = 2.4, 0.6 Hz, 1H). **¹³C-NMR** (75 MHz, CDCl₃, PK-951-13C): δ 19.2, 21.3, 124.4, 124.4, 129.4, 132.0, 135.1,

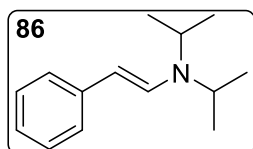
136.4, 137.6, 139.4, 149.6, 150.6, 151.4. The analytical data matched those reported in the literature.^[62]

7.2.7.4 Exemplary procedure

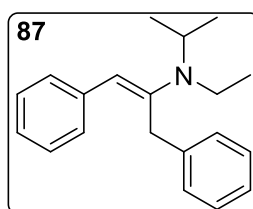
Table 43, entry 11, according to general procedure 6.2.1b) (PK-934). A screw cap vial was charged with IPr-PEPPSI (17.0 mg, 25.0 μmol , 5.0 mol%), and $[\text{Cp}^*\text{IrCl}_2]_2$ (10.0 mg, 25.0 μmol , 2.5 mol%). The vial was introduced into a glovebox. K_2CO_3 (138 mg, 1.00 mmol, 2.0 eq.), 1-bromonaphthalene (98%, 215 μL , 1.50 mmol, 3.0 eq.) and NEt_3 (70.0 μL , 500 μmol , 1.0 eq.) were added in the indicated order. The walls were rinsed with dry DMF (2 mL), the vial was closed with a screw cap and the suspension was stirred for 16 hours at 110 $^\circ\text{C}$ in a pre-heated metal block outside the glovebox. At room temperature, the suspension was filtered over a short pad of Celite (in a Pasteur pipette) directly into a separatory funnel. The pad was rinsed with Et_2O (3 x 2 mL) and the filtrate was diluted with additional Et_2O (50 mL). The organic phase was washed with water (3 x 25 mL), a saturated aqueous solution of NaCl (1 x 25 mL), dried over MgSO_4 , filtered and the solvent was removed under reduced pressure (45 $^\circ\text{C}$, 500 mbar). 1,3,5-Trimethoxybenzene (168.19 g/mol, 23.2 mg, 137.9 μmol) was added as internal standard and the contents of the flask was dissolved in CDCl_3 (800 μL). A sample (500 μL) was transferred to a NMR tube and a ^1H -NMR spectrum ($d_1 = 20$ s, 16 scans) was recorded. NMR file: PK-934-q, AVHD500.

7.2.7.5 Characteristic $^1\text{H-NMR}$ shifts of dehydrogenative coupling β -styryl dialkylamine products

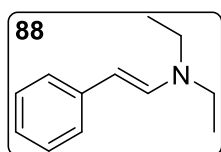
Most characteristic $^1\text{H-NMR}$ shifts of dehydrogenative coupling β -styryl dialkylamine products were indicated; $^1\text{H-NMR}$ signals of phenyl-groups were ignored due to strong overlay of isomers and side-products (homocoupling of ArBr, catalysts...). Coupling constants of alkyl groups were not specified.



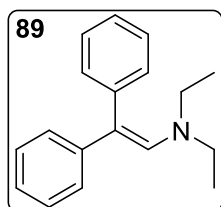
$^1\text{H-NMR}$ (500 MHz, CDCl_3): δ 5.36 (d, $J = 14.0$ Hz), 6.88 (d, $J = 14.0$ Hz).



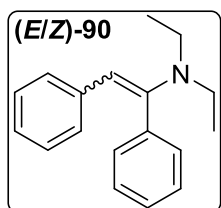
$^1\text{H-NMR}$ (500 MHz, CDCl_3): δ 0.96 (d), 1.17 (t), 3.11 (q), 3.77 (sept.), 3.86 (s), 5.54 (s).



$^1\text{H-NMR}$ (500 MHz, CDCl_3): δ 1.14 (t), 3.16 (q), 5.15 (d, $J = 14.0$ Hz), 6.76 (d, $J = 14.0$ Hz).



$^1\text{H-NMR}$ (500 MHz, CDCl_3): δ 0.96 (q), 2.87 (q), 6.35 (s)



$^1\text{H-NMR}$ (500 MHz, CDCl_3): δ 1.03 (t), 2.98 (q), 5.62 (s).

7.2.8 Heck Coupling of Styrene Derivatives with Pyrimidyl Chlorides

7.2.8.1 General synthesis procedure

General procedure 6.3.1 – Heck coupling of styrene derivatives with 2-chloropyrimidines

A pre-dried Schlenk tube ($<3.0 \cdot 10^{-1}$ mbar, heat-gun) was charged with Pd-precatalyst (5.0 mol%), dried base, (substituted) 2-chloropyrimidine and additive(s) if indicated. The system was evacuated (r.t., $<3.0 \cdot 10^{-1}$ mbar) and backfilled with argon three times. The walls were rinsed with dry solvent (1 mL) and styrene (60.0 μ L, 524 μ mol, 1.0 eq.) was added via 100 μ L Hamilton syringe. After stirring for 18 hours at the indicated temperature in a pre-heated metal block, the suspension was filtered over Celite into a separatory funnel, eluting with Et₂O (3 x 2 mL). Water (25 mL) and Et₂O (50 mL) were added and the phases were separated. The organic phase was washed with water (2 x 25 mL), a saturated solution of NaCl (1 x 25 mL), dried over MgSO₄, filtered and the solvent was removed under reduced pressure (45 °C, 500 mbar). The crude material was diluted in CDCl₃ (800 μ L), tetrachloroethene (50.0 μ L, 473.6 μ mol) was added via 50 μ L Hamilton syringe and a sample (500 μ L) was transferred to an NMR tube. A ¹H-NMR spectrum ($d_1 = 20$ s, 16 scans) was recorded.

7.2.8.2 Exemplary procedure

Table 47, entry 5, according to general procedure 6.3.1 (PK-821). A pre-dried Schlenk tube ($2.3 \cdot 10^{-1}$ mbar, heat-gun) was charged with Pd(OAc)₂ (5.9 mg, 25.0 μ mol, 5.0 mol%), NBu₄DiPP (20.9 mg, 52.4 μ mol, 10.0 mol%), dried K₂CO₃ (145 mg, 1.05 mmol, 2.0 eq.), 2-chloro-4,6-dimethylpyrimidine (112 mg, 786 μ mol, 1.5 eq.). The system was evacuated (r.t., $2.4 \cdot 10^{-1}$ mbar) and backfilled with argon three times. The walls were rinsed with dry DMF (1 mL) and styrene (60.0 μ L, 524 μ mol, 1.0 eq.) was added via 100 μ L Hamilton syringe. After stirring for 18 hours at the indicated temperature in a pre-heated metal block, the suspension was filtered over Celite into a separatory funnel, eluting with Et₂O (3 x 2 mL). Water (25 mL) and Et₂O (50 mL) were added and the phases were separated. The organic phase was washed with water (2 x 25 mL), a saturated solution of NaCl (1 x 25 mL), dried over MgSO₄, filtered and the solvent was removed under reduced pressure (45 °C, 500 mbar). The crude material was diluted in CDCl₃ (800 μ L), tetrachloroethene (50.0 μ L, 473.6 μ mol) was added via 50 μ L Hamilton syringe and a sample (500 μ L) was transferred to an NMR tube. A ¹H-NMR spectrum ($d_1 = 20$ s, 16 scans) was recorded. The reaction showed 47% coupling product along with 30% unreacted styrene.

7.3 References

- [1] D. B. G. Williams, M. Lawton, *J. Org. Chem.* **2010**, *75*, 8351-8354.
- [2] M. Rimoldi, F. Ragaini, E. Gallo, F. Ferretti, P. Macchi, N. Casati, *Dalton Trans.* **2012**, *41*, 3648-3658.
- [3] L. G. Ward, J. Pipal, *Inorg. Synth.* **1972**, *13*, 154-164.
- [4] a) F. DeRosa, L. K. Keefer, J. A. Hrabie, *J. Org. Chem.* **2008**, *73*, 1139-1142; b) Y. Ji, R. E. Plata, C. S. Regens, M. Hay, M. Schmidt, T. Razler, Y. Qiu, P. Geng, Y. Hsiao, T. Rosner, *J. Am. Chem. Soc.* **2015**, *137*, 13272-13281.
- [5] J. Houben, T. Weyl, *Die Methoden Der Organischen Chemie (Weyls Methoden)*, Vol. 4, G. Thieme, **1924**.
- [6] M. M. Maturi, M. Wenninger, R. Alonso, A. Bauer, A. Pöthig, E. Riedle, T. Bach, *Chem. Eur. J.* **2013**, *19*, 7461-7472.
- [7] K.-H. Rimboeck, A. Poethig, T. Bach, *Synthesis* **2015**, *47*, 2869-2884.
- [8] R. Alonso, T. Bach, *Angew. Chem. Int. Ed.* **2014**, *53*, 4368-4371.
- [9] *APEX suite of crystallographic software*, APEX 2, Version 2014.9-0 and APEX 3, Version 2015-5.2, Madison, Wisconsin, USA, **2014/2015**.
- [10] *Saint*, Versions 8.32B, 8.34A and 8.38A, Madison, Wisconsin, USA, **2012/2014/2017**.
- [11] *SADBS*, Versions 2012/1, 2014/5 and 2016/2 and *TWINABS*, Version 2012/1, Madison, Wisconsin, USA, **2012/2014/2016**.
- [12] a) G. Sheldrick, *Acta Crystallogr. A* **2015**, *71*, 3-8; b) G. Sheldrick, *Acta Crystallogr. C* **2015**, *71*, 3-8; c) C. B. Hübschle, G. M. Sheldrick, B. Dittrich, *J. Appl. Crystallogr.* **2011**, *44*, 1281-1284.
- [13] *International Tables for Crystallography*, Vol. C (Ed. A. J. Wilson), Kluwer Academic Publishers, Dordrecht, The Netherlands, **1992**, 6.1.1.4 (pp. 500-502), 4.2.6.8 (pp. 219-222), and 4.2.4.2 (pp. 193-199).
- [14] a) A. Spek, *Acta Crystallogr. D* **2009**, *65*, 148-155; b) C. F. Macrae, I. J. Bruno, J. A. Chisholm, P. R. Edgington, P. McCabe, E. Pidcock, L. Rodriguez-Monge, R. Taylor, J. van de Streek, P. A. Wood, *J. Appl. Crystallogr.* **2008**, *41*, 466-470.
- [15] S. L. Patt, J. N. Shoolery, *J. Magn. Reson.* **1982**, *46*, 535-539.
- [16] a) O. Kühl, *Phosphorus-31 NMR spectroscopy: a concise introduction for the synthetic organic and organometallic chemist*, Springer Science & Business Media, **2008**; b) P.

- D. Stanley, Principles and Topical Applications of ^{19}F -NMR Spectrometry in *Organofluorines*, Springer, **2002**, pp. 1-61.
- [17] H. Nöth, B. Wrackmeyer, *Nuclear magnetic resonance spectroscopy of boron compounds, Vol. 14*, Springer Science & Business Media, **2012**.
- [18] a) S. Mahajan, I. P. Singh, *Magn. Reson. Chem.* **2013**, *51*, 76-81; b) T. Schoenberger, *Anal. Bioanal. Chem.* **2012**, *403*, 247-254.
- [19] S. Koller, J. Gatzka, K. M. Wong, P. J. Altmann, A. Pöthig, L. Hintermann, *J. Org. Chem.* **2018**, *83*, 15009-15028.
- [20] X. Lei, A. Jalla, M. A. A. Shama, J. M. Stafford, B. Cao, *Synthesis* **2015**, *47*, 2578-2585.
- [21] H. tom Dieck, M. Svoboda, T. Greiser, *Z. Naturforsch. B* **1981**, *36*, 823-832.
- [22] L. J. Gooßen, N. Rodríguez, P. P. Lange, C. Linder, *Angew. Chem. Int. Ed.* **2010**, *49*, 1111-1114.
- [23] T. Agrawal, S. P. Cook, *Org. Lett.* **2013**, *15*, 96-99.
- [24] K. M. Khan, S. Rahat, M. I. Choudhary, U. Ghani, S. Perveen, S. Khatoon, A. Dar, A. Malik, *Helv. Chim. Acta* **2002**, *85*, 559-570.
- [25] J. Maddaluno, M. Durandetti, *Synlett* **2015**, *26*, 2385-2388.
- [26] N. Berton, F. Lemasson, J. Tittmann, N. Stürzl, F. Hennrich, M. M. Kappes, M. Mayor, *Chem. Mater.* **2011**, *23*, 2237-2249.
- [27] J. Albaneze-Walker, R. Raju, J. A. Vance, A. J. Goodman, M. R. Reeder, J. Liao, M. T. Maust, P. A. Irish, P. Espino, D. R. Andrews, *Org. Lett.* **2009**, *11*, 1463-1466.
- [28] W. J. Spillane, A. P. Taheny, M. M. Kearns, *J. Chem. Soc., Perkin Trans. 1* **1982**, 677-679.
- [29] S. Bajo, G. Laidlaw, A. R. Kennedy, S. Sproules, D. J. Nelson, *Organometallics* **2017**, *36*, 1662-1672.
- [30] H. Meshram, G. S. Reddy, K. H. Bindu, J. Yadav, *Synlett* **1998**, *8*, 877-878.
- [31] L. Sancineto, C. Tidei, L. Bagnoli, F. Marini, V. Lippolis, M. Arca, E. J. Lenardao, C. Santi, *Eur. J. Org. Chem.* **2016**, *17*, 2999-3005.
- [32] G. J. Perry, J. M. Quibell, A. Panigrahi, I. Larrosa, *J. Am. Chem. Soc.* **2017**, *139*, 11527-11536.
- [33] C. Zarate, R. Martin, *J. Am. Chem. Soc.* **2014**, *136*, 2236-2239.
- [34] W. Liu, X. Yang, Y. Gao, C.-J. Li, *J. Am. Chem. Soc.* **2017**, *139*, 8621-8627.
- [35] L. Niu, H. Zhang, H. Yang, H. Fu, *Synlett* **2014**, *25*, 995-1000.

- [36] M. Chen, S. Ichikawa, S. L. Buchwald, *Angew. Chem. Int. Ed.* **2015**, *54*, 263-266.
- [37] Q. Liu, Y. Lan, J. Liu, G. Li, Y.-D. Wu, A. Lei, *J. Am. Chem. Soc.* **2009**, *131*, 10201-10210.
- [38] D. T. Racys, S. A. Sharif, S. L. Pimlott, A. Sutherland, *J. Org. Chem.* **2016**, *81*, 772-780.
- [39] S. Usui, Y. Hashimoto, J. V. Morey, A. E. Wheatley, M. Uchiyama, *J. Am. Chem. Soc.* **2007**, *129*, 15102-15103.
- [40] D. A. Offermann, J. E. McKendrick, J. J. Sejberg, B. Mo, M. D. Holdom, B. A. Helm, R. J. Leatherbarrow, A. J. Beavil, B. J. Sutton, A. C. Spivey, *J. Org. Chem.* **2012**, *77*, 3197-3214.
- [41] Y. Jiang, S. Pan, Y. Zhang, J. Yu, H. Liu, *Eur. J. Org. Chem.* **2014**, *10*, 2027-2031.
- [42] G. Iakobson, J. Du, A. M. Slawin, P. Beier, *Beilstein J. Org. Chem.* **2015**, *11*, 1494-1502.
- [43] S. Xu, H.-H. Chen, J.-J. Dai, H.-J. Xu, *Org. Lett.* **2014**, *16*, 2306-2309.
- [44] M. A. Stevens, F. H. Hashim, E. S. Gwee, E. I. Izgorodina, R. E. Mulvey, V. L. Blair, *Chem. Eur. J.* **2018**, *24*, 15669-15677.
- [45] L. B. Jimenez, N. V. Torres, J. L. Borioni, A. B. Pierini, *Tetrahedron* **2014**, *70*, 3614-3620.
- [46] H. Kameo, J. Yamamoto, A. Asada, H. Nakazawa, H. Matsuzaka, D. Bourissou, *Angew. Chem. Int. Ed.* **2019**, *58*, 18783-18787.
- [47] R. L. Jezorek, N. Zhang, P. Leowanawat, M. H. Bunner, N. Gutsche, A. K. Pesti, J. T. Olsen, V. Percec, *Org. Lett.* **2014**, *16*, 6326-6329.
- [48] C. F. Lima, J. E. Rodriguez-Borges, L. M. Santos, *Tetrahedron* **2011**, *67*, 689-697.
- [49] S. Sharma, M. Kumar, V. Kumar, N. Kumar, *Tetrahedron Lett.* **2013**, *54*, 4868-4871.
- [50] T. T. Jayanth, M. Jeganmohan, C.-H. Cheng, *Org. Lett.* **2005**, *7*, 2921-2924.
- [51] Z. Jin, S. X. Guo, X. P. Gu, L. L. Qiu, H. B. Song, J. X. Fang, *Adv. Synth. Catal.* **2009**, *351*, 1575-1585.
- [52] Z.-K. Xiao, H.-Y. Yin, J.-M. Lu, *Inorg. Chim. Acta* **2014**, *423*, 106-108.
- [53] E. A. B. Kantchev, G.-R. Peh, C. Zhang, J. Y. Ying, *Org. Lett.* **2008**, *10*, 3949-3952.
- [54] A. Zanardi, J. A. Mata, E. Peris, *Organometallics* **2009**, *28*, 4335-4339.
- [55] L. P. Wu, Y. Suenaga, T. Kuroda-Sowa, M. Maekawa, K. Furuichi, M. Munakata, *Inorg. Chim. Acta* **1996**, *248*, 147-152.
- [56] L.-C. Campeau, P. Thansandote, K. Fagnou, *Org. Lett.* **2005**, *7*, 1857-1860.

- [57] N. Marion, O. Navarro, J. Mei, E. D. Stevens, N. M. Scott, S. P. Nolan, *J. Am. Chem. Soc.* **2006**, *128*, 4101-4111.
- [58] A. Gogoll, H. Grennberg, A. Axén, *Organometallics* **1997**, *16*, 1167-1178.
- [59] D. R. Jensen, M. S. Sigman, *Org. Lett.* **2003**, *5*, 63-65.
- [60] M. R. Furst, C. S. Cazin, *Chem. Commun.* **2010**, *46*, 6924-6925.
- [61] Y.-C. Xu, J. Zhang, H.-M. Sun, Q. Shen, Y. Zhang, *Dalton Trans.* **2013**, *42*, 8437-8445.
- [62] C. J. O'Brien, E. A. B. Kantchev, C. Valente, N. Hadei, G. A. Chass, A. Lough, A. C. Hopkinson, M. G. Organ, *Chem. Eur. J.* **2006**, *12*, 4743-4748.
- [63] D. E. Stephens, J. Lakey-Beitia, G. Chavez, C. Ilie, H. D. Arman, O. V. Larionov, *Chem. Commun.* **2015**, *51*, 9507-9510.
- [64] a) D. P. Bancroft, F. A. Cotton, L. R. Falvello, W. Schwotzer, *Polyhedron* **1988**, *7*, 615-621; b) A. Berenblyum, H. Al-Wadhaf, O. Shishilov, E. Evstigneeva, M. El-Hussien, V. Flid, *Russ. J. Coord. Chem.* **2011**, *37*, 460.
- [65] B. Liu, X. Ma, F. Wu, W. Chen, *Dalton Trans.* **2015**, *44*, 1836-1844.
- [66] A. Beillard, X. Bantreil, T.-X. Métro, J. Martinez, F. Lamaty, *Dalton Trans.* **2016**, *45*, 17859-17866.
- [67] A. J. Briggs, *Synth. Commun.* **2013**, *43*, 3258-3261.
- [68] W. Levason, D. Pugh, G. Reid, *New J. Chem.* **2017**, *41*, 1677-1686.
- [69] C. M. Crudden, H. J. Horton, O. V. Zenkina, I. I. Ebralidze, C. A. Smith (Queen's University at Kingston), US20160199875A1, **2016**.
- [70] F. Mani, M. Peruzzini, P. Stoppioni, *Green Chem.* **2006**, *8*, 995-1000.
- [71] M. Lafrance, K. Fagnou, *J. Am. Chem. Soc.* **2006**, *128*, 16496-16497.
- [72] B. Liegault, D. Lapointe, L. Caron, A. Vlassova, K. Fagnou, *J. Org. Chem.* **2009**, *74*, 1826-1834.
- [73] M. Baghbanzadeh, C. Pilger, C. O. Kappe, *J. Org. Chem.* **2011**, *76*, 8138-8142.
- [74] S. Marhadour, M.-A. Bazin, P. Marchand, *Tetrahedron Lett.* **2012**, *53*, 297-300.
- [75] H. Tomoda, T. Hirano, S. Saito, T. Mutai, K. Araki, *Bull. Chem. Soc. Jpn.* **1999**, *72*, 1327-1334.
- [76] M. Fabris, V. Lucchini, M. Noe, A. Perosa, M. Selva, *Chem. Eur. J.* **2009**, *15*, 12273-12282.
- [77] A. A. Kalathil, A. Kumar, B. Banik, T. A. Ruiter, R. K. Pathak, S. Dhar, *Chem. Commun.* **2016**, *52*, 140-143.
- [78] R. J. Pakula, J. F. Berry, *Dalton Trans.* **2018**, *47*, 13887-13893.

- [79] C. G. Espino, K. W. Fiori, M. Kim, J. Du Bois, *J. Am. Chem. Soc.* **2004**, *126*, 15378-15379.
- [80] H. Nagae, R. Aoki, S. n. Akutagawa, J. Kleemann, R. Tagawa, T. Schindler, G. Choi, T. P. Spaniol, H. Tsurugi, J. Okuda, *Angew. Chem. Int. Ed.* **2018**, *57*, 2492-2496.
- [81] M. Brown, R. Kumar, J. Rehbein, T. Wirth, *Chem. Eur. J.* **2016**, *22*, 4030-4035.
- [82] N. P. Reddy, M. Tanaka, *Tetrahedron Lett.* **1997**, *38*, 4807-4810.
- [83] S. E. Drewes, N. D. Emslie, M. Hemingway, *Synth. Commun.* **1990**, *20*, 1671-1679.
- [84] C. Xu, T. Li, P. Jiang, Y.-j. Zhang, *Tetrahedron* **2020**, *76*, 131107.
- [85] a) M. Hatzimarinaki, M. M. Roubelakis, M. Orfanopoulos, *J. Am. Chem. Soc.* **2005**, *127*, 14182-14183; b) V. Hrobáriková, P. Hrobárik, P. Gajdoš, I. Fitis, M. Fakis, P. Persephonis, P. Zahradník, *J. Org. Chem.* **2010**, *75*, 3053-3068.
- [86] K. Singh, S. J. Staig, J. D. Weaver, *J. Am. Chem. Soc.* **2014**, *136*, 5275-5278.
- [87] G. C. Paul, J. J. Gajewski, *Synthesis* **1997**, *5*, 524-526.
- [88] K. van Alem, G. Belder, G. Lodder, H. Zuilhof, *J. Org. Chem.* **2005**, *70*, 179-190.
- [89] C. Yaroslavsky, A. Patchornik, E. Katchalski, *Tetrahedron Lett.* **1970**, *11*, 3629-3632.
- [90] S. Rej, S. Pramanik, H. Tsurugi, K. Mashima, *Chem. Commun.* **2017**, *53*, 13157-13160.
- [91] C. B. Tripathi, S. Mukherjee, *Angew. Chem. Int. Ed.* **2013**, *52*, 8450-8453.
- [92] a) J. J. Molloy, J. B. Metternich, C. G. Daniliuc, A. J. Watson, R. Gilmour, *Angew. Chem. Int. Ed.* **2018**, *57*, 3168-3172; b) C. Vaccher, P. Berthelot, N. Flouquet, M.-P. Vaccher, M. Debaert, *Synth. Commun.* **1993**, *23*, 671-679.
- [93] M. L. Conner, M. K. Brown, *J. Org. Chem.* **2016**, *81*, 8050-8060.
- [94] G. Zhang, R.-X. Bai, C.-H. Li, C.-G. Feng, G.-Q. Lin, *Tetrahedron* **2019**, *75*, 1658-1662.
- [95] N. Bartalucci, M. Bortoluzzi, S. Zacchini, G. Pampaloni, F. Marchetti, *Dalton Trans.* **2019**, *48*, 1574-1577.
- [96] K. Suzuki, Y. Hori, T. Nishikawa, T. Kobayashi, *Adv. Synth. Catal.* **2007**, *349*, 2089-2091.
- [97] L. Lücke, E. Jassmann (Fahlberg-List Verb.), DE1668830A1, **1967**.
- [98] X. T. Li, Q. S. Gu, X. Y. Dong, X. Meng, X. Y. Liu, *Angew. Chem. Int. Ed.* **2018**, *57*, 7668-7672.
- [99] B. Heyn, B. Hipler, G. Kreisel, H. Schreer, D. Walther, *Anorganische Synthesechemie: ein integriertes Praktikum*, Springer-Verlag, **2013**.

- [100] a) A. Hicken, A. J. White, M. R. Crimmin, *Angew. Chem. Int. Ed.* **2017**, *56*, 15127-15130; b) S. Manabe, C. M. Wong, C. S. Sevov, *J. Am. Chem. Soc.* **2020**, *142*, 3024-3031.
- [101] H. J. Bestmann, R. Dötzer, *Synthesis* **1989**, *3*, 204-205.
- [102] H. J. Bestmann, O. Kratzer, *Chem. Ber.* **1962**, *95*, 1894-1901.
- [103] M. Alcarazo, R. M. Suárez, R. Goddard, A. Fürstner, *Chem. Eur. J.* **2010**, *16*, 9746-9749.
- [104] T. Ohmura, K. Masuda, I. Takase, M. Suginome, *J. Am. Chem. Soc.* **2009**, *131*, 16624-16625.
- [105] S. S. Zaleskiy, V. P. Ananikov, *Organometallics* **2012**, *31*, 2302-2309.
- [106] B. E. Love, E. G. Jones, *J. Org. Chem.* **1999**, *64*, 3755-3756.
- [107] J. W. Dankwardt, *Angew. Chem. Int. Ed.* **2004**, *43*, 2428-2432.
- [108] R. Caraballo, M. Rahm, P. Vongvilai, T. Brinck, O. Ramström, *Chem. Commun.* **2008**, 6603-6605.
- [109] M. Mentel, A. M. Schmidt, M. Gorray, P. Eilbracht, R. Breinbauer, *Angew. Chem. Int. Ed.* **2009**, *48*, 5841-5844.
- [110] X. Huang, K. W. Anderson, D. Zim, L. Jiang, A. Klapars, S. L. Buchwald, *J. Am. Chem. Soc.* **2003**, *125*, 6653-6655.
- [111] J. E. Milne, S. L. Buchwald, *J. Am. Chem. Soc.* **2004**, *126*, 13028-13032.
- [112] N. Hoshiya, S. L. Buchwald, *Adv. Synth. Catal.* **2012**, *354*, 2031-2037.
- [113] J. P. Wolfe, R. A. Singer, B. H. Yang, S. L. Buchwald, *J. Am. Chem. Soc.* **1999**, *121*, 9550-9561.
- [114] H. Tomori, J. M. Fox, S. L. Buchwald, *J. Org. Chem.* **2000**, *65*, 5334-5341.
- [115] M. Oda, K. Okawa, H. Tsuru, S. Kuroda, *Tetrahedron* **2003**, *59*, 795-800.
- [116] M. G. Organ, S. Calimsiz, M. Sayah, K. H. Hoi, A. J. Lough, *Angew. Chem. Int. Ed.* **2009**, *48*, 2383-2387.
- [117] C. Jiang, O. Blacque, T. Fox, H. Berke, *Organometallics* **2011**, *30*, 2117-2124.
- [118] A. M. Belostotskii, H. E. Gottlieb, P. Aped, A. Hassner, *Chem. Eur. J.* **1999**, *5*, 449-455.
- [119] N. C. Bruno, M. T. Tudge, S. L. Buchwald, *Chem. Sci.* **2013**, *4*, 916-920.
- [120] L. Jafarpour, E. D. Stevens, S. P. Nolan, *J. Organomet. Chem.* **2000**, *606*, 49-54.
- [121] A. J. Arduengo III, R. Krafczyk, R. Schmutzler, H. A. Craig, J. R. Goerlich, W. J. Marshall, M. Unverzagt, *Tetrahedron* **1999**, *55*, 14523-14534.

- [122] M. Pompeo, R. D. Froese, N. Hadei, M. G. Organ, *Angew. Chem. Int. Ed.* **2012**, *51*, 11354-11357.
- [123] A. Chartoire, M. Lesieur, L. Falivene, A. M. Slawin, L. Cavallo, C. S. Cazin, S. P. Nolan, *Chem. Eur. J.* **2012**, *18*, 4517-4521.
- [124] F. Izquierdo, C. Zinser, Y. Minenkov, D. B. Cordes, A. M. Slawin, L. Cavallo, F. Nahra, C. S. Cazin, S. P. Nolan, *ChemCatChem* **2018**, *10*, 601-611.
- [125] A. Chartoire, X. Frogneux, A. Boreux, A. M. Slawin, S. P. Nolan, *Organometallics* **2012**, *31*, 6947-6951.
- [126] Q. Cao, J. L. Howard, E. Wheatley, D. L. Browne, *Angew. Chem. Int. Ed.* **2018**, *57*, 11339-11343.

8 APPENDIX

8.1 List of abbreviations

2D	two-dimensional
3-Cl-py	3- Chloropyridine
[CC]	Cross-Coupling precatalyst
[DH]	DeHydrogenation precatalyst
A_λ	absorption maximum at wavelength λ [nm]
ac	acetone
acac	acetylacetonate
act.	activator
Ad	1- Adamantyl
add.	additive
All	Allyl
^tAm	<i>tert</i> - Amyl , -CEtMe ₂
approx.	approximately
aq.	aqueous
Ar	aryl group
Ar _F	3,5-bis(trifluoromethyl)phenyl
a.u.	normalized absorbance
binap	2,2'-bis-diphenylphosphino-1,1'- binaphthyl
bipy	bipyridine
Bn	Benzyl
BQ	BenzoQuinone
caff.	caffeine
calcd	calculated
CAPT	Chiral Anion Phase Transfer

CAS	C hemical A bstract S ervice
cat.	c atalyst or c atalytic
cataCXium [®] A	<i>n</i> -butyl-diadamantylphosphine
CC	(flash) C olumn C hromatography
CCP	C atalyst C omponent P recursor
CHO	C yclo H exene O xide
CHT	C yclo H epta T riene/ C yclo H epta T rienyl
cin	c innamyl
cod	1,5-cyclooctadiene
Cp	C yclopentadiene
Cp*	pentamethylcyclopentadienyl
cryst.	c rystallization
CTA	C etyl T rimethyl A mmonium
CuTC	copper(I) (Cu (I)) T hiophene-2- T arboxylate
d	d ay(s)
DABCO	1,4- D i A za B i C yclo[2.2.2] O ctane
DAD	1,2- D i A za D iene
dba	d ibenzyliden a cetone
DBE	1,2- D i B romo E thane
DBU	1,8- D iaza B icyclo[5.4.0] U ndec-7-ene
DCE	1,2- D i C hloro E thane
DCM	D i C hloro M ethane
DDQ	2,3- D ichloro-5,6- D icyano-1,4-benzo Q uinone
DEC	D i E thoxy C arbonate
DEM	1,1- d iethoxy m ethane

DFT	D iscrete F ourier T ransform
diglyme	bis(2-methoxyethyl)ether
dipp	2,6- d iisopropyl p henyl
DiPP	D iiso P ropyl P ropionate
DiPPA	D iiso P ropyl P ropionoic A cid
disub.	d isubstituted
DMAc	D i M ethyl A cetamide
DMAP	4- D i M ethyl A mino P yridine
dmba	<i>N,N</i> - d imethylbenzylamine
DMC	D i M ethyl C arbonate
dme	1,2- d imethoxyethane
DMI	1,3- D i M ethyl-2- I midazolidinone
DoE	D esign of E xperiments
dpby	4,4'- d iphenyl b ipyridine
dppb	1,4-bis(d iphenyl p hosphino) b utane
dppe	1,2-bis(d iphenyl p hosphino)ethane
dppf	1,1'-bis(d iphenyl p hosphino) f errocene
dppp	1,3-bis(d iphenyl p hosphino) p ropane
ϵ	dielectric constant
E^+	E lectrophile
ee	e nantiomeric e xcess
$E_{x,y}$	E lement of a matrix (entry) at row x and column y
e.g.	Latin: e xempli g ratia, English: for example
EG	E thylene G lycol
eq.	e quivalent(s)

EWG	Electron-Withdrawing Group
exc.	excess
extr.	extraction
f.	and the following
Fc	Ferrocenyl
GC	Gas Chromatography
GP	General Procedure
HAT	Hydrogen Auto-Transfer
HetAr	Heteroaromatic Arene
HiLo	High-Low loading
HMDS	HexaMethylDiSilazide
HOMO	Highest Occupied Molecular Orbital
HPLC	High Performance Liquid Chromatography
HRMS	High Resolution Mass Spectrometry
HTE	High Troughput Experiments
Im	Imidazole/Imidazolium
IMes	1,3-(bis(2,4,6-trimethylphenyl)-imidazol-2-ylidene
IMes-DAD	1,4-bis(2,4,6-trimethylphenyl)diazabutadiene
IMes·HCl	1,3-(bis(2,4,6-trimethylphenyl)-imidazolium chloride
IPr	1,3-(bis(2,6-diisopropylphenyl)-imidazol-2-ylidene
^m IPr	1,3-(bis(2,6-diisopropylphenyl)-imidazol-4-ylidene
IPr·HCl	1,3-(bis(2,6-diisopropylphenyl)-imidazolium chloride
IPr ^{Cl} ·HCl	4,5-dichloro-1,3-(bis(2,6-diisopropylphenyl)-imidazolium chloride
IPr ^{Me} ·HCl	4,5-dimethyl-1,3-(bis(2,6-diisopropylphenyl)-imidazolium chloride
IPr [*] ·HCl	1,3-bis(2,6-benzhydryl-4-methylphenyl)-imidazolium chloride

IPr ^{*OMe} .HCl	1,3-bis(2,6-benzhydryl-4-methoxyphenyl)-imidazolium chloride
IPr-DAD	1,4-bis(2,6-diisopropylphenyl)diazabutadiene
IPr-MeDAD	diacetyl-bis(2,6-diisopropylphenyl)imine or <i>N,N'</i> -(butane-2,3-diylidene)-bis(2,6-diisopropylaniline)
LDA	L ithium D iisopropyl A mide
lit.	l iterature
LUMO	L owest U noccupied M olecular O rbital
max.	m aximum
Men	M enthyl
Mes	M esityl
MFCC	M ultifunctional C omponent C atalyst
MFCCP	M ulti F unctional C omponent C atalyst P rinciple
min	m inute(s)
min.	m inimum
monosubst.	monosubstituted
MTOA	M ethyl T ri O ctyl A mmonium
n	amount of substance
n ₀	initial amount of substance n
NaHMDS	sodium hexamethyldisilazide
Nap	N aphthyl
NBS	<i>N</i> - B rom S uccinimid
n _{caff.}	amount of substance n of caffeine
NCD	N or C ara D iene/ N or C ara D ienyl
n.d.	n ot d etermined
NHP	<i>N</i> - H eterocyclic P hosphine

n_{inj} .	Injected amount of substance n
NMP	N-Methyl-2-Pyrrolidone
NMR	Nuclear Magnetic Resonance
n_{Phcaff} .	amount of substance n of phenylcaffeine
Nuc	Nucleophile
OAVT	One Variable At a Time
ox	oxalate
PEG	PolyEthylene Glycol
PEPSI	Pyridine-Enhanced Precatalyst Preparation Stabilization and Initiation
PET	Positron Emission Tomography
Phcaff.	Phenylcaffeine
PO	Phosphine Oxide
PP	PolyPropylene
ppm	parts per million
precat.	precatalyst
PTC	Phase Transfer Catalyst
PTFE	PolyTetraFluoroEthylene
Py	Pyridine
PyBOP [®]	(benzotriazol-1-yloxy)tripyrrolidinophosphonium hexafluorophosphate
PyBrOP [®]	bromotripyrrolidinophosphonium hexafluorophosphate
Py-2-OH	Pyridin-2-ol
recov.	recovery.
rpm	round(s) per minute
r.t.	room temperature
sat.	saturated

sDoE	sequential D esign of E xperiments
S _E Ar	electrophilic aromatic substitution
SET	S ingle E lectron T ransfer
solv.	s olvent
s.p.	s ide- p roduct
struct.	s tructure
sw	s pectral w idth
t	t ime
T	T emperature (usually in °C)
TBE	T ert- B utyl E thylene
TBME	<i>Tert-ButylMethylEther</i>
TEMPO	2,2,6,6-TE tra M ethyl P iperidiny O xyl
THF	T etra H ydro F uran
TLC	T hin- L ayer C hromatography
TMP	T etra M ethyl P iperidine
Tol	T olyl
TRISPHAT	phosphorous(V) tris(tetrachlorocatecholate)phat
Trop	T ropylium
TsCl	<i>p</i> -toluenesulfonyl chloride
Vin	V inyl
vs.	v ersus
wt.%	weight percent
X _{caff.}	respective peak area of detected caffeine
X _{Phcaff.}	respective peak area of detected phenylcaffeine
XS	e xcess

Xy	Xylene
z.B.	zum B eispiel
λ	wavelength
μ W	micro-wave heating

8.2 Graphs of HPLC reference measures for caffeine and phenylcaffeine

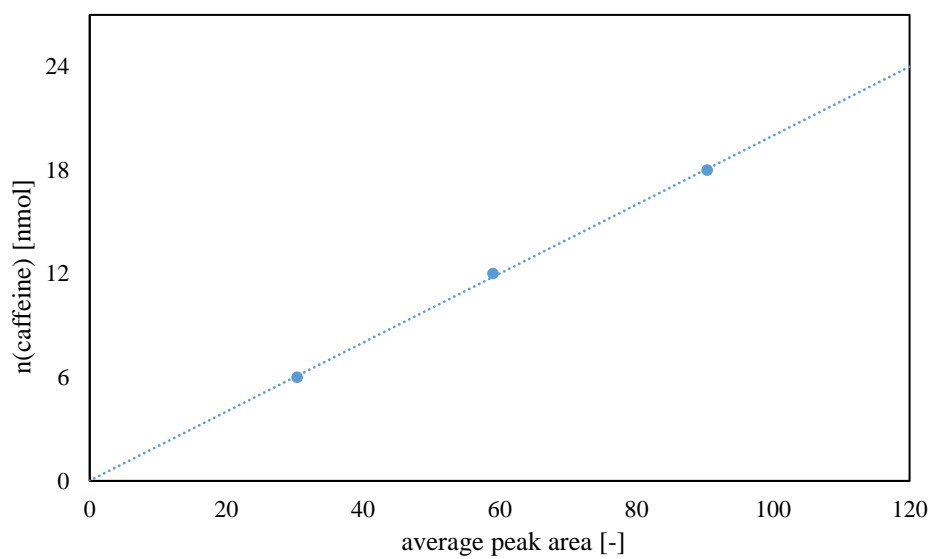


Figure 49. Injected amount of substance of caffeine plotted against the detected peak area. Equation of the trend line: $y_{\text{caff.}} = 0.1998 \cdot x + 0.0176$.

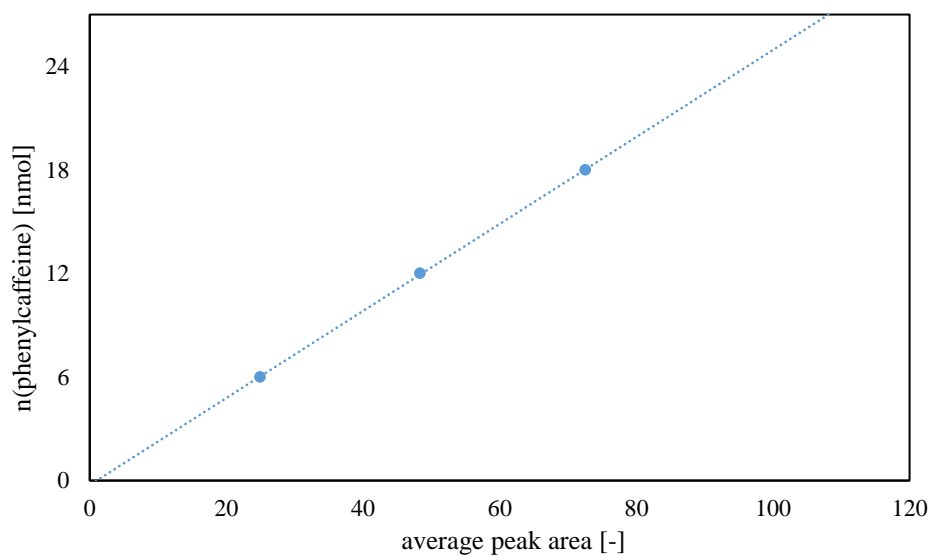


Figure 50. Injected amount of substance of 8-phenylcaffeine plotted against the detected peak area. Equation of the trend line: $y_{\text{Phcaff.}} = 0.252 \cdot x - 0.2553$.

8.3 X-ray structure data

Table 54. Sample and crystal data for KlePh1.

Chemical formula	C ₅₄ H ₇₄ Cl ₆ N ₄ Pd ₂	
Formula weight	1204.67 g/mol	
Temperature	100(2) K	
Wavelength λ	0.71073 Å	
Crystal size	0.018 x 0.129 x 0.180 mm	
Crystal habit	clear intense yellow orange plate	
Crystal system	triclinic	
Space group	P $\bar{1}$	
Unit cell dimensions	a = 11.9615(5) Å	$\alpha = 107.400(2)^\circ$
	b = 13.9958(6) Å	$\beta = 96.952(2)^\circ$
	c = 18.1042(7) Å	$\gamma = 102.204(2)^\circ$
Volume	2771.1(2) Å ³	
Z	2	
Density (calculated)	1.444 g/cm ³	
Absorption coefficient	0.977 mm ⁻¹	
F(000)	1240	

Table 55. Data collection and structure refinement for KlePh1.

Diffractometer	Bruker D8 Venture TXS	
Radiation source	iMS-Microfocus, Mo	
Theta range for data collection	2.28 to 25.47°	
Index ranges	-14 ≤ h ≤ 14, -16 ≤ k ≤ 16, -21 ≤ l ≤ 21	
Reflections collected	57132	
Independent reflections	10219 [R(int) = 0.1280]	
Coverage of independent reflections	99.4%	
Absorption correction	Multi-Scan	
Max. and min. transmission	0.9830 and 0.8440	
Refinement method	Full-matrix least-squares on F ²	
Refinement program	SHELXL-2014/7 (Sheldrick, 2014)	
Function minimized	$\sum w(F_\sigma^2 - F_c^2)^2$	
Data / restraints / parameters	10219 / 0 / 611	
Goodness-of-fit on F²	0.982	
Δ/σ_{\max}	0.002	
Final R indices	7524 data; I > 2σ(I)	R1 = 0.0275, wR2 = 0.0536
	all data	R1 = 0.0592, wR2 = 0.0570
Weighting scheme	w = 1/[σ ² (F _σ ²) + (0.0200 P) ²] where P = (F _σ ² + 2 F _c ²)/3	
Largest diff. peak and hole	0.376 and -0.705 eÅ ⁻³	
R.M.S. deviation from mean	0.078 eÅ ⁻³	

Table 56. Sample and crystal data for KlePh2.

Chemical formula	C ₂₁ H ₂₅ Cl ₃ N ₂ Pd	
Formula weight	518.18 g/mol	
Temperature	100(2) K	
Wavelength λ	0.71073 Å	
Crystal size	0.045 x 0.072 x 0.089 mm	
Crystal habit	clear intense yellow orange fragment	
Crystal system	monoclinic	
Space group	P 1 21/n 1	
Unit cell dimensions	a = 10.4727(9) Å	$\alpha = 90^\circ$
	b = 16.4786(15) Å	$\beta = 105.835(4)^\circ$
	c = 13.1528(13) Å	$\gamma = 90^\circ$
Volume	2183.7(4) Å ³	
Z	4	
Density (calculated)	1.576 g/cm ³	
Absorption coefficient	1.225 mm ⁻¹	
F(000)	1048	

Table 57. Data collection and structure refinement for KlePh2.

Diffractometer	Bruker D8 Venture TXS	
Radiation source	iMS-Microfocus, Mo	
Theta range for data collection	2.21 to 26.46°	
Index ranges	-13 ≤ h ≤ 13, -20 ≤ k ≤ 20, -16 ≤ l ≤ 16	
Reflections collected	25747	
Independent reflections	4497 [R(int) = 0.0353]	
Coverage of independent reflections	99.7%	
Absorption correction	Multi-Scan	
Max. and min. transmission	0.9470 and 0.8990	
Refinement method	Full-matrix least-squares on F ²	
Refinement program	SHELXL-2014/7 (Sheldrick, 2014)	
Function minimized	$\sum w(F_\sigma^2 - F_c^2)^2$	
Data / restraints / parameters	4497 / 0 / 250	
Goodness-of-fit on F²	1.054	
Δ/σ_{\max}	0.001	
Final R indices	3959 data; I > 2σ(I)	R1 = 0.0209, wR2 = 0.0466
	all data	R1 = 0.0273, wR2 = 0.0488
Weighting scheme	w = 1/[σ ² (F _σ ²) + (0.0179 P) ² + 1.8081 P] where P = (F _σ ² + 2 F _c ²)/3	
Largest diff. peak and hole	0.388 and -0.581 eÅ ⁻³	
R.M.S. deviation from mean	0.069 eÅ ⁻³	

Table 58. Sample and crystal data for KlePh3.

Chemical formula	C ₆₆ H ₉₄ Cl ₆ N ₄ O ₄ Pd ₂	
Formula weight	1432.95 g/mol	
Temperature	100(2) K	
Wavelength λ	0.71073 Å	
Crystal size	0.125 x 0.136 x 0.156 mm	
Crystal habit	clear yellow fragment	
Crystal system	monoclinic	
Space group	C 1 2/c 1	
Unit cell dimensions	a = 48.242(5) Å	$\alpha = 90^\circ$
	b = 11.8507(11) Å	$\beta = 97.257(3)^\circ$
	c = 25.228(3) Å	$\gamma = 90^\circ$
Volume	14307.(2) Å ³	
Z	8	
Density (calculated)	1.330 g/cm ³	
Absorption coefficient	0.772 mm ⁻¹	
F(000)	5952	

Table 59. Data collection and structure refinement for KlePh3.

Diffractometer	Bruker D8 Venture TXS	
Radiation source	TXS rotating anode, Mo	
Theta range for data collection	2.20 to 25.34°	
Index ranges	-58 ≤ h ≤ 58, -14 ≤ k ≤ 14, -30 ≤ l ≤ 30	
Reflections collected	153978	
Independent reflections	13075 [R(int) = 0.0335]	
Coverage of independent reflections	99.8%	
Absorption correction	Multi-Scan	
Max. and min. transmission	0.9100 and 0.8890	
Refinement method	Full-matrix least-squares on F ²	
Refinement program	SHELXL-2014/7 (Sheldrick, 2014)	
Function minimized	$\sum w(F_\sigma^2 - F_c^2)^2$	
Data / restraints / parameters	13075 / 39 / 792	
Goodness-of-fit on F²	1.034	
Δ/σ_{\max}	0.002	
Final R indices	11797 data; I > 2σ(I)	R1 = 0.0346, wR2 = 0.0882
	all data	R1 = 0.0396, wR2 = 0.0914
Weighting scheme	w = 1/[σ ² (F _σ ²) + (0.0395 P) ² + 66.3689 P] where P = (F _σ ² + 2 F _c ²)/3	
Largest diff. peak and hole	1.062 and -1.318 eÅ ⁻³	
R.M.S. deviation from mean	0.077 eÅ ⁻³	

Table 60. Sample and crystal data for KlePh4.

Chemical formula	C ₅₂ H ₈₀ Br ₂ P ₂	
Formula weight	926.92 g/mol	
Temperature	100(2) K	
Wavelength λ	0.71073 Å	
Crystal size	0.103 x 0.152 x 0.511 mm	
Crystal habit	clear colorless fragment	
Crystal system	monoclinic	
Space group	P 1 21/n 1	
Unit cell dimensions	a = 19.545(5) Å	$\alpha = 90^\circ$
	b = 11.818(3) Å	$\beta = 96.522(9)^\circ$
	c = 21.256(6) Å	$\gamma = 90^\circ$
Volume	4878.(2) Å ³	
Z	4	
Density (calculated)	1.262 g/cm ³	
Absorption coefficient	1.760 mm ⁻¹	
F(000)	1968	

Table 61. Data collection and structure refinement for KlePh4.

Diffractometer	Bruker D8 Venture Duo IMS	
Radiation source	IMS microsource, Mo	
Theta range for data collection	2.18 to 25.02°	
Index ranges	-23 ≤ h ≤ 23, -14 ≤ k ≤ 14, -25 ≤ l ≤ 25	
Reflections collected	149268	
Independent reflections	8604 [R(int) = 0.1128]	
Coverage of independent reflections	99.9%	
Absorption correction	Multi-Scan	
Max. and min. transmission	0.8390 and 0.4670	
Refinement method	Full-matrix least-squares on F ²	
Refinement program	SHELXL-2014/7 (Sheldrick, 2014)	
Function minimized	$\sum w(F_\sigma^2 - F_c^2)^2$	
Data / restraints / parameters	8604 / 111 / 570	
Goodness-of-fit on F²	1.069	
Δ/σ_{\max}	0.001	
Final R indices	6934 data; I > 2σ(I)	R1 = 0.0398, wR2 = 0.0888
	all data	R1 = 0.0588, wR2 = 0.0838
Weighting scheme	w = 1/[σ ² (F _σ ²) + (0.0278 P) ² + 7.1220 P] where P = (F _σ ² + 2 F _c ²)/3	
Largest diff. peak and hole	0.847 and -0.333 eÅ ⁻³	
R.M.S. deviation from mean	0.066 eÅ ⁻³	

Table 62. Sample and crystal data for KlePh5.

Chemical formula	C ₅₀ H ₈₀ F ₁₂ P ₄	
Formula weight	1033.02 g/mol	
Temperature	100(2) K	
Wavelength λ	0.71073 Å	
Crystal size	0.282 x 0.297 x 0.549 mm	
Crystal habit	clear colorless fragment	
Crystal system	monoclinic	
Space group	P 1 21/c 1	
Unit cell dimensions	a = 19.734(3) Å	$\alpha = 90^\circ$
	b = 14.261(3) Å	$\beta = 108.922(6)^\circ$
	c = 19.211(3) Å	$\gamma = 90^\circ$
Volume	5114.3(14) Å ³	
Z	4	
Density (calculated)	1.342 g/cm ³	
Absorption coefficient	0.225 mm ⁻¹	
F(000)	2192	

Table 63. Data collection and structure refinement for KlePh5.

Diffractometer	Bruker D8 Venture Duo IMS	
Radiation source	IMS microsource, Mo	
Theta range for data collection	2.18 to 25.03°	
Index ranges	-23 ≤ h ≤ 23, -16 ≤ k ≤ 16, -22 ≤ l ≤ 22	
Reflections collected	148541	
Independent reflections	9022 [R(int) = 0.0526]	
Coverage of independent reflections	99.9%	
Absorption correction	Multi-Scan	
Max. and min. transmission	0.9390 and 0.8860	
Refinement method	Full-matrix least-squares on F ²	
Refinement program	SHELXL-2014/7 (Sheldrick, 2014)	
Function minimized	$\sum w(F_\sigma^2 - F_c^2)^2$	
Data / restraints / parameters	9022 / 378 / 778	
Goodness-of-fit on F²	1.034	
Δ/σ_{\max}	0.001	
Final R indices	7845 data; I > 2σ(I)	R1 = 0.0375, wR2 = 0.0894
	all data	R1 = 0.0452, wR2 = 0.0941
Weighting scheme	w = 1/[σ ² (F _σ ²) + (0.0403 P) ² + 4.7400 P] where P = (F _σ ² + 2 F _c ²)/3	
Largest diff. peak and hole	0.642 and -0.327 eÅ ⁻³	
R.M.S. deviation from mean	0.056 eÅ ⁻³	

Table 64. Sample and crystal data for KlePh7.

Chemical formula	C ₂₆ H ₄₂ BrCl ₂ P	
Formula weight	536.37 g/mol	
Temperature	100(2) K	
Wavelength λ	0.71073 Å	
Crystal size	0.122 x 0.221 x 0.249 mm	
Crystal habit	clear colorless plate	
Crystal system	orthorhombic	
Space group	P b c a	
Unit cell dimensions	a = 16.941(8) Å	$\alpha = 90^\circ$
	b = 15.428(7) Å	$\beta = 90^\circ$
	c = 20.947(11) Å	$\gamma = 90^\circ$
Volume	5475.(5) Å ³	
Z	8	
Density (calculated)	1.301 g/cm ³	
Absorption coefficient	1.767 mm ⁻¹	
F(000)	2256	

Table 65. Data collection and structure refinement for KlePh7.

Diffractometer	Bruker D8 Kappa Apex II	
Radiation source	fine-focus sealed tube, Mo	
Theta range for data collection	2.03 to 25.02°	
Index ranges	-20 ≤ h ≤ 19, -18 ≤ k ≤ 18, -24 ≤ l ≤ 24	
Reflections collected	50471	
Independent reflections	4825 [R(int) = 0.0557]	
Coverage of independent reflections	100.0%	
Absorption correction	Multi-Scan	
Max. and min. transmission	0.8130 and 0.6670	
Refinement method	Full-matrix least-squares on F ²	
Refinement program	SHELXL-2014/7 (Sheldrick, 2014)	
Function minimized	$\sum w(F_\sigma^2 - F_c^2)^2$	
Data / restraints / parameters	4825 / 27 / 299	
Goodness-of-fit on F²	1.031	
Δ/σ_{\max}	0.001	
Final R indices	3864 data; I > 2σ(I)	R1 = 0.0359, wR2 = 0.0816
	all data	R1 = 0.0508, wR2 = 0.0885
Weighting scheme	w = 1/[σ ² (F _σ ²) + (0.0334 P) ² + 8.4153 P] where P = (F _σ ² + 2 F _c ²)/3	
Largest diff. peak and hole	0.852 and -0.661 eÅ ⁻³	
R.M.S. deviation from mean	0.063 eÅ ⁻³	

Table 66. Sample and crystal data for KlePh8.

Chemical formula	C ₃₂ H ₄₆ BrCl ₂ P	
Formula weight	612.47 g/mol	
Temperature	100(2) K	
Wavelength λ	0.71073 Å	
Crystal size	0.164 x 0.178 x 0.241 mm	
Crystal habit	clear colorless fragment	
Crystal system	triclinic	
Space group	P-1	
Unit cell dimensions	a = 9.375(7) Å	$\alpha = 93.61(3)^\circ$
	b = 10.363(9) Å	$\beta = 97.32(3)^\circ$
	c = 16.690(14) Å	$\gamma = 105.47(3)^\circ$
Volume	1542.(2) Å ³	
Z	2	
Density (calculated)	1.319 g/cm ³	
Absorption coefficient	1.578 mm ⁻¹	
F(000)	644	

Table 67. Data collection and structure refinement for KlePh8.

Diffractometer	Bruker D8 Kappa Apex II	
Radiation source	fine-focus sealed tube, Mo	
Theta range for data collection	2.05 to 25.03°	
Index ranges	-11 ≤ h ≤ 11, -12 ≤ k ≤ 12, -19 ≤ l ≤ 19	
Reflections collected	25828	
Independent reflections	5405 [R(int) = 0.0541]	
Coverage of independent reflections	99.4%	
Absorption correction	Multi-Scan	
Max. and min. transmission	0.7820 and 0.7020	
Refinement method	Full-matrix least-squares on F ²	
Refinement program	SHELXL-2014/7 (Sheldrick, 2014)	
Function minimized	$\sum w(F_\sigma^2 - F_c^2)^2$	
Data / restraints / parameters	5405 / 0 / 325	
Goodness-of-fit on F²	1.029	
Δ/σ_{\max}	0.001	
Final R indices	4660 data; I > 2σ(I)	R1 = 0.0364, wR2 = 0.0837
	all data	R1 = 0.0463, wR2 = 0.0879
Weighting scheme	w = 1/[σ ² (F _σ ²) + (0.0359 P) ² + 1.3296 P] where P = (F _σ ² + 2 F _c ²)/3	
Largest diff. peak and hole	0.847 and -0.563 eÅ ⁻³	
R.M.S. deviation from mean	0.064 eÅ ⁻³	

Table 68. Sample and crystal data for KlePh9.

Chemical formula	C _{18.50} H ₂₄ Cl _{0.50} P _{0.50}	
Formula weight	279.59 g/mol	
Temperature	100(2) K	
Wavelength λ	0.71073 Å	
Crystal size	0.127 x 0.131 x 0.148 mm	
Crystal habit	clear colorless fragment	
Crystal system	orthorhombic	
Space group	I m a 2	
Unit cell dimensions	a = 17.6373(7) Å	$\alpha = 90^\circ$
	b = 17.2729(7) Å	$\beta = 90^\circ$
	c = 10.1932(4) Å	$\gamma = 90^\circ$
Volume	3105.3(2) Å ³	
Z	8	
Density (calculated)	1.196 g/cm ³	
Absorption coefficient	0.199 mm ⁻¹	
F(000)	1208	

Table 69. Data collection and structure refinement for KlePh9.

Diffractometer	Bruker D8 Venture Duo IMS	
Radiation source	IMS microsource, Mo	
Theta range for data collection	2.31 to 25.01°	
Index ranges	-20 ≤ h ≤ 20, -20 ≤ k ≤ 20, -12 ≤ l ≤ 12	
Reflections collected	36194	
Independent reflections	2840 [R(int) = 0.0274]	
Coverage of independent reflections	99.9%	
Absorption correction	Multi-Scan	
Max. and min. transmission	0.9750 and 0.9710	
Refinement method	Full-matrix least-squares on F ²	
Refinement program	SHELXL-2014/7 (Sheldrick, 2014)	
Function minimized	$\sum w(F_\sigma^2 - F_c^2)^2$	
Data / restraints / parameters	2840 / 333 / 263	
Goodness-of-fit on F²	1.058	
Δ/σ_{\max}	0.001	
Final R indices	2799 data; I > 2σ(I)	R1 = 0.0472, wR2 = 0.1161
	all data	R1 = 0.0478, wR2 = 0.1168
Weighting scheme	w = 1/[σ ² (F _σ ²) + (0.0534 P) ² + 7.9728 P] where P = (F _σ ² + 2 F _c ²)/3	
Largest diff. peak and hole	0.469 and -0.548 eÅ ⁻³	
R.M.S. deviation from mean	0.058 eÅ ⁻³	

Table 70. Sample and crystal data for KlePh10.

Chemical formula	C ₃₃ H ₄₂ F ₆ O ₂ P ₂	
Formula weight	646.60 g/mol	
Temperature	100(2) K	
Wavelength λ	0.71073 Å	
Crystal size	0.096 x 0.235 x 0.320 mm	
Crystal habit	clear colorless fragment	
Crystal system	monoclinic	
Space group	P 1 21/c 1	
Unit cell dimensions	a = 9.5604(4) Å	$\alpha = 90^\circ$
	b = 14.6670(7) Å	$\beta = 96.109(2)^\circ$
	c = 22.5501(11) Å	$\gamma = 90^\circ$
Volume	3144.1(3) Å ³	
Z	4	
Density (calculated)	1.366 g/cm ³	
Absorption coefficient	0.204 mm ⁻¹	
F(000)	1360	

Table 71. Data collection and structure refinement for KlePh10.

Diffractometer	Bruker D8 Venture	
Radiation source	TXS rotating anode, Mo	
Theta range for data collection	2.14 to 25.03°	
Index ranges	-11 ≤ h ≤ 11, -17 ≤ k ≤ 17, -26 ≤ l ≤ 26	
Reflections collected	111304	
Independent reflections	5548 [R(int) = 0.0387]	
Coverage of independent reflections	99.9%	
Absorption correction	Multi-Scan	
Max. and min. transmission	0.9810 and 0.9380	
Refinement method	Full-matrix least-squares on F ²	
Refinement program	SHELXL-2014/7 (Sheldrick, 2014)	
Function minimized	$\sum w(F_\sigma^2 - F_c^2)^2$	
Data / restraints / parameters	5548 / 0 / 390	
Goodness-of-fit on F²	1.038	
Δ/σ_{\max}	0.001	
Final R indices	5139 data; I > 2σ(I)	R1 = 0.0519, wR2 = 0.1273
	all data	R1 = 0.0553, wR2 = 0.1295
Weighting scheme	w = 1/[σ ² (F _σ ²) + (0.0502 P) ² + 6.6960 P] where P = (F _σ ² + 2 F _c ²)/3	
Largest diff. peak and hole	0.918 and -0.508 eÅ ⁻³	
R.M.S. deviation from mean	0.064 eÅ ⁻³	

Table 72. Sample and crystal data for KlePh11.

Chemical formula	C ₄₀ H ₅₆ F ₆ P ₂	
Formula weight	712.78 g/mol	
Temperature	100(2) K	
Wavelength λ	0.71073 Å	
Crystal size	0.045 x 0.082 x 0.219 mm	
Crystal habit	clear colorless fragment	
Crystal system	monoclinic	
Space group	P 1 21/c 1	
Unit cell dimensions	a = 10.8732(5) Å	$\alpha = 90^\circ$
	b = 19.9989(8) Å	$\beta = 92.334(2)^\circ$
	c = 17.0258(6) Å	$\gamma = 90^\circ$
Volume	3699.2(3) Å ³	
Z	4	
Density (calculated)	1.280 g/cm ³	
Absorption coefficient	0.176 mm ⁻¹	
F(000)	1520	

Table 73. Data collection and structure refinement for KlePh11.

Diffractometer	Bruker D8 Venture	
Radiation source	TXS rotating anode, Mo	
Theta range for data collection	2.39 to 25.03°	
Index ranges	-12 ≤ h ≤ 12, -23 ≤ k ≤ 23, -20 ≤ l ≤ 20	
Reflections collected	86821	
Independent reflections	6523 [R(int) = 0.0780]	
Coverage of independent reflections	99.9%	
Absorption correction	Multi-Scan	
Max. and min. transmission	0.9920 and 0.9630	
Refinement method	Full-matrix least-squares on F ²	
Refinement program	SHELXL-2014/7 (Sheldrick, 2014)	
Function minimized	$\sum w(F_\sigma^2 - F_c^2)^2$	
Data / restraints / parameters	6523 / 0 / 440	
Goodness-of-fit on F²	1.047	
Δ/σ_{\max}	0.001	
Final R indices	5412 data; I > 2σ(I)	R1 = 0.0526, wR2 = 0.1237
	all data	R1 = 0.0670, wR2 = 0.1317
Weighting scheme	w = 1/[σ ² (F _σ ²) + (0.0495 P) ² + 6.5030 P] where P = (F _σ ² + 2 F _c ²)/3	
Largest diff. peak and hole	0.726 and -0.395 eÅ ⁻³	
R.M.S. deviation from mean	0.060 eÅ ⁻³	

Table 74. Sample and crystal data for KlePh12.

Chemical formula	C ₃₇ H ₅₀ F ₆ O ₂ P ₂	
Formula weight	702.71 g/mol	
Temperature	100(2) K	
Wavelength λ	0.71073 Å	
Crystal size	0.110 x 0.183 x 0.287 mm	
Crystal habit	clear colorless fragment	
Crystal system	monoclinic	
Space group	P 1 21/c 1	
Unit cell dimensions	a = 9.6697(8) Å	$\alpha = 90^\circ$
	b = 27.476(2) Å	$\beta = 109.332(2)^\circ$
	c = 14.2137(12) Å	$\gamma = 90^\circ$
Volume	3563.4(5) Å ³	
Z	4	
Density (calculated)	1.310 g/cm ³	
Absorption coefficient	0.185 mm ⁻¹	
F(000)	1488	

Table 75. Data collection and structure refinement for KlePh12.

Diffractometer	Bruker D8 Venture	
Radiation source	TXS rotating anode, Mo	
Theta range for data collection	2.35 to 25.03°	
Index ranges	-11 ≤ h ≤ 11, -32 ≤ k ≤ 32, -16 ≤ l ≤ 16	
Reflections collected	52644	
Independent reflections	6299 [R(int) = 0.0398]	
Coverage of independent reflections	99.9%	
Absorption correction	Multi-Scan	
Max. and min. transmission	0.9800 and 0.9490	
Refinement method	Full-matrix least-squares on F ²	
Refinement program	SHELXL-2014/7 (Sheldrick, 2014)	
Function minimized	$\sum w(F_\sigma^2 - F_c^2)^2$	
Data / restraints / parameters	6299 / 0 / 429	
Goodness-of-fit on F²	1.039	
Δ/σ_{\max}	0.001	
Final R indices	5196 data; I > 2σ(I)	R1 = 0.0368, wR2 = 0.0890
	all data	R1 = 0.0491, wR2 = 0.0957
Weighting scheme	w = 1/[σ ² (F _σ ²) + (0.0421 P) ² + 2.2030 P] where P = (F _σ ² + 2 F _c ²)/3	
Largest diff. peak and hole	0.433 and -0.272 eÅ ⁻³	
R.M.S. deviation from mean	0.044 eÅ ⁻³	

Table 76. Sample and crystal data for KlePh14.

Chemical formula	C ₂₂ H ₂₇ F ₆ N ₂ P ₁	
Formula weight	464.413 g/mol	
Temperature	100(2) K	
Wavelength λ	0.71073 Å	
Crystal size	0.081 x 0.148 x 0.274 mm	
Crystal habit	clear colorless fragment	
Crystal system	triclinic	
Space group	P-1	
Unit cell dimensions	a = 9.9944(4) Å	$\alpha = 65.5860(10)^\circ$
	b = 14.8560(4) Å	$\beta = 83.307(2)^\circ$
	c = 11.6068(4) Å	$\gamma = 88.594(2)^\circ$
Volume	1138.52(7) Å ³	
Z	2	
Density (calculated)	1.355 g/cm ³	
Absorption coefficient	0.181 mm ⁻¹	
F(000)	484	

Table 77. Data collection and structure refinement for KlePh14.

Diffractometer	Bruker D8 Venture	
Radiation source	TXS rotating anode, Mo	
Theta range for data collection	2.65 to 26.02°	
Index ranges	-12 ≤ h ≤ 12, -13 ≤ k ≤ 13, -14 ≤ l ≤ 14	
Reflections collected	22271	
Independent reflections	4480 [R(int) = 0.0236]	
Coverage of independent reflections	99.8%	
Absorption correction	Multi-Scan	
Max. and min. transmission	0.9860 and 0.9520	
Refinement method	Full-matrix least-squares on F ²	
Refinement program	SHELXL-2018/3 (Sheldrick, 2018)	
Function minimized	$\sum w(F_\sigma^2 - F_c^2)^2$	
Data / restraints / parameters	4480 / 0 / 284	
Goodness-of-fit on F²	1.043	
Δ/σ_{\max}	0.001	
Final R indices	3987 data; I > 2σ(I)	R1 = 0.0321, wR2 = 0.0814
	all data	R1 = 0.0373, wR2 = 0.0854
Weighting scheme	w = 1/[σ ² (F _σ ²) + (0.0430 P) ² + 0.4930 P] where P = (F _σ ² + 2 F _c ²)/3	
Largest diff. peak and hole	0.245 and -0.419 eÅ ⁻³	
R.M.S. deviation from mean	0.055 eÅ ⁻³	

Table 78. Sample and crystal data for KlePh15.

Chemical formula	C ₆₄ H ₉₀ Cl ₂ N ₄ O ₄ Pd ₂	
Formula weight	1263.09 g/mol	
Temperature	100(2) K	
Wavelength λ	0.71073 Å	
Crystal size	0.222 x 0.248 x 0.275 mm	
Crystal habit	clear yellow fragment	
Crystal system	monoclinic	
Space group	P 1 21/c 1	
Unit cell dimensions	a = 15.4239(14) Å	$\alpha = 90^\circ$
	b = 23.676(2) Å	$\beta = 92.839(3)^\circ$
	c = 20.7488(19) Å	$\gamma = 90^\circ$
Volume	7567.7(12) Å ³	
Z	4	
Density (calculated)	1.109 g/cm ³	
Absorption coefficient	0.585 mm ⁻¹	
F(000)	2640	

Table 79. Data collection and structure refinement for KlePh15.

Diffractometer	Bruker D8 Venture	
Radiation source	TXS rotating anode, Mo	
Theta range for data collection	2.35 to 26.37°	
Index ranges	-19 ≤ h ≤ 19, -29 ≤ k ≤ 29, -25 ≤ l ≤ 25	
Reflections collected	320684	
Independent reflections	15477 [R(int) = 0.0541]	
Coverage of independent reflections	99.9%	
Absorption correction	Multi-Scan	
Max. and min. transmission	0.8810 and 0.8560	
Refinement method	Full-matrix least-squares on F ²	
Refinement program	SHELXL-2014/7 (Sheldrick, 2014)	
Function minimized	$\sum w(F_\sigma^2 - F_c^2)^2$	
Data / restraints / parameters	15477 / 132 / 747	
Goodness-of-fit on F²	1.018	
Δ/σ_{\max}	0.003	
Final R indices	13346 data; I > 2σ(I)	R1 = 0.0287, wR2 = 0.0736
	all data	R1 = 0.0363, wR2 = 0.0775
Weighting scheme	w = 1/[σ ² (F _σ ²) + (0.0372 P) ² + 5.5048 P] where P = (F _σ ² + 2 F _c ²)/3	
Largest diff. peak and hole	0.921 and -0.495 eÅ ⁻³	
R.M.S. deviation from mean	0.054 eÅ ⁻³	

Table 80. Sample and crystal data for KlePh16.

Chemical formula	C ₂₁ H ₃₀ F ₃ OP ₂	
Formula weight	386.42 g/mol	
Temperature	100(2) K	
Wavelength λ	0.71073 Å	
Crystal size	0.230 x 0.257 x 0.265 mm	
Crystal habit	colorless fragment	
Crystal system	triclinic	
Space group	P -1	
Unit cell dimensions	a = 12.029(3) Å	$\alpha = 76.147(9)^\circ$
	b = 13.317(3) Å	$\beta = 82.236(9)^\circ$
	c = 14.809(3) Å	$\gamma = 88.777(11)^\circ$
Volume	2282.0(9) Å ³	
Z	4	
Density (calculated)	1.125 g/cm ³	
Absorption coefficient	0.150 mm ⁻¹	
F(000)	824	

Table 81. Data collection and structure refinement for KlePh16.

Diffractometer	Bruker D8 Venture	
Radiation source	TXS rotating anode, Mo	
Theta range for data collection	2.34 to 26.02°	
Index ranges	-14 ≤ h ≤ 14, -16 ≤ k ≤ 16, -18 ≤ l ≤ 18	
Reflections collected	98495	
Independent reflections	8982 [R(int) = 0.0603]	
Coverage of independent reflections	99.9%	
Absorption correction	Multi-Scan	
Max. and min. transmission	0.9660 and 0.9610	
Refinement method	Full-matrix least-squares on F ²	
Refinement program	SHELXL-2014/7 (Sheldrick, 2014)	
Function minimized	$\sum w(F_\sigma^2 - F_c^2)^2$	
Data / restraints / parameters	8982 / 0 / 477	
Goodness-of-fit on F²	1.037	
Δ/σ_{\max}	0.001	
Final R indices	7938 data; I > 2σ(I)	R1 = 0.0372, wR2 = 0.0996
	all data	R1 = 0.0419, wR2 = 0.1032
Weighting scheme	w = 1/[σ ² (F _σ ²) + (0.0478 P) ² + 1.0826 P] where P = (F _σ ² + 2 F _c ²)/3	
Largest diff. peak and hole	0.328 and -0.292 eÅ ⁻³	
R.M.S. deviation from mean	0.049 eÅ ⁻³	

Table 82. Sample and crystal data for KlePh17.

Chemical formula	C ₃₃ H ₄₃ F ₆ O ₂ P ₂	
Formula weight	629.62 g/mol	
Temperature	296(2) K	
Wavelength λ	0.71073 Å	
Crystal size	0.132 x 0.196 x 0.234 mm	
Crystal habit	clear colorless fragment	
Crystal system	monoclinic	
Space group	P 1 21/c 1	
Unit cell dimensions	a = 9.345(3) Å	$\alpha = 90^\circ$
	b = 24.137(8) Å	$\beta = 107.454(16)^\circ$
	c = 14.119(5) Å	$\gamma = 90^\circ$
Volume	3038.1(18) Å ³	
Z	4	
Density (calculated)	1.377 g/cm ³	
Absorption coefficient	0.205 mm ⁻¹	
F(000)	1328	

Table 83. Data collection and structure refinement for KlePh17.

Diffractometer	Bruker D8 Kappa Apex II	
Radiation source	fine-focus sealed tube, Mo	
Theta range for data collection	2.27 to 26.02°	
Index ranges	-11 ≤ h ≤ 11, -29 ≤ k ≤ 29, -17 ≤ l ≤ 17	
Reflections collected	68576	
Independent reflections	5985 [R(int) = 0.436]	
Coverage of independent reflections	99.9%	
Absorption correction	Multi-Scan	
Max. and min. transmission	0.9730 and 0.9540	
Refinement method	Full-matrix least-squares on F ²	
Refinement program	SHELXL-2018/7 (Sheldrick, 2018)	
Function minimized	$\sum w(F_\sigma^2 - F_c^2)^2$	
Data / restraints / parameters	5985 / 0 / 381	
Goodness-of-fit on F²	1.058	
Δ/σ_{\max}	0.001	
Final R indices	4844 data; I > 2σ(I)	R1 = 0.0510, wR2 = 0.1188
	all data	R1 = 0.0660, wR2 = 0.1267
Weighting scheme	w = 1/[σ ² (F _σ ²) + (0.0469 P) ² + 4.7135 P] where P = (F _σ ² + 2 F _c ²)/3	
Largest diff. peak and hole	0.715 and -0.397 eÅ ⁻³	
R.M.S. deviation from mean	0.063 eÅ ⁻³	

Table 84. Sample and crystal data for KlePh18.

Chemical formula	C ₂₅ H ₅₉ NO ₅	
Formula weight	453.73 g/mol	
Temperature	100(2) K	
Wavelength λ	0.71073 Å	
Crystal size	0.150 x 0.380 x 0.380 mm	
Crystal habit	clear colorless fragment	
Crystal system	monoclinic	
Space group	P 1 21/c 1	
Unit cell dimensions	a = 13.6090(10) Å	$\alpha = 90^\circ$
	b = 14.8330(11) Å	$\beta = 105.270(3)^\circ$
	c = 14.7747(11) Å	$\gamma = 90^\circ$
Volume	2877.2(3) Å ³	
Z	4	
Density (calculated)	1.047 g/cm ³	
Absorption coefficient	0.070 mm ⁻¹	
F(000)	1024	

Table 85. Data collection and structure refinement for KlePh18.

Diffractometer	Bruker D8 Venture Duo IMS	
Radiation source	IMS microsource, Mo	
Theta range for data collection	2.07 to 25.68°	
Index ranges	-16 ≤ h ≤ 16, -18 ≤ k ≤ 18, -18 ≤ l ≤ 18	
Reflections collected	122181	
Independent reflections	5462 [R(int) = 0.0539]	
Coverage of independent reflections	100.0%	
Absorption correction	Multi-Scan	
Max. and min. transmission	0.9900 and 0.9740	
Refinement method	Full-matrix least-squares on F ²	
Refinement program	SHELXL-2017/7 (Sheldrick, 2017)	
Function minimized	$\sum w(F_\sigma^2 - F_c^2)^2$	
Data / restraints / parameters	5462 / 0 / 313	
Goodness-of-fit on F²	1.072	
Δ/σ_{\max}	0.001	
Final R indices	4750 data; I > 2σ(I)	R1 = 0.0346, wR2 = 0.0812
	all data	R1 = 0.0424, wR2 = 0.0881
Weighting scheme	w = 1/[σ ² (F _σ ²) + (0.0330 P) ² + 1.0550 P] where P = (F _σ ² + 2 F _c ²)/3	
Largest diff. peak and hole	0.235 and -0.170 eÅ ⁻³	
R.M.S. deviation from mean	0.033 eÅ ⁻³	

Table 86. Sample and crystal data for KlePh19.

Chemical formula	C ₆₉ H ₅₇ Cl ₃ N ₂ Pd	
Formula weight	1126.91 g/mol	
Temperature	100(2) K	
Wavelength λ	0.71073 Å	
Crystal size	0.131 x 0.187 x 0.225 mm	
Crystal habit	clear intense red fragment	
Crystal system	monoclinic	
Space group	P 1 21/n 1	
Unit cell dimensions	a = 14.1447(7) Å	$\alpha = 90^\circ$
	b = 19.7739(9) Å	$\beta = 90.135(2)^\circ$
	c = 19.5648(8) Å	$\gamma = 90^\circ$
Volume	5472.2(4) Å ³	
Z	4	
Density (calculated)	1.368 g/cm ³	
Absorption coefficient	0.531 mm ⁻¹	
F(000)	2328	

Table 87. Data collection and structure refinement for KlePh19.

Diffractometer	Bruker D8 Venture Duo IMS	
Radiation source	IMS microsource, Mo	
Theta range for data collection	2.05 to 26.37°	
Index ranges	-17 ≤ h ≤ 17, -24 ≤ k ≤ 24, -24 ≤ l ≤ 24	
Reflections collected	330622	
Independent reflections	11190 [R(int) = 0.0371]	
Coverage of independent reflections	99.9%	
Absorption correction	Multi-Scan	
Max. and min. transmission	0.9340 and 0.8900	
Refinement method	Full-matrix least-squares on F ²	
Refinement program	SHELXL-2018/3 (Sheldrick, 2018)	
Function minimized	$\sum w(F_\sigma^2 - F_c^2)^2$	
Data / restraints / parameters	11190 / 0 / 678	
Goodness-of-fit on F²	1.052	
Δ/σ_{\max}	0.004	
Final R indices	10213 data; I > 2σ(I)	R1 = 0.0284, wR2 = 0.0736
	all data	R1 = 0.0326, wR2 = 0.0777
Weighting scheme	w = 1/[σ ² (F _σ ²) + (0.0351 P) ² + 5.6385P] where P = (F _σ ² + 2 F _c ²)/3	
Largest diff. peak and hole	0.665 and -0.499 eÅ ⁻³	
R.M.S. deviation from mean	0.059 eÅ ⁻³	

Table 88. Sample and crystal data for HinKrl.

Chemical formula	C ₁₃₂ H ₁₈₄ Br ₄ Cl ₂ P ₄	
Formula weight	2497.90 g/mol	
Temperature	293(2) K	
Wavelength λ	0.71073 Å	
Crystal size	0.085 x 0.120 x 0.150 mm	
Crystal habit	clear colorless fragment	
Crystal system	monoclinic	
Space group	P 1 n 1	
Unit cell dimensions	a = 11.218(4) Å	$\alpha = 90^\circ$
	b = 16.526(5) Å	$\beta = 98.569(15)^\circ$
	c = 34.004(13) Å	$\gamma = 90^\circ$
Volume	6234.(4) Å ³	
Z	2	
Density (calculated)	1.331 g/cm ³	
Absorption coefficient	1.562 mm ⁻¹	
F(000)	2624	

Table 89. Data collection and structure refinement for HinKrl.

Diffractometer	Bruker D8 Venture Duo IMS	
Radiation source	IMS microsource, Mo	
Theta range for data collection	2.02 to 26.08°	
Index ranges	-13 ≤ h ≤ 13, -20 ≤ k ≤ 20, -42 ≤ l ≤ 42	
Reflections collected	127418	
Independent reflections	24642 [R(int) = 0.0524]	
Coverage of independent reflections	99.98	
Absorption correction	Multi-Scan	
Max. and min. transmission	0.7453 and 0.6817	
Refinement method	Full-matrix least-squares on F ²	
Refinement program	SHELXL-2018/3 (Sheldrick, 2018)	
Function minimized	$\sum w(F_\sigma^2 - F_c^2)^2$	
Data / restraints / parameters	24642 / 2 / 1333	
Goodness-of-fit on F²	1.020	
Δ/σ_{\max}	0.001	
Final R indices	20755 data; I > 2σ(I)	R1 = 0.0376, wR2 = 0.0770
	all data	R1 = 0.0522, wR2 = 0.0834
Weighting scheme	w = 1/[σ ² (F _σ ²) + (0.0273 P) ² + 4.6197 P] where P = (F _σ ² + 2 F _c ²)/3	
Largest diff. peak and hole	0.785 and -0.800 eÅ ⁻³	
R.M.S. deviation from mean	0.064 eÅ ⁻³	

8.4 UV/Vis spectrum of [(Trop)SPhos]PF₆

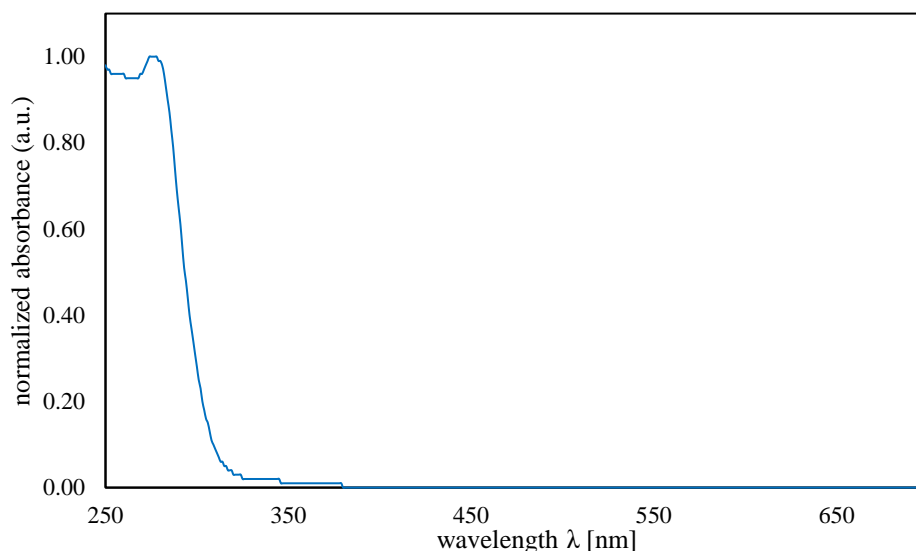
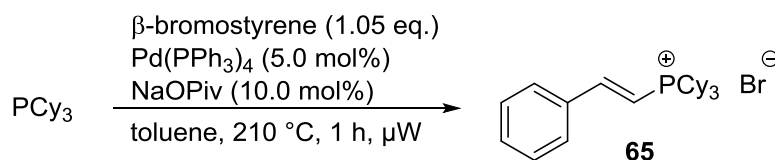


Figure 51. UV/Vis spectrum of [(Trop)SPhos]PF₆ in CHCl₃ (408 μM), normalized to A_{275nm} (absorption maximum, and corrected by a blank measurement of CHCl₃). UV/Vis was recorded from 250 to 700 nm, since chloroforms absorption is too pronounced for wavelengths <250 nm.

8.5 Typical reaction profile of a microwave assisted reaction

A typical reaction profile of a microwave assisted reaction (scheme 77) is shown in figure 52. During a first heating process, the reaction mixture is heated as fast as possible inside an adiabatic reactor (pressure of the closed cavity: green curve) to a target temperature (temperature: orange curve, here 210 °C). The temperature is hold for one hour, which indicates the actual reaction time. In this type of reaction, the pressure usually rises to approx. 7 or 8 bar. Afterwards, the vessel is cooled to 55 °C with the aid of compressed air and placed back into the autosampler. The cooling phase exerts a minor influence on the reaction progress in comparison to the heating phase, during which the educt concentration is maximal. The orange curve indicates the heating power used by the microwave.



Scheme 77. Microwave assisted synthesis of (*E*)-tricyclohexyl(styryl)phosphonium bromide (**65**).

Anton Paar Monowave 300

Serial Number: 80707851
Instrument Software Version: 3.30.8548.5

Processing Protocol

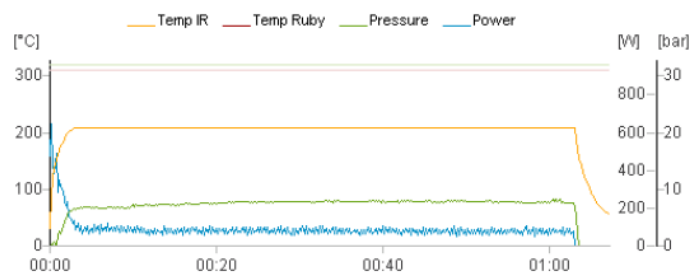
- ▶ Experiment Name: PK-445-2
- ▶ Experiment Date: 2/12/2018 11:32:08 AM
- ▶ User: Administrator
- ▶ Temperature Control: IR
- ▶ Vial Type: Glass vial G10

Steps

Step	Program	Temperature	Time	Cooling	Stirrer Speed
		°C	hh:mm:ss		rpm
1	Heat as fast as possible	210	-	Off	600
2	Hold	-	01:00:00	Off	600
3	Cool down	55	-	On	600

Experiment Result

- ▶ Result: OK



Raw data is accessible for download from the "Browse Results" dialog on Monowave 300 (see serial number above)

Adjustment Information

- ▶ Date of last IR sensor adjustment: 10/12/2017 1:13:24 PM
- ▶ User name of last IR sensor adjustment: Administrator

Figure 52. Reaction profile of microwave assisted reaction; synthesis of (*E*)-tricyclohexyl(styryl)phosphonium bromide (**65**).

8.6 Exemplary analysis of a quantitative NMR spectrum

After an aqueous work-up the crude product was diluted in CDCl_3 (800 μL). The internal standard (here: 1,1,2,2-tetrachloroethane, ρ 1.59 g/mL , M 167.848 g/mol ; 50.0 μL added = 473.6 μmol) was added using a microliter syringe (50 μL Hamilton) and the flask was closed with a yellow cap. The solution was mixed vigorously by swiveling. A part of the sample (500 μL) was transferred to an NMR tube and a proton NMR ($d_1 = 20$ s, 16 scans) was recorded (either AVHD400 or AVHD500). The signals of the expected products were identified by comparing with reported spectroscopic data. An example spectrum of a typical catalytic metalation is shown in figure 53.

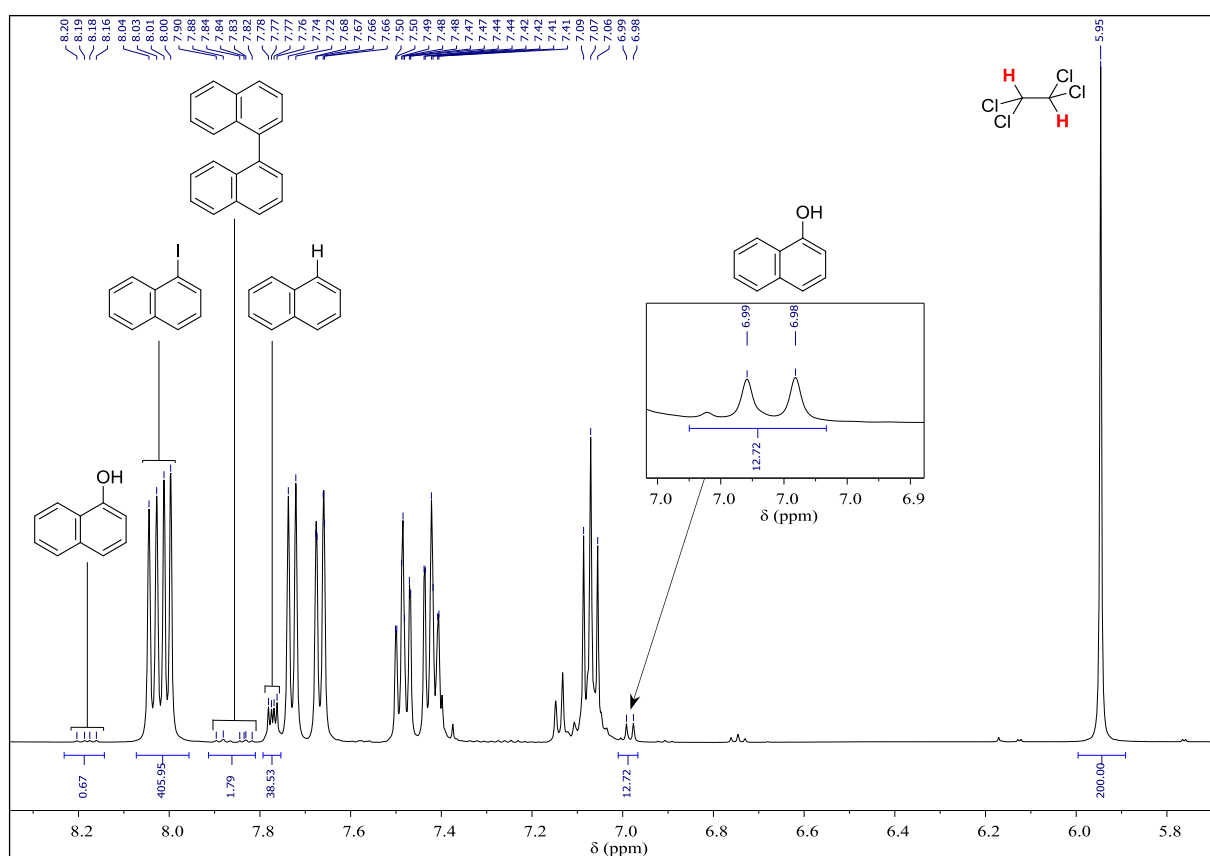


Figure 53. ^1H -NMR spectrum (CDCl_3) of a typical catalytic metalation reaction. The aromatic region as well as the internal standard peak with integrals of the relevant peaks are expanded. The signal of 1-NapOH (black frame) is further magnified.

The yield of the reaction is determined by comparison of the integral of the internal standard with the integral of characteristic signals of the reaction product(s) and starting material(s) in the ^1H -NMR spectra. Area integration of the signals for internal standard

(1,1,2,2-tetrachloroethane in the above case) did not include the ^{13}C satellites. The calculation of the percentage of each reaction product is shown in table 90.

Table 90. Analysis of a quantitative NMR spectrum in CDCl_3 .^a

entry	compound	δ [ppm]	integral	#(protons)	n [μmol]	percentage ω [mol%]
1 ^b	1,1,2,2-tetrachloroethane	5.95	200.00	2	473.6	-
2	1-NapI	8.02	405.95	2	961.3 ^c	96.1 ^d
3 ^e	1-NapH	7.77	38.53	4	45.6	4.6
4	1-NapOH	8.19	0.67	1	3.2	0.3
5	1,1'-binaphthalene	7.86	1.79	4	2.1	0.2

^aReaction scale: 1.00 mmol = 1000 μmol . ^b $V = 50 \mu\text{L}$. $m = \rho \cdot V = 1.59 \text{ mg}/\mu\text{L} \cdot 50 \mu\text{L} = 79.5 \text{ mg} \rightarrow n = 79.5 \text{ mg} : 167.848 \text{ g/mol} = 473.6 \mu\text{mol}$. ^c $n = 405.95 : 2 : 100 \cdot 473.6 \mu\text{mol} = 961.3 \mu\text{mol}$. ^d $\omega = n : 1000 \mu\text{mol} = 961.3 \mu\text{mol} : 1000 \mu\text{mol} = 96.1 \text{ mol\%}$. ^eThe signals of naphthalene overlay with those of 1-NapI.

8.7 Reprint Permission

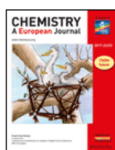
8.7.1 Generation of Organozinc Reagents by Nickel-Diazadiene-Complex Catalyzed Zinc Insertion into Aryl Sulfonates



RightsLink®

?
Help

✉
Email Support



Generation of Organozinc Reagents by Nickel Diazadiene Complex Catalyzed Zinc Insertion into Aryl Sulfonates

Author: Philippe Klein, Vivien Denise Lechner, Tanja Schimmel, et al

Publication: Chemistry - A European Journal

Publisher: John Wiley and Sons

Date: Nov 26, 2019

© 2019 The Authors. Published by Wiley-VCH Verlag GmbH & Co. KGaA.

Open Access Article

This is an open access article distributed under the terms of the [Creative Commons CC BY](#) license, which permits unrestricted use, distribution, and reproduction in any medium, provided the original work is properly cited.

You are not required to obtain permission to reuse this article.

For an understanding of what is meant by the terms of the Creative Commons License, please refer to [Wiley's Open Access Terms and Conditions](#).

Permission is not required for this type of reuse.

Wiley offers a professional reprint service for high quality reproduction of articles from over 1400 scientific and medical journals. Wiley's reprint service offers:

- Peer reviewed research or reviews
- Tailored collections of articles
- A professional high quality finish
- Glossy journal style color covers
- Company or brand customisation
- Language translations
- Prompt turnaround times and delivery directly to your office, warehouse or congress.

Please contact our Reprints department for a quotation. Email corporatesaleseurope@wiley.com or corporatesalesusa@wiley.com or corporatesalesDE@wiley.com.

Chemistry - A European Journal

Published by Wiley on behalf of CPSE (the "Owner")

LICENSE AGREEMENT FOR PUBLISHING CC-BY

Date: October 23, 2019

Contributor name: Lukas Hintermann

Contributor address:

Manuscript number: chem.201904545

Re: Manuscript entitled Generation of Organozinc Reagents by Nickel-Diazadiene-Complex Catalyzed Zinc Insertion into Aryl Sulfonates (the "Contribution")

for publication in Chemistry - A European Journal (the "Journal")

published by Wiley-VCH Verlag GmbH & Co. KGaA ("Wiley")

Dear Contributor(s):

Thank you for submitting your Contribution for publication. In order to expedite the editing and publishing process and enable Wiley to disseminate your Contribution to the fullest extent, we need to have this Agreement executed. If the Contribution is not accepted for publication, or if the Contribution is subsequently rejected, this Agreement will be null and void.

Publication cannot proceed without a signed copy of this Agreement and payment of the appropriate article publication charge.

A. TERMS OF USE

1. The Contribution will be made Open Access under the terms of the [Creative Commons Attribution License](#) which permits use, distribution and reproduction in any medium, provided that the Contribution is properly cited.
2. For an understanding of what is meant by the terms of the Creative Commons License, please refer to [Wiley's Open Access Terms and Conditions](http://www.wileyauthors.com/OAA) (<http://www.wileyauthors.com/OAA>).

3. The Contributor may make use of the submitted and peer reviewed versions of the Contribution prior to publication, provided that the final Contribution is cited appropriately as set forth in paragraph E below. Nothing herein shall permit dual publication in violation of journal ethical practices.
4. The Owner (and Wiley, where Wiley is not the Owner) reserves the right to require changes to the Contribution, including changes to the length of the Contribution, as a condition of acceptance. The Owner (and Wiley, where Wiley is not the Owner) reserves the right, notwithstanding acceptance, not to publish the Contribution if for any reason such publication would in the reasonable judgment of the Owner (and Wiley, where Wiley is not the Owner), result in legal liability or violation of journal ethical practices. If the Owner (or Wiley, where Wiley is not the Owner) decides not to publish the Contribution, no Article Processing Charge or any other fee shall be charged. The Contributor is free to submit the Contribution to any other journal from any other publisher.

B. RETAINED RIGHTS

The Contributor or, if applicable, the Contributor's employer, retains all proprietary rights in addition to copyright, such as patent rights in any process, procedure or article of manufacture described in the Contribution.

C. LICENSE

Owner, Wiley (where Wiley is not the Owner), and users have non-exclusive rights under the terms of the Creative Commons Attribution License.

D. CONTRIBUTIONS OWNED BY EMPLOYER

If the Contribution was written by the Contributor in the course of the Contributor's employment (as a "work-made-for-hire"), and the employer owns the copyright in the Contribution, the employer company/institution must execute this Agreement (in addition to the Contributor) in the space provided below.

E. COPYRIGHT NOTICE

Owner (and Wiley, where Wiley is not the Owner), the Contributor, and the company/institution agree that any and all copies of the Contribution or any part thereof distributed or posted by them in print or electronic format as permitted herein will include the notice of copyright as stipulated in the Journal and a full citation to the final published version of the Contribution in the Journal as published by Wiley.

F. CONTRIBUTOR'S REPRESENTATIONS

The Contributor represents that: (i) the Contribution is the Contributor's original work, all individuals identified as Contributors actually contributed to the Contribution, and all individuals who contributed are included; (ii) if the Contribution was prepared jointly, the Contributor has

informed the co-Contributors of the terms of this Agreement and has obtained their signed written permission to execute this Agreement on their behalf as their agent; (iii) the Contribution is submitted only to this Journal and has not been published before, has not been included in another manuscript, and is not currently under consideration or accepted for publication elsewhere; (iv) if excerpts from copyrighted works owned by third parties are included, the Contributor shall obtain written permission from the copyright owners for all uses as set forth in the standard permissions form or the Journal's Author Guidelines, and show credit to the sources in the Contribution; (v) the Contribution and any submitted Supporting Information contains no libelous or unlawful statements, does not infringe upon the rights (including without limitation the copyright, patent or trademark rights) or the privacy of others, result in any breach of confidentiality, violate a contract or any law, or contain material or instructions that might cause harm or injury and only utilize data that has been obtained in accordance with applicable legal requirements and Journal policies; (vi) there are no conflicts of interest relating to the Contribution, except as disclosed. Accordingly, the Contributor represents that the following information shall be clearly identified on the title page of the Contribution: (1) all financial and material support for the research and work; (2) any financial interests the Contributor or any co-Contributors may have in companies or other entities that have an interest in the information in the Contribution or any submitted Supporting Information (e.g., grants, advisory boards, employment, consultancies, contracts, honoraria, royalties, expert testimony, partnerships, or stock ownership); and (3) indication of no such financial interests if appropriate.

Wiley reserves the right, notwithstanding acceptance, to require changes to the Contribution, including changes to the length of the Contribution, and the right not to publish the Contribution if for any reason such publication would in the reasonable judgment of Wiley, result in legal liability or violation of journal ethical practices.

G. USE OF INFORMATION

The Contributor acknowledges that, during the term of this Agreement and thereafter, the Owner (and Wiley, where Wiley is not the owner) may process the Contributor's personal data, including storing or transferring data outside of the country of the Contributor's residence, in order to process transactions related to this Agreement and to communicate with the Contributor and that the Publisher has a legitimate interest in processing the Contributor's personal data. By entering into this Agreement, the Contributor agrees to the processing of the Contributor's personal data (and, where applicable, confirms that the Contributor has obtained the permission from all other contributors to process their personal data). Wiley shall comply with all applicable laws, statutes and regulations relating to data protection and privacy and shall process such personal data in accordance with Wiley's Privacy Policy located at: <https://www.wiley.com/en-us/privacy>.

I agree to the OPEN ACCESS AGREEMENT as shown above, consent to execution and delivery of the Open Access Agreement electronically and agree that an electronic signature shall be given the same legal force as a handwritten signature, and have obtained written permission from all other contributors to execute this Agreement on their behalf.

Contributor's signature (type name here): Lukas Hintermann

Date: October 23, 2019

SELECT FROM OPTIONS BELOW:

Contributor-owned work

U.S. Government work

Note to U.S. Government Employees

*A contribution prepared by a U.S. federal government employee as part of the employee's official duties, or which is an official U.S. Government publication, is called a "U.S. Government work", and is in the public domain in the United States. If the Contribution was not prepared as part of the employee's duties or is not an official U.S. government publication, it is not a U.S. Government work. Contributor acknowledges that the Contribution will be published in the United States and other countries. Please sign the form to confirm Contributor Representations. If at least one author is **not** a U.S. government employee, then the non-government author should also sign the form, indicating agreement to publication on CC-BY basis and selecting the appropriate additional ownership selection option. If more than one author is not a U.S. government employee, one may sign on behalf of the others.*

U.K. Government work (Crown Copyright)

The rights in a contribution prepared by an employee of a UK government department, agency or other Crown body as part of his/her official duties, or which is an official government publication, belong to the Crown and must be made available under the terms of the Open Government License. Contributors must ensure they comply with departmental regulations and submit the appropriate authorisation to publish. If your status as a government employee legally prevents you from signing this Agreement, please contact the Journal production editor. If this selection does not apply to at least one author in the group, this author should also sign the form, indicating agreement to publication on CC-BY basis and selecting the appropriate additional ownership selection option. If this applies to more than one author, one may sign on behalf of the others.

Other

Including Other Government work or Non-Governmental Organisation work

Note to Non-U.S., Non-U.K. Government Employees or Non-Governmental Organisation Employees

If you are employed by the World Health Organization or UNU-WIDER, please download a copy of the license agreement from <http://www.wileyauthors.com/licensingFAQ> and upload the form to the Wiley Author Services

Dashboard. If your status as a government or non-governmental organisation employee legally prevents you from signing this Agreement, please contact the Journal production editor. If this selection does not apply to at least one author in the group, this author should also sign the form, indicating agreement to publication on CC-BY basis and selecting the appropriate additional ownership selection option. If this applies to more than one author, one may sign on behalf of the others.

Name of Government/Non-Governmental Organisation:

[] Company/institution owned work (made for hire in the course of employment)

If this selection does not apply to at least one author in the group, this author should also sign the form, indicating agreement to publication on CC-BY basis and selecting the appropriate additional ownership selection option. If this applies to more than one author, one may sign on behalf of the others.

Name of Company/Institution:

Authorized Signature of Employer:

Date:

Signature of Employee:

Date:
